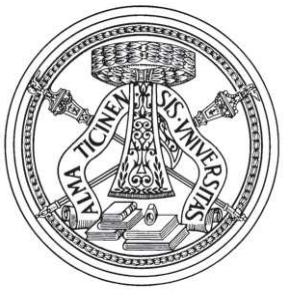

UNIVERSITÀ DEGLI STUDI DI PAVIA

PHD COURSE IN CHEMICAL AND PHARMACEUTICAL SCIENCES AND INDUSTRIAL INNOVATION

XXXIV CYCLE

Department Director: Chiar.ma Prof. Antonella Profumo

PhD Course Coordinator: Chiar.mo. Prof. Giorgio Colombo

COMPUTATIONAL CHEMISTRY: A USEFUL ART TO SUPPORT ASYMMETRIC ORGANIC SYNTHESIS AND ORGANOMETALLIC CHEMISTRY

Supervisor:
Chiar.mo Prof. Lucio Toma

Co-Supervisors:
Chiar.mo Prof. Giuseppe Zanoni
Chiar.ma Prof. Fernanda Duarte Gonzalez (University of Oxford)

PhD Candidate: Emanuele Casali

Anno Dottorale 2020/2021

"I would like to emphasize strongly my belief that the era of computing chemists, when hundreds if not thousands of chemists will go to the computing machine instead of the laboratory for increasingly many facets of chemical information, is already at hand. There is only one obstacle, namely that someone must pay for the computing time. "

Robert S. Mulliken

Contents

Introduction

Computational Chemistry is the science of using computer simulations to understand, predict and help explaining the chemical reactivity.

The predictive power of the simulations is closely related with the characteristics of the machines available for the calculation. The number of floating-point operations per second (FLOPS) and the memory capacity are the most important parameters that determine the possibility of running simulations in a reasonable time. Although the theoretical support for the formulation of models was developed in the early years of the twentieth century, the great step forward in Computational Chemistry began during the last decades of the twentieth century, precisely because sufficiently powerful hardware systems began to be available. Moreover, thanks to the increase in the computational performances, Computational Chemistry has recently become an essential research method not only in Chemistry, but also in the related areas of research in molecular science. The development of new methods like Machine Learning and a new way to implement them, has resulted in a real boom in the past few years. As an example, in the figure below is reported the number of publications per year in different related fields of Computational Chemistry.[1]

It can be easily observed how the increase in the last years has been more than exponential, thus placing this type of Chemistry at the cutting edges of the research. For all the reasons reported above, we focused our attention for this PhD Thesis on the usage of Computational Chemistry applied to the Organic Synthesis and Organometallic Chemistry. However, even if the Computational Chemistry can be considered as the "*Ariadne's thread*" running all across this work, we also focused our research activities on the experimental synthesis, so that one supported the

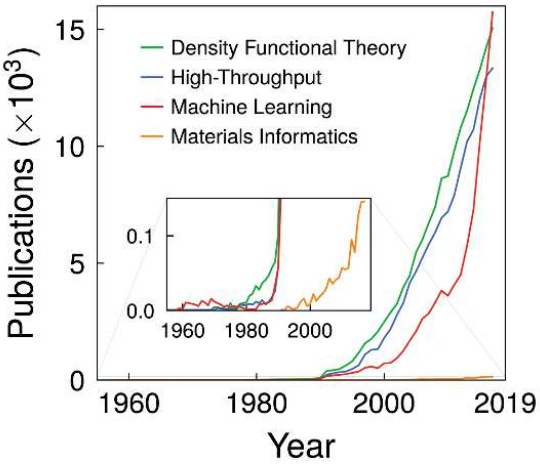

other. The result is a continuous flow of interconnections between experiments and calculations that leads in the contemporary work on multiple projects across the three years.

Here we decided to report the most significative ones that mainly characterized the PhD course and which are ordered in specific chapters.

In the first chapter we will talk about the venerable Tsuji-Trost Asymmetric Allylic Alkylation (AAA). Indeed, in the past years a particular attention was dedicated in our research group to the synthesis of tetrahydrofurans containing metabolites. Specifically, we developed an interesting methodology to govern both the enantio- and the diastereoselectivities through a Tsuji-Trost allylic etherification as a key step for the entire process. However, a very unusual diastereoinversion at position 2 of the furan ring was observed in desymmetrizing a *meso*-diol compound without any erosion in diastereo- and enantio-selectivity. Our efforts were directed both to a computational investigation of this phenomena and to experimental proofs to highlight the most important features of the mechanism involved.

In the second chapter we will report on the research results obtained during the period spent at the University of Oxford in Prof. Duarte's group. There, a new topic in the application of Computational Chemistry as a predicting tool has been investigated. Specifically, we used the state-of-the-art Machine Learning models to manage a big amount of already published data, recover the most important factors that can be stereochemical, electrochemical and thermodynamic properties, and

use them as descriptors to teach the machine the reaction type, how it works and what is more relevant among reactants to give that particular output. In particular, we focused on a predictive tool for enantioselective H-bond catalyzed reactions. We elaborated models capable to predict the enantioselectivity for the Strecker synthesis of α-aminoacids and the Pictet-Spengler cyclizations of hydroxylactams.

In the third one, we report the developments on another project which characterized our group across the years: the synthesis of specifically modified titanocene derivatives for antitumoral proposals. In particular, we developed a new protecting group for the titanium metal center that helps stabilizing the complex during the synthetical approaches, especially those of bioorthogonal click chemistry. We thus prepared a scope of click titanocene reagents (azide, tetrazine, cyclooctyne, cycloalkene, ...) which has been made react with other biomolecular click partners to obtain complex molecules capable in increasing the selectivity of the antitumoral behavior. Moreover, the metal center protecting group can be easily removed and replaced with different types of halogenating reagents. To investigate the mechanism of these ligand exchanges, we run computational calculations which highlighted a large variety of pathways depending on the nature of the halogenating reagent. The biggest goal was achieved by the usage of an innovative fluorinating reagent, where the mechanism of action is a complete novelty in the field.

Finally, in the fourth chapter we report the result of a collaboration between our group and the Prof. Gallo's research group at University of Milan. In particular, they elaborated new stranded porphyrin iron complexes capable to induce cyclopropanation reactions between a carbene precursor (EDA) and an alkene, with good reaction yields and enantio- and diastereo-selectivities. Specifically, we computationally investigated the role of the bis-strapped structure of the catalyst and how the chemical environment around the site where the reaction takes place could influence the final observed output. Doing so, we elaborated a specific mechanism of the reaction which was computationally proven to take in consideration the various oxidation states of the iron metal center.

In each chapter, a specific introduction will lead the reader from the beginning,

with the development of the project, to the results we obtained and, in some cases, published. Supporting information and experimental procedures for each chapter can be found in a dedicated section at the end of the thesis, divided and ordered as the main chapter order [Appendix I (for experimental and computational details) and Appendix II (for cartesians coordinates)].

The main results we obtained during these years of PhD course can be considered as important checkpoints that helped chemists understanding intricated reaction mechanisms, as well as developing new catalysts to improve the outcome of their reactions or achieving new chemical reactivities to lay the foundations of new applications in organometallic chemical synthesis.

References

[1] Schleder, G. R.; Padilha, A. C. M.; Mera Acosta, C.; Costa, M.; Fazzio, A., From DFT to machine learning: recent approaches to materials science - a review, *J. Phys.: Mater.*, **2019**, *2*, 032001.

Chapter 1

Computational studies and asymmetric synthesis of THF-cores obtained through Tsuji-Trost AAA

Five-membered rings are a characteristic structural motif in several natural products and bioactive compounds. Within them, tetrahydrofurans are an extremely recurrent structures in both aqueous and terrestrial metabolites, which most of the times showed biological activities ranging from anti-tumoral to anti-microbial ones. Moreover, they show a too low abundancy on the planet due to the fact that most of them are biosynthetically produced only by few endangered species. For such reasons, a considerable effort was made in the previous years for the development of efficient synthetical pathways that could enable and extend the usage of those compounds in a medical destination being completely environmental friendly. In light of these considerations, a notable effort was directed to the synthetical control of the stereochemistry for the construction of substituted THF rings.[1] The aim of this chapter exactly places in this research field, with the special purpose of computationally explaining the observed selectivities of the reactions used to construct multi-substituted THF-cores. It constitutes the natural prosecution of the experimental PhD work done by Matteo Valli, Davide Sbarbada and Mattia Fredditori.[2]

Before to move to the real discussion of the results of our calculations it is important to give the reader an extensive background of the principal classes of natural products containing substituted tetrahydrofuran systems and to the main reaction we studied in these years.

1.1 THF building blocks in natural metabolites

The principal classes of natural products containing THF systems can be found in acetogenins from annonaceous plant family and lignans. Moreover, also different marine macrolidic metabolites show the huge presence of five-membered oxygenated rings. Let's analyse each of these families in detail.

1.1.1 Acetogenins

Acetogenins are a group of secondary metabolites typically present in the *Annonaceous sp.* plants, diffused in tropical and subtropical regions.[3] The common scaffold is often made by an unbranched C_{32} or C_{34} fatty acid which ends in a γ-lactone (Figure 1.1).

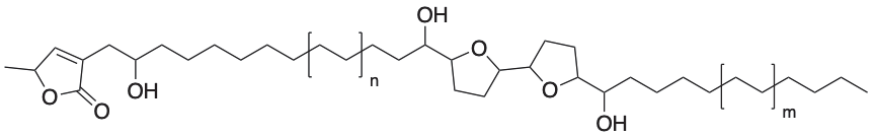

Figure 1.1: *Common skeleton of acetogenins.*[3]

Across the years a high number of acetogenins has been isolated and characterised on the nature of the functional groups which are present. Indeed, several oxygenated functions can be found in the structures, such as hydroxyl, ketone, epoxide, tetrahydrofuran (THF) and tetahydropyran (THP). Also, double and triple bonds were found.[3] Acetogenins were found to exhibit a wide range of biological properties such as cytotoxic, antitumoral, antiparasitic, pesticidal, antimicrobial and immunosuppresive activities.[3] While the mechanism of action of acetogenins is quite known

from studies that highlighted the inhibition of the mitochondrial respiratory chain complex I, the biosynthesis of these metabolites remains unknown and only postulated to involve a first formation of the γ-lactone on a long polyunsaturated fatty acid and then the enzymatic oxidation occurs to form THF and THP rings.[3],[4] Since the high number of acetogenins isolated till now (more than 500 different types), the classification is made following the nature of the functional groups and on the structural characteristics shown in Figure 1.2.

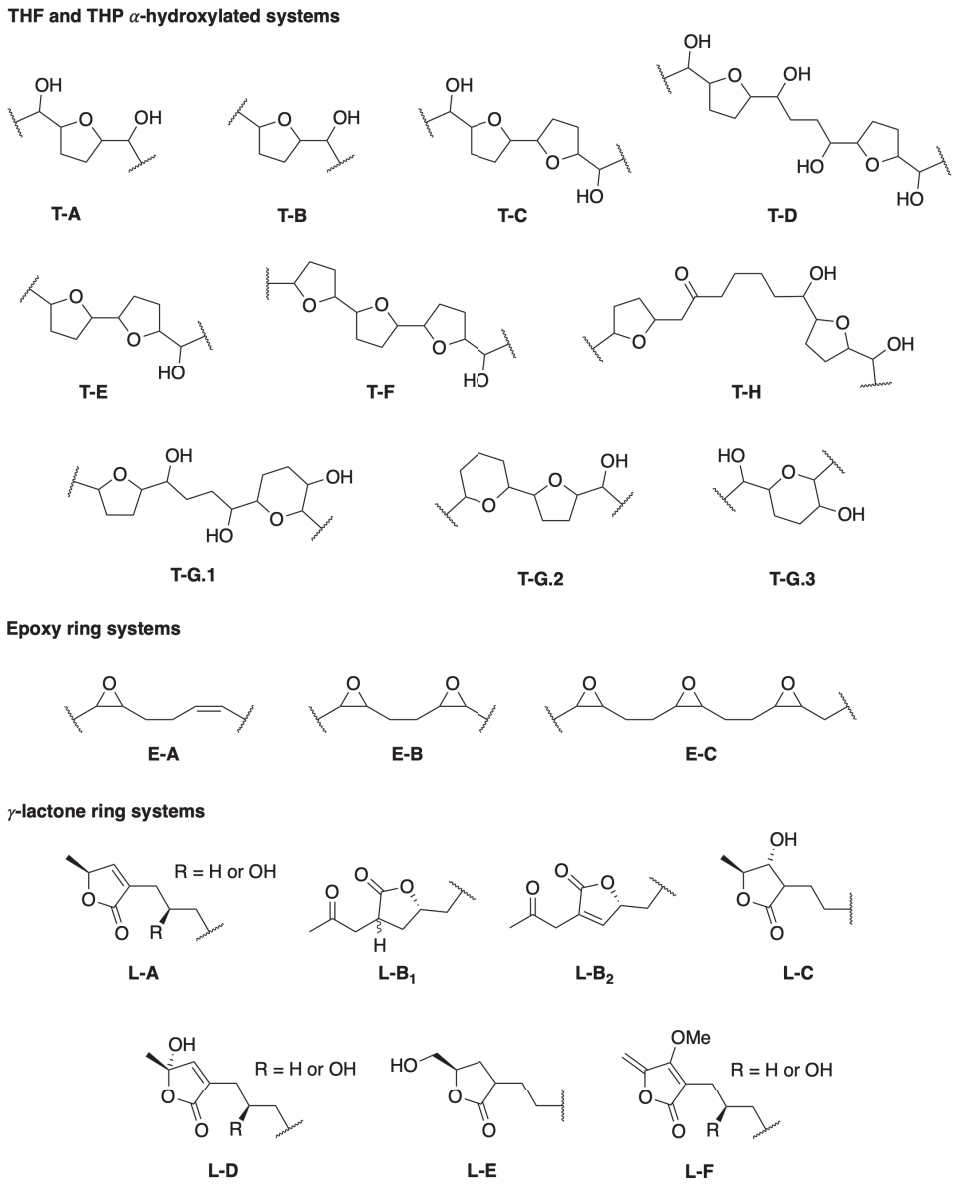

Figure 1.2: *Tetrahydrofuran (THF), tetrahydropyran (THP), epoxy and γ-lactone functional groups in Annonaceous acetogenins.*[3]

It appears clear the importance in having a synthetical control over the stereose-

lectivity in the formation of these oxygenated rings, to provide a reliable synthetical approach to the large-scale preparation of these interesting biologically active compounds.

1.1.2 Lignans

The second class of oxygenated rings compounds is represented by lignans. These molecules are secondary metabolites produced by plants derived from the oxidative dimerization of two phenylpropanoid units.[5] If compared with the above reported acetogenins, lignans show a simpler framework made up of two simple building blocks. However, this must not mislead on the fact that they show an enormous structural diversity.[5] In Figure 1.3 we can see that they usually contain at least one oxygenated five-membered ring, in the form of tetrahydrofuran moiety, or a γ-burtyrolactol, or a γ-burtyrolactone systems.

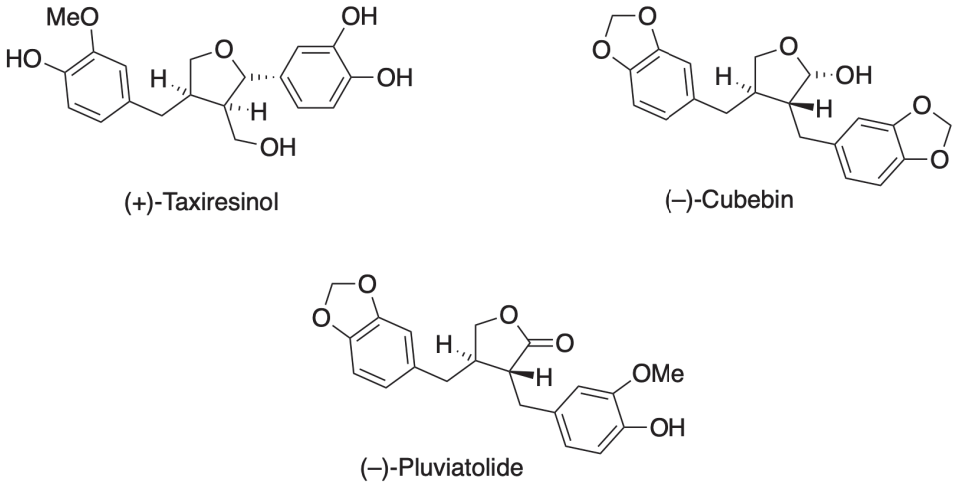

Figure 1.3: *Examples of lignans containing THF, γ-burtyrolactol and γ-burtyrolactone moieties.*

Like in the previous family, also the components of this one showed interesting biological activities, mainly acting as anti-cancer, anti-inflammatory, anti-microbial, anti-oxidative and immunosuppressive compounds.[5]

It appears clear also in this second group of compounds, the necessity in dedicating synthetical efforts to develop stereoselective total synthesis of these molecules.

1.1.3 Marine macrolides containing oxygenated rings

Marine organisms are able to produce a variety of structurally different compounds, with a high biological activity, which derives as an innate natural barrier to environmental aggressions. The high variability of these structures, both from the point of view of the presence of functional groups (mainly oxygenated) and of stereochemistry, makes them excellent candidates for the search for new compounds with pharmacological properties.[6]

In the last years, a significative number of structurally new metabolites have been isolated directly from sponges, dinoflagellates and algae or other marine invertebrates. As can be observed in Figure 1.4, these structures present common features like the high degree of oxygenation associated with complex stereochemical features.

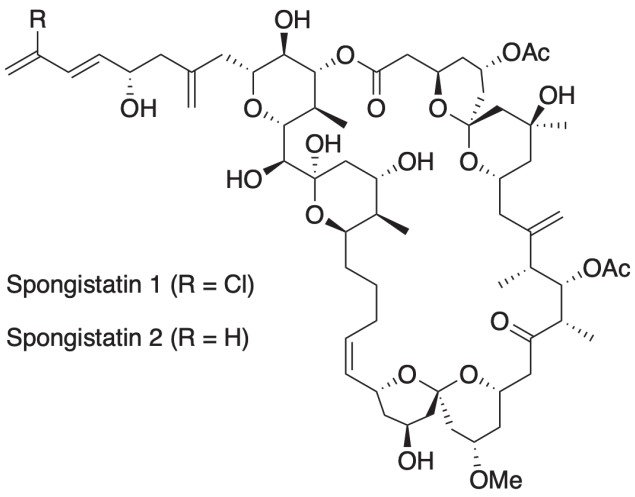

Figure 1.4: *Examples of marine polyketide macrocycles.*

These two combined chemical aspects represent a real challenge both for the characterization techniques of the molecular structure and the determination of biological properties like the bioactivity or the mechanism of action. Moreover, considering the fact that isolation from the natural sources furnish only small sample amounts if compared with the high quantity of organic raw material required for the extraction, it appears clear that the synthesis is necessary not only to increase the supply of these molecules or for structural and stereochemical assignments, but also for further and more extensive medical trials.

Other examples of large molecular size polyketide macrolides containing THP and THF rings can be found in the structures of Briostatin 1 and Eribulin (Figure 1.5).[7] They show diverse and interesting biological activities, as in the case of Eribulin which reached the clinical trial stage as a promising anticancer compound.

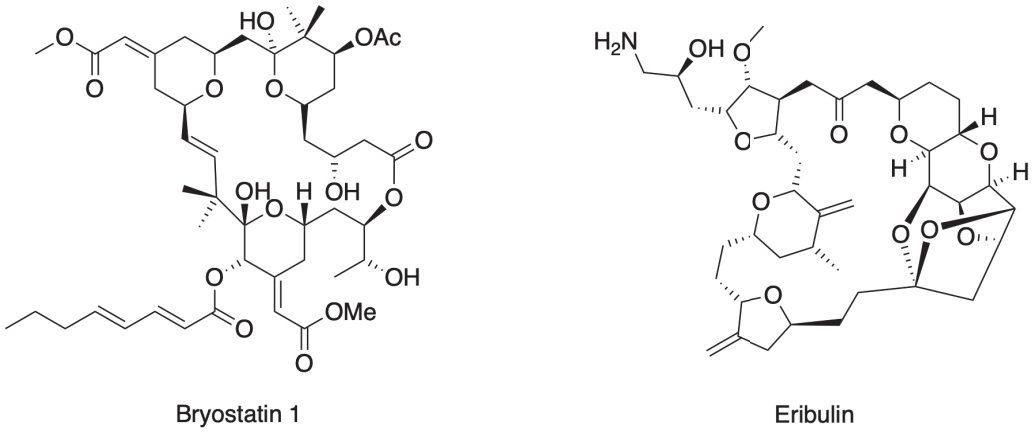

Figure 1.5: *Structures of Bryostatin 1 and Eribulin.*

A common observation can be done by analyzing several marine macrolides: large molecular size THP-containing macrolides rarely include also THF rings in their structures, but in some natural compound like Eribulin both of the two oxygenated ring systems can be found. Recently, THF-containing macrolides structures have achieved more interest as a bioactive compound. This led to an increase in the published description of THF-containing polyketide macrolides, with a concomitant exponential increase in their potential use as drug candidates. One of the main reasons for such a synthetical devotion to these substances, relies in the structure of the macrolides: indeed, they are generally smaller molecules and because of their smaller size, they are the first to have been studied and tested. This observation can be validated by comparing the structures of Bryostatin 1 (Figure 1.5) and the Haterumalide NA (Figure 1.6).

By remaining within the marine macrolides, we have also to remember those derived from the *Amphidium sp.* and other dinoflagellates organisms.

Amphidinolides are a huge class (more than 40 members) of secondary metabolites isolated from *Amphidium sp.*, where 15 of them show a fused or bridged THF

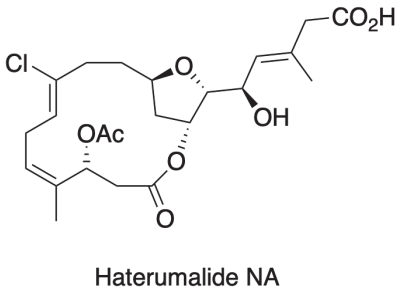

Figure 1.6: *Structure of Haterumalide NA.*

core in the macrolactone scaffold. Besides this important feature that perfectly places these compounds as introductory examples to this chapter, they also show exomethylene units, polyene side chains and other types of oxygenated five-membered rings. It was also reported an interesting biological activity for all the components of this family, being the Amphidinolide C the most striking case, which showed strong cytotoxicity in the nanomolar range against the murine lymphoma L1210 and the human epidermoid carcinoma KB.[8] Some of the most important Amphidinolides are reported in Figure 1.7.

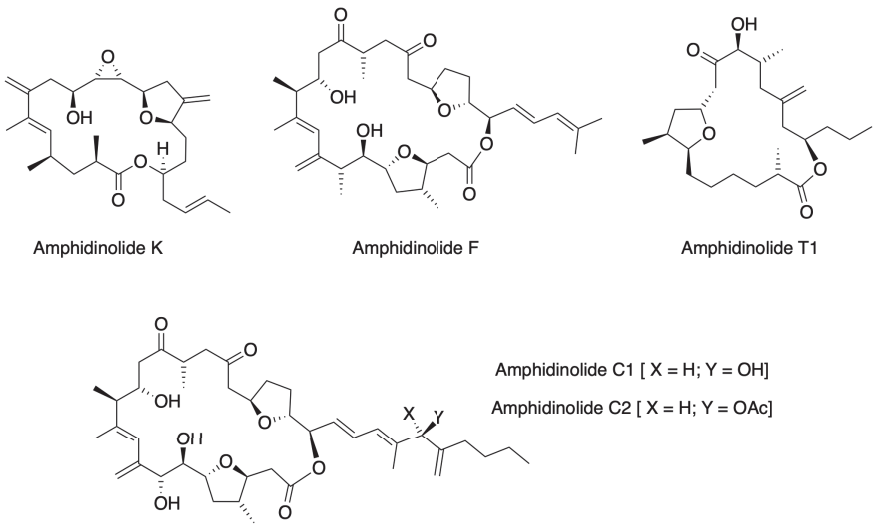

Figure 1.7: *Structures of the most important THF-containing Amphidinolides.*

Another important family is constituted by Haterumalides, a group of chlorinated macrolides firstly isolated in 1999 from sea sponges *Ircinia* and *Lissoclinum sp.*[9] We already reported in Figure 1.6 the most representative member of this class, the Haterumalide NA, which showed a cytotoxic biological activity against

leukemia cells. Its natural diasteromer, the Oocydin A, was isolated from the South American epiphyte *Serratia marcescens*; while oxygenated analogs of heterumalides, also known as biselides, were extracted from the Okinawan ascidian *Didemnidae sp.* (Figure 1.8).[10],[11]

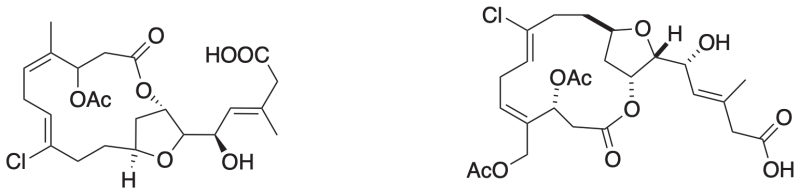

Figure 1.8: *Structures of Oocydin A and Biselide A.*

Structurally speaking, these compounds present different chemically intriguing features like THF ring bridged with a macrocyclic lactone, or a *Z*-chlorovinyl moiety, or two allylic alcohols coupled with several stereogenic centers, highlighting the importance of the stereocontrol in planning their laboratory synthesis.

The last member of marine secondary metabolites is Caribenolide I, which was also isolated from *Amphidinium sp.*[12] It was found to present cytotoxic activity against the human colon carcinoma (HTC 116), by being 100 times more active if compared with the classical Amphidinolide B (Figure 1.9).

Here, we can still find the typical macrocyclic lactone of amphidinolides, but it contains new moieties, like an α-methylene epoxide, one disubstituted THF and one tetrasubstituted THP cores, one keto group, a *E*-double bond, hydroxyl groups and the lateral butyl chain, to which the peculiar biological properties can be ascribed.

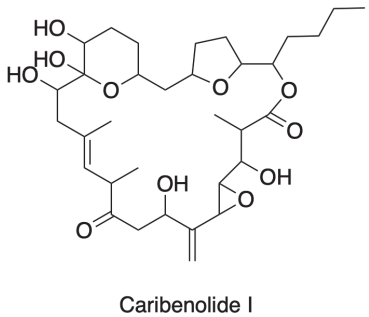

Figure 1.9: *Structure of Caribenolide I.*[12]

1.2 Not only plants and sea: the neurofuran case

In the paragraph above, we reported an extensive series of the common THF containing natural products coming from plants and aquatic organisms. The huge complexity of these structures highlights the synthetical necessity to increase the control over the asymmetric approaches. However, there are also cases of high structural complexity in compounds directly related with the human body and with its health: the neurofurans.

Neurofurans (nFs) are species formed *in vivo* in human brain tissue as a consequence of an increased oxidative stress. The main target in brain tissue is docosahexaenoic acid (DHA), the most abundantly esterified fatty acid within brain cell membranes. Alongside neuroprostans, isofurans and isoprostanes, these molecules have been identified as possible biomarkers of oxidative stress, considered the triggering cause of some diseases such as Huntington's syndrome, Alzheimer's disease and Parkinson's.

The first example of a synthesis of the THF core was reported by Taber and co-workers.[13d-e] Two different asymmetric transformations, a Sharpless asymmetric epoxidation and Sharpless asymmetric dihydroxylation, have been used. However, neither the epoxidation nor the dihydroxylation proceeds with perfect enantiocontrol, and a distereomeric mixture of key tetrahydrofuran building blocks was obtained. Moreover, the key hydroxylic group on C-11 was epimeric to the natural product, and a carbinol inversion by a Mistunobu reaction was then required (Figure 1.10).

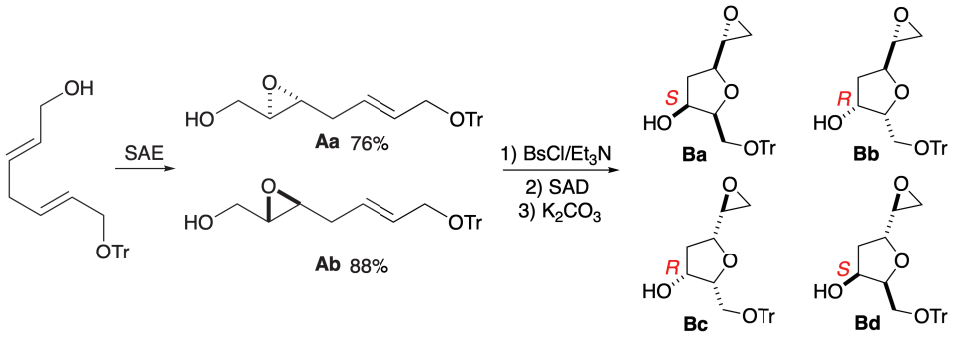

Entry	SAE	SAD	Products	Ratio	Yield (%)
1	D-DET	AD-mix α	**Ba/Bb**	3:1	66
2	D-DET	AD-mix β	**Bb**	>9:1	57
3	L-DET	AD-mix α	**Bc/Bd**	2.2:1	54
4	L-DET	AD-mix β	**Bd**	>9:1	62

[a] Combined yield of the two diastereomers.

Figure 1.10: *Taber's tetrahydrofurans synthesis through sequential SAE and SAD.*[13d-e]

It is within this research sector that our group has studied in the past years a method for synthesis of 7-*epi*-ST-Δ^8-10-neurofuran (Figure 1.11).[14]

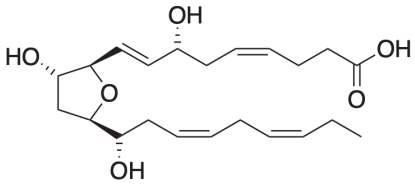

7-epi-ST-Δ^8-10-neurofuran

Figure 1.11: *Structure of 7-epi-ST-Δ^8-10-neurofuran.*[14]

The key step in the formation of the tetrahydrofuran core is the palladium mediated desymmetrization reaction through cyclization of substrate **1**, assisted by one of the ligands of the "Trost Modular Ligands" series (Scheme 1.1), also known as Tsuji-Trost Asymmetric Allylic Alkylation (AAA) reaction in its cycloetherification fashion. The result we have achieved is the possibility of obtaining, in one fell swoop, the tetrahydrofuran core **2** with interesting results of both diastero- and enantiomeric excess.

To define the stereochemistry of the furan core, the same nomenclature method used for neurofurans is considered in this case. Generally, it takes into account the

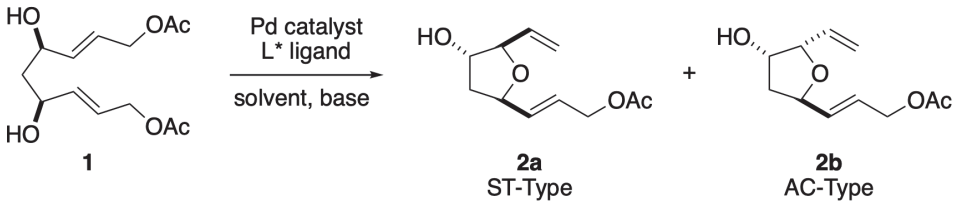

Scheme 1.1: *Desymmetrization of the meso-diol **1** with Tsuji-Trost AAA reaction.*

relative position of the allyl chains on the tetrahydrofuran ring (*syn* or *anti*) and the relationship between the hydroxyl and the olefinic adjacent geminal chain (*cis* or *trans*). These relationships are abbreviated S (*syn*), A (*anti*), C (*cis*), and T (*trans*) and the possible combinations are described in Figure 1.12.

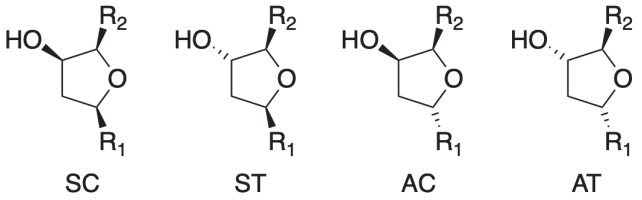

Figure 1.12: *Possible stereochemical combinations in THF synthesis.*

The index "E" or "Z" refers to the configuration of the olefin belonging to the allyl acetate both in the product and in the starting material. This clarification is necessary given the considerations that will be presented in this thesis. Besides the interesting and extremely rapid method to prepare the THF core in one step, it was highlighted an unusual diastereoinversion at position 2 of the furan ring, without any erosion in diastereo- and enantio-selectivity, which was never described in the previous works.[14] This last observation will be the main topic of the current chapter. In the next paragraph a more extended dissertation regarding this uncommon behavior will be addressed. Moreover, extensive computational studies were involved to help in finding an unconventional explanation capable in rationalize the experimental results.

1.3 Tsuji-Trost Asymmetric Allylic Alkylation

Before to move to the specific examination of the case under study, it is important to highlight the most important features of the reaction involved: the Tsuji-Trost

Asymmetric Allylic Alkylation.

This reaction, in the form of an allylic alkylation, was discovered in 1965 by Tsuji and co-workers,[15] while the variation which uses phosphine-based ligands for the Palladium metal centre derives from the studies published by Trost and co-workers in 1973 (Figure 1.13).[16]

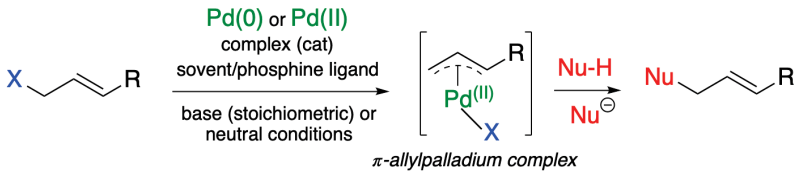

Figure 1.13: *General Tsuji-Trost Allylic Alkylation reaction.*

The mechanism shows that the fundamental intermediate of this reaction (π-allylpalladium complex) can undergo a wide range of substitutions promoted by certain nucleophiles. If we observe in depth the mechanism reported in Scheme 1.2a, a Pd(0) or a Pd(II) source can be used. Of course, if Pd(II) source is used, an *in situ* reduction step needs to be planned. The leaving group X could belong to a wide range of possibilities. After the formation of the η^2-complex, an oxidative addition occurs and the intermediate η^3-complex is formed. A ligand exchange occurs with the solvent (mass effect) and the complex obtained is now prone to undergo the nucleophilic substitution. The nature of the nucleophile group is fundamental and sometimes is necessary a stoichiometric amount of base to generate the soft nucleophile. In the last step, we can observe the formation of a new η^2-complex which than undergo reductive elimination and regenerate the palladium catalyst ready for another cycle.[17]

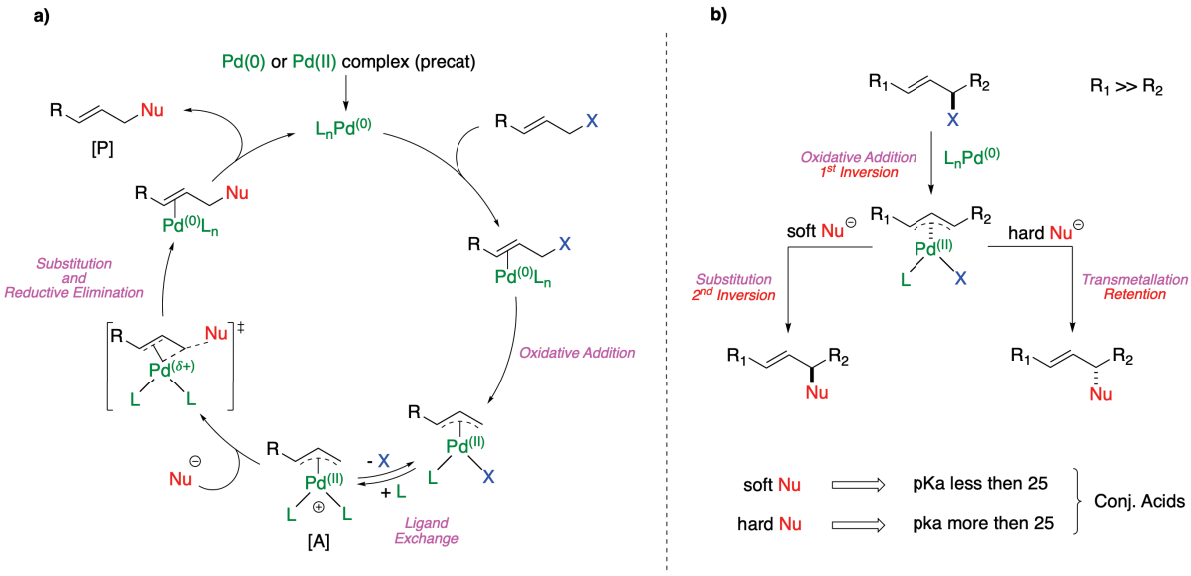

Scheme 1.2: *a) General mechanism; b) Nature of the nucleophile in determining inversion or retention of the configuration.*

The rate of the reaction depends both on the concentration of the Pd(II) cationic complex and on the concentration of the nucleophile (Equation 1.1).

$$\frac{d[P]}{dt} = k^L[A][Nu]$$

Equation 1.1

In particular, in order to accelerate the reaction, addition of a negative specie like NaBAr'F is highly needed. In fact, it has the effect of attenuating the ion-pair return of X and makes the complex prone to the Nu substitution, like the Winstein's "special-salt effect".[17] The acceleration by NaBAr'F, is apparently a balance between having sufficient electron-donation available from the ligands (L) to make abstraction of X energetically accessible, but not having so much electron-donation available that it makes little impact on ion-pair return (k_{IR}) versus nucleophilic attack (k_{Nu}).

The addition of the nucleophile to the unsymmetrical π-allylpalladium complexes is regioselective and oriented through the least substituted allyl terminus. If the allyl substrate is an optically active compound, the result of the substitution depends by the nature of the nucleophile. Soft nucleophiles showed an overall retention of the

configuration through a double inversion mechanism, while hard nucloephiles showed an overall inversion through a π-allyl complexes transmetallation and then followed by reductive elimination (Scheme 1.2b).[17]

When a chiral phosphine-based ligand is used, the streocontrol in the Allylic Alkylation can be performed by developing asymmetrical synthetical strategies. The most used ligand to execute this function are the Trost modular phosphine ligands. The two most important and widely used are the DACH-Ph (from now on **L1**) and the ANDEN-Ph (from now on **L2**) ligands, which will also be involved in the further steps of this work (Figure 1.14).

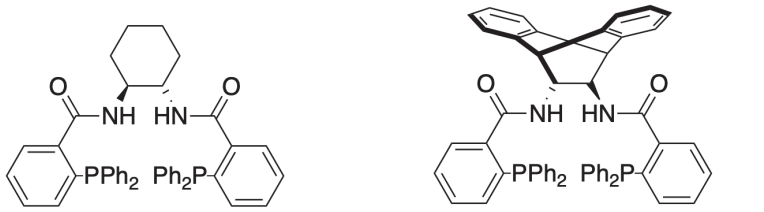

(*S*,*S*)-**L1** [DACH-Ph Trost Ligand] (*R*,*R*)-**L2** [ANDEN-Ph Trost Ligand]

Figure 1.14: *Structures of modular Trost ligands.*

To facilitate the comprehension on how these ligand can induce the observed selectivity, in 1999 Trost and Toste replaced a first-generation mnemonic model that simply predicted torquoselectivity on the basis of ligand configuration, with a second-generation three-dimensional model, which generates a chiral pocket around the η^2-alkene/η^3-allyl coordination plane.[18] The four phenyl rings play key roles by adopting pseudoaxial ('wall') and pseudo-equatorial ('flap') orientations, with the 'walls' acting to selectively impede egress of nucleofuge and entry of nucleophile in one front and one rear quadrant of the allyl plane.[18] For the case of the DACH-Ph ligand in Figure 1.15 can be found the spatial descriptions of the flaps and walls we reported above.

Despite the undeniable utility of what is commonly known in the field as "cartoon model", it is not able to provide detailed information about the intermediates involved in the reactions. In order to provide such an in-depth view of this new model, Lloyd-Jones and co-workers computationally found that two possible structures are

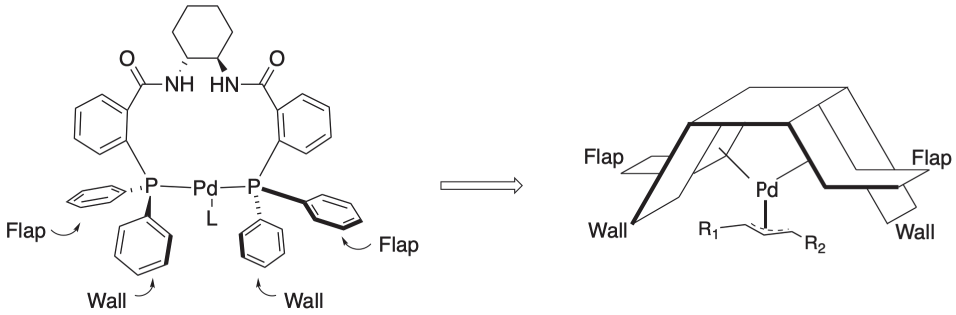

Figure 1.15: *The cartoon model explained.*

available: *exo* and *endo* complexes.[19] For open allyl complexes the difference in energy and population between *endo* and *exo* was lower than the one observed for the cyclic one (where the *exo* structure was the only favored). For several conformations it was observed that the amide N-H points into the concave embrasure, close to one of the allyl terminus (yellow hydrogen in Figure 1.16b). They found that this hydrogen-bond interaction of one N-H unit in Pd-coordinated complex can substantially accelerate both ionization and nucleophilic attack, also directing the delivery of the nucleophile.[19] The high selectivity is thus obtained by selectively favoring one pathway, not by disfavoring all of the undesired paths: a clear example of what is better known as Ligand Accelerated Catalysis.

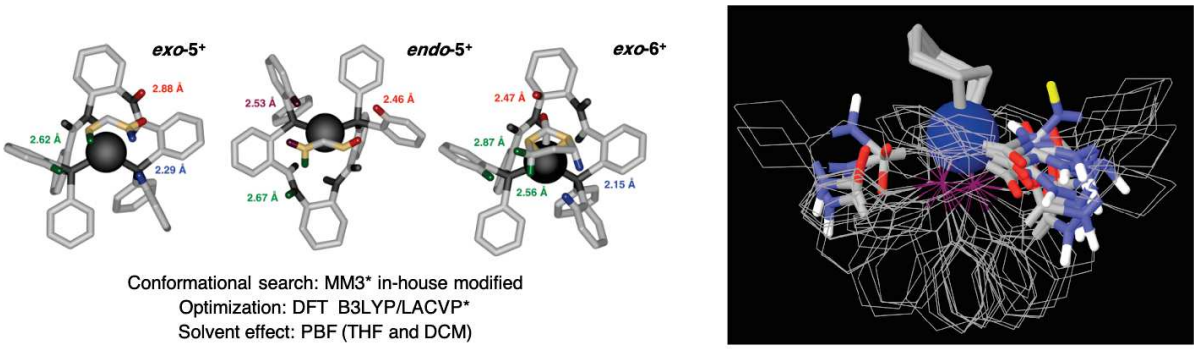

Figure 1.16: *a) The conformational and computational studies done by Lloyd-Jones and co-workers; b) the commonly observed amidic N-H is pointing into the concave embrasure.*[19]

However, their study highlighted that for open-chain allylic substrates, H-bond mediated delivery of the nucleophile is not strained for either isomer (*exo* and *endo*).[19] This factor brought them to predict low selectivities with these types of substrates. But our experimental work, which will be presented in a few, is a proof

that high selectivities can be also obtained by using open-chain allylic substrates.

1.3.1 The origin of the enantio-discrimination

In an enantioselective process, in order to obtain 100% of enantiomeric excess and with an overall yield of 100%, the enantio-discriminant step must necessarily include the ability of the reactive system to accurately recognize a group or one of the two enantiotopic faces of a substituent. Enantioselective reactions catalyzed by metal complexes normally involve additions to the π-allyl system. Contrarily, allylic alkylations involve displacements at sp^3 centers. Furthermore, the possibility of converting an achiral system into an optically active substrate (without the need for kinetic resolution) is quite an unique situation when it involves reactions catalyzed by these metals.[20]

As we reported in Scheme 1.2a, we can formally divide the catalytic cycle in 5 different steps. The first one is the formation of the metal-olefin complex, followed by ionization though oxidative addition. Then, enantiofacial discrimination of the π-allyl complex occurs and nucleophilic attack on the enantiotopic extreme, with the concomitant enantiotopic discrimination by the nucleophile, is performed. It is important to specify that the decomposition of the metal-olefin complex does not change the stereochemistry of the product.

In general, in the reaction of Asymmetric Allylic Alkylation (AAA) five different enantio-discriminating opportunities can be identified (Figure 1.17):[20]

- *Enantiotopic recognition of the faces of an olefin*
- *Enantiotopicity of the leaving groups*
- *Enantiotopic faces of the allyl fragment*
- *Enantiotopic termini of the allyl functionality*
- *Enantiotopic faces of the nucleophile*

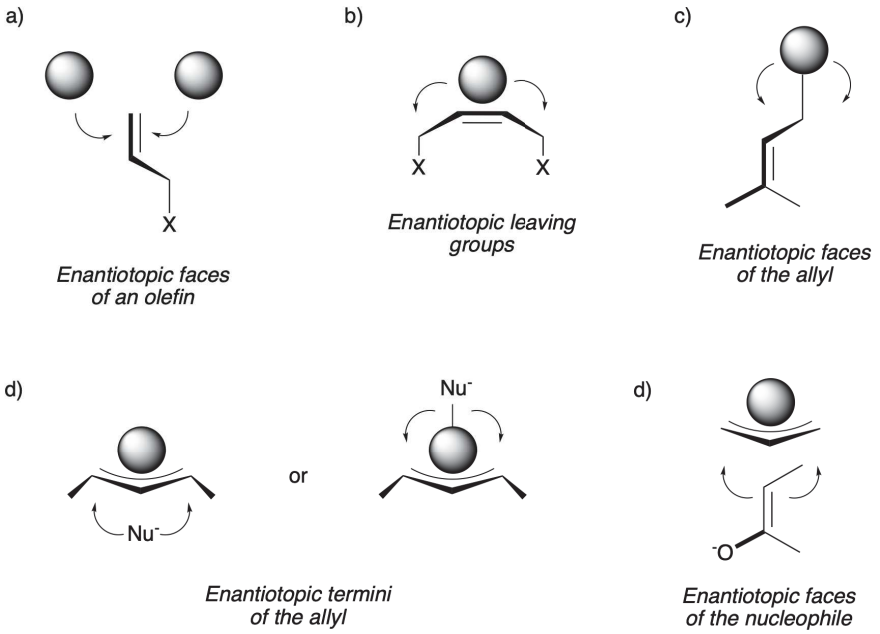

Figure 1.17: *Sources of enantio-discrimination in transition metal-catalyzed allylic alkylations.*[20]

1.3.2 The equilibration η^3-η^1-η^3 and the allylic isomerization

In a substituted olefin, more precisely a disubstituted olefin that has no C_{2h} symmetry (i.e., non-geminal), the transition metal distinguishes the two enantiotopic faces. The stability of the interaction of the metal d^{10}-olefin complex varies widely, reaching up to 14 orders of magnitude, in accordance with the steric and electronic properties of the olefin.[21] Indeed, it is known that electron-withdrawing groups, such as halogens and in particular F, tend to stabilize the complex due to electronic effects, while bulky groups tend to destabilize the complex due to steric hindrance.[21] In a similar way to what has been described above, the argument can also be translated to the ligand that complexes the transition metal: using a bidentate chiral ligand with C_2 symmetry that exposes bulky groups around the metal center, a Pd(0)L* complex is obtained. Thus, when it approaches the olefin, it selectively prefers one of the two enantiotopic faces of the olefin due to the size of the substituents on the ligand, resulting in the formation of two different types of η^3-enantiotopic complexes, where η^n indicates the hapticity number (Figure 1.18).

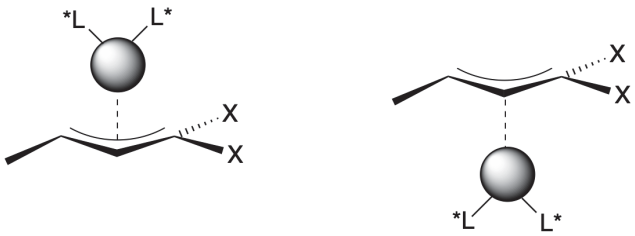

Figure 1.18: *The two different types of η^3-enantiotopic complexes.*

The situation reported so far can be better interpreted in the case the η^3-allyl intermediate is not symmetrically 1,3-disubstituted. Indeed, in such case the enantioselection is related to the face of the allyl fragment which is exposed to the nucleophile, being the other occupied by the complexation with the metal.

However, the selective ionization from one of the two enantiofaces of the olefin is not necessarily a decisive process: indeed, in some cases the metal can exchange the olefin face where it is complexed through an equilibrium process of the η^3-η^1-η^3 type. The enantiofacial transition process can completely cancel enantioselection and this can lead to the formation of racemic mixtures or, in other cases, be fundamental to enable the enantioselection process.[20] This phenomenon is of particular importance in the chemistry of Pd-allyl complexes and it has allowed explaining results otherwise discordant with existing theories. To better understand the η^3-η^1-η^3 equilibration in a substrate with at least two identical substituents on one of the allyl termini, we report in Figure 1.19 the mechanism of this type of face exchange.[22]

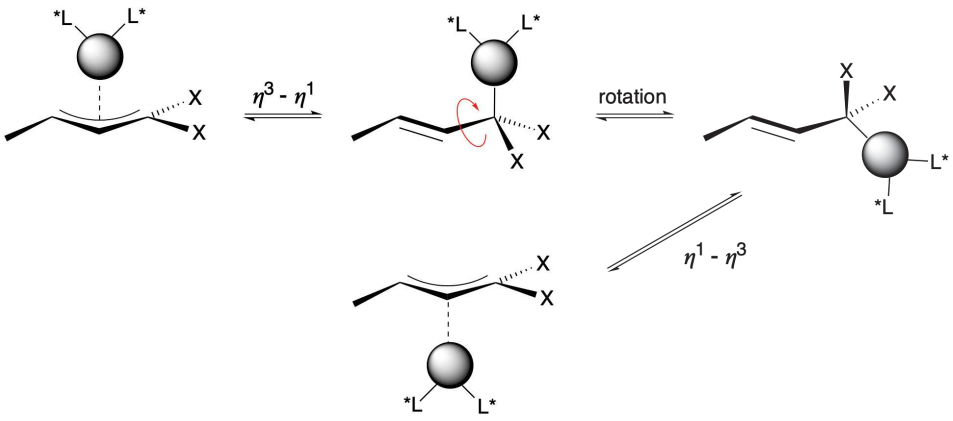

Figure 1.19: *Mechanism of interconversion in the ionized Pd-allyl complex.*

The possibility that the reaction follows a certain path depends not only on the type of substrate or nucleophile, but also on the characteristics of the ligand to the metal center. In cases in which this mechanism is preferred and if facial equilibration is faster than the nucleophilic attack, a high enantiomeric excess can be obtained starting from a racemic substrate with no need to involve a dynamic kinetic resolution.[22] In the present work, we will experimentally investigate also the crucial importance of this equilibration mechanism in determining the observed selectivity.

Besides the possible η^3-η^1-η^3 equilibration that leads to the exchange of the enantiotopic faces of the allyl system, we must also consider another aspect: the Pd-allyl complexes are normally in the state of dynamic equilibrium and the situation around the metal center is never statical.[20] Thus, if we compare the reaction rates of the various steps in the catalytic cycle, there is the possibility that the ligands can dissociate and re-associate multiple times during the reaction, thus resulting in a change in their conformation and geometry.[20] To better understand this aspect it is fundamental to name the substituents on allylic ligands according to their configuration relative to the substituent in position 2 (Figure 1.20).[20]

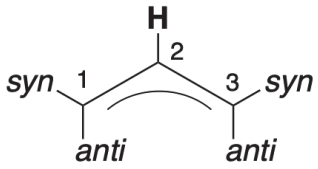

Figure 1.20: *Stereochemical nomenclature for allyl ligands.*

Figure 1.20 shows that the two substituents located on the same side of the hydrogen in position 2 are indicated as "*syn*", while the ones on the opposite side are designated as "*anti*".[20] Thus, considering the time scale of the alkylation reaction, the substituents in *syn*/*anti* positions on the Pd-allyl complex can exchange their position tens or even hundreds of times faster than the reaction itself.[20] The consequence of such exchange can be differentiated if the substituents on an allyl termini are equal or different. In the first case, no particular consequences can be highlighted and the mechanism follows the one reported in Figure 1.19.

Vice versa, when the allyl termini are substituted with different species, the stereochemical output will be strongly affected by the equilibration. Indeed, by considering the interconversion η^3-η^1, it can be seen that the inversion of the initials *syn-anti* positions is obtained by free rotation of the bond between C1 and C2. This inversion can be interpreted as a formal change of the enantiotopic face of the allyl system, which occurs not by changing the complexation face of the Pd-metal but by interconverting the *syn-anti* positions of the allyl substrate.[20] In Figure 1.21 a comprehensive mechanistic model of this interconversion is reported.

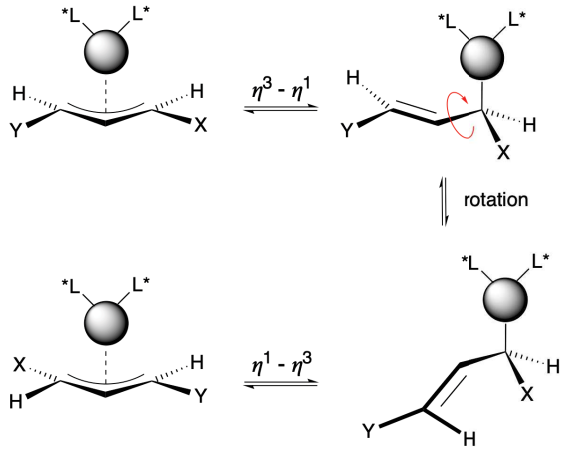

Figure 1.21: Syn/anti *exchange in a π-allyl complex with different substituents in* syn *and* anti *positions.*

This mechanism is of fundamental importance in those systems that can show a high steric interaction between the chiral ligand on the Pd-metal center and the substituents on the allyl-fragment. In such cases, the bulkier is the group interacting with the alkyl (or aryl) portion of the ligand, the faster is the exchange process.[20]

Along with the isomerization reported above, there is also another type: the *apparent allyl rotation.*[20] Indeed, no experimental evidence can be provided regarding the simple mechanism of rotation of the allyl moiety about the Pd-allyl axis. A much more plausible mechanism can be identified in the Figure 1.22, where after a change in the allyl hapticity from η^3 to η^1, a rotation occurs along the C-Pd bond.[20]

At some point before, during or after this rotation, the square-planar complex experiences the change in geometries to open a coordination site on the opposite side

of the B ligand (Figure 1.22). Then, the complex can reestablish the η^3-hapticity of the allyl complex.

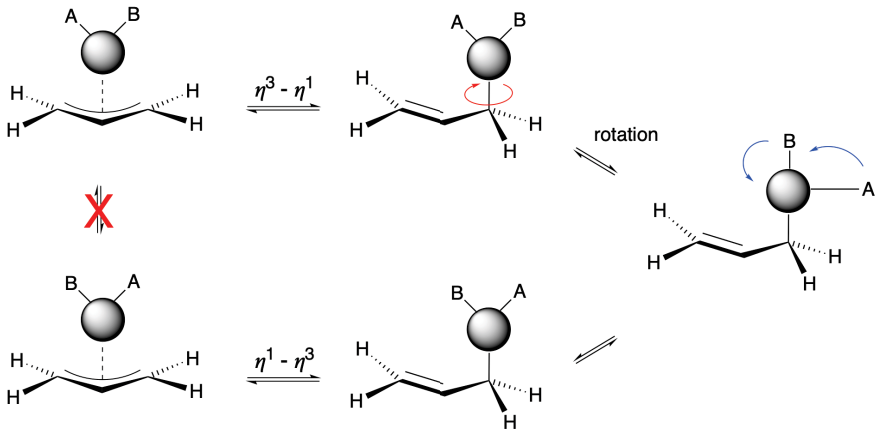

Figure 1.22: *Apparent allyl rotation.*

It should be noted that the *syn*/*anti* interconversion of allyl substituents does not occur in this scenario. Indeed, computational calculations suggest that processes that isomerize d^8 complexes are possible, but are dependent on the donor/acceptor electronic nature of the ligand at the metal center.[24] This aspect is of fundamental importance in the execution of computational modeling: using chiral components, the complexes obtained are formally diasteroisomers and therefore can have different energies and probabilities of state.

The last type of isomerization regards the *apparent isomerization through pseudorotation of the allyl moiety.*[20] This scenario was described in literature when chloride ions are added to the reaction.[17b],[18],[25] In catalytic quantities, this addition can accelerate the apparent rotation process of allyl. For this reason, the use of palladium sources such as (π-allyl)palladium chloride dimer may not be interchangeable with the halogen-free sources such as $Pd_2(dba)_3$ chloroform adduct. However, recent examples shows that the addition of catalytic amounts of a chloride ammonium salt (i.e., Hex_4NCl) in combination with the halogen-free Pd source, can be used in a similar way.[17b]

These effects have been attributed by Åkermark and Vitagliano to a halogen-activated pseudorotation mechanism, where the insertion of the halogen on the metal

center causes the concomitant formation of a coordinative site opposite to the entering halogen, in which a ligand or a part of it (if we are talking about a bidentate ligand) can migrate.[20],[26] The consecutive rearrangement step occurs by ending with an inversion of the geometry of the binder in a similar way to what happens in the case previously examined of *apparent allyl rotation*.[20] In Figure 1.23 the mechanism which involves the presence of a chloride anion is showed.

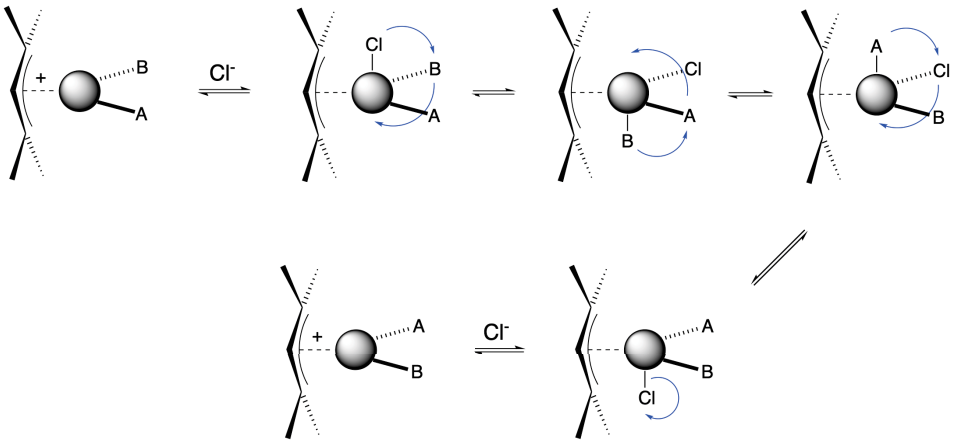

Figure 1.23: *Apparent allyl rotation though chloride catalyzed pseudorotation.*

This last isomerization process will be of particular interest in our work since we will investigate the role of chloride additives in the reaction under study.

In conclusion, from this extended introductory part, it appears clear that due to the different possible sources of enantioselection in this type of reactions, it is sometimes very difficult to rationalize the stereochemical trend. However, we will focus our attention on all these aspects trying to fulfill the unclear gaps and get as much as we can to explain the observed uncommon selectivity in our process.

1.4 The case under study

Now that we have introduced the main features of the chemistry behind this project, we can start talking more extensively about the reaction which will be under examination in the next paragraphs.

We already reported that our group developed a new synthetical way to the

asymmetric total synthesis of neurofurans, being the Tsuji-Trost AAA the key step for the THF-ring closure.[14]

The reaction is more properly defined as a desymmetrization reaction, being the substrate the *meso*-diol **1** prepared as a single (*E*,*E*)-stereoisomer in 55% isolated yield, through a single step *ring-opening cross-metathesis* between *cis*-cyclopent-4-ene-1,3-diol **3** with (*Z*)-1,4-diacetoxybut-2-ene, both commercially available. The catalyst used was the Grubbs IInd generation catalyst and reaction was performed under neat conditions (Figure 1.24).

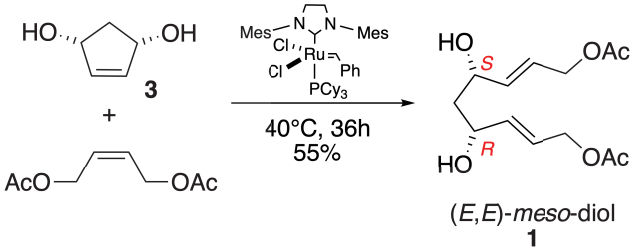

Figure 1.24: *Synthesis of the (E,E)*-meso-*diol **1** through ring-opening cross-metathesis.*[14]

Thus, in the present approach, only one enantioselective reaction, i.e., the Tsuji-Trost AAA, has been used to desymmetrize the substrate with very high enantiomeric excess (see Table 1.1). The overall stereochemical pathway in this case is one of retention, where two inversions occur due to the soft nature of the nucleophile (i.e., alcohol group), as reported before.

Under the conditions reported in Table 1.1, diastereomeric mixture of two tetrahydrofurans ST-like **2a** and AC-like **2b** was obtained (Table 1.1, entry 1).[14] Catalyst loading could be reduced to 8 mol % of ligand and 3 mol % of Pd-precatalyst by adding Cs_2CO_3 which works as a base in increasing the turnover of the catalyst (TON) and using CH_2Cl_2 as a solvent.[14] Under these modified conditions (Table 1.1, entry 2), ST-tetrahydrofuran **2a** was obtained in 80:20 *dr* (HPLC) and 96% *ee*, accompanied by the AC-diastereomer **2b**, 3% *ee*, in an overall yield of 86%.

In order to increase the diastereoselectivity of the cyclisation step, our group decided to change the type of ligand, by using the anthracenyldiamine-derived ligand, but with the opposite absolute stereochemistry: the (*R*,*R*)-**L2**.[14] Surprisingly,

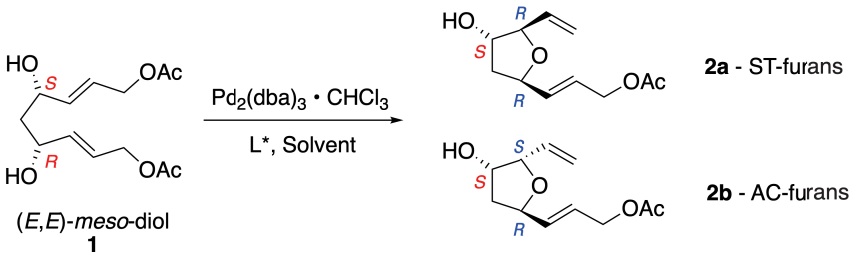

Entry	Ligand	Solvent	*dr* [a]	**2a (ST)** *ee* (%)[b]	**2b (AC)** *ee* (%)[b]	Yield (%)
1	(*S,S*)-**L1**	THF	61:39	94	11	61[c]
2	(*S,S*)-**L1**	CH_2Cl_2	80:20	96	3	86
3	(*R,R*)-**L2**	CH_2Cl_2	34:66	93	88	70
4	(*R,R*)-**L2**	CH_2Cl_2	17:83	95	92	65[d]

Reactions were carried out at r.t. with $Pd_2(dba)_3{\cdot}CHCl_3$ adduct (3 mol %), chiral ligand L* (8 mol %), **1** (0.2 mmol), Cs_2CO_3 (1.05 equiv), Solvent (0.1 M). [a] *d.r.* **2a:2b** determined by HPLC. [b] *e.e.* determined by chiral HPLC (Chiralpak AS-H and AS-3 columns). [c] Cs_2CO_3 not used; $Pd_2(dba)_3{\cdot}CHCl_3$ (8 mol %) and ligand *(S,S)*-**L1** (31 mol %). [d] Carried out at –20 °C.

Table 1.1: *Synthesis of THF substituted cores by using different conditions and ligands.*[14]

we observed an unanticipated inversion in the diastereomeric products distribution which now is in favor of **2b**. This was observed by simply using the (*R*,*R*)-**L2** instead of (*S*,*S*)-**L1**, as you can see from the *dr* values 34:66 of **2a**:**2b** (Table 1.1, entry 3). Furthermore, by lowering the reaction temperature to -20°C resulted in an increase of the *dr* to 17:83 with a concomitant improvement of the enantiomeric excess of both **2b** and **2a** to 92 and 95%, respectively.[14]

Absolute configurations of the obtained cyclized products were established by Mosher esters and NOE NMR spectra.[14] Thus, the counterintuitive results we obtained was that the simple use of (*R*,*R*)-**L2** ligand does not populate the other enantiomer of the ST-furan family, as one should expect by reasoning on the stereochemistry of the ligand, but it enabled a straightforward entry to the AC-furans in good yield and high enantiomeric excess, starting from the same readily available (*E*,*E*)-*meso*-diol **1**.[14]

The idea of a desymmetrization of a meso-diol trough a Tsuji-Trost AAA reaction to form a stereodefined THF core, was already known at the time our group started working on this project. Indeed, a publication by Burke and co-workers appeared

in 2002 showing the same desymmetrization of the (*E*,*E*)-*meso*-diol **1**.[27] However, they worked with only one ligand, specifically the (*R*,*R*)-**L1**, showing the selective formation of the other enantiomer within the ST-furan family (Figure 1.25).[27] By not considering another type of ligand, they missed the opportunity to identify this uncommon behavior in an asymmetric induction.

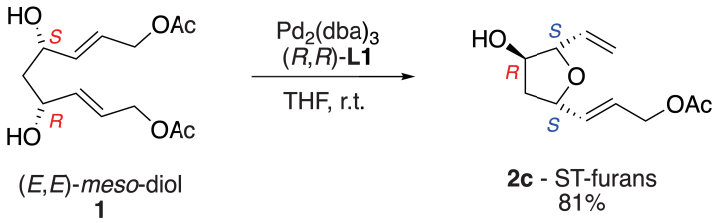

Figure 1.25: *Synthesis of THF substituted cores proposed by Burke and co-workers.*[27]

In accordance with the asymmetric induction model proposed by Trost for the Pd-catalyzed AAA, we speculated that the stereoisomer **2a** would be produced by the preferential coordination of the (*S*,*S*)-**L1**-Pd complex on to the *Si*-face of the allylic acetate moiety in **2a** near the (*S*)-OH group. Furan ring closure would thus result from intramolecular *anti*-attack of the (*R*)-OH group on the *Re*-face of the allyl-Pd complex, affording the prevalent (*R*,*S*,*R*)-stereochemistry observed for **2a** (Scheme 1.3). On the other hand, we assumed that the (*R*,*R*)-**L2**-Pd complex delivered the corresponding diastereoisomer **2b** as preferentially the (*S*,*S*,*R*)-enantiomer by nucleophilic addition of the (*R*)-OH onto the *Si*-face of the (η^3-allyl)palladium complex intermediate. By using the enatiomers of ligands **L1** and **L2**, namely (*R*,*R*)-**L1** and (*S*,*S*)-**L2**, the corresponding enantiomers of **2a** and **2b** were obtained with the same enantio- and diastereomeric excesses.[14]

What appears interesting and somehow quite uncommon is the preference of (*S*,*S*)-**L1** and (*R*,*R*)-**L2** palladium complexes, for the same portion of the molecule in giving the allyl-complex, that is the one close to the (*S*)-OH stereogenic center.

In the next paragraphs we will keep the information reported so far and we will try giving an explanation to the observed uncommon selectivity by the use of computational chemistry.

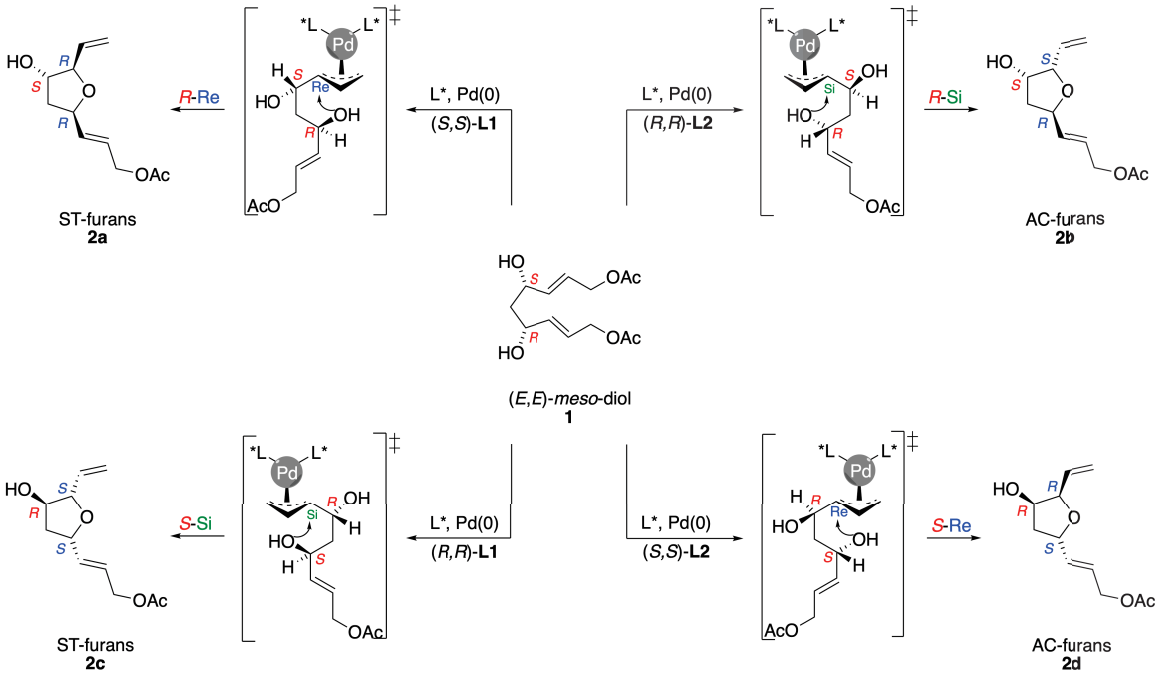

Scheme 1.3: *Proposed mechanism for the asymmetric cyclization of the (E,E)*-meso-*diol* ***1***.

1.5 Synthesis of the ligands and a different synthetical strategy for the (*E*,*E*)-*meso*-diol

Before to move to the computational part of this work, we decided to run again the reactions which were illustrated in the paper published in 2013.[14] In particular, our main concern regarded the presence of Ruthenium by-products in the (*E*,*E*)-*meso*-diol **1** synthetized through the ring-opening cross metathesis. Indeed, when we synthetized the product **1** according with this procedure, we soon identified that the color of the obtained raw product was blackish. Even after multiple chromatographic purifications, we still observed the presence of a grey to black transparency.

We hypothesized that the main candidate to be responsible of such an impurity should have been the ruthenium by-products derived from the Grubbs IInd generation catalyst. Moreover, to exclude the formation of homo-coupling products of *cis*-cyclopent-4-ene-1,3-diol it was necessary to operate in the absence of solvent and in large excess of (*Z*)-1,4-diacetoxybut-2-ene, which is actually used as a solvent. This expedient not only avoids polymerization reactions, but also ensures that

the reaction intermediate derived from the mono-reaction metathesis, statistically prefers the cycloaddition with another diacetate molecule rather than with the other termini of the mono-intermediate.

It appears clear that if a precise mechanistic investigation has to be performed, we cannot look the other way on the presence of that impurity. For such reason, we decided to set up a new synthetical strategy that follows a *total synthesis* motif. It is true that it will be longer in steps than the single step of the ring-opening cross metathesis, but in such a way we will exclude the presence of other organometallic by-products from the final product.

The total synthesis we ideated starts with the TBS protection of the alcohol moieties of the commercially available *cis*-cyclopent-4-ene-1,3-diol **3** to obtain the compound **4**. This one is subsequently subjected to ozonolysis to obtain the respective dialdehyde **5** which cannot be isolated for stability reasons. Indeed, after the work-up the just-formed **5** is subjected directly and without purification to Horner-Wittig olefination reaction in THF with the appropriate phosphonium ylide to obtain the α,β-unsaturated diester **6** as a mixture of isomers, with (*E*,*E*)- and (*E*,*Z*)-configuration, respectively. Thus, the mixture of diester **6** is purified with classical chromatographic methods to obtain only the (*E*,*E*)-isomer, in high purity. Then, it is converted into the respective allyl alcohol **7** by reaction with DIBAL-H in THF. The acetylation of the alcohol **7** with acetic anhydride and pyridine in DCM gave us the opportunity to obtain the protected product **8**.

The final step consists in deprotecting the silyl ethers, by using aqueous HF in acetonitrile. The overall yield of the synthesis is around 60%, with reference to the initial quantity of *cis*-cyclopent-4-ene-1,3-diol **3**. In Figure 1.26, the complete synthetical scheme is reported.

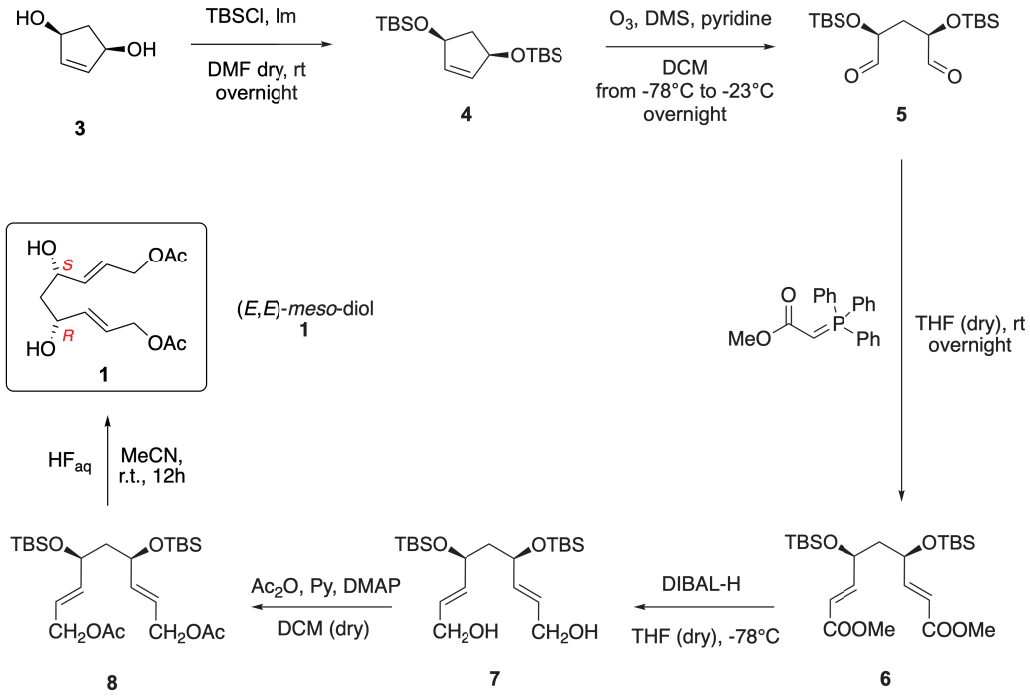

Figure 1.26: *Synthetical pathway for the total synthesis of the (E,E)*-meso-*diol* ***1***.

However, we have to observe that the starting *cis*-cyclopent-4-ene-1,3-diol **3** can be particularly expensive, especially if purchased as it is. Another suitable solution could be the laboratory photochemical synthesis of **3** starting from the much cheaper cyclopentadiene. The reaction consists in the Diels-Alder reaction between cyclopentadiene and singlet oxygen, which is generated *in situ* by irradiating with a Hg vapor lamp the solution where oxygen is bubbling and by using Rose Bengal as photosensitizer. In this phase it is of extreme importance not only the control of the temperature during the whole reaction, but also the quality of the starting cyclopentadiene, which must be freshly distilled just before the photochemical reaction setup. After the decomposition of the endoperoxide intermediate by reaction with thiourea and the complicated purification of the reaction mixture to remove the photosensitizer, the precious diol **3** is obtained with an acceptable yield of 30% (Figure 1.27).

We also decided to synthetize the two chiral ligands, since we observed better values of both enantio- and diastereoselectivity if the ligands were freshly prepared if compared with the results obtained with the commercial ones. The synthesis of the two ligands consists in a simple condensation reaction between the commer-

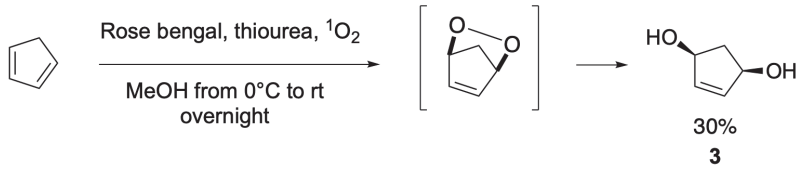

Figure 1.27: *Photochemical synthesis of the diol **3**.*

cially available (1*S*,2*S*)-1,2-diamino cyclohexane **9** or the (11*R*,12*R*)-11,12-diamino-9,10-dihydro-9,10-ethanoanthracene **10** and the 2-(diphenylphosphino)benzoic acid. The reaction occurs in a smooth way, in dichloromethane in the presence of *N*,*N*'-dicyclohexylcarbodiimide (DCC) as carboxyl activating agent and with good isolated yields (Figure 1.28).

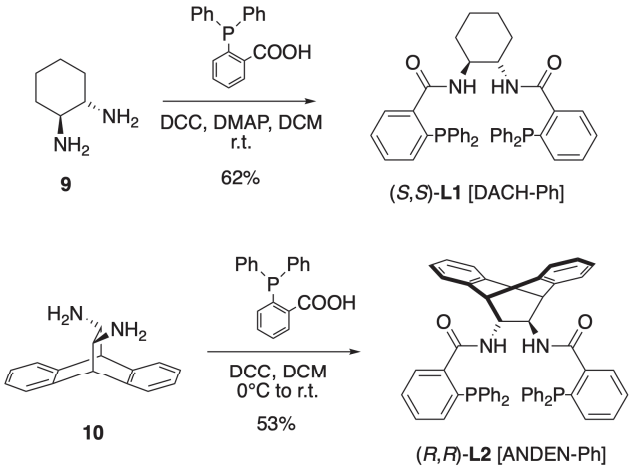

Figure 1.28: *Synthesis of the ligands (S,S)-**L1** and (R,R)-**L2**.*

1.6 Cyclization reactions

Now that we prepared the starting substrate **1** and the two ligands, we can move to rerun the cyclizations trials. Indeed, another important observation has to be done: in the reaction performed by our group in the previous years, we can commonly find the presence of Cs_2CO_3 as an additive. We already reported in Table 1.1 that it works as a base in increasing the turnover of the catalyst (TON). This information is correct, but the main role of the base is not to directly interact with the catalyst, but with the acetic acid that is naturally formed as by-product from the cyclization reaction. From this point of view, the base helps in moving the equilibrium to the

product, by neutralization of the acetic acid. However, it is known that the reaction works also in the absence of the base and for such reason, to place the experiments as close as possible to the next computational calculations, we decided to run the cyclizations in the absence of the base. Moreover, we changed also the solvent: by running the reaction in toluene we can eliminate the Cs_2CO_3 by maintaining high values both for *ee* and yield. The quantities of catalyst and ligand were maintained as before, being 3% mol the $Pd_2(dba)_3{\cdot}CHCl_3$ catalyst and 8% mol the ligand. Also, the molarity of the solution was 0.1M as before.

Let's report now the results we obtained. In the case of the (*R*,*R*)-**L2** ligand the (*S*)-portion of the molecule is involved in the complexation of the Pd and it brings favorably to the AC-*SSR* isomer when the hydroxyl nucleophile attaches preferentially on to the *Si*-face of the allyl, while the ST-*RSR* derives from the attach on to the *Re*-face, as we explained in the proposed mechanism of Scheme 1.3. The *dr* we got is in favor of the AC furans like before (32.6:67.4, ST:AC), while we experienced a small decrease in the *ee* values (84.0%, ST; 85.0%, AC), which are a little bit less than the ones we reported before (see Table 1.1). This change in enantiomeric excess can be due to the absence of Cs_2CO_3, but we consider mainly the change in the properties of the solvent to be the main cause for that variation. Regarding the isolated yield, it was still good at 79% (Figure 1.29).

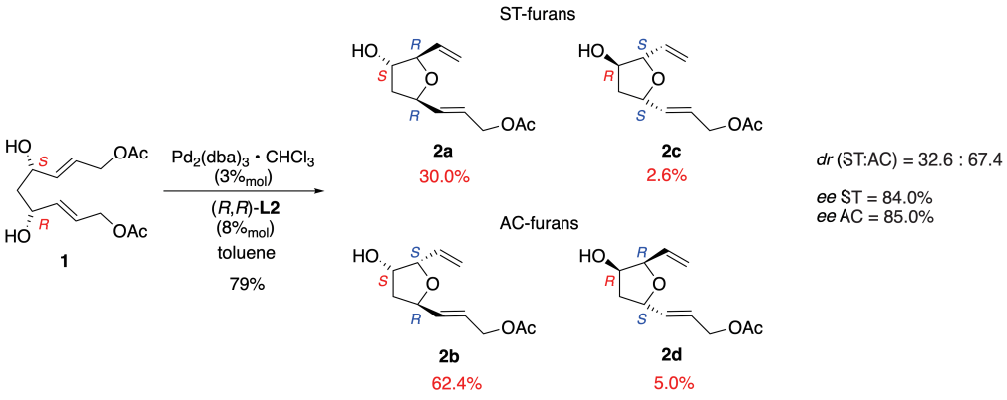

Figure 1.29: *New cyclization with (R,R)-**L2** ligand and in toluene.*

In Figure 1.30 it is reported the HPLC chromatogram from which we obtained the selectivity results reported above. Specifically, we used a Chiralpak AS-H column with 80:20 Heptane:iPrOH isocratic eluent mixture.

The molecular assignations reported on the chromatogram were placed in accordance with the experimental work done in the previous years.[2]

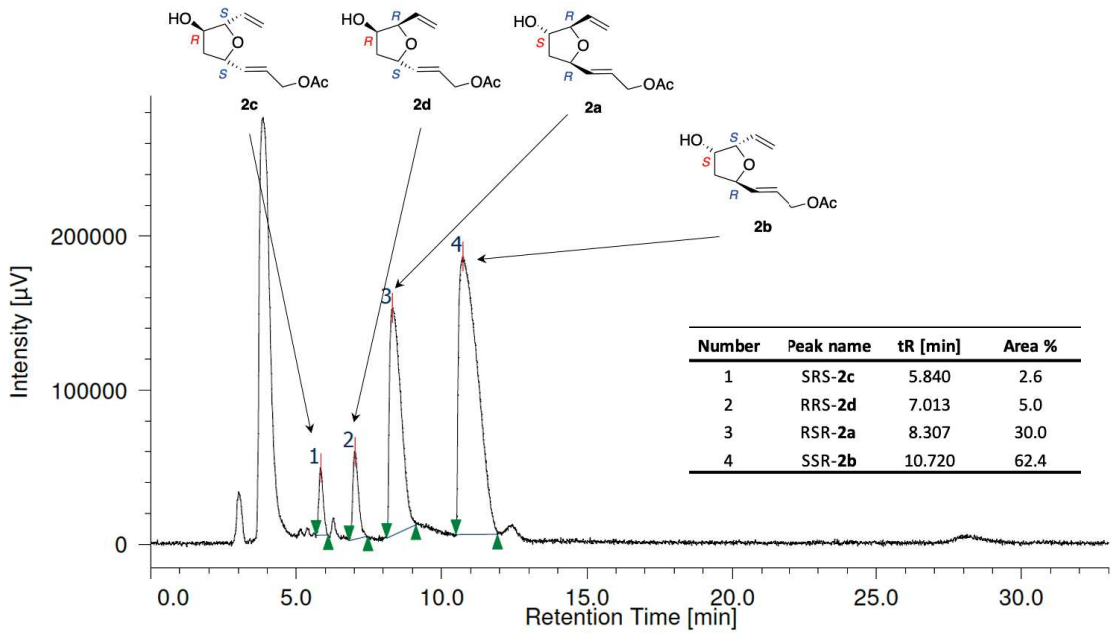

Figure 1.30: *HPLC profile for the (R,R)-**L2** promoted cyclization and the corresponding integrations.*

As can be seen, a huge peak appears below 5.0 min: this peak can be due to the presence of dba residues which were not perfectly removed from the product mixture. Indeed, not to alter the relative percentage of the obtained isomers, we decided to perform a very fast filtration over silica and not a complete chromatographic purification.

In the case of the **L1** ligand, we decided to use not the (*S*,*S*)-one as before used in the paper, but the (*R*,*R*)-**L1** one, which can be synthetized accordingly with the same procedure reported above (Figure 1.28). This because it helps more in highlighting the real differences between these two catalysts, which furnish a complete different stereochemical output even if bearing the same absolute configuration. Indeed, according to our proposed mechanism, the usage of (*R*,*R*)-**L1** should interests

now the (*R*)-portion of the molecule for the complexation of the Pd, thus bringing favorably to the ST-*SRS* isomer since the hydroxyl nucleophile attaches preferentially on to the *Si*-face, while the AC-*RRS* derives from the attach on to the *Re*-one. The *dr* we got now is in favor of the ST furans like before (59.2:40.8, ST:AC) and the *ee* values, show a quasi-complete enantioselectivity between the ST-furans in favor of the *SRS* one (97.0%), while the AC-furans *SSR* and *RRS* appeared to be a racemic mixture (0.3%). Regarding the isolated yield, it was still good at 85% (Figure 1.31).

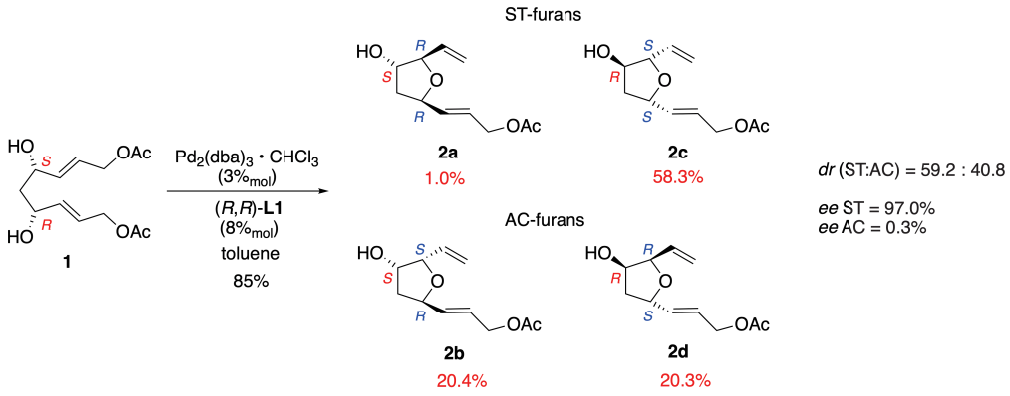

Figure 1.31: *New cyclization with (R,R)-**L1** ligand and in toluene.*

In Figure 1.32 it is reported the HPLC chromatogram from which we obtained the selectivity results reported above. Again we used a Chiralpak AS-H column with 80:20 Heptane:iPrOH isocratic eluent mixture.

It appears clear, just by looking at the two chromatograms obtained with the (*R*,*R*)-**L2** and the (*R*,*R*)-**L1**, how these two ligands completely rely on a different mechanistic behavior, where the absolute configuration of them is not the only factor that has to be taken in consideration.

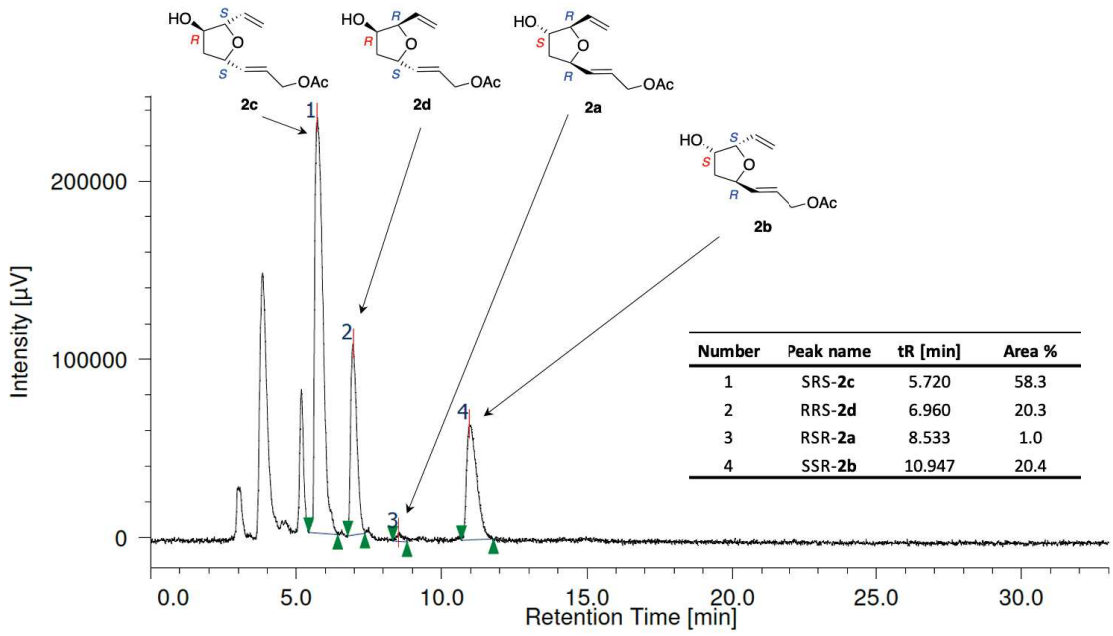

Figure 1.32: *HPLC profile for the (R,R)-**L1** promoted cyclization and the corresponding integrations.*

However, not to confuse the reader with the continuous exchange in configurations for the ligands, we decided to computationally investigate the mechanism using the originals (*R*,*R*)-**L2** and (*S*,*S*)-**L1**. Thus, to obtain the percentage for this last one, we can rely on the mutual exchange between the enantiomers of the ligands and thus simply revert the data reported in Figure 1.31. For completion of discussion, the Figure 1.33 reports the data already reverted.

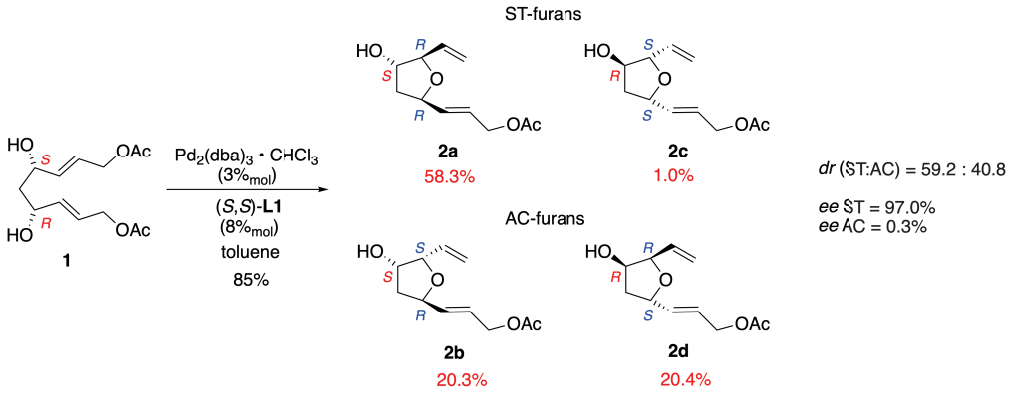

Figure 1.33: *Data from the cyclization with (R,R)-**L1** ligand reverted for the (S,S)-**L1**.*

1.7 Computational investigation of the mechanisms

In the previous sections we reported on the proposed mechanism which can be involved in this reaction: namely the preference of the (*S*,*S*)-**L1** in coordinating the *Si*-face of the allyl on to the (*S*)-portion of the molecule, while the (*R*,*R*)-**L2** prefers the *Re*-one on to the same portion. However, no explanation can be proposed for such a selectivity.

For such reasons, we decided to undertake computational investigations to highlight the hidden features which regulates the facial selectivity and the final stereochemical output.

Before to approach the calculations, we looked at the published literature for these types of reactions and we observed that a similar work, but with a different substrate and ligand, was investigated by Roulland and co-workers in 2012 with the aim of explaining the selectivity in the formation of the THF through Tsuji-Trost reaction for the synthesis of the haterumalide NA (see Figure 1.6 for the structure).[28] Specifically, their reaction involved a Pd-catalyzed cyclization of the diol **11**, to form the corresponding THF core with the usage of the achiral phosphine ligand like PPh_3 and $P(4\text{-}MeOC_6H_4)_3$, as reported in Figure 1.34.

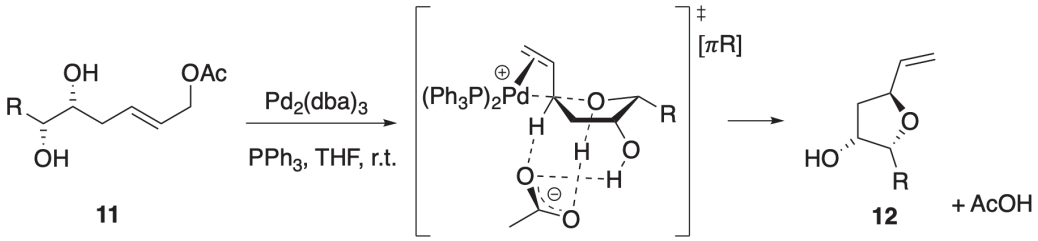

Figure 1.34: *Cyclization reaction investigated by Roulland and co-workers.*[28]

They firstly highlighted the importance of the acetate anion in giving a *counterion-directed catalysis* (CDC). The high diastereoselective synthesis of THF ring is strictly dependent on the presence of the carboxylate counterion derived by the acetate living group.[28]

Indeed, they proposed a mechanism, based on DFT calculations and chemical experiments, which indicates that the formation of an unusual non-covalent bond

between the counteranion and the two hydroxy groups of the cationic π-allyl/Pd complex is of fundamental importance in stabilizing the transition states.[28] Moreover, the presence of a third H-bond interaction leads preferentially to the highly organized chiral transition state $[\pi R]^{\ddagger}$, which favors the formation of the product **12**.[28] They also claimed that the cyclization transition states could not be found if the acetate counteranion was not taken into account.[28] In Figure 1.35, the results of their calculations are reported along with the Gibbs free energies and the structures of each reactive specie.

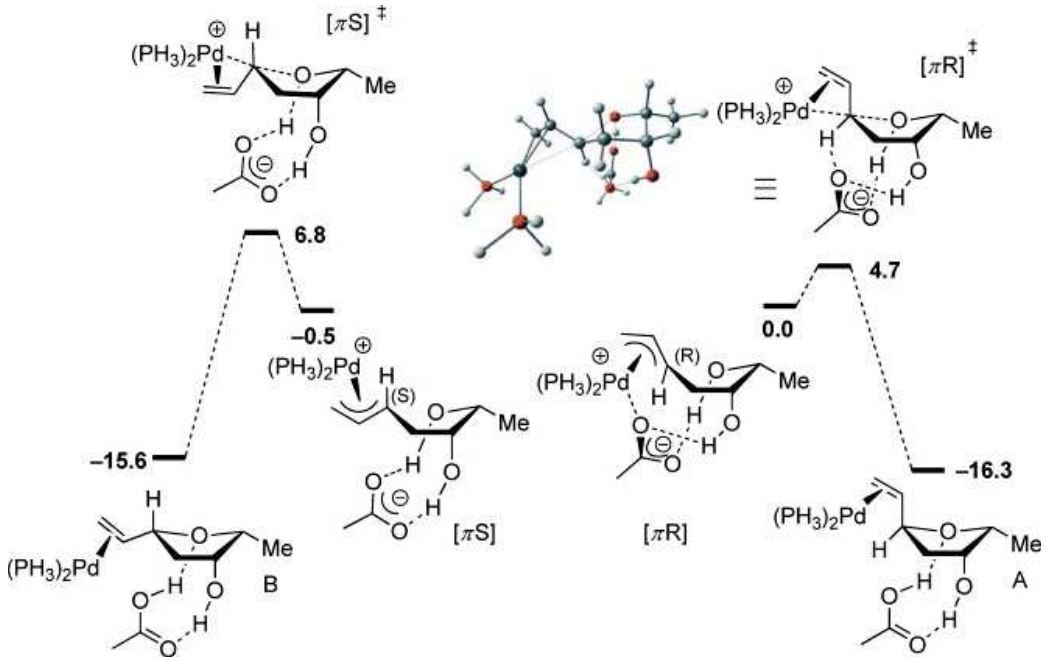

Figure 1.35: *DFT calculations of the two pathways leading to the major (A-through $\pi R^{\ddagger}$) and the minor (B-through $\pi S^{\ddagger}$) products. Level of theory: B3LYP/6-31G(d) & ECP28MWB; ligand structure approximation to PH_3.*[28]

For the reasons showed by Roulland and co-workers, we considered that also in our calculations it would have resulted fundamenal to insert the acetate anion, because it helps in the exit of the proton from the hydroxyl group directly involved in the cyclization. In particular, the aceteate anion, released from the formation of the π-allyl Pd complex, can be able to operate on our (*E*,*E*)-*meso*-diol **1** in a similar way to the one reported above. Indeed, it can coordinate both its oxygens with hydrogens of hydroxyl groups on the substrate **1**. This strategy let us to observe all the possible conformations that could occur during the various TS of the catalytic

cycle.

However, in order to define which of those is the most important one in order to promote the reaction, a detailed population analysis is needed.

We thus started organizing our computational work, by defining a computational method which follows the known steps for this reaction. First of all, we have to give a close look to the most important reaction steps, which are reported in a simplified version in Figure 1.36.

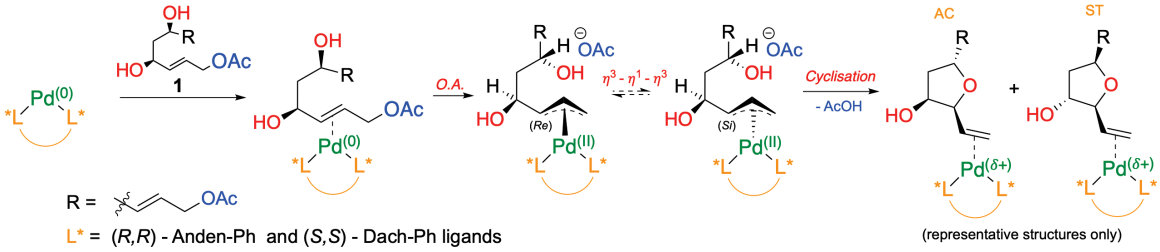

Figure 1.36: *Most important reaction steps for the desymmetrization of the (E,E)-*meso*-diol **1**.*

Thus, the reaction starts with the first step which is formation of the palladium-olefin η^2-complex and then the oxidative addition with the formation of the η^3-palladium allyl complex occurs in the second one. Next, in accordance with the pre-existent models, the third step involves the equilibration which brings the palladium changing the faces of the allyl system. Finally, the cyclisation step occurs.

We mainly focused our attention on to the second and fourth steps. We thus decided not to consider the formation of the first complex due to the low importance in the formation of a more labile complex than the one involved next for the oxidative addition. Anyway, to fulfill all the possible structures for this first initial complex, we considered all the different palladium-olefin orientations in giving the second step. Moreover, the consideration of the subsequent equilibration step would have resulted in a consistent increase of the computational difficulty. Since the structures of the ligands cannot be simplified to smaller ones not to lose important descriptors, it results that to face the equilibration step not only the variation of simple bond or a dihedral should be considered, but all the molecule needs to move synchronously to pander the change in conformation. Furthermore, if something could be done,

it is not guaranteed that such a particular motion is the realistic one, which has to involve all the system for the location of the equilibration transition state. For such reason, the starting complexes for the fourth step were investigated with different orientations of the Pd-allyl system, thus to consider all the possible structures populated by the equilibration.

All the calculations were performed applying the DFT theory by the usage of Gaussian 09 program package.[29] We worked with a similar computational approach to the one reported by Roulland and co-workers.[28] Specifically, we remained within the B3LYP functional (i.e., the Becke three-parameter hybrid exchange functional (B3) in its variation provided by Lee, Yang and Parr correlation functional (LYP)),[30] and by using a specified basis set for each atom: for H, C, O, N, P we used 6-31g(d), while for Pd we used the effective core potential basis set LanL2DZ.[31] Conformational analysis was performed manually: due to the extreme high degrees of freedom of the molecules and complexes under examination we focused our attention on the most realistic conformational changes. Indeed, we already reported that to satisfy all the possible interactions involved in the selectivity, we decided not to simplify the structures of the catalysts. This for sure will help in having a clear and more realistic idea of what is the discriminant in the reaction, but it penalizes in the amount of time required for the calculation. The only simplification we operated was on the substrate, where we replaced the uncoordinated allyl-acetate portion, with a vinyl-methyl group (Figure 1.37).

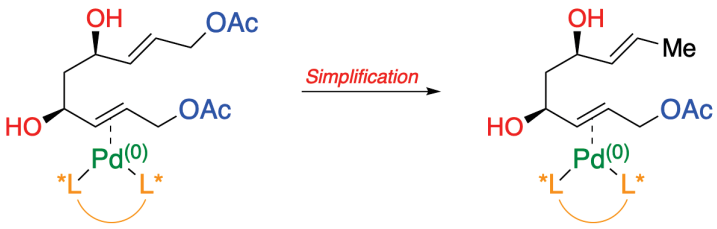

Figure 1.37: *Simplification on the substrate.*

Now that we introduced the computational method we used, we can start by showing the results we obtained in the two cases: namely the investigation of the second (i.e., oxidative addition) and fourth (i.e., cyclization) steps for both the

(*R*,*R*)-ANDEN-Ph [(*R*,*R*)-**L2**] and the (*S*,*S*)-DACH-Ph [(*S*,*S*)-**L1**] Trost ligands.

1.7.1 (*R*,*R*)-ANDEN-Ph [(*R*,*R*)-L2] Trost Ligand

We started our computational studies from the most sterically demanding between the two ligands. Indeed, the ANDEN-Ph ligand appeared us not to be so widely used as the DACH-Ph one. This prompted us to increase our efforts in the possibility of uncovering a new mode of action for this ligand.

The oxidative addition step was the first area of investigation. Indeed, after the complexation and the formation of the initial η^2-Pd complex, the removal of the acetate leaving group and the change in hapticity appeared us to be the very first step where a discrimination can occur. Thus, to approach this reactive step, we manually populated different types of conformers, mainly by rotating the uncoordinated portion of the molecule, but a particular attention was dedicated to the relative orientation of the acetate leaving group and the allyl-Pd system. Indeed, the carbonyl-oxygen atom of the acetate can point "inwards" the allyl system (Figure 1.38a), or "outwards" the allyl system (Figure 1.38b). To identify those two relative orientations, we called A the one which points the acetate "inwards", while B the other (see Figure 1.38).

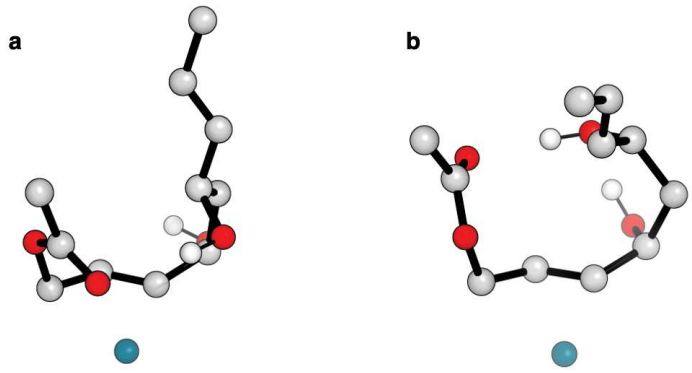

Figure 1.38: *Relative orientations of the acetate leaving group "inwards" (A, left) or "outwards" (B, right).*

By continuing looking at the substrate, we also identified another important interaction, which will be fundamental in the location of the oxidative addition

transition states (TSs): the H-bond interaction between the carbonyl-oxygen atom of the acetate and the hydroxyl group on the unreactive portion of the molecule (see Figure 1.38). In the absence of this non-covalent interaction, we were not able to locate the corresponding TSs, thus finding a connection point with the work done by Roulland and co-workers and pointing trough a CDC catalysis.[28]

Having clarified these initial observations, we moved to the in-depth investigation of the oxidative addition step, by locating the TSs for each possible orientation and portion of the molecule. In the very next developments, we will report only the most stable between all the possible conformers investigated for each portion of the molecule. Specifically, we will refer here to Pro-S or Pro-R depending on the allylic portion involved in the coordination of the Pd, always together with the A or B denomination to distinguish the relative acetate orientation.

The results of our computational investigation for the first step showed a good match between the experiments and the calculations as can be observed from the Table 1.2, which reports the data of population analysis.

	E (a.u.)	Population Percentage	Computational	Experimental
TS Pro-S-A	-3883.333112	52.4	**99.8**	**92.4**
TS Pro-S-B	-3883.333018	47.4		
TS Pro-R-A	-3883.327896	0.2	**0.2**	**7.6**
TS Pro-R-B	No results			
	Sum	**100.0**	**100.0**	**100.0**

Table 1.2: *Electronic energies and population analysis for the oxidative addition step with (R,R)-**L2** ligand. DFT level of theory: B3LYP/6-31G(d) & LanL2DZ (only the most stable conformer for each portion are reported).*

According with the calculations, the favored portion of the molecule in giving the complexation with the palladium is the one which contains the *S* stereogenic center (i.e., Pro-S). During this first step we observed that the removal of the acetate leaving group and the formation of the η^3-complex starting from the η^2-one from the *S*-portion of the molecule, appeared to be 3.2 kcal/mol favored over the Pro-R-one (Chart 1.1).

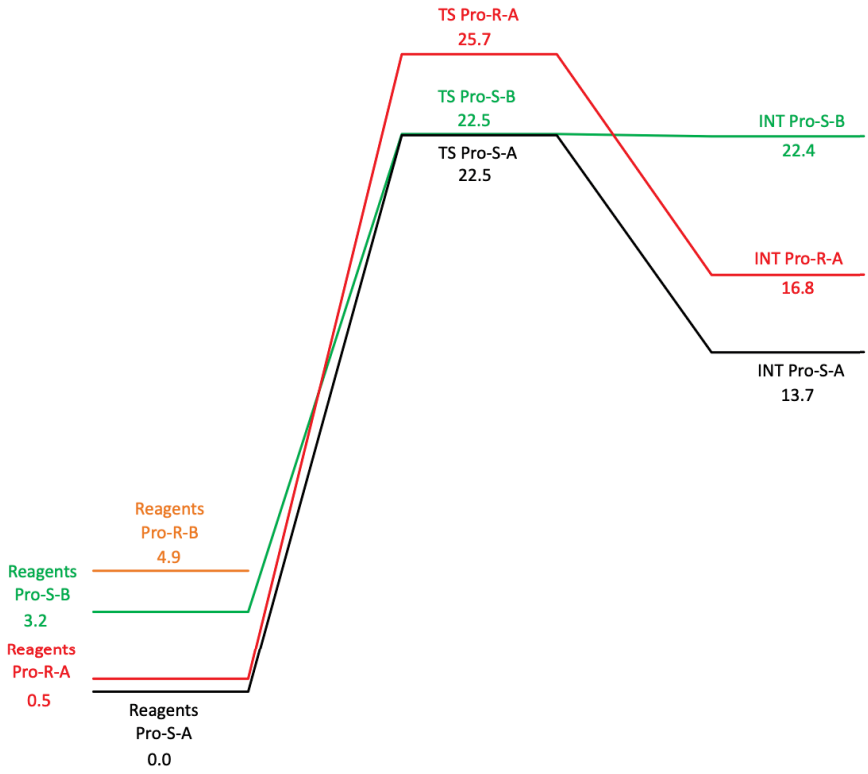

Chart 1.1: *DFT calculations of the four main possible conformational pathways to the oxidative addition step with the usage of (R,R)-**L2** ligand. Level of theory: B3LYP/6-31G(d) & LanL2DZ (values reported in kcal/mol).*

Besides the **Pro-R-B** conformer that did not result in any transition state during our investigation, we can clearly see from Chart 1.1 that the selection of the reactive portion of the molecule directly occurs during this step. Indeed, the 3.4 kcal/mol which differentiates the **TS Pro-R-A** from the other two **TS Pro-S**, are more than enough to explain the quasi-absolute preference for this last portion over the other.

By looking at the TS structures, it becomes clear the reason for this discrimination in the two possible coordination to the allyl-moieties. Indeed, the most favored **TS Pro-S-A**, showed an intricate network of non-covalent interactions that helps in stabilizing both the substrate within the catalyst environment and the exit of the acetate leaving group (Figure 1.39).

This network in **TS Pro-S-A** shows the already reported H-bond interaction

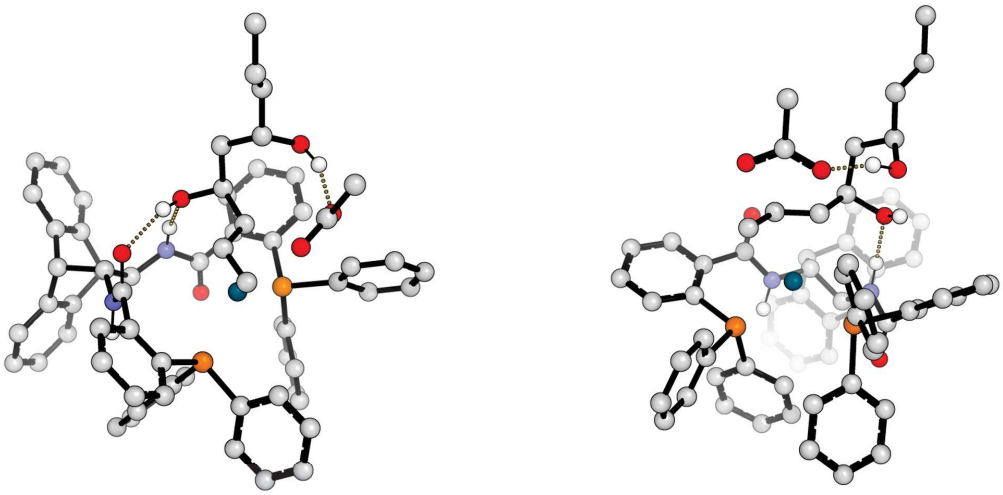

Figure 1.39: *Transition state structures for the most favored* ***Pro-S-A*** *conformer and the least favored* ***Pro-R-A*** *one (non-covalent bonds highlighted in yellow dashed lines).*

between the carbonyl-oxygen atom of the acetate and the *R*-hydroxyl group (1.79 Å), together with other two ones. Indeed, the *S*-hydroxyl group, which is the one belonging with the coordinated portion of the molecule, also interacts with H-bonds with the amidic groups on to the (*R*,*R*)-**L2** ligand. Specifically, it both acts as an H-bond donor, with the carbonyl-oxygen on one side (1.93 Å), but it is also prone to accept the incoming H-bond from the N-H amide moiety on the opposite one (2.08 Å). All those non-covalent interactions, with a distance which is in perfect accordance with the H-bond type, helps in stabilizing the **TS Pro-S-A** over the **TS Pro-R-A**. This last one, indeed, shows the same acetate/*S*-hydroxyl group interaction, but due to the different orientation of the *R*-hydroxyl group (which now belongs to the coordinated portion of the substrate) only one intermolecular interaction with the ligand can be established. Thus, the *R*-hydroxyl group can only act as a H-bond acceptor form the N-H amide moiety of the ligand (2.00 Å), but no intermolecular H-bond donation can be established due to the different orientation in the space. In light of this, a very small H-bond interaction for **TS Pro-R-A** can be identified intramolecularly between the two hydroxyl groups of the substrate, with a distance of 2.21 Å which is not depicted in the Figure 1.39. However, it appears that this intramolecular non-covalent interaction between the two hydroxyl groups

seems not to be so predominant in discriminating the selectivity of the reaction, like the two other intermolecular ones highlighted in the **TS Pro-S-A** case.

Moreover, the last observation for this first oxidative addition step, regards the face of the allyl system involved in the complexation with the Pd. Indeed, according to our proposed mechanism reported in Scheme 1.3, we hypothesized that the complexation should have been preferential on the *Re*-face of the allyl-moiety of the *S*-portion, to provide the desired stereochemistry after the cyclization. As a confirmation, by looking at the results we got from computations, we can see that the preferred face of the allyl to give the oxidative addition is the *Re*-one (Figure 1.39). This means, that the oxidative addition directly populates the definitive face of the η^3-complex which will be involved in the next cyclization step. An equilibration step can occur in inverting the two faces of the η^3-complex and bringing to the possible different orientation for obtaining the observed experimental stereochemical output. We already reported that due to the molecular complexity of the complexes under examination, we were not able to face computationally the equilibration between the two η^3-complexes, but considering the activation energies of the oxidative addition step being over 20 kcal/mol, we will expect the one for this equilibration to be consistently smaller, due to the absence of an event like the break or formation of a covalent bond.

Thus, we can conclude from the analysis of this first reaction step, that the selection of the two molecular portions in giving the Pd-η^3-complex occurs during the oxidative addition. We can refer to this selectivity as an enantioselection, being the presence of two stereocenters in the starting substrate, but correlated by a plane of symmetry in the *meso*-compound.

Now that we concluded the study on the first step of the reaction, we can move to the fourth one, namely the cyclization. We already extensively reported the reasons why we did not investigate the equilibration step, so as starting intermediates for the cyclization, we manually prepared all possible conformers populated by the equilibration, like it has occurred without our control. This furnished us the output structures to continue the study and to investigate the stereochemical control in the

cyclisation step. Also for this second investigation, our computational results match with the experimental ones, as can be observed from the Table 1.3, which reports the data of population analysis for the cyclization step.

	E (a.u.)	Computational	Experimental
SSR-TS	-3883.349415	**65.4**	**62.4**
RSR-TS	-3883.348815	**34.6**	**30.0**
RRS-TS	-3883.335529	**0.0**	**5.0**
SRS-TS	-3883.341745	**0.0**	**2.6**
	Sum	**100.0**	**100.0**

Table 1.3: *Electronic energies and population analysis for the cyclization step with (R,R)-**L2** ligand. DFT level of theory: B3LYP/6-31G(d) & LanL2DZ (only the most stable conformer for each portion are reported).*

Again, we observed the crucial role of the acetate leaving group in helping during the removal of the proton from the hydroxyl group that is involved in the cyclization and thus increasing the nucleophilicity of the oxygen atom. Then, the network of interactions we talked about in the previous pages, still governs the selectivity in this cyclization step, by helping in decreasing the activation energy of the cyclization product on the *S*-portion of the molecule (i.e., the *R*-hydroxyl group is the one involved in the cyclization). In the following Chart 1.2, we can easily observe how these H-bond interactions can stabilize the relative energy for the **SSR-TS** and **RSR-TS** to 2.7 and 3.1 kcal/mol, respectively. On the other hand, the two isomeric **RRS-TS** and **SRS-TS** which describe the cyclization on the *R*-portion of the *meso*-diol (i.e., the *S*-hydroxyl group is the one involved in the cyclization), showed an increase in the relative energy to 11.4 and 7.5 kcal/mol, respectively (Chart 1.2).

By looking at the Chart 1.2 and the Table 1.3, one can argue that the results can be considered a quite good match for the **SSR-TS** and **RSR-TS** product ratio, while for the other two the results are poor. This is true, but we have always to consider the intrinsic error of the method, that relies approximately on 2 kcal/mol for the functional and basis set we used. This means that the results which showed a large preference for a particular isomer are in good accordance, but with low per-

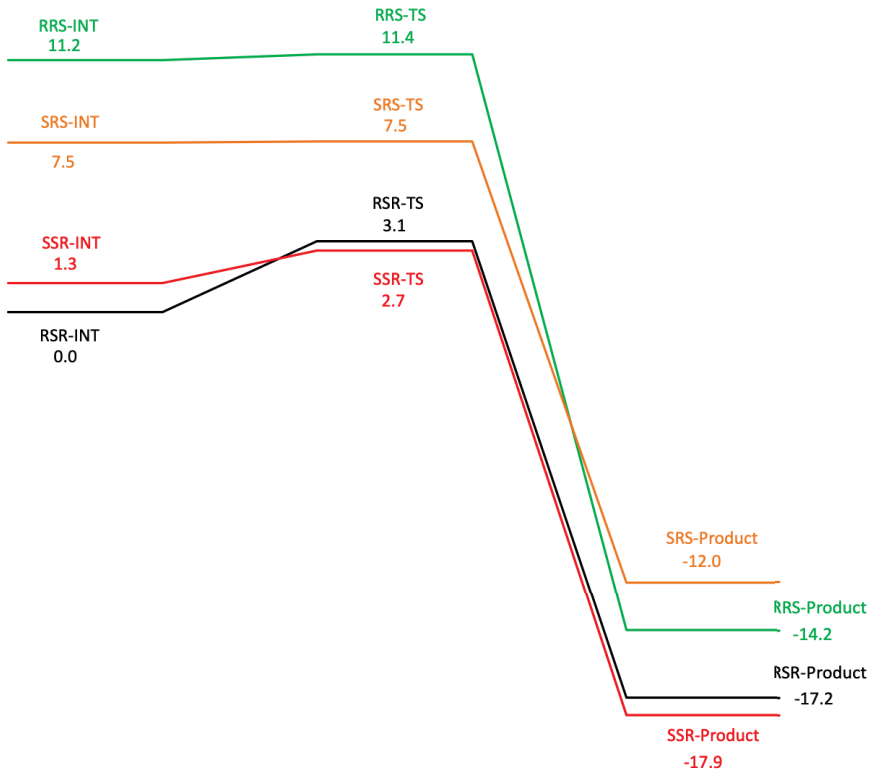

Chart 1.2: *DFT calculations of the four main possible conformational pathways to the cyclization step with the usage of (R,R)-**L2** ligand. Level of theory: B3LYP/6-31G(d) & LanL2DZ (values reported in kcal/mol)*

centage values like those of **RRS-TS** and **SRS-TS**, it can be possible to have a discordance in the match. The most important thing in our opinion, is the maintenance of the match for those isomers which were preponderant in the reaction output.

From the TS structures, it becomes clear the reason the way the H-bond interactions regulates the discrimination of the four possible isomeric products. Indeed, if we compare the two TS structures which bring to the enantiomeric products **SSR** and **RRS**, we can soon observe for the second one the lack of the H-bond between the *R*-hydroxyl group and the amidic proton of the ligand (Figure 1.40).

Specifically, if we look at the *S*-hydroxyl group in **SSR-TS**, it again shows its capacity in acting as both an H-bond donor, with the acetate anion on one side (1.61 Å), but it is also prone to accept the incoming H-bond from the N-H amide moiety on the opposite one (1.94 Å) like before. Moreover, the second oxygen of the acetate

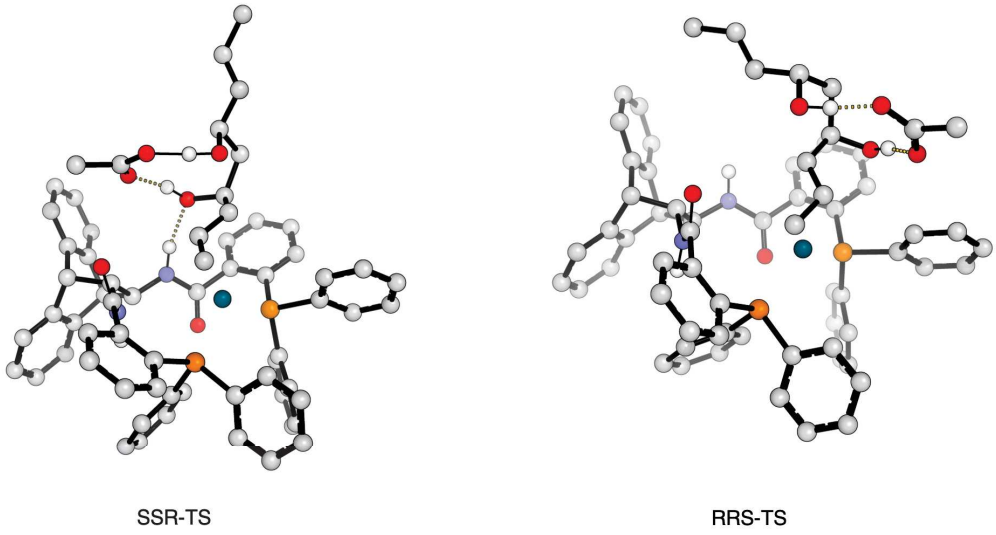

Figure 1.40: *Transition state structures for the cyclization towards the most favored **SSR** isomer and the least favored **RRS** one (non-covalent bonds highlighted in yellow dashed lines).*

anion helps in extracting the proton on the *R*-hydroxyl group, with a distance in the TS that is shorter than the ones found for the H-bonds (1.44 Å).

On the other hand, the enantiomeric **RRS-TS**, shows the same intramolecular interactions between the acetate anion and the two hydroxyl groups of the substrate with distances comparable with the ones highlighted for the **SSR-TS** isomer. However, the big difference occurs in the orientation of the *R*-hydroxyl group away from the ligand amidic cores, thus resulting the completely absence of the intermolecular stabilizing interactions. A similar situation can also be found by comparing the TS structures of the two enantiomeric **RSR**, **SRS** transition states.

Like in the previous step, those non-covalent intermolecular H-bond type interactions, helps in stabilizing more than the intramolecular ones, favoring the *S*-portion products over the *R*-derived ones. Regarding the faces of attack, we can confirm our prediction in the proposed mechanism, where the **SSR** product is obtained by the cyclization of the *R*-OH group on the *Si*-face of the Pd-allyl complex, while the **RRS** product by the cyclization of the *S*-OH group on the *Re*-one. Vice versa, the **RSR** and the **SRS** derived from the cyclization of the *R*-OH group on the *Re*-face of the allyl system and of the *S*-OH group on the *Si*-one, respectively.

We can conclude our analysis of the cyclization reaction of the (*E*,*E*)-*meso*-diol **1** promoted by the (*R*,*R*)-**L2**, by observing that during this reactive step a diastereoselection of the two diastereotopic faces of each allylic portion of the molecule is operated. Thus, the final crucial points in our study occurs in the first step with the oxidative addition and in the fourth one with the cyclization. In the former, we operate an enantioselection of the two portions of the molecule, being the *S*-one the most preferred; while in the latter we observe a diastereoselective process for the ring-closure on the two diastereotopic faces of each allylic system. Moreover, the equilibration step helps in changing the faces between the intermediates obtained from of the oxidative addition and the ones involved in the cyclization step, but we strongly think that it has no role in the regulation of the final stereochemical output. In our idea, it has the mere role in the facial exchange before the real diastereoselective cyclization step.

1.7.2 (*S*,*S*)-DACH-Ph [(*S*,*S*)-L1] Trost Ligand

Due to the interesting results we obtained from the computational investigation of the mechanism and the stereoselective steps with the (*R*,*R*)-**L2** ligand, we decided to approach in a similar way also the reaction promoted by the usage of the (*S*,*S*)-**L1** ligand. Specifically, we used the same approach as before and level of theory, being particularly interested in what regulates the selectivity of the two portions of the substrate **1**, namely the initial oxidative addition enantioselective step. Indeed, we have to remember that the reaction showed a counterintuitive stereochemical output, by favoring again the isomeric products derived by the cyclization on the *S*-portion of the molecule rather than those from the *R*-one, as one should expect from the change in stereochemistry on the ligand.

Thus, we followed the same approach as before, by manually populating the different types of conformers through the rotation of the uncoordinated portion of the molecule. Moreover, we also adopted the same Pro-S or Pro-R denomination depending on the allylic portion involved in the coordination of the Pd, always together with the A or B definition to distinguish the relative acetate orientation.

When we compared the results of our computational investigation for the first step with the experimental ones, soon we observed a huge discordance, as evinced in the Table 1.4, which reports the data of population analysis.

	E (a.u.)	Population Percentage	Computational	Experimental
TS Pro-R-A	-3501.073492	95.3	**100.0**	**21.4**
TS Pro-R-B	-3501.070645	4.7		
TS Pro-S-A	-3501.065696	0.0	**0.0**	**78.6**
TS Pro-S-B	No results			
Sum		**100.0**	**100.0**	**100.0**

Table 1.4: *Population analysis for the oxidative addition step with (S,S)-**L1** ligand. DFT level of theory: B3LYP/6-31G(d) & LanL2DZ (only the most stable conformer for each portion are reported).*

Thus, according with the calculations, the favored portion of the molecule in giving the complexation with the palladium is now the one which contains the *R* stereogenic center (i.e., Pro-R), as we should reasonably expect and not the really experimental observed *S*-one. In particular, the removal of the acetate leaving group and the formation of the η^3-complex starting from the η^2-one from the *R*-portion of the molecule, appeared now nearly 5.0 kcal/mol favored over the Pro-S-one, as described by the Chart 1.3. This explains the huge difference in the observed computational selectivity, which is almost completely selective through the *R*-portion.

Like in the previous examination we were not able to identify the TS for the **Pro-S-B** conformer. However, the above highlighted 5.0 kcal/mol which differentiates the **TS Pro-R-A** from the most unstable **TS Pro-S-A**, are at the origin of the completely selectivity observed in the calculations on to the wrong portion of the molecule (i.e., the *R*-one). A careful examination of the TS structures, easily shows the reasons behind this selectivity which follow the theoretically expected one. Indeed, the most favored **TS Pro-R-A**, showed the same intricate network of non-covalent interactions we reported for the **TS Pro-S-A** when the (*R*,*R*)-**L2** ligand was used. The same H-bond type interactions that helped in that case in stabilizing the transition state, also act now in the same manner by stabilizing both

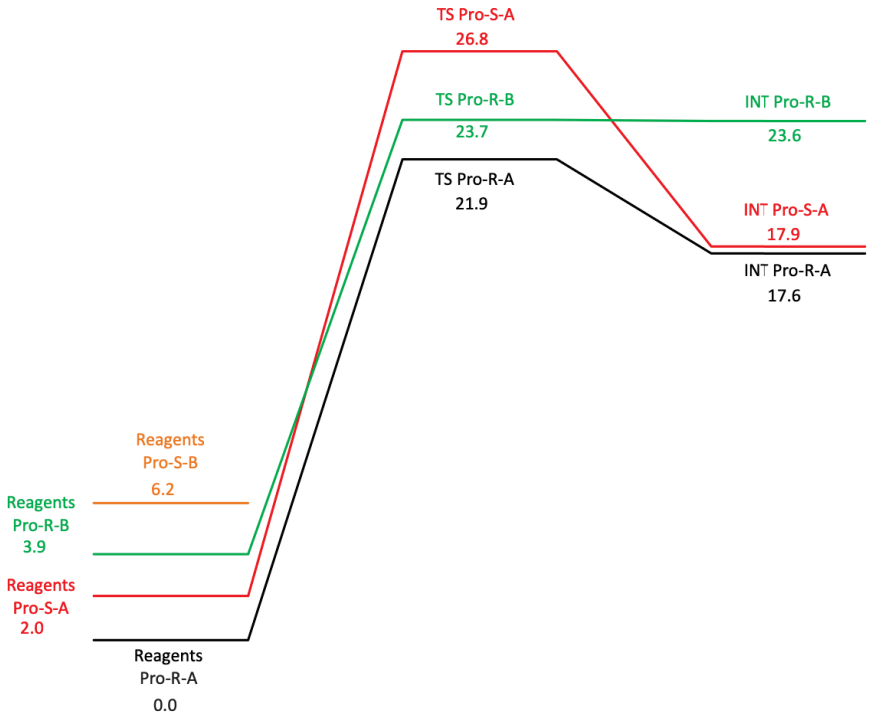

Chart 1.3: *DFT calculations of the four main possible conformational pathways to the oxidative addition step with the usage of (S,S)-**L1** ligand. Level of theory: B3LYP/6-31G(d) & LanL2DZ (values reported in kcal/mol)*

the substrate within the catalyst environment and the exit of the acetate leaving group (Figure 1.41).

A close look at the **TS Pro-R-A** structure highlight again the presence of the double intermolecular interactions provided now by the *R*-hydroxyl group with the ligand's amidic moieties. Indeed, this *R*-OH group can act as previously reported for the *S*-one in the (*R*,*R*)-**L2** case, by establishing two H-bonds both as a donor and acceptor group. It donates the H-bond to the carbonyl oxygen of the ligand (2.01 Å), while accepting it from the N-H amidic group on the opposite side of the ligand (1.87 Å). Simultaneously, we can still find the intramolecular interaction between the acetate leaving group and the *S*-hydroxyl group belonging to the portion not involved in the complexation. On the opposite side, due to the different spatial orientation of the *S*-hydroxyl group in the **TS Pro-S-A**, it is only able to establish

a single H-bond interaction by accepting the N-H amidic proton (1.96 Å). The intramolecular one, namely the interaction between the acetate leaving group and the *R*-OH group is still present.

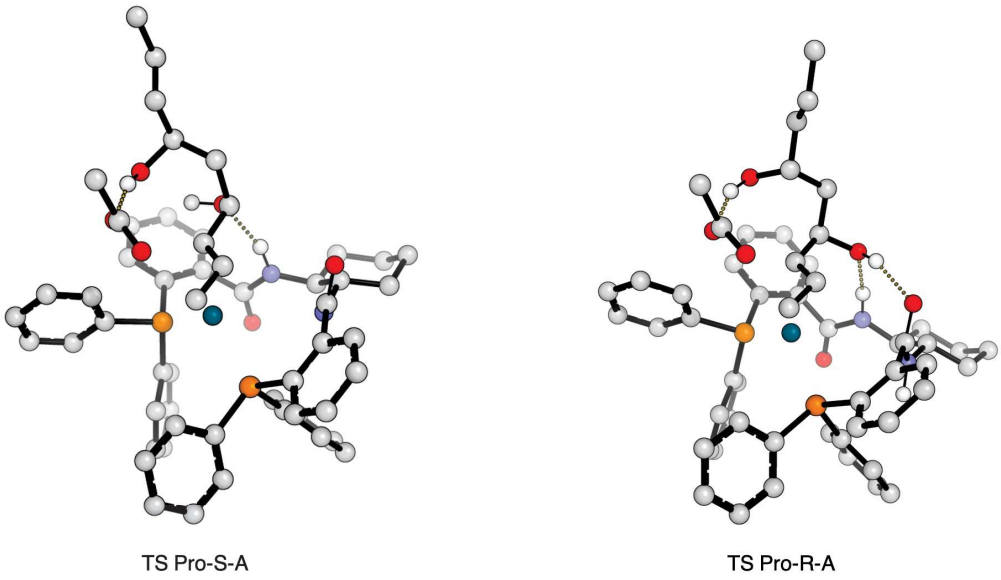

Figure 1.41: *Transition state structures for the most favored* ***Pro-R-A*** *conformer and the least favored* ***Pro-S-A*** *one (non-covalent bonds highlighted in yellow dashed lines).*

Moreover, if we look now at the face of the allyl moiety in the most favored **TS Pro-R-A** involved in the complexation with the Pd atom, we can see again a parallelism with the situation observed in the (*R*,*R*)-**L2** case. Indeed, the proposed face for the complexation with our mechanism was the *Si*-one on to the *S*-portion of the (*E*,*E*)-*meso*-diol **1**, and as a confirmation here we can clearly see that the *Si*-face of the substrate is involved in the complexation both on the *S*- and *R*-portions.

To sum up, the situation that our calculations described, is the typical specular one we would have expected with the application of the classical stereochemical theory, where the inversion in the stereochemistry of the ligand results in the specular inversion of the observed stereochemical output in the products. We can say that the change in the stereochemistry of the ligand can be translated in the opposite enantioselection between the two enantiotopic faces of the two portions of the substrate.

However, the main crucial point is that our calculations did not found a match with the experimental observed selectivities, which appeared to be absolutely counterintuitive. To solve the problems we encountered, we still analyzed in more detail the chromatograms reported in Figures 1.30 and 1.32, but we did not find any problem or misunderstanding in the observed selectivities. The mismatch we observed between the good results obtained with the (*R*,*R*)-**L2** ligand and the poor ones for the (*S*,*S*)-**L1** ligand, prompted us to focus our attention on this first step of the reaction, considering that a proper understanding of the oxidative addition step in the case of the (*S*,*S*)-**L1** ligand could have been the key to explain the observed experimental selectivities.

We thus decided to start from the computations and the method we used to evaluate and model the system. First of all, we tried approaching the same structures with a different functional and specifically we tried using the same basis set under the Minnesota M06-2X functional.[32] However, no particular differences were observed in terms of selectivities for this first step, being again the *R*-portion largely preferred over the *S*-one. We then tried to remain in the same functional we used before (i.e., the B3LYP), but by changing the basis set. In particular, we decided to apply the Ahlrichs all-electron def2-TZVP basis set to all the atoms.[33] Also in this case we did not observed any significative variation in the previously reported selectivities. After these failures, we kept thinking that both the two functional used are not so well parametrized to describe such an intricate network of non-covalent interactions. The usage of corrections to the dispersion appeared us to be the first available choice to test on the problem. We thus decided to introduce in the B3LYP calculations the GD3-BJ Gaussian keyword to describe the D3 version of Grimme's dispersion with Becke-Johnson damping.[34] However, also in this case no positive change was achieved. We remained with only one last option: the investigation of the role of the solvent, thinking at a crucial role of it during the reaction. To do so, we modeled our calculations in the presence of toluene and by using two different polarizable continuum solvent models: the PCM and the SMD.[35] Again, no difference was highlighted by the usage of a solvent model.

It thus appeared us that a different model could be involved for the oxidative

addition step using the (*S*,*S*)-**L1** ligand. Indeed, with all the modifications we tried in the previous trials, we should have observed some variation, while we did not get any appreciable difference. By looking at the structure of the complex, we soon recognized another possible interaction which involves the acetate leaving group and helps its exit. Indeed, we considered since now that the acetate leaves the allylic position by the help of an intramolecular interaction within the substrate itself driven by the hydroxyl group on to the uncoordinated portion of the (*E*,*E*)-*meso*-diol **1**.

However, if we rotate the acetate carbonyl group towards the ligand scaffold, we can find that the amidic N-H moiety of the ligand can establish an intermolecular H-bond too, by stabilizing the exit of the acetate. Considering the general increase in stabilization we found for the previous analysis on the (*R*,*R*)-**L2**, where the intermolecular interactions fully governed the selectivity over the intramolecular ones, we can still consider a similar scenario in this case. Moreover, this new type of intermolecular interaction appeared us to be unfeasible on to the (*R*,*R*)-**L2** ligand, due to the intrinsically bigger dimensions of the ligand scaffold and to the different orientation of the amidic proton respect with the acetate, thus making practically impossible an H-bond stabilizing interaction.

We thus started approaching the transition states for this new hypothesis and the results of we got for the new first step finally showed a proper match between the experiments and the calculations. Table 1.5 reports the data we obtained as a result of the population analysis.

	E (a.u.)	Population Percentage	Computational	Experimental
TS Pro-R-A-new	-3501.075482	7.1	**7.1**	**21.4**
TS Pro-R-B-new	No results			
TS Pro-S-A-new	-3501.077905	92.9	**92.9**	**78.6**
TS Pro-S-B-new	-3501.066887	0.0		
	Sum		**100.0**	**100.0**

Table 1.5: *Population analysis for the new oxidative addition step with (S,S)-**L1** ligand. DFT level of theory: B3LYP/6-31G(d) & LanL2DZ (only the most stable conformer for each portion are reported).*

As a first observation we can see that the absolute energies for this new model of

oxidative addition are lower than those reported before. This is the first macroscopic confirmation that again the intermolecular interactions help in stabilizing more than the intramolecular ones. The key H-bond can be observed from the TS structures of the two most stable conformations **TS Pro-S-A-new** and **TS Pro-R-A-new**, reported in Figure 1.42.

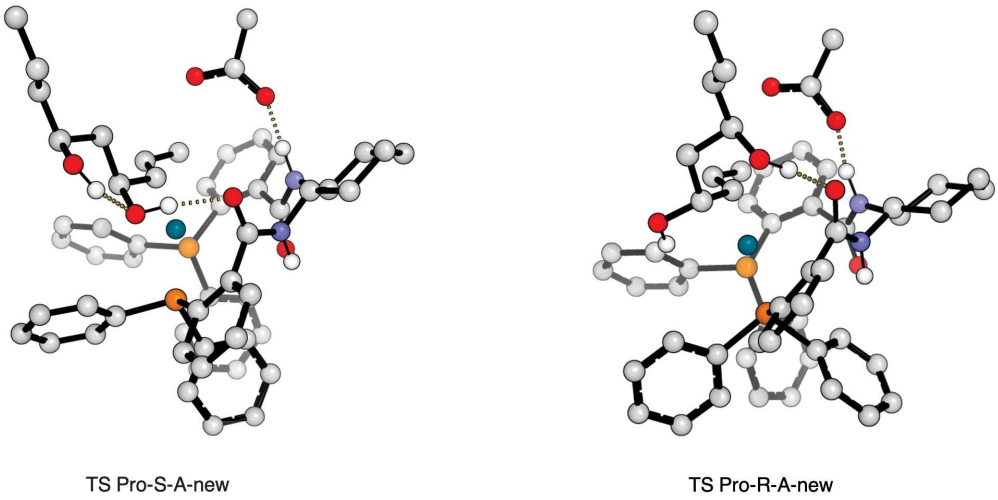

Figure 1.42: *Transition state structures for the most favored* ***Pro-S-A-new*** *conformer and the least favored* ***Pro-R-A-new*** *one (non-covalent bonds highlighted in yellow dashed lines).*

These two H-bond are almost the same length in both of them, being around 1.68 Å, and we can say that it helps in the general stabilization of the complex. However, another key interaction regulates the selectivity within this new approach. Specifically, we have to move observing the network of the other inter- and intramolecular contacts. By looking at **TS Pro-R-A-new**, we can see that the *S*-hydroxyl group, which belongs to the non-coordinated portion of the molecule, everts from the upper side of the substrate to donate its proton in a H-bond with the carbonyl moiety of the ligand amide (1.85 Å). On the opposite side, the *S*-hydroxyl group is completely oriented far from the ligand scaffold and cannot directly interact with it. Moreover, the substate undergoes a conformational change to make the *R*-OH group interacting with the ligand, moving away the two hydroxyl groups from a possible intramolecular stabilizing interaction. This last one is the key feature that distinguish the **TS Pro-S-A-new**. Indeed, in this Pro-S transition state along with the already

mentioned N-H···OAc interaction, we can observe at least other two ones. The first one, in terms of importance, still remains the intermolecular H-bond between the *S*-hydroxyl group belonging to the coordinated portion of the molecule and the carbonyl moiety of the ligand amide (1.84 Å). This time, the *S*-OH group is already oriented towards the amidic moieties of the ligand and no conformational change has to be planned to fulfill this interaction where the hydroxyl group donates its proton to the carbonyl one. Moreover, another important interaction can now occur intramolecularly within the coordinated substrate. The non-necessity to conformationally accommodate the orientation of the *S*-hydroxyl group, makes it possible to direct the *R*-one to donate its proton in an intramolecular H-bond between them. Specifically, the *R*-hydroxyl results already oriented to give the interaction to a distance of 1.87 Å. By looking more in-depth within this network, we can also identify another important feature arising from this H-bond: namely, the formation of a six-membered ring which contains the two oxygen atoms of the substrate, together with the proton and the other three carbon atoms insisting on them (Figure 1.42). Moreover, the proposed *Si*-face complexation by the Pd-catalyst was confirmed also by our new calculations. Indeed, we can see that both in the case of the *S*-portion and in the *R*-one, the *Si*-face of the allyl system is the favored one to give the coordination to the Pd.

Altogether, all the features described above helps in stabilizing the first oxidative addition step again on the *S*-portion of the molecule, rather than on the intuitive *R*-one. We can thus conclude that also in the case of the (*S*,*S*)-**L1** ligand, the first oxidative addition step is the enantioselective one, as already reported for the (*R*,*R*)-**L2** ligand. However, the way this enantioselection is achieved is completely different in the two cases. We showed in the previous case, that the regulation of the selectivity was operated by a specific intermolecular network of interactions, where the acetate leaving group was assisted by an intramolecular H-bond. In this last case, the intermolecular interactions still govern the whole process, but in a different way. Acting directly on the acetate leaving group, completely change the network we saw for the (*R*,*R*)-**L2**. Furthermore, another and extremely discriminative H-bond arises now intramolecularly, by forming a six-membered ring characterized by a huge

stability, thus helping in the final expression of the enantioselectivity.

Recently this year, the same H-bond between the acetate leaving group and the N-H moiety of the (*S*,*S*)-**L1** ligand we highlighted, was also reported in a literature masterpiece, showing the first *parallel-kinetic-resolution* (PKR) achieved through a Tsuji-Trost asymmetric allylic alkylation in the total synthesis of the (-)-Arborisidine alkaloid.[36]

1.7.3 Experimental evaluation of the NH···OAc H-Bond

We were particularly proud of the models we were able to elaborate and of the interactions and features we highlighted. However, an experimental evaluation of the role of that NH···OAc H-bond interaction should have been extremely useful to validate all of our hypothesis and results. To do so we decided to operate in the opposite manner: the removal of that interaction.

Soon we imagined possible different ways to remove that N-H proton and thus exclude the possibility to observe the corresponding effect. The first real problem was due to the nature of that N-H bond. Indeed, being part of an amidic system, thinking to a deuterative process would have resulted in an unsuccess, due to the lability of that bond as a result of the classical resonance equilibrium over the amide core. Due to the presence of the acetic acid as the direct byproduct of the cyclization reaction, the deuterium atom would be easily replaced from the N-D moiety with another proton which occurs in a stochiometric amount.

We thus thought to use a more stable bond, but whose effect was minimal on to the chiral environment where the reaction occurs. This is fundamental in order not to modify again the stereochemical output of the reaction. The best solution we found as the least invasive both in terms of electrical modification over the ligand and steric hindrance, was the selective methylation of the two amidic groups of the ligand.

We firstly synthetized the new (*S*,*S*)-**L1**-Me ligand by following the same condensation procedure adopted for the other ones. Specifically we started from the commercially available (1*S*,2*S*)-*N*,*N*'-dimethylcyclohexane-1,2-diamine **13** and the

2-(diphenylphosphino)benzoic acid. The reaction again occurred in a smooth way, in dichloromethane. The only variation from the previous approach was the usage of the 1-Ethyl-3-(3-dimethylaminopropyl)carbodiimide (EDCI) as activating agent and 4-Dimethylaminopyridine (DMAP) (Figure 1.43).

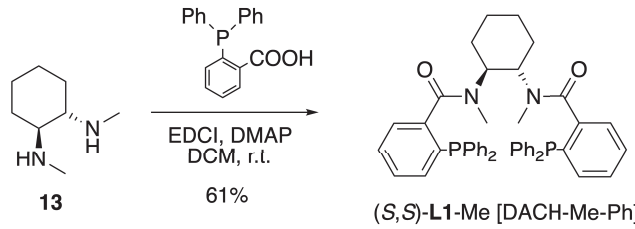

Figure 1.43: *Synthesis of the ligand (S,S)-**L1**-Me.*

With the so obtained ligand, we approached the reaction on the (*E*,*E*)-*meso*-diol **1** in the same condition as reported for the other two cases. In particular, we used again toluene as solvent and no stoichiometric amount of a base was used in the reaction. The quantities of catalyst and ligand were maintained as before, being 3% mol the $Pd_2(dba)_3{\cdot}CHCl_3$ catalyst and 8% mol the ligand. Also, the molarity of the solution was 0.1M as before.

The results we got are reported in the following Figure 1.44.

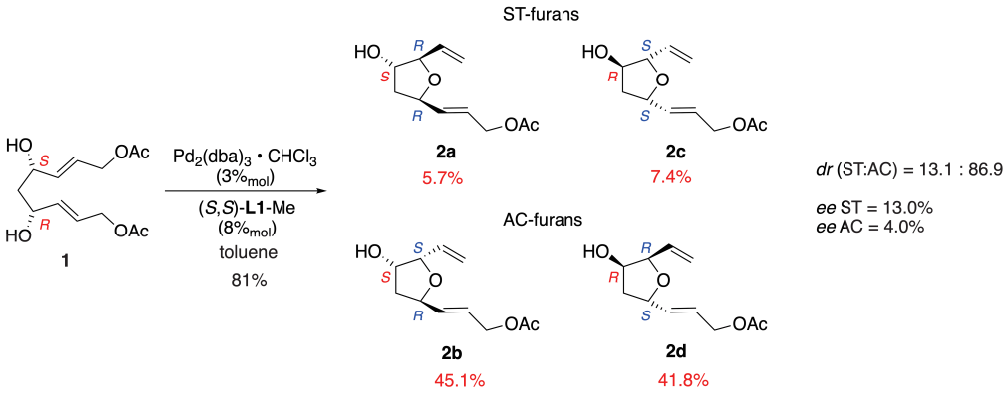

Figure 1.44: *New cyclization with (S,S)-**L1**-Me ligand and in toluene.*

By comparing these results with those of the previous two cyclizations and reported in Figures 1.29 and 1.33, we can easily find a diastereoselective behavior similar with the one achieved by the usage of the (*R*,*R*)-**L2** ligand (Table 1.6). Indeed, now we can find again a slight preference over the *S*-portion of the molecule,

Entry	Ligand	Solvent	*dr* [a]	**2a (ST)** *ee* (%)[b]	**2b (AC)** *ee* (%)[b]	Yield (%)
1	(*R,R*)-**L2**	Toluene	33:67	84	85	79
2	(*S,S*)-**L1**	Toluene	59:41	97	0.3	85
3	(*S,S*)-**L1**-Me	Toluene	13:87	-13	4	81

[a] *dr* **ST:AC** determined by HPLC. [b] *ee* determined by chiral HPLC (Chiralpak AS-H column – 80:20 Heptane:iPrOH).

Table 1.6: *Comparison of the selectivities obtained by using the three different ligands in the same experimental conditions.*

but the *dr* (13.1:86.9) is strongly moved towards the AC-furans and not to the ST-ones, as we observed with usage of the (*R*,*R*)-**L2** ligand. Furthermore, the decrease in the *ee* for both the ST-furans (13.0%) and the AC-ones (4.0%) can be explained by considering the obvious increase in sterical hindrance within the catalyst reactive site. Finally, the isolated yield still remained to quite high values (81%). These results, are in accordance with the model we elaborated computationally, by showing a fundamental role of the N-H moiety, intervening directly in the govern of the stereoselectivity observed. However, the usage of a non-sterically-innocent methyl group, strongly modified the ratios in terms of enantioselectivity.

For completeness, in Figure 1.45 we report the HPLC chromatogram from which we obtained the selectivity results reported above. Again we used a Chiralpak AS-H column with 80:20 Heptane:iPrOH isocratic eluent mixture.

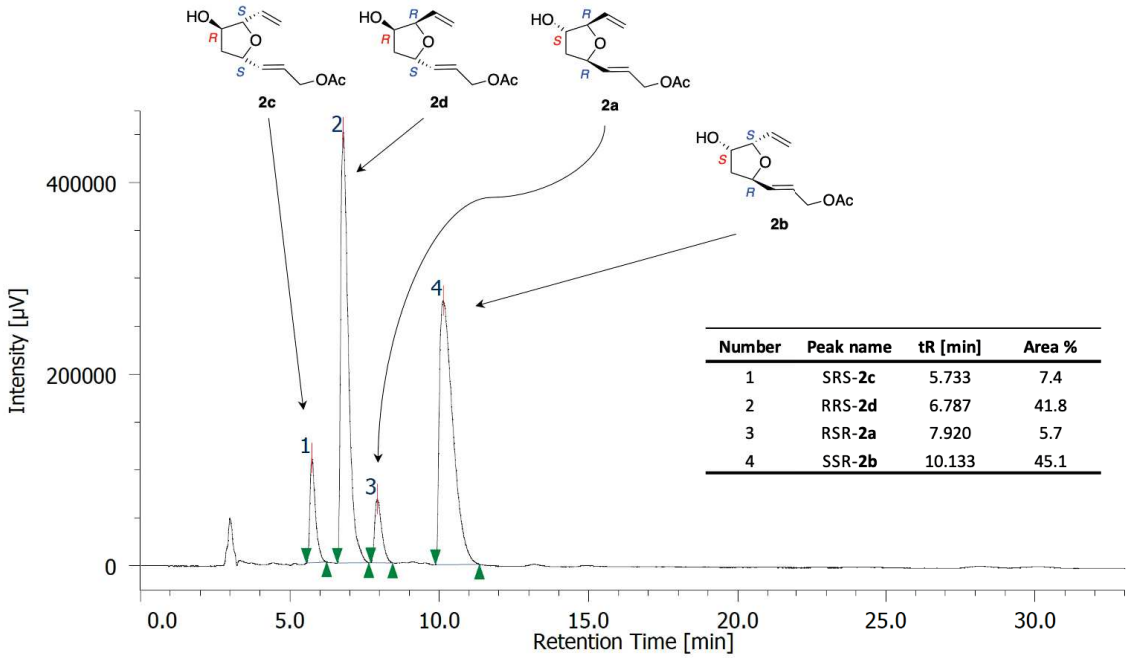

Figure 1.45: *HPLC profile for the (S,S)-**L1**-Me promoted cyclization and the corresponding integrations.*

1.8 Investigations on the equilibration step: the role of additives

In the initial section of this chapter, we highlighted that different mechanistic pathways can control the exchange between the coordination of the Pd on to the two diastereotopic faces of the allyl system in the (*E*,*E*)-*meso*-diol **1**. This process, also known as η^3-η^1-η^3 equilibration can be achieved in different ways, as we reported in the previous sections. However, by looking at our computational studies it appears clear that another important factor is the relative orientation between the acetate leaving group and the allyl moiety. It derives also that the relative orientation between the Pd-ligand complex and the allyl plays a fundamental role in regulating what we called as A or B orientations. Indeed, some stabilizing interactions can only be established if the acetate, the allyl and the Pd-ligand complex are placed with a specific orientation, as for example in the case of the (*S*,*S*)-**L1**.

By looking in-depth within this process, we can see that a particular pseudorotation of the allyl system can result in an apparent rotation of the Pd-ligand complex. We referred to this in the previous sections as the *apparent isomerization through pseudorotation* of the allyl moiety.[20] Moreover, it was also reported in literature that the addition of chloride ions, for example as *tetra*-alkylammonium salts, could help in increasing the rate of this equilibration.[17b],[18],[25] The mechanism of this particular isomerization can be found in Figure 1.23.

In light of what we computationally discovered to be discriminating in the regulation of the selectivity for this reaction on our diol **1**, we thought that it could have been interesting to experimentally investigate the behavior of the reaction in the presence of a source of chloride anions. Specifically, we decided to add catalytic quantities of Hex_4NCl as described by Evans and co-workers in 2008. We still used the same catalytical amount of the $Pd_2(dba)_3{\cdot}CHCl_3$ complex (3% mol) and the two ligands (*R*,*R*)-**L2** and (*S*,*S*)-**L1** (8% mol). The loading of the ammonium salt we choose was 30% mol, as the authors identified to be a good choice in the published paper.[17b] The solvent we used was now changed to dichloromethane, due to solubility problems of the ammonium additive in toluene. This solvent modification

should not influence drastically the result of our experiments, since it was used as best solvent choice during the studies in our publication.[14]

The results we obtained are reported in Table 1.7, while the HPLC chromatograms are available in the experimental section in support to this chapter at the end of this thesis.

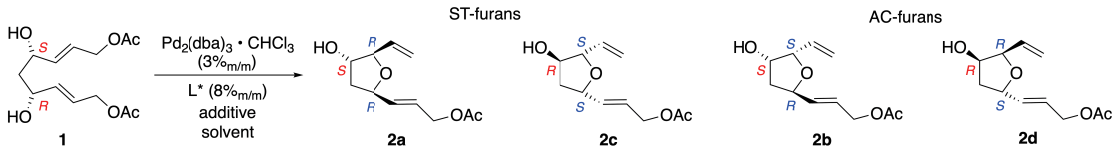

Entry	Ligand	Solvent	Additive	Amount of Additive	*dr* [a]	2a (ST) *ee* (%)[b]	2b (AC) *ee* (%)[b]	Conversion (%)[c]	Yield (%)
1	(*R,R*)-**L2**	Toluene	none	0	33:67	84	85	100	79
2	(*R,R*)-**L2**	DCM	Hex_4NCl	30%	30:70	82	80	80	90
3	(*S,S*)-**L1**	Toluene	none	0	59:41	97	0.3	100	85
4	(*S,S*)-**L1**	DCM	Hex_4NCl	30%	70:30	99	0.2	100	81

[a] *dr* **ST:AC** determined by HPLC. [b] *ee* determined by chiral HPLC (Chiralpak AS-H column – 80:20 Heptane:iPrOH). [c] After 24 hours.

Table 1.7: *Comparison for the synthesis of THF substituted cores in the absence or in presence of catalytic amounts of* Hex_4NCl *additive.*

A close look at Table 1.7 shows that no extremely significant modifications to the stereochemical output are obtained by the addition of the chloride anion. This means that the equilibration in the pseudorotation is already fast enough with both the two ligands, also without the addition of the additive.

By comparing the two run with the (*R,R*)-**L2** ligand, we can see that both in terms of *dr* and *ee* the results are almost the same. Only a small increase in isolated yield can be noted in the usage of the additive. Moreover, after 24h we observed that the percentage in conversion of the starting material was only at 80% and not to the observed completeness when no additive was used. This fact can be interpreted as a secondary result of the increase in equilibration rate. Indeed, by increasing a bit the rate of the equilibration step can result in the decrease of the time available by the substrate to orient, establish interactions and cyclize. However, we can refer to this as a general delay in the reactivity and not something that can influence the stereochemistry of the products, as can be seen from the practically unchanged values of enantio- and diastereoselectivity.

On the other hand, the usage of the ammonium salt with the (*S*,*S*)-**L1** ligand, resulted in the same identical values of *ee* if compared with the ones obtained in absence of chloride anions. The yield was also practically the same. The only variation we observed was an increase in the diastereoselectivity to values closer to the ones of our publication (see Table 1.1). This increase from nearly 60:40 to 70:30 (*dr* ST:AC), can be due mainly to two different causes. For sure the presence of the additive can help in populating more the most stable species to give the diastereoselective cyclization step, but also the role of the change in solvent has not to be excluded. Indeed the 80:20 (*dr* ST:AC) reported as the best result in our published paper, was obtained in dichloromethane and thus a role of the solvent in increasing the *dr* by stabilizing the more reactive intermediates cannot be excluded.

Anyhow, the most important observation that has to be done from these results, is the practical no influence of the additive in changing the reactive portion of the molecule. The *S*-portion remained favoured with both of the two ligands also in the presence of the additive. We should point out that the role of the addition of chloride anion is to act on to the already formed η^3-complex, and thus could have resulted in a greater effect on to the diastereoselectivity rather than on to the enantioselectivity. Indeed, we showed that according to our calculations, it is during the first oxidative addition step that the portion-discrimination occurs. Not involving this step already formed η^3-complexes, it results basically indifferent to the presence of the additive, which can only exert its potential on to the next steps.

1.9 Investigations on the η^3-η^1-η^3 equilibration step: the *Z*,*Z*-*meso*-diol

We extensively reported in the previous sections on the peculiar features of the (*E*,*E*)-*meso*-diol **1**, especially on the stereochemical descriptors of its structure. Indeed, according with the commonly accepted IUPAC rules, we can define as diastereotopic the two faces of each allyl system and name them as *Re* or *Si* one.

Since we showed and computationally investigated that the catalyst preferentially complexes one of the two prochiral faces of the allyl system, we thought that

by reversing the stereochemistry of the two double bonds from *E* to *Z*, we would have obtained the reversal of the prochiral faces of the fragment. In this way the catalyst is theoretically forced to complex the molecule's allyl systems on the opposite side with respect to the previous (*E*,*E*)-case. This new approach should help us in studying with an increased detail the η^3-η^1-η^3-equilibration step we were not able to investigate computationally. We already talked about the mechanism of this equilibration and how it can be achieved (Figures 1.19 and 1.21). Along with that dissertation, we have now to introduce the ligand discrimination proposed by Trost when a soft nucleophile (i.e., like our hydroxyl group with a pKa $\approx$ 15) is involved in an Asymmetric Allylic Alkylation reaction.[20]

According to their studies, it is possible to divide the Pd-ligand complexes in two main different categories:[37]

- *Equilibrating complexes*: where the PdL* complex is able to equilibrate between the two allyl faces faster than the nucleophilic attack;

- *Non-equilibrating complexes*: where the nucleophilic attack is faster than the PdL* complex equilibration between the two allyl faces.

According to the data collected so far, the two main ligands discussed in this work, due to their possibility of accessing the ST and AC cores with an excellent enantiomeric excess, can respectively generate two complexes Pd-(*S*,*S*)-**L1** and Pd-(*R*,*R*)-**L2**, where the first one belongs to the non-equilibrating class and the second to the equilibrating one.[37] However, we computationally demonstrated that in the case of the (*E*,*E*)-diol **1**, the oxidative addition occurs already on to the preferred final faces of the allyl systems of the diol. This means that on the same *S*-portion, the *Re*-face is preferred in giving the oxidative addition step with the (*R*,*R*)-**L2** ligand, while the *Si*-one is the preferred with the (*S*,*S*)-**L1**. Those faces are also the most stable in giving the next cyclization products, thus underlying that in our situation a possible absence of this equilibration cannot be excluded.

To prove the possibility of this equilibration we started thinking at a different substrate that can exert better the role of the equilibration in populating the com-

plexation on to the most stable faces of the allylic systems: the (*Z*,*Z*)-*meso*-diol **14** (Figure 1.46).

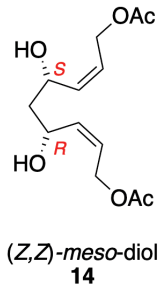

Figure 1.46: *The (Z,Z)*-meso-*diol we will use in the equilibration studies.*

Given that the Pd-(*S*,*S*)-**L1** complex is non-equilibrating, the step that determines the diastereoselection is the enantiofacial recognition of the olefin. Therefore, through a modification of the reactive substrate configuration, we force the Pd-ligand complex to approach the allyl moiety from the opposite side of the molecule: indeed, according with the Cahn, Ingold and Prelog rules (CIP), by changing the configuration of the double bond from *E* to *Z* the topicity of the two faces is reversed (Figure 1.47).

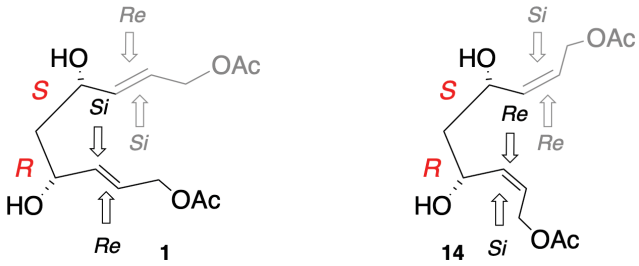

Figure 1.47: *The exchange in the face topicity resulted from the inversion in configuration of the double bonds from* ***1*** *to* ***14****.*

For completeness, we will report also the cyclization in the presence of the (*R*,*R*)-**L2** ligand. Moreover, we will investigate the role of the Hex_4NCl additive in the stereochemical output.

We have now to start with the synthesis of the desired (*Z*,*Z*)-*meso*-diol **14**. As we reported for the diol **1**, the fastest way to obtain the product should be the cross-metathesis strategy. In this case we could think to use the same *ring-opening*

cross-metathesis between *cis*-cyclopent-4-ene-1,3-diol **3** with (*Z*)-1,4-diacetoxybut-2-ene and by involving now the Grubbs *Z*-selective catalyst,[38] as reported in Figure 1.48.

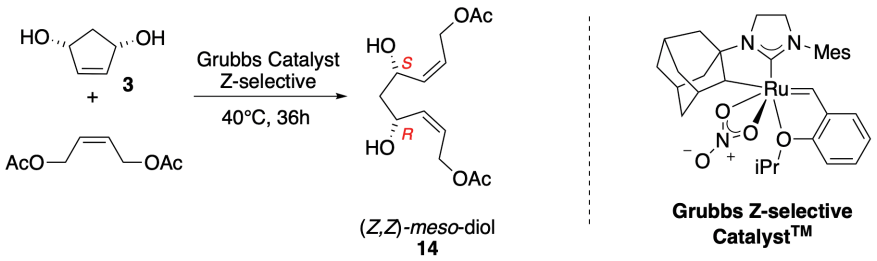

Figure 1.48: *Synthesis of the (Z,Z)*-meso-*diol* ***14*** *through ring-opening cross-metathesis.*

This synthetical approach was attempted in the previous years in our lab, but only traces of raw product were obtained.[2] Indeed, we speculated that the Grubbs *Z*-selective catalyst is capable in promoting *Z*-selective metathesis where no ring opening has to be performed. An extensive research in the current literature shows that it is widely adopted in circumstances where no strained cycloalkenes are present as reactive partners.[38] Moreover, we observed a huge presence of Ru-complex byproducts of difficult purification and, accordingly to our mechanistic studies, we cannot tolerate the presence of other metal traces in our reaction mixture.

We thus decided to follow a synthetical approach similar to the one set up for the diol **1** (Figure 1.49). Specifically, we started from the same intermediate **5** and we operated firstly a Wittig reaction to obtain the bis-olefin **15** with an isolated yield of 76%. In this olefination reaction the anion obtained from chloromethyl-triphenylphosphonium chloride is used to generate the active species using a slight defect of *t*BuOK in anhydrous THF. Thus, the so obtained compound **15** was subjected to a one-pot lithiation with *n*BuLi and then homologation with paraformaldehyde, to give the corresponding bis-propargylic diol **16** in 56% of yield. The bis-propargylic diol **16** was firstly esterified with acetic anhydride and pyridine in DCM by exploiting the nucleophilic catalysis of DMAP to obtain derivative **17**. The latter was then subjected to orthogonal deprotection of the silyl ethers with TBAF in THF to furnish the diol **18** in 37% of isolated yield. As last step, we performed a catalytic

hydrogenation by using the Lindlar catalyst and ethyl acetate as solvent in hydrogen atmosphere. The final (*Z*,*Z*)-*meso*-diol **14** was obtained with a quantitative yield. The whole process is described in Figure 1.49.

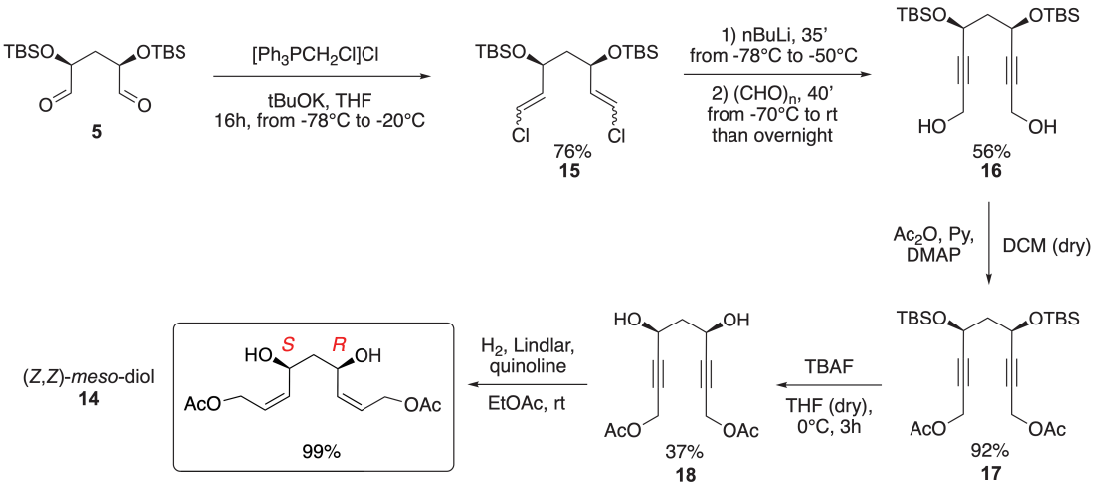

Figure 1.49: *Synthetical pathway for the total synthesis of the (Z,Z)*-meso-*diol **14**.*

Before to move to the cyclization reaction, it is important to define an analytical strategy that could help us in identifying the order of elution of the stereoisomers from the chiral HPLC. The most effective way we identified was to directly correlate the cyclized products from the (*Z*,*Z*)-*meso*-diol **14** with those obtained from the (*E*,*E*)-*meso*-diol **1**. However, due to the inversion in the configuration of the double-bond, a different retention time could be at the origin of a non-perfect coincidence between the results observed from the previous cyclization with those new ones. To unify the situation, we thus decided to reduce the both of the double bonds in the cyclized stereoisomers so that a direct correlation between the two systems can be operated by depending only from the stereochemistry on to the THF ring (Figure 1.50).

To do so, we hydrogenated the stereoisomeric mixtures obtained from the cyclization of **1** with the two ligands (*S*,*S*)-**L1** and (*R*,*R*)-**L2**. Due to the reduction of the two alkenes, we were obliged to change the HPLC method, by using the Chiralpak IA-3 column with 90:10 Heptane:iPrOH as eluent mixture. The chromatograms of these reductions were thus compared with the ones obtained before the reductive step to establish the nature of the specific stereoisomer. Thus, we directly compared

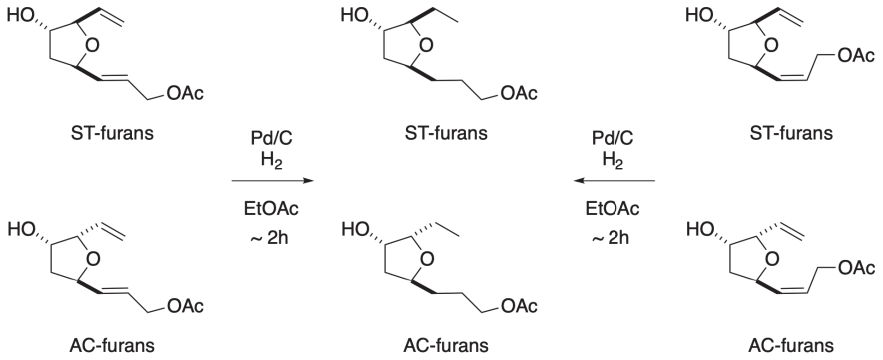

Figure 1.50: *Correlation strategy between (E,E)-*meso*-diol* ***1*** *products and (Z,Z)-*meso*-diol* ***14*** *ones.*

the integrated areas of each peak, by considering that no product went lost during the catalytic reduction (i.e., no byproduct was observed during the TLC controls). The so obtained chromatograms can be found in the experimental part at the end of this thesis, while here we report the legend correlation chromatogram obtained from one of the previous studies done by our group.[2] Specifically, it reports the reduced products from the cyclization promoted by the 1,2-bis(diphenylphosphino)etane (dppe) ligand on to **1**, which resulted to be specifically selective for the preferential formation of the AC-furans.[2],[14] On to that chromatogram, we then assigned also the species we got as a result from our last reductive analysis (Figure 1.51).

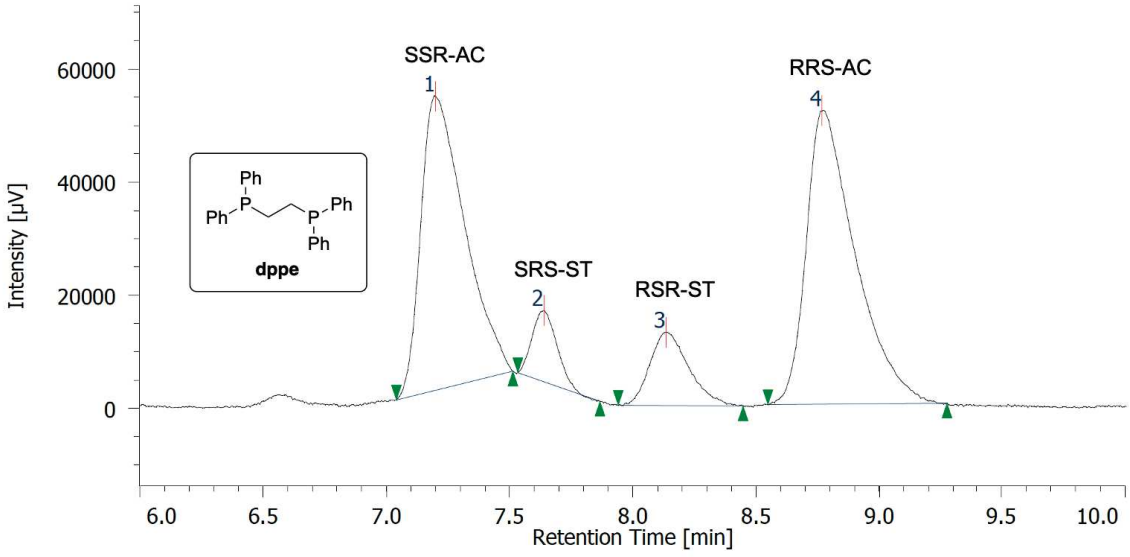

Figure 1.51: *HPLC legend correlation profile for the reduced species (Chiralpak IA-3 column, 90:10 Heptane:iPrOH).*

Now that we defined the synthesis of the diol **14** and the analytical procedure we can use to correlate the results with those from **1**, we can move to the cyclization step, to the investigation of the equilibration step and how the Hex_4NCl can now influence the stereochemical output. We operated as for the cyclization with the diol **1**, by using the same amount of palladium catalyst (3% mol) and ligands (8% mol). Again, we run the reactions in toluene when the additive was absent, while we moved to dichloromethane when Hex_4NCl was used.

When we approached the first reaction by using the (*R*,*R*)-**L2** ligand, we soon got an important result. Indeed, we did not observed a similar situation to the one obtained with the (*E*,*E*)-*meso*-diol **1**. This was the expected result according with the consideration reported above, where we referred to the (*R*,*R*)-**L2** ligand as an equilibrating one. Differently form that situation, we observed now a drastic inversion in the diastereoselectivity, which results now to be in favor of the ST-furans (63.2:36.8 *dr* ST:AC). Moreover, we can see how now the most preferred portion of the molecule in giving the coordination to the Pd-metal center is the R-one, the exact opposite of the previous case (Figure 1.52).

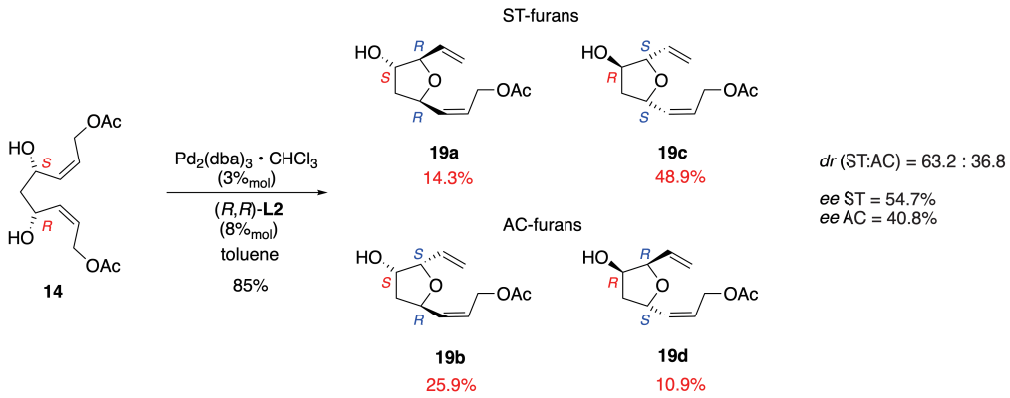

Figure 1.52: *New cyclization of the (Z,Z)*-meso-*diol* ***14*** *with the (R,R)-****L2*** *ligand in toluene.*

By comparing these results with the ones showed in Figure 1.29, it appears clear that the (*R*,*R*)-**L2** catalyst prefers not to act as before, thus selecting the same *S*-portion and then equilibrate to furnish the expected identical results as before, but it completely changes the preferred portion of coordination to the *R*-one. This means that the new substrate **14** behaves in a completely different way to the ones

experimentally and computationally investigated. Moreover, also the *ee* are different than before. We can see a general decrease in the enantioselectivity in both the ST-enantiomers (54.7%) and the AC-ones (40.8%), but the most intriguing observation relies on the exact inversion in the population of the species obtained. Indeed, the most populated isomer for the diol **1** was the **SSR** AC-furan, while now we have as the most preferred the **SRS** ST-furan. Both of these results can be explained by considering the different orientations of the polar groups by moving from the substrate **1** to the **14**. The dramatic change in the directionality of the acetate leaving group and of the hydroxyls, due to the change in the configuration of the double bond, results in a different orientation during the coordination step to the palladium. Thus, it will end up in a new type of oriented non-covalent interactions that will stabilize or destabilize, both inter- and intramolecularly, the main steps of the reaction and so resulting in a different population of the final stereochemical output. Regarding the decrease in the *ee* we have also to remember the notable increase in the sterical hindrance during the cyclization step. Indeed, the non-coordinated portion of the molecule remains in the *Z*-configuration on the double bond, thus increasing the crowding at the reactive center and reducing the conformational freedom which is needed to obtain the proper network of interactions. The chromatogram relating to this reaction and operated on to the reduced species can be observed in the experimental section dedicated to this chapter and placed at the end of this thesis.

By moving now to the reaction operated in the presence of the (*S*,*S*)-**L1** ligand we observed another non-conventional situation, which is even stranger than the previous ones. Indeed, we again did not obtained the expected equilibration with the identical distribution in isomers population like before, but we observed a quasi-identical result to the ones just reported for the (*R*,*R*)-**L2** ligand. This situation is exactly the same as we reported with the (*E*,*E*)-*meso*-diol **1**, where the two different ligands populated the isomers by preferring the same specific portion of the molecule. In that case the portion was the *S*-one, while now we can find again with (*S*,*S*)-**L1**, the same *R*-portion to be the most preferred. However, by comparing the results we obtained with the (*R*,*R*)-**L2** ligand and the ones just obtained, we can see that

there is a practically identical distribution in the population, which favors again the **SRS** ST-furan (Figure 1.53).

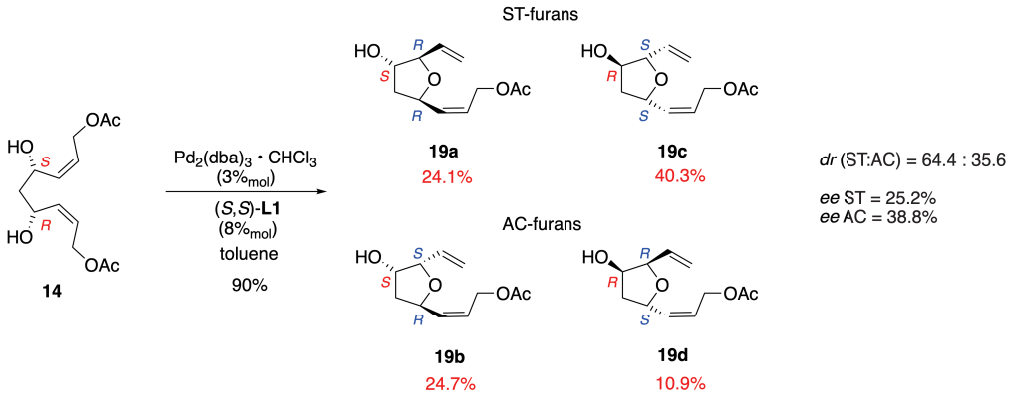

Figure 1.53: *New cyclization of the (Z,Z)*-meso-*diol **14** with the (S,S)-**L1** ligand in toluene.*

This result is extremely unconventional, because in the previous studies on the substate **1** we observed at least the change between the **SSR** AC-furan [with the (*R*,*R*)-**L2**] and the **RSR** ST-furan [with the (*S*,*S*)-**L1**]. Now, we have the same identical situation, with a *dr* that remains again in favor of the ST-furans (64.4:35.6 *dr* ST:AC) and *ee* values that are slightly decreased than before. Specifically, we registered a higher decrease for the *ee* of the ST-enantiomers (25.2%) rather than the one observed for the AC-ones (38.8%).

As the principal reasons to explain the observed results, we can still call in to question the typical non-covalent interactions that can drastically modify the preference in the initial coordination and then regulate all the next steps of the reaction. We also cannot completely exclude the non-equilibrating nature which is recognized for this ligand.[20] Indeed, it can also be that the substrate itself can furnish these results as a non-equilibrating one, as this category was reported by Trost as another possible way of governing the selectivity.[20] Anyhow, no explanation can be referred to this nature on the basis of the preferred coordination on to the opposite portion of the molecule rather than before, if not the one that involves the already cited interaction network.

After these studies, it appears clear that the idea of using the new substrate **14** resulted in more questions than answers, and right now did not helped in giving a

straightforward explanation to the equilibration step we were not able investigating during our computations.

We thus decided, to also test the role in the addition of additives like in the studies previously done with the (*E*,*E*)-*meso*-diol **1**. The results we obtained are again extremely unnatural and added another big question to what really occurs in the mechanism of these reactions. Indeed, differently from what we reported before, when practically no change was observed both in the diastereo- and the enantioselectivity when the addition of Hex_4NCl was operated in the reaction with the substrate **1**, here we got an extremely changed situation. Specifically, the addition of the additive in the reaction with (*R*,*R*)-**L2** ligand resulted in an unchanged diastereoselectivity, which remained to 70:30 (ST:AC) and in a similar decrease in conversion after 24h like the one observed with the diol **1**. This implies a direct dependence between this decrease in conversion and the specific ligand we are using and thus not correlates with the different nature of the substate. However, the greatest modification was observed in terms of enantioselectivity. In the case of the AC-furans, the *ee* remained to values similar to those in absence of the additive (44%) and showing that the same **SSR** AC-furan was the most favored between the two enantiomers. Vice versa, the situation for the ST-furans resulted to be the most affected by the addition of the chloride salt. Indeed, not only we registered a decrease in the *ee* to a value closer to zero (-9%) and thus underling the formation of a quasi-racemic mixture of the two enantiomers, but also the **RSR** ST-furan resulted now to be the slightly favored between the two. This suggest that the addition of the additive, could result in an equilibration that can favor again the complexation on to the *S*-portion of the molecule, suggesting a mix between an apparent isomerization through pseudorotation of the allyl moiety and the above cited η^3-η^1-η^3-equilibration which favours again the **RSR** ST-furan, like in the (*E*,*E*)-*meso*-diol **1** studies with the (*R*,*R*)-**L2** ligand (Table 1.8).

The situation changed again when the addition of the additive was performed in the reaction promoted by the (*S*,*S*)-**L1** ligand. Indeed, even if also here we maintained the same degree of diastereoselection in favour of the ST-furans (64:36 *dr* ST:AC) and a complete conversion, the enantioselectivities are completely changed.

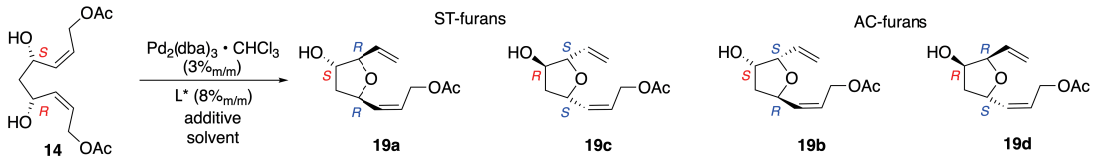

Entry	Ligand	Solvent	Additive	Amount of Additive	*dr* [a]	**19c (ST)** *ee* (%) [b]	**19b (AC)** *ee* (%) [b]	Conversion (%) [c]	Yield (%)
1	(*R,R*)-**L2**	Toluene	none	0	63:37	55	41	100	85
2	(*R,R*)-**L2**	DCM	Hex_4NCl	30%	70:30	-9	44	80	71
3	(*S,S*)-**L1**	Toluene	none	0	64:36	25	39	100	90
4	(*S,S*)-**L1**	DCM	Hex_4NCl	30%	64:36	-33	-48	100	94

[a] *dr* **ST:AC** determined by HPLC. [b] *ee* determined by chiral HPLC (Chiralpak IA-3 column – 90:10 Heptane:iPrOH after idrogenation of the olefins). [c] After 24 hours.

Table 1.8: *Comparison for the synthesis of THF substituted cores in the absence or in presence of catalytic amounts of Hex_4NCl additive for the substrate **14**.*

The addition of the chloride salt resulted in the quasi-exact inversion in the population of the two couples of enantiomers. Indeed, while before we had for the ST-furans the 25% of *ee* favouring the **SRS** enantiomer, now we registered the 33% in favour of the other **RSR** one (i.e., -33% if referred to the same isomer as before). Moreover, the same situation was observed also in the case of the AC-furans, were we moved from the 39% of *ee* for the **SSR** enantiomer, to the 48% in favour of the **RRS** one (i.e., -48% if referred to the same isomer as before) (Table 1.8).

The HPLC chromatograms relative to these experiments with the addition of additives are available in the experimental section in support to this chapter at the end of this thesis.

It appears clear, that in both the cases the result is due to a combination of equilibration steps that appears to be promoted by the presence of the chloride anion. Of particular interest is the fact that the addition of the additive differently populates the two portion of the molecules, by favouring in the reaction with the (*S,S*)-**L1** ligand the *S*-portion for the ST-furans, while the *R*-one for the AC-furans, thus resulting in a complete enantioselective inversion respect with the reaction without additive.

1.10 Conclusions

In this chapter we reported the newest results we obtained in explaining the very unnatural selectivity highlighted by our group in the previous years. Thanks to the extensive computational studies, we identified what can be referred to as a "molecular-wide network" of interactions that both occurs within the substate **1** intramolecularly and between the *meso*-diol and the ligand in an intermolecular fashion. We also highlighted a completely different behaviour of the ligand in regulating the H-bond interactions: the (*R*,*R*)-**L2** cannot provide the non-covalent bond between one of its amide NH groups and the acetate leaving specie, whether the (*S*,*S*)-**L1** can act in such a way and thus stabilize more the outcoming group. To the best of our knowledge, this is the first time that such a study is operated on *meso*-diol compounds that undergo desymmetrization through an Asymmetric Allylic Alkylation reaction.

Most of the results we got are of extreme importance to shed some light in the comprehension of the real mechanism involved in the reaction. Especially, the role of the chloride anion additive which showed to be ineffective in the first diol **1**, but extremely important in regulating the selectivity with the second substrate **14**.

Moreover, the usage of a different substrate like the compound **14**, gave us the possibility to increase the level of the mechanistic comprehension, by showing that also the substrate and not only the ligand can express an equilibrating or non-equilibrating nature. Even if the answers that we got are still less than the questions to be addressed, we can say that most of the uncertainties have been solved. To fulfil our purpose of a complete comprehension of the mechanism, we are still investigating what remained as hidden reasons behind this unconventional behaviour in the desymmetrisation reaction. In our group are still ongoing both experimental and computational proofs to try to accommodate the last missing pieces for the full comprehension on the mechanism. Moreover, recent studies obtained by our group confirmed that our synthetical strategy can be used to prepare differently and stereodefined THF cores, useful as readily available building block for the natural product synthesis.

References

[1] Wolfe, P.; Hay, M. B., Recent advances in the stereoselective synthesis of tetrahydrofurans, *Tetrahedron*, **2007**, *63*, 261-290.

[2] PhD Thesis of: Matteo Valli, Davide Sbarbada and Mattia Fredditori.

[3] Bermejo, A.; Figad, B.; Zafra-Polo, M.-C.; Barrachina, I.; Estornell, E.; Cortes, D. Acetogenins from Annonaceae: recent progress in isolation, synthesis and mechanisms of action, *Nat. Prod. Rep.*, **2005**, *22*, 269-303.

[4] Polo, M.; Figad, B.; Gallardo, T.; Tormo, J. R.; Cortes, D. Natural acetogenins from annonaceae, synthesis and mechanisms of action, *Pythochemistry*, **1998**, *48*, 1087-1117.

[5] Saleem, M.; Kim, H.; Ali, M.; Lee, Y. S. An update on bioactive plant lignans, *Nat. Prod. Rep.*, **2005**, *22*, 696-716.

[6] Bhatnagar, I.; Kim, S. K. Marine Antitumor Drugs: Status, Shortfalls and Strategies, *Mar. Drugs*, **2010**, *8*, 2702-2720.

[7] Jackson, K. L.; Henderson, J. A.; Phillips, A. J. The Halichondrins and E7389, *Chem. Rev.*, **2009**, *109*, 3044-3079.

[8] Kobayashi, J., Amphidinolides and Its Related Macrolides from Marine Dinoflagellates, *J. Antibiot.*, **2008**, *61*, 271-284.

[9] Ueda, K.; Hu, Y., Haterumalide B: A new cytotoxic macrolide from an Okinawan ascidian Lissoclinum sp., *Tetrahedron Lett.*, **1999**, *40*, 6305-6308.

[10] Strobel, G.; Li, J.-Y.; Sugawara, F.; Koshino, H.; Harper, J.; Hess, W. M., Oocydin A, a chlorinated macrocyclic lactone with potent anti- oomycete activity from Serratia marcescens, *Microbiology*, **1999**, *145*, 3557-3564.

[11] Challa, V. R.; Kwon, D.; Taron, M.; Fan, H.; Kang, B.; Wilson, D.; Haeckl, F. P. J.; Keerthisinghe, S.; Linington, R. G.; Britton, R., Total synthesis of biselide A, *Chem. Sci.*, **2021**, *12*, 5534-5543.

[12] Bauer, I.; Maranda, L.; Young, K. A.; Shimizu, Y.; Fairchild, C.; Cornell, L.; MacBeth, J.; Huang, S., Isolation and Structure of Caribenolide I, a Highly Potent Antitumor Macrolide from a Cultured Free-Swimming Caribbean Dinoflagellate, Amphidinium sp. S1-36-5, *J. Org. Chem.*, **1995**, *60*, 1084-1086.

[13] a) Jahn, U.; Galano, J.-M.; Durand, T., Beyond Prostaglandins?Chemistry and Biology of Cyclic Oxygenated Metabolites Formed by Free-Radical Pathways from Polyunsaturated Fatty Acids, *Angew. Chem. Int. Ed.*, **2008**, *47*, 5894-5955; b) Sayre, L. M.; Perry, G.; Smith, M., Oxidative Stress and Neurotoxicity, *Chem. Res. Toxicol.*, **2008**, *21*, 172-188; c)

Andersen, J. K., Oxidative stress in neurodegeneration: cause or consequence?, *Nature Med.*, **2004**, *10*, S18-S25; d) Taber, D. F.; Pan, Y.; Zhao, X., A Flexible Enantioselective Synthesis of the Isofurans, *J. Org. Chem.*, **2004**, *69*, 7234-7240; e) Taber, D. F.; Pieming, G.; Li, R., A Divergent Synthesis of the Δ^{13}-9-Isofurans, *J. Org. Chem.*, **2009**, *74*, 5516-5522.

[14] Valli, M.; Bruno, P.; Sbarbada, D.; Porta, A.; Vidari, G.; Zanoni, G., Stereodivergent Strategy for Neurofuran Synthesis via Palladium-Catalyzed Asymmetric Allylic Cyclization: Total Synthesis of 7-*epi*-ST-Δ^8-10-Neurofuran, *J. Org. Chem.*, **2013**, *78*, 5556-5567.

[15] Tsuji, J.; Takahashi, H.; Morikawa, M., Organic syntheses by means of noble metal compounds XVII. Reaction of π-allylpalladium chloride with nucleophiles, *Tetrahedron Lett.*, **1965**, *6*, 4387-4388.

[16] Trost, B. M.; Fullerton, T. J., New synthetic reactions. Allylic alkylation., *J. Am. Chem. Soc.*, **1973**, *95*, 292-294.

[17] a) Kürti, L.; Czakó, B., Strategic Applications of named reactions in Organic Synthesis, *Elsevier*, **2005**, 458-459; b) Evans, L. A.; Fey, N.; Harvey, J. N.; Hose, D.; Lloyd-Jones, G. C.; Murray, P.; Orpen, G.; Osborne, R.; Owen-Smith, G. J. J.; Purdie, M., Counterintuitive Kinetics in Tsuji-Trost Allylation: Ion-Pair Partitioning and Implications for Asymmetric Catalysis, *J. Am. Chem. Soc.*, **2008**, *130*, 14471-14473.

[18] Trost, B. M.; Toste, F. D., Regio- and Enantioslective Allylic Alkylation of Unymmetrical Substrate: A working model., *J. Am. Chem. Soc.*, **1999**, *121*, 4545-4554.

[19] Butts, C. P.; Filali, E.; Lloyd-Jones, G. C.; Norrby, P.-O.; Sale, D. A.; Schramm, Y., Structure-Based Rationale for Selectivity in the Asymmetric Allylic Alkylation of Cycloalkenyl Esters Employing the Trost 'Standard Ligand' (TSL): Isolation, Analysis and Alkylation of the Monomeric form of the Cationic η^3-Cyclohexenyl Complex $[(\eta^3\text{-}c\text{-}C_6H_9)Pd(TSL)]^+$, *J. Am. Chem. Soc.*, **2009**, *131*, 9945-9957.

[20] Trost, B. M.; Van Vranken, D. L., Asymmetric transition metal-catalyzed Allylic Alkylations, *Chem. Rev.*, **1996**, *96*, 395-422.

[21] Tolman, C. A., Olefin complexes of nickel(0). III. Formation constants of (olefin)bis(tri-o-tolyl phosphite)nickel complexes, *J. Am. Chem. Soc.*, **1974**, *96*, 2780-2789.

[22] Maitlis, P. M., The Organic Chemistry of Palladium, *Academic Press*, **1971**, New York.

[23] a) Mackenzie, P. B.; Whelan, J.; Bosnich, B., Asymmetric synthesis. Mechanism of asymmetric catalytic allylation, *J. Am. Chem. Soc.*, **1985**, *107*, 2046-2054; b) Keinan, E.; Sahai, M.; Roth, Z.; Nudelman, A.; Herzig, J., Organotin nucleophiles. 6. Palladium-catalyzed allylic etherification with tin alkoxides, *J. Org. Chem.*, **1985**, *50*, 3558-3566; c) Murahashi,

S. I.; Taniguchi, Y.; Imada, Y.; Tanigawa, Y., Palladium(0)-catalyzed azidation of allyl esters. Selective synthesis of allyl azides, primary allylamines, and related compounds, *J. Org. Chem.*, **1989**, *54*, 3292-3303.

[24] Tatsumi, K.; Hoffmann, R.; Yamamoto, A.; Stille, J. K., Reductive Elimination of d^8-Organotransition Metal Complexes, *Bull. Chem. Soc. Jpn.*, **1981**, *54*, 1857-1867.

[25] a) Gogoll, A.; Ornebro, J.; Grennberg, H.; Backwall, J. E., Mechanism of Apparent ?-Allyl Rotation in (?-Allyl)palladium Complexes with Bidentate Nitrogen Ligands, *J. Am. Chem. Soc.*, **1994**, *16*, 3631-3632; b) Andersson, P. G.; Harden, A.; Tanner, D.; Norby, P. O., Studies of Allylic Substitution Catalysed by a Palladium Complex of a C_2-Symmetric Bis(aziridine): Preparation and NMR Spectroscopic Investigation of a Chiral π-Allyl Species, *Chem. Eur. J.*, **1995**, *1*, 12-16.

[26] Hansson, S.; Norrby, P. O.; Soegren, M. P. T.; Aakermark, B.; Cucciolito, M. A.; Giordano, F.; Vitagliano, A., Effects of phenanthroline type ligands on the dynamic processes of (η^3-allyl)palladium complexes. Molecular structure of (2,9-dimethyl-1,10-phenanthroline)[(1,2,3-η)-3-methyl-2-butenyl]chloropalladium, *Organometallics*, **1993**, *12*, 4940-4948.

[27] Jiang, L.; Burke, S. D., A Novel Route to the F-Ring of Halichondrin B. Diastereoselection in Pd(0)-Mediated *meso* and *C2* Diol Desymmetrization, *Org. Lett.*, **2002**, *4*, 3411-3414.

[28] Arthuis, M.; Beaud, R.; Gandon, V.; Roulland, E., Counteranion-Directed Catalysis in the Tsuji-Trost Reaction: Stereocontrolled Access to 2,5-Disubstituted 3-Hydroxy-Tetrahydrofurans, *Angew. Chem. Int. Ed.*, **2012**, *51*, 10510-10514.

[29] Frisch, M. J.; Trucks, G. W.; Schlegel, H. B.; Scuseria, G. E.; Robb, M. A.; Cheeseman, J. R.; Scalmani, G.; Barone, V.; Mennucci, B.; Petersson, G. A.; Nakatsuji, H.; Caricato, M.; Li, X.; Hratchian, H. P.; Izmaylov, A. F.; Bloino, J.; Zheng, G.; Sonnenberg, J. L.; Hada, M.; Ehara, M.; Toyota, K.; Fukuda, R.; Hasegawa, J.; Ishida, M.; Nakajima, T.; Honda, Y.; Kitao, O.; Nakai, H.; Vreven, T.; Montgomery, J. A., Jr.; Peralta, J. E.; Ogliaro, F.; Bearpark, M.; Heyd, J. J.; Brothers, E.; Kudin, K. N.; Staroverov, V. N.; Keith, T.; Kobayashi, R.; Normand, J.; Raghavachari, K.; Rendell, A.; Burant, J. C.; Iyengar, S. S.; Tomasi, J.; Cossi, M.; Rega, N.; Millam, J. M.; Klene, M.; Knox, J. E.; Cross, J. B.; Bakken, V.; Adamo, C.; Jaramillo, J.; Gomperts, R.; Stratmann, R. E.; Yazyev, O.; Austin, A. J.; Cammi, R.; Pomelli, C.; Ochterski, J. W.; Martin, R. L.; Morokuma, K.; Zakrzewski, V. G.; Voth, G. A.; Salvador, P.; Dannenberg, J. J.; Dapprich, S.; Daniels, A. D.; Farkas, O.; Foresman, J. B.; Ortiz, J. V.; Cioslowski, J.; Fox, D. J. Gaussian 09, Revision B.01; *Gaussian, Inc.*, Wallingford, CT, **2010**.

[30] a) Becke, A. D. Density-functional thermochemistry. III. The role of exact exchange. *J. Chem. Phys.*, **1993**, *98*, 5648-5652; b) Lee, C.; Yang, W.; Parr, R. G. Development of the

Colle-Salvetti correlation-energy formula into a functional of the electron density. *Phys. Rev. B*, **1988**, *37*, 785-789.

[31] (a) Becke, A. D. Density-functional thermochemistry. III. The role of exact exchange. *J. Chem. Phys.*, **1993**, *98*, 5648-5652. (b) Lee, C.; Yang, W.; Parr, R. G. Development of the Colle-Salvetti correlation-energy formula into a functional of the electron density. *Phys. Rev. B*, **1988**, *37*, 785-789; c) Hehre, W. J.; Ditchfield, R.; Pople, J. A. Self-Consistent Molecular-Orbital Methods. IX. An Extended Gaussian-Type Basis for Molecular-Orbital Studies of Organic Molecules. *J. Chem. Phys.*, **1971**, *54*, 724-728; d) Hehre, W. J.; Ditchfield, R.; Pople, J. A. Self-Consistent Molecular Orbital Methods. XII. Further Extensions of Gaussian-Type Basis Sets for Use in Molecular Orbital Studies of Organic Molecules. *J. Chem. Phys.*, **1972**, *56*, 2257-2261; e) Hay, J. P.; Wadt, W. R., Ab initio effective core potentials for molecular calculations. Potentials for K to Au including the outermost core orbitals, J. Chem. Phys., 1985, 82, 299-310; (f) Wadt, W. R.; Hay, P. J. *Ab initio* effective core potentials for molecular calculations. Potentials for main group elements Na to Bi. *J. Chem. Phys.* **1985**, *82*, 284; (g) Hay, P. J.; Wadt, W. R. Ab initio effective core potentials for molecular calculations. Potentials for the transition metal atoms Sc to Hg. *J. Chem. Phys.*, **1985**, *82*, 270.

[32] Zhao, Y.; Truhlar, D. G., The M06 suite of density functionals for main group thermochemistry, thermochemical kinetics, noncovalent interactions, excited states, and transition elements: two new functionals and systematic testing of four M06-class functionals and 12 other functionals, *Theor. Chem. Acc.*, **2008**, *120*, 215-241.

[33] a) Weigend, F.; Ahlrichs, R., Balanced basis sets of split valence, triple zeta valence and quadruple zeta valence quality for H to Rn: Design and assessment of accuracy, *Phys. Chem. Chem. Phys.*, **2005**, *7*, 3297-3305; b) Weigend, F, Accurate Coulomb-fitting basis sets for H to Rn, *Phys. Chem. Chem. Phys.*, **2006**, *8*, 1057-1065.

[34] Grimme, S.; Ehrlich, S.; Goerigk, L., Effect of the damping function in dispersion corrected density functional theory, *J. Comp. Chem.*, **2011**, *32*, 1456-1465.

[35] For SMD solvation model see: Marenich, A. V.; Cramer, C. J.; Truhlar, C. G. Universal solvation model based on solute electron density and a continuum model of the solvent defined by the bulk dielectric constant and atomic surface tensions, *J. Phys. Chem. B*, **2009**, *113*, 6378-6396; for PCM solvation model see: a) (a) Tomasi, J.; Mennucci, B.; Cances, E. The IEF version of the PCM solvation method: An overview of a new method addressed to study molecular solutes at the QM ab initio level. *J. Mol. Struct. Theochem.*, **1999**, *464*, 211-226. (b) Mennucci, B.; Tomasi, J. Continuum solvation models: A new approach to the problem of solute's charge distribution and cavity boundaries. *J. Chem. Phys.*, **1997**, *106*, 5151. (c) Mennucci, B.; Cances, E.; Tomasi, J. Evaluation of Solvent Effects in Isotropic and Anisotropic Dielectrics and in Ionic Solutions with a Unified Integral Equation Method:

Theoretical Bases, Computational Implementation, and Numerical Applications. *J. Phys. Chem. B*, **1997**, *101*, 10506-10517; d) Tomasi, J.; Mennucci, B.; Cammi, R., Quantum mechanical continuum solvation models, *Chem. Rev.*, **2005**, *105*, 2999-3093.

[36] Wang, F.-Y.; Jiao, L., Total Synthesis of (-)-Arborisidine, *Angwe. Chem. Int. Ed.*, **2021**, *60*, 12732-12736.

[37] Trost, B. M.; Krische, M. J.; Radinov, R.; Zanoni, G., On Asymmetric Induction in Allylic Alkylation via Enantiotopic Facial Discrimination, *J. Am. Chem. Soc.*, **1996**, *118*, 6297-6298.

[38] a) Keitz, B. K.; Endo, K.; Patel, P. R.; Herbert, M. B.; Grubbs, R. H., Improved Ruthenium Catalysts for Z-Selective Olefin Metathesis, *J. Am. Chem. Soc.*, **2012**, *134*, 693-699; b) Marx, V. M.; Herbert, M. B.; Keitz, B. K.; Grubbs, R. H., Stereoselective Access to Z and E Macrocycles by Ruthenium-Catalyzed Z-Selective Ring-Closing Metathesis and Ethenolysis, *J. Am. Chem. Soc.*, **2013**, *135*, 94-97; c) Dumas, A.; Tarrieu, R.; Vives, T.; Roisnel, T.; Dorcet, V.; Basl.; Mauduit, M., A Versatile and Highly Z-Selective Olefin Metathesis Ruthenium Catalyst Based on a Readily Accessible N-Heterocyclic Carbene, *ACS Catal.*, **2018**, *8*, 3257-3262.

Chapter 2

Machine-Learning Guided catalyst design

During the second year of PhD, I had the opportunity to join Prof. Fernanda Duarte's Group at University of Oxford. The research field of this group is centered on the computational chemistry in all its meanings: from the physical organic chemistry, to the supramolecular and biomimetic design, as well as biomolecular modelling and non-covalent catalysis. Moreover, alongside with the classical and well-established computational methods, the group focuses its attention also on how integrate with the modern and state of the art computational approaches, like the innovative application of different forms of Artificial Intelligence in the field of synthetical organic chemistry.

This last field is the one I followed during my period there: specifically, I was involved in the project designed by Dr. Stamatia Zavitsanou whose aim was the elaboration of a Machine Learning method to assist the experimental chemist in the catalyst design step. This aspect appears most of the times underestimated and results in the random trial and error approach to identify the best conditions and structure for the catalyst. Even better: in some cases the solution obtained is not the best at all!

The necessity to have a practical and fast strategy that can help the chemist during its experiments without losing time and money in random approaches appears

to be fundamental. For all such reasons we worked together to elaborate a fast and reliable method that can assist the chemist in planning its experiments and helping or at least reducing the investigation area around a specific part of the molecule. To do so, Machine Learning is the first-choice tool because of the possibility to have under control tents or hundreds of data and descriptors that a human cannot physiologically control. Moreover, the classical experimental approach starts most of the times from already known catalyst structures that can be bought or prepared according with the procedures present in the scientific literature. Thanks to the huge capabilities of Machine Learning coupled with data analysis, the already published data constitutes a pool of information from which extract and elaborate a model that "tests" the reaction *in silico* before to be run in the real laboratory. Here summed up are all the reasons why we decided to refer to this approach as a methodology "guided" by the Machine Learning. Thus, before starting with the presentation of the work and the result we got, it is important to have a fast recall on Machine Learning and how data can be treated with a proper analytical method.

2.1 Machine Learning and data analysis

By simply looking at a dictionary, we can define the main field of "Artificial Intelligence" (AI) as the study which models the human mental functions through the use of a computer.[1] Among the different tasks that can be operated by means of AI, one of the cornerstones of AI appears to be the ability of the computer to automatically improve the algorithms through experience. This concept constitutes the basis of Machine Learning (ML) which can thus be defined as the science of getting computers to act without being explicitly programmed.[1]

Machine learning tasks are typically classified into three broad categories, depending on the nature of the "signal" used for learning or the "feedback" available to the learning system. These categories, are:

- *Unsupervised Learning*

- *Supervised Learning*

- *Reinforcement Learning*

The first one represents the ability to detect patterns that can occur in a list of inputs without any type of intervention from the human helping in categorizing them.[2]

The second one is a type of learning where the human has to operate initial categorizations: indeed, it includes both *classification* of data by the human and *numerical regression*.[2],[3] Classification is the first step and is used to determine to which category certain data belong; the numerical regression is the second step, where the machine tries to identify a function that describes the relationships occurring between inputs and outputs. Form this point of view the aim of the ML is trying to learn a function that regulates and correlates the two data set of input and output by predicting also how the output could be affected form variations in the input set.[2],[3]

In the last one, the reinforcement learning, the model interacts with a dynamic environment in which it seeks to achieve a goal by being directed from a "super-user" that only knows if the result provided is correct or wrong.[2] Starting from this negative of positive response, the algorithm can improve its knowledge of the pattern of data and "reinforce" the validity of the prediction. Besides this novel and fascinating part were computers seems act without being controlled by an external person, we have to remember that ML algorithms do not constitute a recent discovery in the field of computer science: the mathematical models which are based on, have been developed over the past 70 years.[4] However, it is only with the powerful computers that has been made available in these last years, that ML algorithms have become available to everyone, including chemists.

Once introduced the three big categories of ML, it is noteworthy to talk about the different types of ML approaches that can be followed. Specifically, by remaining in the field of computational chemistry, different approaches have been used to correlate experimental results and chemical "descriptors". Form this point of view, ML can be seen as a new type of quantitative structure-reactivity relationship (QSRR) method, which starts form a pool of chemical features to extract information capable to describe the molecules and their reactions.[5] The descriptors can

be obtained in the form of one-dimensional (InChI, SMILES, or SELFIES) graphical notation, or chemical descriptors obtained from electronic structure calculations (partial atomic charges, electrostatic potentials, orbital energies, ionization energies and electron affinities, bond orders, and geometrical descriptors at minima and transition states).[5]

With those descriptors in the hands, ML approaches, including multivariate linear regression (MLR), support vector machines (SVMs), decision trees (DTs), random forests (RFs), and neural networks (NNs),[6],[7] have been used to develop quantitative predicting models for the selectivity of the reactions. Before to proceed in the project we investigated, it is important to give also a general explanation for these approaches.

Multivariate Linear Regression (MLR) is a model which tries to find and establish a linear relationship between the dependent variable (e.g. y) and a pool of independent variables (e.g. x_a , x_b , x_c ,...), and it is one of the most used methods to simulate the classical QSRR ones in predicting reaction selectivities and other features like reaction rate or yield.[5] These models have the advantages of being easy to be implemented, robust and readily interpretable, because the function that regulates the relation between the variables can be checked by classical linear interpolation techniques, being the one of a straight line.[5] However, they have also problems and drawbacks that can be summed up in the high sensitivity to outliers (i.e., data values out of the trend followed by the multitude of the others) and multicollinearity, (i.e., where two or more variables are strongly correlated).[5] Sigman and co-workers are one of the pioneers for this Multivariate Linear and Polynomial Regression analysis method to predict reaction selectivity of ketone substrates in the field of organocatalysis (Figure 2.1).[8] Specifically, by using 313 between electronical and sterical descriptors, they were able to elaborate a model on 350 reactions capable of explaining the enantioselectivity induced in the Chiral-Phosphoric-Acids (CPA)-catalyzed nucleophilic additions to imines.[5],[8] They demonstrated the model was able to recognize the importance of steric factors around the imine and categorizing the E vs Z geometry assumed in the transition state (TS). Specifically, the high steric hindrance provided by large substituents on both the catalyst and the imine

favored the imine-TS *E* geometry, while with smaller ones the *Z* form for the TS was found to be preferred.[8] This behavior appears to be identical to the one commonly accepted and elaborated on the classical qualitative origin of enantioselectivity based on the steric bulk.

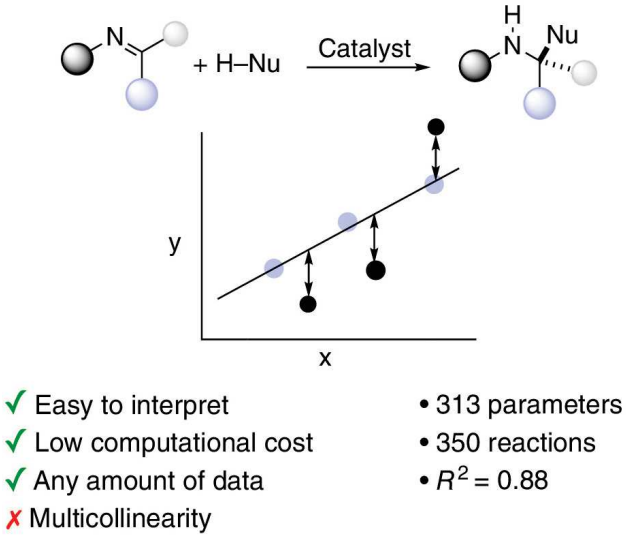

Figure 2.1: *MLR model features and example which shows the data reported by Sigman and co-workers on the prediction in enantioselectivity for the CPA-catalyzed additions to imines.*[5],[8]

The *Support Vector Machines* (SVM) models are another typical approach for ML in computational chemistry to predict enantioselectivities in organocatalytic reactions. Specifically, they are based on a binary approach to the classifiers: given a set of examples for training, each of which is labeled with the class to which the two possible classes belong, an SVM training algorithm builds a model that assigns the new examples to one of the two classes, thus obtaining a linear binary classifier.[2] Thus, an SVM model is a representation of the examples as points in space, mapped in such a way that the examples belonging to the two different categories are clearly separated by as large a space as possible. The new examples are then mapped in the same space and the prediction of the category to which they belong is made on the basis of the side in which it falls.[2] Formally, a support vector machine constructs a hyperplane or set of hyperplanes in a multi-dimensional space, which can be used for classification or regression. Being the separation of categories the

main goal of this approach, a good result can be obtained from the hyperplane that has the greatest distance from the closest point of each of the classes; in general, the greater the margin between these points, the smaller the generalization error made by the classifier.[2] Besides having a low computational cost and a high accuracy, the main drawback of this method relies in the increasing difficulty in visualizing the boundary between classes as the number of descriptors keeps increasing.[5] The pioneer for this ML approach were Denmark *et al.*, which have used SVM to predict enantioselectivity for the nucleophilic addition of thiols to *N*-acyl imines (Figure 2.2).[9] They built the model by using 1075 reactions and 16384 between average steric occupancy descriptors and electronical parameters (then reduced to 2000 after feature selection and principal component analysis).[5] With this model in the hands, they were able to achieve high level of prediction of higher-performing catalysts (over 96.5% *ee* also confirmed experimentally) even by only using previous experimental data near to 80% of *ee*, thus demonstrating the power of the method in predicting new more selective catalysts.

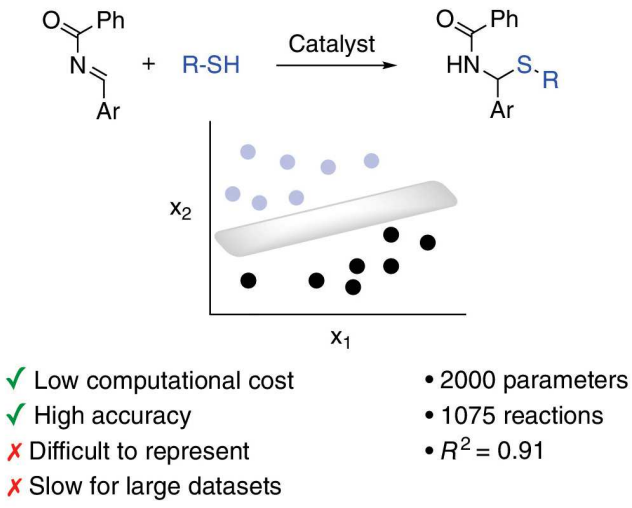

Figure 2.2: *SVM model features and example which shows the data reported by Denmark and co-workers on the prediction in enantioselectivity for the nucleophilic addition of thiols to N-acyl imines.*[5],[9]

Next type of ML approach is based on *Neural Networks* (NNs), where the machine tries reasoning and taking the same sequence of actions which typically occurs in the human brain.[5] This model consists of a group of interconnections made up of

artificial neurons and processes that use a computational connectionism approach. In most cases, an artificial neural network is an adaptive system able to change its structure based on external or internal information which flow through the network itself during the learning phase. The whole process can be divided in the following steps:[5]

- The initial *input layer* receives the descriptors information for the model and passes the information on to the hidden layers
- The *hidden layer* applies a series of transformations to the descriptors by applying an activation function
- Finally, the *output layer* takes the information elaborated by the hidden one and returns the prediction value

Thanks to their ability to process data faster than other approaches and yielding to high accuracy and performances, they are widely used in regression and classification analysis.[5] However, one of their main drawbacks relies on the difficulty of interpreting the output. For such reasons, not so many works are present to these days using NNs. One of them was reported in 2017 by Jensen and co-workers. They used 1055 chemical features to construct a NNs model to predict the output of 15000 reactions by focusing their attention on the main product that should have been obtained, achieving an accuracy of nearly 72% (Figure 2.3).[10] Another example was provided by Sunoj and co-workers, which in 2018 elaborated a NNs model, based on 63 chemical features, to predict the regiochemical output of 66 regioselective difluorination reactions of alkenes by means of catalytical amounts of hypervalent iodine.[11] The accuracy achieved in this second example was increased to 90%.

The most classical way of thinking as a computer is to follow a flowchart regulated by different statements. In the field of ML, if these statements can be summed up as a sequence of "if" or "then" clauses, together with a series of questions that can help in calculating the probability that a certain value belong to a class, we are talking about *Decision Trees* (DTs).[5] Generally, as the tree gets deep, the highest accuracy can be achieved. DT models are easy to understand, but they suffer from overfitting

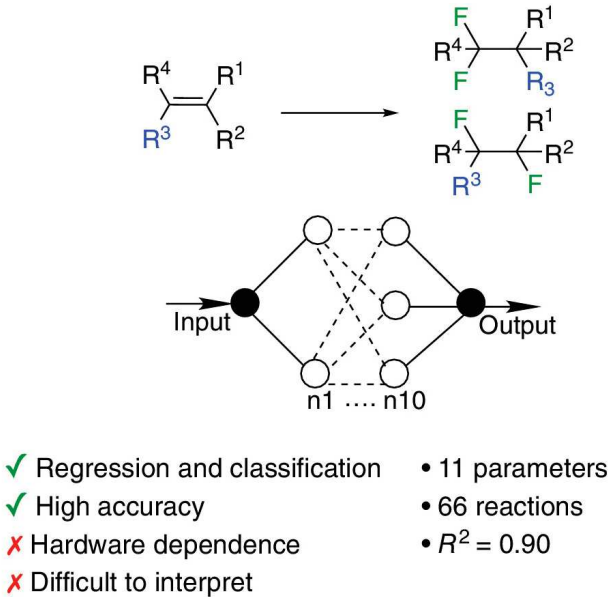

Figure 2.3: *NNs model features and example which shows the data reported by Sunoj and co-workers on the prediction in regioselectivity for the difluorination reactions of alkenes catalyzed by hypervalent iodine.*[5],[11]

due to the rules and specificity that has to be followed by the statements in the model.[5] To overcome this issue, a solution was found in increasing the aggregation between DTs, thus creating what is better known as *Random Forest* (RF).[5] In a RF, each DT operates independently by making its own decisions to achieve a certain degree of prediction. In the end, all the singular predictions are unified together to generate a final collective predictive model.[5] Thus, while the main problem of DTs is intrinsically solved within the RFs, another main problem arises: the computational cost increases as well as the time required to achieve a good training.[5] Two examples can be reported for this type of ML approach. The first one was reported in 2018 by Doyle and co-workers which employed RFs to predict reaction yield in the Buchwald-Hartwig amination reaction.[12] While another recent example was reported in 2020 by Hong and co-workers (Figure 2.4).[13] They elaborated a RF model that predicts the regioselectivity of radical C-H functionalization reactions with an accuracy of 90% by using 50 types of different chemical features for both sterics and electronics for 8580 reactions.[5]

After this general overview a conclusion can be drawn: MLR and SVM are approaches more suitable for small to medium sized datasets, being easily interpretable

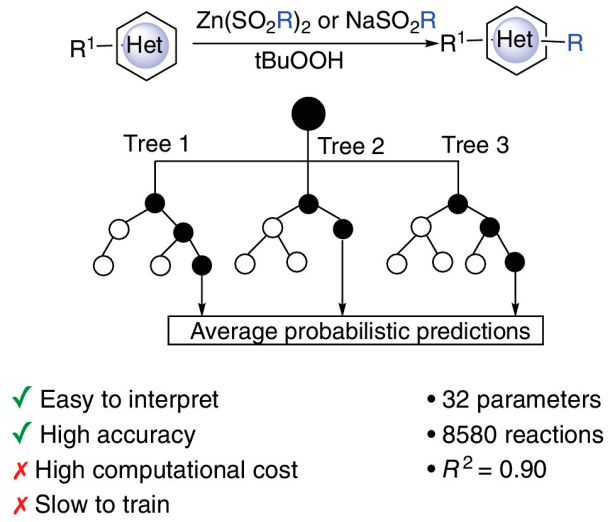

Figure 2.4: *RFs model features and example which shows the data reported by Hong and co-workers on the prediction in regioselectivity of radical C-H functionalization reactions.*[5],[11]

and less prone to overfitting. On the other hand, for large data sets it is better to use approaches like NNs or RFs, because they are more capable in identifying complex patterns in larger amount of data.[5]

Another important observation relies on the way data are split: indeed, three different mutually exclusive subsets are needed for a ML model.[5],[14] The first one is the *training set*, which constitutes the set of data used to train and generate the model. Ideally, the higher the degree of molecular diversity, the larger the range of molecular properties to train the model.[5],[14] The second one is the *validation set*, which constitutes a sort of a "fine-tuning training set" and is used to compare models by estimating the prediction error. It is important to remember that those data are not used during the main training of the model and thus are different from the ones that constitutes the training set.[5],[14] The third one is the *test set*, which is a set of data used once choosen the final model to estimate its prediction error. The most important aspect is that the data belonging to this last set are independent from the ones reported in the previous two and thus are not involved neither in the initial training, neither in its fine tuning.[5],[14]

When the data set is not larger enough to extrapolate and divide data between three different sets, they can be safely split in the only two *training* and *test* sets:

while the *test* set remains the same, the *training* one becomes repeatedly split in other two subset which work as *training* and *validation* sets. This process in better known as *cross-validation* and is particularly suitable for small sized data sets, helping also in controlling and even diminishing problems associated with the overfitting.[5],[14]

Regardless of how a particular model is fitted, the final result can be reported in a graph which represents the observed versus the predicted target properties values. As a standard measure of the quality of the model usually the *coefficient of determination* R^2 is used. However, even if it is one of the most used parameters, not always it constitutes the best choice to evaluate a model.[14] Before to introduce the aspects associated to this choice, lets introduce in a better way the coefficient itself.

The coefficient R^2 is defined as the square of the correlation coefficients (also known as Pearson's r) which relies between the observed and the predicted values in a regression.[14] The most simple and informative formula to define the value of R^2 was suggested by Kvalseth, and is reported in Equation 2.1:

$$R^2 = 1 - \frac{\sum(y_i - \widehat{y})^2}{\sum(y_i - \overline{y})^2}$$

Equation 2.1: *R^2 definition as proposed by Kvalseth.[15]*

where the y_i is the observed variable, $\hat{y}$ is its predicted value and $\overline{y}$ is its mean.[14],[15] The real aim hidden behind the Equation 2.1 is the measure of the size of the residuals derived from the model compared with the size of the residuals from the mean value.[14] Moreover, the numerator in the fraction of Equation 2.1 is the sum of the squared residuals and constitutes the real core of the coefficient R^2: indeed, the better the model, the smaller the residuals.[14] For such reason, the highest the value of R^2, the best is the model: a perfect one should have $R^2 = 1$.[14] Another important parameter is the *Root-Mean-Square Error* (RMSE), which is defined as the square root of the ratio between the squared residuals and the number of observations n (Equation 2.2).[14]

$$RMSE = \sqrt{\frac{1}{n}\sum_{i=1}^{n}(y_i - \widehat{y})^2}$$

Equation 2.2: *RMSE definition.*

Together with R^2, the RMSE should be always added to model since it furnishes the standard deviation of the residuals and constitutes a meaningful measure of the model fit, while R^2 measures how the model fit a specific data set.[14] In this very last sentence is contained the essence of the role of those two model descriptors: the quality of a model generally depends on its overall accuracy and precision and not how a specific data set is successfully explained. This means that RMSE as a measure of the general standard deviation of a model is a better indicator for the model utility, rather than the R^2.[14] This concept can be also better explained by looking directly at Equation 2.1: by augmenting the number of data, the observed values will increase their variation by maintaining the same accuracy. This means that the denominator in the fraction of Equation 2.1 becomes larger and contextually the R^2 increases, but neither the RMSE and thus the practical utility of the model should be affected by the addition of new data points.[14] Figure 2.5 shows exactly what we reported above. The gain in the data range (red triangles) help in increasing the R^2, but practically the usefulness of the method (which is described by the RMSE) is not affected at all, because the distribution of the residuals has been maintained identical.[14]

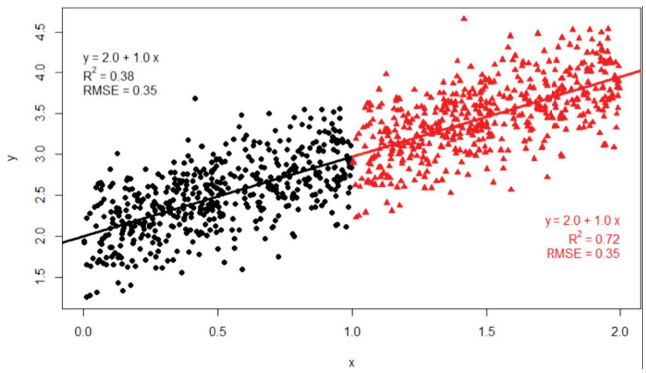

Figure 2.5: *The RMSE of the model is the same in each case, being identical the red and black residuals, but by increasing the data range increases the R^2.*[14]

Thus, as a final conclusion we can assume that even if a model shows low values for R^2 (i.e., at least $R^2 > 0.6$ to assure a proper fit of the data), it could still be useful if the RMSE is low: the user will then decide how low, depending on the situation under examination and the intended use of the model.[14]

2.2 Project idea: a ML tool to guide catalyst design

The aim of this project was elaborated during the years by Dr. Zavitsanou within the Duarte's group with the idea to tackle the long time required for classical trial and error experimental approach, with the alternative provided by computational chemistry in rationally design new catalysts with enhanced reactivity or selectivity. The protocol adopted during the computational workflow focuses its attention on the prediction of the enantiomeric excess (*ee*) of chemical reactions, by employing DFT based descriptors as features in a MLR model. This type of ML approach was chosen thanks to the easy interpretability of the results and due to the fact that not always the dimension of the data set (i.e., the experimental data from which extrapolate the chemical descriptors) is big enough to prefer a different approach. By having in mind this idea, the reactions that have been tested experimentally play the role of a training set for the model. The so obtained model can then be used to give an estimation of the *ee* for reactions that have not yet been investigated experimentally. Additionally, the function extrapolated from the MLR method provides information about the chemical features that directly influence the outcome of the reaction the most, thus giving a specific idea to the experimental chemist where the catalyst could be modified to satisfy a higher request in *ee*. To sum up, the crucial point of this methodology is to guide the design of new reactions.

In the next subsections, a short explanation of the methodology involved in this project, as well as the systems studied, the descriptors used and the ML approach will be examined. For a detailed explanation of the methodology and all the tests done to achieve the best model results, please refer to the PhD thesis of Dr. Zavitsanou.

2.3 Computational workflow and methodology

The main advantage of the protocol elaborated is that multiple steps can be automated so that the test of this methodology can be easily operated on different types of reactions: this not only helps in training the method in the best way, but constitutes a natural benchmark to test the soundness of method itself as a general tool that can be applied to different reactions.

In our studies we tested this method on two different types of reactions: the enantioselective Strecker synthesis of α-aminoacids (Scheme 2.1a),[16] and the Pictet-Spengler cyclization of hydroxylactams (Scheme 2.1b).[17]

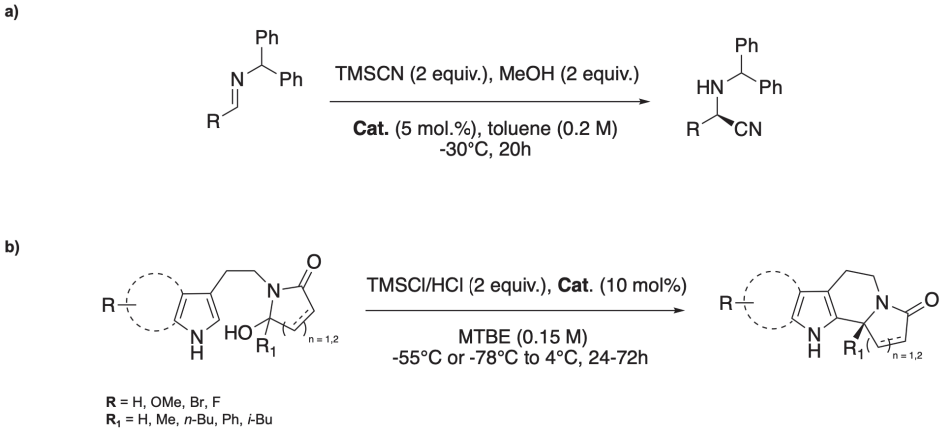

Scheme 2.1: *Reactions under study. a) enantioselective Strecker synthesis of α-aminoacids promoted by thiourea catalysts; b) Pictet-Spengler cyclization promoted by thiourea catalysts.*

All these organocatalyzed reactions will be explained in details in the next sections of this chapter, when they will be directly analyzed in the application of the methodology.

Thus, following the workflow elaborated by Dr. Zavitsanou, the first step is the manual selection of the experimental data directly obtained from the literature papers or from the laboratory notes: indeed, one of the biggest drawbacks in using only published material is due to the natural and diffused manner in publishing preferentially only the best results, while to train in the best way a model it is

fundamental inserting also in the dataset the wrong ones. This helps in reducing the overfitting and also in maintain a good and uniform distribution of the data.

After the data and the reaction has been selected, the second important step is to start retrieving and categorizing data. This is the second manual step and mainly relies in the extraction of the experimental *enantioselectivity* values reported in literature:[16-17] for each reaction *ee* or *e.r.* values are converted to their corresponding $\Delta\Delta G^{\ddagger}$ (kJ/mol) using the following relationship (Equation 2.3):

$$[\Delta\Delta G]^{\ddagger} = -RTln(e.r.)$$

Equation 2.3: *Correlation between* $\Delta\Delta G^{\ddagger}$ *and the enantiomeric ratio (e.r.).*

where *e.r.* is the enantiomeric ratio, T is the temperature (K) at which the reaction was performed, and R is the gas constant (8.3145 J/K mol). The so obtained data will be associated to each corresponding reaction descriptors vector during the ML step.

We then manually prepared the catalyst molecular structures and the substrate ones: we also bound the anions (CN^-, Cl^-) through H-bonds within the urea or thiourea cores.

At this point different models were tested in the years with the aim of getting the best from the chemical descriptors of the molecules. Each of them contains information about the steric effects around the anion (CN^-, Cl^-) as well as the information about the temperature (in °C) and the solvent of each reaction. However, they differ in the type of input used to describe both the substrates and catalyst-anion (CN^-, Cl^-) complexes, and how the conformational flexibility is considered during the calculations. Here we focused the attention on the finally selected and used in our project (i.e., *Model 4*) with the idea of testing and verifying its prediction skills in different chemical reactions. To have a more specific idea regarding all the other models, please refer to the PhD thesis of Dr. Zavitsanou.

We decided to choose *Model 4* as election approach to test our reactions, thanks to a practically identical level of accuracy for the prediction (if compared with most time-consuming *Model 3* and *5*), by contemporarily decreasing a lot the cost of the

computations.

To better sample the conformational space available for these systems and to assure the proper and most populated conformer to be studied, we planned a conformation search by using the opensource *SIMAN* tool associated with the *xTB* software, by specifying the solvents involved in the reaction as well as possible charges already present in the starting materials.[18] The level of theory used in this software relies in the region of the semiempirical extended tight binding [*xTB (GFN2-xTB)*] approach, which is a perfect compromise in terms of chemical space sampling, but shows a limited accuracy for thermochemical properties calculations and thus requires additional higher level calculations.[18] The most stable conformer of the catalyst-anion complex is directly provided as an output by the *xTB* programme and we used its structure directly in the following single-point high-level calculations by using *ORCA v. 4.1* package at PBE-D3BJ/def2-SVP level of theory, by applying the resolution of identity (RI) approximation and an auxiliary basis set (generated using the 'AutoAux' keyword).[19] The parameters and the descriptors extracted from these calculations will be discussed later (Figure 2.6).

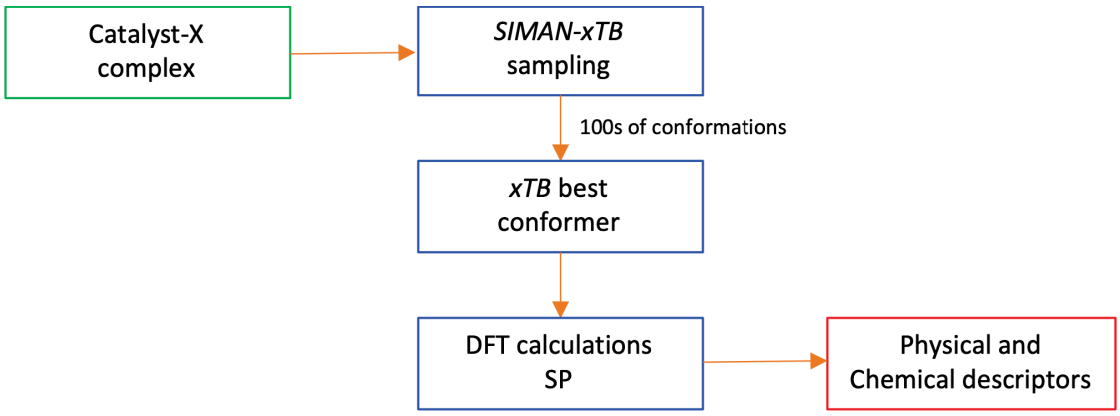

Figure 2.6: *Flowchart which highlights the steps applied to the catalyst-anion complex to get the physical and chemical descriptors.*

For the substrate, once generated the conformers, we selected the singles by excluding the duplicates using another home-made Python script which looks for the RMSD of the coordinates of the atoms in a spatial region of diameter 1.0 Å. The so obtained structures were firstly optimised by using *ORCA v. 4.1* package at PBE-D3BJ/def2-SVP level of theory, with RI approximation and the use of an auxiliary

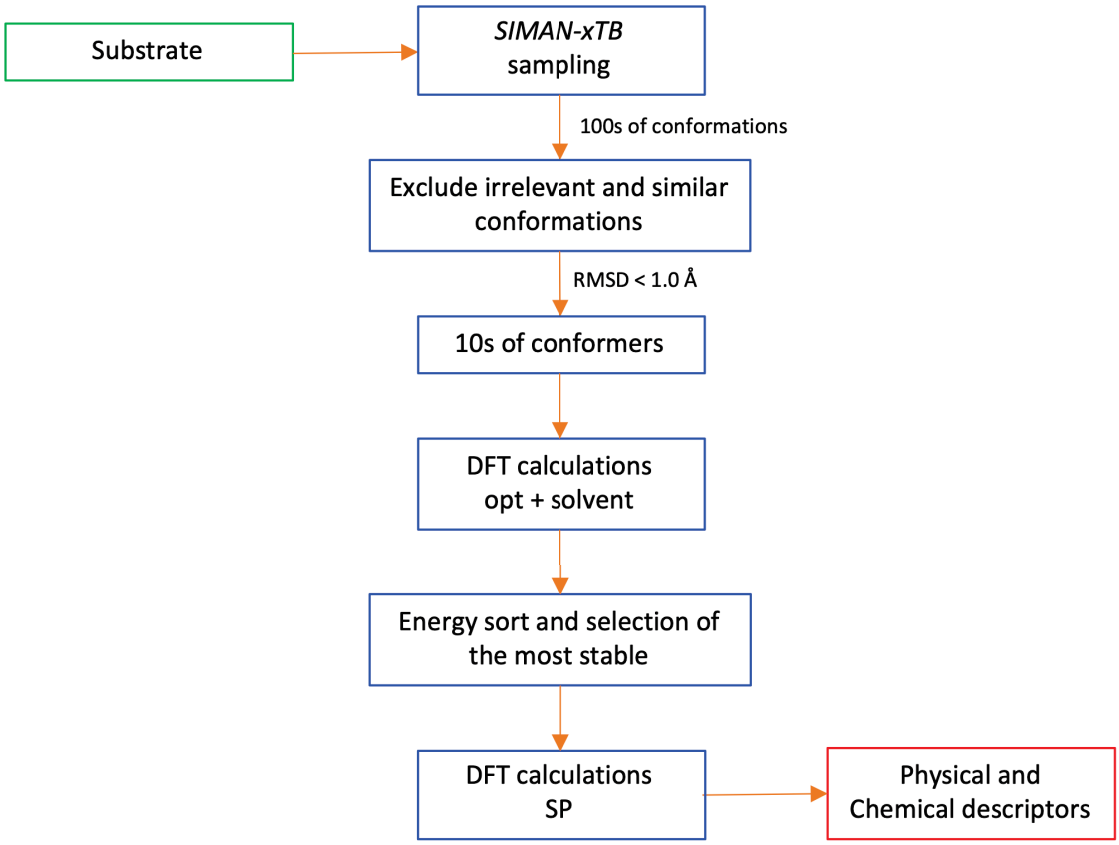

Figure 2.7: *Flowchart which highlights the steps applied to the substate to get the physical and chemical descriptors.*

basis set, but by considering also the role of the solvent with the SMD polarizable continuum solvation model.[19] The so obtained list of optimized substrate molecules in solvent was then sorted in terms of energies and the most stable one was selected as most preferred conformation to run single point calculation and extract the needed chemical descriptors (Figure 2.7).

Now, that the starting structure has been obtained for the catalyst-anion complexes and the substrates, we have to discuss about the chemical descriptors we need to better represent the reactions. *Model 4* relies on specific chemical descriptors capable in giving a detailed evaluation of both the electronic and steric parameters that could influence the reaction. Anyway, a distinction has to be observed for the catalyst-anion complexes and the substrates.

For the complex between catalyst and anion we decided to get the following electronic descriptors: 1) HOMO and LUMO energies (eV), 2) dipole moment ($Debye$),

3) ^{1}H, ^{13}C, ^{35}Cl NMR shielding tensors (*ppm* - GIAO)[20] for the urea or thiourea moiety and the anion, 4) bond order (BO - Mayer)[21] of the hydrogen bonding interaction between the anion and the urea or thiourea hydrogen atoms, BO of the nitrogen-urea/thiourea hydrogen atoms and BO of the nitrogen-urea/thiourea carbon atoms and 6) atomic charges (*e* - Hirshfeld)[22] of the anion and the urea or thiourea hydrogens. As the numbers of atoms may differ between catalyst scaffolds, the number of descriptors varies for each system. To ensure consistency across different catalysts, these descriptors were aligned according to the atoms they represent.

For the substrates we took again as electronic descriptors the HOMO and LUMO energies, as well as the dipole moment and the atomic charges, but we didn't consider the bond orders and the NMR shielding tensors. In Table 2.1 all the descriptors we used are summed up and divided in catalyst-anion complex ones and substrate ones.

Descriptors for ML model	
Catalyst	*Substarte*
HOMO energy (eV)	
LUMO energy (eV)	HOMO energy (eV)
Dipole Moment (Debye)	LUMO energy (eV)
Atomic Charges (e) - *Hirshfeld*	Dipole Moment (Debye)
Bond Orders - *Mayer*	Atomic Charges (e) - *Hirshfeld*
NMR Shielding tensors (ppm) - *GIAO*	Sterimol parameters (Å)
Sterimol parameters (Å)	

Table 2.1: *Different type of electronic and chemical descriptors used for catalyst-anion complexes and substrates.*

Moreover, the specific *Model 4* uses the average values of the NMR shifts (per atom type), the average values of charges (per atom type) and the sum of the values of bond orders (per bond type). This approach ensures the possibility of a full automation of the protocol, because it avoids the need for a manual alignment of the descriptors as reported above.

However, it should be noted that till now we only kept in consideration the chemical descriptors which accounts for the electronic properties of the molecules involved in the reaction. To gain information regarding the sterics and the spatial

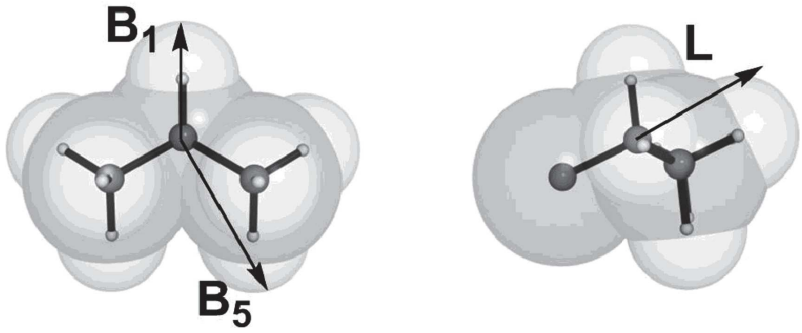

Figure 2.8: *Graphical representation of Sterimol parameters (*B_1*,* B_5*, and* L*).*[23]

encumbrance of the three-dimensional molecules we decided to use the Sterimol parameters.[23] In 2012, Sigman and co-workers introduced Sterimol parameters to construct a Quantitative Structure Activity Relationship (QSAR) between sterics and enantioselectivity. Since then, Sterimol parameters have also been applied in medicinal chemistry and asymmetric catalysis.[23] Sterimol parameters are obtained using Corey-Pauling-Koltun (CPK) molecular models, where the principal axes B_1, B_5, and L can be defined starting from the point of attachment of a given substituent through the van der Waals sphere of the nearby atoms (Figure 2.8).

To better comprehend the nature of those vectors we can define each of them as:

- L is the vector representing the total distance from the point of attachment following the primary axis of attachment (i.e., the total length of the substituent);

- B_1 is the vector which represents the shortest distance perpendicular from the primary axis of attachment (i.e., minimum width of a substituent);

- B_5 vector represents the longest distance starting from the point of attachment (i.e., maximum width of a substituent).

To calculate the B_1, B_5, and L values, we used the automated Python workflow (named Sterimol) developed by Paton and co-workers.[24]

2.4 Machine Learning Method

Now that the methodology and the descriptors has been treated, we have to report on the specific method we used for the ML to investigate the two organocatalytic cases. Again, this method was extensively treated and experimented by Dr. Zavitsanou and here we will report only few aspects of it. For a more detailed discussion, please refer to her PhD thesis.

We already reported on the various approaches that can be implemented in ML and we anticipated our one relies on the MLR, where it is assumed a linear relationship between the dependent variable y (i.e., $\Delta\Delta G^{\ddagger}$) and the independent one x (i.e., the electronical or sterical first-order parameters P_i and their coefficients ρ_i), unless a constant C that takes in count the regression which do not interpolates through the origin (Equation 2.4).

$$[\Delta\Delta G]^{\ddagger} = C + \sum_i \rho_i P_i$$

Equation 2.4: *LR relationship between* $\Delta\Delta G^{\ddagger}$ *and the chemical descriptors.*

However, to make sure that the importance of each descriptor is preserved within the coefficients figures, we applied the mean normalization of the parameters.

We already reported in the previous paragraphs that a good linear correlation (R^2 close to 1.0) between the predicted $\Delta\Delta G^{\ddagger}$ and the measured $\Delta\Delta G^{\ddagger}$ indicates that the obtained model adequately approximates the system under study, but a particular attention has to be paid to the RMSE of both the training and test set. By controlling that the discrepancy between the two appears as lower as possible, together with a general low estimated error, assures another important feature that could help in establishing the usefulness of the method. It is ideal having an RMSE within the one due to the computational methods used (i.e., lower than 2 kcal/mol).

To evaluate the error and to modify and improve the prediction accuracy we choose the least absolute shrinkage and selection operator (*Lasso*), which selects between variables and penalizes the large feature coefficients.

We already talked also about the *cross-validation* as a good choice to reduce overfitting problems in small data sets. In our ML approach, a *100-fold cross-validation* is implemented, thus meaning that the splitting iteration of the dataset in subsets is repeated 100 times, by forming each run random subsets and thus different error in the predictions (RMSE and R^2). By running each model 100 times, we present the average values for the RSME and R^2, for each of them. Specifically, in the random data splitting step, 90% of the data are used as a training set and the other subset contains the remaining 10% of the data as a test set.

Till now we extensively talked about the *overfitting*, but we do not have explained it in detail yet. To understand the origin of the overfitting, we have to recall the way the error is estimated.

Indeed, to estimate the error properly, the number of descriptors should be less than the data points. Vice versa, if the number of descriptors is higher than the data points, the model will be too flexible for the amount of training data: in one word it will overfit the dataset. A general dependence of the model flexibility from the number of the variable can be depicted: the larger the number of variables, the higher the possibility of fitting random fluctuations in the training data that do not represent the true distribution. This problem does not affect only the training of the model, but each time this model will be used to return information regarding a new test set it will result in poor performances. Thus, the idea of employing the above statistical strategies (Lasso, 100-fold cross-validation, validation over unseen data - test set), is an extremely valid choice to reduce the chance of overfitting.

2.5 First dataset: the enantioselective Strecker synthesis of α-aminoacids

Usually, the best dataset is constituted both on data recovered form published literature and from experimental data directly obtained by collaborating with the experimental group. This way of proceeding is the one adopted by Dr. Zavitsanou in her PhD thesis. What if the data can only be recovered from the literature and not

from a pool of experimental tested reactions? We already reported how publishing only the best results is the norm in experimental chemistry. Thus, will the usage of data only taken from literature affect the performances of our method? This is the main question we wanted to address in this part of the thesis.

To prove this, we decided to remain in the field of H-bond organocatalysis by investigating the enantioselective Strecker synthesis of α-aminoacids reaction developed by Jacobsen and co-workers.[16] Since this reaction takes place by an ion-pairing step, therefore served as a useful test to expand the applicability of our approach.

We know very well how α-aminoacids and their derivatives constitutes important building blocks for the synthesis of biologically important moelcules. One of the election reactions to realize them is the Strecker synthesis of α-aminoacids, where an aldehyde is transformed in the corresponding imine to be then involved in a nucleophilic addition promoted by hydrogen cyanide and thus forming the corresponding α-aminonitrile product. The further hydrolytic step provides the formation of the α-aminoacid derivative (Figure 2.9).[16]

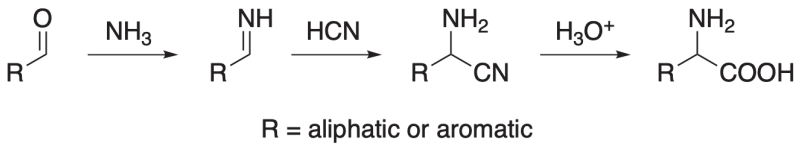

Figure 2.9: *Strecker's synthesis of α-aminoacids*

As in can be easily observed, the reaction stereochemical output cannot be controlled if any kind of asymmetric induction is absent in the system. The possibility to induce a level of enantioselectivity in the final product is highly recommended because it can open the way to a family of unnatural α-aminoacids that cannot be easily synthetized by the simple usage of chemo-enzymatic methods.[16] To solve this problem Jacobsen and co-workers developed an asymmetric synthetical pathway by exploiting the urea and thioureas ability in operating as hydrogen-bond donors by coordinating the cyanide anion and then delivering it on to the imine substrate.[16] Specifically, if the urea/thiourea brings also a chiral information in its structure, then a high level of enantioselectivity can be achieved.

The reaction involves the *in-situ* production of HCN from TMSCN and MeOH, which protonates the imine leading to the formation of a cyanide anion that coordinates to the thiourea moiety. $^{-}$CN then undergoes nucleophilic addition on the iminium cation to form a stereo-defined C-C bond (Figure 2.10).[16b-g] Hydrolysis of the cyanide group leads to the final α-amino acid.[16g] This reaction has been used extensively by Jacobsen and co-workers since the beginning of 2000, with high yields and *ee* values over 98%.[16]

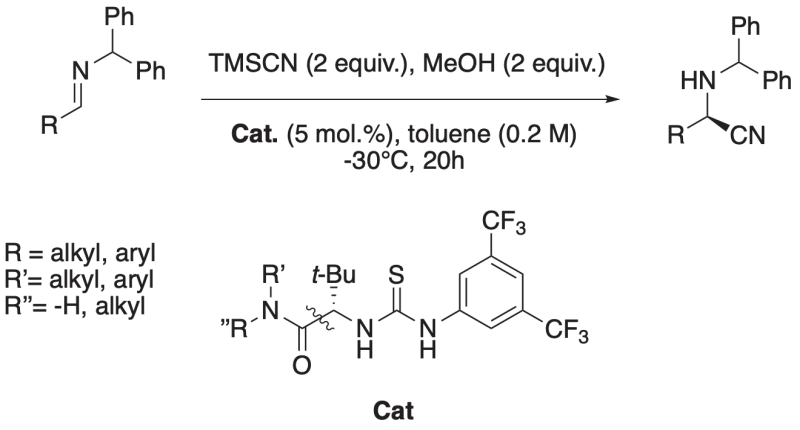

Figure 2.10: *Thiourea-catalysed enantioselective Strecker reaction.*

Authors investigated also the mechanism of this reaction by means of different techniques like Hammett, SAR, isotope labelling and traditional computational studies: all of them underlined a catalyst-bound cyanide-iminium ion pair as well as noncovalent interactions that are the basis for the enantioselectivity.[16b]

Authors computationally evaluated two different pathways: the direct imine activation from the thiourea catalyst and the cyanide or isocyanide binding from the thiourea (Figure 2.11a).[16g] The first one was found to be the less favored due to a huge increase in terms of activation energy in the nucleophilic addition, which resulted 23.2 kcal/mol higher than the second one. Thus, in the favored pathway, a proton transfer from thiourea-bound HCN (or HNC) to imine occurs by generating a catalyst-bound cyanide·iminium ion pair.[16g] Authors also reported that between the cyanide or isocyanide binding, the former one seems to be the most favored during the initial steps of the reaction, while in the crucial reactive one the isocyanide binding form becomes the most stable.[16b] The so formed ion pair undergoes a rear-

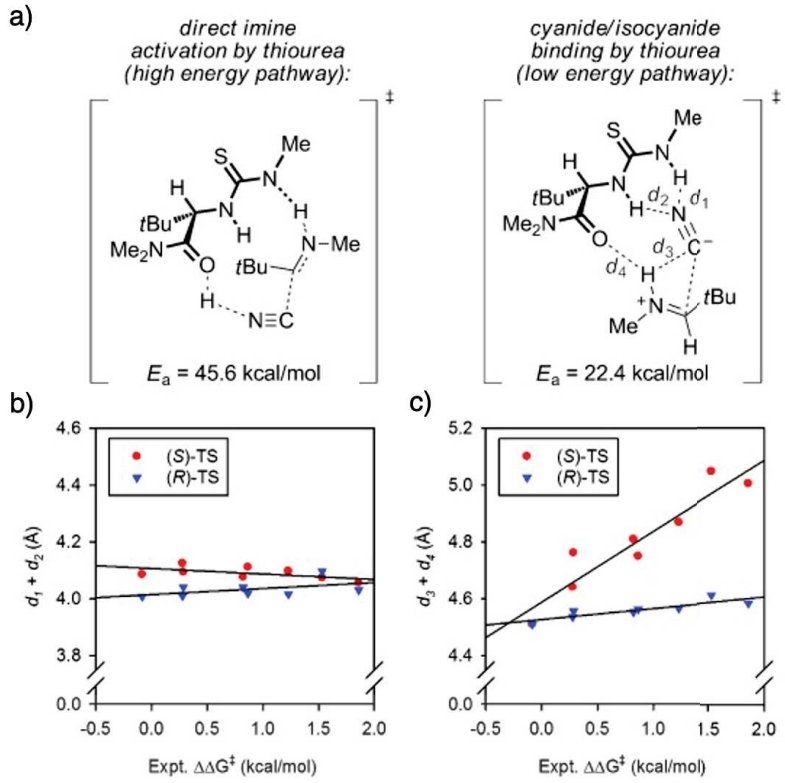

Figure 2.11: *Mechanistic studies to explain the observed enantioselectivity: a) two ways of potential activation mechanism; b) correlation between the sum of thiourea-cyanide bond lengths* (d_1+d_2) *versus enantioselectivity; c) correlation between the bond lengths of hydrogen-bonding interaction of the iminium ion from the cyanide to the carbonyl of the catalyst amide* (d_3+d_4) *versus enantioselectivity.*[16b]

rangement which both controls the rate of the reaction and the final enantioselection. The key separation of the two charged species occurs through the transfer of the hydrogen-bonding interaction of the iminium ion from the cyanide to the carbonyl of the catalyst amide. The subsequent step is a simultaneous stereospecific collapse to the α-aminonitrile product.[16g] This proposed mechanism was validated by comparing the experimental and calculated enantioselectivities for eight different thiourea catalysts, by showing high levels of correlation.[16]

The authors also investigated the basis for enantioselectivity, by looking at relationships between enantioselectivity and various hydrogen-bond lengths in the calculated transition-states structures. When they plotted the sum of the thiourea-cyanide bond lengths (d_1+d_2) versus enantioselectivity, no particular trend was observed (Figure 2.11b), thus showing that the observed enantioselectivity cannot only

rely on the degree of stabilization of the cyanide nucleophile.[16g] When they tried plotting the enantioselectivity against the calculated lengths of the stabilizing hydrogen bonds to the iminium ion N-H from the cyanide anion and amide carbonyl (d_3+d_4), they observed a good positive correlation (Figure 2.11c).[16g] This last one is of particular importance because it means that the enantioselectivity can derive from different stabilization of the iminium cation during the ion pair rearrangement, by highlighting the role of the diastereomeric transition states.[16g]

Now that we gave to the reader a comprehensive review of the chemistry involved in this reaction and of what it is known regulating the selectivity, we can move by reporting our results. With the data extracted from five publications by Jacobsen and co-workers, consisting of 63 substrates and 14 catalysts (a total of 99 experimentally tested reactions),[16] we built a new MLR model. It has to be observed that with our approach we are treating separately the substrates and the catalysts, thus no information can be directly obtained regarding the distances we talked about above. However, we can still get interesting results by observing features deriving from patterns in the data that cannot be extrapolated by considering a classical approach on a single catalyst-substrate adduct.

Based on our previous results, *Model 4* was used to obtain the DFT descriptors, which correlate with selectivity of $R^2 = 0.73$ (RMSE = 1.15 kJ/mol) for the training set and an $R^2 = 0.64$ (RMSE = 1.23 kJ/mol) for the test set (Figure 2.12).

The first analysis involves again the two statistical features we are commonly using: R^2 and RMSE. First of all, the R^2 appears to be quite low, but we have to remember that this feature is also strongly correlated on the number of data used and on their distribution. Indeed, we showed how the addition of data could cause the variation in R^2. For such reason, we have to base our analysis here again on the RMSE, which shows that an error for the MLR model lower than that of the computational methods involved (i.e., 2 kcal/mol $\approx$ 8 kJ/mol). By looking at this feature we can conclude that our model approach is still useful to make prediction on the reactive features provided by our dataset.

By analyzing the important coefficients included in the model as they arise from

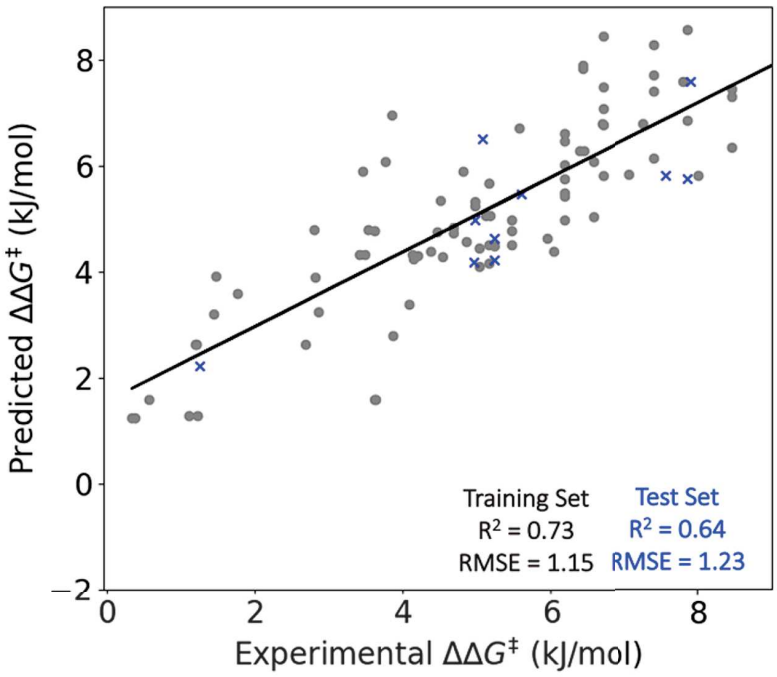

Figure 2.12: *MLR* Model 4 *for α-aminoacid formation dataset. In grey spots, the data points used as training set. In blue crosses, the data points used as test set.*

Lasso, we obtained the following Equation 2.5.

$$\Delta\Delta G^{\ddagger} = 1.95 + 15.25N_1charge_{sub} + 5.52N_8C_9(B_1)_{cat} + 1.55N_8C_9(L)_{cat} + 0.82N_5C_4(B_5)_{cat} + 0.79N_1C_{42}(B_1)_{cat} + 0.61N_1C_0(B_1)_{sub} + 0.33N_1C_2(L)_{sub} + 0.20N_1C_2(B_5)_{sub} - 0.16Dipole_{sub} - 0.36N_1C_0(B_5)_{sub} - 0.46HNMR_{cat} - 0.95N_1C_2(B_1)_{sub} - 4.69CNcharge - 3.21N_8H_{26}(B_1)_{cat} - 30.43Tot(H_{Charge-cat})$$

Equation 2.5: *Linear dependency of the* $\Delta\Delta G^{\ddagger}$ *from the chemical descriptors of the α-aminoacid formation reaction.*

Equation 2.5 identifies the most important chemical descriptors which regulates the observed experimental selectivity and that can be used in the designing process of new catalysts. Descriptors have been separated in those with a positive coefficient (which helps in increasing the selectivity) and those with a negative one (which decrease the selectivity). In Figure 2.13 all the important descriptors are highlighted on the 3D-structure of a model catalyst and substrate.

The data set analysis of the substrate parameters in *Model 4* indicates a larger number of descriptors to be involved in the selectivity. In particular, the charge on the substrate's N_1 contribute the most. This highlights the importance of stabilizing

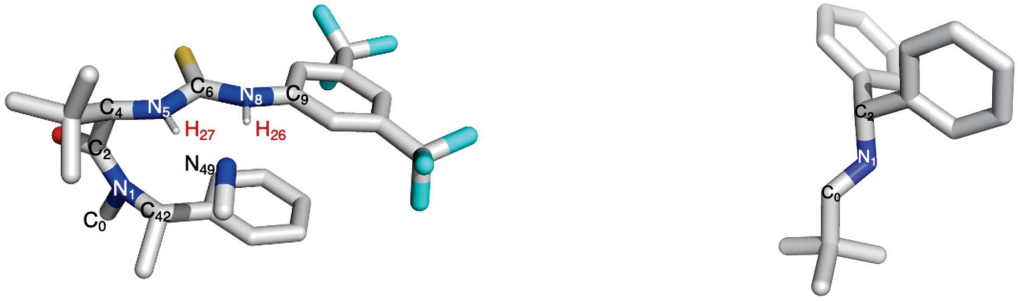

Figure 2.13: *Model 3D-structures of both catalyst and substrate, with the most important descriptors highlighted.*

the iminium ion during the reaction, where electron withdrawing and electron poor groups are present. This also holds for the difference between the aldimine and ketoimines, where aldimines have a lower charge on the nitrogen, therefore reducing their predicted $\Delta\Delta G^{\ddagger}$. The presence of the molecular dipole coefficient, confirms what reported above in the structural and electronic differences of the substrates.

The dependence from the Sterimol factors directly related to the site where the reaction takes place is also important. The presence of $N_1C_0(B_1)_{sub}$ and $N_1C_0(B_5)_{sub}$ distances can be rationalized as a tradeoff between steric bulk being needed for high selectivity, but bulky ketoimines being less reactive and selective due to steric congestion at the reaction center. Distances $N_1C_2(L)_{sub}$, $N_1C_2(B_1)_{sub}$ and $N_1C_2(B_5)_{sub}$ select for groups where steric bulk on the imine protecting group can cause steric congestion. This explains how the sterics onto the substrate play an important role in determining the attack of the nucleophile and in governing the difference in distances reported in the introductory part of this chapter.

On the other side, the steric parameters associated with the catalyst's moieties N_5-C_4, N_1-C_{42}, N_8-C_9 and N_8-H_{26}, play an important role (see Figure 2.13). Indeed, the $N_5C_4(B_5)$ is directly related with the chiral information expressed on carbon C_4 and on the size of the substituent selected on that position. Another important feature is described by the sterical information of $N_1C_{42}(B_1)$ which accounts for the different substitutions on the amidic nitrogen N_1. By moving on the other side of the catalyst structure, we find the sterical information related to the substitutions on the aromatic core enclosed in features $N_8C_9(B_1)$ and $N_8C_9(L)$. The descriptor

$N_8C_9(B_1)$ is also related to the same part of the molecule, by the fact that represents the perpendicular vector to the N_8-H_{26} bond and thus can be directed in the region of the aromatic core.

Moreover, $\Delta\Delta G^{\ddagger}$ is also strongly influenced by the charge on the two thiourea hydrogens, which are directly involved in the coordination of the anion, and the charge on the cyanide ion itself. Those two descriptors show the highest negative coefficients and for such reason a good compromise in the stabilization of the cyanide anion has to be found. Indeed, a possible deprotonation of the catalyst promoted by the anion could result in loose protons H_{26} and H_{27}, and in a corresponding decrease in selectivity. Contemporarily, if the cyanide is not properly coordinated, the high charge on it can induce a similar result. For such reasons, not only the chiral part of the molecule has to be tuned, but also a fine research on the substituents on the thiourea moiety has to be performed in order to setup the perfect electronical conditions. Noteworthy is the average of the hydrogen NMR shielding tensor, which accounts for the change in substituents on the catalyst core. These results agree with the DFT study carried out by Jacobsen *et al.* on the origin of enantioselectivity for this type of reaction.[16b] We already reported at the beginning of the paragraph that they showed a variation in the distances of the iminium cation from the carbonyl moiety of the catalyst and the cyanide ion as the origin of the observed enantioselectivity.[16b-g] This property can also be deduced from our analysis: specifically, from the steric factors related with the amide moiety (i.e., N_5-C_4, N_1-C_{42}). Especially the $N_1C_{42}(B_1)$ is important because depends on the substituents at the nitrogen atom of the amide group. Indeed, the authors conclude that the main influence on the difference in those distances relies on the substitutions on the amide core of the catalyst.[16b-figure18]

Besides all the interesting information reported above, we were not completely satisfied by the low amount of data in the lower region of the chart, which represent the low scoring to 0 *ee* catalyst zone. This was mainly due to the absence of bad results in the published literature we used to set up the model. For such reason we decided to test if the addition of unselective catalyst data could help in giving a better response from the model. To do so, we prepared 5 catalysts with no chiral

centres or with symmetric substitutions on both sides of the thiourea or on the amide group (see the experimental section at the end of the chapter for the full structures). We operated in accordance with some preliminary results obtained from the single paper which reported very few bad results.[16e] Operating in such a way, we included 20 reactions with 0 *ee* (5 catalysts with 4 selected substrates). The new data set obtained by the addition of the new catalysts consists now of 119 reactions, with 63 substrates and 18 catalysts.[16] *Model 4* was again used to obtain the DFT descriptors, which now correlate with selectivity of $R^2 = 0.83$ (RMSE = 1.15 kJ/mol) for the training set and an $R^2 = 0.75$ (RMSE = 1.53 kJ/mol) for the test set (Figure 2.14).

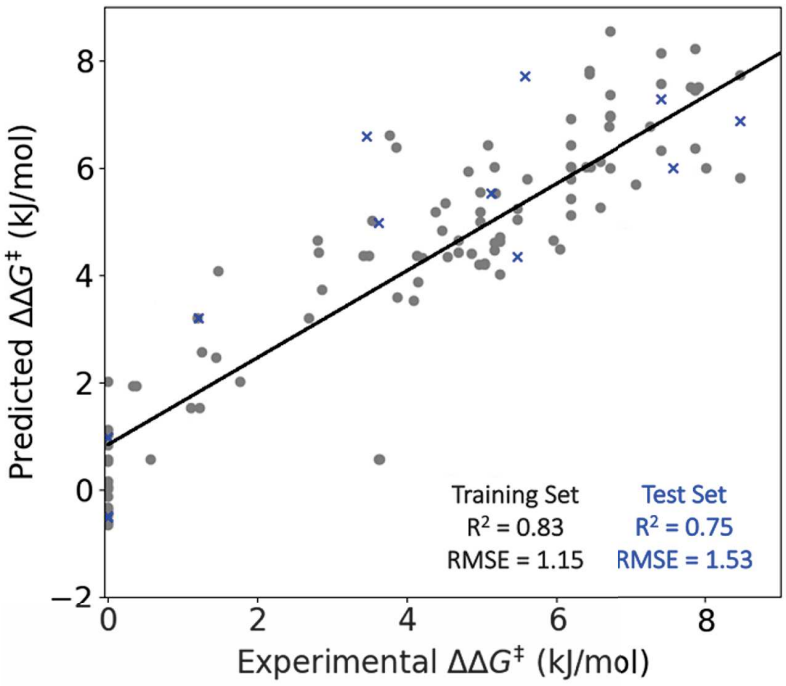

Figure 2.14: *MLR* Model 4 *for α-aminoacid formation dataset including unselective reactions. In grey spots, the data points used as training set. In blue crosses, the data points used as test set.*

As expected, the addition of new data with the aim of populating the lowest region of the chart resulted in an increase of the R^2, but that is not the important fact. Indeed, the fundamental observation that we should do is the practical no variation of the RMSE in both of the sets. This is another big proof that the model approach is useful to make prediction on the data provided by this type of reaction.

By analyzing the important coefficients we now obtained from the model, we can represent the following Equation 2.6.

$$\Delta\Delta G^{\ddagger} = 0.90 + 20.96 N_1 charge_{sub} + 3.29 N_8 C_9(B_1)_{cat} + 1.74 N_1 C_{42}(B_1)_{cat} + 0.58 N_1 C_0(B_1)_{sub} + 0.52 N_5 C_4(L)_{cat} + 0.48 N_5 C_4(B_5)_{cat} + 0.27 N_1 C_2(L)_{sub} + 0.15 N_1 C_2(B_5)_{sub} - 0.16 N_1 C_{42}(L)_{cat} - 0.28 N_1 C_0(B_5)_{sub} - 0.34 N_1 C_0(L)_{cat} - 0.49 HNMR_{cat} - 0.50 N_1 C_2(B_1)_{sub} - 1.88 N_8 H_{26}(B_1)_{cat} - 6.01 CN_{charge}$$

Equation 2.6: *Linear dependency of the* $\Delta\Delta G^{\ddagger}$ *from the chemical descriptors of the* α*-aminoacid formation reaction.*

The important parameters highlighted in Equation 2.6 show again the dependence from the steric parameters associated with the N_1-C_0, the N_1-C_{42}, the N_5-C_4, the N_8-C_9 and the N_8-H_{26} moieties, (Figure 2.13). The charge of the two hydrogens of the thiourea is not present here as an important parameter suggesting its importance may be as a catalyst identifier rather than in the enatiodetermining reaction. Noteworthy is the average of the hydrogen NMR shielding tensor, which depends on the substitutions made on the catalysts and strictly related to C_0, C_4, C_9 and C_{42}. The charge of the cyanide anion is still present with a high and negative coefficient, highlighting the importance to stabilize it in the reaction through H-bonds.

The presence of the coefficients related to the amide core (N_1-C_0 and N_1-C_{42}) are in accordance also in this case with the explanation reported above. Regarding the coefficients related to the substrate, the coefficient of the N_1 charge seems to remain high in value, highlighting the importance of the stabilization provided by the substituents on the N atom and then during the formation of the non-covalent bonds with the catalyst.

In conclusion, the addition of unreactive data shows not only that the RMSE remained practically unvaried, but also that our model is able to predict the output for unselective reactions. Furthermore, the better distribution of $\Delta\Delta G^{\ddagger}$ values lead also to a better correlation. We once again showed, that computationally expensive transition state analysis is not necessary to identify important dependencies between the substrate/catalyst and the reaction outcome. And not only that: by having a general point of view on the molecules, we were able to highlight also different, but

comparable features to those of the classical study (both electronical and sterical) that can be tailored to increase the selectivity of the reaction.

2.6 Second dataset: the enantioselective Pictet-Spengler cyclizations of hydroxylactams

To enlarge further the applicability of our approach, we investigated also its use to predict the reactivity of another thiourea-catalysed asymmetric ion-pairing reaction, again reported by Jacobsen *et al.*[17] In particular, we decided to approach the enantioselective Pictet-Spengler type cyclisation of hydroxylactams, being extremely important in the synthetical preparation of six-membered heterocyclic cores for natural product synthesis.[17]

The Pictet-Spengler reaction involves the cyclization of electron-rich aryl groups onto iminium electrophiles. In its asymmetric variant was firstly developed by Jacobsen and Taylor by the usage of chiral thioureas to catalyze the cyclization of indoles onto *N*-acyliminium ions (Figure 2.15a). By following this procedure, they were also able to efficiently operate the total synthesis of the (+)-yohimbine (Figure 2.15b).[16f]

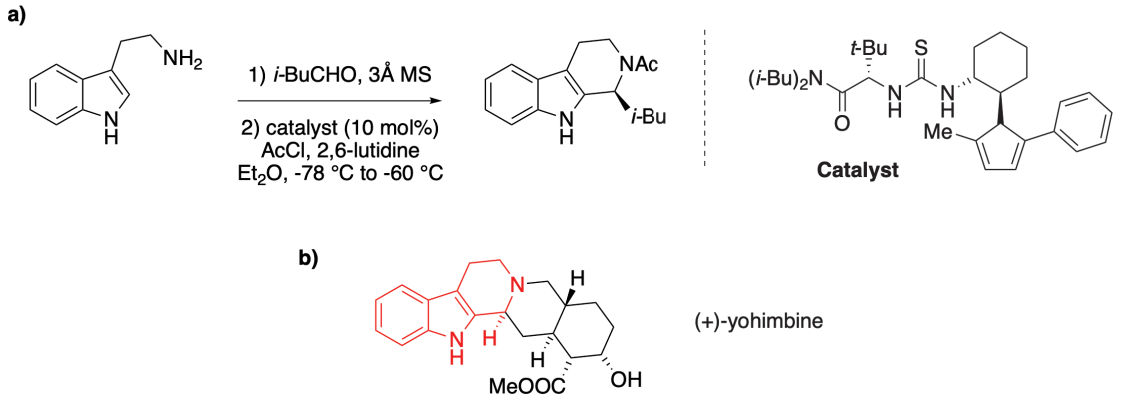

Figure 2.15: *a) Thiourea catalyzed acyl-Pictet-Spengler reaction; b) (+)-yohimbine structure (highlighted in red the core prepared through a Pictet-Spengler reaction.*[16f]

The authors then tried to increase the scope of the reaction by investigating also the possibility of generate *N*-acyliminium ions from the *in-situ* dehydration of

hydroxylactams (Figure 2.16). This reaction resulted particularly important because gave the first idea of the real natural interaction between the substrate and the catalyst.[16f]

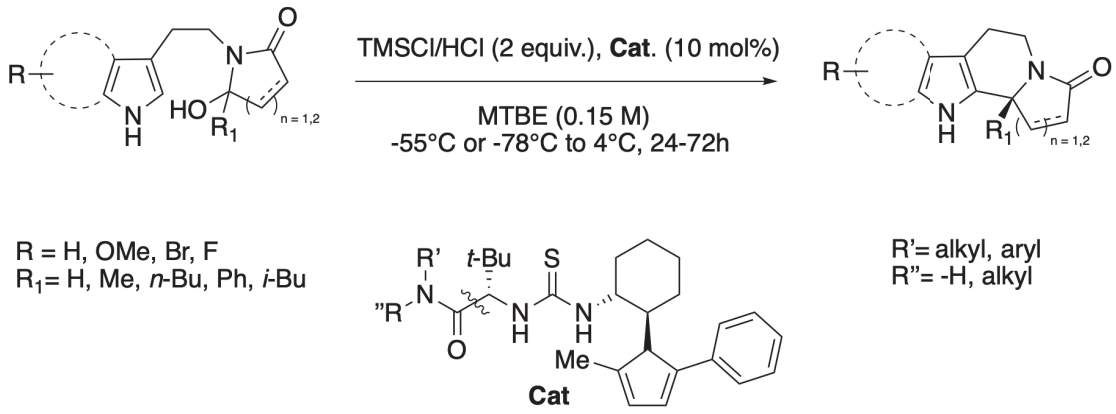

Figure 2.16: *Thiourea-catalysed enantioselective Pictet-Spengler cyclisation of hydroxylactams.*[16f]

Specifically, from NMR studies it was found the role of the dehydrating reagent in the TMSCl or HCl. By following the most clear mechanism which was proposed by Jacobsen and co-workers,[18b] the hydroxylactam undergoes a formal exchange of the alcoholic group with the chloride anion deriving from the HCl or TMSCl, used as *in situ* chlorinating agents. This reaction which lead to the formation of the corresponding chlorolactam was found to be fast and irreversible (Figure 2.17).[18b] After an equilibration where the Cl anion is removed by the catalyst's thiourea moiety, the so formed iminium ion undergoes intramolecular cyclisation being promoted by the nearby indolic/pyrrolic group.[17] The resulting cyclised product then deprotonates and reconstitutes the aromaticity of the system (Figure 2.17).

Hydroxylactam derivatives generated by imide alkylation (R=Me) showed experimentally an increase in reactivity in respect with imide reduction (R=H), thus suggesting that a S_n1-type mechanism is involved in the cyclization step.[16f] However, even if these experiments established the presence of an *N*-acyliminium ion during the reaction pathway, the way the catalyst interacts with the substrate during the enantiodetermining transition state was still undefined. Authors also tried explaining the reactivity by the usage of DFT calculations, but each trial in iden-

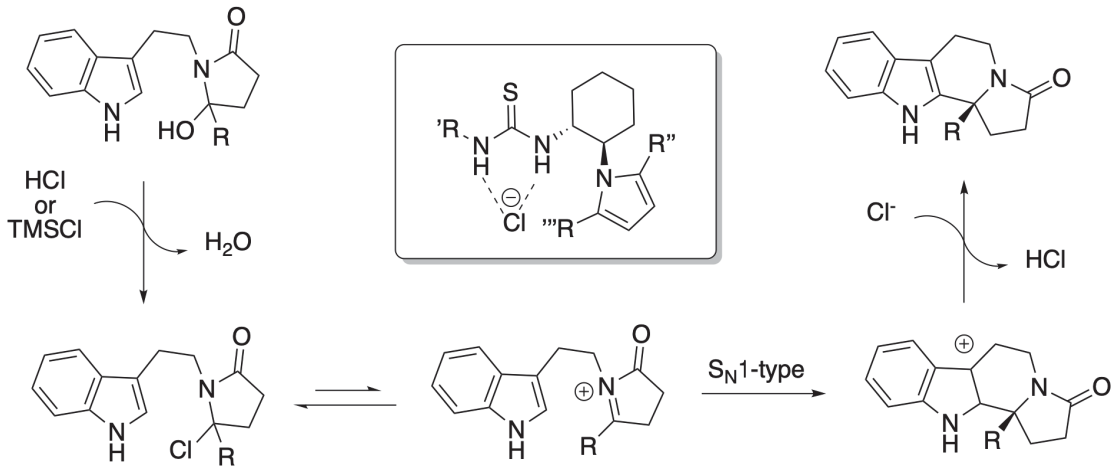

Figure 2.17: *Porposed chlorolactam formation and anion-binding mechanism.*[18b]

tifying the thiourea bound to the *N*-acyliminium ion carbonyl failed.[16f] However, a notable interaction was identified between the thiourea and the α-chloroamide, involving the α-chloro substituent. Therefore it was proposed the enantioselective reaction to occur via an ion pair constituted by the chiral thiourea-bound and *N*-acyliminium chloride.[16f] This specie results from the dissociation of the chloride in α-position induced by the thiourea's proton catalyst. To support the idea of an anion-binding model, the authors highlighted halide counterion effects which increased as the dimension of the anion increased (i.e., Cl, 97% *ee*; Br, 68% *ee*; I, <5% *ee*) together with solvent effects (TBME, 97% *ee*; CH_2Cl_2, <5% *ee*). Moreover, in agreement with the proposed S_n1-type mechanism, a rate acceleration was observed with the increase in substituents at the electrophilic center.[16f]

We reported how classical DFT calculations answered only to few questions about the mechanism involved in the enantio-induction for this reaction. It could thus be useful to see if the generalized approach we developed could provide deep insights on the electronic and sterical features governing this mechanism.

To do so we extracted data from two papers by Jacobsen and co-workers, consisting of 35 substrates and 45 catalysts (a total of 90 experimentally tested reactions),[17] and we built a new MLR model to account for the reaction under examination. Since in our model we are considering the catalyst and substrates as separated entities and the reaction under examination shows a displacement of the chloride from substrate to the catalyst, we decided to adopt a convention in this third case. We both

considered the presence of a chloride anion coordinated on to the catalyst and a chlorine atom linked to the substrate. Thanks to this expedient, we can account for the equilibration that moves the chloride from the substrate to the catalyst: indeed, in a given instant of time after the beginning of the reaction, we will have molecules of catalysts with the anion coordinated, together with molecules of substrate still chlorinated. This situation will evolve in the time after the cyclization occurs, that is when the chloride anion will be lost by the catalyst to provide the basic specie capable in removing the proton after the S_n1 step.

Based on our previous results, *Model 4* was used to obtain the DFT descriptors. The statistical features we obtained correlate with selectivity of R^2= 0.71 (RMSE = 1.20 kJ/mol) for the training set and an R^2=0.55 (RMSE = 1.41 kJ/mol) for the test set (Figure 2.18).

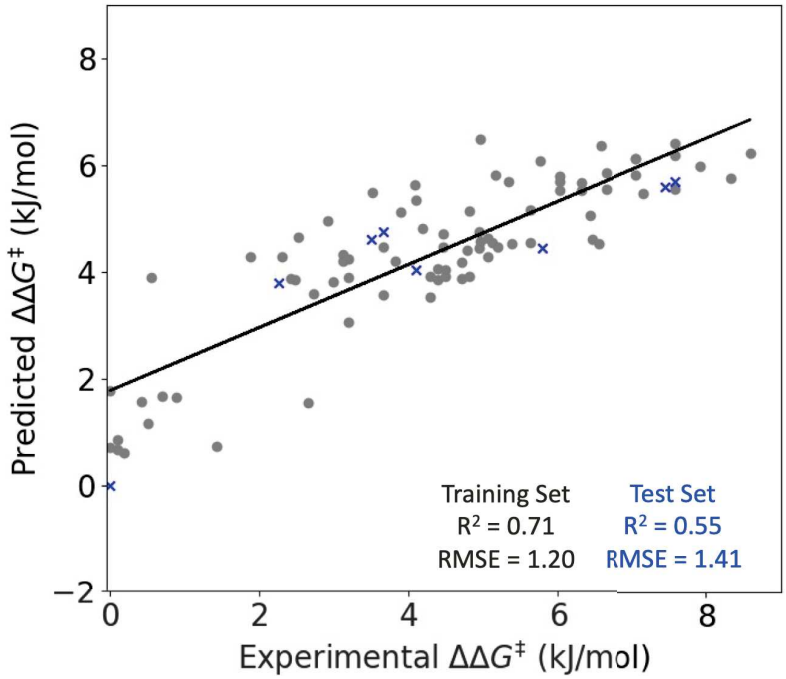

Figure 2.18: *MLR* Model 4 *for Pictet-Spengler cyclisation of hydroxylactams dataset. In blue crosses, the data points used as test set.*

As in the previous case we have to analyze the two statistical features R^2 and RMSE. The R^2 for the test set appears to be lower than what we found for the other case. This can be due to two main reasons: firstly, the number of data used is lower respect with the other one. Furthermore, the reaction shows a different

situation respect with the previous case: here the nucleophile involved in the reaction is already present in the substrate structure, thus showing an intramolecular fashion. This means that the role of the catalyst is not in the delivery of the anion, as we encountered before, but it is merely helping in the removal of the chloride providing a chiral environment during the ion pair formation. For such reason, if we want to use our model approach to make prediction on the reactive features provided by our dataset, we have to establish again our analysis on the RMSE. The error for the MLR model appeared again to be lower than that of the computational methods involved (i.e., 2 kcal/mol $\approx$ 8 kJ/mol), thus prompting to the conclusion that our model approach is still useful to make predictions.

By analyzing the important coefficients we now obtained from the model, we can represent the following Equation 2.7.

$$\Delta\Delta G^{\ddagger} = 1.80 + 195.16 N_2 charge_{sub} + 61.24 C_{19} charge_{sub} + 15.44 N_2 C_{43}(L)_{cat} + 1.02 C_{19} H_{27}(B_1)_{sub} + 0.19 N_{26} C_{52}(B_5)_{cat} + 0.10 N_{26} C_{51}(B_5)_{cat} + 0.08 N_{26} C_{52}(B_1)_{cat} + 0.05 N_2 C_3(L)_{sub} + 0.02 N_9 C_{10}(L)_{cat} - 0.06 N_2 C_{43}(B_1)_{cat} - 1.37 CNMR_{cat} - 0.02 Temp$$

Equation 2.7: *Linear dependency of the $\Delta\Delta G^{\ddagger}$ from the chemical descriptors of the Pictet-Spengler cyclisation of hydroxylactams reaction.*

As for the other case, Equation 2.7 identifies the most important chemical descriptors in regulating the experimental selectivity and shows separately those with a positive coefficient (which helps in increasing the selectivity) and those with a negative one (which decrease the selectivity). In Figure 2.19 all the important descriptors are highlighted on the 3D-structure of a model catalyst and substrate.

The data set analysis of the parameters in *Model 4* shows that the charge on the substrate's N_2 and the indolic/pyrrolic C_{19} contribute the most. These observations are in line with the reactivity observed in the reaction mechanism: the formation of the iminium cation and its interception by the indolic/pyrrolic carbon to give the cyclization highlight the importance of the charge on these two atoms. Noteworthy is the fact that the ML method, even if we did not consider the species as ionic couples, was able to identify the most important atoms to be involved in the cyclization step and the charge modifications associated to them. It is also important

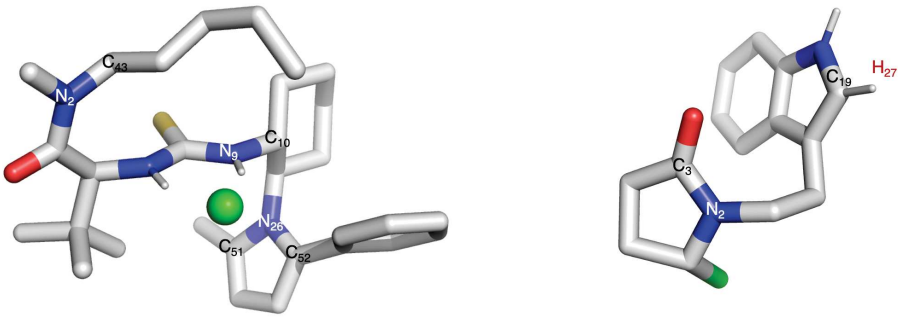

Figure 2.19: *Model 3D-structures of both catalyst and substrate, with the most important descriptors highlighted.*

to highlight that the main reaction step is an intramolecular cyclization and thus the highest electronic coefficients associated with the substrate are in accordance with this aspect.

By remaining on the substrate descriptors, we can identify also the Sterimol parameters for $N_2C_3(L)$ and $C_{19}H_{27}(B_1)$. The first one accounts for the substitutions on the lactam core of the substrate; the second one, representing a steric parameter orthogonal with the bond C-H direction, correlates with the substitutions on the indole/pyrrole and highlights also the presence of protecting groups on the nearby nitrogen atom (i.e., TIPS groups).

While the descriptors for the substrates all showed a positive coefficient, the ones of the catalyst presented a more variegate situation. The highest value is now showed by the Sterimol parameter $N_2C_{43}(L)$, which is directly related with the dimensions of the substituents on the nitrogen atom of the amide. This result is of particular importance because suggest a similar situation with the one observed in the Strecker reaction. Indeed, also here the importance of the substituents on the amide moiety is fundamental in defining the chiral space that will induce the selectivity in getting the reaction product. On the same bond region, but with a small negative coefficient value, there is also the $N_2C_{43}(B_1)$ which depends on the substituents on the other carbon atom linked to the same amidic nitrogen. The descriptor $N_9C_{10}(L)$ accounts for the substitutions on the other side of the molecule, which involve different moieties on the cyclohexyl core. Of particular interest are the three descriptors on the N_{26}-C_{51} and N_{26}-C_{52}, because they are in strict correlation with the substitutions

placed on the pyrrole core. This last information is of particular importance because our method spontaneously highlighted the two most relevant part of the molecule involved in defining the chiral space around the catalyst: the amidic core and the pyrrole with its substituents on the cyclohexyl one. This suggest that a fine tune of the substituents of these two regions of the molecule will have a dramatic influence on the stereochemical outcome. By looking back to the work done by the authors, it is easily understandable that precisely these two parts of the catalyst molecule were extensively studied with a trial-and-error approach to get the highest performing one.[17]

Lastly, we have to highlight the presence of a negative coefficient for the carbon NMR shielding tensor, which represents the change in substituents on the catalyst core and the temperature, which was found to have a negative effect on the enantioinduction as it increases.

In conclusion, we already said that this reaction appears different in respect with the previous one, because it is an intramolecular reaction where the anion is not delivered from the catalyst to the substrate. Thus, not being the catalyst directly involved in delivering the anion, it acts simply by preparing a chiral environment around the substrate, where the intramolecular reaction takes place. However, the novelty of our approach provided a new insight in the way the asymmetry is transferred, which was not reported with the previous computational studies. Indeed, the presence of the same descriptors related to the amide core, like the ones of the Strecker's reaction, suggest that a similar mechanism of interactions between the amide, the chloride and the iminium-cation intermediate, could be active also in this case.

2.7 Conclusions

In this chapter, we reported the results we obtained through the application of a new computational workflow designed by Dr. Zavitsanou to predict and design new catalytic structures. The protocol is automated and easy to follow, and it allows for the rapid identification of the important parameters (electronic and steric) which

govern and regulate the stereochemical output of the reaction, helping chemists in the guided design of new effective catalysts. It has been tested on two different models of H-bond catalyzed reaction.

The application of the model to the enantioselective Strecker synthesis of α-aminoacids showed that different descriptors were more relevant in determining *ee*. Specifically, we were able to identify the same chemical relationships highlighted by the authors during the classical computational studies, but in a newer and faster way. Our computational workflow can thus accurately predict the *ee* of reactions and give reliable feedback to the chemists, allowing them to design the next steps of their experiments based on a mathematical model.

By investigating the Pictet-Spengler cyclisation of hydroxylactams, we found similar features to the ones observed in the Strecker case. This result can be useful in concluding that this last reaction, even if very different in terms of chemical behavior if compared with previous one, could be regulated by a similar mechanism of interactions between the two reactants, which differentiates the two pathways to the stereodefined product.

References

[1] Definitions from *Collins Dictionary* and *Stanford University*.

[2] Russell, S.; Norvig, P., Artificial Intelligence: A Modern Approach (2nd ed.). **2003**, Prentice Hall.

[3] Poole, D.; Mackworth, A.; Goebel, R., Computational Intelligence: A Logical Approach. **1998**, New York: Oxford University Press, 397-439.

[4] a) Samuel, A. L., Eight-move opening utilizing generalization learning. **1959**, *IBM J.* 3, 210-229; b) Kohavi & Ron. Glossary of terms. Spec. Issue Appl. Mach. Learn. Knowl. Discov. Process, **1998**, *30*, 127-132; c) Yadav, N.; Yadav, A.; Kumar, M.; An Introduction to Neural Network Methods for Differential Equations. *SpringerBriefs Appl. Sci. Technol.*, **2015**, *16*, 13-15; d) Nilsson, N.J., Learning machines, **1965**, McGrawHill: New York; e) Duda, R. O.; Hart, P. E.; Stork, D. G., Pattern Classiication and Scene Analysis 2nd ed. Part 1: Pattern Classification., **2000**, Wiley: New York; f) Harnad, S., The Annotation Game: On Turing (1950) on Computing, Machinery, and Intelligence., **2008**, Springer.

[5] Sterling, A. J.; Zavitsanou, M.; Ford, J.; Duarte, F., Selectivity in organocatalysis-From qualitative to quantitative predictive models., *WIREs Comput. Mol. Sci.*, **2021**, e1518.

[6] Shalev-Shwartz, S.; Ben-David, S., Understanding machine learning: from theory to algorithms. Vol XVI., **2014**, Cambridge University Press:New York.

[7] Elton, D. C.; Boukouvalas, Z.; Fuge, M. D.; Chung, P. W., Deep learning for molecular design-a review of the state of the art., *Mol. Syst. Design Eng.*, **2019**, *4*, 828-849.

[8] a) Santiago, C. B.; Guo, J. Y.; Sigman, M. S., Predictive and mechanistic multivariate linear regression models for reaction development., *Chem. Sci.*, **2018**, *9*, 2398-2412; b) Reid, J. P.; Sigman, M. S., Holistic prediction of enantioselectivity in asymmetric catalysis., *Nature*, **2019**, *571*, 343-348; c) Milo, A.; Neel, A. J.; Dean Toste, F.; Sigman, M. S., A data-intensive approach to mechanistic elucidation applied to chiral anion catalysis., *Science*, **2015**, *347*, 737-743; d) Milo, A.; Bess, E.; Sigman, M. S., Interrogating selectivity in catalysis using molecular vibrations., *Nature*, **2014**, *507*, 210-214; e) Bess, E. N.; Bischoff, A. J.; Sigman, M. S.; Jacobsen, E. N., Designer substrate library for quantitative, predictive modeling of reaction performance., *Proc. Natl. Acad. Sci. U. S. A.*, **2014**, *111*, 14698-14703.

[9] a) Zahrt, A. F.; Henle, J. J.; Rose, B. T.; Wang, Y.; Darrow, W. T.; Denmark, S. E., Prediction of higher-selectivity catalysts by computer-driven workflow and machine learning., *Science*, **2019**, *363*, eaau5631; b) Zahrt, A.; Denmark, S. E., Evaluating continuous chirality measure as a 3D descriptor in chemoinformatics applied to asymmetric catalysis., *Tetrahedron*, **2019**, *13*, 1841-1851.

[10] Coley, C. W.; Barzilay, R.; Jaakkola, T. S.; Green, W. H.; Jensen, K. F., Prediction of organic reaction outcomes using machine learning., *ACS Central Sci.*, **2017**, *3*, 434-443.

[11] Banerjee, S.; Sreenithya, A.; Sunoj, R. B., Machine learning for predicting product distributions in catalytic regioselective reactions., *Phys Chem Chem Phys.*, **2018**, *20*, 18311-18318.

[12] Ahneman, D. T.; Estrada, J. G.; Lin, S.; Dreher, S. D.; Doyle, A. G., Predicting reaction performance in C-N cross-coupling using machine learning., *Science*, **2018**, *360*, 186-190.

[13] Li, X.; Zhang, S.-Q.; Xu, L.-C.; Hong X., Predicting regioselectivity in radical C-H functionalization of heterocycles through machine learning., *Angew. Chem. Int. Ed.*, **2020**, *59*, 13253-13259.

[14] Alexander, D. L. J.; Tropsha, A.; Winkler, D. A., Beware of R2: Simple, Unambiguos Assessment of the Prediction Accuracy of QSAR and QSPR Models., *J. Chem. Inf. Model*, **2015**, *55*, 1316-1322.

[15] Kvalseth, T. O., Cautionary Note about R^2, *Am. Stat.*, **1985**, *39*, 279-285.

[16] a) Vachal, P., Jacobsen, E. N., Enantioselective Catalytic Addition of HCN to Ketoimines. Catalytic Synthesis of Quaternary Amino Acids, *Org. Lett.*, **2000**, *6*, 867-870; b) Zuend, S. J., Jacobsen, E. N., Mechanism of Amido-Thiourea Catalyzed Enantioselectiv Imine Hydrocyanation: Transition State Stabilization via Multiple Non-Covalent Interactions, *J. Am. Chem. Soc.*, **2009**, *131*, 15358-15374; c) Sigman, M. S., Jacobsen, E. N., Schiff Base Catalysts for the Asymmetric Strecker Reaction Identified and Optimized from Parallel Synthetic Libraries, *J. Am. Chem. Soc.*, **1998**, *120*, 4901-4902; d) Sigman, M. S.; Zuend, S. J.; Jacobsen, E. N., A General Catalyst for the Asymmetric Strecker Reaction, *Angew. Chem. Int. Ed.*, **2000**, *39*, 1279-1281; e) Pan, S. C.; List, B., The Catalytic Acylcyanation of Imines, *Chem. Asian J.*, **2008**, *3*, 430-437; f) Brak, K., Jacobsen, E. N., Asymmetric Ion-Pairing Catalysis., *Angew. Chem. Int. Ed.*, **2013**, *52*, 534-561; g) Zuend, S. J., Coughlin, M. P., Lalonde, M. P., Jacobsen, E. N., Scaleable catalytic asymmetric Strecker syntheses of unnatural ?-amino acids, *Nature*, **2009**, *461*, 968-971.

[17] a) Raheem, I. T.; Thiara, P. S.; Peterson, E. A.; Jacobsen, E. N., Enantioselective Pictet-Spengler-Type Cyclizations of Hydroxylactams: H-Bond Donor Catalysis by Anion Binding, *J. Am. Chem. Soc.*, **2007**, *129*, 13404-13405; b) Raheem, I. T.; Thiara, P. S.; Jacobsen, E. N., Regio- and Enantioselective Catalytic Cyclisation of Pyrroles onto N-Acyliminium Ions, *Org. Lett.*, **2008**, *10*, 1577-1580.

[18] a) Grimme, S.; Neese, F., Fully Automated Quantum-Chemistry-Based Computation of Spin-Spin-Coupled Nuclear Magnetic Resonance Spectra, *Angew. Chem. Int. Ed.*, **2017**, *56*, 14763-14769; b) Bannwarth, C.; Ehlert, S.; Grimme, S., GFN2-xTB-An Accurate and Broadly Parametrized Self-Consistent Tight-Binding Quantum Chemical Method with Multipole Electrostatics and Density-Dependent Dispersion Contributions, *J. Chem. Theory Comput.*, **2019**, *15*, 1652-1671; c) Pracht, P.; Bohle, F.; Grimme, S., Automated exploration of the low-energy chemical space with fast quantum chemical methods, *Phys. Chem. Chem. Phys.*, **2020**, *22*, 7169-7192.

[19] a) Neese, F.; Wennmohs, F.; Becker, U.; Riplinger, C., The ORCA quantum chemistry program package, *J. Chem. Phys.*, **2020**, *152*, 224108; b) for the PBE functional see: (i) Perdew, J. P.; Burke, K.; Ernzerhof, M., Generalized gradient approximation made simple, *Phys. Rev. Lett.*, **1996**, *77*, 3865-3868; (ii) Perdew, J. P.; Burke, K.; Ernzerhof, M., Errata: Generalized gradient approximation made simple, *Phys. Rev. Lett.*, **1997**, *78*, 1396; c) for the D3BJ empirical dispersions see: Grimme, S.; Ehrlich, S.; Goerigk, L., Effect of the damping function in dispersion corrected density functional theory, *J. Comp. Chem.*, **2011**, *32*, 1456-1465; d) for the def2-SVP basis set see: (i) Weigend, F.; Ahlrichs, R., Balanced basis sets of split valence, triple zeta valence and quadruple zeta valence quality for H to Rn: Design and assessment of accuracy, *Phys. Chem. Chem. Phys.*, **2005**, *7*, 3297-305; (ii) Weigend, F., Accurate Coulomb-fitting basis sets for H to Rn, *Phys. Chem. Chem. Phys.*, **2006**, *8*,

1057-65; e) for the RI and AutoAux approximatons please refer to the Orca manual 4.1.0 or the Orca Input Library (https://sites.google.com/site/orcainputlibrary/).

[20] a) London, F., The quantic theory of inter-atomic currents in aromatic combinations, *J. Phys. Radium*, **1937**, *8*, 397-409; b) McWeeny, R., Perturbation Theory for Fock-Dirac Density Matrix, *Phys. Rev.*, **1962**, *126*, 1028; c) Ditchfield, R., Self-consistent perturbation theory of diamagnetism. 1. Gauge-invariant LCAO method for N.M.R. chemical shifts, *Mol. Phys.*, **1974**, *27*, 789-807; d) Wolinski, K.; Hilton, J. F.; Pulay, P., Efficient Implementation of the Gauge-Independent Atomic Orbital Method for NMR Chemical Shift Calculations, *J. Am. Chem. Soc.*, **1990**, *112*, 8251-8260; e) Cheeseman, J. R.; Trucks, G. W.; Keith, T. A.; Frisch, M. J., A Comparison of Models for Calculating Nuclear Magnetic Resonance Shielding Tensors, *J. Chem. Phys.*, **1996**, *104*, 5497-5509.

[21] Mayer, I., Bond order and valence indices: A personal account, *J. Comput. Chem.*, **2007**, *28*, 204-221.

[22] Hirshfeld, F. L., Bonded-Atom Fragments for Describing Molecular Charge Densities, *Theoret. Chim. Acta*, **1977**, *44*, 129-138.

[23] a) Harper, K. C.; Bess, E. N.; Sigman, M. S., Multidimensional steric parameters in the analysis of asymmetric catalytic reactions, *Nature Chemistry*, **2012**, *4*, 366-374; b) Brethomé, A. V.; Fletcher, S. P.; Paton, R. S., Conformational Effects on Physical-Organic Descriptors: The Case of Sterimol Steric Parameters, *ACS Catal.*, **2019**, *9*, 2313-2323.

[24] Sterimol: GitHub repository; https://github.com/bobbypaton/Sterimol

Chapter 3

Ligand exchange on Titanocene complexes: a computational study towards easy and fast way to biotarget compounds

In the last decades, an increasing number of people are affected by some form of cancer. The typical ways to treat these health problems are surgeries, radiotherapy or the subministrations of specific drugs.

Nowadays, amongst the wide number of drugs used, the most common are *cis*-platin [*cis*-diamminedichloroplatinum(II)] or 5-fluorouracil and their derivatives. These drugs, as for all the compounds used in this type of treatment, present some problems due to their widespread aggression against not only cancer, but also the whole body. Furthermore, Platinum derivatives are inefficient against Platinum-resistant tumour.[16] As an additional drawback, the target of these drugs is said to be "ubiquitous", but we generally accept that the main interaction is between Platinum anticancer drug and DNA.[17]

For all these reasons, the need of alternative, more selective and more efficient drugs is essential.[1]

Recently, *organometallic compounds* - metal complexes in which there is at least

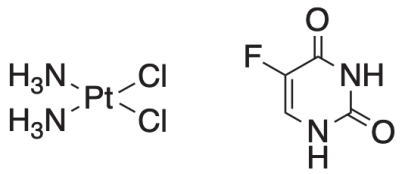

Figure 3.1: *Chemical structures of cis-platin (left) and 5-fluorouracil (right).*

one direct metal-carbon bond - have been found to be excellent candidates as anticancer drugs.[1] These molecules could present a broad structural variety, passing from linear to octahedral ones.[1] As additional advantages, these compounds show a different stereochemistry compared to organic compounds and the possibility to change ligand design whatever we want provide us the control over specific kinetic properties.[1] They are also kinetically stable, uncharged, quite lipophilic and with the metal in a low oxidation state. For all these reasons, they offer wide opportunities in novel classes of medicinal compounds design.[1] As an example, all the organometallics used for catalysis or in synthetic chemistry - metallocenes, half-sandwich, carbene-, CO-, or π-ligands - have recently found an important application in medicinal chemistry.[1] Organometallic chemists collaborate in these branch of studies with biochemists, biologist and medicinal chemists, by employing all the knowledge of modern biomedical research: with new instruments like computer-aided design they can also deeply understand why a cell could be a possible target and how the molecule studied could interact with the target inside the cell.[1]

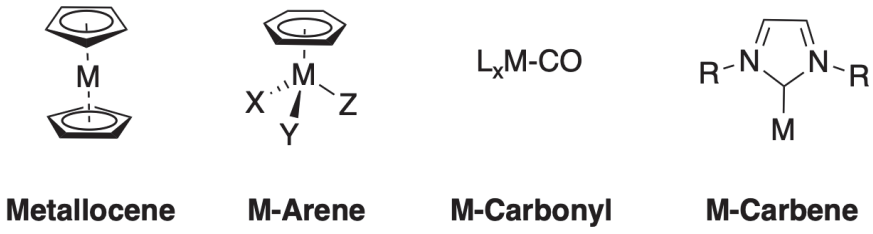

Figure 3.2: *Typical classes of organometallic compounds in medicinal chemistry.*[1]

With all this information, we decided to focus our research on Titanium derived organometallics, paying particular attention on Titanocene derivatives.

3.1 Titanium: a wonderful element

Titanium, discovered for the first time by Gregor in 1791, is the 22nd element inside the periodic table of elements and it presents an atomic weigh of 47.867 g/mol. It can have valence number of 2, 3 or 4 and the preferred coordination number is 6. Natural Titanium consist of five isotopes which present atomic masses from 46 to 50, all perfectly stable, but the 48 is the most abundant one. Additionally, there are also eighteen unstable isotopes. Its name comes from the Latin mythological figure of *Titans*, Earth's first son. In its pure form, Titanium was prepared by heating $TiCl_4$ with Sodium inside a steel bomb.[2] The element is the ninth most abundant in Earth's crust and it can be found inside igneous rocks, making us thinking that a consistent percentage of this metal dominates the composition of the internal substrates of the Earth. As mineral, it can be found on the Earth in three allotropic forms: *rutile*, *ilmenite* and *sphene*.[2] It is also present inside titanates and iron ores. This metal can be found also inside the ash of coal, inside the plants and in the human body.[2] Titanium became a commercial metal when in 1946 Kroll discovered how it could be prepared from titanium tetrachloride by reduction with Magnesium. When pure, it is a lustrous, white metal, with low density, good strength and strong corrosion resistance. It is the only element which can burn in nitrogen, producing Titanium Nitride (TiN), that has an important role in thin film deposition: in fact, it is a very strong material, only second to diamond, according to Vickers Hardness. Because of its metallic gold colour, it is used for decorative purposes.[2] This element, in its metallic form, is also resistant to dilute hydrochloric, sulphuric and most of organic acids. Stronger as steel, but 45% lighter, makes Titanium one of the most important material for application in all branches of new technologies. It has a dimorphic structure: the hexagonal α form passes very slowly to the cubic β form when heated at 880°C. It should be noted that Titanium, in its metal form, has an excellent resistance to the corrosion by sea water.[2] Additional important information about this element is the possibility to use it as an *alloying agent* with Aluminium, Molybdenum, Manganese, Iron and Vanadium. These alloys are principally used for aircraft and missiles, where lightness and hardness are the two

most important discriminants.[2] It is considered physiologically inert: this property is due to the superficial oxide layer which can interact with the bone tissue. This property is used in order to realise metal hip or knee, surgical equipment and dental implants.[2] Another important application of titanium derivatives is the possibility to use the high index of reflection of pure titanium dioxide to realise optical lenses. It is also extensively used in house paint due to its bright white colour.[2]

As said before, Titanium presents three valence numbers: as Ti^{2+} it is prone to form numerous diamagnetic metal complexes, but it can also form complexes when it is present as Ti^{3+}, which is rapidly oxidised by the oxygen in the air to the more stable Ti^{4+}.

3.1.1 Metallocenes: a brief introduction inside the chemistry of these compounds

In principle, studies and research were directed towards cytostatically active compounds which included only one atom of the metal. Taking this in mind, we can imagine to create three main groups of metal containing antitumour agents: inorganic complexes with inorganic ligands, organometallic complexes and those which does not have direct carbon-metal bond and therefore cannot be defined as organometallic.[3] Considering the first group, this is the one in which history of metal-containing antitumour agents begun. Indeed, *cis*-diamminedichloroplatinum - better known as *cisplatin* - was the first metal complex which showed antitumour properties (Figure 3.1).[18] The phenomenal success of this inorganic drug led to a strong research in this direction for further Platinum antitumour compounds. This work discovered other platinum complexes like diammine(cyclobutane-1,1-dicarboxylato)platinum(II) - the so called *carboplatin*; acquo[1,1-bis(aminomethyl)-cyclohexane](sulfato)platinum(II) - *spiroplatin*; bis(isopropylamine)-cis-dichloro-trans-dihydroxoplatinum(IV) - *iproplatin* (Figure 3.3).[19] All these compounds were characterized by a similar activity in comparison to *cisplatin*, but a reduced nephrotoxicity and an increased myelotoxicity.[3]

In further studies, a wide range of complexes containing platinum-group metals

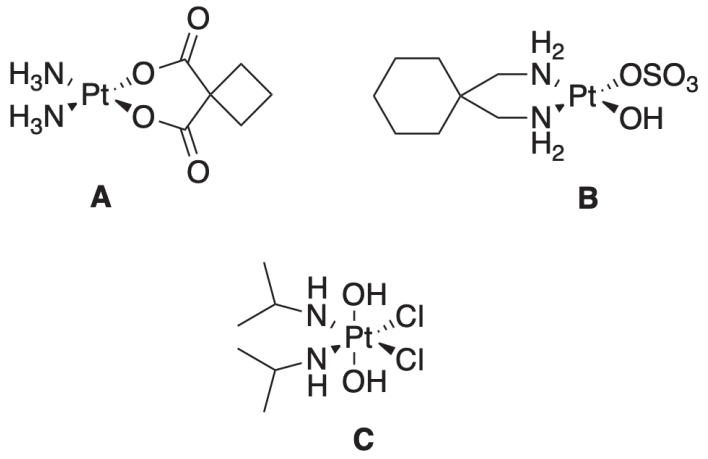

Figure 3.3: *Complexes derived from cisplatin: A) carboplatin, B) spiroplatin and C) iproplatin.*[3]

- Ruthenium, Rhodium, Palladium - were characterised.[3]

However, as everytime happens in research, studies were directed also inside the others metal groups: from these studies antitumour agents like Gallium salts, Germanium compounds and Tin organo-complexes were discovered.[3] Important studies were also performed within transition-metal compounds, where early transition metals like Titanium and Vanadium, or medium transition metals like Iron, were involved. The complexes studied assumed the typical structure of "*Metallocene*" or "*Metallocenium*" derivatives.[3] Metallocene is the name attributed to those compounds which presents two π-bonded *cyclopentadienyl* (Cp) ligands on the metal atom. Research inside this area started in 1952 when the structure of *ferrocene* [bis-cyclopentadienyl iron(II)] was firstly discovered: this presents a C_5-symmetric structure with two Cp rings equivalently (η^5 - hapticity number) bonded. These types of structures are named "*sandwich complex*" (Figure 3.4).[1]

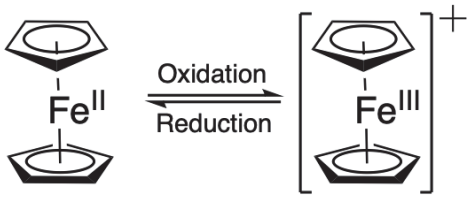

Figure 3.4: *Classical structure of "sandwich complex" for ferrocene and ferrocenium-ion.*[1]

The importance for the ferrocenium structure is due to recent studies explaining

the antitumour activity - observed for the first time in 1984 against Ehrlich ascite tumour (EAT) - as a result of a Fenton-type reaction, with the formation of hydroxyl radicals that could damage the DNA.[1],[3]

However, this type of structure is not a general behaviour for these compounds: in fact, recently was observed that Ru(arene) complexes (Figure 3.5) - albeit if they have not a double cyclopentadienyl ligand - are considered metallocenes. The difference is the "*half-sandwich complex*" which is the typical structure of these compounds. Today metal complexes which carry cyclic π-ligand are sometimes named metallocenes.[1]

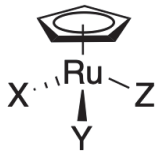

Figure 3.5: *Classical structure of "half-sandwich complex" for Ru(arene).*

Furthermore, bis-cyclopentadienyl complexes can be classified in two groups: the "classical" ones, with a sandwich structure, and the "*bent*" ones, which presents other ligands bonded to the metal in addition to the Cp rings (Figure 3.6). These particular structures are those typical for early transition metals like Titanium, Zirconium, Vanadium, Niobium and Molybdenum.[1]

Figure 3.6: *Classical structure of "bent complex" for Titanocene dichloride.*

Observing the structure of all medicinally important bent-metallocenes, we can find a disposition for the halides which resembles the *cis*-structure typical for cisplatin and its derivatives.[1] A more detailed observation of these bent complexes shows a characteristic distorted tetrahedral structure (Figure 3.6), in which two cyclopentadienyl ligands and two halide or acido ligands are coordinated to the central metal. This one, as said before, is typically an early transition metal, generally in

the fourth (IV) oxidation state. Also in this case, like the classical one, the hapticity number for the two Cp rings is 5 (η^5): this indicates that each carbon within the cyclic ring, is equivalently bonded to the central metal.[4]

These metallocenes dihalides were studied for long time as antitumour organometallic agents and it was found that they exhibit antitumour and antiproliferative properties *in vitro* against numerous tumoral cell lines, such as leukaemias P388 and L1210, colon 38, Lewis lung carcinomas, Ehrlich ascites tumour and B16 melanoma, but also against several xenografted human carcinomas transplanted into athymic mice. In these studies, using animal models, it showed also antiviral, anti-inflammatory and insecticide properties.[3],[4] For these compounds structure-activity relationship studies were established, both for halides and for substituents on Cp rings, trying to use amino acids, nucleic acids, plasma and proteins.[1]

All these studies revealed that the most active compounds were those of Titanium and for that reason Titanocene dichloride (Figure 3.6) also underwent clinical trials until Phase II. The possible formation of metallocene-DNA complexes should be implicated inside these antitumour compounds mechanism of action. More recent studies investigated the possibility for Titanium - inside metallocenes - to link and strictly interact with DNA or RNA, by inhibiting their synthesis or proteins like topoisomerase, or by inducing the apoptosis.[20] A further proof of this mechanism is the presence of Titanium in those regions inside the cell which are rich of nucleic acids.[1] However, despite the similarity between Titanocene dichloride and cisplatin, there is not the evidence of a clear mode of action for the first one, whereas the latter and the platinum-based anticancer drugs are well characterised.[1],[4] Recent studies, aiming at investigating stability of Titanocene compounds against the hydrolysis at different values of pH and the possible direct interactions with nucleic acids, highlighted different mechanism of action for different Titanocenes.[4]

3.1.2 Antitumor properties and studies of Titanocene dichloride

Titanocene dichloride (Figure 3.6) is one of the most studied and reviewed new antitumour agents based on early-transition metals complexes. Most of this work was carried out by Köpf and Köpf-Mayer research group. Despite other antitumour drugs based on metallocenes, those containing Titanium in the 4^{th} oxidation state, showed a higher potential of cure for antitumour therapy.[21] This metal complex was involved in pre-clinical studies by Köpf-Mayer *et al.* since 1970, against Ehrlich ascite tumour (EAT) using animal tumour models. Those studies showed an optimum cure rate of 100% against EAT and Colon 38 adenocarcinoma inhibition (80%) was better than cisplatin.[4],[5]

Taking this in mind, further studies were conducted on other types of tumour which presented receptivity against Titanocene dichloride: in particular, carcinomas in the gastrointestinal tract, lungs and breasts were tried.[22] It also showed an increased activity against some xenografted human carcinomas if compared to cisplatin.[4],[5] The results obtained from these pre-clinical tests using animal models highlighted toxicity at liver (bilirubinaemia) and intestinal (stomach and mucosa damage) level, but, in contrast to the cisplatin activity, they did not show nephrotoxicity or bone marrow depletion.[22] However, hepatic and intestinal diseasess showed a partial reversibility as the level of creatinine returned within normal ranges during 1 - 10 weeks later the subministration. Also the metallic taste observed few hours after infusion is reversible.[5]

All these promising pre-clinical results - in particular absence of nephrotoxicity in mice models - culminated in 1998 in Phase I clinical trials.[6] In contrast to the tests conducted on animal tumours, the application of Titanocene dichloride to humans does not showed - as dose-limiting side effect - hepatic or intestinal toxicity. The limiting factor became the nephrotoxicity along with similar symptom to those reported by infusion of cisplatin (nausea, metallic taste, hypoglycaemia and pain). However, bone marrow diseases were not observed.[4] One of the reason of this failure could be the triphasic elimination of Cp_2TiCl_2 from the plasma, with a long half-life

of 165 hours.[6] These results showed that data obtained from animal studies were deceptive and could not be used as a model for humans. For that reason, Phase II clinical trials were planned by combining synergistically the activity of Cp_2TiCl_2 with that of 5-fluorouracil, as observed by *in vitro* tests.[23]

Further work was planned in order to comprehend the reasons for the clinical failure of Titanocene dichloride. Nowadays this mechanism is not cleared yet, but numerous theories were proposed to explain the results observed in humans. One of the most entangling one is that under physiological conditions, Cp_2TiCl_2 could undergo a rapid hydrolysis.[6] This theory was elaborated and reported by Harding and Mokdsi group by considering the hydrolytic instability of Titanocene dichloride at values of pH lower than 5.[4] In fact, while the stability of most metallocenes dihalides in organic solvents - where they are soluble - is very good, in aqueous solutions the hydrolysis of the two halides and of the Cp rings is favoured.[4] According to the metal atom in the centre of the complex, the rate of the hydrolysis process could vary. Typology of halide and the solution pH could influence this process too.[4]

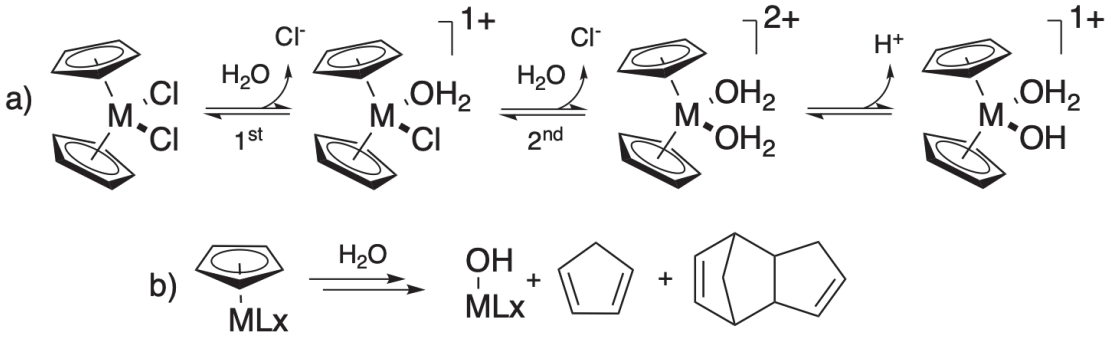

Figure 3.7: *Hydrolysis of a) halide and b) cyclopentadienyl ligands in Cp_2MCl_2 complexes.*[4]

It was demonstrated that a solution prepared with some metallocenes dissolved in water shows pH values between 2 and 3. If pH is brought to values closer to 6 (nearly the physiological value) insoluble precipitates are formed, while the soluble products resulting from hydrolysis are not biologically active. This process can be observed sketched in Figure 3.7.[4]

In the case of Titanocene dichloride, first the rapid hydrolysis of one chloride ligand occurs - rate no measurable due to the half-life too short - giving an aquated

intermediate which undergoes the second hydrolysis - now measurable - in about 50 minutes.[24] The other metallocenes tried - V, Zr, Mo - showed lower amounts of time.[24] The resulting precipitate may contain TiO_2 and polymeric species like $[(CpTiO)_4O_2]_n$.[4] The estimated stabilities and half lives for the Cp ligands hydrolysis for Cp_2TiCl_2 showed a $t_{1/2}$ of 57 hours.[24] It is possible conclude that both pathways of hydrolysis process are strictly dependent by pH and the metal present.[4]

In order to overcome these problems during clinical phase tests, buffered solution was prepared. In particular Titanocene dichloride was dispensed as a saline solution made of DMSO (10%) and malate as buffer in order to stabilise pH around 3: this made the solution stable against hydrolysis for at least 4 hours.[25] Another useful formulation involves lyophilisation of Cp_2TiCl_2 in the presence of a salt and mannitol, which confers over 1 hour of stability.[6] However, it was observed that buffered formulates showed reduced antitumour properties after administration.[26]

Looking at the results reported above, it appears clear that research pointed towards new synthetic studies in order to increase the hydrolytic stability of Titanocenes dichlorides, increasing at the same time toxicity and antitumour activity for further clinical tests.

3.1.3 Transport inside cells and first attempt to define biological targets of Cp_2TiCl_2

As we said in previous paragraphs, a lot of biological and chemical studies were carried out on Titanocene dichloride in order to comprehend the antitumour action mechanism and the biological transport inside the tumoral cells. Nowadays only the second purpose has been elucidated, whereas for the first one it is not fully understood yet.[4] Titanium species nevertheless are transported into cells, so stabilisation and transport of Titanocene dichloride *in vivo* must be considered in the antitumour action.[4] The presence of Titanium complexes inside plasma could be explained considering the presence of *transferrin*, a protein involved in regulation of Iron and its transport as Iron(III) complex from plasma through cell membrane, thanks to an endocytosis mechanism. This protein could represent a possible access route to the

tumour cell, because of the possibility to bind Titanium atom to one of its two domains.[27] As an additional information, tumour cells presents a higher number of receptors for transferrin compared to that in normal cells.[27] In particular, as regards the intracellular activity, every metallocene shows a specific mechanism of action, which culminates in the irreversible structural modification of DNA which cannot be repaired. Another possible interaction could be adenosine tri-phosphate (ATP).[5]

Concerning the mechanism of interaction between proteins and Titanium compounds, one of the most important study, realised by Tinoco and Valentine, showed how Titanium (IV) is linked more strictly to human transferrin than Iron (III).[8] However, human blood plasma contains up to 600 different proteins and interaction between metal complexes with them needs to be considered.[28] For example, recent studies conducted with glycine and L-alanine have shown that their coordination to the Titanium atom occurs in preference to chloride if some condition are respected.[29] However, these amino acid ligands rapidly undergo dissociation if nucleotides or their derivatives are present.[29] For this reason, considering sulphur or nitrogen coordination sites inside proteins is much more useful.[4]

As already mentioned, transferrin seems to play a fundamental role in Titanocene dichloride antitumour activity, because it was found that more than 70% of this metal complex is protein bound in plasma after intravenous injection.[4] Titanium (IV) derived from Cp_2TiCl_2 forms a strong complex with human transferrin: the only way to form this particular complex is the presence of a specific hydrophobic area in which cyclopentadienyl rings could be stabilised.[30] Titanium atom has been found to be coordinated to each of the two specific Iron (III) binding sites of the protein and a Ti_2-transferrin complex is obtained by removing one of the Cp ring and one of the chloride ligands. This metal complex is stable in the range of pH between 5.5 and 9.0. Titanium (IV) may be transported inside the cell membrane by transferrin and subsequently undergoes on binding DNA.[4],[5]

Recent studies showed also the possibility of interaction between Titanocene dichloride and topoisomerase II, resulting in inhibition of its unwinding properties.[31] This was firstly observed when metallocenes were found able to inhibit *in vitro*

cellular DNA synthesis by arresting cells at the G_2 or G_1/G_2 phases of the cell cycle (Figure 3.8). However, this inhibition may be possible only if a $TiCp_2$ derivative enters the cell.[31]

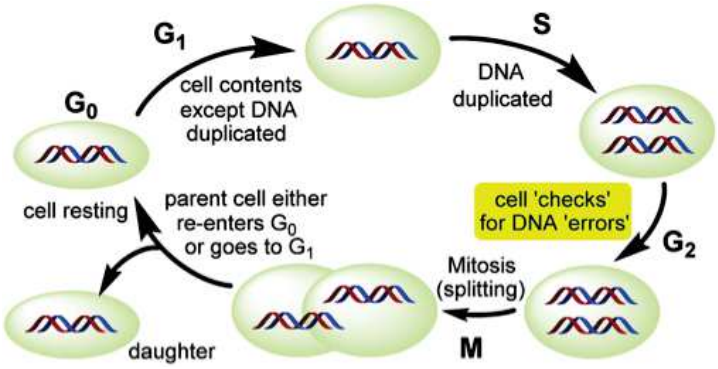

Figure 3.8: *Representative scheme of the cell cycle.*[32]

Going forward we must talk about the interactions between metallocenes and the building blocks of DNA and RNA. Those targets are certainly D-ribose-5'-phosphate, nucleobases, nucleosides and nucleotides. Unlike the so long studied mechanism of action for cisplatin and its derivatives - with a direct crosslink of DNA which creates problems during replication - interaction of Titanium derivatives with DNA is poorly understood. Nevertheless, Titanium-DNA interaction has recently been studied for Titanocenes.[33] The study made by electron energy loss spectroscopy revealed that DNA is the prime cellular target for Cp_2TiCl_2; that research showed that the metal derived from that complex, accumulate in the regions rich in nucleic acids.[33] The same result was obtained also in xenografted human tumours: titanium was detected firstly, after 12 hours of administration in a near phosphorous rich area.[33] Significant inhibition of DNA and RNA synthesis was also demonstrated both *in vivo* and *in vitro*.[4],[5]

In order to identify potential interaction which lead to a coordination complex, nucleic acids constituents were tried.[29] As reported in Figure 3.9, this study highlighted the possibility for Titanium to bind both nitrogens and oxygens of phosphate group present in nucleotides: this can happen because under pH = 3, Cp_2Ti^{2+} species are formed and an immediate coordination occurs.[29] When pH increased to values higher than 4, the protonation of cyclopentadienyl ligands was favoured, with the

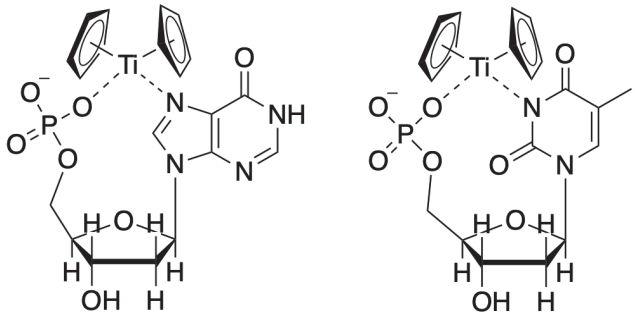

Figure 3.9: *Representative examples of mode of coordination for Cp_2TiCl_2 complexes.*[4]

concomitant loss of those ligands and formation of insoluble Titanium derivatives biologically inactives.[4],[9]

The first experimental data which supports the formation of Titanocene-DNA complexes were found by characterization of metallocenes dihalides-DNA adducts by inductively coupled plasma (ICP).[34] The use of tritium labelled DNA showed that two distinct adducts were formed. When pH increase from a value of 5.3, in which both Cp rings are present inside the adduct, to a value of 7.0, only one Cp ring was associated with DNA adduct.[34] Recent analysis using atomic absorption spectroscopy has shown that the Titanium atom binds DNA.[4] Is it also possible to use UV spectroscopy to characterize the interaction of metallocenes with DNA, with a decrease in UV absorbance of DNA when the adduct is formed.[4] The quantification of adduct formation increases with time and within physiological conditions of pH close to 7.4, in this case, more than 90% of DNA coordinates Titanium after 46 hours from the administration.[10]

Sadler and co-workers proposed a different target: ATP.[35] However, as they also stated for transferrin, Cp rings lability is fundamental to generate Titanium (IV) species.[27] This explains also the lack of activity for methyl substituted Cp derivatives which are stable to hydrolysis, an argument that will be well explained in the next section.[4]

Obviously, such a great biological efficiency can be interpreted as the high affinity between Titanium and phosphate groups present in DNA. Further confirmation for the formation of these adducts comes from the tumoral protein p53, which is found to be incremented in those cells treated with Titanocene dichloride.[23] This could be

interpreted as the result of a DNA-damage which could be attributed to Cp_2TiCl_2. Subsequently, this process brings to a severely invalidated cell cycle which ends up in the apoptosis of the cell.[5]

Thus, in order to sum up the result of the studies, we now know that Titanium (IV) is transported in bloodstream by transferrin and, when pH is 5.5, it is released. This happens in cancer cells which presents over-expressed transferrin receptor than the healthy ones. In addition, pH values inside a tumour cell is lower than in the surrounding space, so Titanium (IV) is released inside the tumour cell and most probably it binds ATP. From this latter one, it will be available for complexation with DNA, or for activation of ATP dependent proteins like topoisomerase II, involved in apoptosis.[4]

3.1.4 Need to develop new modified Titanocenes

Studies related to the antitumour activity of Titanocenes dihalides - as previously described - showed a consistent activity against those cancers which were resistant to general chemotherapy. Results obtained by *in vitro* and by animal model studies, demonstrate that there was the possibility to start clinical trials. However, when Phase I and Phase II were tried on human patients, results observed were discordant compared to ones registered before. For that reason, attempts were made in order to improve the stability of these compound against physiologically promoted hydrolysis and to enhance the cytotoxicity of the original compound. The first site where the molecule could be modified is the replacement of the two halide or pseudo-halide ligands. However, the most innovative modification that was introduced on these complexes was the presence of substituents on cyclopentadienyl rings. These functionalization in some cases enormously increased the antitumour behaviour of the molecule in comparison to Cp_2TiCl_2.[9],[7]

Before start speaking about Cp-substituted Titanocenes, we have to remember also the first Titanium based antitumour drugs without cyclopentadienyl rings: the [*cis*-diethoxybis-(1-phenylbutane-1,3-dionate) Titanium(IV)], simply called "*Budotitane*", Figure 3.10.[36] An important observation that stands out immediately is the cis structure of the two ethoxy labile groups: the same thing was observed for chloride

ligands in cisplatin and Titanocene dichloride.[9]

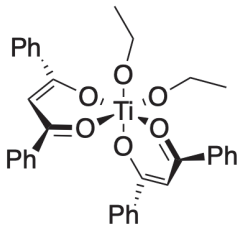

Figure 3.10: *Representative structure of a budotitane stereoisomer complex.*[5]

Otherwise, there is also a significant difference between the cytotoxic mechanism of Platinum and that of Titanium in budotitane: in fact, cisplatin hydrolysis of Cl-Pt bond occurs inside the tumour cell.[37] In contrast to this mechanism, budotitane showed a fast cleavage of Ti-OEt bonds through an hydrolysis pathway, which reasonably happens outside the tumour cell.[36] These results are confirmed during Phase I and II of clinical trials using Titanocene dichloride and observing a consistent complexation of Titanium mediated by blood proteins.[5]

Main targets for budotitane are gastrointestinal tract tumours. Preclinical studies showed an increased toxicity against sarcoma 180 and carcinosarcoma Walker 256.[36] Despite the activity of cisplatin and metallocenes anticancer drugs, budotitane activity against leukaemias P338 and L1210 was marginal.[38] As an additional information, the antitumour activity of budotitane against colon rectal tumours was greater than those of cisplatin and 5-fluorouracil.[5]

Furthermore, budotitane undergoes to hydrolysis evolving toward polynuclear forms, where O(oxo) atoms bridge Titanium metals. For that reason, the development of this drug was difficult: the use of ethanol was necessary to counterbalance the bond cleavage, but inevitably further restricted the formulation variety. It is also not soluble in water and in most of organic solvents it undergoes hydrolysis too rapidly.[36] For these reasons attempts were made in order to realise a formulation which could be applied in clinical Phase I. The best one used was composed - besides Ethanol - of Cremophore propylene glycol.[39]

In animal model trials a notable liver toxicity was observed. However, Phase I clinical trials were performed and a recommended dosage was determined to be 180

mg/m^2. No subsequent clinical evaluation was made because of the impossibility to meet modern clinic standard for this drug.[40]

Taking in mind what we saw for budotitane, it appears an obvious consequence that research groups direct their effort on Titanocene derivatives.

The two main problems observed for Titanocene dihalides were poor aqueous solubility and hydrolytic instability. In order to overcome these problems a huge range of Cp_2TiCl_2 derivatives with Cp rings substituted by electron-withdrawing or electron-donating groups - aromatic rings, alkyl, cyclic amines - were prepared and their activity was tested.[1],[11] The possibility to select hydrolytically stable ligands could realise Titanium derivatives which do not need the presence of any protein like transferrin for cellular uptake and stabilisation.[41]

The incorporation of polar electron-withdrawing groups on Cp rings increased the Lewis acidity of Titanium atom, enhancing the possible interaction with nucleobases within DNA, which shows a typical Lewis base behaviour.[6] Some tests were made *in vitro* in order to observe the difference between carbomethoxy mono- and di-substituted Cp rings (Figure 3.11): it was shown that the di-substituted one presented an higher cytotoxicity in contrast to the mono-substituted compound.[41] The main reason of this behaviour was attributed to different hydrolytic capabilities of the two derivatives. However, none of these two complexes showed an interesting antitumour activity for further applications.[6]

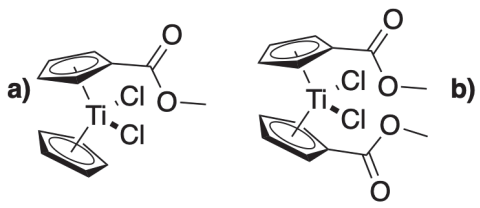

Figure 3.11: *Representative structure of a) mono-carbomethoxy and b) di-carbomethoxy Titanocene dichloride.*

In order to increase the aqueous solubility of Titanocene dichloride, researchers introduced a range of protonated amino and aryl side chains on Cp rings.[11] These "ionic titanocenes" showed an enhanced activity and stability if compared to the classical one. Such electro-donating groups are expected to stabilise and prevent

protonolysis, penalizing the classical uptake of the vacant Titanium (IV) by transferrin.[11] For that reason, tests were conducted both on di-cationic and mono-cationic derivatives: water soluble analogs of Titanocene dichloride containing two alkylammonium substituents, were proved to be more cytotoxic in lung and ovarian cancer cells line than the corresponding mono-alkylammonium ones. These differences may be related to the different hydrolysis rates of Cp-Ti bonds.[6],[11]

Recently, a range of heteroaryl and *ansa*-derivatives were realised by the group of Tackle, developing a new synthetic route to cyclopentadienyl-substituted Titanocenes *via fulvene*.[42] This new class of compounds is easily accessible through a Knoevenagel condensation, as reported in Figure 3.12.[1]

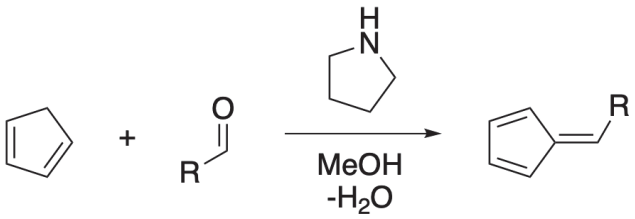

Figure 3.12: *Classical fulvene synthesis trough Knoevenagel condensation.*

This approach let Tackle and his group to realise unbridged (through hydridolithiation) or *ansa*-bridged Titanocenes (through carbolithiation) with an antitumour activity which was changed from the classical ones.[42] For example, the inclusion of dimethylamino groups in Titanocene C (Figure 3.13 a) aid solubility and stability of the metal centre, properties related to an intramolecular coordination to the central Titanium upon displacement of chloride ligands.[42] With the same approach, they realised Titanocene Y (Figure 3.13 b), which brings two *p*-methoxybenzyl derivatives on Cp rings.[42] This latter derivative showed an increased cytotoxicity against prostate cancer cells and it was found more capable than cisplatin to induce apoptosis.[6]

Between these two compounds, Titanocene C was the most cytotoxic agent, with an Inhibitory Concentration of 50% (IC_{50}) close to the value of cisplatin. It was also four hundred times more cytotoxic than classical Titanocene dichloride.[41] In order to comprehend more deeply the mechanism of action of this compound, Olszewski

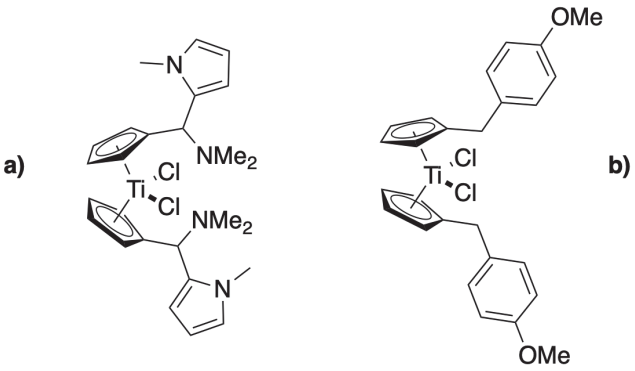

Figure 3.13: *Representative sketched structures for a) Titanocene C and b) Titanocene Y.*

and Hamilton investigated the whole process which occurs inside a tumour cell when Titanocene C is administered.[6] This mechanism is difficult to understand because it involves several steps, from cellular uptake, to nucleic acids and proteins interaction.

However, it is important to introduce the synthesis developed by Tackle and his group for Titanocene C. Titanocene C is a 6-*N*,*N*-dimethylammino-functionalised Ti-complex and the synthesis could be planned starting from a carbolithiation reaction of 6-*N*,*N*-dimethylamino fulvene with Lithium *N*-methylpyrrolate. The product obtained undergoes a transmetallation reaction with titanium tetrachloride producing the target molecule, as reported in Figure 3.14.[12]

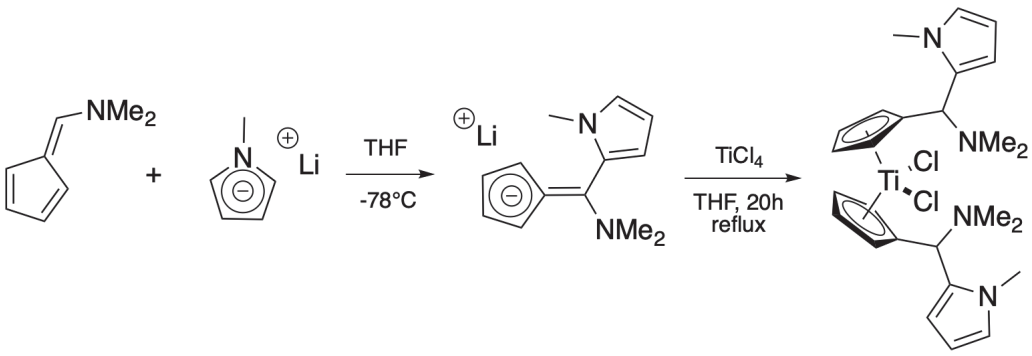

Figure 3.14: *Synthesis of Titanocene C elaborated by Tackle and his group through carbolithiation.*[12]

As we said before, the most active derivative Titanocene C, has shown an antiproliferative activity against human small cell lung tumour line. Moreover, Olszewski and Hamilton conducted several studies in order to comprehend the mechanism of action.[6] These studies started from other works realised on the distribution

of Titanocene dichloride both in cell lines and in xenografted tumours: they observed that Titanium was associated with vesicles and lysosomes during uptake and extrusion.[43],[27] Therefore, introduction of Titanocene C within the cell occurs through bound to some serum proteins - like transferrin - followed by incorporation via endocytosis by clathrin-coated vesicles.[27] Typically, Cp_2TiCl_2 analogues are released from vesicles inside the cell and then hydrolysed in cytoplasm. The loss of chloride ligands, in contrast to classical behaviour of Titanocene, does not evolve with the replacement by hydroxyl or aqua ligands, because in this case *N*-methyl groups provide the intramolecular coordination.[44] After the cell uptake, Ti^{2+} is transported to the nucleus and there interacts with metalloenzymes or transcription factors (TFs) inside cytoplasm.[6] Most of these metalloenzymes target are metallothioneins, which are cysteine rich proteins that bind Zn^{2+} ions as reserve of metal for the synthesis of apoenzymes and zinc finger motive-containing TFs.[45] These metalloproteins are fundamental in nucleic acid metabolism, cell replication and growth. The Zn^{2+} ion is a fundamental element, but toxic at excessive concentrations and its homeostasis is critical for normal cell healthiness.[46] Furthermore, the possible exchange mechanism between Zn^{2+} and metal cations used inside antitumour metal-based drugs, could increase the concentration of free Zn^{2+} in cytoplasm.[6] This disturbed homeostasis lead to accumulation of misfolded proteins and to modifications of transcription factors, which directly decrease the transcription of topoisomerases and histones.[6] The absence of these enzymes ends up with an impairment of DNA transcription, replication and cell cycle progression. For all these reasons, which are strictly linked together, Ti^{2+}-mediated DNA damage lead also to the shutdown of glycolytic and respiratory cycles, resulting in loss of vital energy followed by apoptotic cell death.[6]

In Figure 3.15, it is possible to observe all of these processes represented schematically. However, it seems that the final result of this mechanism is due to the interference inside homeostatic equilibrium of Zn^{2+} mediated by Ti^{2+}. Further studies are under way in order to determine if it is a mechanism specific for Titanocene C or it could have a more general sense.[6]

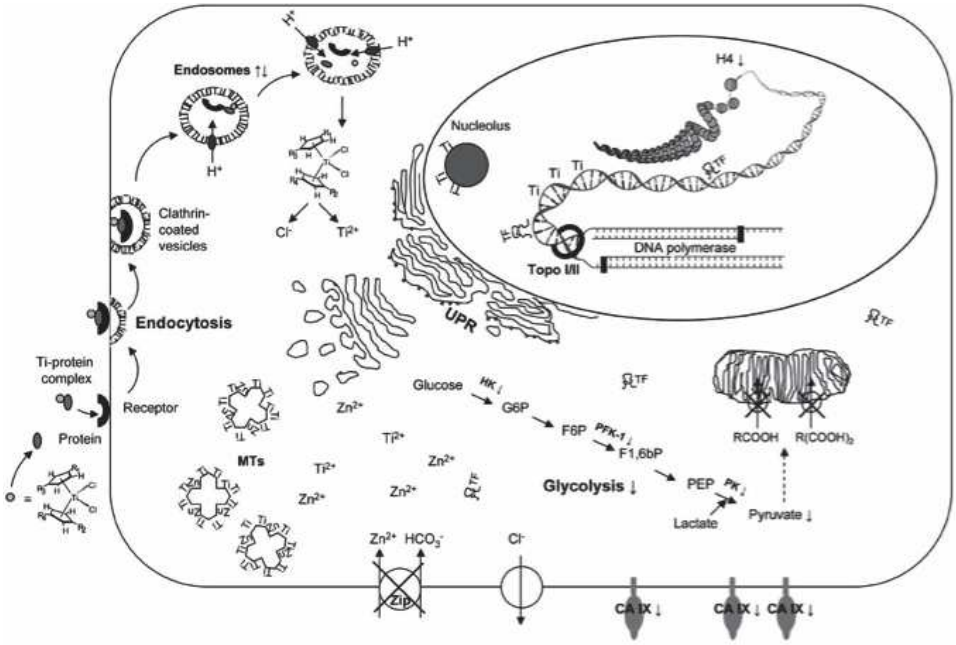

Figure 3.15: *Proposed mechanism of action of Titanocene C anticancer drug.*[6]

In this paragraph we have treated only the internal behaviour of these anticancer drugs, but recent studies have shown how the transport and the uptake process are also fundamental steps in determining the effective antitumour activity.[47] An important study which describe this behaviour was realised on Titanocene Y (Figure 3.13 b): it was observed that the incremented cytotoxicity - compared to Cp_2TiCl_2 - relies on the mode in which this drug is transported.[48] In contrast to what happens for Titanocene dichloride, which is primarily transported by transferrin, Titanocene Y is transferred from plasma to cell membrane by *albumin*.[48] This is possible thanks to a cavity in which there is a serine residue that is able to realise a hydrogen bond with one of the two methoxy groups on Cp-benzyl ligands.[12]

Research in these last years focuses its attention on selective carriers, for a specific antitumour drug.

3.1.5 Novel development in Titanocene based drug synthesis

In order to overcome all of problems mentioned above new efforts were made recently, to improve functionalization of these drugs using biomolecules. For exam-

ple, a wide range of tumour cells presents a high absorption of sugars compared to the healthy ones, with particular interest in D-glucose uptake *in vivo*, which exceed by one order of magnitude that of the normal tissues. This behaviour is known as the "*Warburg effect*".[13] This situation can be observed on the other side on tumour cell membrane, where D-glucose transporters (GLUTs) are overexpressed.[49] Taking in account what we reported in previous paragraphs, it is possible to use glucose receptors for the selective transport of anticancer drugs inside the cancerous cell. It is important to observe that GLUT receptor can also transport simple monosaccharides like D-xylose, D-ribose and α-D-ribofuranose.[50] Generally, if a transition-metal undergoes conjugation with an organic molecule, the result is a reduced toxicity, better biocompatibility and increased solubility in aqueous media.[13] Additionally, if the biomolecule constitutes a target for overexpressed receptors, selectivity and cytotoxicity could be enormously enhanced.[13]

Using this information, Titanocene dichloride was made with substituents on its Cp rings.[13] In particular it was observed that the presence of α-D-ribofuranose as substituent on cyclopentadienyl rings (Figure 1.16), showed an increased cytotoxicity which can be modified by varying the position of substituents in the order: 4<1<2<3 (see Figure 1.16).[13] In particular, the highest cytotoxicity observed (complex 3 in Figure 3.16) can be compared with that of cisplatin. These compounds, due to their increased activity, were recently patented.[51]

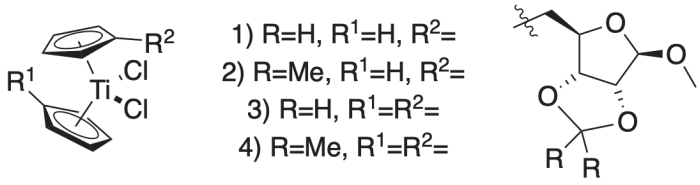

Figure 3.16: *Representative substitution possibilities on Titanocene dichloride with α-D-ribofuranose derivatives.*[13]

It is also worth mentioning the effort made in order to support these Titanocenes derivatives on solid materials like mesoporous silica-based KIT-6, where the cytotoxic activity observed was the highest reported.[14] In addition, it was found an higher Titanium uptake of the cells when treated with this material respect to the

classical Titanocenes free derivatives. These results may be due to a different process in which Titanium is released, combined with changes to the morphological and functional dynamics of apoptosis.[14] We can conclude that these nano-structured materials should be considered as safe vehicles for delivering Titanocene complexes.

Last but not least, there is the possibility to functionalise Cp rings with substituents able to achieve *radiotheranostic* (a mix between radiotherapy and diagnostic). A novel Ti/^{111}In heterometallic complex was studied thanks to the design of new trackable Titanium based therapeutics.[15] In fact, to the date only a few trackable titanium complexes were described. Some initial studies have reported the use of ^{45}Ti (a β^+ emitter with $t_{1/2}$ = 3.1 hours), in order to perform *PET* (Positron Emission Tomography).[52] The main problem in the use of this isotope is the low availability in nature and the difficulty to generate *in situ* transferrin-Ti complexes.[15] What about *in vitro* tracking, no study was performed, except that of Dillon who reported the use of X-ray fluorescence in order to map the distribution of Titanocene dichloride inside cells, which anyway presented a consistent lack of sensitivity.[53]

In a recent work, Pierre Le Gendre and co-workers, synthesized Titanocene complexes functionalised with a fluorescent probe (BODIPY) which was the ideal solution for *in vitro* visualisation through confocal microscopy.[15] The possibility to do the same thing using complexes functionalised with a chelating agent (DOTA) for a radiometal, highlighted the possibility to use this latter one for *in vivo* imaging through SPECT (Single Photon Emission Computed Tomography) or PET (see Figure 3.17).[15]

Thanks to the study of Gansäuer, they were able to functionalise *a posteriori* Titanocene derivatives, passing through a highly electrophilic Titanocene-acyl chloride. This method results also in the formation of cationic Titanocenes, improving in one fell swoop both water solubility and reactivity in order to bind BODIPY and DOTA derivatives. Also stability in physiological media resulted enhanced for several hours.[54]

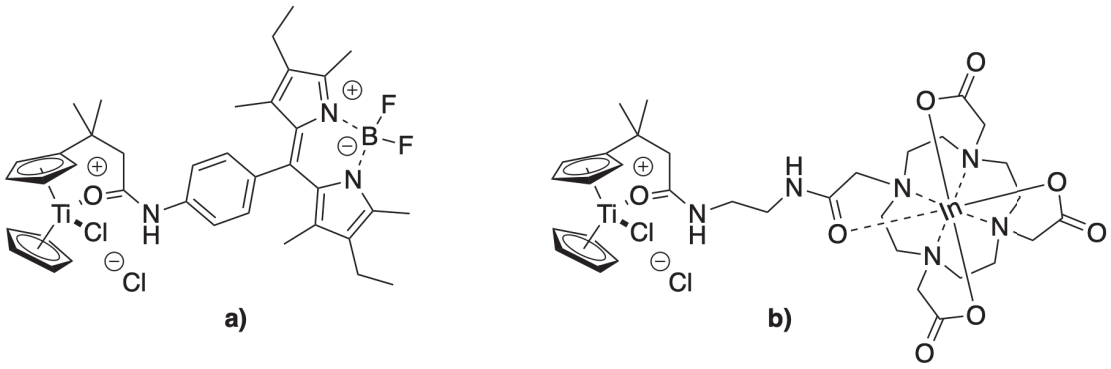

Figure 3.17: *Representative structures for a) BODIPY-Titanocene and b) DOTA-In-Titanocene.*[15]

3.2 Case under study

By following the ideas reported in the introductory part of this chapter, in order to improve the stability of these compounds against physiologically promoted hydrolysis and to enhance the cytotoxicity of the original (Cp_2TiCl_2) compound,[3],[9],[7] our research group started studying and developing new titanocene based compounds.[153] Specifically, we concentrated our efforts to the synthesis of modified cyclopentadienyl ligands that can be involved in click-chemistry reactions to further conjugate biomolecules on to the titanocene complex in an "add-on" fashion.[153] To achieve this result, we investigated possible collateral reactions between the titanocene compound and the classical moieties mostly involved in click-chemistry (i.e. azides and tetrazines). Unfortunately, we found some articles reporting on the reactivity between Titanium centre and azide- or tetrazine- derivatives.[57],[58] In particular, a notable reaction was found between Titanocenes and tetrazine by forming molecular squares and rectangles through self-assembly reactions as described in Figure 3.18.[58]

However, we made a simple experiment leaving the commercially available tetrazine derivative [4-(1,2,4,5-Tetrazin-3-yl)phenyl]methanamine, together with commercial Cp_2TiCl_2 at room temperature for 48h in toluene.[58] No products were found, probably due to the steric crowding at the site of binding and the greater delocalization of the charge between two conjugated aromatic rings.

Another important observation we made by looking at azide-derivatives used

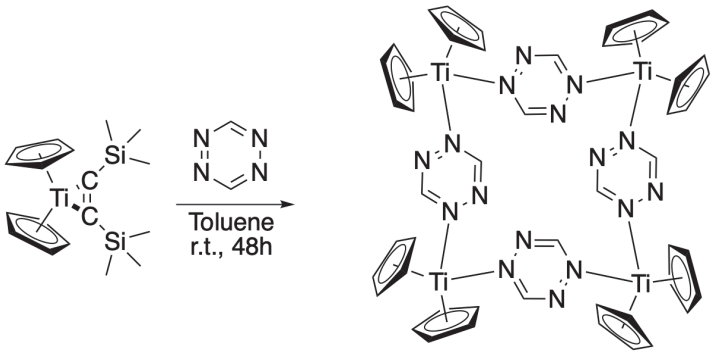

Figure 3.18: *Reaction between Titanocene [$Cp_2Ti\eta^2$-$C^2(SiMe_3)_2$] and tetrazine giving the tetrazine-bridged complex.*[58]

in click-chemistry for strain-promoted alkyne-azide cycloaddictions (SPAAC) is the possibility to give a direct reaction with Titanocene derivatives.[57] In an article written by Coutts and Surtees in late 1965, they observed that bis(cyclopentadienyl)-Titanium(III)chloride reacts with organic azides with the liberation of nitrogen through a vigorous reaction and the formation of Ti(IV) nitrogen-bridged compounds.[57] Such complexes show a different thermal stability directly dependent on the nature of the substituent, which links the azide group, and the solvent used: for example, in THF such compounds are rapidly transformed into mixtures of $Cp_2TiCl(NR)$.[57] The general reaction is reported in the following equation.

$$2Cp_2TiCl + RN_3 \longrightarrow (Cp_2TiCl)_2NR + N_2$$

Such products presented also hydrolytic sensitivity if exposed to the atmosphere by forming Ti-O-Ti groups, especially those which contain aromatic rings such as Phenylazide. However, Cp_2TiCl_2 was not hydrolysed to $(Cp_2TiCl)_2O$ under the same conditions.[71]

It should be suggested that the mechanism which brings to the rapid disproportionation of N-bridged compounds may be due to the presence of $Cp_2Ti^{III}Cl$ which directs a chloride abstraction from the bridged compound, as reported below.[57]

$$Cp_2Ti^{III}Cl + ClTi^{IV}Cp_2{-}NR{-}Cp_2Ti^{IV}Cl \longrightarrow Cp_2Ti^{IV}Cl + Cp_2Ti^{III}{-}NR{-}Cp_2Ti^{IV}Cl$$

The new formed Ti(III) could then attack another azide and continue the process until the formation of high molecular weight material. If the specie $Cp_2Ti^{III}Cl$ is not

present inside the reaction, it could be possible that $(Cp_2Ti^{IV}Cl)_2NR$ undergoes a homolytic decomposition of the Ti-N bond, with the formation of radical species and $(Cp_2Ti^{III}Cl)_2NR$, which can undertake the same reaction reported above.[57] Alternatively, another possible way is a heterolytic process, which could be strictly dependent on the nature of the group -R, as reported in Figure 3.19.[57]

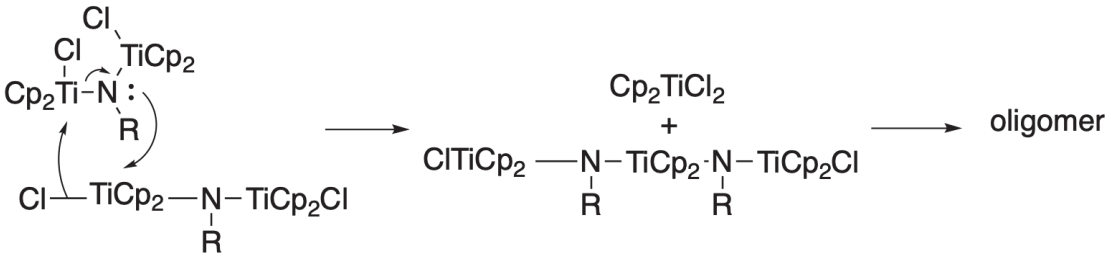

Figure 3.19: *Heterolytic process for disproportionation of N-bridged compounds.*[57]

All those studies made us thinking about the necessity of some ligand that could "protect" and block the Titanium centre during our transformation on the Cp linker, without interfering during these reactions. Thanks to recent studies made on Titanium ligands, we opted for sulphur-based linker and particularly the benzene-1,2-dithiol.[153]

3.3 The benzenedithiolate way

We opted for such ligand because we know how important are in nature, and in particular in some biological processes which involve enzymes like *molybdopterin*, the electronic interaction between metals and dithiolenes.[60] In particular such interactions are gaining more importance in recent times in materials field of research, in particular they are optimal in applications like sensors, photochemical and electronic devices for catalysis. In this latter use, dithiolene ligand is used in order to stabilise the metal centre in multiple oxidation states during processes of electron transfer.[59]

In order to improve the knowledge about the nature of metal-dithiolene electronic interactions in Titanocene derviatives, Enemark, Lichtenberger *et al.* used photoelectron spectroscopy in gas-phase to provide, together with valence ionization

energy, a unique quantitative energy measure of valence orbital overlap interactions between the orbitals of metal and sulphur.[59]

Fundamental studies of electronic interactions between metal and dithiolenes were reported in 1976 by Lauher and Hoffmann by using the classic molecular orbital description for metallocene complexes.[72] They realised that dithiolene ligand can use its *HOMO* orbital in order to donate electron density to the metal centre by forming a covalent bonding interaction. Such theory is also supported by the fact that the metal has an empty *d* orbital, with the suitable energy and symmetry to interact with sulphur ligand.[72] A schematic overlap interaction of the *HOMO* of the ligand benzenedithiolate (bdt) and a metal centre with an empty *d* orbital is shown in Figure 3.20.

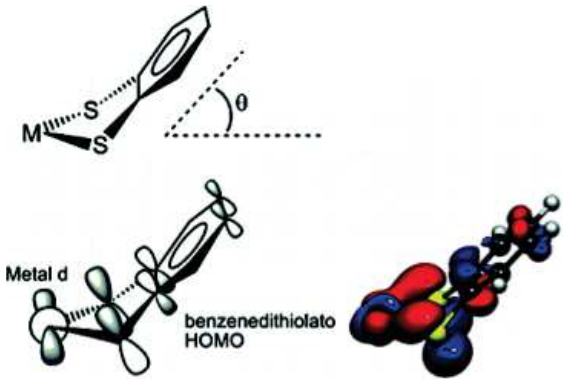

Figure 3.20: *Schematic of interaction between metal* d *empty orbital and* HOMO *of bdt.*[59]

As it is possible to see from the picture, the overlap interaction is modulated by the folded angle of bdt.[59] In fact, because the principal interaction occurs between p_π orbitals of sulphur ($S_{\pi+}$) and metal *d* empty orbital, the only way to maximise the overlap is by increasing the fold angle θ, passing from 0° (when $S_{\pi+}$ and *d* metal orbitals are nearly orthogonal) to a higher value which depends strictly on the metal centre we are dealing with.[59] It is also noteworthy that there is a small but important contribution which is given by the ene π bond, that being antibonding with respect to the S p_π orbitals ($S_{\pi+}$), it exercises a destabilisation of $S_{\pi+}$, increasing in this way the overlapping.[59]

It was found that there is a strong correlation between the metal electron count in

d orbitals and the folding angle.[73],[74],[75] As it is possible to observe in Figure 3.21, where are reported different metal centres at the same oxidation state - but with different electron number inside d orbitals - the interaction with bdt shows different folding angles. In particular, when the d metal orbital is doubly occupied (Mo-d^2), the interaction with $S_{\pi+}$ is an antibonding filled-filled interaction and in order to minimize the overlapping the folding angle is near to 0°.[73] When the d metal orbital is unoccupied like in Ti complex (d^0), the $S_{\pi+}$ orbital can interact directly with the d orbital and donate electrons to the metal centre.[74] Such bonding interaction which can be seen at the bottom of Figure 3.21, provides the stabilisation of the complex and it is as optimal as the folding angle increases, reaching in this case values above 40°.[74] The case of V is also reported in order to confirm the fact that the single electron present in the d orbital (d^1) influence the folding angle which is, in this case, comprehended between the values observed for Mo and Ti.[75]

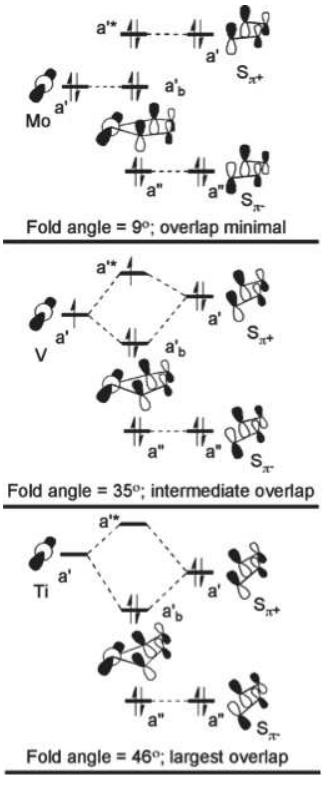

Figure 3.21: *Schematic of MO depiction of interaction between metal* d^0*(Ti),* d^1*(V) and* d^2*(Mo) metal orbitals and* HOMO *of bdt.*[59]

It is also interesting to observe that the next occupied orbitals - which are not depicted in Figure 3.21 - are those occupied of Cp π which are able to donate

electronic density to the metal centre.[59]

An other interesting observation is directly related to the nature of σ bonds which link the bdt ligand to the metal.[59] Such bonds, if treated with the classical molecular orbital description of the full complex, are shown to be orthogonal to the frontier orbitals, as in broad terms reported in Figure 3.20 and 3.21 by the use of single plain "lines".[59] These "lines" are inserted on the metal near the nodes of the idealised metal d orbital. For this reason, the σ-interaction which constitute the direct metal-sulphur bonding is less pronounced with the lowest metal d orbital, maybe because of the avoided overlapping and the large energy separation between orbitals.[59]

In the specific case of $Cp_2Ti(bdt)$, Ti(IV) has a d^0 electronic configuration and the a'* orbital is unoccupied. For this reason it is not possible to measure its ionisation energy.[59] However, the benzenedithiolate ligand can be considered as a six-electron donor group. In fact, each of the bdt orbitals involved in σ-bonding to the metal centre, provides two electrons to the metal. Other two electrons are then added to the Ti(IV) centre by the overlapping with $S_{\pi+}$ orbital. For all these reasons the bdt ligand stabilises $Cp_2Ti(bdt)$ because this complex can reach the ideal state of an 18-electron complex.[60] This last compound presents also the highest value for the folding angle (46°) provided by $S_{\pi+}$ and metal d-orbital mixing in energy.[59]

In conclusion, from the study conducted in previous years, the bdt folding stabilises the molecule, also lowering the total energy of the system. However, there is an other important last observation we have to report: the degree of folding destabilises also the Cp-Ti bonding, with the increase of the total energy of the system.[60] This mutual influence between bdt ligand and Cp ligand brings to a balanced situation in which stabilising effect of folded bdt and destabilising effect of Cp-Ti bonding are paired. Such balance controls the degree of folding observed in the bis-dentate ligand bdt.[60] Computational studies made by Jeanet Conradie using Density functional theory (DFT), the principal method of choice for computational studies of this kind of molecules, confirmed the studies made in previous years, highlighting the importance of the out of plane folding for maximum π-backdonation from bdt ligand to Ti metal centre.[61]

3.3.1 Our improvements with Cp*CpTi(bdt)

Bearing all these studies in mind, we decided that benzene-1,2-dithiol could have been the perfect ligand we were looking for in order to preserve the transition metal inside the complex during our planned transformations on the Cp linkers.

In order to contrast the hydrolytic instability of classical Titanocene dichloride - which could undergo hydrolysis also in physiological condition, as said in the introductory paragraph - we decided to work on asymmetric Titanocene dichloride, where one of the two Cp rings is substituted by a penta-methyl cyclopentadiene ligand **1** (Figure 3.22).[153] This product was synthetized according to the procedures found in literature, starting from the commercially available (pentamethylcyclopentadienyl)titanium trichloride (Cp^*TiCl_3) and, through a reaction of ligand exchange (Figure 3.22) operated by sodium cyclopentadienide, we obtained the desired product **1** as red-purple crystals (yield = 82%) for ligand exchange trials.[77]

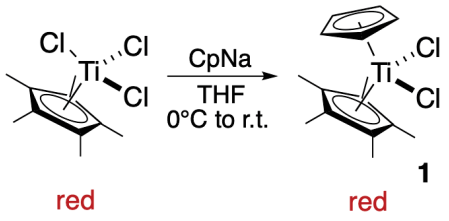

Figure 3.22: *Synthetical procedure for the pentamethylcyclopentadiene Titanocene dichloride **1** ($Cp^*CpTiCl_2$)*

Before starting with the bioorthogonal chemistry in order to modify the upper Cp ring, we decided to plan some trials to evaluate if bdt could constitute an optimal ligand, able to replace the two chloride ligands and which can resist under the condition used for the bioorthogonal transformations. For that reason, we realised the ligand exchange on **1** by using commercial benzene-1,2-dithiol (**bdt**-H_2). This protection of the Ti metal center involves the exchange of the two chloride ions of **1** with the benzenedithiolate ligand (**bdt**) in order to obtain the product **2**. The reaction occurs by heating gently to 38°C in THF, providing the dark-green complex Cp*CpTi(bdt) **2** in high yields (80%). The purification of **2** occurs easily in silica-gel without significant loss in product due to the increased stability given by the bdt ligand. It is important to remember that this reaction happens only in the presence

of trimethylamine, as reported in Figure 3.23. For such reason, we started thinking that the presence of Et_3N not only helps as a scavenger of HCl, but it is important during the initial deprotonation of the dithiol in order to form a sulfide anion which readily undergoes the ligand substitution.

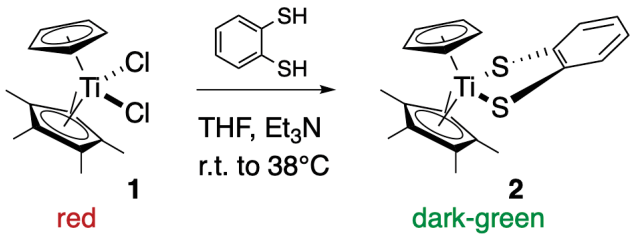

Figure 3.23: *Reaction between **1** ($Cp^*CpTiCl_2$) and **bdt**-H_2 gives the dark-green complex **2**.*

However, in order to better comprehend the real mechanism which regulates the ligand exchange we started a huge research in current and old literature: to our great surprise, we did not find a literature item which clearly explains the mechanism involved in this kind of exchange on Titanium metal centre. For such reason besides the experimental investigation on the ligand exchange, we carried out a detailed computational study, in order to define how **bdt** replaces the two chloride ligands in titanocene dichloride and also how the so obtained protected titanocene could constitute a suitable starting point to achieve the preparation of new titanocene dihalides. Indeed, as we can see below, the protecting group can be easily removed by reaction with *in situ* generated HCl (**1**), HBr (**4**), HI (**5**), and HF (**3**) in anhydrous solvents (Figure 3.24).

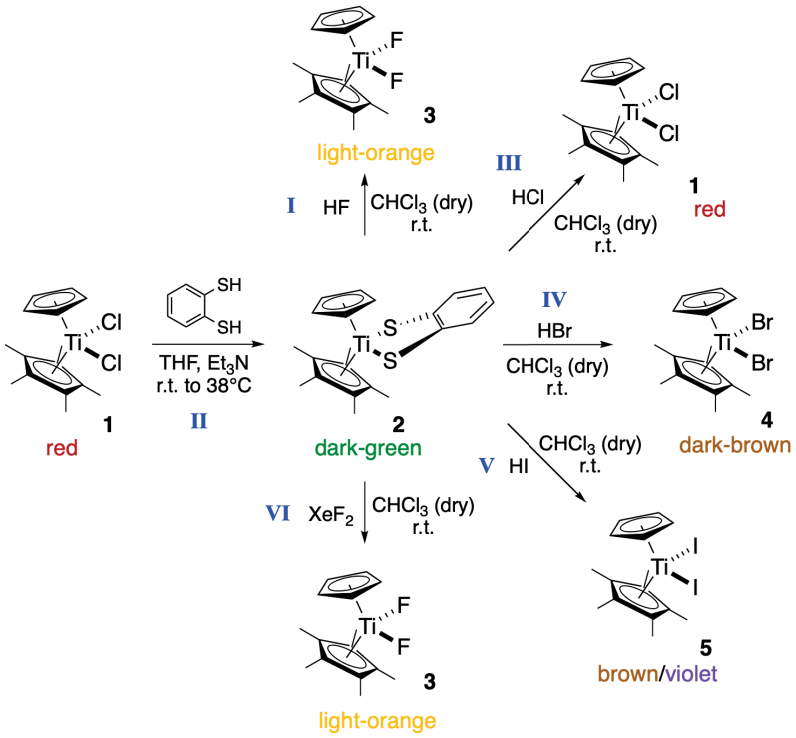

Figure 3.24: *Reaction pathways for protection and de-protection of Titanium metal centre by obtaining a range of dihalides.*

Specifically, HCl, HBr, HI were obtained *in situ* from a reaction between the corresponding acetyl derivative and methanol, while HF was prepared by the *in situ* reaction between benzoyl fluoride and methanol.[64] The so prepared solution was then added to a portion of the stock one of **2** in dry chlorofom. This general strategy let us obtain products **1**, **3**, **4**, and **5** with high yields, as reported in the Table 3.1.

HX	t (min)	Temperature (°C)	eqv	yield (%) [c]	colour	product
HCl [a]	(within seconds)	25	3	96	red	**1**
HBr [a]	(within seconds)	25	3	71	dark-brown	**4**
HI [a]	(within seconds)	25	3	84	brown/violet	**5**
HF [b]	5 minutes	25	3	81	light-orange	**3**

Table 3.1: *Ligand exchange data for different inorganic hydrogen halides. a) HCl, HBr, HI: the compound is obtained in situ from a reaction between the corresponding acetyl derivative and methanol; b) HF: the compound is obtained by the in situ reaction between benzoyl fluoride and methanol; c) isolated yield.*

As it could be seen from the table, the yields are quite high and the range of colours observed for each metal complex let us follow the reaction through a colorimetric way. What strikes one immediately is that the substitution of ligands in

the deprotection is quite instantaneous respect to the protection one reported above. For that reason, the removal of the bdt ligand does not need to be thermostated like the previous one.

Furthermore, the possibility to perform the exchange between (**bdt**)-ligand and fluoride, as reported in the last entry, showed that (**bdt**)-ligand is an optimal solution in order to obtain fluorinated products without heating to reflux overnight the chlorinated reagent together with alkaline fluoride salts.[154] Thus, this new strategy inspired us to pave the way for further studies the substitution between **bdt** and fluoride, relieing on the possibility to use the Titanocene difluoride for application in diagnosis, by simple switching ^{19}F in ^{18}F using marked reagents.[76] This is one of the most sensitive radionuclides in positron emission tomography (PET) imaging technique. Such radionuclide presents a typical β^+ decay by the emission of a positively charged particle, the positron (e^+), as reported in the equation below.

$$^{18}_{9}\mathrm{F} \rightarrow ^{18}_{8}\mathrm{O} + e^+ + \nu_e$$

This kind of decay let us visualize most interactions between physiological targets and ligands such as analogs of cellular nutrients, neurotransmitters, tumor markers and brain receptors. However, such strategy seems to be more interesting if compared to the one which involves as metal centre ^{45}Sc which then undertake a β^- decay giving ^{45}Ti, but we have to bring in mind that ^{18}F has an half-life of only 109 minutes, so all the ligand exchange and the injection in the patient has to be done within this range of time.[62] Another major drawback is the cost for ^{18}F production: indeed, the most advantageous way which is used today to produce that radionuclide in high yield involves the H_2O enriched in ^{18}O ($> 95\%$), which is treated then with a beam of protons to an energy of 16 MeV.[62] However, one of the most important advantages of $Cp_2Ti^{18}F_2$ is the high strength of the Ti-F bond (140 kcal/mol): an additional point in order to avoid undesired release of fluoride ions inside of the human body.[66] One of the biggest goals of our work was the reaction of ligand exchange promoted by XeF_2 in dry $CHCl_3$. Xenon difluoride, is a colourless crystalline solid (mp 129°C), which can be weighed and transferred in air. Most reactions with XeF_2 can be conducted in PTFE apparatus with no apparent diminution in yield. For all

such reasons, XeF_2 can be imagined as a mild version of F_2.[78] This is also one of the sporadic cases that a reaction involves XeF_2 as a "ligand exchanger" without obtaining M-F-Xe-F-M' bridged complexes, as reported in literature with similar reactions.[155] That particular reactivity let us obtaining the product **3** with a completely different strategy to the one reported above, avoiding the use of aggressive HF dry. We prepared as before a solution of the Cp*CpTi(bdt) in dry $CHCl_3$ and only in a second time we added the so prepared solution to the crystals of XeF_2. The reaction (Figure 3.25) proceeds instantaneously by leading to the desired product with 67% in yield.

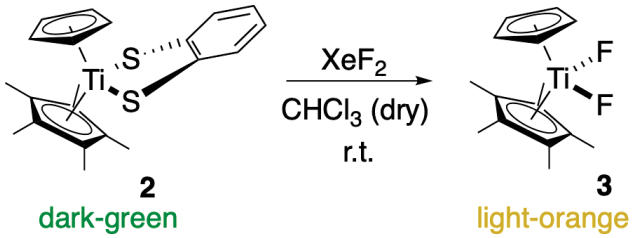

Figure 3.25: *De-protection reaction with ligand exchange taken into account.*

Xenon difluoride can be easily obtained as the ^{18}F marked analogue $[^{18}F]XeF_2$ with a proton-only cyclotron in a clinical setting, according to the $^{18}O(p,n)$ - ^{18}F nuclear reaction from $^{18}O_2$ (Figure 3.26).[80],[81]

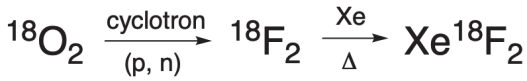

Figure 3.26: *Nuclear reaction to produce $^{18}F_2$ and the further formation of the marked analogue of XeF_2.*[80],[81]

This paves the way not only for the labelling of this compound as a fast way to obtain a PET tracer, but potentially constitutes a new useful and rapid alternative for labelling novel radiotracers with fluorine-18.[79]

3.4 Theoretical studies on ligand exchange mechanisms

To gain a better insight in the reaction mechanism which regulates both the chloride-(**bdt**) and the (**bdt**)-fluoride exchange we performed computational chemistry calculations. The ligand exchange process was investigated using the Gaussian 09 program package[156] in the framework of the Density Functional Theory (DFT). All the calculations were carried out using, as hybrid functional for DFT calculation, the Becke three-parameter hybrid exchange functional (B3)[157] in its variation provided by Lee, Yang and Parr correlation functional (LYP).[158] In the reaction with xenon difluoride both restricted and unrestricted calculations were performed; in the latter case, the stability of the wave function was checked to verify the most stable electronic state. We choose different basis sets for atoms which could present neat differences in the electronic distribution. In particular, we used 6-311+G(d,p) for C, H and F, and 6-311+G(2df,p) for S and Cl.[160] The LanL2DZ[159] basis set was chosen for the Ti as well as Xe atoms as they need to be treated with an effective core potential basis set which let us take in account also the pseudo-potentials. Frequency calculations were performed for each species in order to confirm the effective minimum or transition state nature of the optimized structures. Intrinsic reaction coordinate (IRC) calculations were also used to confirm that every transition state structure is linked with that of reactants, intermediates, or products.[161] Single point calculations, performed by using a polarizable continuum model (PCM)[162] on the optimized structure of all reagents, intermediates, products, and transition states, allowed to take into account solvent effects. All data reported below, are referred to this level of theory and the discussions are based on the values of (E) and activation (E_{att}) relative energies in kcal/mol, summed with the zero-point correction to energy of each species.

3.4.1 Titanocene structures

First of all, we investigated the structure and the geometry of the titanocene dithiolate **2** and its synthetic precursor **1**. When proper starting geometries were

optimized at the above reported level of theory, only one conformer was located for **1** whereas two different conformers, **2A** and **2B**, were obtained for **2**, due to the significant deviation of the benzene ring from the plane of titanium and the two sulphur atoms, definable by the so called folding angle θ [166] (Figure 3.27).

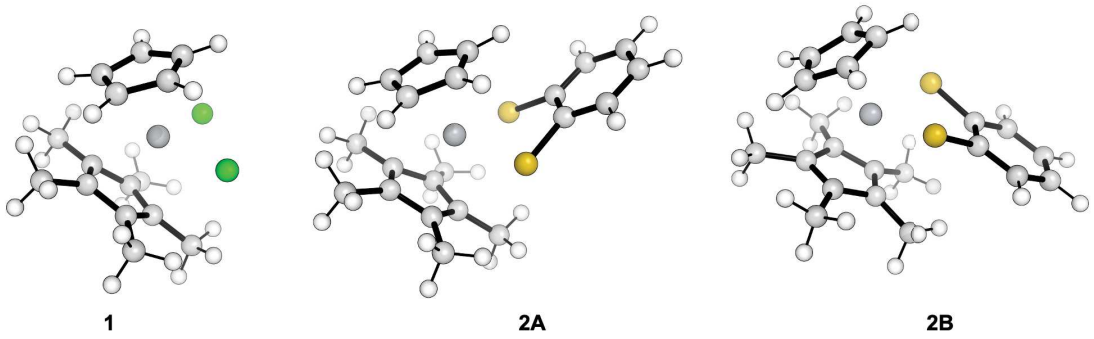

Figure 3.27: *Three-dimensional plot of the located conformers of titanocenes **1**, **2A** and **2B**.*

The importance of this out-of-plane folding has already been highlighted in a DFT computational study[61] as it allows the maximum π-backdonation from the benzenedithiolate ligand to the metal centre. It can be seen that in all the cases the methyl groups on the substituted cyclopentadienyl are bent away from the face complexing titanium, which results in a minimized steric strain. **1**, **2A** and **2B** show the typical distorted tetrahedral shape with Cl-Ti-Cl and S-Ti-S angles of 94° and 83°, respectively. The Ti-Cl bonds of **1** (2.36 Å) are slightly shorter than the Ti-S bonds of **2** (2.42 Å). The folding angle is 43° in **2A** and 40° in **2B**, with deviation of the benzene ring in opposite directions, not equivalent due to the structural difference between the two cyclopentadienyl moieties. This deviation from planarity improves the overlapping between the titanium d^0 and sulphur π orbitals which is optimal when the folding angle reaches values above 40°.[61],[17b] Though slightly smaller than the value reported by Enemark *et al.* for the crystal structure of bis(cyclopentadienyl)titanium dithiolate (46°),[59] such deviation provides the stabilization of the complex **2**, in particular in the preferred conformer **2A**, more stable by about 3 kcal/mol than **2B**, which shows a lower folding angle for the presence of methyl substituents on the substituted cyclopentadienyl ring. For such reason, all the below reported results refer to structures with the same fold as in **2A**.

3.4.2 Conversion of 2 into 1 by reaction with HCl

We started studying the transformation of titanocene dithiolate **2** into its dihalogenated derivatives with the computational approach, in order to highlight similarities and differences among the reaction mechanism underlying the different experimental procedures. The transformation of **2** into **1** appears to be a multistep reaction with several transition states and intermediates along the reaction coordinate (Chart 3.1).

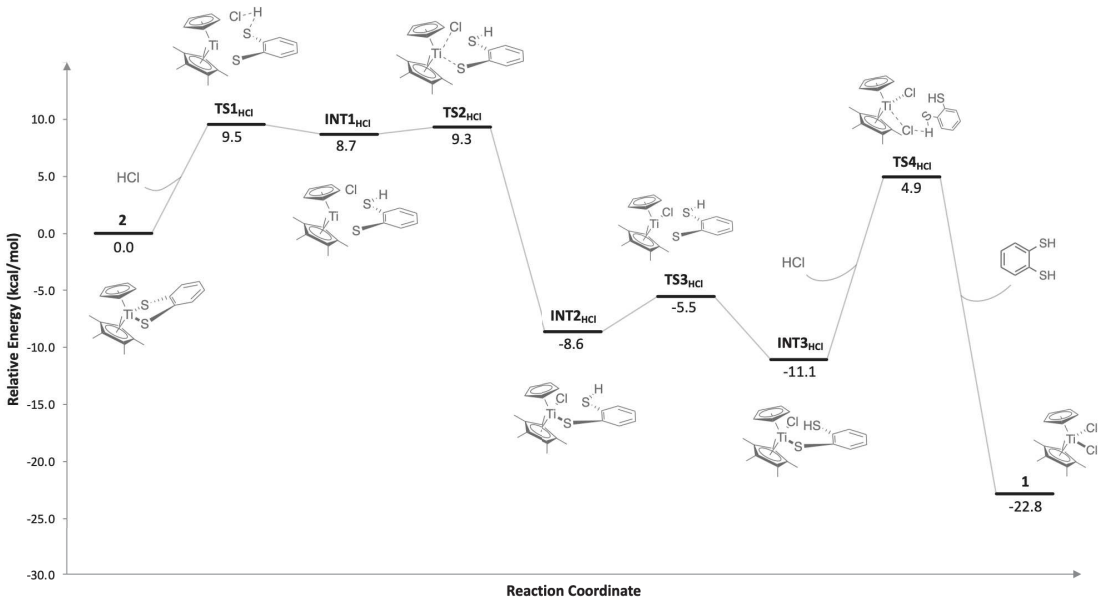

Chart 3.1: *Relative energy + ZPE diagram for the conversion of **2** into **1** by reaction with HCl in anhydrous $CHCl_3$.*

The addition of HCl results in a weak hydrogen bond towards one of the sulphur atoms of **2** and close proximity of the chloride-substituent to the titanium. The first transition state $\mathbf{TS1_{HCl}}$ results from the breakage and formation of two bonds. Via $\mathbf{TS1_{HCl}}$, the first intermediate $\mathbf{INT1_{HCl}}$ is formed in which the titanium is pentacoordinate accompanied with an elongation of the Ti-S bonds from 2.42 to 2.68 Å (Table 3.2).

After passing a very low barrier, characterized by $\mathbf{TS2_{HCl}}$, intermediate $\mathbf{INT1_{HCl}}$ transforms into the tetracoordinate mixed complex $\mathbf{INT2_{HCl}}$, in which the original length of the bond of titanium with the resting sulphur atom is restored to 2.43 Å

Specie	Ti-S(r) (Å)	Ti-Cl(r) (Å)	Ti-S(l) (Å)	Ti-Cl(e) (Å)	∠S(r)-Ti-S(l) (°)	∠S(r)-Ti-Cl(e) (°)	∠S(l)-Ti-Cl(e) (°)	∠Cl(r)-Ti-S(l) (°)	∠Cl(r)-Ti-Cl(e) (°)
2	2.42		2.42		82.73				
TS1$_{HCl}$	2.50		2.61	3.47	72.93	133.08	60.16		
INT1$_{HCl}$	2.68		2.68	2.59	68.30	136.84	68.55		
TS2$_{HCl}$	2.60		3.04	2.52	64.28	130.54	66.71		
INT2$_{HCl}$	2.43		4.39	2.37	45.64	97.30	56.94		
TS3$_{HCl}$	2.43		4.39	2.37	44.29	96.75	53.55		
INT3$_{HCl}$		2.39	2.42				57.03	96.54	
TS4$_{HCl}$		2.48	2.79	3.12			66.34	74.27	139.70
1		2.36		2.36					94.48

Table 3.2: *Optimized bond and angles measurements for the HCl promoted deprotection reaction (r = resting; l = leaving; e = entering).*

and the entered chloride substituent is bonded to the metal center with a value of 2.37 Å.

The calculation shows that the initially formed conformation of $\mathbf{INT2_{HCl}}$ is not the most stable intermediate, as rotation of the thiol group around the C-S bond allows to easily obtain $\mathbf{INT3_{HCl}}$, about 3 kcal/mol more stable than the previous intermediate. Finally, a second molecule of hydrochloric acid attacks titanium from the opposite side to that already hosting the first chloride substituent and leads directly to the final product **1** via transition state $\mathbf{TS4_{HCl}}$. It is worthy pointing out that the energy of this transition state is about 4.5 kcal/mol lower than that of $\mathbf{TS1_{HCl}}$; however, the activation barrier of the second substitution step is the highest of the entire process (about 16 kcal/mol), thus making it the rate determining step. Table 3.2 reports all the specific variations in geometry of bonds and angles observed for each species.

3.4.3 Conversion of 2 into 3 by reaction with HF

The transformation of **2** in **3** with dry HF needs longer than with HCl. The computed energy profile showed a huge difference if compared with the multistep mechanism highlighted for HCl both in the height of the energy barriers and in the

number of mechanism steps (Chart 3.2).

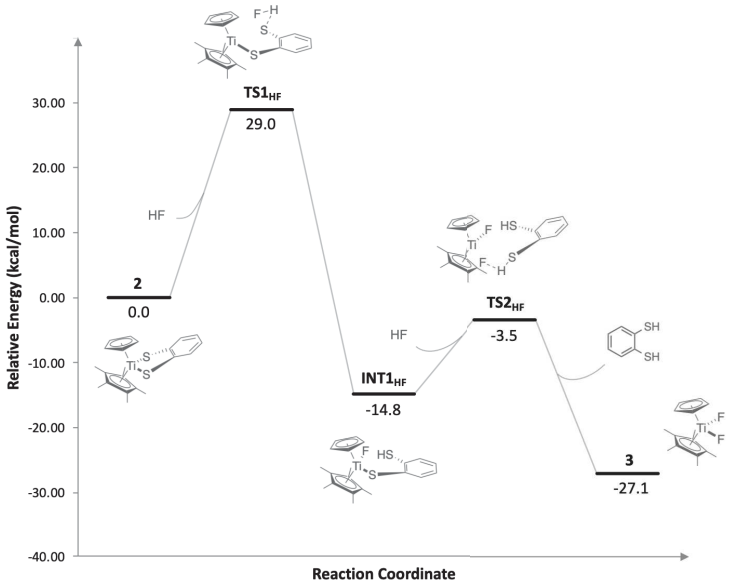

Chart 3.2: *Relative energy + ZPE diagram for the for the conversion of **2** into **3** with dry HF in $CHCl_3$.*

The first substitution represents the rate determining step of the reaction and shows an activation energy (about 29 kcal/mol) much higher than that found in the reaction with HCl, explaining the experimentally observed increased reaction time. The structure of $\mathbf{TS1_{HF}}$ shows the fluorine atom interacting with the titanium metal centre, while the hydrogen atom linked to it interacts with the leaving sulphur atom causing an elongation of the HF bond. The process is then completed when the fluoride ion binds the titanium metal centre and simultaneously loses the hydrogen atom connected by one of the sulphur atoms in the intermediate $\mathbf{INT1_{HF}}$. A pentacoordinate structures, as observed in the HCl reaction is not observed, since the direct formation of the Ti-F bond final value of 1.88 Å is energetically preferred (Table 3.3).

The second fluorine atom approaches the titanium centre in a process characterized by the $\mathbf{TS2_{HF}}$ transition state without any rotation of the S-H bond required. This second step shows a much lower activation energy than the previous one and the two products, titanocene **3** and benzene-1,2-dithiol are obtained. Again, Table 3.3 reports all the specific variations in geometry of bonds and angles observed for each species.

Specie	Ti-S(r) (Å)	Ti-F(r) (Å)	Ti-S(l) (Å)	Ti-F(e) (Å)	∠S(r)-Ti-S(l) (°)	∠S(r)-Ti-F(e) (°)	∠S(l)-Ti-F(e) (°)	∠F(r)-Ti-S(l) (°)	∠F(r)-Ti-F(e) (°)
2	2.42		2.42		82.73				
TS1HF	2.32	2.56	2.50		83.69	92.88	65.27		
INT1HF	2.42	1.88	4.30		52.18	95.85	49.57		
TS2HF		1.90	2.81	2.32			61.88	77.34	139.11
3		1.85		1.85					98.32

Table 3.3: *Optimized bond and angles measurements for the HF promoted deprotection reaction (r = resting; l = leaving; e = entering).*

3.4.4 Conversion of 2 into 3 by reaction with XeF_2

The transformation of **2** into **3** with XeF_2 proceeds much faster than with HF. At a first glance, HF might be produced when XeF_2 reacts with the used solvent. However, this scenario can be ruled out since the formation of HF from chloroform is a very slow process as long the solvent is pure and anhydrous.[78] Reaction of XeF_2 with metal complexeses is a well-known procedure to prepare the corresponding fluorides. However, mechanistically, the process involves an electrophilic attack of an F^+ with a subsequent oxidation of the metal centre.[163] Since titanium IV is the most stable oxidation state, the electrophilic mechanism can be ruled out.[164] However, the oxidative fluorination of the ditiolate sulfur ligand triggers the Ti-ligand dissociation process, thus, favoring the formation of highly reactive Ti(IV) species.[165] This process typically requires the presence of either HF or heating at temperatures of at least 80°C. Neither of them corresponds to the experimental working conditions. It should be pointed out that XeF_2 is a reagent with multiple chemical reactivity, capable of transferring fluorine as a nucleophile, electrophile and radical species. Albeit XeF_2 radical reaction on metal complexes, at the best of our knowledge, is still an unexplored area and we could anticipate that computed radical reaction manifold is able to account for the experimental data.

For all these reasons, different reaction paths were explored by performing unrestricted B3LYP calculations, in the singlet and triplet spin states, alongside the restricted calculations useful to evaluate the closed-shell singlet state. However, by applying the same high level of theory approach we used before, we were able to

locate the transition states corresponding to the initial attack of xenon difluoride to **2** only in the case of the closed-shell reaction, but not for the open-shell states. So, we tried to locate them at a lower level of theory, namely at the B3LYP/6-31g(d)&LanL2DZ level and we succeeded in finding them; the corresponding three energy profiles are reported in Chart 3.3.

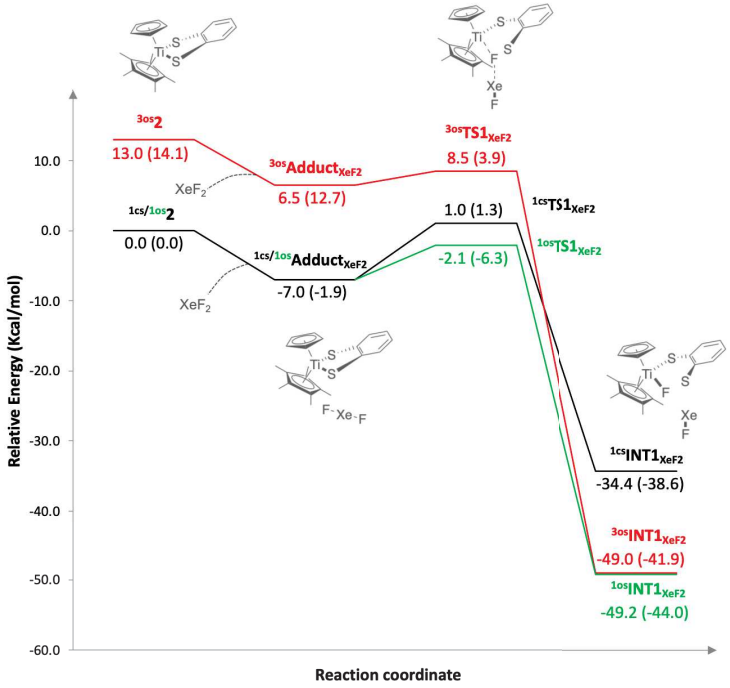

Chart 3.3: *Relative energy + ZPE diagram for the de-protection reaction with XeF_2 in $CHCl_3$. In parenthesis are reported the values for the high level of theory calculations.*

It can be seen that they are very easy processes, characterized by very low energy barriers, where the transition state $^{1os}\mathbf{TS1_{XeF_2}}$ located on the open-shell singlet surface is even more stable than the starting reagents. Then, we performed single point calculations at the usual higher level obtaining the corresponding energy value for the significant points, i.e. isolated starting reagents, reactant complex, transition state, and first intermediate, all reported in parentheses in Chart 3.3. Not unexpectedly, the open-shell reactions were shown to be downhill processes without any barrier, thus justifying our failure in locating the corresponding transition states. These barrier-less processes should not be considered a methodological error, as it is known that radical reactions often happen without a real transition state.

Anyway, a complex between the intermediate $^{1os}\mathbf{INT1_{XeF_2}}$ and the radical F-Xe

fragment, about 50 kcal/mol more stable than the starting reactants, is obtained. The xenon atom is located at a distance of 4.49 Å and 3.59 Å from the nearest sulphur and the coordinated fluoride atoms, respectively. An analysis of the spin densities showed that in the transition state $^{1os}\mathbf{TS1_{XeF_2}}$ the spin is principally located onto the sulphur atom which is directly interacting with the XeF_2 reagent (0.186) and the XeF_2 (-0.345). Furthermore, in $^{1os}\mathbf{INT1_{XeF_2}}$ an entire unpaired electron is located onto the radical ·XeF fragment (0.930) while the other one is mainly distributed among the two sulphur atoms (-0.267 and -0.372) and the benzene moiety (-0.256). Like above, in Table 3.4 are reported all the specific values of bonds and angles for the species investigated.

Specie	Ti-S(r) (Å)	Ti-S(l) (Å)	Ti-F(e) (Å)	∠S(r)-Ti-S(l) (°)	∠S(r)-Ti-F(e) (°)	∠S(l)-Ti-F(e) (°)
^{1cs}**2**	2.42	2.42		82.93		
^{1os}**2**	2.42	2.42		82.93		
^{3os}**2**	2.55	2.55		80.13		
^{1cs}**Adduct** $_{XeF2}$	2.43	2.43	4.31	82.55	148.13	66.08
^{1os}**Adduct** $_{XeF2}$	2.42	2.44	4.31	82.55	148.10	66.04
^{3os}**Adduct** $_{XeF2}$	2.55	2.55	4.04	80.00	136.29	56.63
^{1cs}**TS1** $_{XeF2}$	2.51	2.48	2.69	79.01	143.88	64.88
^{1os}**TS1** $_{XeF2}$	2.45	2.48	3.63	82.03	139.85	57.96
^{3os}**TS1** $_{XeF2}$	2.55	2.54	3.61	80.18	137.40	57.42
^{1cs}**INT1** $_{XeF2}$	2.76	2.79	1.86	70.93	136.82	66.91
^{1os}**INT1** $_{XeF2}$	2.82	2.60	1.87	72.72	141.90	69.22
^{3os}**INT1** $_{XeF2}$	2.82	2.60	1.87	72.79	141.90	69.12

Table 3.4: *Optimized bond and angles measurements for the XeF_2 promoted deprotection reaction (r = resting; l = leaving; e = entering).*

To confirm the real identity of the radical open-shell singlet species, we operated also a spin contamination analysis by observing if some contamination derives from the triplet state. While in the case of $^{1os}\mathbf{Adduct_{XeF_2}}$ the $<S^2>$ value was consistent with the ones of a perfect singlet specie (i.e. 0.00), in the case of $^{1os}\mathbf{TS_{XeF_2}}$ and $^{1os}\mathbf{INT_{XeF_2}}$, a non-negligible contamination effect arriving from higher spin states was found. In order to evaluate that effect, Yamaguchi's correction was applied to the

energy values of the open-shell singlet.[169] In both the cases a consistent stabilization of the singlet was achieved, with a transition state that becomes 2.6 kcal/mol more stable than the previous one (Table 3.5). That result is in complete accordance with the ones observed at the higher level of theory, were the reaction seems to occur without activation barrier: thus, it seems that the observed transition state derives from a spin contamination by the triplet state. This is another important plus point for a radical fashion reaction.

	E (a.u.)	$\langle S^2 \rangle$ before annihilation	$\langle S^2 \rangle$ after annihilation	f_{sc}	$E_{correction}$ (a.u.)	$E_{correction}$ (kcal/mol)
$^{1os}TS_{XeF2}$	-1884.216011	0.3603	0.0046			
triplet in OSS geometry	-1884.197424	2.0101	2.0001	0.218	-0.00406	-2.6
$^{1os}INT_{XeF2}$	-1884.289725	0.9468	0.0572			
triplet in OSS geometry	-1884.289425	2.0092	2.0000	0.891	-0.00027	-0.2

Table 3.5: *Yamaguchi's corrections for the open-shell singlet species of Titanocene species.*

The second sulphur/fluorine replacement was not computationally investigated. We suggest that spontaneous breaking of the Xe-F bond in the ·XeF fragment might lead to xenon and a fluorine radical able to replace, in a barrierless process the second sulphur atom to yield the final titanocene difluoride **3**. We only report the thermodynamics of this second step. The overall energy of titanocene **3**, a xenon atom, and the probable bicyclic byproduct **6** is 106.7 kcal/mol lower than $^{1os}\mathbf{INT1_{XeF_2}}$ and 155.9 kcal/mol lower than the starting reactants.

3.4.5 Conversion of 1 into 2 by reaction with benzene-1,2-dithiol

In this section we report the energy profile for the preparation of titanocene benzenedithiolate **2** from titanocene dichloride **1** with benzene-1,2-dithiol. It is clear that a simply reverse of the energy profile in Chart 3.1 cannot account for the experimental data, mainly for the reason that the process would be not thermodynamically favored, with a final energetical cost of about 23 kcal/mol. From our experimental trials, we know that the reaction occurs only in the presence of trimethylamine, thus

suggesting an acid-base reaction. To have a proof of this behaviour, we calculated with the method reported by Pliego *et al.*[167] the pK_a of the species involved in the reaction. However, before to proceed with the reporting of the data we obtained, it is important to give a brief summary on the method we adopted.

The value of pK_a of a specific proton in a molecule cannot be simply evaluated with a command-like input in Gaussian 09, but we need to think to the whole reaction itself and to what happens to the species involved during the removal and the solvation of the proton. Concisely, we need to think to the whole thermodynamic cycle reported in Figure 3.28, rather than the classical simple equation $HA \rightarrow A^- + H^+$.

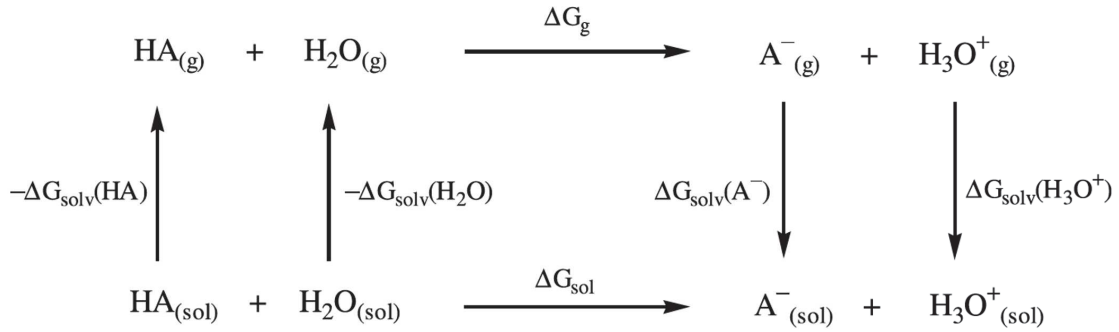

Figure 3.28: *Thermodynamic cycle used in the calculation of pK_a.*[167]

The reason is that the free proton is not a species that can be easily treated in theoretical calculations of the solvation free energy.[167] To overcome this problem, by considering the solvation of the proton as hydronium ion, helps in getting a more reliable result without the errors and problems associated with the proton alone. The translation of the above reported cycle in an algebraic equation avoids missing terms that are fundamental for the entire process. Specifically, we can consider the definition of the chemical potential μ of a specie X in solution:

$$\mu_{sol}(X) = \mu^*_{gas}(X) + \Delta G^*_{solv}(X) + RTln[X]$$

where the first term is the chemical potential of the specie X in gas phase behaving as an ideal gas in a concentration of 1M; the second is the Ben-Naim solvation free energy term in a concentration of 1M, while the last one is related to the concentration of X in solution.[167] By substituting the species involved in our case and

considering the upper chemical equation in cycle depicted in Figure 3.28, we can write down the following equation for each chemical potential of each species:

$$\mu_{sol}(A^-) + \mu_{sol}(H_3O^+) - \mu_{sol}(HA) - \mu_{sol}(H_2O) = 0$$

And substituting the general equation for each specific term leads to:

$$\Delta G^*_{solv} = -RTln\frac{[A^-][H_3O^+]}{[HA][H_2O]}$$

where

$$\Delta G^*_{solv} = \Delta G^*_{gas} + \Delta\Delta G^*_{solv} = \\ \Delta G^*_{gas} + \Delta G^*_{solv}(A^-) + \Delta G^*_{solv}(H_3O^+) - \Delta G^*_{solv}(HA) - \Delta G^*_{solv}(H_2O)$$

By moving now from the logarithmic equation to the exponential one we can re-write the second-last equation as:

$$K_a = \frac{[A^-][H_3O^+]}{[HA]} = e^{-\frac{\Delta G^*_{solv}}{RT}}[H_2O]$$

which can be rewritten in negative base-10 logarithms as:

$$pK_a = \frac{\Delta G^*_{solv}}{1.364} - log[H_2O]$$

The bulk concentration of water is taken as 55.49M. The authors, after having benchmarked the computational method, also added a correction factor to the final result as reported in the following equation:[167]

$$pK_a(corrected) = pK_a(calculated) - 4.54$$

The computational method we followed is the same we reported above: we performed geometry optimization both *in-vacuo* and water by using B3LYP functional and the same differentiated basis set. Frequency calculations were performed to obtain the thermochemical descriptors for the free energy terms. For the in-solvent

calculations we opted this time for a CPCM solvent model, following the same choice as Pliego.[167] The pK_a for the first deprotonation of benzene-1,2-dithiol resulted in a value of 3.08, while the calculated pK_a value of triethylammonium ion was 10.95, in complete agreement with the experimental value of 10.78.[168] This confirms that triethylamine is able to deprotonate benzene-1,2-dithiol to give a thiolate anion stabilized by the presence of an intramolecular hydrogen bond with the adjacent sulfhydryl group (Figure 3.29).

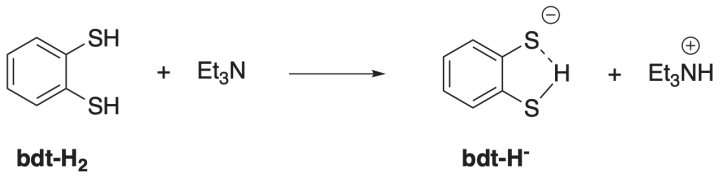

Figure 3.29: *First deprotonation of benzene-1,2-dithiol forming* ***bdt-H$^-$***.

We explored the reaction of the thiolate anion with **1** and succeeded to locate the corresponding transition state $\mathbf{TS1_{rev}}$ which can be connected to the mixed titanocene complex $\mathbf{INT1_{rev}}$ (Figure 3.30-a).

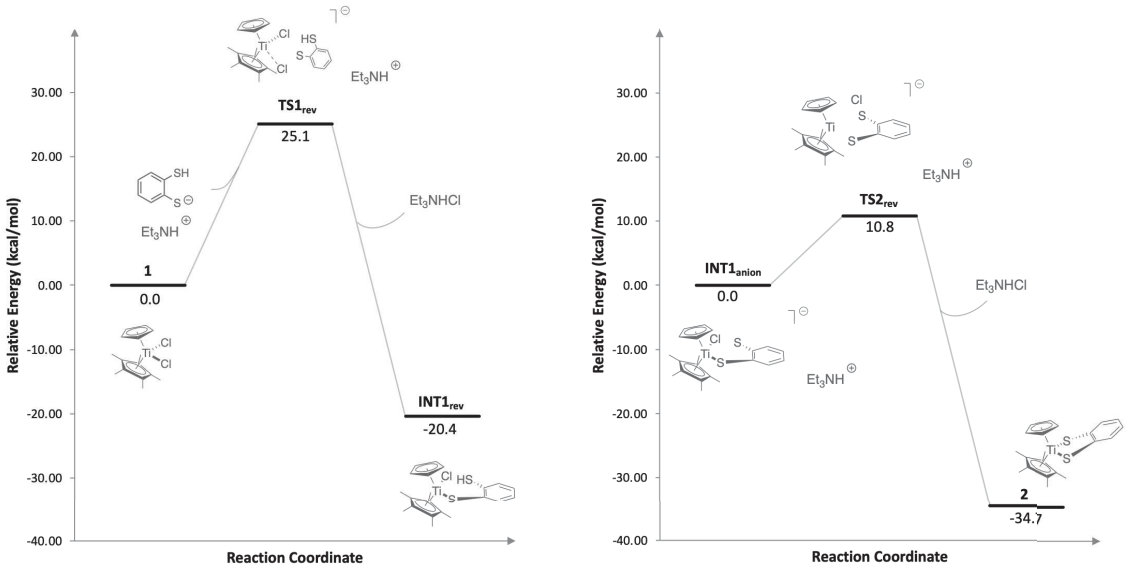

Figure 3.30: *(a-left) Relative energy + ZPE diagram for the reaction of titanocene dichloride* ***1*** *with the anion of benzene-1,2-dithiol; (b-right) Relative energy + ZPE diagram for the second step of the protection reaction.*

In agreement with the experimental conditions, a reasonable energy barrier to give an intermediate much more stable than the reagents is observed. $\mathbf{TS1_{rev}}$ is an

early transition state with the incoming sulphur atom still far from titanium (3.43 Å) even if the Cl-Ti-Cl angle is already considerably enlarged (from 94° to 129°) and ready to accommodate it. Simultaneously, the Ti-Cl bonds show a small increase from 2.36 to 2.44/2.46 Å (Table 3.6). The process completes with the definitive break of one of the Ti-Cl bonds and the formation of the new Ti-S one to give $\mathbf{INT1_{rev}}$, about 20 kcal/mol more stable than the reagents.

Specie	Ti-Cl(r) (Å)	Ti-S(r) (Å)	Ti-Cl(l) (Å)	Ti-S(e) (Å)	∠Cl(r)-Ti-Cl(l) (°)	∠Cl(r)-Ti-S(e) (°)	∠Cl(l)-Ti-S(e) (°)	∠S(r)-Ti-Cl(l) (°)	∠S(r)-Ti-S(e) (°)
1	2.36		2.36		94.48				
TS1rev	2.44		2.46	3.43	128.94	68.77	61.67		
INT1rev	2.39			2.42		96.54			
INT1anion		2.36	2.41	4.72			72.24	95.21	40.13
TS2rev		2.43	2.47	3.49			65.83	122.87	63.35
2		2.42		2.42					82.73

Table 3.6: *Optimized bond and angles measurements for the protection reaction (r = resting; l = leaving; e = entering).*

In an additional step, another equivalent of triethylamine performs a second deprotonation on the $\mathbf{INT1_{rev}}$ intermediate to give the corresponding thiolate anion $\mathbf{INT1_{anion}}$ (Figure 3.31).

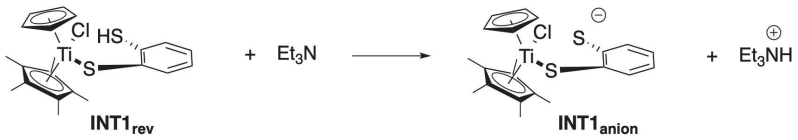

Figure 3.31: *Second deprotonation, form* $\boldsymbol{INT1_{rev}}$ *to* $\boldsymbol{INT1_{anion}}$.

The computed pK_a value for this second deprotonation was found to be 9.10. Then, the second chlorine displacement by the thiolate anion proceeds intramolecularly and very fast (Figure 3.30-b). The located transition state $\mathbf{TS2_{rev}}$ is characterized by a lower activation energy than $\mathbf{TS1_{rev}}$ to give the final product **2**, which is even more stable than $\mathbf{INT1_{rev}}$.

3.5 Experimental modifications to the Cp* ligand and click-chemistry

In parallel with the computational studies, we worked following the research line of cyclopentadienyl modifications that could be further involved in bio-orthogonal click-chemistry reactions, as we depicted before at the beginning of the chapter.[153] The modifications we performed can be divided in three big subgroups:

1) Modifications with strained alkyne moieties that can be involved in SPPAC reactions;

2) Modifications with strained alkenes and alkynes that could undergo iEDDA reactions;

3) Modification with carboxyl acid group that can easily undergo condensation forming stable amidic bond.

Before to start showing the synthesis of the linkers we developed, it is important to give a fast explanation on the types of click reactions we are going to perform: specifically, SPAAC and iEDDA.

3.5.1 Strain-promoted azide-alkyne cycloaddition (SPAAC)

In order to find the best conditions to modify our Titanocene derivative on one of the two cyclopentadienyl ligands, we looked for some studies conducted in the field of bioorthogonal cycloadditions. In particular, a work reported by Houk and co-workers, showed a beautiful computational analysis for the mechanism and reactivity of bioorthogonal reactions.[122] As it is possible to observe from this article, they investigated with the *Distortion/Interaction Model* the relative reactivities of a series of 1,3-dipoles, the tendencies for cycloaddition reactivities of cyclic alkenes and alkynes, and the mutual orthogonality of different bioorthogonal cycloadditions.[122] All such studies were realised by looking at the influences of electronic and steric factor, as well as regio- and stereo-chemistries.[122] They focalised their attention on those reactions that could be easily accessible in order to form five-membered

heterocycles (1,3-dipolar cycloadditions) and six-membered carbocycles or heterocycles (Diels-Alder reaction and its variants).[122] An essential condition for *in vivo* applications of bioorthogonal targeting, is that the rate constants for the cycloaddition reactions should be 1 $M^{-1}s^{-1}$ or higher: only this condition let us decrease the concentrations needed for the reaction by entering in the safety range for the subministration in a living system.[122]

In the field of bioorthogonal reactions, several groups tried to accelerate the rate of the reaction not by using a metal catalyst, but by activating the alkyne substrate. In fact, the presence of metal like Copper (I) salts or Rutenium (II) salts in order to catalyse azide-alkyne cyclodditions, could not be translated for *in vivo* applications due to the high cytotoxicity of these metals.[82] This successful development was at the basis of what we now know as ***Strain-promoted azide-alkyne cycloaddition*** (SPAAC): the copper-free click-chemistry.[93] The first example of this new type of reactions was reported for the first time in 2004 by Bertozzi and co-workers. They used a cyclooctyne derivative (OCT) where the ring strain was used in order to provide the activated partner for the reaction with an azide by giving stable 1,2,3-triazoles, as reported in Figure 3.32.[94]

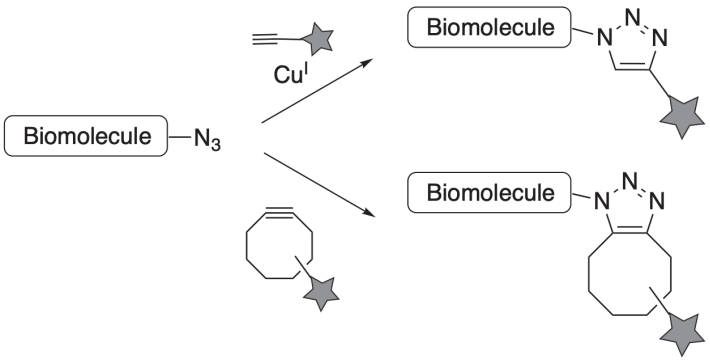

Figure 3.32: *General scheme to differentiate the CuAAC mechanism (specific for terminal alkynes) from SPAAC mechanism (specific for strained alkynes).*[86]

This type of chemistry was found to be very useful in labelling proteins, and also in protein modification and tissues reengineering.[123] Other interesting applications for such reactions were recently found in material sciences.[124] The interest in SPAAC is emerged thanks to the possibility to exclude toxic metals, but also we

have to remember that such reactions are highly efficient even at room temperature in physiological conditions.[126]

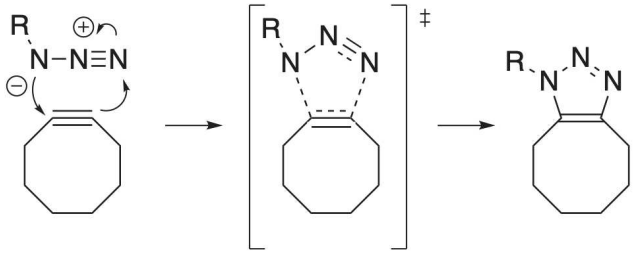

Figure 3.33: *The general reaction showing the strain-release azide-alkyne cycloaddition.*

In order to better comprehend the real mechanism for this reaction, density functional theory calculations were made under the B3LYP hybrid functional parameters.[125] By looking at the transition states of cycloadditions of phenyl azide with acetylene and cyclooctyne it was found that the fast rate of the SPAAC reaction is due to a lower energy required for the distortion ($\Delta E_d^{\ddagger}$) of the 1,3-dipole and the alkyne during the transition state (Figure 3.34).[125],[127]

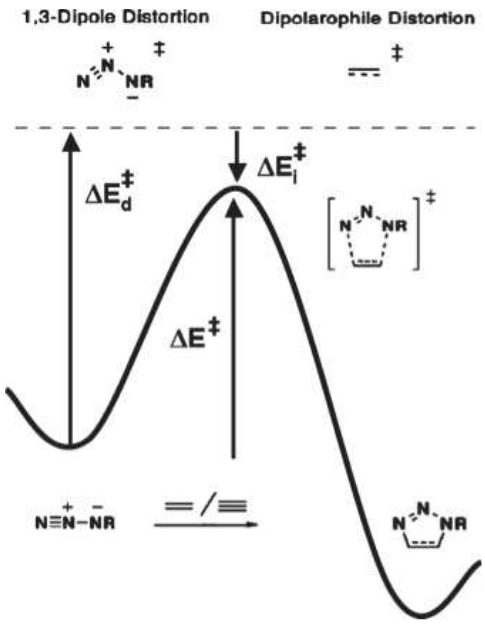

Figure 3.34: *Relationship between activation ($\Delta E^{\ddagger}$), distortion ($\Delta E_d^{\ddagger}$) and interaction energies ($\Delta E_i^{\ddagger}$).*[127]

In recent years, a greater number of cyclooctyne derivatives were reported in order to increase the rate of the reaction. As it is possible to observe in Figure 3.35,

they contain heteroatoms inside of the cyclooctyne ring and it was found that the inclusion of a cyclopropane ring could enhance up to 70-fold the reactivity.[95]

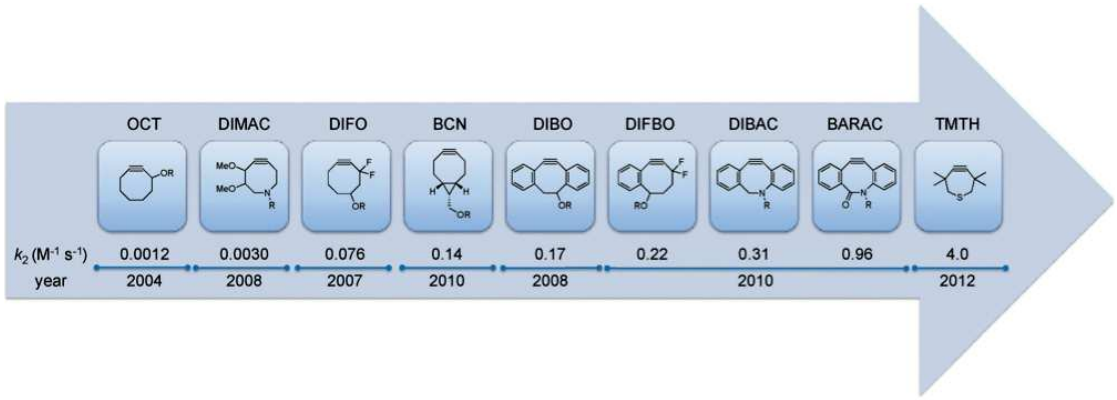

Figure 3.35: *General scheme that shows the evolution of strained alkynes and the improved kinetics for SPAAC reactions.*[82]

3.5.2 Inverse-Electron Demand Diels-Alder (iEDDA): tetrazine ligation

The reaction between an alkene and a 1,2,4,5-tetrazine was found to be an extremely fast, with the second-order rate constant near to 2000 $M^{-1}s^{-1}$.[98] The so called ***Tetrazine ligation*** was reported separately for the first time by the groups of Fox[98] and Hilderbrand[99] in 2008 and it was inspired by the previous work of Sauer.[100]

In particular, this type of reaction presents a specific behaviour which is interesting to observe. Firstly, this is an "*inverse Electron demand Diels-Alder*", better known with its acronym as iEDDA or Carboni-Lindsey reaction.[130] Such type of reaction was firstly used for the synthesis of pyridazines[130], but quite soon (2008) was admitted their importance as potential metal-free click chemistry reactions.[98],[99]

In order to better comprehend this reaction and how they could be assimilated to Diels-Alder reactions, we have to look at the intimate mechanism that is involved (Figure 3.36).

Tetrazine (Tz) and an opportune dienophile react in an inverse electron demand hetero-Diels-Alder (ihDA, TS) -retro-Diels-Alder (rDA, a) reaction cascade[132] to

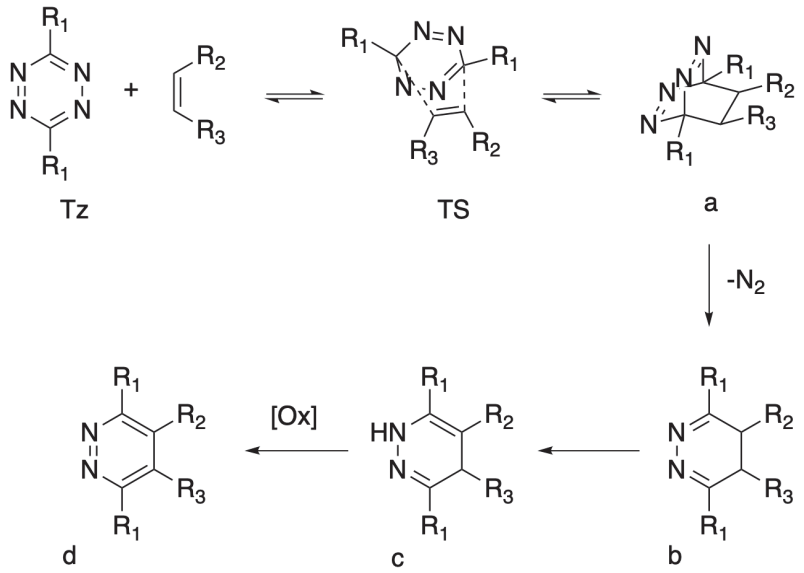

Figure 3.36: *The general reaction mechanism for iEDDA reactions.*[131]

form dihydropyridazines (b) which could be successively oxidised to the corresponding pyridazines.[131] In particular, the highly strained bicyclic intermediate (a) is the product of the iEDDA [4+2] cycloaddition: this is the RDS of the whole concerted reaction, due to the second-order kinetics between tetrazine (Tz) as diene and alkene as dienophile.[131] Thus, the initially formed bicyclic adduct (a) could undergo a rapid conversion in a retro-Diels-Alder step, with release of N_2 to form the corresponding 4,5-dihydropyridazine (b).[131] Then, a 1,3-prototropic isomerisation leads to the 1,4-dihydro-isomer (c): this one could be oxidised to finally produce the stable pyridazine product (d).[131] The in-depth study for these final steps is still missing: firstly, due to the poor importance in the study of the steps which follows the rDA one, and secondly the low interest in studying the site of conjugation when iEDDA are used as a conjugation tool.[131] However, the peak observed for the NH group is still present near to 8.5-9 ppm after some time. Of course we could not make a general rule because of the dependence from the type of the alkene used for stability of intermediate (c). In order to achieve the final (d) product sometimes oxidants are needed.[131] It is worth mentioning that if alkynes are used as dienophiles, the final product will be directly the (c) pyridazine, without passing from oxidation steps.[131]

Fox and co-workers reported the reaction of *trans*-cyclooctene with dipyridyltetrazine to form the ligation product as reported in the Figure 3.37.[98]

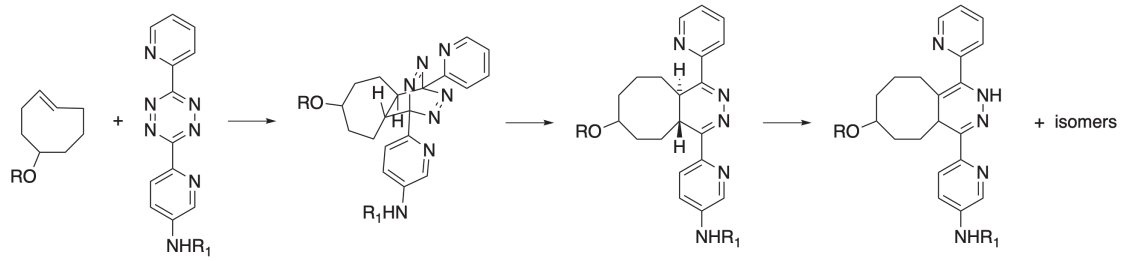

Figure 3.37: *Reaction developed by Fox and co-workers for the first tetrazine ligation trough an iEDDA mechanism.*[86]

As it is possible to observe, the reaction proceeds through an intermediate that evolves by loosing N_2 to yield the final product. Some isomerisations may occur in order to provide the more stable products.[86]

Hildebrand and co-workers discovered another interesting application of this reaction. They tried to react a tetrazine group with a norbornene as a strained alkene in order to increase the rate of the reaction. This reaction proceeds with the same mechanism of the previous one, but it does not occur as rapidly as the tetrazine ligation reported by Fox and co-workers (Figure 3.38).[99]

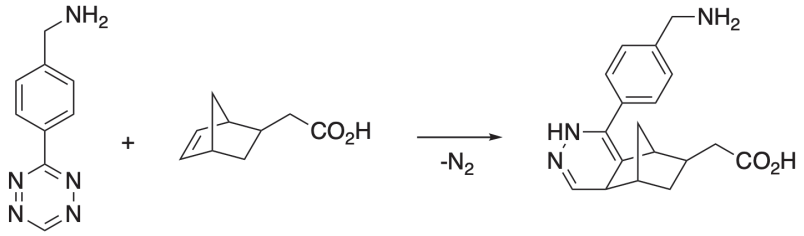

Figure 3.38: *Reaction developed by Hildebrand and co-workers for the first tetrazine-norbornene ligation.*[99]

Because of the consistent dimensions of both norbornene and *trans*-cyclooctene, in order to increase the rate of the reaction for tetrazine ligation, the groups of Devaraj and Prescher developed independently a new activated reaction partner. It was the smallest strained alkene: cyclopropene.[102],[103] It is an interesting bioorthogonal reporter due to its absence in most eukaryotes cells and thanks to its small size. However, it has not only *pros*, but it has also a challenging *con*: at room temperature the non-substituted cyclopropene is susceptible of both nucleophilic attack and polymerisation.[82] To overcome these problems the group of Devaraj developed a strategy to increase its stability against polymerisation, without lose reactivity with

tetrazines. In particular, they added a methyl group on the alkene, as reported in Figure 3.39.[103]

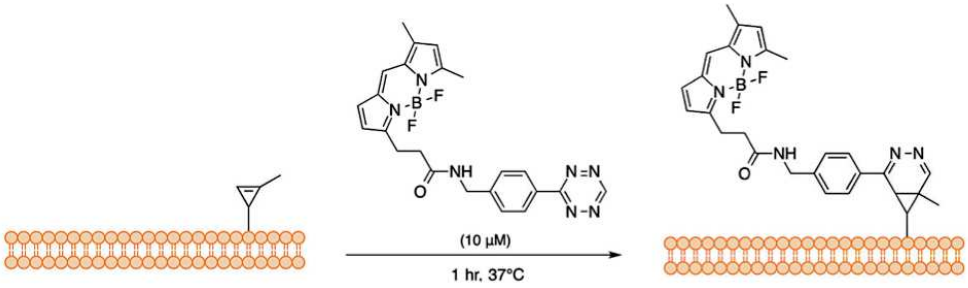

Figure 3.39: *Cell-surface labelling via tetrazine ligation using cyclopropene as a bioorthogonal reporter.*[82]

It is interesting to observe that further researches were conducted in order to increase the reactivities and to find the best partners to realise the iEDDA reaction. This work was firstly realised by Sauer *et al.*, who conducted studies on mechanisms and kinetic optimisations.[133],[134]

In Figure 3.40 we report a summary of their studies to better comprehend the general trends of reactivities.

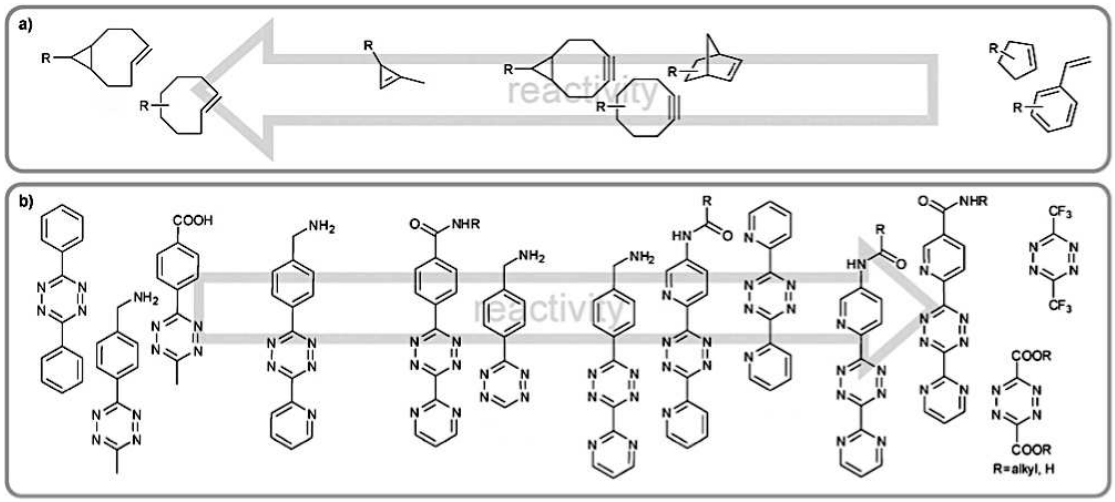

Figure 3.40: *General trends of reactivities for dienophiles (a)*[133] *and tetrazines (b)*[134] *used in iEDDA reactions.*[131]

In order to decide how a substituent could influence the reaction, it should be interesting to remember the frontier orbital theory.[132] In particular, Diels-Alder reactions can be divided into three types (Figure 3.41): (a) *neutral* Diels-Alder additions show a similar ΔE between HOMO and LUMO of both the reactants; (b) *normal* Diels-Alder additions show a reduced separation between $HOMO_{diene}$ and $LUMO_{dienophile}$ and this governs the reactivity; (c) *inverse electron demand* Diels-Alder additions show the opposite situation respect to the *normal*-DA, with a reduced separation between $HOMO_{dienophile}$ and $LUMO_{diene}$.[135]

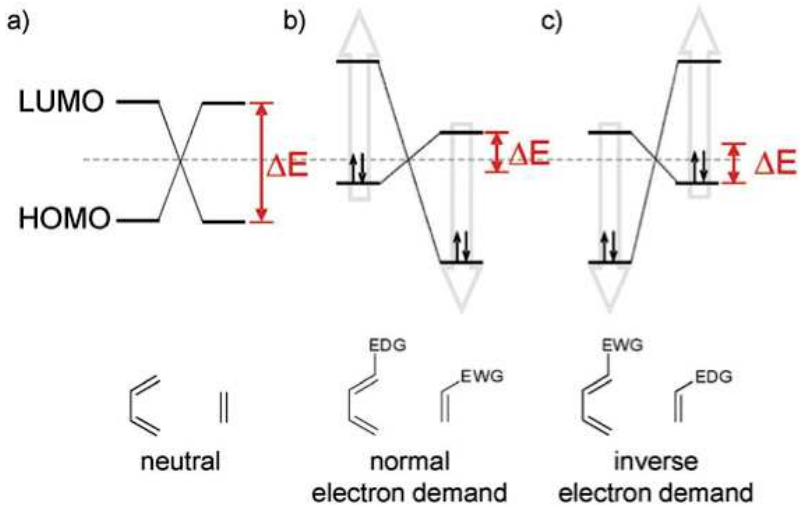

Figure 3.41: *Frontier orbital model for (a) neutral, (b) normal and (c) inverse electron demand Diels-Alder additions.*[131]

It is interesting to observe that electron-withdrawing groups (EWG) at 3- and 6-positions of the tetrazine, lower the LUMO of the diene, while the presence of an electron-donating group (EDG) on the dienophile raises the energy of the HOMO of the dienophile: both these two crossed mechanisms accelerate the iEDDA rates.[132]

Another remarkable topic is the steric effect: sterically demanding substituents on both tetrazine and dienophile, raise the distortion energy ($\Delta E_d^{\ddagger}$) needed to achieve the TS as mentioned before.[136] On the other side the presence of ring strained dienophiles (cyclooctyne, norbornene, cyclopropene, ecc.) facilitates the iEDDA reaction because of the reduction in activation energy ($\Delta E^{\ddagger}$).[136]

Finally, the role of the solvent used, and in particular its polarity, was found to be small and only the presence of water could increase drastically the rate of the

reaction.[135]

It is interesting to observe now three most impressive features of iEDDA reactions: fast reaction rates, bioorthogonality and mutual orthogonality with other click reactions.[131]

Firstly, despite the other classical click chemistry reactions, in iEDDA both reaction partners can be used to modulate the reaction speed, reaching sometimes a range of reactivity that spans nine orders of magnitude. Such high reactivity inspired some research groups to prepare ^{18}F-labeled PET-tracers by iEDDA conjugation to a biomolecular compound, perfectly remaining within the time limit of 110 minutes, which corresponds to the half-life of ^{18}F.[131]

Secondly, for bioorthogonal reactions a general prerequisite is needed: the functionalities used in the conjugation chemistry must be absent in natural biomolecules and, of course, the perturbation in the biomolecule imposed by conjugation must be irrelevant in order to grant the natural bioactivity.[138] In this case, the advantage of iEDDA not only cover the absence of tetrazine groups in biomolecules, but also the lack of need of copper catalyst pave the way for life science applications.[138] Interesting is the possibility also to operate DNA modifications and genetic encoding by operating on the "amber" UAG codon.[131]

Thirdly, iEDDA showed a very extended mutual orthogonality with other click reactions. In particular one of the most appealing feature is the complete orthogonality with azide-alkyne chemistry, allowing these two reactions to take place together in a "one-pot fashion".[98] However, under harsh conditions the respective "cross-reactions" between iEDDA on alkenes and AAC on strained cycloalkynes were observed, as shows Figure 3.42.[131]

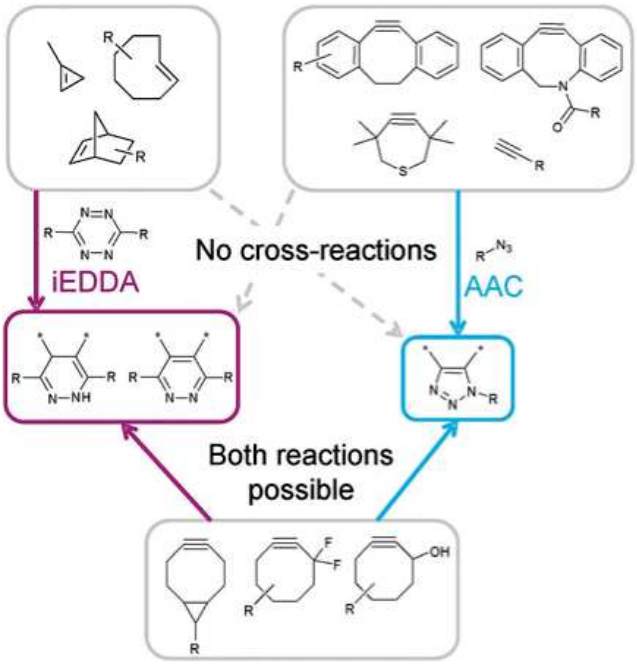

Figure 3.42: *Mutually orthogonal partners for azide-alkyne and iEDDA click chemistry.*[131]

3.5.3 Strained alkyne-ligand synthesis

The first synthesis of the strained alkyne for a selective SPAAC reaction was firstly performed years ago in our laboratory by Dr. Andrea Gandini.[153] Specifically, we opted for the cyclooctyne structure, because (as reported in the above figure) it opens wide possibilities in both the SPAAC and iEDDA reactions, by maintaining in both the cases high reaction rate and fast kinetics. The cyclooctyne partner can be simply prepared with a four-step synthesis starting from commercial cycloheptene. With a first reaction which involves the dibromocarbene - prepared by using potassium *tert*-butoxide as base and bromoform - the 8,8-dibromobicyclo[5.1.0]octane **6** is obtained. Then, with an oxidative insertion promoted by $AgClO_4$, the smaller ring is broken to form the enlarged eight-membered ring. The presence of the 1,6-hexanediol in the same reaction, promoted also the ligation of a linker which will be useful in the future applications of this molecule. The so obtained 6-[(3-bromocyclooct-2-en)-1-oxy]hexan-1-ol **7**, in presence of DBU, eliminates HBr in order to form 6-(cyclooct-2-in-1-oxy)hexan-1-ol **8**. Thus, this latter one is transformed in the final product 3-[(6-iodohexyl)oxy]cyclooct-1-yne **9** through a

Mitsunobu-like reaction, by using iodine and triphenylphosphine in presence of imidazole. In Figure 3.43 is reported the total synthetic process described above.

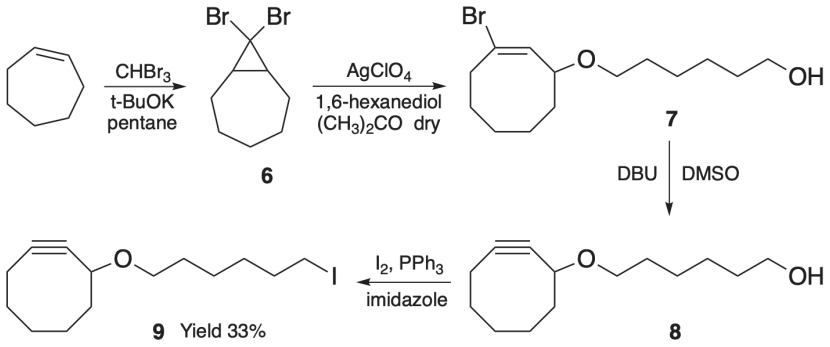

Figure 3.43: *Synthetic procedure for the synthesis of 3-[(6-iodohexyl)oxy]cyclooct-1-yne* ***9****.*[153]

Starting from this molecule we operated a S_n2 reaction with sodium cyclopentadienylide in order to replace the Iodine leaving group with the Cyclopentadinyl entering group to give 3-[6-(cyclopenta-2,4-dien-1-yl)hexyl]oxycyclooct-1-yne **10**, with an isolated yield of 92% (Figure 3.44).

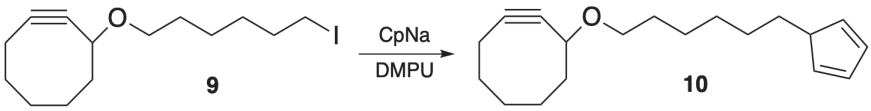

Figure 3.44: *Synthesis through* S_n2 *reaction of 3-[6-(cyclopenta-2,4-dien-1-yl)hexyl]oxycyclooct-1-yne* ***10****.*

After that, we operated the key step in order to link this ligand to the titanium metal centre. Thus we operated a ligand substitution on the commercial available (Pentamethylcyclopentadienyl)titanium(IV) Trichloride [$Cp(Me)_5TiCl_3$] in order to obtain the 3-[6-(cyclopentadienyl)hexyl]oxycyclooct-1-yn-(Pentamethylcyclopentadienyl) titanium(IV) dichloride **11**, with an isolated yield of 47% (Figure 3.45).

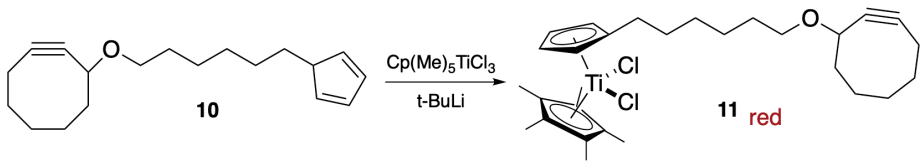

Figure 3.45: *Synthesis through ligand exchange reaction of 3-[6-(cyclopentadienyl)hexyl]oxycyclooct-1-yn-(Pentamethylcyclopentadienyl)titanium(IV) dichloride* ***11****.*

Thanks to this reaction we introduced the alkyne group on the cyclopentadienyl ligand, offering us the possibility to realise a SPAAC reaction. However, before to report that reaction, we decided to "protect" the Titanium metal centre with a benzenedithiolate (**bdt**) ligand, as reported in the previous sections. This ligand substitution let us preserve the metal from possible interactions with azido moieties acting as ligands. For such reason, we realised the dark-green 3-[6-(cyclopentadienyl)hexyl]oxycyclooct-1-yn-(Pentamethylcyclopentadienyl)-titanium(IV) (**bdt**) **12**, with an isolated yield of 56% (Figure 3.46).

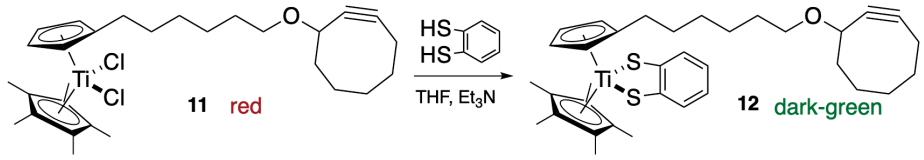

Figure 3.46: *Synthesis through ligand exchange reaction of 3-[6-(cyclopentadienyl)hexyl]oxycyclooct-1-yn-(Pentamethylcyclopentadienyl)-titanium(IV) (****bdt****)* ***12****.*

3.5.4 Strained alkene-ligand synthesis

For a selective iEDDA reaction we opted for a norbornene-based ligand, in order to assure the right tension that speeds-up the click reaction rate. We started from the commercial available 2,5-norbornadiene **13** in order to obtain the alcohol derivative *exo*-bicyclo[2.2.1]hept-5-en-2-ol **15** that will be used in the linkage on the cyclopentadienyl ligand. It is important that only the *exo* isomer has to be obtained, because of its higher stability and the possibility to have a favourable not hindered orientation for the hydroxyl group in the further steps. To prepare it we followed a procedure reported in an article by Posner and co-workers.[146] They reported a

classical addition of an organic acid on an alkene. In particular they heated freshly distilled **13** and 0.5 eqv of acetic acid at 188°C in a sealed tube for 24h.[146] We followed this procedure by using a pressure-tube in order to prevent releasing vapours. After work up we obtained the *exo*-bicyclo[2.2.1]hept-5-en-2-yl acetate **14** with an isolated yield of 15% (Figure 3.47).

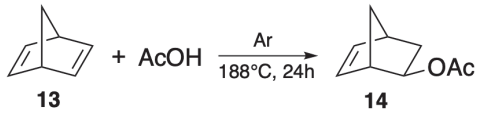

Figure 3.47: *Synthesis through addition reaction of exo-bicyclo[2.2.1]hept-5-en-2-yl acetate **14**.*

Then, in order to obtain the alcohol **15** we operated a basic hydrolysis of the ester **14**.[146] After acidification and purification, we obtained the product *exo*-bicyclo[2.2.1]hept-5-en-2-ol **15** with an isolated yield of 90% (Figure 3.48).

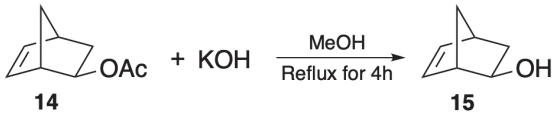

Figure 3.48: *Synthesis through transesterification reaction of exo-bicyclo[2.2.1]hept-5-en-2-ol **15**.*

We have now to illustrate how this new norbornene group could be linked to the cyclopentadienyl ligand. In fact, we cannot bind directly the hydroxyl functionality to the Cp for a very important reason: we have to avoid the possible lack of reactivity between tetrazine and a much more hindered norbornene. The use of a long linker that pushes the norbornene moiety away from the titanium centre is in this case highly recommended. For such reasons, we found in literature the possibility to realise a benzyl-norbornenyl ether by the reaction between the alcohol **15** and α,α'-dibromo-*p*-xylene.[147] We obtained the desired product α-bromo-α'-(*exo*-5-norbornene-2-ol)-*p*-xylene **16** with an isolated yield of 20% (Figure 3.49).

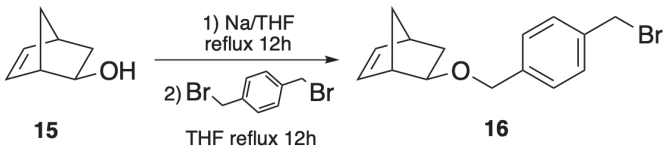

Figure 3.49: *Synthesis through S_n2 reaction promoted by alkoxide formation of α-bromo-α'-(exo-5-norbornene-2-ol)-p-xylene* ***16****.*

A second S_n2 reaction by using sodium cyclopentadienylide in order to replace the bromine leaving group with the cyclopentadienyl entering group, gives the product α-cyclopentadienyl-α'-(*exo*-5-norbornene-2-ol)-*p*-xylene **17**, with an isolated yield of 70% (Figure 3.50).

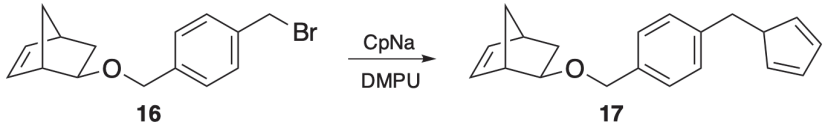

Figure 3.50: *Synthesis through S_n2 reaction of α-cyclopentadienyl-α'-(exo-5-norbornene-2-ol)-p-xylene* ***17****.*

With the so prepared ligand **17**, we used the same conditions reported above for cyclooctyne in order to realise the key step to link this new ligand to the titanium metal centre. Thus we operated, as before, a ligand substitution on the commercial available (Pentamethylcyclopentadienyl)titanium(IV) Trichloride $Cp(Me)_5TiCl_3$ in order to obtain the [α'-(*exo*-5-norbornene-2-ol)-*p*-xylene]-α-cyclopentadienyl-(Pentamethylcyclopentadienyl) titanium(IV) dichloride **18**, with an isolated yield of 48% (Figure 3.51).

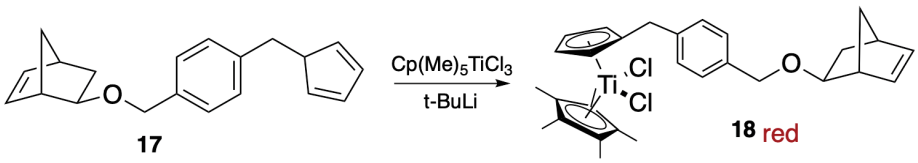

Figure 3.51: *Synthesis through ligand exchange reaction of [α'-(exo-5norbornene-2-ol)-p-xylene]-α-cyclopentadienyl-(Pentamethylcyclopentadienyl) titanium(IV) dichloride* ***18****.*

Thanks to this reaction we have introduced the alkene group on the norbornene ligand, offering us the possibility to realise a iEDDA reaction. Now, in the same

manner used for the cyclooctyne partner, we performed the "protection" of the metal centre with a benzenedithiolate (**bdt**) ligand. This ligand substitution let us preserve the metal from possible interactions with tetrazine as a possible ligand. For such reason we realised the dark-green [α'-(*exo*-5-norbornene-2-ol)-*p*-xylene]-α-cyclopentadienyl-(Pentamethylcyclopentadienyl) titanium(IV) (**bdt**) **19**, with an isolated yield of 53% (Figure 3.52).

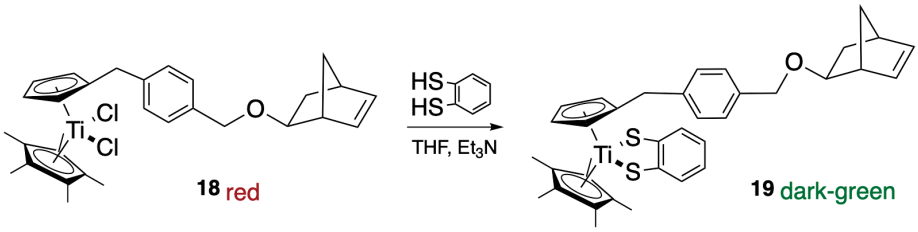

Figure 3.52: *Synthesis through ligand exchange reaction of [α'-(exo-5-norbornene-2-ol)-p-xylene]-α-cyclopentadienyl-(Pentamethylcyclopentadienyl) titanium(IV) (**bdt**) **19**.*

3.5.5 Click-reactions and Bio-imaging trials

By having these two linkers available for the click step of the synthesis, we decided to proceed in a way that could have helped us determining not only if the click-reaction has occurred, but also to further test the permeation and distribution of the titanocene complex within tumoral cells. After some research we found that a class of fluorescent dyes known as boron-dipyrromethene (BODIPY) could be used in confocal fluorescence microscopy in order to enhance the fluorescence intensity of the Titanocene derivative.[139] In particular such method could enable the non-invasive visualisation of the real mechanism of anti-tumour action for these Titanocene derivatives. In literature it is well established the BODIPY-tetrazine ligation, an useful tool in order to define the mechanism of action of some anti-tumour drugs like Taxol.[99],[101]

If we consider the typical properties of BODIPY dyes, we have to report firstly their small Stokes shift. Noteworthy, they also show high fluorescence quantum yields, sharp excitation and emission peaks that contribute to overall brightness, and high solubility in many organic solvents. The combination of all these qualities

makes this fluorophore an important tool in chemistry in order to be applied to a variety of imaging techniques.[148]

All the properties above reported are due to the presence of the 4,4-difluoro-4-bora-3a,4a-diaza-s-indacene group, which is the real core of BODIPY fluorophore (Figure 3.53).

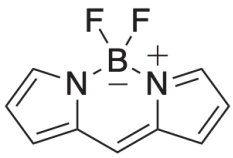

Figure 3.53: *The core of BODIPY dyes (4,4-difluoro-4-bora-3a,4a-diaza-s-indacene).*

The presence of particular substituents on the two pyrrole groups, let chemists to change and regulate the colour emitted in a very broad range of wavelengths.

Bearing all this information in mind, we decided to synthesise a BODIPY dye in order to operate a further functionalization with an azide or a tetrazine. The introduction of these functional groups will allow us to realise the same SPAAC and iEDDA reaction that we have talked about in the previous sections.

We report the whole process of synthesis for the BODIPY-FL molecule. Pyrrole **21** was prepared through a sequence of Wittig olefination reaction and catalytic hydrogenation on the commercially available 1*H*-pyrrole-2-carbaldehyde, with an overall yield of 64%. The condensation between the pyrrole **21** and the aldehyde group on the other pyrrole, followed by $POCl_3$ olefination, allowed us to obtain the asymmetric BODIPY **22** with an isolated yield of 46%.[150],[151] Then, the acid hydrolysis of the methyl ester, produced the carboxylic acid **23** of BODIPY-FL, with and isolated yield of 58% (Figure 3.54).[152]

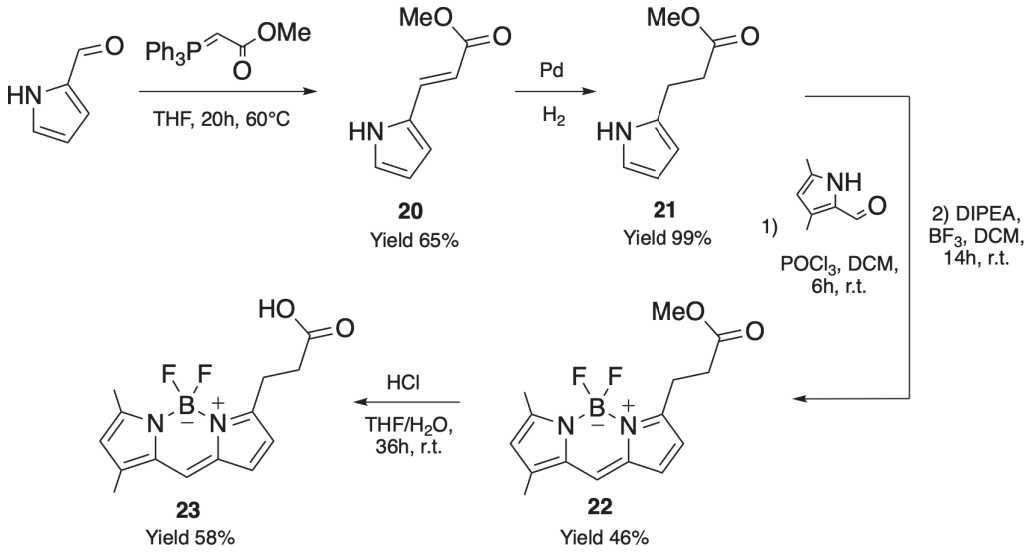

Figure 3.54: *BODIPY-FL synthesis starting from its components.*

The product **23**, was then activated as an NHS ester in order to promote the condensation with 3-azidopropanmine **24**.[120],[152] This is fundamental to introduce the azido group for the further SPAAC reaction on Titanocene cyclooctyne **12**, by obtaining the final product **25**, with an isolated yield of 38% (Figure 3.55).

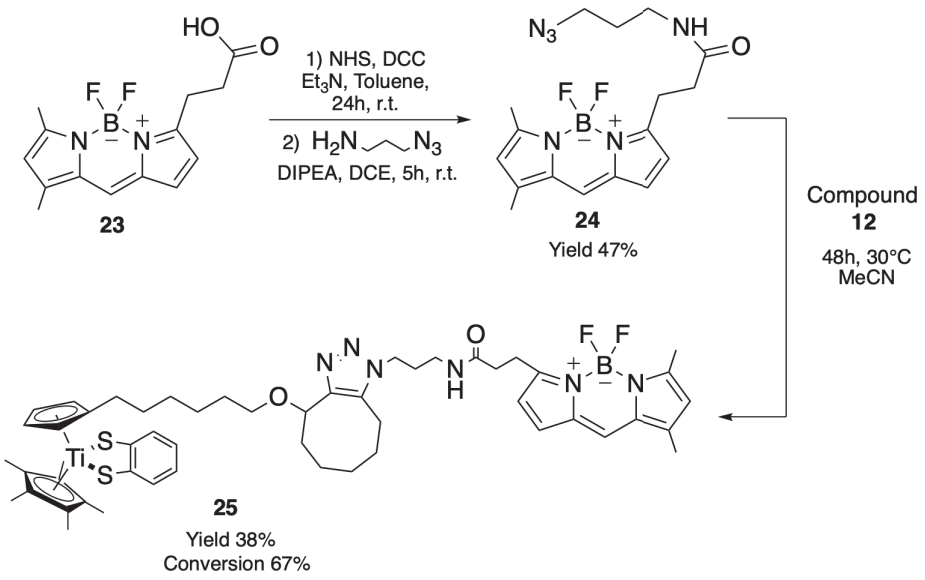

Figure 3.55: *Azido-BODIPY-FL synthesis and Titanocene cyclooctyne-**bdt** SPAAC reaction.*

Starting from product **25** we operated the ligand exchange on Titanium centre in order to obtain the difluoro complex. For such reason, we used the XeF_2 in the

same condition we reported above, obtaining the product **26** with an isolated yield of 93% (Figure 3.56).

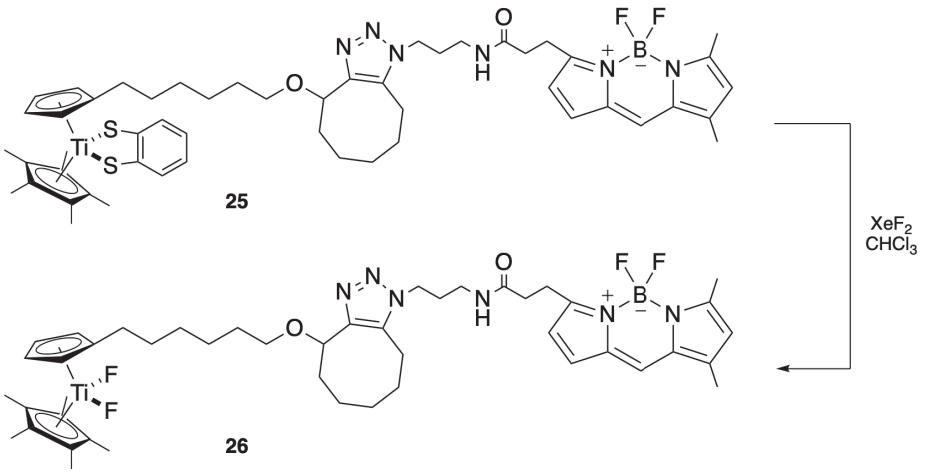

Figure 3.56: *Xenon difluoride ligand exchange reaction on BODIPY Titanocene-**bdt**.*

The so prepared BODIPY-targeted Titanocene compound **26** was further involved in biological tests in order to provide - thanks to the fluorescent dye we introduced - a first detailed overview in the location of the titanium complex within the tumoral cell. In collaboration with Policlinico San Matteo Hospital in Pavia, we run a first infusion of our complex in Pleural Malignant Mesothelioma Cells (H2452) by using a 1-10-100 μM DMSO buffered solution. *Confocal fluorescence microscopy technique* was performed by the usage of an OLYMPUS FV10i - Confocal Laser Scanning Microscope. The results we obtained after few hours of infusion with 100 μM solution of **26** were particularly encouraging, especially considering the area in which the fluorescence was located and the different shape adopted by the cells. Indeed, we were able to identify a particular *perinuclear* behaviour for the absorbed Ti-complex that can be easily understood from Figure 3.57. The three images there reported refers to the visible-fluorescence superimposed image (a), the nuclei coloured with DAPI selective stain (b) and BODIPY-only fluorescence at 503 nm (c). Soon can be observed that the Ti-BODIPY complex entered the cell and located around the nucleus. This particular behaviour is of fundamental importance because one of the most common way metal complexes exploit their cytotoxic property is to interfere directly with the DNA within the nucleus (i.e. *cis*-platin). The

other important information we can extract from this test is that the cells soon modified their shape: abandoning their slender shape and becoming more rounded is the very first qualitative data that predict an imminent apoptotic ending.

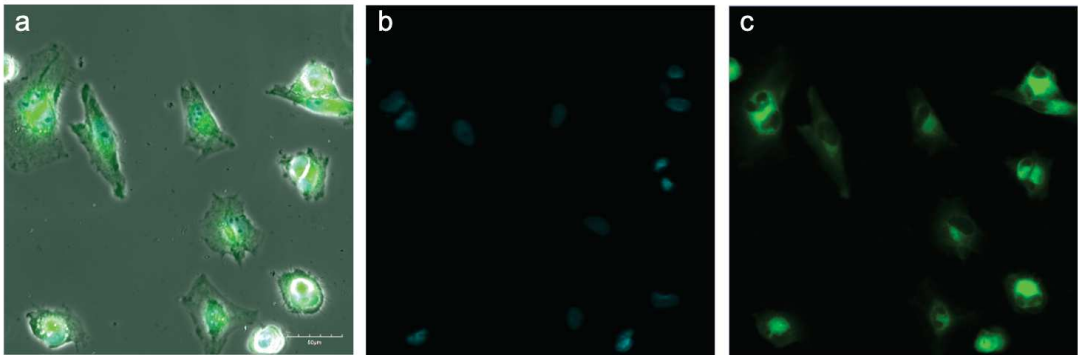

Figure 3.57: *Confocal fluorescence microscopy images with 100 μM DMSO buffered solution. a) visible light -fluorescence superimposed; b) nuclei (DAPI); c) Ti-BODIPY-26 (503 nm). OLYMPUS FV10i - Confocal Laser Scanning Microscope.*

Having obtained these important results and knowing the very well-established methodology involving BODIPY and tetrazine ligation, we performed and identical synthesis of a tetrazine-BODIPY capable to undergo iEDDA reaction with our norbornene linker.[99],[101],[153]

Specifically, we started form the commercially available [4-(1,2,4,5-Tetrazin-3-yl)phenyl]methanamine hydrochloride, which was involved in the condensation reaction with **23** in the presence of HOBt and EDCI as condensating reagent, to give tetrazine-BODIPY-FL product **27** with an isolated yield of 83%. The further click reaction with the norbornene-substituted titanocene **19** was performed in dry-THF at room temperature and after 48h the formation of product **28** was complete with and isolated yield of 92% (Figure 3.58).

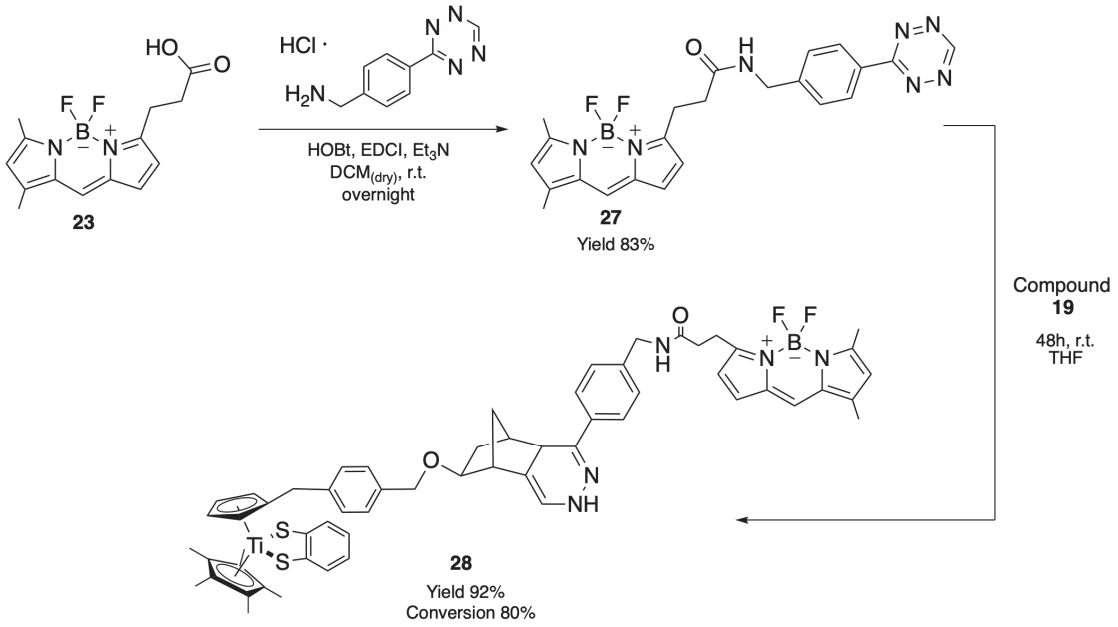

Figure 3.58: *Tetrazine-BODIPY-FL synthesis and Titanocene norbornene-**bdt** iEDDA reaction.*

3.5.6 Click-reactions with relevant biomolecular-compounds

By observing the very good results we obtained with the BODIPY-FL substituent, we decided to move our research towards an increase in the cellular uptake by using commercially available click-reagents with a biomolecular-moiety in their structures. After a very fast screening of the commercially available azide- and tetrazine-substituted biomolecules, we choose the cholesteryl-TEG-azide, the 1-[(2R,4S,5S)-4-azido-5-(hydroxymethyl)oxolan-2-yl]-5-methyl-1,2,3,4-tetrahydropyrimidine-2,4-dione and the methyltetrazine-PEG4-biotin. The first two reactant were reacted with the cyclooctyne product **12**, while the tetrazine with the norbornene substituted one **19**. Moreover, we also prepared an ethyl- and TBS-protected derivative of alendronic acid **30**. The synthesis of this protected derivative was developed in order to manage the solubility of alendronic acid, otherwise insoluble in most organic solvents. The synthetic strategy we followed was the same elaborated by Alani and co-workers in 2006, as shown in Figure 3.59.[170] Starting from commercial 4-chlorobutyryl chloride we firstly operated a one-pot Arbuzov-Pudovik reaction, obtaining the protected chloride-alendronate derivative **29** with 32% of isolated yield and subsequently we replaced the chlorine with an azide through a nucleophilic

substitution reaction, giving the azido-alendronate derivative **30** in 84% of isolated yield.

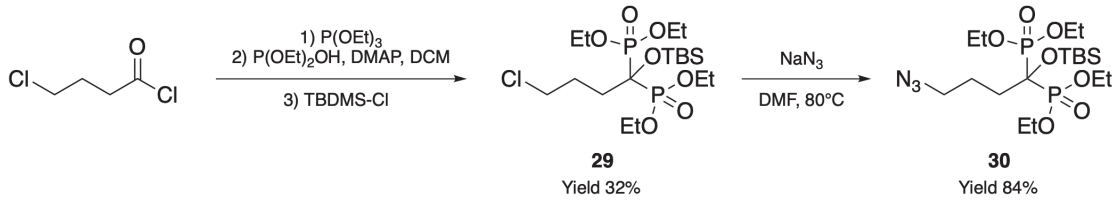

Figure 3.59: *Synthesis of protected azido-alendronate derivative **30**.*

We choose these molecules thanks to their particular properties: cholesteryl derivatives are known to be widely diffused in the body and to be metabolized in the liver though oxidative processes;[171] thymidine derivatives are known to show anticancer and antiviral properties;[172] alendronic acid derivatives mainly interact within the bone tissue by exploiting antiosteoporotic, anti-inflammatory and antitumor properties.[173] Thus, by integrating the click chemistry we reported before on our titanocenes with those bio-compounds, we are aiming not only to increase the cellular uptake, but also to add additional therapeutical properties. In Figure 3.60, the preparation of cholesteryl- **31**, thymidine- **32** and alendronate- **33** titanocene derivatives is reported. The reaction conditions are the same as reported for the previous click reactions, except for the solvent that in most of the cases involves a solution of anhydrous DCM with the addition of a small drop of DMSO to help increase the solubility of the biomolecule in the organic solvent.

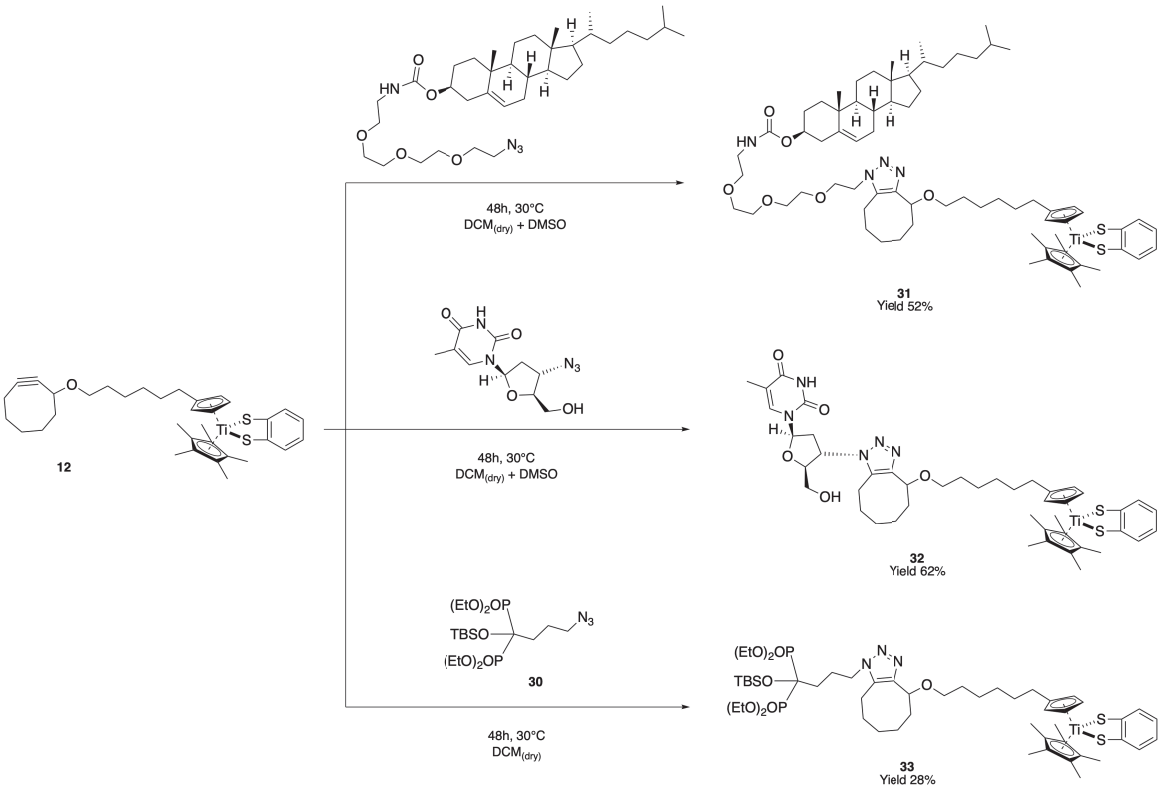

Figure 3.60: *Synthesis of titanocene-cyclooctine click products with biomolecular compounds.*

In the case of the norbornene substituted titanocene **19** we operated the click reaction with the methyltetrazine-PEG4-biotin reactant, by operating in the same conditions as above, with DCM and DMSO as solubilizing additive, just increasing the reaction temperature from 25°C to 30°C. The product **34** was obtained in 54% of isolated yield (Figure 3.61).

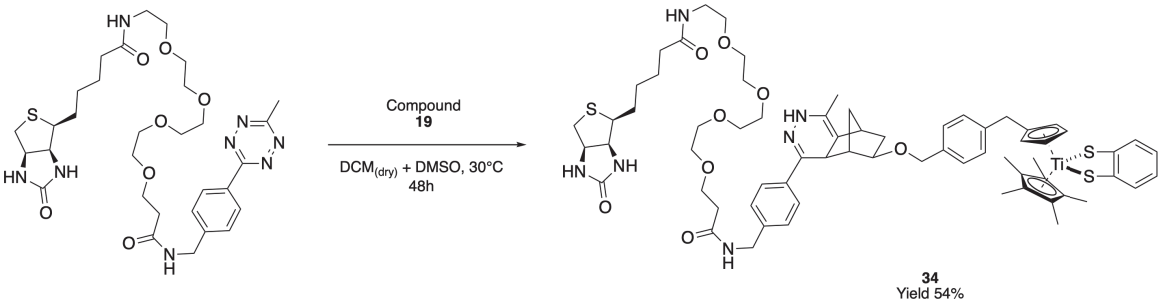

Figure 3.61: *Synthesis of titanocene-norbornene click product with biotin-tetrazine biomolecular compound.*

3.5.7 Increasing the modularity and expandability of titanocene-substituted click-reactants

The results we reported so far are extremely encouraging and constitute themselves a big step forward in tailoring the specific activity and selectivity of titanocene-based antitumoral compounds. To increase further the expandability of the possible modifications on the titanocene complex we looked for a functionality that could be easily modified, thus giving access to other different types of titanocene-click reactants. By looking at the increasing in reactivity towards a click-reaction as the tension of the unsaturated ring increase (see Figure 3.40), we would like to substitute the titanocene core with cyclopropane- or *trans*-cyclooctene-based derivatives. Contemporarily, the possibility to invert the functional reactivity by preparing titanocene-azide or tetrazine, could also increase the final applicability of the click reaction to more commercially available or easy to prepare click partners. By giving a fast look at the realm of organic chemistry bond-type, the easiest way to prepare very strong and widely usable bond is to condense an acidic moiety with a terminal amine to form the well-known *amidic bond*. This bond-type is characterized by a very strong stability mainly due to polarization and resonance equilibrium that help in stabilizing and increase its strength. Noteworthy, the main bond that is responsible of the primary structure in proteins is the amidic bond.

We thus started thinking how to realize a titanocene-acid complex capable to undergo amide-condensation with a primary amine reagent. Fortunately, in the previous years our research group developed a similar structure for different purposes: the *t*-Bu-titanocene ester **35**.[153] Indeed, this complex could easily be transformed in the corresponding acid-derivative by simply treating with concentrated TFA, giving access to the product **36** ready to be further involved in the condensation with an amine derivative (see Figure 3.62).

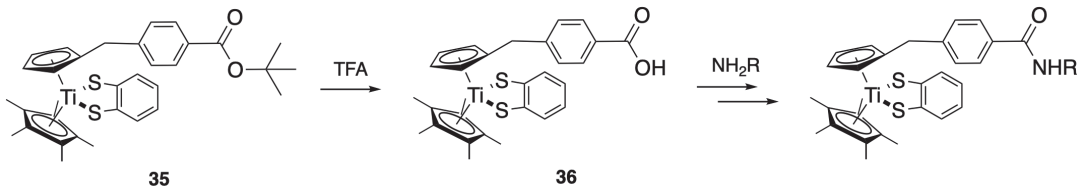

Figure 3.62: *Scheme of synthesis of titanocene-acid complex and subsequent condensation with primary amine.*

Let's report now on the synthesis of complex **35**. The synthesis of titanocene-acid **36** was planned starting from the commercially available 4-(bromomethyl)benzoic acid with its transformation to the corresponding *tert*-buthyl-4-(bromomethyl)benzoate **37** in the presence of *tert*-butyl-2,2,2-trichloroacetimidate and $BF_3{\cdot}Et_2O$, with an isolated yield of 79% (Figure 3.63). By following the same procedure adopted for the other two types of Cp-substituted titanocene complexes (see **12** and **19**), we operated a S_n2 reaction with sodium cyclopentadienylide (CpNa) to install the cyclopentadienyl moiety in the product **38**, which will be involved in the formation of the Ti-complex. The isolated yield for this second step was 76% (Figure 3.63).

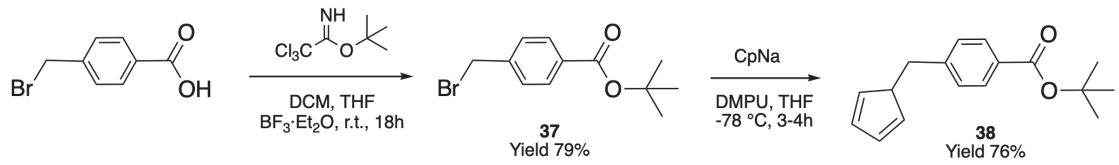

Figure 3.63: *Synthesis of tert-buthyl-4-(bromomethyl)benzoate **37** and tert-buthyl-4-(cyclopenta-2,4-dien-1-il)benzoate **38**.*

Proceeding as already shown, once obtained the ligand **38** we operated the substitution on the Cp^*TiCl_3 to give the intermediate complex **39** in 62% of isolated yield; this last one was then protected on the Ti-metal center by the use of (**bdt**)-H_2 ligand, thus obtaining the product **35** with an isolated yield of 70% (Figure 3.64).

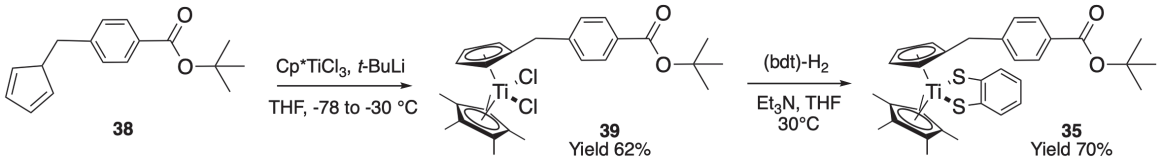

Figure 3.64: *Synthesis of tert-buthyl-4-(cyclopentadien-1-ylmethyl)benzoate-(pentamethylcyclopentadienyl)-titanium (IV) dichloride **39** and tert-buthyl-4-(cyclopentadien-1-ylmethyl)benzoate-(pentamethylcyclopentadienyl)-titanium (IV) (**bdt**) **35**.*

The final step is the ester hydrolysis promoted by the trifluoracetic acid (TFA): during this reaction step we envisioned a reaction drawback due to the presence of the trifluoroacetate anion released in solution and capable in coordinating the Ti-metal center. This particular behavior can be easily observed in the solution color, which moves from the dark green typical of Ti-(**bdt**) complexes to the dark-orange one. To avoid this undesired reactivity we solved the issue by the addition of a slight excess of (**bdt**)-H_2 ligand which moves the complexation equilibrium far from the trifluoroacetate one and towards the green titanocene-acid product **36**, with an isolated yield of 56% (Figure 3.65).

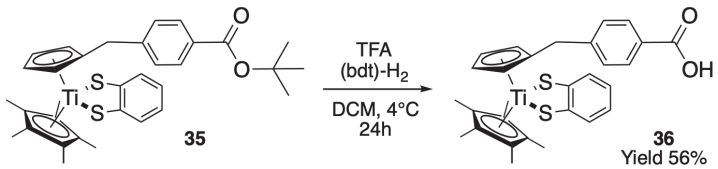

Figure 3.65: *Synthesis of acid-4-(cyclopentadien-1-ylmethyl)-benzoic-(pentamethylcyclopentadienyl)-titanium (IV) (**bdt**) **36**.*

With the so obtained titanocene acid **36** we planned a series of functionalisations by using the acid moiety and condensing it with primary amines to form amidic bonds. By having in mind the increase in reactivity depicted in Figure 3.40, we decided to use commercially available methylcyclopropene-PEG3-amine and the *trans*-cyclooctene-amine as HCl salts. Moreover, we also planned to invert the reactivity around the Ti-complex and specifically we condensed the acid with the 3-azidopropanamine and with the benzylamino-tetrazine hydrochloride. The procedure we followed for all those substituents was the same and involved the usage of EDCI and HOBt as condensing agents. The reaction was run in DCM for

3 to 4 hours and with the addition of equimolar amounts of Et_3N to neutralize the presence of HCl both in the amine salts and in the EDCI reagent. We obtained the methylcyclopropene-titanocene **40**, the *trans*-cyclooctene-titanocene **41**, the benzylamino-tetrazine-titanocene **42** and the azido-titanocene **43** products with 59%, 98%, 88% and 51% of isolated yield, respectively (Figure 3.66).

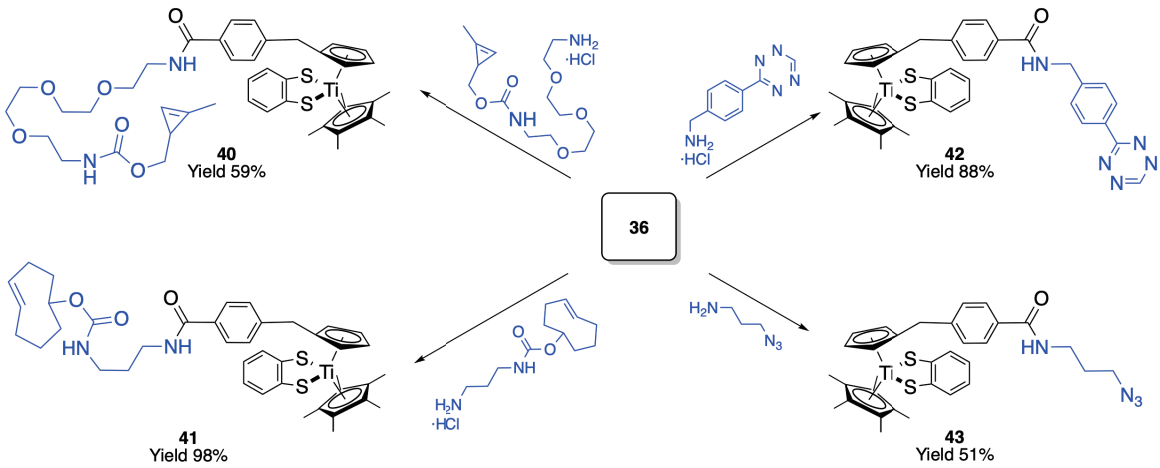

Figure 3.66: *Synthesis of titanocene-decorated products **40**, **41**, **42** and **43**. General procedure: amine-HCl salt, EDCI, HOBt, Et_3N, DCM, 0°C to r.t., 3-4h.*

3.5.8 Synthesis of the Titanocene-folate derivative

To have a last and final idea of the wide applicability of the molecules we prepared so far, we decided to test a click reaction between the product **43** and a cyclooctyne substituted folic acid derivative.[153] The folic acid is an important enzymatic cofactor which participates in numerous metabolic processes, including the synthesis of purines and pyrimidines, therefore indispensable both for the creation of new nucleic acids and for cell division. Consequently, rapidly proliferating tissues, including tumor tissues, exhibit increased expression of membrane folate receptors (FOLR1).[174] We can therefore combine our coordination complexes with Titanium (IV) with a folic acid derivative to obtain a better delivery of this within the neoplastic cell. The greatest expression of these receptors was found in renal, ovarian and mammary tumor tissues.[175] We therefore decided to use a new highly tensioned alkyne to functionalize the folic acid: the bicycle[6.1.0]-nonyne (BCN). This probe

allows to perform extremely efficient bioorthogonal click reactions even with large molecules, such as peptides, nucleic acids and monoclonal antibodies.[176] Furthermore, the BCN shows a strong hydrophilicity which turns out to be particularly suitable for bioconjugation reactions in aqueous solvents. Therefore, the strategy adopted for its synthesis starting from the commercial cyclooctadiene is reported below and follows the once proposed by Tirrell and co-workers.[177] The first reaction leads to the formation of two conformers, *endo* **44** and *exo* **45**, as shown in Figure 3.67, with isolated yields of 30% and 45% respectively.

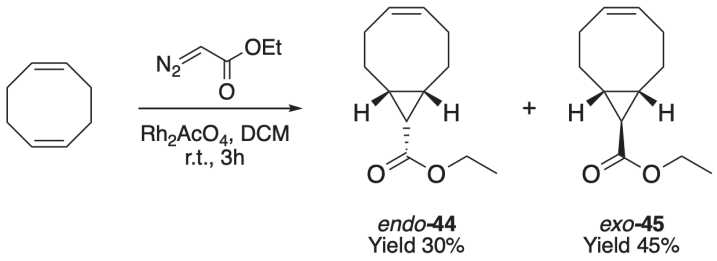

Figure 3.67: *Synthesis of (1R,8S,9s,Z)-ethyl bicyclo[6.1.0]non-4-en-9-carboxylate (endo-**44**) and (1R,8S,9r,Z)-ethyl bicyclo[6.1.0]non-4-en-9-carboxylate (exo-**45**).*

According with the studies performed by Tirrell and co-workers, they discovered that the *endo*-conformer showed the highest reactivity and for that reason we used it for the further steps of the synthesis. Specifically, the BCN-OH molecule was obtained in two steps, with the $LiAlH_4$ promoted reduction of the ethyl-ester followed by the bromination reaction of the double bond to give the crude product **46** which was further involved in the elimination step promoted by potassium *tert*-butoxide to obtain the (1*R*,8*S*,9*s*)-bicyclo[6.1.0]non-4-yn-9-ylmethanol **47** with an isolated yield of 28%. The alcoholic moiety was then activated with *N*,*N*'-disuccinimidyl carbonate (DSC) to the corresponding (1*R*,8*S*,9*s*)-bicyclo[6.1.0]non-4-yn-9-ylmethyl-(2,5-dioxopyrrolidin-1-yl)carbonate (**48**, BCN-O*Su*) with an isolated yield of 98% (Figure 3.68).

The so prepared activated BCN-O*Su* **48** will be involved in the synthesis of the folate-BCN derivative, but a few synthetical steps are also required on the commercially available folic acid to prepare a suitable functionality able to interact with **48**. Specifically, we followed the procedure reported by Afonso and co-workers with some

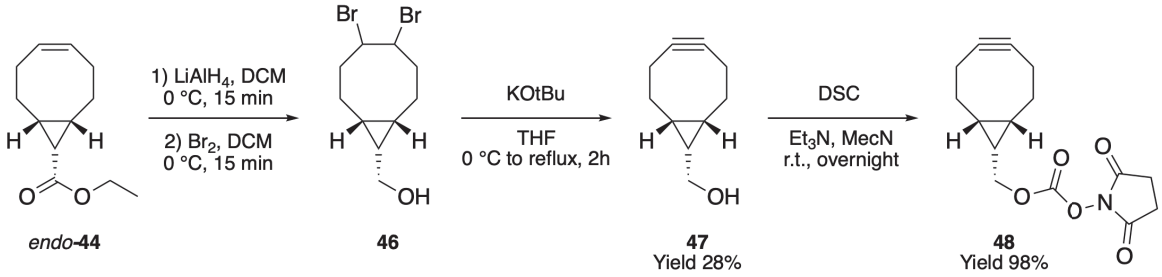

Figure 3.68: *Synthesis of BCN-OH **47** and BCN-OSu **48**.*

very small modifications.[178] The first reaction step shows a condensation between the primary acidic moiety of the folic acid with the 1,3-propanediamine, to give the 1,3-propanediamine folate **49** with an isolated yield of 73% after precipitation and centrifuge (Figure 3.69).[179]

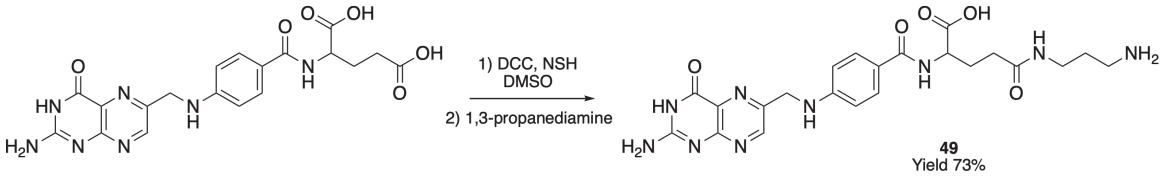

Figure 3.69: *Synthesis of 1,3-propanediamine folate **49**.*

The nucleophilic bimolecular substitution can be now performed between **49** and **48** in the presence of DIPEA to give the BCN-1,3-propanediamine folate product **50** in 73% of isolated yield. The usage of DMSO was fundamental in order to properly solubilize the reagent **49** and it constitutes also a fast choice to recover the product **50**: by washing several timed with diethyl ether and acetone, the BCN-1,3-propanediamine folate precipitates and can be collected by means of a centrifuge (Figure 3.70).

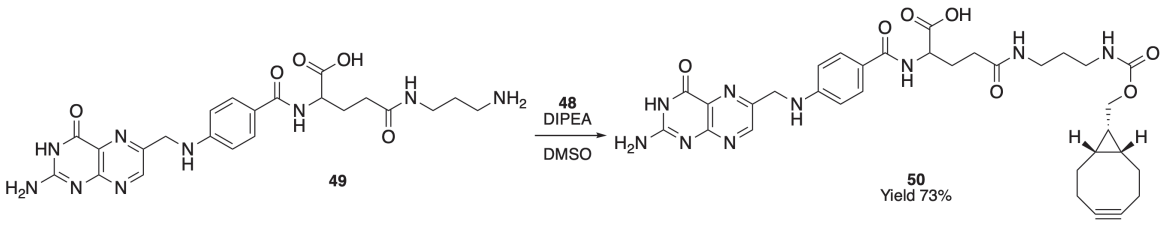

Figure 3.70: *Synthesis of BCN-1,3-propanediamine folate product **50**.*

The click reaction between Titanocene-azide **43** and the synthesized BCN-1,3-propanediamine folate **50** can finally take place: the reaction was carried out in

DMSO and the product left under stirring at room temperature for 48 hours (Figure 3.71). The so obtained titanocene-**bdt**-folate product **51**, was purified as for the previous intermediates by precipitation, centrifugation and washing with Et_2O and acetone to give 69% of isolated yield. We also deprotected the titanium metal center from the **bdt** ligand by the usage of XeF_2 reagent - as we extensively described before in the chapter - obtaining the titanocene-fluoride-folate product **52** in almost quantitative yields after 15 minutes (Figure 3.71). The only variation was the choice of DMSO as solvent due to the solubility problems of regent **51** in chloroform.

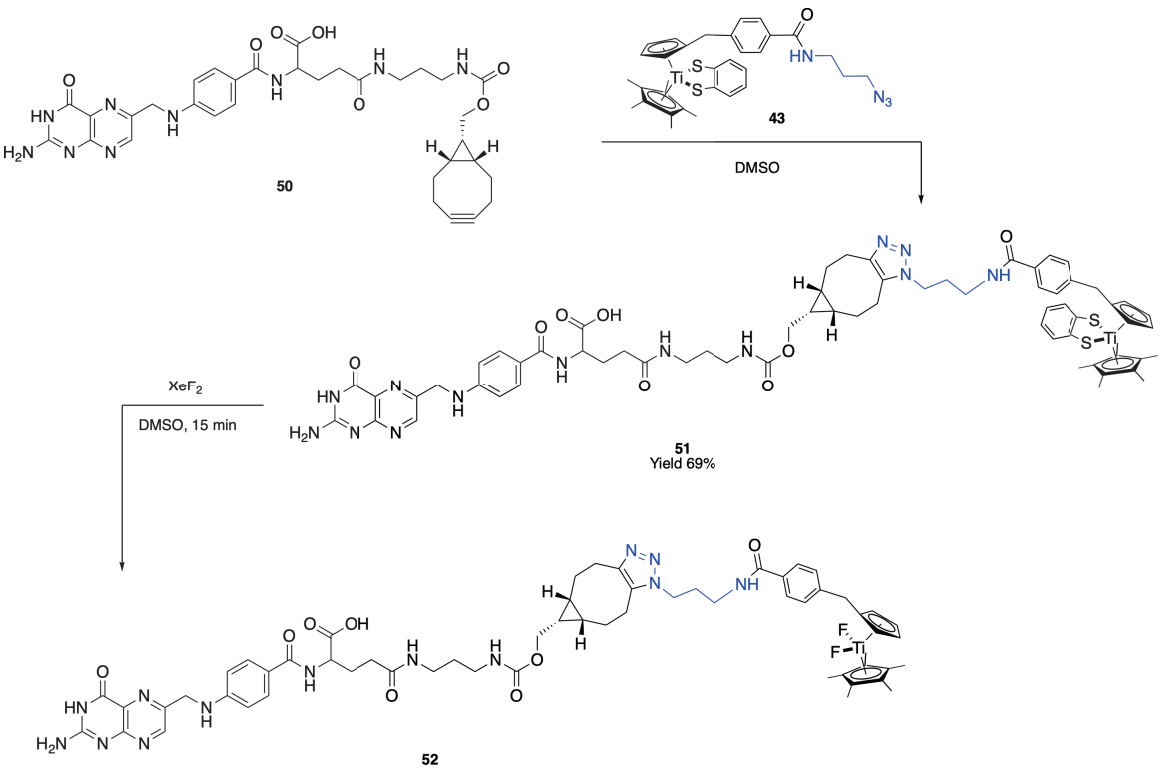

Figure 3.71: *Synthesis of titanocene-**bdt**-folate **51** and titanocene-fluoride-folate **52**.*

3.6 Conclusions

In all the ligand exchange cases investigated in this chapter, a common conclusion can be drawn. The mechanism involved in this reaction it is not just a simple associative substitution mechanism, but rather it is an *associative interchange* ($\mathbf{I_a}$) ligand substitution mechanism. The confirmation of this process derives from the

analysis of the transition states, showing that the formation of the bond between the incoming ligand and the metal is more crucial than the breaking of the bond between the departing ligand and the metal. It is also important to observe that product **3** is more stable (-27.1 kcal/mol) than product **1** (-22.8 kcal/mol). This result can be explained by the differences in dissociation energy for the bonds Ti-F (136 kcal/mol) and Ti-Cl (120 kcal/mol).[67] Furthermore, since fluorine is more electronegative than chlorine, it isn't necessary to plan pre-coordination or rotation steps: once the fluoride ion begins to interact with the electron-poor titanium metal center, the formation of the bond is the natural consequence of that interaction. This happens both during the first step and in the second one. Therefore, by observing the trend and change in behavior passing from HCl to HF, we can conclude that the reaction of deprotection operated by the use of HBr and HI will show a mechanism similar to the one found for HCl. This conclusion can be further rationalized by considering the rate reported in this work, which is similar to the one for the HCl deprotection and the decrease in electronegativity passing from HCl to HI: a condition far from the one observed for HF. The transformation of **2** in **3** using XeF_2 can be considered similar to those reported before, with the specific difference to be a process that is radical rather than ionic. No conclusions can be drawn regarding the RDS of this reaction, because of the investigation of only a single step. However, the extremely low energy barrier fits well with the immediate reaction we observed during our experimental work. This is also one of the sporadic cases that a reaction involves XeF_2 as a "ligand exchanger" without obtaining M-F-Xe-F-M' bridged complexes.[155] Moreover, we demonstrated that the protection of the Ti metal center with the easily removable bdt-ligand helps in increasing the stability of the complex during the classical silica gel purification steps and also during the click-chemistry reactions. Indeed, we were able to prepare a suitable scope of variously decorated Ti-complexes capable to undergo click reactions with biomolecules, aiming to help in increasing the activity and the cellular uptake of the metal complex. The culmination of this approach was achieved in the synthesis of the titanocene-fluoride-folate product **53**: being the folic acid an important enzymatic cofactor and the well-known behavior of tumoral cellular to overexpress the folate FLOR1 receptors, this last

compound appeared us to be particularly promising. Biological *in vitro* tests will be planned in future for the purpose of assessing its chemical-physical characteristics and any cytotoxic and anti-reproaching activity. The cells selected for this purpose are the *HeLa* ones, an immortalized tumor cell line isolated from a cervical uterine cancer.

References

[1] G. Gasser, I. Ott, N. Metzler-Nolte, Organometallic Anticancer Compounds, *J. Med. Chem.*, **2011**, *54*, 3-25.

[2] W. M. Haynes, T. J. Bruno, D. R. Lyde, C. R. Hammond, CRC Handbook of Chemistry and Physics, *CRC Press*, **2016**, 95$^{\text{th}}$ edition, 38.

[3] P. Köpf-Maier, H. Köpf, Non-Platinum-Group Metal antitumour agents: History, current status, and perspectives, *Chem. Rev.*, **1987**, *87*, 1137-1152.

[4] M. M. Harding, G. Mokdsi, Antitumour Metallocenes: Structure-Activity Studies and Interactions with Biomolecules, *Current Medicinal Chemistry*, **2000**, *7*, 1289-1303.

[5] F. Caruso, M. Rossi, Antitumour Titanium Compounds, *Mini-Reviews in Medicinal Chemistry*, **2004**, *4*, 49-60.

[6] U. Olszewski, G. Hamilton, Mechanism of Cytotoxicity of Anticancer Titanocenes, *Anti-Cancer Agents in Medicinal Chemistry*, **2010**, *10*, 302-311.

[7] Y. Dang, Cooridination chemistry of cyclopentadineyl titanium carboxylates and related complexes, *Coord. Chem. Rev.*, **1994**, *135/136*, 93-128.

[8] A. D. Tinoco, E. V. Eames, A. M. Valentine, Reconsideration of serum Ti(IV) transport: albumin and transferrin tracking of Ti(IV) and its complexes, *J. Am. Chem. Soc.*, **2008**, *20*, *130*, 2262-2270.

[9] C. V. Christodoulou, D. R. Ferry, D. W. Fyfe, A. Young, J. Doran, T. Sheehan, A. Eliopoulos, K. Hale, J. Baumgart, G. Sass, D. J. Kerr, Phase I trial of weekly scheduling and pharmacokinetics of titanocene dichloride in patients with advanced cancer, *J. Clin. Oncol.*, **1998**, *16*, 2761-2769.

[10] J. L. Vera, F. R. Roman, E. Melenex, Study of titanocene-DNA and molybdocene-DNA interactions by inductively coupled plasma-atomic emission specroscopy, *Anal. Bioanal. Chem.*, **2004**, *379*, 399-403.

[11] P. M. Abeysinghe, M. M. Harding, Antitumour bis(cyclopentadienyl) metal complexes: titanocene and molybdocene dichloride, *Dalton Trans.*, **2007**, *28*, 3474-3482.

[12] M. Hogan, M. Tacke, Titanocenes: Cytotoxic and Anti-angiogenic Chemotherapy against avanced renal-cell cancer, *Top Organomet. Chem.*, **2010**, *32*, 119-140.

[13] T. Hodík, M. Lamac, L. C. St'stnà, J. Karban, L. Koubkòva, R. Hrstka, I. Cìsarova, J. Pinkas, Titanocene dihalides and Ferrocenes bearing a pendant D-Xylofuranos-5-yl or D-Ribofuranos-5-yl moiety. Synthesis, Characterization, and Cytotoxic activity, *Organometallics*, **2014**, *33*, 2059-2070.

[14] J. Ceballos-Torres, P. Virag, M. Cenariu, S. Prashar, M. Fajardo, E. Fischer-Fodor, S. Gòmez-Ruiz, Anti-cancer applications of Titanocene-functionalised nanostructured systems: an insight into cell death mechanism, *Chem. Eur. J.*, **2014**, *20*, 10811-10828.

[15] O. Flores, A. Trommenschlager, S. Amor, F. Marques, F. Silva, L. Gano, F. Denat, M. P. Cabral Campello, C. Goze, E. Bodio, P. Le Gendre, In vitro and in vivo trackable titanocene-based complexes using optical imaging or SPECT, *Dalton Trans.*, **2017**, *46*, 14548-14555.

[16] D. Wang, S. J. Lippard, Cellular processing of platinum anticancer drugs, *Nat. Rev. Drug Discovery*, **2005**, *4*, 307-320.

[17] B. Lippert, Cisplatin, Chemistry and Biochemistry of a leading Anticancer Drug, *Verlag Helvetica Chimica Acta*: Zrich, Switzerland, **1999**.

[18] B. Rosenberg, L. Van Camp, J. E. Trosko, V. H. Mansour, Platinum compounds: a new class of potent antitumour agents, *Nature*, **1969**, *222*, 385.

[19] (a) M. J. Cleare, P. C. Hydes, D. R. Hepburn, B. W. Malerbi, In *Cisplatin: Current Status and New Developments*, Academic: New York, **1980**; (b) J. J. Roberts, In *Metal Ions in Genetic Information Transfer*, Eichhorn, G. L., Marzilli, L. G., Eds.; Elsevier: New York, **1981**.

[20] (a) M. Guo, Z. Guo, P. J. Sadler, Ti(IV) targets phosphoesters on nucleotides: implications for the mechanism of action of anti-cancer drug titanocene dichloride, *J. Biol. Inorg. Chem.*, **2001**, *6*, 698-707; (b) G. Mokdsi, M. M. Harding, Topoisomerase II inhibition by the antitumour metallocenes, *J. Inorg. Biochem.*, **2001**, *83*, 205-209; (c) C. V. Cristodoulou, A. G. Eliopoulos, L. S. Young, L. Hodgkins, D. R. Ferry, D. J. Kerr, Anti-proliferative activity and mechanism of action of titanocene dichloride, *Br. J. Cancer*, **1998**, *77*, 2088-2097.

[21] P. Köpf-Maier, H. Köpf, In *Metal Compounds in Cancer Therapy*, Chapman and Hall: London, **1994**, 109-146.

[22] P. Köpf-Maier, S. Gerlach, Pattern of toxicity by titanocene dichloride in mice. Blood and urine chemical parameters, *J. Cancer Res. Clin. Oncol.*, **1986**, *111*, 243-247.

[23] C. V. Christodoulou, A. G. Eliopoulos, L. S. Young, L. Hodgkins, D. R. Ferry, D. J. Kerr, Anti-proliferative activity and mechanism of action of titanocene dichloride, *Brit. J. Cancer*, **1998**, *77*, 2088-2097.

[24] J. H. Toney, T. J. Marks, Hydrolysis Chemistry of the Metallocene Dichlorides M(η^5-$C_5H_5)_2Cl_2$, M=Ti, V, Zr. Aqueous Kinetics, Equilibria, and Mechanistic Implications for a New Class of Antitumour Agents, *J. Am. Chem. Soc.*, **1985**, *107*, 947-953.

[25] P. Köpf-Maier, H. Köpf, Transition and main-group metal cyclopentadienyl complexes: Preclinical studies on a series of antitumor agents of different structural type, *Struct. Bonding*, **1988**, *70*, 103-185.

[26] P. Köpf-Maier, B. Hesse, R. Voigtler, H. Köpf, Tumor inhibition by metallocenes: Antitumor activity of titanocene dihalides $(C_5H_5)_2TiX_2$ (X=F, Cl, Br, I, NCS) and their application in buffered solutions as a method for suppressing drug-induced side effects *J. Cancer Res. Clin. Oncol.*, **1980**, *97*, 31-39.

[27] M. Guo, H. Sun, H. J. McArdle, L. Gambling, P. J. Sadler, TiIV Uptake and Release by Human Serum Transferrin and Recognition of TiIV-Transferrin by Cancer Cells:? Understanding the Mechanism of Action of the Anticancer Drug Titanocene Dichloride, *Biochemistry*, **2000**, *39*, 10023-10033.

[28] F. Kratz, In *Metal Complexes in Cancer Chemotherapy*, VCH Ed., **1993**, 391-429.

[29] M. M. Harding, G. Mokdsi, Hydrolytically stable derivatives of the antitumour agent titanocene dichloride and Binding studies with nucleotides, *J. Organomet. Chem.*, **1998**, *565*, 29-35.

[30] P. Köpf-Maier, W. Kahl, N. Klouras, G. Hermann, H. Köpf, *Eur. J. Med. Chem.*, **1981**, *16*, 275.

[31] M. M. Harding, G. Mokdsi, Inhibition of human topoisomerase II by the antitumour metallocenes, *J. Inorg. Biochem.*, **2001**, *83*, 205.

[32] M. Cini, T. D. Bradshawb, S. Woodward, Using titanium complexes to defeat cancer: the view from the shoulders of titans, *Chem. Soc. Rev.*, **2017**, *46*, 1040.

[33] P. Köpf-Maier, Intracellular localization of titanium within xenografted sensitive human tumours after treatment with the antitumour agent titanocene dichloride, *J. Struct. Biol.*, **1990**, *105*, 35-45.

[34] M. L. McLaughlin, J. M. J. Cronan, T. R. Schaller, R. D. Sneller, DNA-metal binding by antitumour-active metallocene dichlorides from inductively coupled plasma spectroscopy analysis: titanocene dichloride forms DNA-Cp_2Ti or DNA-CpTi adducts depending on pH, *J. Am. Chem. Soc.*, **1990**, *112*, 8949-8952.

[35] M. Guo, H. Sun, P. J. Sadler, Uptake and release of a titanium anticancer complex by human transferrin, *J. Inorg. Biochem.*, **1999**, *74*, 150.

[36] B. K. Keppler, C. Friesen, H. Vongerichten, E. Vogel, In *Metal Complexes in Cancer Chemotherapy*, VCH Ed., **1993**, 297-323.

[37] P. Pil, S. Lippard, In *Encyclopedia of Cancer*, J. R. Bertino, Ed.; Academic Press, San Diego USA, **1997**, 392-410.

[38] M. R. Berger, M. H. Seelig, A. Galeano, In *Metal Complexes in Cancer Chemotherapy*, B. K. VCH Ed., **1993**, 327-349.

[39] K. B. Keppler, M. E. Heim, *Drugs of the Future*, **1988**, *13*, 637.

[40] T. Pieper, K. Borsky, B. K. Keppler, In *Topics in Biological Inorganic Chemistry*, M. J. Clarke, Springer Ed.: Berlin, **1999**, 172-199.

[41] E. Melez, Titanium complexes in cancer treatment, *Crit. Rev. Oncol. Hematolog.*, **2002**, *42*, 309-315.

[42] K. Strohfeldt, M. Tacke, Bioorganometallic fulvene-derived Titanocene anti-cancer drugs, *Chem. Soc. Rev.*, **2008**, *37*, 1174-1187.

[43] P. Köpf-Maier, Histologic and ultrastructural alterations of a xenografted human colon adenocarcinoma after treatment with titanocene dichloride, *J. Cancer Res. Clin. Oncol.*, **1988**, *114*, 250-258.

[44] I. Kostova, Titanium and vanadium complexes as anticancer agents, *Anticancer Agents Med. Chem.*, **2009**, *9*, 827-842.

[45] S. G. Bell, B. L. Vallee, The metallothionein/thionein system: an oxidoreductive metabolic zinc link, *Chembiochem*, **2009**, *10*, 55- 62.

[46] M. Murakami, T. Hirano, Intracellular zinc homeostasis and zinc signalling, *Cancer Sci.*, **2008**, *99*, 1515-1522.

[47] J. Schur, C. M. Manna, A. Deally, R. W. Köster, M. Tacke, E. Y. Tshuva, I. Ott, A comparative chemical-biological evaluation of titanium(IV) complexes with a salan or cyclopentadienyl ligand, *Chem. Commun.*, **2013**, *49*, 4785-4787.

[48] R. Barro Soria, M. Spitzner, R. Schreiber, K. Kunzelmann, Bestrophin-1 Enables Ca2+-activated Cl^- Conductance in Epithelia, *J. Biol. Chem.*, **2009**, *284*, 29405-29412.

[49] E. C. Calvaresi, P. J. Hergenrother, Glucose conjugation for the specific targeting and treatment of cancer, *J. Chem. Sci.*, **2013**, *4*, 2319-2333.

[50] G. P. Lefevre, Sugar transport in the red blood cell: structure-activity relationships in substrates and antagonists, *Pharmacol. Rev.*, **1961**, *13*, 39-70.

[51] F. Sasse, G. Erker, G. Kehr, B. Meyer, H. Redlich, DE102006053690A1, **2008**

[52] (a) G. W. Severin, C. H. Nielsen, A. I. Jensen, J. Fonslet, A. Kjær, F. Zhuravlev, Bringing Radiotracing to Titanium-Based Antineoplastics: Solid Phase Radiosynthesis, PET and ex Vivo Evaluation of Antitumor Agent [^{45}Ti](salan)Ti(dipic), *J. Med. Chem.*, **2015**, *58*, 7591-7595; (b) A. L. Vavere, M. J. Welch, Preparation, Biodistribution, and Small Animal PET of ^{45}Ti-Transferrin, *J. Nucl. Med.*, **2005**, *46*, 683-690.

[53] J. B. Waern, H. H. Harris, B. Lai, Z. Cai, M. M. Harding, C. T. Dillon, Intracellular mapping of the distribution of metals derived from the antitumor metallocenes, *J. Biol. Inorg. Chem.*, **2005**, *10*, 443-452.

[54] A. Gansäuer, D. Franke, T. Lauterbach, M. Nieger, A Modular and Efficient Synthesis of Functional Titanocenes, *J. Am. Chem. Soc.*, **2005**, *127*, 11622-11623.

[55] C. H. Langford, H. B. Gray, *Ligand substitution processes*, W. A. Benjamin, **1966**, New York, 1-16.

[56] G. L. Miessler, P. J. Fischer, D. A. Tarr, *Inorganic Chemistry*, 5$^{\text{th}}$ Ed., Pearson, *2013*, 437-445.

[57] R. S. P. Coutts, J. R. Surtees, The reaction of bis(cyclopentadienyl)Titanium(III) chloride with organic azides, *Aust. J. Chem.*, **1966**, *19*, 387-392.

[58] S. Kraft, E. Hanuschek, R. Beckhaus, D. Hasse, W. Saak, Titanium-based molecular squares and rectangles: synthesis by self-assembly reactions of Titanocene fragments and aromatic *N*-heterocylces, *Chem. Eur. J.*, **2005**, *11*, 969-978.

[59] N. J. Wiebelhaus, M. A. Cranswick, E. L. Klein, L. T. Lockett, D. L. Lichtenberger, J. H. Enemark, Metal-sulfur valence orbital interaction energies in metal-dithiolene complexes: determination of charge and overlap interaction energies by comparison of core and valence ionization energy shifts, *Inorg. Chem.*, **2011**, *50*, 11021-11031.

[60] J. J. A. Cooney, M. A. Cranswick, N. E. Gruhn, H. K. Joshi, J. H. Enemark, Electronic structure of bendt Titanocene complexes with chelated dithiolate ligands, *Inorg. Chem.*, **2004**, *43*, 8110-8118.

[61] J. Conradie, A computational study and fragment analysis of the back-bonding in titanocenyl complexes containing a five-member L,L'-cyclic ligand, L,L'= O,O'; S,S' or Se,Se', *Theochem*, **2009**, *915*, 51-57.

[62] S. M. Ametamey, M. Honer, P. A. Schubiger, Molecular imaging with PET, *Chem. Rev.*, **2008**, 1501-1516.

[63] F. E. Hahn, W. W. Seidel, Synthesis and coordination chemistry of ortho-functionalised dimercaptobenzene: building blocks for tripodal hexathiol ligands, *Angew. Chem. Int. Ed. Engl.*, **1995**, *34*, 2700-2703.

[64] W. W. Seidel, F. E. Hahn, T. Lügger, Coordination chemistry of *N*-alkylbenzamide-2,3-dithiolates as an approach to poly(dithiolate) ligands: 1,4-bis[(2,3-dimercaptobenzamido)methyl]benzene and its chelate complex with the (C_5H_5)Ti fragment, *Inorg. Chem.*, **1998**, *37*, 6587-6596.

[65] K. Osakada, Y. Kawaguchi, T. Yamamoto, Thiolato ligand transfer from bis(thiolato)titanocenes to platinum(II) complexes, *Organometallics*, **1995**, *14*, 4542-4548.

[66] J. E. Huheey, *Inorganic chemistry: Principles of structure and reactivity*, 3rd Ed., Herper and Row, New York, **1983**, 845.

[67] L. T. Cottrel, *The strengths of chemical bonds*, 2nd Ed., Butterworth, London, **1958**.

[68] *Encyclopaedia of Inorganic Chemistry*, John Wiley and Sons, **2006**, on-line

[69] S. Glasstone, K. S. Laidler, H. Eyring, *The theory of rate processes*, McGraw-Hill, New York, **1947**.

[70] C. K. Ingold, *Structure and mechanism in organic chemistry*, Cornell University Press, Ithaca, N.Y., **1953**, Chap. V

[71] D. C. Bradley, A. H. Westlake, Structures of Polymeric Titanium Ethoxide and Titanium Oxide Ethoxides, *Nature*, **1961**, *191*, 273.

[72] J. W. Lauher, R. J. Hoffmann, Structure and chemistry of bis(cyclopentadienyl)-ML_n complexes, *J. Am. Chem. Soc.*, **1976**, *98*, 1729-1742.

[73] A. Kutoglu, H. J. Kopf, Metallocen-dithiolen-chelate. Strukturaufklng und synthese von benzol-1,2-dithiolato di(π-cyclopentadienyl)molybdän(IV), *Organomet. Chem.*, **1970**, *25*, 455-460.

[74] A. Z. Kutoglu, Strukturbestimmungen an nichtlinearen Metallocenen. II. Die Molekül- und KristallStruktur von Benzol-1,2-Dithiolato-di(π-Cyclopentadienyl)-Titan (IV), *Anorg. Allg. Chem.*, **1972**, *390*, 195-209.

[75] D. W. Stephan, Sulfur-hydrogen and sulfur-sulfur oxidative addition to low-valent vanadium: synthesis and structure of monocyclopentadienyl- and dicyclopentadienylvanadium dithiolate derivatives, *Inorg. Chem.*, **1992**, *31*, 4218-4223.

[76] A. Gandini, M. Pazzi, A. Porta, G. Zanoni, Metallocene compounds and labelled molecules comprising the same for in vivo imaging, EP2774930A1

[77] J. Chen, Y. Kai, N. Kasai, Steric effect of allyl substituent on the molecular structures of allyltitanium complexes, *Journal of Organometallic Chemistry*, **1991**, *407*, 191-205.

[78] M. A. Tius, Xenon difluoride in synthesis, *Tetrahedron*, **1995**, *51*, 6605-6634.

[79] S. Lu, V. W. Pike, Synthesis of [^{18}F]xenon difluoride as a radiolabeling reagent from [^{18}F]fluoride ion in a micro-reactor and at production scale, *Journal of Fluorine Chemistry*, **2010**, *131*, 1032-1038.

[80] R. J. Nickles, M. E. Daube, T. J. Ruth, An $^{18}O_2$ target for the production of [^{18}F]F_2,*Int. J. Appl. Radiat. Isot.*, **1984**, *35*, 117.

[81] R. Chirakal, G. Firnau, G. J. Schrobilgen, J. Mckay, E. S. Garnett, The Synthesis of [^{18}F]Xenon Difluoride from [^{18}F]Fluorine Gas, *Int. J. Appl. Radiat. Isot.*, **1984**, *35*, 401-404.

[82] C. P. Ramil, Q. Lin, Bioorthogonal chemistry: strategies and recent developments, *Chem. Commun.*, **2013**, *49*, 11007-11020.

[83] O. Shimomura, F. H. Johnson, Y. Saiga, Extraction, purification and properties of aequorin, a bioluminescent protein from the luminous hydromedusan, Aequorea, *J. Cell. Physiol.*, **1962**, *59*, 223-239.

[84] D. Rideout, Self-assembling cytotoxins, *Science*, **1986**, *233*, 561-653.

[85] J. A. Prescher, C. R. Bertozzi, Chemistry in living systems, *Nat. Chem. Biol.*, **2005**, *1*, 13-21.

[86] E. M. Sletten, C. R. Bertozzi, Bioorthogonal chemistry: fishing for selectivity in a sea of functionality, *Angew. Chem. Int. Ed.*, **2009**, *48*, 6794-6998.

[87] R. Huisgen, 1,3-Dipolar Cycloadditions. Past and Future, *Angew. Chem. Int. Ed. Engl.*, **1963**, *2*, 565-598.

[88] V. V. Rostovtsev, L. G. Green, V. V. Fokin, K. B. Sharpless, A stepwise Huisgen cycloaddition process: copper(I)-catalyzed regioselective "ligation" of azides and terminal alkynes, *Angew. Chem. Int. Ed. Engl.*, **2002**, *41*, 2596-2599.

[89] C. W. Tornoe, C. Christensen, M. Meldal, Peptidotriazoles on solid phase: [1,2,3]-triazoles by regiospecific copper(I)-catalyzed 1,3-dipolar cycloadditions of terminal alkynes to azides, *J. Org. Chem.*, **2002**, *67*, 3057-3064.

[90] F. Himo, T. Lovell, R. Hilgraf, V. V. Rostovtsev, L. Noodleman, K. B. Sharpless, V. V. Fokin, Copper (I)-catalyzed synthesis of azoles. DFT study predicts unprecedented reactivity and intermediates, *J. Am. Chem. Soc.*, **2005**, *127*, 210-216.

[91] B. T. Worrell, J. A. Malik, V. V. Fokin, Direct evidence of a dinuclear copper intermediate in Cu(I)-catalyzed azide-alkyne cycloadditions, *Science*, **2013**, *340*, 457-460.

[92] T. R. Chan, R. Hilgraf, K. B. Sharpless, V. V. Fokin, Polytriazoles as copper(I)-stabilizing ligands in catalysis, *Org. Lett.*, **2004**, *6*, 2853-2855.

[93] D. C. Kennedy, C. S. McKay, M. C. Legault, D. C. Danielson, J. A. Blake, A. F. Pegoraro, A. Stolow, Z. Mester, J. P. Pezacki, Cellular consequences of copper complexes used to catalyze bioorthogonal click reactions, *J. Am. Chem. Soc.*, **2011**, *133*, 17993-18001.

[94] N. J. Agard, J. A. Prescher, C. R. Bertozzi, A strain-promoted [3+2] azide-alkyne cycloaddition for covalent modification of biomolecules in living systems, *J. Am. Chem. Soc.*, **2004**, *126*, 15046-15047.

[95] H. Meier, C. Schuh-Popitz, H. Peiersen, Isolation of a Highly Strained Bicyclic Alkyne, *Angew. Chem., Int. Ed. Engl.*, **1981**, *20*, 270-271.

[96] J. Dommerholt, S. Schmidt, R. Temming, L. J. Hendriks, F. P. Rutjes, J. C. van Hest, D. J. Lefeber, P. Friedl, F. L. van Delft, Readily accessible bicyclononynes for bioorthogonal labeling and three-dimensional imaging of living cells, *Angew. Chem., Int. Ed.*, **2010**, *49*, 9422-9425.

[97] A. Padwa, *1,3-Dipolar Cycloaddition Chemistry*, Vol. 1, 1st ed., Wiley-Interscience Publication, New York, **1984**

[98] M. L. Blackman, M. Royzen, J. M. Fox, Tetrazine ligation: fast bioconjugation based on inverse-electron-demand Diels-Alder reactivity, *J. Am. Chem. Soc.*, **2008**, *130*, 13518-13519.

[99] N. K. Devaraj, R. Weissleder, S. A. Hilderbrand, Tetrazine-based cycloadditions: application to pretargeted live cell imaging, *Bioconjugate Chem.*, **2008**, *19*, 2297-2299.

[100] (a) J. Sauer, D. K. Heldmann, J. Hetzenegger, J. Krauthan, H. Sichert, J. Schuster, 1,2,4,5-Tetrazine: Synthesis and Reactivity in [4+2] Cycloadditions, *Eur. J. Org. Chem.*, **1998**, 2885-2896; (b) F. Thalhammer, U. Wallfahrer, J. Sauer, Reaktivität einfacher offenkettiger und cyclischer dienophile bei Diels-Alder-reaktionen mit inversem elektronenbedarf, *Tetrahedron Lett.*, **1990**, *31*, 6851-6854; (c) J. Balcar, G. Chrisam, F. X. Huber, J. Sauer, Reaktivität von stickstoff-heterocyclen genenüber cyclooctin als dienophil, *Tetrahedron Lett.*, **1983**, *24*, 1481-1484.

[101] N. K. Devaraj, S. Hilderbrand, R. Upadhyay, R. Mazitschek, R. Weissleder, Bioorthogonal turn-on probes for imaging small molecules inside living cells, *Angew. Chem., Int. Ed.*, **2010**, *49*, 2869-2872.

[102] D. M. Patterson, L. A. Nazarova, B. Xie, D. N. Kamber, J. A. Prescher, Functionalized cyclopropenes as bioorthogonal chemical reporters, *J. Am. Chem. Soc.*, **2012**, *134*, 18638-18643.

[103] J. Yang, J. Seckut. M. Cole, N. K. Devaraj, Live-cell imaging of cyclopropene tags with fluorogenic tetrazine cycloadditions, *Angew. Chem., Int. Ed.*, **2012**, *124*, 7594-7597.

[104] K. Lang, L. Davis, S. Wallace, M. Mahesh, D. J. Cox, M. L. Blackman, J. M. Fox, J. W. Chin, Genetic Encoding of bicyclononynes and trans-cyclooctenes for site-specific protein labeling in vitro and in live mammalian cells via rapid fluorogenic Diels-Alder reactions, *J. Am. Chem. Soc.*, **2012**, *134*, 10317-10320.

[105] (a) A. D. de Araujo, J. M. Palomo, J. Cramer, O. Seitz, K. Alexandrov, H. Waldmann, Diels-Alder Ligation of Peptides and Proteins, *Chem. Eur. J.*, **2006**, *12*, 6095-6109; (b) A. D. de Araujo, J. M. Palomo, J. Cramer, M. Kohn, H. Schroder, R. Wacker, C. Niemeyer, K. Alexandrov, H. Waldmann, Diels-Alder Ligation and Surface Immobilization of Proteins, *Angew. Chem. Int. Ed.*, **2006**, *45*, 296-301; (c) X. L. Sun, L. C. Yang, E. L. Chaikof, Chemoselective immobilization of biomolecules through aqueous Diels-Alder and PEG chemistry, *Tetrahedron Lett.*, **2008**, *49*, 2510-2513; (d) V. Steven, D. Graham, Oligonucleotide conjugation to a cell-penetrating (TAT) peptide by Diels-Alder cycloaddition, *Org. Biomol. Chem.*, **2008**, *6*, pp 3781-3787.

[106] M. A. Tasdelen, Y. Yagci, Light-induced Click Reactions, *Angew. Chem., Int. Ed.*, **2013**, *52*, 5930-5938.

[107] W. Song, Y. Wang, J. Qu, M. M. Madden, Q. Lin, A photoinducible 1,3-dipolar cycloaddition reaction for rapid, selective modification of tetrazole-containing proteins, *Angew. Chem. Int. Ed.*, **2008**, *47*, 2832.

[108] X. Ning, R. P. Temming, J. Dommerholt, J. Guo, D. B. Ania, M. F. Debets, M. A. Wolfert, G. J. Boons, F. L. van Delft, Protein modification by strain-promoted alkyne-nitrone cycloaddition, *Angew. Chem., Int. Ed.*, **2010**, *49*, 3065-3068.

[109] K. Kodama, S. Fukuzawa, H. Nakayama, K. Sakamoto, T. Kigawa, T. Yabuki, N. Matsuda, M. Shirouzu, K. Takio, S. Yokoyama, K. Tachibana, Site-specific functionalization of proteins by organopalladium reactions, *ChemBioChem*, **2007**, *8*, 232-238.

[110] A. Ojida, H. Tsutsumi, N. Kasagi, I. Hamachi, Suzuki coupling for protein modification, *Tetrahedron Lett.*, **2005**, *46*, 3301-3305.

[111] E. Brustad, M. L. Bushey, J. W. Lee, D. Groff, W. Liu, P. G. Schultz, A genetically encoded boronate-containing amino acid, *Angew. Chem., Int. Ed.*, **2008**, *47*, 8220-8223.

[112] (a) S. J. Miller, R. H. Grubbs, Synthesis of Conformationally Restricted Amino Acids and Peptides Employing Olefin Metathesis, *J. Am. Chem. Soc.*, **1995**, *117*, 5855-5856; (b) T. D. Clark, M. R. Ghadiri, Supramolecular Design by Covalent Capture. Design of a Peptide Cylinder via Hydrogen-Bond- Promoted Intermolecular Olefin Metathesis, *J. Am. Chem. Soc.*, **1995**, *117*, 12364-12365; (c) H. E. Blackwell, R. H. Grubbs, Highly Efficient Synthesis of Covalently Cross-Linked Peptide Helices by Ring-Closing Metathesis, *Angew. Chem. Int. Ed.*, **1998**, *37*, 3281-3284; (d) H. D. Maynard, S. Y. Okada, R. H. Grubbs, Inhibition of

Cell Adhesion to Fibronectin by Oligopeptide-Substituted Polynorbornenes, *J. Am. Chem. Soc.*, **2001**, *123*, 1275-1279.

[113] Y. A. Lin, J. M. Chalker, N. Floyd, G. J. L. Bernardes, B. G. I. Davis, Allyl sulfides are privileged substrates in aqueous cross-metathesis: application to site-selective protein modification, *J. Am. Chem. Soc.*, **2008**, *130*, 9642-9643.

[114] H. Stockmann, A. A. Neves, S. Stairs, K. M. Brindle, F. J. Leeper, Exploring isonitrile-based click chemistry for ligation with biomolecules, *Org. Biomol. Chem.*, **2011**, *9*, 7303-7305.

[115] (a) E. M. Sletten, C. R. Bertozzi, A Bioorthogonal Quadricyclane Ligation, *J. Am. Chem. Soc.*, **2011**, *133*, 17570-17573; (b) P. Agarwal, J. van der Weijden, E. M. Sletten, D. Rabuka, C. R. Bertozzi, A Pictet-Spengler ligation for protein chemical modification, *Proc. Natl. Acad. Sci. U. S. A.*, **2013**, *110*, 46-51.

[116] M. J. Han, D. C. Xiong, X. S. Ye, Enabling Wittig reaction on site-specific protein modification, *Chem. Commun.*, **2012**, *48*, 11079-11081

[117] Q. Li, T. Dong, X. Liu, X. Lei, A bioorthogonal ligation enabled by click cycloaddition of o-quinolinone quinone methide and vinyl thioether, *J. Am. Chem. Soc.*, **2013**, *135*, 4996-4999.

[118] S. I. van Kasteren, H. B. Kramer, H. H. Jensen, S. J. Campbell, J. Kirkpatrick, N. J. Oldham, D. C. Anthony, B. G. Davis, Expanding the diversity of chemical protein modification allows post-translational mimicry, *Nature*, **2007**, *446*, 1105-1109.

[119] L. I. Willems, M. Verdoes, B. I. Florea, G. A. van der Marel, H. S. Overkleeft, Two-step labeling of endogenous enzymatic activities by Diels-Alder ligation, *ChemBioChem*, **2010**, *11*, 1769-1781.

[120] L. I. Willems, N. Li, B. I. Florea, M. Ruben, G. A. van der Marel, H. S. Overkleeft, Triple Bioorthogonal Ligation Strategy for Simultaneous Labeling of Multiple Enzymatic Activities, *Angew. Chem., Int. Ed.*, **2012**, *51*, 4431-4434.

[121] M. R. Karver, R. Weissleder, S. A. Hilderbrand, Bioorthogonal reaction pairs enable simultaneous, selective, multi-target imaging, *Angew. Chem. Int. Ed.*, **2012**, *51*, 920-922.

[122] F. Liu, Y. Liang, K. N. Houk, Bioorthogonal cycloadditions: computational analysis with the Distortion/Interaction Model and Predictions of reactivities, *Acc. Chem. Res.*, **2017**, *50*, 2297-2308.

[123] (a) E. M. Sletten, C. R. Bertozzi, Bioorthogonal chemistry: fishing for selectivity in a sea of functionality, *Angew. Chem. Int. Ed.*, **2009**, *48*, 6974-6998; (b) G. J. Boons, in *Carbohydrate Chemistry: Chemical and Biological Approaches*, Vol. 36 (Eds.: A. Pilar Rauter, T. K. Lindhorst), RSC, Cambridge, **2010**, 152-167; (c) M. F. Debets, C. W. J. van der Doelen,

F. P. J. T. Rutjes, F. L. van Delft, Azide: A Unique Dipole for Metal-Free Bioorthogonal Ligations, *ChemBioChem*, **2010**, *11*, 1168-1184; (d) J. C. Jewett, C. R. Bertozzi, Cu-free click cycloaddition reactions in chemical biology, *Chem. Soc. Rev.*, **2010**, *39*, 1272-1279.

[124] (a) J. A. Johnson, J. M. Baskin, C. R. Bertozzi, J. T. Koberstein, N. J. Turro, Copper-free click chemistry for the in situ crosslinking of photodegradable star polymers, *Chem. Commun.*, **2008**, 3064-3066; (b) C. Ornelas, J. Broichhagen, M. Weck, Strain-Promoted Alkyne Azide Cycloaddition for the Functionalization of Poly(amide)-Based Dendrons and Dendrimers, *J. Am. Chem. Soc.*, **2010**, *132*, 3923-3931; (c) P. A. Ledin, F. Friscourt, J. Guo, G. J. Boons, Convergent Assembly and Surface Modification of Multifunctional Dendrimers by Three Consecutive Click Reactions, *Chem. Eur. J.*, **2011**, *17*, 839-846.

[125] K. Chenoweth, D. Chenoweth, W. A. Goddard, Cyclooctyne-based reagents for uncatalyzed click chemistry: A computational survey, *Org. Biomol. Chem.*, **2009**, *7*, 5255-5258.

[126] N. E. Mbua, J. Guo, M. A. Wolfert, R. Steet, G. J. Boons, Strain-Promoted Alkyne-Azide Cycloadditions (SPAAC) Reveal New Features of Glycoconjugate Biosynthesis, *ChemBioChem*, **2011**, *12*, 1912-1921.

[127] F. Schoenebeck, D. H. Ess, G. O. Jones, K. N. Houk, Reactivity and Regioselectivity in 1,3-Dipolar Cycloadditions of Azides to Strained Alkynes and Alkenes: A Computational Study, *J. Am. Chem. Soc.*, **2009**, *131*, 8121-8133.

[128] (a) J. M. Baskin, J. A. Prescher, S. T. Laughlin, N. J. Agard, P. V. Chang, I. A. Miller, A. Lo, J. A. Codelli, C. R. Bertozzi, Copper-free click chemistry for dynamic in vivo imaging, *Proc. Natl. Acad. Sci. USA*, **2007**, *104*, 16793-16797; (b) J. A. Codelli, J. M. Baskin, N. J. Agard, C. R. Bertozzi, Second-Generation Difluorinated Cyclooctynes for Copper-Free Click Chemistry, *J. Am. Chem. Soc.*, **2008**, *130*, 11486-11493.

[129] X. H. Ning, J. Guo, M. A. Wolfert, G. J. Boons, Visualizing metabolically labeled glycoconjugates of living cells by copper-free and fast Huisgen cycloadditions, *Angew. Chem. Int. Ed.*, **2008**, *47*, 2253-2255.

[130] R. A. Carboni, R. V. Lindsey, Reactions of Tetrazines with Unsaturated Compounds. A New Synthesis of Pyridazines, *J. Am. Chem. Soc.*, **1959**, *81*, 4342.

[131] A. C. Knall, C. Slugovc, Inverse electron demand Diels-Alder (iEDDA)-initiated conjugation: a (high) potential click chemistry scheme, *Chem. Soc. Rev.*, **2013**, *42*, 5131.

[132] R. A. A. Foster, M. C. Willis, Tandem inverse-electron-demand hetero-/retro-Diels-Alder reactions for aromatic nitrogen heterocycle synthesis, *Chem. Soc. Rev.*, **2013**, *42*, 63, and references therein.

[133] J. Sauer, D. K. Heldmann, J. Hetzenegger, J. Krauthan, H. Sichert, J. Schuster, 1,2,4,5-Tetrazine: Synthesis and Reactivity in [4+2] Cycloadditions, *Eur. J. Org. Chem.*, **1998**, 2885-2896, and references therein.

[134] (a) W. Chen, D. Wang, C. Dai, D. Hamelberg, B. Wang, Clicking 1,2,4,5-tetrazine and cyclooctynes with tunable reaction rates, *Chem. Commun.*, **2012**, *48*, 1736-1738; (b) M. T. Taylor, M. L. Blackman, O. Dmitrenko, J. M. Fox, Design and Synthesis of Highly Reactive Dienophiles for the Tetrazine-trans-Cyclooctene Ligation, *J. Am. Chem. Soc.*, **2011**, *133*, 9646-9649; (c) M. R. Karver, R.Weissleder, S. A. Hilderbrand, Synthesis and Evaluation of a Series of 1,2,4,5-Tetrazines for Bioorthogonal Conjugation, *Bioconjugate Chem.*, **2011**, *22*, 2263-2270; (d) K. Lang, L. Davis, J. Torres-Kolbus, C. Chou, A. Deiters, J. W. Chin, Genetically encoded norbornene directs site-specific cellular protein labelling via a rapid bioorthogonal reaction, *Nat. Chem.*, **2012**, *4*, 298-304.

[135] J. Sauer, R. Sustmann, Mechanistic Aspects of Diels-Alder Reactions: A Critical Survey, *Angew. Chem., Int. Ed. Engl.*, **1980**, *19*, 779.

[136] Y. Liang, J. L. Mackey, S. A. Lopez, F. Liu, K. N. Houk, Control and design of mutual orthogonality in bioorthogonal cycloadditions, *J. Am. Chem. Soc.*, **2012**, *134*, 17904-17907.

[137] C. H. Wong, S. C. Zimmermann, Orthogonality in organic, polymer, and supramolecular chemistry: from Merrifield to click chemistry, *Chem. Commun.*, **2013**, *49*, 1679, and references therein.

[138] J. C. Jewett, C. R. Bertozzi, Cu-free click cycloaddition reactions in chemical biology, *Chem. Soc. Rev.*, **2010**, *39*, 1272, and references therein.

[139] K. Kang, J. Park, E. Kim, Tetrazine ligation for chemical proteomics, *Proteome Science*, **2017**, 15:15.

[140] (a) K. A. Hofmann, O. Ehrhart, Einwirkung von Hydrazin auf Dicyandiamid, *Ber. Dtsch. Chem. Ges.*, **1912**, *45*, 2731-2740; (b) E. Müller, L. Herrdegen, Einwirkung von wasserfreiem Hydrazin auf Nitrile, *J. Prakt. Chem.*, **1921**, *102*, 113-155; (c) T. Curtius, A. Hess, Einwirkung von Hydrazin auf m-Cyanbenzoesäure, *J. Prakt. Chem.*, **1930**, *125*, 40-53.

[141] J. Yang, M. R. Karver, W. Li, S. Sahu, N. K. Devaraj, Metal-Catalyzed One-Pot Synthesis of Tetrazines Directly from Aliphatic Nitriles and Hydrazine, *Angew. Chem. Int. Ed.*, **2012**, *51*, 5222-5225.

[142] (a) A. Pinner, Ueber die Einwirkung von Hydrazin auf Imidoäther, *Ber. Dtsch. Chem. Ges.*, **1893**, *26*, 2126-2135; (b) S. A. Lang, B. D. Johnson, E. Cohen, Novel synthesis of unsymmetrically substituted s-tetrazines, *J. Heterocycl. Chem.*, **1975**, *12*, 1143-1153; (c) W. Skorianetz, E. S. Kovats, Eine neue Synthese von 3,6-Dialkyl-1,2,4,5-tetrazinen, *Helv. Chim. Acta*, **1971**, *54*, 1922-1939.

[143] (a) H. Neunhoeffer, P. F. Wiley, *Chemistry of 1,2,3-Triazines, Tetrazines, and Pentazines*, Wiley, New York, **1978**, 1073; (b) P. Audebert, S. Sadki, F. Miomandre, G. Clavier, M. C. Vernieres, M. Saoud, P. Hapiot, Synthesis of new substituted tetrazines: electrochemical and spectroscopic properties, *New J. Chem.*, **2004**, *28*, 387-392.

[144] (a) P. Oxley, M. W. Partridge, W. F. Short, Amidines. Part VII. Preparation of amidines from cyanides, aluminium chloride, and ammonia or amines, *J. Chem. Soc.*, **1947**, 1110-1116; (b) W. O. Siegl, Metal ion activation of nitriles. Syntheses of 1,3-bis(arylimino)isoindolines, *J. Org. Chem.*, **1977**, *42*, 1872-1878; (c) Z. P. Demko, K. B. Sharpless, Preparation of 5-Substituted 1H-Tetrazoles from Nitriles in Water, *J. Org. Chem.*, **2001**, *66*, 7945-7950; (d) J. F. Wang, F. Xu, T. Cai, Q. Shen, Addition of Amines to Nitriles Catalyzed by Ytterbium Amides:? An Efficient One-Step Synthesis of Monosubstituted N-Arylamidines, *Org. Lett.*, **2008**, *10*, 445-448; (e) V. Y. Kukushkin, A. J. L. Pombeiro, Additions to Metal-Activated Organonitriles, *Chem. Rev.*, **2002**, *102*, 1771-1802; (f) G. Rousselet, P. Capdevielle, M. Maumy, Copper(I)-induced addition of amines to unactivated nitriles: The first general one-step synthesis of alkyl amidines, *Tetrahedron Lett.*, **1993**, *34*, 6395-6398.

[145] P. Mayo, G. Orlova, J. D. Goddard, W. Tam, Remote substituent effects on the oxymercuration of 2-substituted norbornenes: an experimental and theoretical study, *J. Org. Chem.*, **2001**, *66*, 5182-5191.

[146] G. H. Posner, J. S. Ting, M. Lentz, A mechanistic and synthetic study of organocopper substitution reactions with some homo allylic and cyclopropylcarbinyl substrates application to isoprenoid synthesis, *Tetrahedron*, **1976**, *32*, 2281-2287.

[147] K. J. Watson, S. T. Nguyen, C. A. Mirkin, The synthesis and ring-opening metathesis polymerisation of an amphiphilic redox-active norbornene, *Journal of Organometallic Chemistry*, **2000**, *606*, 79-83.

[148] I. J. Arroyo, R. Hu, G. Merino, B. Z. Tang, E. Peabrera, The Smallest and One of the Brightest. Efficient Preparation and Optical Description of the Parent Borondipyrromethene System, *J. Org. Chem.*, **2009**, *74*, 5719-5722.

[149] L. E. Greene, R. Lincoln, G. Cosa, Rate of Lipid Peroxyl Radical Production during Cellular Homeostasis Unraveled via Fluorescence Imaging, *J. Am. Chem. Soc.*, **2017**, *139*, 15801-15811.

[150] A. M. Hansen, A. L. Sewell, R. H. Pedersen, D. Long, N. Gadegaard, R. Marqueza, Tunable BODIPY derivatives amenable to click and peptide chemistry, *Tetrahedron*, **2013**, *69*, 8527-8533.

[151] M. R. Sorkin, J. A. Walker, J. S. Brown, C. A. Alabi, Versatile Platform for the Synthesis of Orthogonally Cleavable Heteromultifunctional Cross-Linkers, *Bioconjugate Chem.*, **2017**, *28*, 907-912.

[152] PhD Thesis of Dr. Andrea Gandini, Master degree Thesis of Emanuele Casali, Master degree Thesis of Vittoria Salomoni.

[153] P. G. Gassman, W. H. Campbell, D. W. Macomber, An unusual relationship between titanium-49 chemical shift and Ti(2p3/2) binding energy. The use of titanium-49 NMR in evaluating the electronic effect of methyl substitution on the cyclopentadienyl ligand, *Organometallics*, **1984**, *3*, 385-387.

[154] G. Tavcar, M. Tramsek, XeF2 as a ligand to a metal center, an interesting field of noble gas chemistry, *Journal of Fluorine Chemistry*, **2015**, *174*, 14-21.

[155] Frisch, M. J.; Trucks, G. W.; Schlegel, H. B.; Scuseria, G. E.; Robb, M. A.; Cheeseman, J. R.; Scalmani, G.; Barone, V.; Mennucci, B.; Petersson, G. A.; Nakatsuji, H.; Caricato, M.; Li, X.; Hratchian, H. P.; Izmaylov, A. F.; Bloino, J.; Zheng, G.; Sonnenberg, J. L.; Hada, M.; Ehara, M.; Toyota, K.; Fukuda, R.; Hasegawa, J.; Ishida, M.; Nakajima, T.; Honda, Y.; Kitao, O.; Nakai, H.; Vreven, T.; Montgomery, J. A., Jr.; Peralta, J. E.; Ogliaro, F.; Bearpark, M.; Heyd, J. J.; Brothers, E.; Kudin, K. N.; Staroverov, V. N.; Keith, T.; Kobayashi, R.; Normand, J.; Raghavachari, K.; Rendell, A.; Burant, J. C.; Iyengar, S. S.; Tomasi, J.; Cossi, M.; Rega, N.; Millam, J. M.; Klene, M.; Knox, J. E.; Cross, J. B.; Bakken, V.; Adamo, C.; Jaramillo, J.; Gomperts, R.; Stratmann, R. E.; Yazyev, O.; Austin, A. J.; Cammi, R.; Pomelli, C.; Ochterski, J. W.; Martin, R. L.; Morokuma, K.; Zakrzewski, V. G.; Voth, G. A.; Salvador, P.; Dannenberg, J. J.; Dapprich, S.; Daniels, A. D.; Farkas, O.; Foresman, J. B.; Ortiz, J. V.; Cioslowski, J.; Fox, D. J. *Gaussian 09, Revision B.01*; Gaussian, Inc., Wallingford, CT, **2010**.

[156] Becke, A. D. Density-functional thermochemistry. III. The role of exact exchange. *J. Chem. Phys.*, **1993**, *98*, 5648-5652.

[157] Lee, C.; Yang, W.; Parr, R. G. Development of the Colle-Salvetti correlation-energy formula into a functional of the electron density. *Phys. Rev. B*, **1988**, *37*, 785-789.

[158] (a) Hay, P. J.; Wadt, W. R. Ab initio effective core potentials for molecular calculations. Potentials for K to Au including the outermost core orbitals. *J. Chem. Phys.*, **1985**, *82*, 299; (b) Wadt, W. R.; Hay, P. J. Ab initio effective core potentials for molecular calculations. Potentials for main group elements Na to Bi. *J. Chem. Phys.*, **1985**, *82*, 284; (c) Hay, P. J.; Wadt, W. R. Ab initio effective core potentials for molecular calculations. Potentials for the transition metal atoms Sc to Hg. *J. Chem. Phys.*, **1985**, *82*, 270.

[159] (a) Rassolov, V. A.; Ratner, M. A.; Pople, J. A.; Redfern, P. C.; Curtiss, L. A. 6-31G* basis set for atoms K through Zn. *J. Comput. Chem.*, **2001**, *22*, 976-984. (b) Hehre, W. J.; Ditchfield, R.; Pople, J. A. Self-Consistent Molecular Orbital Methods. XII. Further Extensions of Gaussian-Type Basis Sets for Use in Molecular Orbital Studies of Organic

Molecules. *J. Chem. Phys.*, **1972**, *56*, 2257-2261. (c) Hariharan, P. C.; Pople, J. A. The influence of polarization functions on molecular orbital hydrogenation energies. *Theor. Chim. Acta*, **1973**, *28*, 213-222.

[160] (a) Gonzalez, C.; Schlegel, H. B. Reaction path following in mass-weighted internal coordinates. *J. Chem. Phys.*, **1990**, *94*, 5523-5527. (b) Gonzalez, C.; Schlegel, H. B. An improved algorithm for reaction path following. *J. Chem. Phys.*, **1989**, *90*, 2154.

[161] (a) Tomasi, J.; Mennucci, B.; Cances, E. The IEF version of the PCM solvation method: An overview of a new method addressed to study molecular solutes at the QM ab initio level. *J. Mol. Struct. Theochem*, **1999**, *464*, 211-226. (b) Mennucci, B.; Tomasi, J. Continuum solvation models: A new approach to the problem of solute's charge distribution and cavity boundaries. *J. Chem. Phys.*, **1997**, *106*, 5151. (c) Mennucci, B.; Cances, E.; Tomasi, J. Evaluation of Solvent Effects in Isotropic and Anisotropic Dielectrics and in Ionic Solutions with a Unified Integral Equation Method: Theoretical Bases, Computational Implementation, and Numerical Applications. *J. Phys. Chem. B*, **1997**, *101*, 10506-10517.

[162] a) Engle, K. M.; Mei, T. S.; Wang, X.; Yu, J. Q. Bystanding F^+ Oxidants Enable Selective Reductive Elimination from High-Valent Metal Centers in Catalysis. *Angew. Chem. Int. Ed.*, **2011**, *50*, 1478-1491. b) Vigalok, A. Electrophilic Halogenation-Reductive Elimination Chemistry of Organopalladium and -Platinum Complexes. *Acc. Chem. Res.*, **2015**, *48*, 238-247. c) Vigalok, A. Electrophilic Fluorination of Group 10 Organometallic Complexes: Chemistry beyond Oxidative Addition. *Organometallics*, **2011**, 30, 18, 4802-4810.

[163] (a) Mazej, Z.; Goreshnik, E. A. Largest perfluorometallate $[Ti_{10}F_{45}]^{5-}$ oligomer and polymeric $([Ti_3F_{13}]^-)_\infty$ and $([TiF_5]^-)_\infty$ anions prepared as $[XeF_5]^+$ salts. *New J. Chem.*, **2016**, *40*, 7320-7325. (b) Radan, K.; Goreshnik, E.; Zemva, B. Xenon(II) Polyfluoridotitanates(IV): Synthesis and Structural Characterization of $[Xe_2F_3]^+$ and $[XeF]^+$ Salts. *Angew. Chem. Int. Ed.*, **2014**, *53*, 13715-13719.

[164] (a) Zupan, M.; Zajc, B. Fluorination with xenon difluoride. Part 18. Reactivity of diphenyl sulphide and substituted thiochromanones. *J. Chem. Soc., Perkin Trans.*, **1978**, *1*, 965-967. (b) Marat, R. K.; Janzen, A. F. Reaction of xenon difluoride. Part III. Oxidative-fluorination and α-fluorination of sulfur(II) compounds. *Can. J. Chem.*, **1977**, *55*, 3031-3034.

[165] (a) Kutoglu, A.; Kopf, H. J. Metallocen-dithiolen-chelate. Strukturaufklärung und synthese von benzol-1,2-dithiolato di(π-cyclopentadienyl)molybdän(IV). *Organomet. Chem.*, **1970**, *25*, 455-460. (b) Kutoglu, A. Strukturbestimmungen an nichtlinearen Metallocenen. II. Die Molekül- und Kristall Struktur von Benzol-1,2-Dithiolato-di(π-Cyclopentadienyl)-Titan (IV). *Z. Anorg. Allg. Chem.*, **1972**, *390*, 195-209. (c) Stephan, D. W. Sulphur-hydrogen and sulphur-sulphur oxidative addition to low-valent vanadium: synthesis and

structure of monocyclopentadienyl- and dicyclopentadienylvanadium dithiolate derivatives. *Inorg. Chem.*, **1992**, *31*, 4218-4223.

[166] Pliego Jr., J.R. Thermodynamic cycles and the calculation of pK_a. *Chem. Phys. Lett.*, **2003**, *367*, 145-149.

[167] Riddick, J.A., W.B. Bunger, Sakano T.K. *Techniques of Chemistry* 4^{th} ed., Volume II. Organic Solvents. New York, NY: John Wiley and Sons., **1985**, 638.

[168] Kitagawa, Y.; Saito, T.; Ito, M.; Shoji, M.; Koizumi, K.; Yamanaka, S.; Kawakami, T.; Okumura, M.; Yamaguchi, K. Chem. *Phys. Lett.*, **2007**, *442*, 445.

[169] P. Vachal, J. J. Hale, Z. Lu, E. C. Streckfuss, S. G. Mills, M. MacCoss, D. H. Yin, K. Algayer, K. Manser, F. Kesisoglou, S. Ghosh, L. L. Alani, Synthesis and Study of Alendronate Derivatives as Potential Prodrugs of Alendronate Sodium for the Treatment of Low Bone Density and Osteoporosis. *J. Med. Chem.*, **2006**, *49*, 3060-3063.

[170] N. B. Javitt, Bile acid synthesis from cholesterol: regulatory and auxiliary pathways. *FASEB Journal.*, **1994**, *15*, 1308-1311.

[171] a) P. H. Ellims, Thymidine as an anticancer agent, alone or in combination. *Cancer Chemotherapy and Pharmacology*, **1982**, *10*, 1-6; b) F. Mao, T. M. Rechtin, R. Jones, A. A. Cantu, L. S. Anderson, A. Radominska, M. P. Moyer, R. R. Drake, Synthesis of a Photoaffinity Analog of 3'-Azidothymidine, 5-Azido-3'-azido-2',3'-dideoxyuridine.: INTERACTIONS WITH HERPESVIRUS THYMIDINE KINASE AND CELLULAR ENZYMES, *Journal of Biological Chemistry*, **1995**, *270*, 13660-13664.

[172] a) S. C. L. M. Cremers, R. van Hogezand, D. Bfer, J. den Hartigh, P. Vermeij, S. E. Papapoulos, N. A. T. Hamdy, Absorption of the oral bisphosphonate alendronate in osteoporotic patients with Crohn's disease. *Osteoporosis International*, **2005**, *16*, 1727-1730; b) J. C. Frith, J. Mönkkönen, S. Auriola, H. Mönkkönen, M. J. Rogers, The molecular mechanism of action of the antiresorptive and antiinflammatory drug clodronate: Evidence for the formation in vivo of a metabolite that inhibits bone resorption and causes osteoclast and macrophage apoptosis. *Arthritis & Rheumatism*, **2001**, *44*, 2201-2210; c) V. B. Andela, *Cancer Research*, **2004**, *64*, 2936.

[173] N. Parker, M. Turk, E. Westrick, Folate receptor expression in carcinomas and normal tissues determined by a quantitative radioligand binding assay, *Analytical Biochemistry*, **2005**, *338*, 284-293

[174] https://www.proteinatlas.org/ENSG00000110195-FOLR1/cell

[175] J. Dommerholt, O. Rooijen, A. Borrmann, Highly accelerated inverse electron-demand cycloaddition of electron-deficient azides with aliphatic cyclooctynes, *Nature Communications*, **2014**, *5*, 5378.

[176] C. DeForest, D. Tirrell, *Nature Materials*, NMAT4219, Method S1.

[177] A. F. Trindade, R. F. M. Frade, E. M. S. Mas, C. Gra C. A. B. Rodrigues, J. M. G. Martinho, C. A. M. Afonso, "Click and go": simple and fast folic acid conjugation. *Org. Biomol. Chem.*, **2014**, *12*, 3181-3190.

[178] R. I. Pinhassi, Y. G. Assaraf, S. Farber, M. Stark, D. Ickowicz, S. Drori, A. J. Domb, Y. D. Livney, Arabinogalactan-Folic Acid-Drug Conjugate for Targeted Delivery and Target-Activated Release of Anticancer Drugs to Folate Receptor-Overexpressing Cells, *Biomacromolecules*, **2010**, *11*, 294-303.

Chapter 4

Cyclopropanation reactions promoted by Fe(Porphyrin)OMe complexes: a Computational study

Compounds containing cyclopropanes units constantly play an important role in chemistry: many pharmaceuticals and natural product base their properties of high reactivity and biological activity on the presence of a three membered cyclic core.[1],[2],[3] For instance, biological properties can range from enzyme inhibitions to insecticidal, antifungal, herbicidal, antimicrobial, antibiotic, antibacterial, antitumor and antiviral activities.[2] Pyrethrums (Figure 4.1) extracted from the *Chrysanthemum cinerariafolium* and *C. coccineum* plants have been known to exhibit insecticidal activities.[2]

In the field of antiviral compounds, nucleoside analogues containing substituted cyclopropylidene groups in place of sugar moiety can be found (Figure 4.2). The synthesis of such nucleoside analogue (*Z*)-1-[(*z*-guanidino-carbomoylcyclopropyledene)methyl]-4,5,7,8-tetrahydro-6*H*-6-iminoimidazo(4,5-*e*)[1,3]diazipine-4,6-dione (Figure 4.2) can be achieved starting from methyl imidazole-4,5-dicarboxylate by sequential condensations with 2-bromo-2-ethyl cyclopropane-1-carboxylate and guanidine.[2]

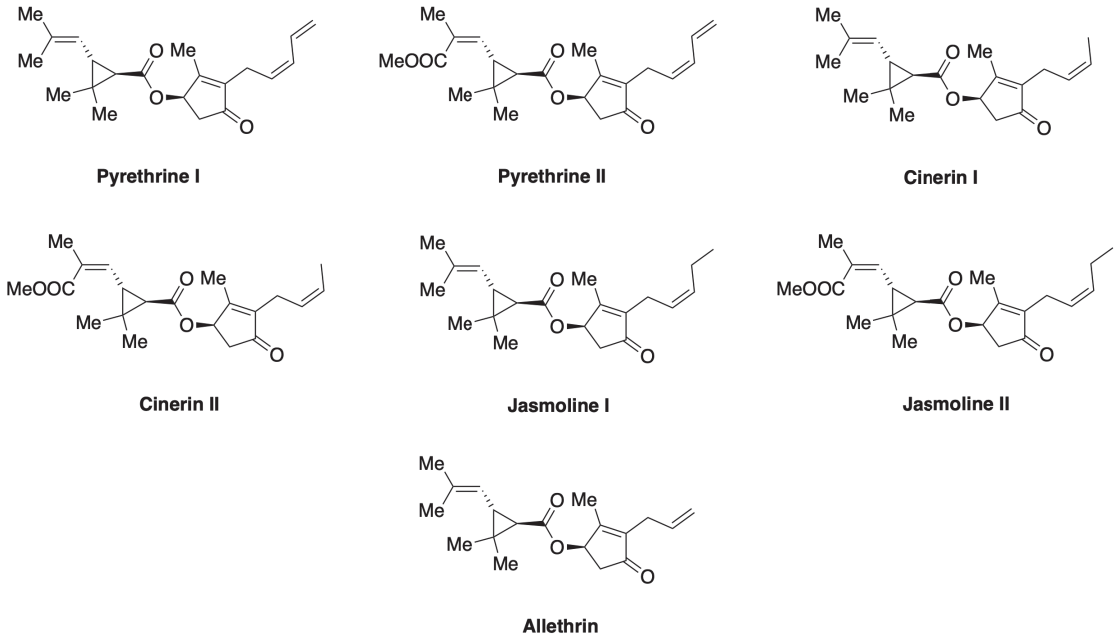

Figure 4.1: *Pyrethrums extracted from natural sources which exhibits insecticidal activities.*

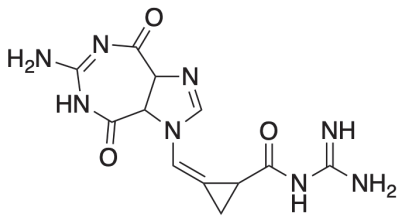

Figure 4.2: *Nucleoside analogue which exhibits antiviral activity.*

Other applications rely on the wide possibility to use the cyclopropane unit as intermediate group to undergo further modifications, like the ones reported by Carreira and co-workers in which the total synthesis of (±)-horsfiline (Figure 4.3) is achieved through the construction of heterocyclic compounds from the activated cyclopropane moiety.[3]

Besides all of these examples, different strategies were adopted for the construction of the cyclopropane ring which all converged in the widely adopted one-pot metal-catalyzed reaction between a diazocompound and an olefin, being an atom-efficient strategy and the generation of gaseous N_2 as only byproduct.[4] This approach is one of the best examples of how a fine-tuning of eco-compatibility of processes can develop a sustainable synthetic chemistry.[10] A crucial role in the

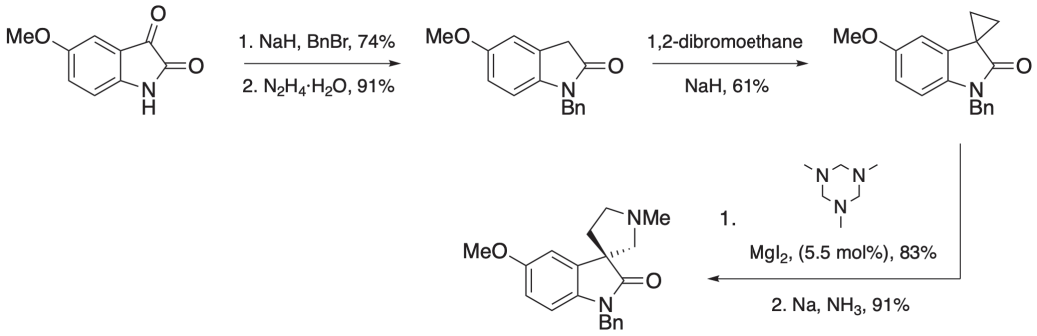

Figure 4.3: *Carreira's total synthesis of (±)-horsfiline.*

cyclopropanation reactions had already been reported in 1986 in a seminal review paper by Doyle, showing the widely use of metal catalysis to promote the cyclization between diazoesters and substituted olefins partners (Scheme 4.1).[5]

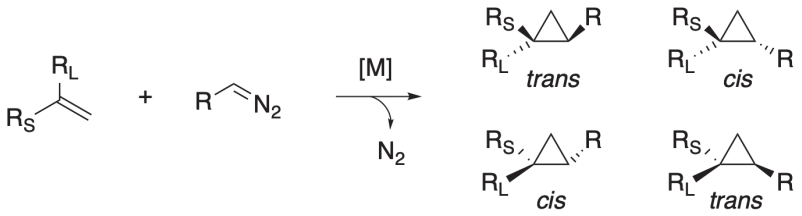

Scheme 4.1: *Metal-catalyzed one-pot reaction of diazo compounds with alkenes.*

In the next years, many literature paper were published by showing chiral complexes of Copper[6] and Rhodium[7] as catalysts to effect cyclopropanation with high enantioselectivity, even if the diastereoselectivity of *cis*/*trans* mixtures achieved with these compounds were generally poor.[8]

The first example of the use of porphyrin ligands for the metal was reported in 1980 and the further work done by Kodadek using Rh(III)-tetramesitylporphyrin showed a feasible cyclopropanation by involving EDA as carbene source.[9]

Before to continue the dissertation regarding the cyclopropanation reactions it is important to introduce the reader to peculiar properties of these type of ligands. Porphyrins are a group organic compounds consisting of heterocyclic macrocycle composed of four modified pyrrole subunits linked at their α-carbon atoms through methine bridges (=CH-) (Figure 4.4). This so formed unit, in absence of a metal cation inside the ring and substituents on to the carbon scaffold, takes the name of **porphin**. The most important property of this system relies on the number of elec-

trons in the macrocycle: with a total of 26 π-electrons, of which 18 π-electrons form a planar, continuous cycle, the porphin ring structure is often described as aromatic.[16] This results in a large conjugated system that typically absorbs light in the visible region of the electromagnetic spectrum. As a proof of facts, the name "porphyrin" derives from the Greek word $\pi o \rho \phi \upsilon \rho \alpha$ (porphyra), which means purple.[17]

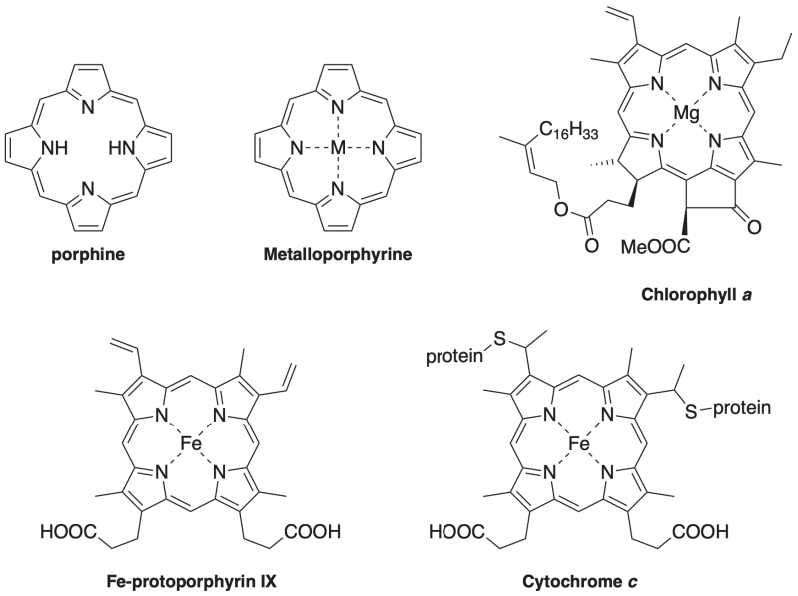

Figure 4.4: *Porphyne, porphyrine and related compounds.*[17]

The synthesis of the porphin ring can be easily addressed in laboratory following the well-known Rothemund reaction, by condensing the required aldehyde and the desired pyrrole, to form respectively the methine bridges and the pyrrole rings (Scheme 4.2).[18]

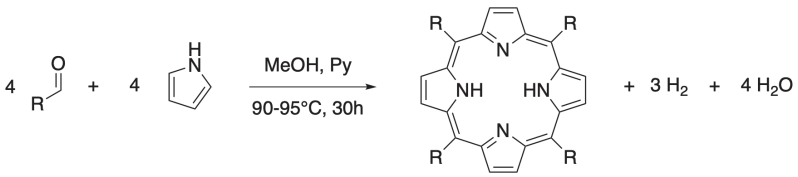

Scheme 4.2: *Rothemund's porphin synthesis.*

When a metal is coordinated in the center, the porphin core acts as a X-type ligand with a -2 total charge: the so formed **porphyrin** can be interpreted as the conjugated basis of ligand that bind the metal to form the complex. The metal ion

typically involved in complexation belong to transition metal or to the alkaline earth metal groups and usually has a charge of +2 or +3. Exhaustive examples can be observed in Figure 4.4, where Fe-porphyrin IX (an exemplified form of heme group), Cytochrome-c core or Chlorophyll a (with Mg^{2+} cation) can be found.[17]

By returning back to our proposal, metal porphyrins were extensively adopted: Ruthenium,[11] Osmium,[12] Rhodium,[13] and Iridium [14] porphyrins showed excellent efficiency and high enantio- and diastereoselective control in olefin cyclopropanations. In spite of the good catalytic efficiency of the above-mentioned metal porphyrin catalysts, their high cost and toxicity prompted the scientific community to investigate the eco-friendlier first-row transition metal porphyrins complexes.[10] The election metal-candidates for such derivatives were found in Cobalt [15] and Iron.[16] In this context, iron porphyrins have constantly gained a leading role in cyclization of olefins. They were firstly introduced in oxygenation catalysis, while in 1995 it was reported their use as cyclopropanting catalysts by Kodadek and co-workers[8] and in 1999 by Gross *et al.* which for the first time reported their extensive use.[15] Since then, numerous iron porphyrin complexes have been synthesized to be applied to carbene transfer reactions and several structural modifications of the ligand skeleton have been performed to increase the catalyst efficiency through a metal/periphery synergy.[10]

In the next sections of the chapter, we are going to present the experimental work done by our collaborators in the group of Prof. Emma Gallo at University of Milan, which constitutes the basis on which we planned our computational studies in order to explain the in-depth mechanism of such an observed reactivity.

4.1 The bis-strapped porphyrin study

In 2008, Gallo and co-workers started working on the employment of "non-innocent" ligands with which porphyrin cores can me modified.[19] Specifically, they started working on Co(II)-binaphtyl porphyrins to achieve asymmetric cyclopropanations: the so good results they got prompted them to the further functionalization of porphyrin ring with bis-strapped chiral binapthyl prophyrine scheleton **2**. It can

be easily prepared by one single Suzuki coupling step, from the corresponding porphyirine **1** (Scheme 4.3).[4]

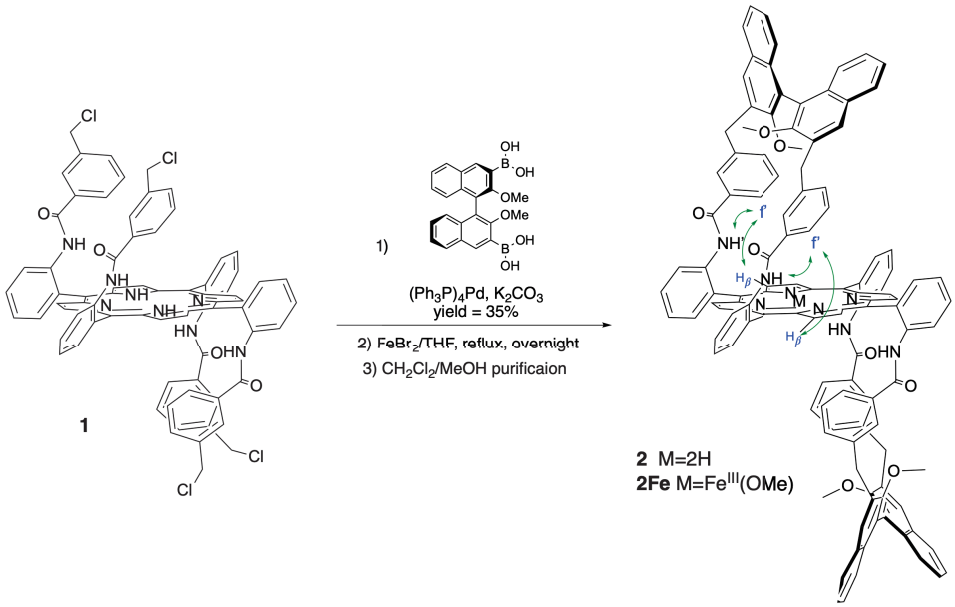

Scheme 4.3: *Synthesis of C2-symmetrical binol-bis-strapped porphyrin* ***2*** *and its iron(III) complex* ***2Fe****.*

Thanks to the bis-strapped moiety that is bridged in 5-15 position of the porphyrin ring, an appropriate group is inserted near to the reactive site, with a chiral structure that can overhang above the metal center and induce a reaction stereoselectivity.[4],[19] Structure of **2** was extensively characterized by the use of X-ray crystallography and NMR, showing a structure that is pre-organized, but enough flexible to assure the entrance of the reactive species. The conformation proposed for the bis-strap of **2** in Scheme 4.3, was further deduced by NOE-effects between H_f and both amidic proton and the H_β.[4] The so obtained structure of **2** presents a C_2 axis of symmetry, with two open spaces (above and below the plane) to assure the substrate access, by maintaining the steric chiral bulk on the porphyrine core.[4] By reacting **2** with $FeBr_2$ the corresponding iron(II)porphyrin was obtained and the consequent oxidation promoted by atmospheric oxygen in the presence of methanol formed the iron(III) **2Fe** porphyrin complex.[4] To assure the so achieved oxidation state and the methoxy ligand, ESR spectroscopy and HRMS-ESI analysis were performed.[4] The catalytic activity of these iron-complexes was tested by

authors in a benchmark reaction between α-methylstyrene and ethyl diazoacetate (EDA), obtaining excellent results in terms of yield and diastereoselectivities even by using very low catalyst loading, which was optimized at 0°C with the following ratios: **2Fe**:Alkene:EDA = 1:10000:10000. This means a catalytic loading of 0.01% and a TON of 10000; in some cases, the reaction was so fast that it was completed in less than 5 minutes, thus showing a TOF equal to 120000 h^{-1}, a so low value has never been reported for porphyrin mediated cyclopropanations (see Scheme 4.4 and Table 4.1, entry 1-5).[4],[10]

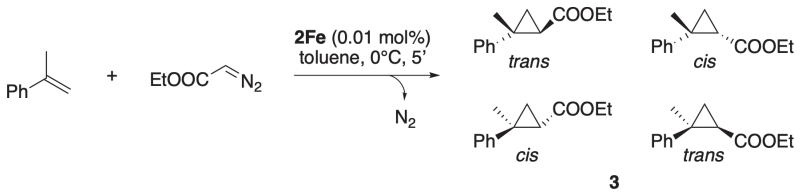

Scheme 4.4: *Cyclopropanation of α-methylstyrene by EDA.*[4]

Moreover, authors provided an extensive study of both substituents role on the alkene and on the diazo-compound always getting good results on the *trans*/*cis* selectivity and only a slight decrease in terms of enantioselectivity when highly steric demanding substituents were placed on the reactant partners (Table 4.1 and 4.2).[4],[10]

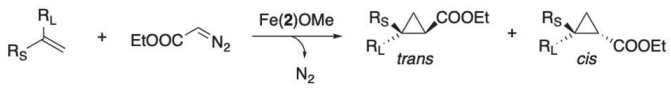

Entry	Alkene	Cat/alkene/EDA	T [°C]	t [min]	Product, yield$_{trans}$ [%]	*trans/cis* ratio	*ee* $_{trans(R,R)}$ [%]
1		1:1000:1000	25	5	75	97:3	68
2		1:1000:1100	25	5	85	98:2	70
3		1:1000:1100	0	5	76	98:2	69
4		1:1000:1100	-40	15	98	98:2	87
5		1:10000:10100	0	5	98	96:4	76
6	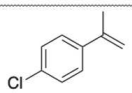	1:10000:10100	0	30	80	97:3	70
7	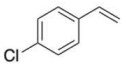	1:10000:10100	0	20	62	97:3	57
8	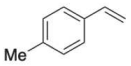	1:10000:10100	0	15	53	97:3	64
9	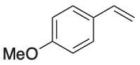	1:10000:10100	0	30	74	95:5	60
10	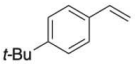	1:10000:10100	0	5	70	98:2	40
11		1:1000:1100	-40	120	25	—	48
12	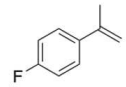	1:1000:1100	-40	120	30	91:9	71
13	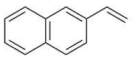	1:1000:1100	-40	90	45	97:3	40
14	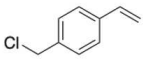	1:1000:1100	-40	90	60	98:2	n.d.

Table 4.1: *Alkene substrate scope for cyclopropanation by EDA.*[4],[10]

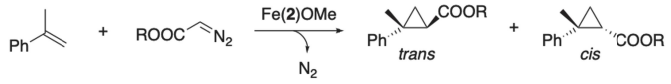

Entry	R	Cat/alkene/EDA	T [°C]	t [min]	Product, yield$_{trans}$ [%]	*trans/cis* ratio	*ee* $_{trans(R,R)}$ [%]
1	Et	1:1000:1100	25	5	85	98:2	70
2	*i*- Pr	1:1000:1100	25	120	60	98:2	67
3	*n*- Pr	1:1000:1100	25	90	73	98:2	40
4	*t*- Bu	1:1000:1100	25	42	42	63:37	7

Table 4.2: *Different substituent on diazocompound effect on cyclopropanation reaction.*[4],[10]

To explain this dependency of the reaction output from the steric demands of the reactants, authors suggested that during the formation of the reactive carbene intermediate, the iron center cannot freely interact with such reactants if inserted in a crowded place like the bis-stranded porphyrin **2**.[10]

Another important data, which will be fundamental in the study of the reaction mechanism in the next sections, is the recovery and the reuse of the catalyst. The authors tried firstly the consecutiveness of the reaction, by adding again reactants to the reaction mixture for three times and found a strong dependency from the amount of EDA used in the second and third cycle.[4] Since it is known that EDA can show a reductive activity,[8],[20] the authors started thinking about its role in the initial reduction of Fe^{III}**2**OMe complex to the corresponding Fe^{II}**2**OMe^- anion and in avoiding any oxidative degradation.[4] To also evaluate the catalyst recovery and recycling in a non-protected reaction medium, the authors operated in the same way described above, but after every run the catalytic mixture was evaporated to dryness, exposed to air and then used for the next reaction step. The results they got showed a decrease in yield and chemoselectivity, till obtaining traces in the third run.[10] Viceversa, by operating in the same way and adding EDA in slight excess (1:1000:1100 ratio, see above) they observed reaction occurring with the same high chemoselectivity observed before, thus underling the importance of EDA in avoiding degradation pathways of the active species due to the presence of air.[10] Even by running the reaction in air, by using a properly equipped flask with a calcium chloride drying tube, when in excess of EDA no consistent variation in yield and chemoselectivity were observed.[10]

As an additional information, the authors reported also the experimental procedure to recover the catalyst, showing that the methoxy ligand was always present in the coordination sphere of the iron metal, thus excluding any mechanistic pathway that could result in the complete dissociation of it during the reaction.[10] As a proof of this result, authors analyzed through ESI-MS spectroscopy the crude product, observing the presence of the Fe^{III}**2**OMe starting complex.[10] This result is of fundamental importance for the further developments of this chapter.

4.2 The carbene formation and the electronic structure study

We already reported that the role of EDA is that of generating a carbene specie: this happens during the first step of the mechanism, involving the formation of an iron=carbene complex that will be attached by the alkene moiety of the other reactant in the next cyclopropanation step. Before to start reporting the results of our calculations, it is important to introduce the properties of this active carbene specie involved in the reaction. An excellent analysis of those properties was reported by Shaik and co-workers in 2016, by working on a similar iron complex but with a thiomethyl axial ligand instead of Gallo's methoxy one.[21] Arnold, Fasan and co-workers[22] reported of a reduced porphyrin carbene as the active species, thus thinking to an overall monoanionic electronic structure: with a dianionic porphyrin ring and a monoanionic thiomethyl axial ligand the overall charge on the iron atom and the connected carbene has to be +2.[21] To achieve this charge distribution, two different solutions can be proposed: firstly, we can think of having a Fe oxidation state in its third oxidation state [Fe^{III} - d^5] and a carbene radical (formally a radical anion). This situation can be found in the Open-Shell Singlet (OSS) and the Triplet solutions, as reported in Figure 4.5.[21]

Specifically, by looking at section b of the same figure, it can be observed an antiferromagnetic coupling in the case of the OSS state between the carbene carbon-centered radical and the unpaired electron in the iron d-orbital. Vice versa, a ferromagnetic coupling is involved in the triplet state.[21] Another possible solution is the Closed-Shell Singlet (CSS) state, which presents a charge distribution with the iron in its second oxidation state [Fe^{II} - d^6] and a carbene with all the electrons paired.[21] According to their DFT calculations, which where operated at the (U)B3LYP level of theory with a differently specified basis set [geometries: Fe (LanL2DZ), other atoms (6-31G(d)); single-points: all atoms (def2-TZVP)], they observed that the lowest in energy spin state was the OSS one, being the CSS the highest and the Triplet the intermediate one.[21] Moreover, the OSS and the Triplet states showed the most similar geometrical properties (i.e. Fe-C carbene distance and Fe-C-C-O

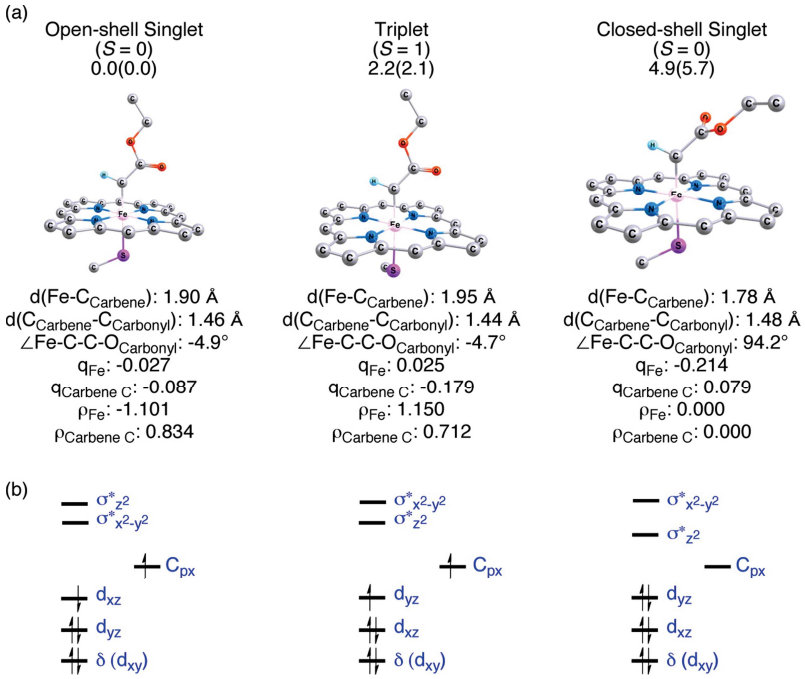

Figure 4.5: *Structures, parameters and electronic configuration of iron-carbene porphyrin species.*[21]

dihedral angles, see Figure 4.5), respect to the CSS one that appears with a 90° twisted dihedral angle.

To gain a higher degree of detail in the electronic configuration of the iron-carbene, the authors decided to investigate, with the same level of calculation reported before, what happens during the interaction between the iron metal center and the carbene fragment. When orbitals of the two species start interacting, the situation reported in Figure 4.6, which shows the molecular orbital interaction diagram for the OSS lowest state, can be observed.[21]

Interaction involves a sp^2 carbene orbital which orients one of its lobes towards the iron and donates its electron pair to the empty d_{z^2} orbital. This initial interaction generates two molecular orbitals (MO) and by populating the bonding-MO forms the Fe-C σ bond in the iron porphyrin carbene. Contemporarily, the doubly occupied d_{xz} Fe orbital, which presents a π symmetry, can mix weakly with the empty symmetrical carbene p_x-orbital, thus forming a combination of MOs which is only weakly bonding and antibonding. Being the interaction so small, the "bonding" orbital mostly resides on the iron atom and it is called here d_{xz} to underline

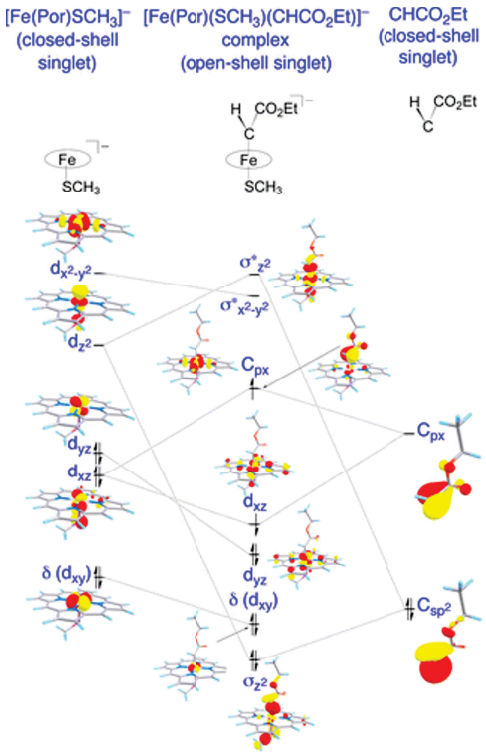

Figure 4.6: *Molecular orbital interaction diagram for the OSS lowest state.*[21]

that specific character. Analogously, the other "antibonding" orbital is mostly on carbene's carbon and, in the same way as above, it is named C_{px}. The other iron d-orbital of π symmetry (d_{yz}) cannot overlap with any carbene orbital, so it shows a non-bonding character.[21] In order to get insight view on the d_{xz}/C_{px} MO couple, authors performed the Spin-Natural Orbitals (SNO) calculations obtaining the values of occupancies reported in Figure 4.7.[21] Specifically, in the case of OSS, C_{px} showed an occupancy of 0.88, while d_{xz} an occupancy of -0.88: this non-unitary result clearly illustrates a mutual interaction between these two orbitals, with the two electrons neither interacting together, nor perfectly isolated from each other (Figure 4.7a).[21] This situation was further investigated by considering the Natural Orbitals (NO, Figure 4.7b) and the Kohn-Sham Corresponding Orbitals (KSCO, Figure 4.7c), by arriving to the same conclusions that the two electrons have some degree of separation and that all the system can be thought as an iron-bound carbene radical.[21]

While the CSS is an excited singlet state with a not stable wave function, the Triplet one deserves more attention that goes over the simple spin flip of OSS.[21]

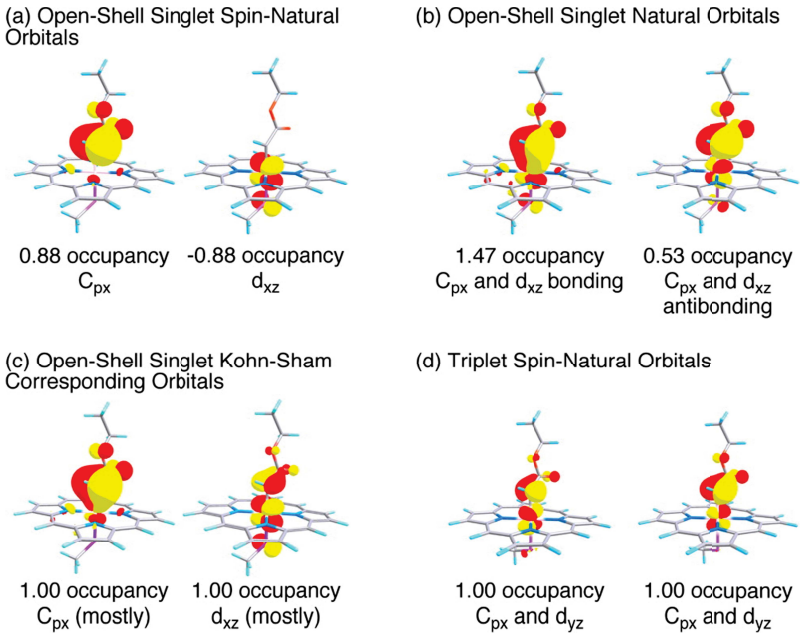

Figure 4.7: *SNO, NO, KSCO occupancy analysis for OSS and Triplet states.*[21]

From calculations reported in Figure 4.7d, it can be seen that there is a single occupancy in SNO: now, besides the previous reported C_{px}, the d_{yz} is singly occupied. This means that the two electrons reside now in perpendicular orbitals and not in parallel ones, like in OSS. This particular feature allows for a minimization in the repulsion between the two identically oriented spins, but slightly increases the distance between Fe and C not being a stabilizing interaction like in OSS (see Figure 4.5, Fe-C distance).[21] Moreover, the concomitant decrease of dihedral angle close to 0°, opens the possibility to delocalize the electron of the carbene portion onto the near carbonyl group.[21]

4.3 The in-depth computational study of Fe(Porphyrin)(OMe) catalyzed cyclopropanation

Propelled by the results reported before, we decided to investigate, with a high-definition study, the mechanism of the reaction using catalysts elaborated by Gallo's group and published some years ago.[23] As we described above, lots of efforts have

been employed to disclose the mechanism of carbene formation, as well as studies of the subsequent carbene transfer reaction to C=C and C-H bonds with the fundamental contribution of theoretical calculations. In order to describe properly the electronic features of these systems, very simplified computational models of the porphyrin complexes have been usually used, e.g. simple porphine, thus without taking care of the contribution of the organic environment in which porphyrin is operating, whether it is a protein or the ligand skeleton of a bio-inspired system. One of the most interesting situations occurs when chiral moieties are mounted onto the tetrapyrrolic core of the catalyst: in such systems stereoselective reactions can be achieved, which mimic the selectivity of the corresponding engineered metalloenzyme-catalyzed reactions.[24] With the usage of the iron(III) porphyrin methoxy complex [Fe(**1**)(OCH_3)] (Figure 4.8), bearing suitable chiral C_2 symmetrical moieties onto the porphyrin core, as catalysts for cyclopropanation reactions, Gallo and co-workers showed very high *turnover number* (TON) and *turnover frequency* (TOF) values, as well as high diastereo and enantioselectivity.[4] In the previous years, stereochemical outcome of these reactions was rationalized through theoretical calculations by focusing on the tridimensional arrangement of the ligand framework of the catalyst.[10] However, an in-depth investigation on the various steps of the catalytic cycle is still missing. So, we decided to investigate the mechanism of the reaction between **EDA** and ethylene, first using the simplified model catalyst containing simple porphine [Fe(Por)(OCH_3)] (**FP**) (Por = porphine), then expanding the study, for the main mechanistic step, to the more complex *mono*-strapped catalyst [Fe(**2**)(OCH_3)] (**FP-2**), in which one chiral organic moiety is mounted onto the porphyrin core (Figure 4.8).

We already showed above that **EDA** is capable of reducing iron from the Fe(III) to the Fe(II) oxidation state,[8],[20] and for such reason both electronic states should be taken into account in the mechanistic investigation. Thus, the reaction pathway involving [Fe^{III}(Por)(OCH_3)] (**FP**) and that involving the reduced methoxy porphyrin [Fe^{II}(Por)(OCH_3)]$^-$ (**FP$^-$**) complex should be both determined during the theoretical investigation of the reaction mechanisms.

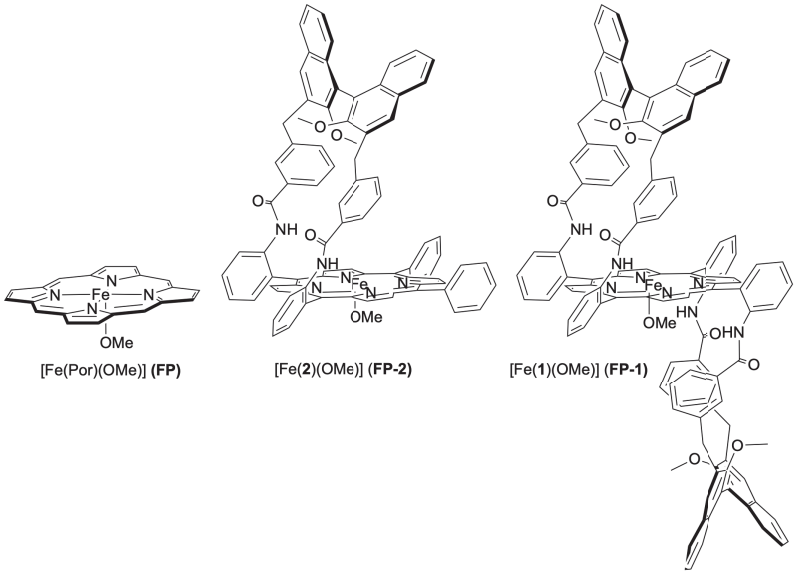

Figure 4.8: *Molecular structures of iron-methoxy porphyrin complexes.*[23]

A generic overall picture of the proposed reaction mechanism is depicted in Scheme 4.5: by moving from the starting reactants to the cyclopropane product (**CP**), the picture shows that the initial attack of **EDA** to [Fe(Por)(OCH_3)] (**FP**) and the concomitant loss of dinitrogen give rise to the carbene intermediate [Fe(Por)(OCH_3)($CHCO_2Et$)]. This last one can exist in the two different modes, *terminal*-carbene **TC** and *bridging*-carbene **BC**, though usually the former is considered to lay along the reaction pathway whereas the latter constitutes a form in equilibrium with it.[10],[25] The next reaction of ethylene with the intermediate affords the cyclopropane adduct **CP** and restores the catalyst **FP** in its starting state.

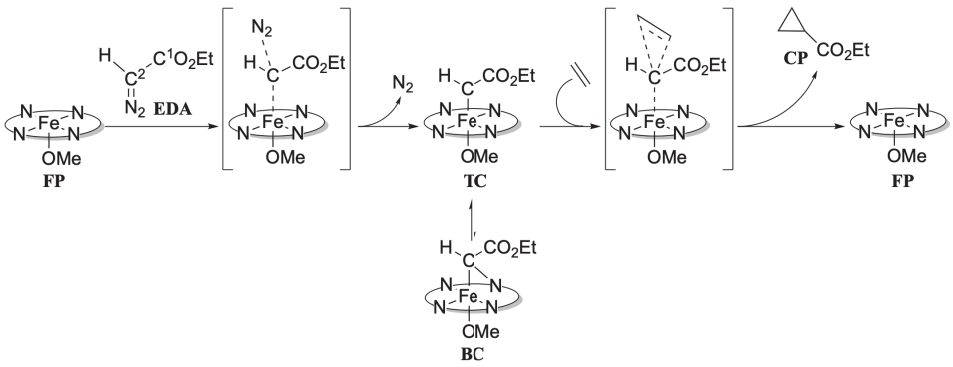

Scheme 4.5: *General scheme of the cyclopropane formation catalyzed by [Fe^{III}(Por)(OCH_3)] (**FP**).*[23]

A similar distinction between *terminal* and *bridged* carbene was also reported

by Shaik and co-workers.[21] They highlighted that in the case of the thiomethyl iron porphyrin carbene [Fe(Por)(SMe)($CHCO_2Et$)], when the oxidized species were involved in the calculations, the *bridged* and the *terminal* forms can exist as minima in the doublet spin state, which is the lowest possible in energy.[21] The difference appeared when compared the two carbene forms together: while in the case of the reduced specie they reported only on the *terminal* form as the lowest in energy, they found that in the oxidized one the *bridged* became the most stable one.[21] In particular, they showed that not only the bridged oxidized carbene was over 20 kcal/mol more stable than the terminal one, but also the barrier to form the bridged species form the terminal ones was found to be very low.[21]

All these observations were also supported by experimental and computational studies suggesting that the oxidized specie can exist in a bridged form and can be an intermediate in the carbene-mediated reactions.[26]

4.3.1 Reaction catalyzed by $[Fe^{II}(Por)(OMe)]^-$ (FP^-)

To start our computations, we decided to follow the same level of theory reported by Shaik and co-workers, also to create all the possible circumstances to give comparisons between the two catalysts.[21]

Specifically, all the reactants, intermediates, and transition states along the reaction pathway were optimized by using toluene as solvent and the unrestricted UB3LYP functional at the 6-31G(d) level[27] for all the atoms, but iron for which the effective core potential LanL2DZ was used. Once obtained the optimized geometries, single-point energy calculations in toluene were performed using the all-electron def2-TZVP basis set for all atoms. Dispersion corrections were computed with the Grimme's D3 method not to underestimate the metal-ligands interactions.[35] The stability of the wavefunction was always checked for the open-shell structures, optimizing it when found unstable. For all the reduced species containing iron, the closed-shell singlet, open-shell singlet, triplet, and quintet spin states were investigated.

We decided to start the modelling of the catalyst system by using the simple

porphine ligand **FP** reported in Figure 4.8. The use of a such simplified ligand structure was reported also in the publications of our research group and Shaik's one, showing that it is a good simplification choice to decrease computational cost without affecting so much the results of the calculations.[10],[21]

EDA and **FP**$^{-}$ were separately optimized and the iron ground state in **FP**$^{-}$ was determined to be the high spin quintet state, ^{5}**FP**$^{-}$, preferred by 9.2 kcal/mol over the triplet state ^{3}**FP**$^{-}$ and by almost 14 kcal/mol over both the closed and open-shell singlet states ^{1cs}**FP**$^{-}$ and ^{1os}**FP**$^{-}$. In **EDA** approaching **FP**$^{-}$, a **FP**$^{-}$**-EDA** loose complex initially forms with a distance between iron and the **EDA** C_2 atom ($d_{C2\text{-}Fe}$) longer than 3.5 Å. In the formation of this complex species, the singlet states remained the less stable ones and the energy gap with respect to the quintet state ^{5}**FP**$^{-}$**-EDA** even increases (Figure 4.9 and Table 4.3). This ^{5}**FP**$^{-}$**-EDA** local energy minimum geometry is 9.7 kcal/mol more stable than the isolated **EDA** and ^{5}**FP**$^{-}$ reactants in terms of energy but, due to the entropy penalty, it is slightly less stable than the reactants in terms of Gibbs free energy.

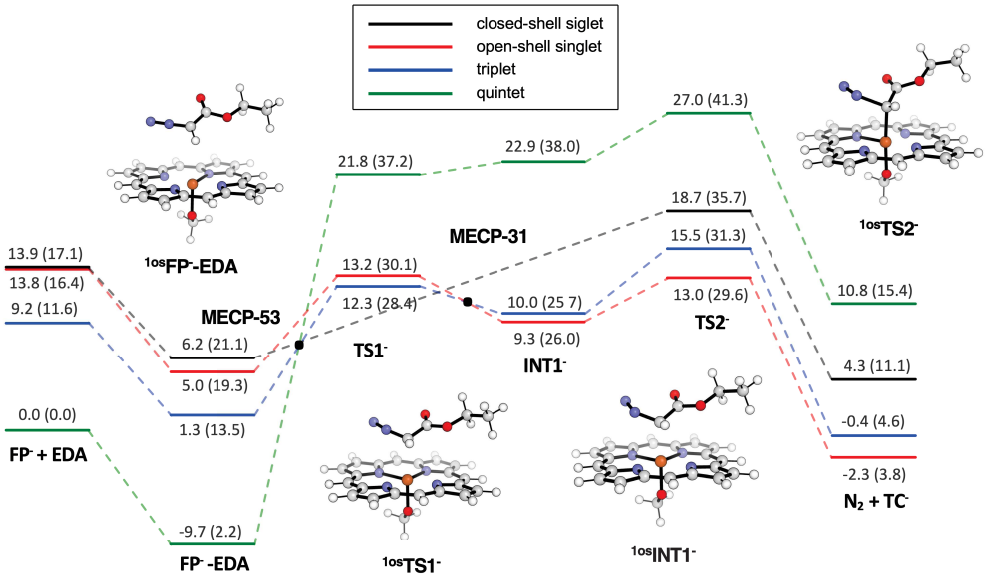

Figure 4.9: *Energy profiles for the reaction of carbene intermediate formation from* ***EDA*** *and [Fe^{II}(Por)(OCH$_3$)]$^{-}$,* ***FP***$^{-}$*. Energy values are from single-point def2-TZVP calculations in toluene on geometries optimized at the UB3LYP/6-31G(d) level (LanL2DZ for iron) in toluene with zero-point correction; the corresponding Gibbs free energy are reported in parenthesis. All values are dispersion corrected.*[23]

	E_{rel}	G_{rel}	$d_{C2\text{-}N\alpha}$	$d_{C2\text{-}Fe}$	$d_{C2\text{-}N}$	$d_{Fe\text{-}O}$
^{1cs}**FP$^-$ + EDA**	13.9	17.1				1.898
^{1os}**FP$^-$ + EDA**	13.8	16.4				1.935
^{3}**FP$^-$ + EDA**	9.2	11.6				2.008
^{5}**FP$^-$ + EDA**	0.0	0.0				1.901
^{1cs}**FP$^-$-EDA**	6.2	21.1	1.307	3.468	3.855	1.900
^{1os}**FP$^-$-EDA**	5.0	19.3	1.306	3.575	3.887	1.937
^{3}**FP$^-$-EDA**	1.2	13.5	1.305	3.772	3.805	1.977
^{5}**FP$^-$-EDA**	-9.7	2.2	1.306	3.929	3.592	1.895
^{1os}**TS1$^-$**	13.2	30.1	1.367	2.460	3.048	1.853
^{3}**TS1$^-$**	12.2	28.4	1.345	2.768	3.160	1.798
^{5}**TS1$^-$**	21.8	37.2	1.439	2.283	2.935	1.892
^{1os}**INT1$^-$**	9.3	26.0	1.452	2.231	2.899	1.853
^{3}**INT1$^-$**	10.0	25.7	1.447	2.251	2.912	1.849
^{5}**INT1$^-$**	22.9	38.0	1.455	2.223	2.921	1.868
^{1cs}**TS2$^-$**	18.7	35.7	1.740	1.987	2.687	1.934
^{1os}**TS2$^-$**	13.0	29.6	1.815	2.064	2.794	1.878
^{3}**TS2$^-$**	15.4	31.3	1.857	2.104	2.801	1.863
^{5}**TS2$^-$**	27.0	41.3	1.844	2.081	2.827	1.872
N_2 + ^{1cs}TC$^-$	4.3	11.1		1.798	2.698	1.947
N_2 + ^{1os}TC$^-$	-2.3	3.8		1.939	2.734	1.904
N_2 + ^{3}TC$^-$	-0.4	4.6		1.971	2.752	1.891
N_2 + ^{5}TC$^-$	10.8	15.4		1.959	2.767	1.884
N_2 + ^{1cs}TS3$^-$	15.7	22.4		1.874	1.985	1.942
N_2 + ^{1os}TS3$^-$	12.7	19.8		1.925	1.980	1.902
N_2 + ^{3}TS3$^-$	16.7	22.9		1.994	2.004	1.875
N_2 + ^{5}TS3$^-$	23.9	28.5		2.081	2.136	1.876
N_2 + ^{1cs}BC$^-$	4.9	11.9		2.058	1.452	1.896
N_2 + ^{1os}BC$^-$	-1.1	5.7		2.005	1.472	1.866
N_2 + ^{3}BC$^-$	-0.7	5.2		2.011	1.467	1.865
N_2 + ^{5}BC$^-$	-10.5	-5.9		2.491	1.418	1.898

Table 4.3: *Relative electronic energy, with zero-point correction, and the corresponding Gibbs free energy (kcal/mol) of the transition states and intermediates in the reaction of carbene intermediate formation from ethyl diazoacetate (**EDA**) and [Fe^{II}(Por)(OCH_3)]$^-$ (**FP$^-$**) determined through single-point def2-TZVP calculations in toluene on geometries optimized at the UB3LYP/6-31G(d) level (LanL2DZ for iron) in toluene. The distances (Å) between **EDA** C2 atom and leaving N_2 ($d_{C2\text{-}N\alpha}$), iron ($d_{C2\text{-}Fe}$), and the closest porphyrin nitrogen atom ($d_{C2\text{-}N}$) are reported for each stationary point.*[23]

The energy profile which brings to the loss of dinitrogen and formation of the *terminal* carbene species **TC$^-$** was determined and it resulted more intricate than in Scheme 4.5 (Figure 4.9). Among the four **FP$^-$-EDA** complexes, the radical or diradicaloid species are not directly connected to the transition states of the dinitrogen loss, but in the first reaction step, three intermediate structures can be identified, the so-called close complexes **^{1os}INT1$^-$**, **^{3}INT1$^-$**, and **^{5}INT1$^-$**, in which the distance between the C2 and Nα ($d_{\text{C2-N}\alpha}$) atoms of **EDA** is still a bond distance (∼1.45 Å). The interaction between **EDA** and iron is already significant in these structures ($d_{\text{C2-Fe}}$ shows a decrease to a bond distance, 2.22-2.25 Å). Moreover, the stability order of the various spin states resulted reversed, being the broken-symmetry solution of the singlet **^{1os}INT1$^-$** and the triplet **^{3}INT1$^-$** the most stable ones, while **^{5}INT1$^-$** becomes the least stable. Another important observation concerns the significant values of spin density observed in these intermediates: contrarily to the **FP$^-$-EDA** complexes, where no spin density is present on the atoms, in **^{1os}INT1$^-$** it mainly resides on iron (ρ_{Fe} = -1.001) and the nitrogen atoms of the **EDA** moiety ($\rho_{\text{N}\beta}$ = 0.733 and $\rho_{\text{N}\alpha}$ = 0.134); a small spin density is also observed on C2 (ρ_{C2} = 0.120) and the methoxy oxygen atom (ρ_{O} = -0.103). Simultaneously, a significant charge transfer is observed, as the neutral **EDA** moiety of **^{1os}FP$^-$-EDA**, with an entire charge hosted by **FP$^-$**, gains an overall charge of -0.490 with only 0.510 left on the iron porphyrin moiety. An interesting observation arises from the inspection of the structures of **FP$^-$-EDA** and **INT1$^-$**, showing that they differ mainly in two geometrical features: the already mentioned distance between iron and the C2 carbon atom of **EDA** and the geometry of the first nitrogen atom (Nα) of **EDA**, which is linear in the complexes **FP$^-$-EDA**, while trigonal planar in the intermediates **INT1$^-$**, suggesting that a change of its hybridization can be involved in this step. As a proof of this variation, we were able to locate the transition state **TS1$^-$** corresponding to their interconversion, which is characterized by a very strong negative frequency and a correct correlation to **FP$^-$-EDA** and **INT1$^-$**, through IRC calculations. Energy barriers of 12-13 kcal/mol with respect to isolated **EDA** and **^{5}FP$^-$** were found for **^{1os}TS1$^-$** and **^{3}TS1$^-$**, while **^{5}TS1$^-$** is less stable by 10-11 kcal/mol.

By proceeding along the reaction coordinate, further shortening of $d_{\text{C2-Fe}}$ leads

to the three open-shell transition states ^{1os}**TS2$^-$** , ^{3}**TS2$^-$**, and ^{5}**TS2$^-$**, here reported in order of stability. The closed-shell transition state ^{1cs}**TS2$^-$**, which is directly accessible from the reactant complex ^{1cs}**FP$^-$-EDA**, is less stable than ^{3}**TS2$^-$**, but more stable than ^{5}**TS2$^-$**. The preferred transition state ^{1os}**TS2$^-$** is characterized by $d_{\text{C2-Fe}}$ = 2.06 Å and $d_{\text{C2-N}\alpha}$ = 1.81 Å and by a spin density on C2 significantly improved (ρ_{C2} = 0.424), which corresponds to the concomitant decrease on the nitrogen atoms ($\rho_{\text{N}\beta}$ = 0.444 and $\rho_{\text{N}\alpha}$ = 0.029), and an almost unchanged value on the other atoms (ρ_{Fe} = -0.955 and ρ_{O} = -0.100). This spin change is also accompanied by a partial charge return towards the iron porphyrin moiety (overall charge on **EDA** 0.351). In ^{1os}**TS2$^-$** the electronic energy barrier is 13 kcal/mol with respect to isolated **EDA** and ^{5}**FP$^-$**, which is much higher if the Gibbs free energy is considered, 29.5 kcal/mol, a value which seems too high for a viable reaction pathway. The examination of this energy barrier shows that it might be overestimated due to over-stabilization of the higher spin state precursors provided by the B3LYP hybrid functional. Moreover, it should be also considered that the investigations reported so far on the reaction mechanism are referred to a very simplified reaction model, whereas the real reaction is experimentally performed with [Fe(**1**)(OCH_3)] catalyst, with a C_2 symmetrical steric chiral bulk surrounding the tetrapyrrolic core (Figure 4.8). As a matter of fact, it is known that in the enzyme-catalyzed reactions, the barrier from the reactant complex to the transition state is lowered by the enzyme environment.[28] The "ligand environment" installed in **1**, due to the large organic moiety composed by the pickets and the surmounting binaphtyl hat that surrounds the reaction site for **EDA**, might act in a similar way. To confirm this hypothesis, transition states including the entire *bis*-strapped porphyrin **1**, instead of the simple porphine present in ^{1os}**TS2$^-$**, should be located, but this is beyond our today's computational possibilities. In previous papers[10],[29] our group showed that the behavior of the [Fe(**1**)(OCH_3)] complex can be accurately reproduced in calculations by the corresponding single-stranded porphyrin model complex [Fe(**2**)(OCH_3)] (**FP-2**) (Figure 4.8). So, we tried to locate the corresponding transition state ^{1os}**TS2-2$^-$**, succeeding in the goal after considerable computational efforts. While the geometrical data of **EDA** inside the reaction site found for ^{1os}**TS2-2$^-$** are very similar to

those of ^{1os}**TS2**$^{-}$, the electronic energy barrier is significantly lower, 5 kcal/mol for the former (Table 4.4) and 13 kcal/mol for the latter (Table 4.3). The decrease is significant also in terms of relative free energy as the barrier approaches the value of 24 kcal/mol, 5.5 kcal/mol lower than in the simplified model and thus evidencing the large effect of the organic environment on the energy barriers. Another important factor that should be remarked, is that the barrier from the isolated reactants overestimates the entropy involved. In fact, the computed free energy barrier from the reactant complex ^{5}**FP-2**$^{-}$**-EDA** shows an even lower value (21.5 kcal/mol), compatible with the fast reaction catalyzed by the [Fe(**1**)(OCH_3)] complex, able to promote cyclopropanation reactions even below room temperature.[10] We can thus envisage that the energy barrier of the reaction mediated by the *bis*-strapped [Fe(**1**)(OCH_3)] complex should be about the same or even lower than that calculated in the presence of the *mono*-strapped [Fe(**2**)(OCH_3)] (**FP-2**), being the second strap not directly involved in the carbene formation.

	E_{rel}	G_{rel}	$d_{C2\text{-}N\alpha}$	$d_{C2\text{-}Fe}$	$d_{C2\text{-}N}$	$d_{Fe\text{-}O}$
^{5}**FP-2**$^{-}$ **+ EDA**	0.0	0.0				1.896
^{5}**FP-2**$^{-}$**-EDA**	-10.1	2.5	1.304	6.594	4.836	1.896
^{1os}**INT1-2**$^{-}$	2.2	21.4	1.453	2.224	2.949	1.850
^{1os}**TS2-2**$^{-}$	5.0	24.0	1.818	2.055	2.809	1.874

Table 4.4: *Relative electronic energy, with zero-point correction, and the corresponding Gibbs free energy (kcal/mol) of the transition states in the reaction of terminal-carbene intermediate formation from ethyl diazoacetate* ***EDA*** *and* $[Fe^{II}(\mathbf{2})(OCH_3)]^{-}$, ***FP-2***$^{-}$, *determined through single-point def2-TZVP calculations in toluene on geometries optimized at the UB3LYP/6-31G(d) level (LanL2DZ for iron) in toluene. The distances (Å) between* ***EDA*** *C2 atom and leaving N_2 ($d_{C2\text{-}N\alpha}$), iron ($d_{C2\text{-}Fe}$), and the closest porphyrin nitrogen atom ($d_{C2\text{-}N}$) are reported for each stationary point.*[23]

Going back to the simple porphine model, the intrinsic reaction coordinate (IRC) calculations performed on the four transition states **TS2**$^{-}$ allowed to connect them, on the forward side, to the *terminal* carbene intermediate species $[Fe^{II}(Por)(OCH_3)(CHCO_2Et)]^{-}$ (**TC**$^{-}$) and dinitrogen as by product. The stability order of these *terminal* carbenes reflects that of the transition state leading to them, being the broken-symmetry solution of the open-shell singlet ^{1os}**TC**$^{-}$ the most stable one, with energy

comparable, even lower, than that of the starting reactants (Table 4.3 and Figure 4.10). In agreement with previous experimental and computational data,[30] the singlet state resulted preferred for this carbene species. To gain more information on these intermediate structures and transition states, we investigated this step in more detail. The spin density in ^{1os}**TC**$^{-}$ *terminal* carbene resides on iron (ρ_{Fe} = -0.960) and the carbon atom linked to it (ρ_{C} = 0.834) evidencing an antiferromagnetic coupling between the carbon-centered radical and the unpaired electron on iron as already found in the corresponding terminal carbene bearing a methylthiolate instead of the methoxy group as the other axial ligand on iron.[21] The diradicaloid structure of ^{1os}**TC**$^{-}$ terminal carbene resembles that of the cobalt carbene radical species.[31] Specifically, a positive NPA charge was found on iron (q_{Fe} = +0.159) while the two atoms directly linked to it are negatively charged (q_{C2} = -0.119 and q_{O} = -0.628). The overall charge on the carbene moiety (-0.195) further highlights the charge shift towards the iron porphyrin moiety. The distance between iron and the methoxy oxygen atom remains almost the same during the reaction (from 1.901 Å in ^{5}**FP**$^{-}$ to 1.853 Å in ^{1os}**INT1**$^{-}$ and 1.905 Å in ^{1os}**TC**$^{-}$, see Table 4.3).

The experimental evidences indicated that, regardless of the nature of the active carbene intermediate, the methoxy ligand of the catalyst is not lost during cyclopropanation.[10]

Starting from the *terminal* carbenes $[Fe^{II}(Por)(OCH_3)(CHCO_2Et)]^{-}$ (**TC**$^{-}$) we moved to the corresponding *bridging* structures **BC**$^{-}$ and the transition states connecting them, **TS3**$^{-}$. The lowest energy transition state was found in ^{1os}**TS3**$^{-}$, occurring on the singlet open-shell surface with a barrier of 15 kcal/mol with respect to ^{1os}**TC**$^{-}$ and giving a *bridging* structure ^{1os}**BC**$^{-}$ almost isoenergetic to ^{1os}**TC**$^{-}$ (Table 4.3 and Figure 4.10). The most stable *bridging* carbene was identified in the high spin quintet ^{5}**BC**$^{-}$, 9.4 kcal/mol more stable than ^{1os}**BC**$^{-}$.

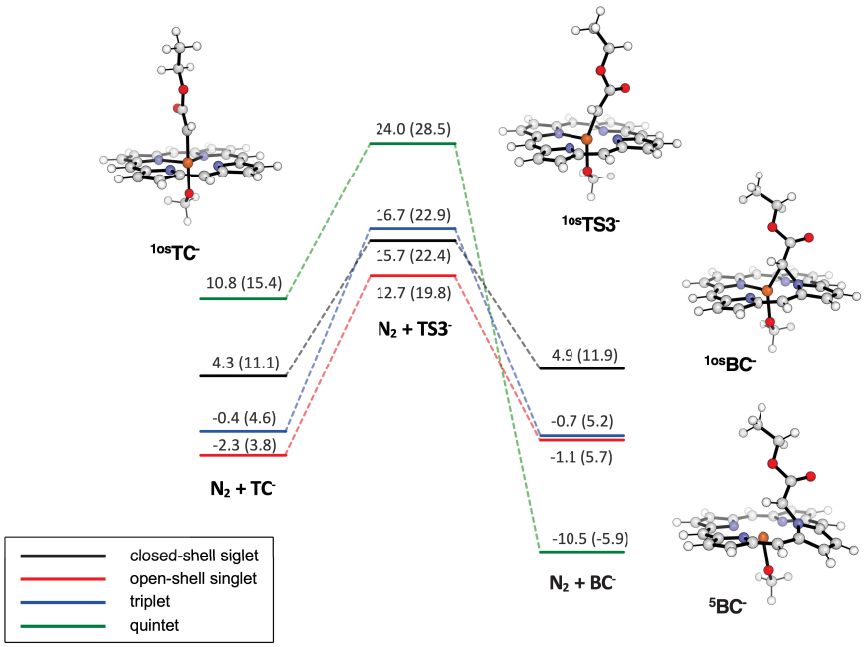

Figure 4.10: *Energy profiles for the terminal-carbene* ***TC*** *and bridging-carbene* ***BC*** *interconversion. Energy values are from single-point def2-TZVP calculations in toluene on geometries optimized at the UB3LYP/6-31G(d) level (LanL2DZ for iron) in toluene with zero-point correction; the corresponding Gibbs free energy are reported in parenthesis. All values are dispersion corrected. The energy values are referred to the starting reactants* ***5FP*** *and* ***EDA****.*[23]

In the above results the broken-symmetry solutions of the singlet species could have been corrected for spin contamination using the Yamaguchi correction.[32] The reason why we looked for those corrections relies on to the fact that during DFT calculations performed using an unrestricted functional (UB3LYP in our case), spins are left to gain another degree of freedom, which is represented by the possibility to populate orbitals with a different spatial orbital distribution for the electrons (Figure 4.11).

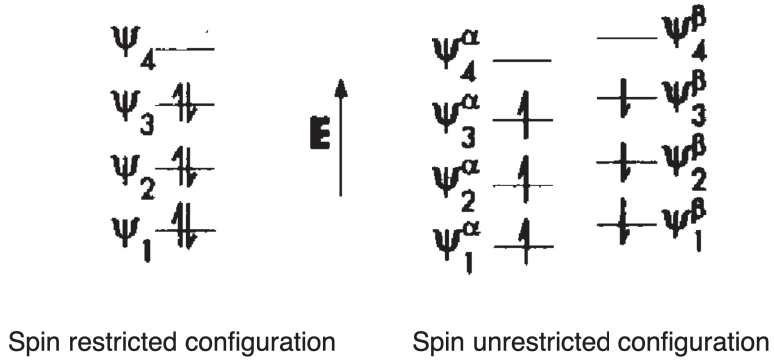

Figure 4.11: *Schematic representation of restricted and unrestricted wafefunctions.*

The spatial distribution for electrons with α spins and β spins can therefore describe the *spin polarization*. Spin polarization occurs due to exchange-correlations effects via the interactions of the electrons of the same spin as an unpaired electron in the open shell (e.g. radical) system.

One consequence of allowing spin-up and spin-down orbitals to have different spatial parts is that the wavefunction so obtained, no longer corresponds to a definite or "pure" spin state.[33] For a system with n_α α electrons and n_β β electrons, then the projection of the overall spin on the z-axis (i.e. the quantum number s_z) is given by:

$$s_z = \frac{1}{2}(n_\alpha - n_\beta)$$

Another way to characterize the spin state of a system is in terms of the quantum mechanical operator $\hat{S}^2$, the square of the total spin and its expectation value for the wavefunction is:

$$\left\langle \widehat{S}^2 \right\rangle = s_z(s_z + 1)$$

for a pure spin state.[33]

This means that, for example, for a doublet, where $n_\alpha = n_\beta + 1$, the expectation value for $\hat{S}^2$ would be 0.75; vice versa, for a triplet, where $n_\alpha = n_\beta + 2$, it would be 2.[33] Here the problem arises: unrestricted calculated wavefunctions do not correspond to pure spin states and thereby suffer from the so-called *spin contamination*

by states of higher spin (i.e. they are not eigenfunctions of $\hat{S}^2$).[33] These wavefunctions return expectation values of $\hat{S}^2$ larger than expected based on the number of α and β electrons. For example, singlet states will be contaminated (have an admixture) of triplet, quintet etc. states, while doublets will be contaminated by quartets, sextets etc.[33] To have an idea of the magnitude and from where mathematically derives such contamination, we can have a close look to the following equation for the expectation value of $\hat{S}^2$ in the case of UHF wavefunction:

$$\int \psi \widehat{S}^2 \psi dr = s_z(s_z+1) + n_\beta - \sum_{i=1}^{n_\alpha} \sum_{j=1}^{n_\beta} \left(\int \psi_i^\alpha(r) \psi_j^\beta(r) dr \right)$$

The first term on to the right is the pure-spin value of the expectation value of $\hat{S}^2$; the second one is the number of β electrons and the last term is the sum of the overlap integrals of the spatial parts of all the occupied α molecular orbitals with all the occupied β molecular orbitals. This last term is the most interesting one because it can assume values from 0 to 1 depending on the nature of the orbitals: if two orbitals are completely different or *orthogonal*, the overlap will be equal to 0; if the two orbitals are exactly the same, the overlap will be 1.[33] Now, in the case of an unrestricted wavefunction, differences arise when α and β spatial orbitals are different and as a consequence the resulting calculated wavefunction will suffer from spin contamination (i.e. the expectation value of $\hat{S}^2$ is slightly larger than the one obtained with a pure-spin value).[33] This situation arises an unrealistic representation of the electronical system and a wrong estimation of orbital energy values.

To solve this problem, Yamaguchi and co-workers reported on a mathematical way to add corrections to the intrinsic problem of unrestricted calculations.[32] Specifically they elaborated and demonstrated a geometry optimization method that approximates the spin projection, efficiently eliminating the spin contamination in the total energy of broken-symmetry low-spin species.[32] Following the Yamaguchi mathematical approach, in the case of *OSS* contaminated by Triplet state, it has been demonstrated that by working under the Heisenberg-Hamiltonian approach [34] the value that takes in count the spin contamination can be expressed as:

$$f_{sc} = \frac{\langle S^2 \rangle_{OSS}}{\langle S^2 \rangle_{triplet\ in\ OSS\ geometry} - \langle S^2 \rangle_{OSS}}$$

Thus, the correction to the electronic energy can be obtained by simply multiplying the spin contamination factor f_{sc} by the difference in electronic energy of *OSS* and the Triplet state in the *OSS* geometry.[33]

$$E_{correction} = f_{sc} \cdot (E_{OSS} - E_{triplet\ in\ OSS\ geometry})$$

Summing up, the correction to the electronic energy can be evaluated by simply obtaining the electronic energies and the annihilation values for $\langle S^2 \rangle$ of both *OSS* and the same geometry of *OSS*, but treated in the Triplet state.

In order to apply these corrections to our specific case, we evaluated energies at the UB3LYP(GD3BJ)/def2tzvp/SMD(toluene) level of theory for the *OSS* geometries and the same ones evaluated in the Triplet state, by checking the stability of the wave function for each species.[23] Thus, annihilation values for $\langle S^2 \rangle$ were extracted. The results we obtained are reported in Table 4.5.

As it can be observed, the correction further stabilizes the broken-symmetry solution of the *OSS* (see Table 4.5) and do no not qualitatively change the discussion reported so far. The analysis we operated constitutes another proof in favor of the broken-symmetry *OSS* as the lowest energy species along the reaction profile. For such reasons, the corrected values for energy have not been added in the Figures and Tables showed above. Moreover, these findings suggest the reason why the *OSS* is lower in energy respect to the *CSS*: this can be easily explained by considering what happens during the carbene formation. As reported by Shaik and co-workers, the electron donation during the carbene formation is a one-electron process.[21] In order for one electron to be transferred from iron to EDA/forming N_2 species, it has to become initially unpaired or become unpaired during the course of the reaction. In the case of *OSS*, the electron is already unpaired and therefore no energy is required to broke the symmetry; vice versa, in a *CSS* state by definition no unpaired electrons can exist and therefore the requirements in energy to undergo the same type of reactivity without accessing broken symmetry solutions are considerably higher.[21]

	E (a.u.)	$\langle S^2 \rangle$ before annihilation	$\langle S^2 \rangle$ after annihilation	f_{sc}	$E_{correction}$ (a.u.)	$E_{correction}$ (kcal/mol)
^{1os}**FP**$^-$	-2367.955395	0.6281	0.0966			
triplet in OSS geometry	-2367.961532	2.4546	2.0219	0.344	0.00211	1.3
^{1os}**FP**$^-$**-EDA**	-2784.110044	0.6245	0.1011			
triplet in OSS geometry	-2784.115668	2.4137	2.0190	0.349	0.00196	1.2
^{1os}**TS1**$^-$	-2784.095122	0.8616	0.2251			
triplet in OSS geometry	-2784.091468	2.0439	2.0008	0.729	-0.00266	-1.7
^{1os}**INT1**$^-$	-2784.103969	1.0194	0.2553			
triplet in OSS geometry	-2784.103125	2.0265	2.0004	1.012	-0.00085	-0.5
^{1os}**TS2**$^-$	-2784.095544	0.9364	0.2101			
triplet in OSS geometry	-2784.090433	2.0267	2.0004	0.859	-0.00439	-2.8
^{1os}**TC**$^-$	-2674.548627	0.8397	0.1443			
triplet in OSS geometry	-2674.537042	2.0279	2.0004	0.707	-0.00819	-5.1
^{1os}**TS3**$^-$	-2674.52511	0.6884	0.0970			
triplet in OSS geometry	-2674.513662	2.0427	2.0010	0.508	-0.00582	-3.7
^{1os}**BC**$^-$	-2674.549237	0.9415	0.1489			
triplet in OSS geometry	-2674.547637	2.0735	2.0020	0.832	-0.00133	-0.8
^{1os}**TS4**$^-$	-2753.172532	0.9016	0.2679			
triplet in OSS geometry	-2753.165206	2.0435	2.0010	0.79	-0.00578	-3.6
^{1os}**INT2**$^-$	-2753.205822	1.0202	0.2023			
triplet in OSS geometry	-2753.206204	2.0352	2.0006	1.005	0.00038	0.2
^{1os}**TS5**$^-$	-2753.197051	0.951	0.3135			
triplet in OSS geometry	-2753.200643	2.1226	2.0036	0.812	0.00292	1.8

Table 4.5: *Yamaguchi's corrections for the open-shell singlet species of iron-porphyrin species.*[23]

By returning back to the case under study, focus was placed on the right side of the cyclopropanation reaction (Scheme 4.5) by looking for the transition states deriving from the attack of ethylene to the porphyrin carbene intermediates $[Fe^{II}(Por)(OCH_3)(CHCO_2Et)]^-$ (**TC**$^-$). The most stable TS was found to be ^{1os}**TS4**$^-$ (Table 4.6 and Figure 4.12), lying on the open-shell singlet surface and being characterized by a very low energy barrier (4.8 kcal/mol from ^{1os}**TC**$^-$), much smaller than that of the corresponding *terminal-bridging* interconversion.

Once again, ^{1os}**TS4**$^-$ is preferred over ^{3}**TS4**$^-$ and largely preferred over ^{1cs}**TS4**$^-$ and ^{5}**TS4**$^-$. IRC analysis from ^{1os}**TS4**$^-$ leads in the forward direction to an intermediate with a diradicaloid character, ^{1os}**INT2**$^-$. This intermediate shows the spin density residing on iron (ρ_{Fe} = -1.000) and the farthest carbon atom of the attacking ethylene (ρ_C = 1.047); one new C-C bond is already formed (1.55 Å) while the other

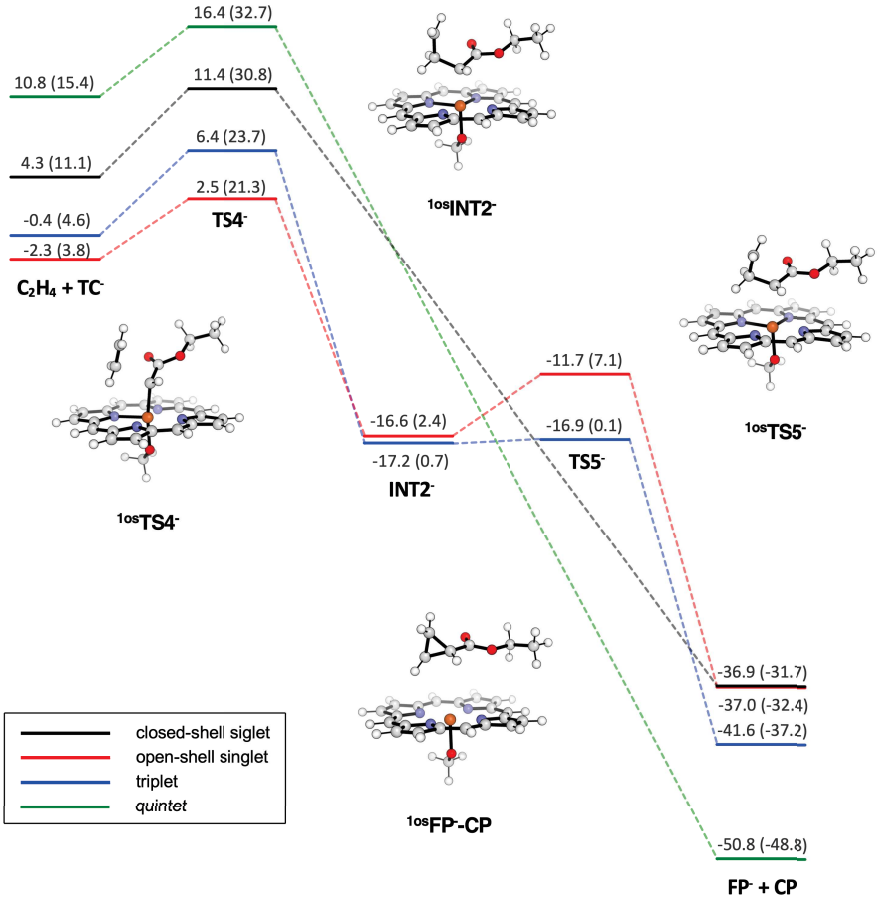

Figure 4.12: *Energy profiles for the reaction of the terminal-carbene* $[Fe^{II}(Por)(OCH_3)(CHCO_2Et)]^-$ (***TC***$^-$) *with ethylene. Energy values are from single-point def2-TZVP calculations in toluene on geometries optimized at the UB3LYP/6-31G(d) level (LanL2DZ for iron) in toluene with zero-point correction; the corresponding Gibbs free energy are reported in parenthesis. All values are dispersion corrected. The energy values are referred to the starting reactants* ^{5}***FP***$^-$ *and* ***EDA***.[23]

one far to be formed (2.52 Å), all suggesting that it is a reaction intermediate with a radical nature. However, the IRC path from ^{3}**TS4**$^-$ gives access to a structure, ^{3}**INT2**$^-$, separated by the final products by a very low energy barrier, which disappears in terms of free energy. Moreover, both the closed-shell ^{1cs}**TS4-** and the highest spin ^{5}**TS4**$^-$ transition states are directly connected to the final products. Thus, it cannot be excluded that the pathways cross after the ^{1os}**TS4**$^-$ transition state to generate the cyclopropane product without passing the ^{1os}**INT2**$^-$ intermediate (see Section 4.4). The ring closure to get the cyclopropane product occurs after transition state, ^{1os}**TS5**$^-$, with a very low energy barrier (5 kcal/mol from

^{1os}**INT2**$^{-}$). Then, the process ends in a deep valley, about 50 kcal/mol below the starting reactants, both in terms of electronic energy and free energy (Table 4.6) with the formation of cyclopropane **CP** and the regeneration of the catalyst which is ready for a new reaction cycle after the crossover to the most stable quintet ground state (see Section 4.4).

	E_{rel}	G_{rel}	$d_{C2\text{-}CE1}$	$d_{C2\text{-}CE2}$	$d_{C2\text{-}Fe}$	$d_{C2\text{-}N}$	$d_{Fe\text{-}O}$
^{1cs}**TS4**$^{-}$	11.4	30.8	2.129	2.656	1.942	2.627	1.938
^{1os}**TS4**$^{-}$	2.5	21.3	2.221	2.954	2.022	2.710	1.898
^{3}**TS4**$^{-}$	6.4	23.7	2.269	3.033	2.078	2.761	1.881
^{5}**TS4**$^{-}$	16.4	32.7	2.270	2.995	2.043	2.793	1.890
^{1os}**INT2**$^{-}$	-16.6	2.4	1.553	2.520	2.190	2.898	1.887
^{3}**INT2**$^{-}$	-17.2	0.7	1.549	2.499	2.204	2.898	1.890
^{1os}**TS5**$^{-}$	-11.7	7.1	1.524	2.191	2.461	3.023	1.901
^{3}**TS5**$^{-}$	-16.9	0.1	1.512	2.203	2.551	3.070	1.951
CP + ^{1cs}**FP**$^{-}$	-36.9	-31.7					
CP + ^{1os}**FP**$^{-}$	-37.0	-32.4					
CP + ^{3}**FP**$^{-}$	-41.6	-37.2					
CP + ^{5}**FP**$^{-}$	-50.8	-48.8					

Table 4.6: *Relative electronic energy, with zero-point correction, and the corresponding Gibbs free energy (kcal/mol) of the transition states and intermediates in the reaction of ethylene with the terminal-carbene [Fe^{II}(Por)(OCH_3)($CHCO_2Et$)]$^-$ intermediates* ***TC***$^-$ *determined through single-point def2-TZVP calculations in toluene on geometries optimized at the UB3LYP/6-31G(d) level (LanL2DZ for iron) in toluene. The energy values are referred to the starting reactants* ^{5}***FP***$^-$ *and* ***EDA***. *The distances (Å) between the carbene C2 atom and the incoming ethylene carbon atoms (*$d_{C2\text{-}CE1}$ *and* $d_{C2\text{-}CE2}$*), iron (*$d_{C2\text{-}Fe}$*), and the closest porphyrin nitrogen atom (*$d_{C2\text{-}N}$*) are reported for each stationary point.*[23]

4.3.2 Reaction catalyzed by [Fe^{III}(Por)(OMe)] (FP)

To gain a general view on the reaction and the reactivity of the system, we decided to investigate also the oxidized form of the iron catalyst. The computational approach was the same as above described. In this case, the doublet, quartet, and sextet spin states were investigated for all the species containing iron. When the oxidized iron porphyrin [Fe^{III}(Por)(OCH_3)] (**FP**) was optimized, the preferred ground state was now found to be the high spin sextet state, ^{6}**FP**, preferred over the quartet and doublet states ^{4}**FP** and ^{2}**FP** by 3.2 and 8.5 kcal/mol, respectively

(Figure 4.13 and Table 4.7). The most stable reactant complex **^{6}FP-EDA** is 8.4 kcal/mol more stable than the isolated **EDA** and **^{6}FP** in terms of energy, but less stable in terms of Gibbs free energy, as observed for $[Fe^{II}(Por)(OCH_3)]^-$ (**FP$^-$**). Moving from the reactant complexes by decreasing the $d_{C2\text{-}Fe}$ distances, once more the lowest spin state becomes preferred. Differently from what reported above, no intermediate structure was observed and the transition state **^{2}TS2** for dinitrogen loss, is directly reached. The electronic energy barrier with respect to isolated **EDA** and **^{6}FP** is higher than with the reduced catalyst (22.6 kcal/mol) and becomes extremely high if the Gibbs free energy is considered (37 kcal/mol). The free energy barrier computed from the reactant complex **^{6}FP-EDA** shows a lower, but still high value (33.3 kcal/mol). Operating as before and using the model single-stranded porphyrin complex $[Fe^{III}(\mathbf{2})(OCH_3)]$ (**FP-2**) a significant decrease of about 6 kcal/mol of the electronic energy barrier was observed (Table 4.8). The decrease is significant also in terms of relative free energy (about 4 kcal/mol) and the barrier approaches the value of 30 kcal/mol as computed free energy barrier from the reactant complex **^{6}FP-2-EDA**. Even if this barrier represents a significant improvement, with respect to the initial value of 37 kcal/mol, it remains much higher than in the case of the reaction catalyzed by the reduced form $[Fe^{II}(Por)(OCH_3)]^-$ (**FP$^-$**). An IRC analysis from **^{2}TS2** in the forward direction, connected it to the *terminal* carbene **^{2}TC** and dinitrogen. The investigation of the transition states for the N_2 loss on the quartet and sextet surfaces, resulted in **^{4}TS2** and **^{6}TS2** that were found to be much less stable than **^{2}TS2** (Figure 4.13 and Table 4.7).

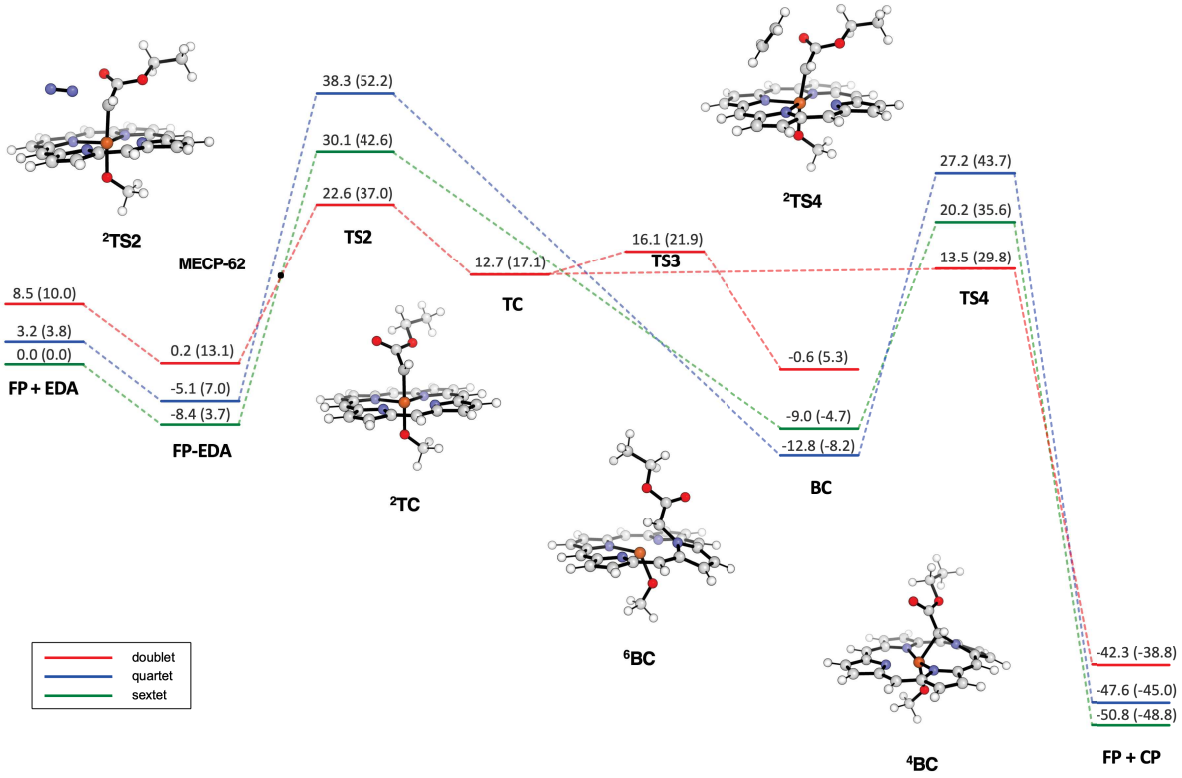

Figure 4.13: *Energy profiles for the reaction of carbene intermediate formation from ethyl diazoacetate* ***EDA*** *and [Fe^{III}(Por)(OCH$_3$)] (**FP**) and subsequent reaction with ethylene. Energy values are from single-point def2-TZVP calculations in toluene on geometries optimized at the UB3LYP/6-31G(d) level (LanL2DZ for iron) in toluene with zero-point correction; the corresponding Gibbs free energy are reported in parenthesis. All values are dispersion corrected.*[23]

Contrarily to **^{2}TS2**, IRC calculations from these higher spin transition states gave direct access to the *bridging* carbenes **^{4}BC** and **^{6}BC**, the former being the most stable carbene species, more than 25 kcal/mol more stable than **^{2}TC**. The carbene species **^{2}BC**, not directly obtained through IRC calculations, was instead located and optimized together with the transitions state **^{2}TS3** that directly interconverts the *terminal-bridging* structures. The geometry of this transition state resembles the one of the *terminal*-structure and shows a very low energy barrier from the *terminal* carbene **^{2}TC** (3.3 kcal/mol).

	E_{rel}	G_{rel}	$d_{C2\text{-}N\alpha}$	$d_{C2\text{-}Fe}$	$d_{C2\text{-}N}$	$d_{Fe\text{-}O}$
^{2}FP + EDA	8.5	10.0				1.780
^{4}FP + EDA	3.2	3.8				1.856
^{6}FP + EDA	0.0	0.0				1.819
^{2}FP-EDA	0.2	13.1	1.307	3.644	4.151	1.780
^{4}FP-EDA	-5.1	7.0	1.306	3.701	4.101	1.859
^{6}FP-EDA	-8.4	3.7	1.306	3.865	4.026	1.819
^{2}TS2	22.6	37.0	1.979	1.989	2.613	1.821
^{4}TS2	38.3	52.2	1.971	2.008	2.576	1.815
^{6}TS2	30.1	42.6	1.990	2.364	2.361	1.823
N_2 + ^{2}TC	12.7	17.1		1.852	2.672	1.833
N_2 + ^{2}TS3	16.1	21.9		1.871	2.367	1.828
N_2 + ^{2}BC	-0.6	5.3		1.994	1.472	1.829
N_2 + ^{4}BC	-12.8	-8.2		2.034	1.438	1.830
N_2 + ^{6}BC	-9.0	-4.7		2.181	1.431	1.852

Table 4.7: *Relative electronic energy, with zero-point correction, and the corresponding Gibbs free energy (kcal/mol) of the transition states and intermediates in the reaction of carbene intermediate formation from ethyl diazoacetate* ***EDA*** *and [Fe^{III}(Por)(OCH_3)] (**FP**), determined through single-point def2-TZVP calculations in toluene on geometries optimized at the UB3LYP/6-31G(d) level (LanL2DZ for iron) in toluene. The distances (Å) between* ***EDA*** *C2 atom and leaving N_2 ($d_{C2\text{-}N\alpha}$), iron ($d_{C2\text{-}Fe}$), and the closest porphyrin nitrogen atom ($d_{C2\text{-}N}$) are reported for each stationary point.*[23]

	E_{rel}	G_{rel}	$d_{C2\text{-}N\alpha}$	$d_{C2\text{-}Fe}$	$d_{C2\text{-}N}$	$d_{Fe\text{-}O}$
^{6}FP-2 + EDA	0.0	0.0				1.819
^{6}FP-2-EDA	-12.0	2.6	1.306	5.656	6.831	1.820
^{2}TS2-2	16.9	33.2	1.966	1.978	2.665	1.822

Table 4.8: *Relative electronic energy, with zero-point correction, and the corresponding Gibbs free energy (kcal/mol) of the transition states in the reaction of terminal-carbene intermediate formation from ethyl diazoacetate* ***EDA*** *and [Fe^{III}(**2**)(OCH_3)] (**FP-2**), determined through single-point def2-TZVP calculations in toluene on geometries optimized at the UB3LYP/6-31G(d) level (LanL2DZ for iron) in toluene. The distances (Å) between* ***EDA*** *C2 atom and leaving N_2 ($d_{C2\text{-}N\alpha}$), iron ($d_{C2\text{-}Fe}$), and the closest porphyrin nitrogen atom ($d_{C2\text{-}N}$) are reported for each stationary point.*[23]

In investigating the reaction of the carbene intermediates with ethylene, the most stable transition state was found again to be the one on the lowest spin state surface, **^{2}TS4** (Table 4.9 and Figure 4.13), characterized by a very small energy

barrier (0.8 kcal/mol) from the **^{2}TC** carbene intermediate, even lower than that of the terminal-bridging interconversion. Once again, **^{2}TS4** is largely preferred over **^{4}TS4** and **^{6}TS4**. The **^{2}TS4** transition state is concerted, showing an asynchronous fashion, and the IRC path from it connects to the terminal carbene **^{2}TC** and directly to the cyclopropane product **CP**. Simultaneously, the regeneration of the catalyst occurs and, after a spin crossing, regains the most stable sextet state.

	E_{rel}	G_{rel}	$d_{C2\text{-}CE1}$	$d_{C2\text{-}CE2}$	$d_{C2\text{-}Fe}$	$d_{C2\text{-}N}$	$d_{Fe\text{-}O}$
^{2}TS4	13.5	29.8	2.611	2.874	1.929	2.482	1.827
^{4}TS4	27.2	43.7	2.243	2.623	2.145	2.171	1.825
^{6}TS4	20.2	35.6	2.328	2.700	2.288	2.117	1.852
CP + ^{2}FP	-42.3	-38.8					
CP + ^{4}FP	-47.6	-45.0					
CP + ^{6}FP	-50.8	-48.8					

Table 4.9: *Relative electronic energy, with zero-point correction, and the corresponding Gibbs free energy (kcal/mol) of the transition states in the reaction of ethylene with the [Fe^{III}(Por)(OCH_3)($CHCO_2Et$)] carbene intermediates determined through single-point def2-TZVP calculations in toluene on geometries optimized at the UB3LYP/6-31G(d) level (LanL2DZ for iron) in toluene. The energy values are referred to the starting reactants **^{6}FP** and **EDA**. The distances (Å) between the carbene C2 atom and the incoming ethylene carbon atoms ($d_{C2\text{-}CE1}$ and $d_{C2\text{-}CE2}$), iron ($d_{C2\text{-}Fe}$), and the closest porphyrin nitrogen atom ($d_{C2\text{-}N}$) are reported for each stationary point.*[23]

4.4 Minimum Energy Crossing Points (MECP)

Observing the general shape of the potential energy surfaces (PES) reported above, it can be easily seen that in some regions the PES of different spin states results to be very close to each other. Crossovers can also be detected along the reaction coordinate: the hyperlines between the two PES where the crossover happens, are called Minimum Energy Crossing Point (MECP) and constitute the natural pathway to help increasing or decreasing the energetic barriers for the overall process.[36] To better understand what happens in those cases we need to make a step backwards and report on the theory behind these processes.

Many chemical reactions occur involving a change in spin-state. To describe those reactions, the classical Transition State Theory (TST) cannot be simply applied, but

a specific modification of it can accounts for the kinetics of these reactions.[37] These reactions are treated as *non-adiabatic* in the sense that they occur not by following a singular energy surface, but their pathway belongs to more than one PES.[37] Thus, the transformation of reactants in products occurs through "hopping" of the system from one PES corresponding to the initial spin state onto that corresponding to the product or intermediate state, by following also multiple hops.[37] To increase the depth of the theoretical analysis we have to remember the two natures of the PES: *adiabatic* or *diabatic*. In the first case, surfaces are described within the Born-Oppenheimer approximation by the eigenvalue of the energy of a given solution to the electronic Schrödinger equation at each geometry.[37] The solutions of the wavefunction equation are obtained through the full electronic Hamiltonian (i.e. it has to include Coulomb, scalar relativistic and spin-orbit terms).[37] Vice versa, the diabatic PES can be defined as solutions derived from the eigenvalues of the Schrödinger equation solved by the use of Hamiltonian with the omission of the spin-orbit terms.[37] In Figure 4.14, diabatic and adiabatic surfaces are reported, showing also the surfaces-cross in the MECP.

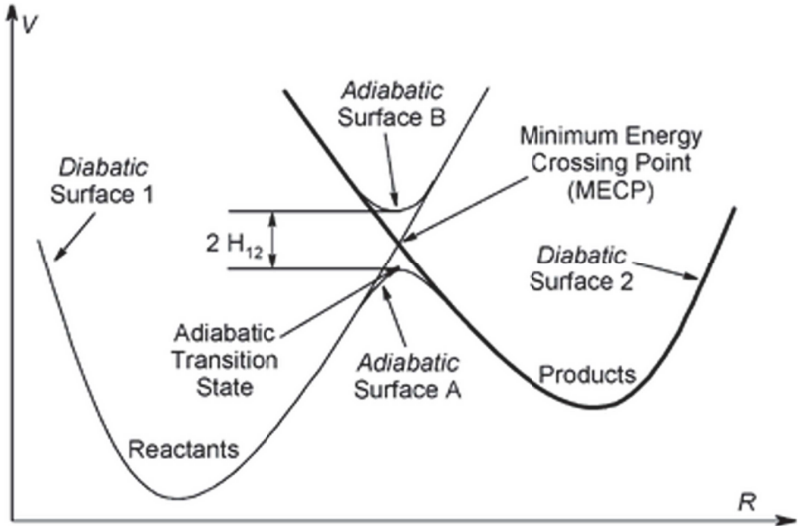

Figure 4.14: *Schematic diabatic and adiabatic PES for a spin-forbidden reaction.*[37]

By having a look at Figure 4.14, it can be observed that despite the two diabatic surfaces cross, this is not the same for the two adiabatic ones (i.e., A and B). The reason is that the spin-orbit coupling matrix element is non-zero and when it

is included in the Hamiltonian, it results in eigenfunctions which are mixtures of different spin states.[37] This behavior means that on the lower surface there should be - at least in principle - a transition state that can be described in the usual TST standard way.[37] However, in practice what happens in most of the times is that the mixing is not so strong, resulting in a non-adiabatic behavior that can be described only within the non-Born-Oppenheimer situation. To be able in describing the reactivity, we have to think about the "hopping" of the system from one surface to the other.[37] These hops can occur at any coordinate along the reaction pathway, but the probability in happening increases in those regions where is located the crossing point (MECP) and where the two surfaces are close in energy.

To sum up, a simple model can be sketched that will be useful in the next part of this paragraph. First, the system has to access the crossing seam within the two PES of different spin state, resulting in an activation energy for the reaction. Then, the system needs to hop from one diabatic surface to the other and this can preferably occur in the region surrounding the seam, as reported above. To achieve that it is necessary that spin-orbit coupling between the two PES occurs.[37] Thus, the determination of the energy of the MECP represents a relative activation energy measure to achieve the spin crossing, while the amplitude of the spin-orbit coupling element in the Hamiltonian matrix regulates the probability of hopping form one surface to the other.[37]

Being that the MECP provides the natural choice to achieve the hopping coordinate, the necessity in identifying and locating where the PESs cross, as well as the electronic properties and energies associated to the specific geometry adopted by the system, is of fundamental importance to describe the reaction pathway in the most realistic way. Besides the different types of strategies adopted by theoretical chemists to gain this information,[38] the one described by Harvey and co-workers is noteworthy, thanks to the low computational cost required.[39] To circumvent the necessity of a full optimization of the MECP using an high level of theory, they developed a hybrid approach that permits to determine the MECP at one level of theory and gradients to a more convenient one.[39] It is easy to understand this approach by thinking to the comparison with the simpler procedure used for locating

the MECP using energies and gradients at the same level.[38]

The energies E_i on the two PESs and the corresponding energy gradients $\frac{\delta E_i}{\delta q}$ respect to the nuclear coordinates q, can be interpreted as combinations of themselves to yield two effective gradients vectors $\boldsymbol{f}$ and $\boldsymbol{g}$.[39] The so obtained vectors are orthogonal and tend to zero at the MECP (i.e., they both assume value zero in correspondence of the MECP), being parallel the energy gradients on the two surfaces.[39]

$$f = (E_1 - E_2)\left[\left(\frac{\partial E_1}{\partial q}\right) - \left(\frac{\partial E_2}{\partial q}\right)\right] = (E_1 - E_2)\, x_1$$

$$g = \left(\frac{\partial E_1}{\partial q}\right) - \frac{x_1}{|x_1|}\left[\left(\frac{\partial E_1}{\partial q}\right) \cdot \frac{x_1}{|x_1|}\right]$$

Extremely important is to remember the spatial orientation of these two vectors: while the $\boldsymbol{f}$ is orthogonal to the crossing hyperline around the MECP, the $\boldsymbol{g}$ is parallel to it and points towards the minimum.[39] This treatment gives the possibility to choose the most appropriate calculation level to derive the gradients, provided that the method chosen is correct for the problem under study.[39] The geometry optimization of the MECP can thus be performed using a minimization algorithm that follows the sum of the two gradient vectors $\boldsymbol{f}$ and $\boldsymbol{g}$.[39] The convergence criteria can then be selected by simply modifying the steepest descent method used until getting the proper result in terms of chemical accuracy.

In the hybrid method we can thus approximate the above-mentioned vectors $\boldsymbol{f}$ and $\boldsymbol{g}$ with the closely similar terms $\boldsymbol{f'}$ and $\boldsymbol{g'}$, which are defined as follows:

$$f' = \left({E_1}^{high} - {E_2}^{high}\right)\left[\left(\frac{\partial {E_1}^{low}}{\partial q}\right) - \left(\frac{\partial {E_2}^{low}}{\partial q}\right)\right] = \left({E_1}^{high} - {E_2}^{high}\right){x_1}^{low}$$

$$g' = \left(\frac{\partial {E_1}^{low}}{\partial q}\right) - \frac{{x_1}^{low}}{|{x_1}^{low}|}\left[\left(\frac{\partial {E_1}^{low}}{\partial q}\right) \cdot \frac{{x_1}^{low}}{|{x_1}^{low}|}\right]$$

where the superscript *high* and *low* refers to the level of theory used to calculate the corresponding number of vectors.[39] The idea behind using the low-level gradients is that by using a lower level of theory, the overall shape of the two surfaces will be anyway correctly reproduced, even if their relative energies are not.[39] Thus, the difference gradient ${x_1}^{low}$ should have the correct orientation, as should the approximate gradient $\boldsymbol{g'}$ and the real $\boldsymbol{g}$. Thus, following the approximate gradients $\boldsymbol{f'}$ and $\boldsymbol{g'}$ will lead to a point where they are equal to zero: this point should be in most cases a good approximation for the high-level MECP.[39]

To sum up the theory reported so far, we can say that the standard method for locating MECPs is the same as a full geometry optimization on one of the PESs, with the constraint that the difference in energy of the PESs is zero.[38] On the contrary, the hybrid method elaborated by Harvey and co-workers, is a low-level geometry optimization on one of the PESs, under the constraint that the difference of the high-level calculated energies is zero.[39] The so located approximate MECP is then the low-level minimum along the high-level crossing hyperline.[39] This approach is practically equivalent to that used in classical DFT approaches, when calculating high-level single point energies at stationary points which were optimized at a lower level.[39]

One last theoretical consideration has to be done before moving to the presentation of our results. As Harvey reported, the stationary point located in the 3N-7 dimensions across the hyperline (MECP) can be both a minimum or a higher-order stationary point. This aspect makes the classical standard frequency analysis not feasible, because the MECP is not a stationary point in neither of the full 3N-6 dimension of the PESs.[39] Anyway, a procedure to achieve this result can be found if the second-order Taylor expansion for the energy is performed for both the surfaces with the conditions of remaing near the MECP and using a Δq displacement along the crossing hyperline which is orthogonal to x_1:

$$E = E_{MECP} + \frac{1}{2}\Delta q^T \left(\frac{\left|\frac{\partial E_2}{\partial q}\right| H_2}{|x_1|} - \frac{\left|\frac{\partial E_2}{\partial q}\right| H_1}{|x_1|} \right) \Delta q = E_{MECP} + \frac{1}{2}\Delta q^T H_{eff} \Delta q$$

where H_1 and H_2 are the Hessian matrices of the second derivatives of the energy respect to the nuclear coordinates on the two PESs.[39]

The further diagonalization of the effective Hessian H_{eff}, should result in a set of normal modes and force constants which describes the movement along the crossing hyperline. Noteworthy, the above reported equation is only valid if the displacements occur orthogonally to x_1. It is thus necessary to project out of H_{eff} the 6 rotations and translations and the direction of the difference gradient x_1 in the space before the diagonalization step. The mathematical approach to achieve this projection is well known,[40] and thus it is easy to generate, project, then diagonalize the H_{eff}, yielding a set of 3N-7 force constants along the crossing hyperline.[39] These can be useful for verifying that the MECP is a minimum, and not a higher-order stationary point in the region of the crossing hyperline.[39]

Harvey and co-workers also translated all this mathematical discussion in a Fortran based computer program.[39] However, due to the more common and today's increase in the use of Python as the main language in data science, we decided to use the open-source Python-based EasyMECP program elaborated by Jaime Rodrìguez-Guerra and co-workers.[41] The script they elaborated, follows the same identical approach of the original Harvey work, but constitutes a wrap that greatly simplifies the calculation setup using Gaussian. For such reasons, we used this last distribution and we were able to locate the most important MECP that help in decreasing the activation energy of the reaction through the hop between on spin state and the other. Calculations were approached with the same level of theory adopted before, but an important observation has to be done: by following to the low-level of theory MECP search, the corresponding high-level single point, we will not be able to have a good correspondence in energy with the points in the graph. The reason relies on the fact that evaluating the energy as a single point using a different level of theory respect to the one used in the geometry optimization, will result in a different way the PES is represented and shaped, thus in a non-perfect correlation between the range energy where the MECP is located. A better correspondence could be achieved by using the same level of theory used in the geometry optimization, but that will result in a different type of chart respect to the ones reported above. For

all such reasons, we decided to locate the MECP only for the starting region of the mechanisms and giving an analysis on the basis of the geometry observed in those points.

By looking at the reaction mechanism catalyzed by the $[Fe^{II}(Por)(OMe)]^-$ specie (Figure 4.9), we observed before that the lowest spin state for the starting adduct **FP-EDA** is the quintet one. The PES of the quintet sate crosses the triplet one in correspondence of the **MECP-53** (Figure 4.9), thus giving the possibility to achieve the much more stable **TS1$^-$** on the triplet PES (12.26 kcal/mol), respect to the quintet one (21.81 kcal/mol). This results in a further decrease in the activation energy for the first step to a value of ∼22 kcal/mol which is compatible with the conditions involved in the experimental reactions. The geometrical features of **MECP-53** can be summed up as in Table 4.10 and a schematic representation of its structure is given in Figure 4.15.

	$d_{C2\text{-}N\alpha}$	$d_{C2\text{-}Fe}$	$d_{C2\text{-}N}$	$d_{Fe\text{-}O}$
^{3}FP$^-$-EDA	1.305	3.772	3.805	1.977
^{5}FP$^-$-EDA	1.306	3.929	3.592	1.895
MECP-53	1.305	3.765	4.167	1.979
^{3}TS1$^-$	1.345	2.768	3.160	1.798
^{5}TS1$^-$	1.439	2.283	2.935	1.892

Table 4.10: *Geometries features for **MECP-53** obtained through calculations at the UB3LYP/6-31G(d) level (LanL2DZ for iron) in toluene. The distances (Å) between **EDA** C2 atom and leaving N_2 ($d_{C2\text{-}N\alpha}$), iron ($d_{C2\text{-}Fe}$), and the closest porphyrin nitrogen atom ($d_{C2\text{-}N}$) are reported for each point.*

Specifically, we can see that no particular modifications occur in the distances between the C2 atom of **EDA** and the Nα close to it, as well as between the same C2 atom and the iron metal center. However, a significant increase in the distance between **EDA** C2 atom and the closest porphyrin nitrogen atom ($d_{C2\text{-}N}$) underlines a slide of the **EDA** moiety respect to the porphyrin plane. The distance between the iron and the oxygen of the methoxy ligand still doesn't show any strong modification.

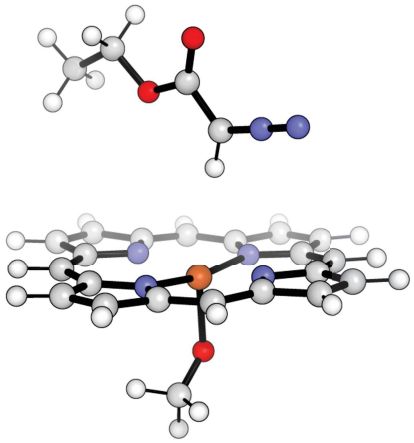

Figure 4.15: *Structural representation of* ***MECP-53****.*

Moving now to the next step, we can observe that after the **TS1**$^{-}$ transition state, the triplet PES and the open-shell singlet one cross together in correspondence of **MECP-31** (Figure 4.9). The location of this point is of fundamental importance: even if the energy gain in **INT1**$^{-}$ is not so high, it populates the singlet spin state which will be the lowest state for all the further steps of the mechanism. The geometrical features of **MECP-31** can be summed up as in Table 4.11 and in Figure 4.16 can be observed its tridimensional representation.

	$d_{C2\text{-}N\alpha}$	$d_{C2\text{-}Fe}$	$d_{C2\text{-}N}$	$d_{Fe\text{-}O}$
^{1os}**TS1**$^{-}$	1.367	2.460	3.048	1.853
^{3}**TS1**$^{-}$	1.345	2.768	3.160	1.798
MECP-31	1.371	2.426	3.007	1.879
^{1os}**INT1**$^{-}$	1.452	2.231	2.899	1.853
^{3}**INT1**$^{-}$	1.447	2.251	2.912	1.849

Table 4.11: *Geometries features for* ***MECP-31*** *obtained through calculations at the UB3LYP/6-31G(d) level (LanL2DZ for iron) in toluene. The distances (Å) between* ***EDA*** *C2 atom and leaving N_2 ($d_{C2\text{-}N\alpha}$), iron ($d_{C2\text{-}Fe}$), and the closest porphyrin nitrogen atom ($d_{C2\text{-}N}$) are reported for each point.*

Also in this case, no particular differences can be highlighted for the distances under evaluation in the point, respect to the range of structures in which is located. By making a comparison between the transition state structures and the next intermediates ones, we can conclude that the **MECP-31** structure is much more similar

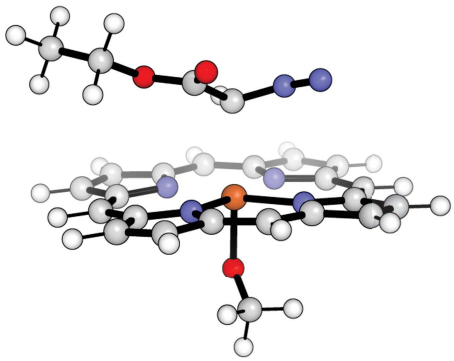

Figure 4.16: *Structural representation of* ***MECP-31****.*

to the ones of the transition states, respect to those of the intermediates.

We then moved to the reaction mechanism catalyzed by the [Fe^{III}(Por)(OMe)] specie (Figure 4.13). Here the lowest spin state for the **FP-EDA** adduct is the sextet one, but all the next lowest steps of the mechanism rely on the doublet as the most stable PES. Thus, by looking at the profile depicted in Figure 4.13, we identified that a possible crossing point could be located in the very first step between the sextet and the doublet PES. By proceeding with the same protocol, we located the **MECP-62** between those surfaces: it not only helps decreasing the very high activation energy in **TS1**, but also it assures the change in spin state fundamental for the next steps of the reaction. The gain in energy is noteworthy: the possibility to achieve the much more stable **TS1** on the doublet PES (22.61 kcal/mol), respect to the sextet one (38.33 kcal/mol), thus decreasing the activation energy to nearly 31 kcal/mol. This step still remains unfavored respect to the one proposed for the reduced catalyst specie over nearly 10 kcal/mol. The geometrical features of **MECP-62** are resumed in Table 4.12 and the structure taken in the crossing point is represented in Figure 4.17.

	$d_{C2\text{-}N\alpha}$	$d_{C2\text{-}Fe}$	$d_{C2\text{-}N}$	$d_{Fe\text{-}O}$
^{2}FP-EDA	1.307	3.644	4.151	1.780
^{6}FP-EDA	1.306	3.865	4.026	1.819
MECP-62	1.307	3.712	4.155	1.804
^{2}TS2	1.979	1.989	2.613	1.821
^{6}TS2	1.990	2.364	2.361	1.823

Table 4.12: *Geometries features for **MECP-62** obtained through calculations at the UB3LYP/6-31G(d) level (LanL2DZ for iron) in toluene. The distances (Å) between **EDA** C2 atom and leaving N_2 ($d_{C2\text{-}N\alpha}$), iron ($d_{C2\text{-}Fe}$), and the closest porphyrin nitrogen atom ($d_{C2\text{-}N}$) are reported for each point.*

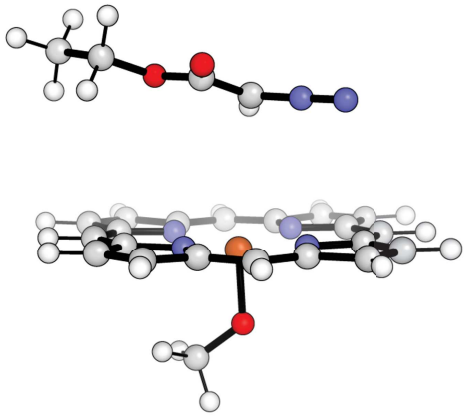

Figure 4.17: *Structural representation of **MECP-62**.*

By looking at the geometrical features of this point, we can give a similar conclusion as before: the structure at which the crossing can be obtained is much more similar to that of the starting adduct respect to the transition state ones. As reported in Table 4.12, a quantity that seems not to be affected before and after the MECP is the distance between the iron ion and the oxygen atom of the methoxy ligand, but for all the other quantities huge variations are reported.

4.5 Redox potential calculation

The last argument that remains uninvestigated is how the EDA is capable in reducing the Fe(III)-OMe prophyrin to the corresponding [Fe(II)-OMe]$^{-}$ complex. We already reported that this behavior was described by many authors: starting from the seminal paper in 1995 by Woo and co-workers,[8] this particular reductive

property of EDA was always widely cited and used, but it was never proved through experimental analysis how it can occur.[20] Also we referred to that reactivity on the basis of what we observed, and based our calculation according to the experimental proof of Gallo's group and other authors.[4],[10],[21],[23] However, to the best of our knowledge, no computational proof or even speculative mechanism was reported so far.

For all such reasons, we decided to try investigating from the beginning this particular redox activity. One of the first things that we thought, was the availability of redox potentials in order to achieve a very initial, even if qualitative, answer to the EDA capability in reducing iron species. Discussing with the experimental group based in Milan about possible experiments of Cyclic Voltammetry (CV) resulted in trials that gave unsatisfactory results, both in the case of the catalyst and in the case of the diazocompound. In particular, the catalyst was found to decompose during the CV experiment, while the high instability of EDA in normal CV experimental conditions, resulted in another stalemate.

To overcome all those experimental problems, we started thinking at a computational evaluation of the redox potential of the two species. It is well known that a computational approach to the redox potential, could give a quite realistic result if compared with the experimental one. These calculations can be performed having in mind the Nernst equation and the Born-Haber cycle (Scheme 4.6). Before to move to the results we obtained, it is noteworthy to give a fast and effective mathematical explanation as a fundament of the method followed.

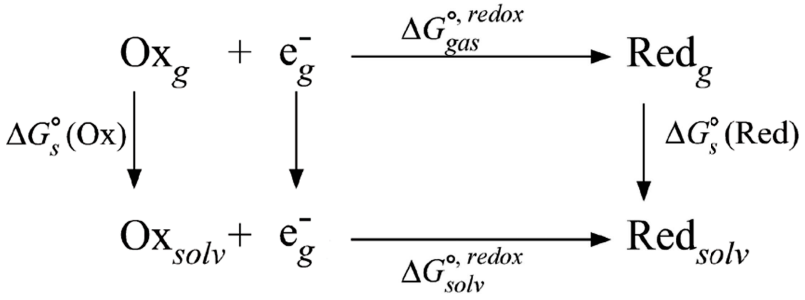

Scheme 4.6: *Born-Haber Cycle.*[42]

The basic principle is that if known the $\Delta G^{o,redox}_{solv}$ of the redox reaction, we can

obtain directly the redox potential through the Nernst equation:

$$\Delta G^{o,redox}_{solv} = -nFE^{o}_{calc} \qquad \Rightarrow \qquad E^{o}_{calc} = -\frac{\Delta G^{o,redox}_{solv}}{nF}$$

where n is the number of electrons, F is the Faraday's constant (23.06 kcal/mol) and ΔE^{o}_{calc} is the calculated redox potential.[42] Thus, to obtain the $\Delta G^{o,redox}_{solv}$ we have to remember that it consists of the free energy change in the gas phase and the solvation free energies of the oxidized and reduced species.[42] The equation below can be used to obtain the $\Delta G^{o,redox}_{solv}$ introducing the specific values required.

$$\Delta G^{o,redox}_{solv} = \Delta G^{o,redox}_{gas} + \Delta G^{o}_{s} = \left[\Delta G^{o,Red}_{gas} - \Delta G^{o,Ox}_{gas}\right] + \left[\Delta G^{o,Red}_{s} - \Delta G^{o,Ox}_{s}\right]$$

What remains now is to explain how to obtain these data from the calculation output. We used also in this case Gaussian 09[45] and through frequency calculations it is easy to obtain the thermochemical parameters and corrections. The free energy G can be easily streamed out from the Gaussian output file as "Sum of electronic and thermal Free Energies", which directly reports the sum of the electronic calculated energy (ε^0) and the thermal correction to Gibbs Free energy (G_{corr}).

$$G = \varepsilon^0 + G_{corr}$$

Following this strategy, the $\Delta G^{o,redox}_{gas}$ for the gas phase can be obtained by taking the difference between the free energy values of product and reactant, (i.e., the Reduced product and the Oxidized reactant) thus following the upper part of Scheme 4.6.

$$\Delta G^{o,redox}_{gas} = \left(\varepsilon^0_{gas} + G_{corr}\right)^{Red} - \left(\varepsilon^0_{gas} + G_{corr}\right)^{Ox}$$

The intricacy arises now for the evaluation of the free energy for the solvated reaction. It has been reported that a proper solvation model is required for such of analysis, like COSMO, but the computational cost of such a model can be deleterious when metal-complex systems are the object of the investigation. Instead of that

one, results can be also reproduced, even if at a qualitative level, by the usage of a less expensive model such as a polarizable continuum model (PCM) or SMD.[43] By observing the $\Delta G_{solv}^{o,redox}$ equation, we can therefore calculate the ΔG_s^o terms by using the following expressions:

$$\Delta G_s^{o,Red} = \left(\varepsilon_{solv}^0 + G_{corr}^{gas}\right)^{Red} - \left(\varepsilon_{gas}^0 + G_{corr}^{gas}\right)^{Red} = \varepsilon_{solv}^{0,Red} - \varepsilon_{gas}^{0,Red} = \varepsilon_{solvation}^{Red}$$

$$\Delta G_s^{o,Ox} = \left(\varepsilon_{solv}^0 + G_{corr}^{gas}\right)^{Ox} - \left(\varepsilon_{gas}^0 + G_{corr}^{gas}\right)^{Ox} = \varepsilon_{solv}^{0,Ox} - \varepsilon_{gas}^{0,Ox} = \varepsilon_{solvation}^{Ox}$$

The so calculated ΔG_s^o terms accounts for the "vertical" correlation in the Born-Haber cycle between gas phase and solvent phase, as reported in Scheme 4.6. Thus, the $\Delta G_{solv}^{o,redox}$ equation can be reformulated in the following way:

$$\Delta G_{solv}^{o,redox} = \left(\varepsilon_{gas}^0 + \varepsilon_{solvation} + G_{corr}\right)^{Red} - \left(\varepsilon_{gas}^0 + \varepsilon_{solvation} + G_{corr}\right)^{Ox}$$

Now the $\Delta G_{solv}^{o,redox}$ value can be included in the Nernst equation to get the calculated potential redox potential, E_{calc}^o, which can also be referenced to the Standard Hydrogen Electrode (SHE)[44] or Standard Calomel Electrode (SCE)[43] by the following conversions:

$$E_{calc}^{o,SHE} = E_{calc}^o - 4.43V$$

$$E_{calc}^{o,SCE} = E_{calc}^o - 4.1888V$$

We decided to follow the procedure described by Friesner and Baik,[43] using Gaussian 09 software with the following level of theory: optimization of the geometries were conducted by the usage of UB3LYP as a functional and a differentiated basis set with LanL2DZ for Fe and 6-31g(d,p) for all the other atoms.[45] The calculation in toluene solvent was performed with the same level of theory and by the usage of SMD solvation model. Then, once the geometries were established, single point calculations were performed with the level of theory reported by Friesner:[43]

UB3LYP as functional, LanL2DZ for Fe and Dunning's correlation-consistent triple-ξ basis set cc-pVTZ for all the other atoms. As reported before, the effects of toluene as solvent were simulated with SMD solvation model also in the single point calculations. What we want to report now is the calculated potentials at which the reduction of the [Fe^{III}(Por)(OCH_3)] to [Fe^{II}(Por)(OCH_3)]$^-$ complex occurs promoted by the oxidation of EDA to EDA^+. This procedure was operated both for the reduced and oxidized forms of both the reactants (i.e. [Fe(Por)OMe] and EDA) by simply adding a negative or positive charge to all the system or leaving it neutral. For the open-shell species, calculations were operated by working on the lowest energy spin state for the system under investigation. Let's start from the iron-porphirin complex as starting specie: by following the convention of reporting redox potentials in the direction of the reduction, the equation that should be investigated is the following:

$$^6\left[Fe^{III}\,(Por)\,(OCH_3)\right] + e^- \quad \rightarrow \quad ^5\left[Fe^{II}\,(Por)\,(OCH_3)\right]^-$$

We already reported that the lowest spin state for the Fe^{III} neutral species was the sextet while for the Fe^{II} anionic one was the quintet. Following the procedure reported above, we obtained the redox potential reported below, here referred to the SHE electrode.

$$E^o_{SHE}\,(Fe - porphyrin) = -1.43V$$

In the case of EDA we used the closed-shell singlet state for the reduced form, while the open-shell doublet state was found to be the most stable state for the oxidized form. Thus, we followed the equation reported below to describe the redox reaction of EDA reported in the direction of the reduction:

$$^2EDA^+ \; + \; e^- \quad \rightarrow \quad ^{1CS}EDA$$

Operating in the same manner as above, we obtained the following redox potential result:

$$E^o_{SHE}\,(EDA) = +3.11V$$

According to the generally accepted consideration, in the standard electrode potential series the species that is more positive in term of E^o is capable of oxidizing the one less positive by reducing itself and, vice versa, the less positive is able to reduce the more positive one by oxidizing itself. Adopting this explanation to our specific case, soon appears clear that as the result of the calculation we performed EDA is not able to reduce the Fe-porphirin species. This result has to be discussed before to give unattended conclusions. First of all, the level of theory we adopted is not really identical to the one reported by Friesner and Baik,[43] due to the impossibility in Gaussian 09[45] to easily modify the basis set as they did with Jaguar 1.4: specifically they used cc-pVTZ-(-f) where f orbitals functions were removed instead of the cc-pVTZ we used.[46] Moreover, they used the LACVP** or its modified version LACV3P** to treat the transition state metals: this basis set was not available for Gaussian09 and even if we tried to include it in its non-modified version, we were not able to make the program fit to it.

As last observation, the situation we investigated is a "statical" version of what can happen in the reality: specifically, by simply modifying the charge on the species (even if we evaluated each single spin state when required) we can't explain what really occurs during the redox reaction. The nitrogen of EDA could be dissociated, bended, as well as the -OMe ligand on iron can move from the internal coordination sphere to the external one or even completely dissociate, giving access to intermediates that could present redox potentials similar or completely different to the ones we obtained and reported above. For all such reasons, the results we got cannot be interpreted as wrong data, but they should be considered as intrinsically correct respect to the situation investigated. Not having experimental information of the mechanism of reduction promoted by EDA, we can only speculate on how it can occur, and based on our results this cannot be achieved by a simple electron transfer reaction between the reactive species as they are intended as starting materials.

Our research group is currently investigating all the possible pathways that could explain such a reductive process and a plausible reaction mechanism that involves radical species is now under study in our laboratories.

4.6 Conclusions

In this Chapter the overall mechanism of cyclopropanation reaction catalyzed by an iron porphyrin methoxy complex was investigated with the aid of a computational approach. The catalyst used to perform the experimental reactions, [Fe^{III}(**1**)(OCH_3)], shows the iron in the +3 oxidation state: authors of the experiments reported that it can be recovered as such at the end of the reaction to be used again with virtually unmodified catalytic performances.[10] However, a lot of works can be found in literature on comparable systems suggesting to consider its reduced form, [Fe^{II}(**1**)(OCH_3)]$^-$, as the catalytically active form, where the resting iron(III) species derives by the *in situ* reducing action of ethyl diazoacetate.[8],[20] During the catalyst recovery, the reduced iron(II) species is oxidized again by atmospheric oxygen to iron(III), as normally occurs during the synthetical procedure to obtain [Fe^{III}(**1**)(OCH_3)] from $FeBr_2$ as the iron source.[4] For such reasons, both the profiles for the reactions catalyzed by the oxidized as well the reduced iron species were investigated and compared by locating all the transition states and intermediates along the reaction pathways using the model catalyst [Fe(Por)(OCH_3)], where the simple porphine is used instead of the iron ligand **1**. However, to account the effect on the energy profiles of the tridimensional arrangement of the porphyrin skeleton, *i.e.* the organic environment of **1** surrounding the reaction site, the crucial stationary points were determined by using the single-stranded methoxy iron porphyrin [Fe(**2**)(OCH_3)] complex.

In the situations we reported before, both the reduced iron(II) and oxidized iron(III) form of the catalyst prefer high spin states, the quintet and sextet state, respectively. By moving from the starting complexes, all the transition states encountered along the reaction coordinate, as well as all the intermediates, preferred low spin states, in particular the broken-symmetry solution of the singlet for iron(II). However, in this solution spin density might be merely a reminiscence of the triplet spin state contaminants and the real singlet species may present an electronic structure which is a compromise between the closed-shell and the broken-symmetry singlet solutions. The rate determining step was found to be for both the cases the one leading to the *terminal*-carbene intermediate with simultaneous dinitro-

gen loss, thus showing that $[Fe^{II}(Por)(OCH_3)]^-$ (**FP$^-$**) performs much better than $[Fe^{III}(Por)(OCH_3)]$ (**FP**) due to a much smaller energy barrier (29.5 with respect to 37 kcal/mol in terms of Gibbs free energy). Contrarily to the iron(III) profile in which the carbene intermediate can be directly obtained from the starting complex, the favored iron(II) is a more intricate process, as already reported in literature in the case of $[Fe^{II}(Por)(SCH_3)]^-$ [21] or $[Fe^{II}(Por)(Cl)]^-$.[36] The reaction shows initially a far complex between the starting catalyst $[Fe^{II}(Por)(OCH_3)]^-$ (**FP$^-$**) and ethyl diazoacetate which is converted into a close complex, that ends into the *terminal* iron porphyrin carbene intermediate $[Fe^{II}(Por)(OCH_3)(CHCO_2Et)]^-$ (**TC$^-$**), passing through the main transition state. The transition state between the far and close complexes was located and we found that it is almost isoenergetic with the main transition state. This observation raises the question whether the rate determining step corresponds to dinitrogen loss or to an electronic and structural rearrangement in ethyl diazoacetate. The change from the linear to the trigonal planar geometry of its first nitrogen atom and the significant shortening of the Fe-C2 distance, all accompanied a by a severe change of the spin density and charge distribution was observed as the main structural and electronical modifications that occurs during this transition from far to close complex. Thus, being the two barriers comparable, whatever the highest barrier can be between the two, the reaction rate is almost unaffected.

The ethylene addition to the *terminal*-carbene is a downhill process which, on the broken-symmetry solution of the singlet surface, presents an elusive intermediate, which is badly defined on the triplet surface, to be than inexistent on the closed-shell singlet and quintet surfaces.

To sum up the computational data obtained with the single-stranded porphyrin catalyst $[Fe^{II}(\mathbf{2})(OCH_3)]^-$, it appears clear the very significant effect on the reaction profile of the organic environment surrounding the reaction site, underlining the strong influence of the entire catalyst on its performance. With the presence of the single stranded **2** catalyst (which resembles the double strand in **1**) the energy barrier becomes much lower (a Gibbs free energy value of 21.5 kcal/mol with respect to the reactant complex), making feasible an apparently unfeasible reaction. In a similar

way, we can think that the second strand in **1**, even if not directly involved in the reaction site, could help in decreasing a bit more the energy barrier of the reaction.

Thanks to the evaluation of MECP, we were able to identify the exact point where the PESs of two different spin states crosses and thus where the surface hop is much more probable. This not only helped us in gaining a more insight view on the mechanism, but opened the way of thinking as a possible reduction in the activation energies through multiple crossing points until the lowest in energy spin state is populated to continue the mechanism to the end of the reaction.

The results we obtained during the redox potential calculation both for iron-porphirin species and EDA, showed that by considering a statical situation EDA is not able to reduce the iron complex. By the way, as we reported above, the mismatched result could be addressed to the different type of basis sets available under Gaussian 09[45] software environment and the real chemical system which could undergo modifications both in structure and electronics during the reduction reaction. The hypothesis of a mechanism which involves radical species cannot be completely excluded and it is currently under investigations in our laboratories.

References

[1] Tang, P. and Qin, Y., Recent Applications of Cyclopropane-Based Strategies to Natural Product Synthesis, *Synthesis*, **2012**, *44*, 2969-2984.

[2] Kumar, A. K., Brief Review On Cyclopropane Analogs: Synthesis And Their Pharmacological Applications, *Int. J. Pharm. Pharm. Sci.*, **2013**, *5*, 467-472.

[3] Carson, C. A. and Kerr, M. A., Heterocycles from cyclopropanes: applications in natural product synthesis, *Chem. Soc. Rev.*, **2009**, *38*, 3051-3060.

[4] Intrieri, D.; Le Gac, S.; Caselli, A.; Rose, E.; Boitrel, B.; Gallo, E., Highly diastereoselective cyclopropanation of α-methylstyrene catalysed by a C_2-symmetrical chiral iron porphyrin complex, *Chem. Comm.*, **2014**, *50*, 1811-1813.

[5] Doyle, M. P., Catalytic methods for metal carbene transformations, *Chem. Rev.*, **1986**, *86*, 919-939.

[6] (a) Evans, D. A.; Woerpel, K. A.; Hinman, M. M.; Faul, M. M., Bis(oxazolines) as chiral ligands in metal-catalyzed asymmetric reactions. Catalytic, asymmetric cyclopropanation of

olefins, *J. Am. Chem. Soc.*, **1991**, *113*, 726-728; (b) Lowenthal, R. E.; Abiko, A.; Masamune, S., Asymmetric catalytic cyclopropanation of olefins: bis-oxazoline copper complexes, *Tetrahedron Lett.*, **1990**, *31*, 6005-6008; (c) Pfaltz, A., Chiral semicorrins and related nitrogen heterocycles as ligands in asymmetric catalysis, *Acc. Chem. Res.*, **1993**, *26*, 339-345.

[7] (a) Doyle, M. P.; Brandes, B. D.; Kazala, A. P.; Pieters, R. J.; Jarstfer, M. B.; Watkins, L. M.; Eagle, C. T., Chiral rhodium(II) carboxamides. A new class of catalysts for enantioselective cyclopropanation reactions, *Tetrahedron Lett.*, **1990**, *31*, 6613-6616; (b) Doyle, M. P.; Pieters, R. J.; Martin, S. F.; Austin, R. E.; Oalmann, C. J.; Muller, P. J., High enantioselectivity in the intramolecular cyclopropanation of allyl diazoacetates using a novel rhodium(II) catalyst, *J. Am. Chem. Soc.*, **1991**, *113*, 1423-1424.

[8] Wolf, J. R.; Hamaker, C. G.; Djukic, J. P.; Kodadek, T.; Woo, L. K., Shape and stereoselective cyclopropanation of alkenes catalyzed by iron porphyrins, *J. Am. Chem. Soc.*, **1995**, *117*, 9194-9199.

[9] (a) Callot, H. J.; Schaeffer, E., *Nouv. J. Chim.*, **1980**, *4*, 307; (b) Callot, H. J.; Metz, F.; Piechocki, C., Sterically crowded cyclopropanation catalysts. *Syn*-selectivity using rhodium(III) porphyrins, *Tetrahedron*, **1982**, *38*, 2365-2369; (c) Maxwell, J.; O'Malley, S.; Brown, K.; Kodadek, T., Shape-selective and asymmetric cyclopropanation of alkenes catalyzed by rhodium porphyrins, *Organometallics*, **1992**, *11*, 645-652; (d) Maxwell, J. L.; Brown, K. C.; Bartley, D.; Kodadek, T., Mechanism of the Rhodium Porphyrin-Catalyzed Cyclopropanation of Alkenes, *Science*, **1992**, *256*, 1544-1547.

[10] Cariminati, D. M.; Intrieri, D.; Caselli, A.; Le Gac, S.; Boitrel, B.; Toma, L.; Legnani, L.; Gallo, E., Designing 'Totem' C_2-Symmetrical Iron Porphyrin Catalysts for Stereoselective Cyclopropanations, *Chem. Eur. J.*, **2016**, *22*, 13599-13612.

[11] (a) Rose, E.; Raoul, N.; Gallo, E, Synthesis of chiral ruthenium and cobalt (*meso*-2-amidophenyl) porphyrins and their catalytic activity in cyclopropanation reactions, *J. Porphyrins Phthalocyanines*, **2011**, *15*, 602-611; (b) Zhang, J.-L.; Chan, P. W. H.; Che, C.-M., Ruthenium(II) porphyrin catalyzed cyclopropanation of alkenes with tosylhydrazones, *Tetrahedron Lett.*, **2003**, *44*, 8733-8737; (c) Zhou, C.-Y.; Huang, J.-S.; Che, C.-M., Ruthenium-Porphyrin-Catalyzed Carbenoid Transfer Reactions, *Synlett*, **2010**, 2681-2700.

[12] (a) Djukic, J.-P.; Smith, D. A.; Young, V. G. Jr.; Woo, L. K., Properties and Molecular Structures of Osmium(II) Porphyrin Carbene Complexes: (5,10,15,20-tetra-p-tolylporphyrinato) osmium Di-p-tolylmethylidene and (5,10,15,20-tetra-p-tolylporphyrinato)osmium (Trimethylsilyl) methylidene, *Organometallics*, **1994**, *13*, 3020-3026; (b) Smith, D. A.; Reynolds, D. N.; Woo, L. K., Cyclopropanation catalyzed by osmium porphyrin complexes, *J. Am. Chem. Soc.*, **1993**, *115*, 2511-2513.

[13] (a) Bartley, D. W.; Kodadek, T., Identification of the active catalyst in the rhodium porphyrin-mediated cyclopropanation of alkenes, *J. Am. Chem. Soc.*, **1993**, *115*, 1656-1660; (b) Rosenberg, M. L.; Vlasana, K.; Sen, G. N.; Wragg, D.; Tilset, M., Highly *cis*-Selective Rh(I)-Catalyzed Cyclopropanation Reactions, *J. Org. Chem.*, **2011**, *76*, 2465-2470.

[14] Anding, B. J.; Ellern, A.; Woo, L. K., Olefin Cyclopropanation Catalyzed by Iridium(III) Porphyrin Complexes, *Organometallics*, **2012**, *31*, 3628-3635.

[15] Gross, Z.; Galili, N.; Simkhovich, L., Metalloporphyrin catalyzed asymmetric cyclopropanation of olefins, *Tetrahedron Lett.*, **1999**, *40*, 1571-1574.

[16] (a) Ivanov, A. S.; Boldyrev, A. I., Deciphering aromaticity in porphyrinoids via adaptive natural density partitioning, *Org. Biomol. Chem.*, **2014**, *12*, 6145-6150; (b) Lash, T. D., Origin of aromatic character in porphyrinoid systems, *J. Porphyrins Phthalocyanines*, **2011**, *15*, 1093-1115.

[17] Miessler, G. L.; Tarr, D. A., *Chimica Inorganica*, IV Ed., **2012**, 633.

[18] (a) Rothemund. P, A New Porphyrin Synthesis. The Synthesis of Porphin, *J. Am. Chem. Soc.*, **1936**, *58*, 625-627; (b) Rothemund, P., Formation of Porphyrins from Pyrrole and Aldehydes, *J. Am. Chem. Soc.*, **1935**, *57*, 2010-2011; (c) Adler, A. D.; Longo. F. R.; Finarelli, J. D.; Goldmacher, J.; Assour, J.; Korsakoff, L., A simplified synthesis for *meso*-tetraphenylporphine, *J. Org. Chem.*, **1967**, *32*, 476.

[19] Fantauzzi, S.; Gallo, E.; Rose, E.; Raoul, N.; Caselli, A.; Issa, S.; Ragaini, F.; Cenini, S., Asymmetric Cyclopropanation of Olefins Catalyzed by Chiral Cobalt(II)-Binaphthyl Porphyrins, *Organometallics*, **2008**, *27*, 6143-6151.

[20] (a) Salomon, R. G.; Kochi, J. K., Copper(I) catalysis in cyclopropanations with diazo compounds. Role of olefin coordination, *J. Am. Chem. Soc.*, **1973**, *95*, 3300-3310; (b) Cheng, G.; Mirafzal, G. A.; Woo, L. K., Iron Porphyrin-Catalyzed Olefination of Carbonyl Compounds with Ethyl Diazoacetate, *Organometallics*, **2003**, *22*, 1468-1474; (c) Lai, T. S.; Chan, F. Y.; So, P. K.; Ma, D. L.; Wong, K. Y.; Che, C. M., Alkene cyclopropanation catalyzed by Halterman iron porphyrin: participation of organic bases as axial ligands, *Dalton Trans.*, **2006**, 4845-4851.

[21] Sharon, D. A.; Mallick, D.; Wang, B.; Shaik, S., Computation Sheds Insight into Iron Porphyrin Carbenes' Electronic Structure, Formation, and N-H Insertion Reactivity, *J. Am. Chem. Soc.*, **2016**, *138*, 9597-9610.

[22] (a) Coelho, P. S.; Brustad, E. M.; Kannan, A.; Arnold, F. H., Olefin Cyclopropanation via Carbene Transfer Catalyzed by Engineered Cytochrome P450 Enzymes, *Science*, **2013**, *339*, 307-310; (b) Coelho, P. S.; Wang, Z. J.; Ener, M. E.; Baril, S. A.; Kannan, A.; Arnold, F. H.; Brustad, E. M., A serine-substituted P450 catalyzes highly efficient carbene transfer to

olefins in vivo, *Nat. Chem. Biol.*, **2013**, *9*, 485-487; (c) Wang, Z. J.; Peck, N. E.; Renata, H.; Arnold, F. H., Cytochrome P450-catalyzed insertion of carbenoids into N-H bonds, *Chem. Sci.*, **2014**, *5*, 598-601; (d) Sreenilayam, G.; Fasan, R., Myoglobin-catalyzed intermolecular carbene N-H insertion with arylamine substrates, *Chem. Commun.*, **2015**, *51*, 1532-1534.

[23] Casali, E.; Gallo, E.; Toma, L., An In-Depth Computational Study of Alkene Cyclopropanation Catalyzed by Fe(porphyrin)(OCH_3) Complexes. The Environmental Effects on the Energy Barriers, *Inorg. Chem.*, **2020**, *59*, 11329-11336.

[24] Intrieri, D.; Carminati, D. M.; Gallo, E., The ligand influence in stereoselective carbene transfer reactions promoted by chiral metal porphyrin catalysts, *Dalton Trans.*, **2016**, *45*, 15746-15761.

[25] Hayashi, T.; Tinzl, M.; Mori, T.; Krengel, U.; Proppe, J.; Soetbeer, J.; Klose, D.; Jeschke, G.; Reiher, M.; Hilvert, D., Capture and characterization of a reactive haem-carbenoid complex in an artificial metalloenzyme, *Nat. Catal.*, **2018**, *1*, 578-584.

[26] (a) Artaud, I.; Gregoire, N.; Leduc, P.; Mansuy, D., Formation and fate of iron-carbene complexes in reactions between a diazoalkane and iron-porphyrins: relevance to the mechanism of formation of N-substituted hemes in cytochrome P-450-dependent oxidation of sydnones, *J. Am. Chem. Soc.*, **1990**, *112*, 6899-6905; (b) Artaud, I.; Gregoire, N.; Battioni, J.-P.; Dupre, D.; Mansuy, D., Heme model studies related to cytochrome P-450 reactions: preparation of iron porphyrin complexes with carbenes bearing a β-oxygen atom and their transformation into iron-N-alkylporphyrins and iron-metallacyclic complexes, *J. Am. Chem. Soc.*, **1988**, *110*, 8714-8716; (c) Baumann, L. K.; Mbuvi, H. M.; Du, G.; Woo, L. K., Iron Porphyrin Catalyzed N-H Insertion Reactions with Ethyl Diazoacetate, *Organometallics*, **2007**, *26*, 3995-4002; (d) Comanescu, C. C.; Vyushkova, M.; Iluc, V., Palladium carbene complexes as persistent radicals, *M. Chem. Sci.*, **2015**, *6*, 4570-4579.

[27] (a) Becke, A. D., Density-functional Thermochemistry. III. The Role of Exact Exchange, *J. Chem. Phys.*, **1993**, *98*, 5648-5652; (b) Lee, C.; Yang, W.; Parr, R. G., Development of the Colle-Salvetti Correlation-energy Formula into a Functional of the Electron Density, *Phys. Rev. B.*, **1988**, *37*, 785-789.

[28] Zhang, Y., Computational Investigations of Heme Carbenes and Heme Carbene Transfer Reactions, *Chem. Eur. J.*, **2019**, *25*, 13231-13247.

[29] Gallo, E.; Rose, E.; Boitrel, B.; Legnani, L.; Toma, L., DFT Conformational Studies of Chiral Bis-Binaphthyl Porphyrins and Their Metal Complexes Employed as Cyclopropanation Catalysts, *Organometallics*, **2014**, *33*, 6081-6088.

[30] Khade, R. L.; Fan, W.; Ling, Y.; Yang, L.; Oldfield, E.; Zhang, Y., Iron Porphyrin Carbenes as Catalytic Intermediates: Structures, Mössbauer and NMR Spectroscopic Properties, and Bonding, *Angew. Chem. Int. Ed.*, **2014**, *53*, 7574-7578.

[31] (a) Paul, N. D.; Chirila, A.; Lu, H.; Zhang, X. P.; de Bruin, B., Carbene Radicals in Cobalt(II)-Porphyrin-Catalysed Carbene Carbonylation Reactions; A Catalytic Approach to Ketenes, *Chem. Eur. J.*, **2013**, *19*, 12953-12958; (b) Lu, H.; Dzik, W. I.; Xu, X.; Wojtas, L.; de Bruin, B.; Zhang, X. P., Experimental Evidence for Cobalt(III)-Carbene Radicals: Key Intermediates in Cobalt(II)-Based Metalloradical Cyclopropanation, *J. Am. Chem. Soc.*, **2011**, *133*, 8518-8521; (c) Dzik, W. I.; Zhang, X. P.; de Bruin, B., Redox Noninnocence of Carbene Ligands: Carbene Radicals in (Catalytic) C-C Bond Formation, *Inorg. Chem.*, **2011**, *50*, 9896-9903; (d) Dzik, W. I.; Xu, X.; Zhang, X. P.; Reek, J. N. H.; de Bruin, B., 'Carbene Radicals' in CoII(por)-Catalyzed Olefin Cyclopropanation, *J. Am. Chem. Soc.*, **2010**, *132*, 10891-10902.

[32] Kitagawa, Y.; Saito, T.; Ito, M.; Shoji, M.; Koizumi, K.; Yamanaka, S.; Kawakami, T.; Okumura, M.; Yamaguchi, K., Approximately spin-projected geometry optimization method and its application to di-chromium systems, *Chem. Phys. Lett.*, **2007**, *442*, 445-450.

[33] Harvey, J., *Computational Chemistry*, Oxford Chemistry Primers, **2018**, 24-25.

[34] Yamaguchi, K.; Takahara, Y.; Fueno, T.; Houk, K. N., Extended Hartree-Fock (EHF) theory of chemical reactions, *Theor. Chim. Acta*, **1988**, *73*, 337-364.

[35] Chirila, A.; Brands, M. B.; de Bruin, B., Mechanistic investigations into the cyclopropanation of electron deficient alkenes with ethyl diazoacetate using [Co(MeTAA)], *Journal of Catalysis*, **2018**, *361*, 347-360.

[36] Torrent-Sucarrat, M.; Arrastia, I.; Arrieta, A.; Cossio, F. P., Stereoselectivity, Different Oxidation States, and Multiple Spin States in the Cyclopropanation of Olefins Catalyzed by Fe-Porphyrin Complexes, *ACS Catalysis*, **2018**, *8*, 11140-11153.

[37] Harvey, J. N., Understanding the kinetics of spin-forbidden chemical reactions, *Phys. Chem. Chem. Phys.*, **2007**, *9*, 331-343.

[38] (a) Yarkony, D.R., Systematic determination of intersections of potential energy surfaces using a Lagrange multiplier constrained procedure, *J. Phys. Chem.*, **1993**, *97*, 4407-4412; (b) Bearpark, M. J.; Robb, M. A.; Schlegel, H. B., A direct method for the location of the lowest energy point on a potential surface crossing, *Chem. Phys. Lett.*, **1994**, *223*, 269-274; (c) Koga, N.; Morokuma, K., Determination of the lowest energy point on the crossing seam between two potential surfaces using the energy gradient, *Chem. Phys. Lett.*, **1985**, *119*, 371-374; (d) Cui, Q.; Morokuma, K., Ab initio MO studies on the photodissociation of C_2H_2 from the $S_1(1A_u)$ state. II. Mechanism involving triplet states, *Chem. Phys. Lett.*, **1997**, *272*, 319; (e) Farazdel, A.; Dupuis, M., On the determination of the minimum on the crossing seam of two potential energy surfaces, J. Comput. Chem., 1991, 12, 276-282; (f) De Vico, L.; Olivucci, M.; Lindh, R., New General Tools for Constrained Geometry Optimizations, *J. Chem. Theory Comput.*, **2005**, *1*, 1029-1037.

[39] Harvey, J. N.; Aschi, M.; Schwarz, H.; Koch, W., The singlet and triplet states of phenyl cation. A hybrid approach for locating minimum energy crossing points between non-interacting potential energy surfaces, *Theor. Chem. Acc.*, **1998**, *99*, 95-99.

[40] Miller, W. H.; Handy, N. C.; Adams, J. E., Reaction path Hamiltonian for polyatomic molecules, *J. Chem. Phys.*, **1980**, *72*, 99.

[41] Rodríguez-Guerra, J.; Funes-Ardoiz, I.; Maseras, F. EasyMECP, *Zenodo*, **2018**, doi: 10.5281/zenodo.4293421

[42] Roy, L. E.; Jakubikova, E.; Guthrie, M. G.; Batista, E. R., Calculation of One-Electron Redox Potentials Revisited. Is It Possible to Calculate Accurate Potentials with Density Functional Methods?, *J. Phys. Chem. A.*, **2009**, *113*, 6745-6750.

[43] Baik, M. H.; Friesner, R. A., Computing Redox Potentials in Solution: Density Functional Theory as A Tool for Rational Design of Redox Agents, *J. Phys. Chem. A.*, **2002**, *106*, 7407-7412.

[44] Trasatti, S., The absolute electrode potential: an explanatory note, *Pure Appl. Chem.*, **1986**, *58*, 955-966.

[45] Frisch, M. J.; Trucks, G. W.; Schlegel, H. B.; Scuseria, G. E.; Robb, M. A.; Cheeseman, J. R.; Scalmani, G.; Barone, V.; Mennucci, B.; Petersson, G. A.; Nakatsuji, H.; Caricato, M.; Li, X.; Hratchian, H. P.; Izmaylov, A. F.; Bloino, J.; Zheng, G.; Sonnenberg, J. L.; Hada, M.; Ehara, M.; Toyota, K.; Fukuda, R.; Hasegawa, J.; Ishida, M.; Nakajima, T.; Honda, Y.; Kitao, O.; Nakai, H.; Vreven, T.; Montgomery, J. A., Jr.; Peralta, J. E.; Ogliaro, F.; Bearpark, M.; Heyd, J. J.; Brothers, E.; Kudin, K. N.; Staroverov, V. N.; Keith, T.; Kobayashi, R.; Normand, J.; Raghavachari, K.; Rendell, A.; Burant, J. C.; Iyengar, S. S.; Tomasi, J.; Cossi, M.; Rega, N.; Millam, J. M.; Klene, M.; Knox, J. E.; Cross, J. B.; Bakken, V.; Adamo, C.; Jaramillo, J.; Gomperts, R.; Stratmann, R. E.; Yazyev, O.; Austin, A. J.; Cammi, R.; Pomelli, C.; Ochterski, J. W.; Martin, R. L.; Morokuma, K.; Zakrzewski, V. G.; Voth, G. A.; Salvador, P.; Dannenberg, J. J.; Dapprich, S.; Daniels, A. D.; Farkas, O.; Foresman, J. B.; Ortiz, J. V.; Cioslowski, J.; Fox, D. J. *Gaussian 09, Revision B.01*; Gaussian, Inc., Wallingford, CT, **2010**.

[46] Bochevarov, A.D.; Harder, E.; Hughes, T.F.; Greenwood, J.R.; Braden, D.A.; Philipp, D.M.; Rinaldo, D.; Halls, M.D.; Zhang, J.; Friesner, R.A., Jaguar: A high-performance quantum chemistry software program with strengths in life and materials sciences, *Int. J. Quantum Chem.*, **2013**, *113*, 2110-2142.

Ringraziamenti

E anche stavolta siamo giunti alla fine... Ma non come le altre volte, in cui comunque ci sarebbe stata l'idea di una continuazione. Questa volta no. Con il dottorato finisce ufficialmente il mio percorso formativo universitario. Tante sono le cose che restano ancora da imparare, ma mi accompagneranno negli anni a venire.

È quantomeno doveroso ricordare ora tutti coloro i quali mi hanno assistito in questo lungo viaggio, accompagnandomi e sostenendomi giorno per giorno.

Il mio primissimo grazie va a chi ha creduto in me sin dall'inizio, quando ancora non pensavo di poter perseguire anche quest'ultimo traguardo nella formazione universitaria.

Il Professor Lucio Toma, mio tutor ufficiale, è stato un ottimo mentore che mi ha trasmesso in questi anni gran parte del suo sapere sulla Chimica Computazionale. Numerosi sono stati gli spunti che sono nati da semplici chiacchierate e che hanno poi condotto a notevoli svolte dal punto di vista scientifico. Grazie davvero, Prof., per il supporto che mi ha dato anche nei momenti difficili. Alla notizia del suo pensionamento mi sono rattristato, perché sarebbe stato bello poter proseguire ancora a fare scienza insieme, ma le prometto che il sapere che mi ha tramandato verrà custodito e fatto fruttare nel migliore dei modi. Auspico, inoltre, di poter continuare a collaborare come in questi anni e a tener vivo quello che è stato il nostro gruppo di ricerca. Grazie per avermi insegnato a camminare da solo.

A seguire, ma non secondo, il Professor Giuseppe Zanoni (il Beppe) che mi ha cresciuto dal punto di vista sperimentale. Nel Lab B2 ho mosso i miei primi passi, quando ancora non ero uno studente universitario, per poi portare a termine gli studi della tesi magistrale e di gran parte del lavoro sperimentale nel dottorato.

Grazie per avermi sempre sostenuto, per essere stato severo quando necessario, per aver assecondato ogni mia strana idea, anche se sapevi non avrebbe portato a nulla di buono. Tanti sono stati i progetti su cui abbiamo collaborato assieme e spero di poter continuare anche in futuro a fare ricerca di alto livello, come abbiamo sempre fatto. Grazie Beppe.

Altro doveroso ringraziamento va alla Professoressa Fernanda Duarte che mi ha accolto nel suo gruppo di ricerca all'Università di Oxford e che mi ha supportato durante i momenti difficili del COVID. Assieme a lei ringrazio tutti gli amici del gruppo e in particolare Matina. È stato un onore lavorare con voi e avervi come mentori in un campo di ricerca a me totalmente sconosciuto come il Machine Learning.

Giunge ora il momento di ringraziare i miei colleghi e tutti i ragazzi che hanno popolato in questi anni le mie giornate in B2. In primis devo ringraziare Max Brochetta, Gando, Arbas, Viro, Diesel, Max Andreoli, Bacca, Paolino, Chicco, Stef., Chad, Ervis, Eugenio (il malvagio), Zigo e Teo. Grazie anche ai tesisti che in questi anni ho avuto modo di seguire e che mi hanno trasmesso tanto, anche dal punto di vista didattico. Grazie alla Vittooooooo, alla Sofi, al buon Livio e alle due nuove gemelle M&M. Come non ringraziare poi il Nando, la vera anima del laboratorio, sempre super informato sulle ultime novità tecnologiche dell'azienda di Cupertino.

Un doveroso ringraziamento va poi al Professor Alessio Porta (ALP) che ha sempre dispensato consigli utili e che mi ha seguito in alcuni momenti di difficoltà nell'interpretazione di spettri NMR o nella messa a punto di nuovi metodi HPLC.

Terminati i ringraziamenti agli "addetti ai lavori", un non minore riguardo va dedicato a chi in questi anni ha lavorato con me dietro le quinte, quando, tolto il camice, ritornavo ad essere figlio, parente e compagno. A tal riguardo un grande, enorme, immenso ringraziamento va ai miei genitori Doriana e Mario che mi hanno supportato in questo percorso sia mentalmente, sia caratterialmente. Scusatemi se a volte è stato difficile interagire con me, costantemente assorto nelle problematiche da risolvere in laboratorio e se in certi momenti c'è stata qualche mancanza. Un grosso grazie va anche ai miei nonni, le mie guide spirituali che, oltre ad avermi cresciuto e accompagnato, vivono tutt'oggi per me: Edda e Natalino che mi seguono nella vita

di tutti i giorni e Mariarosa e Pietro che mi guardano da lassù. Vi voglio bene.

Sacrosanto è poi il ringraziamento a mio cugino, il Dr. Enrico Maggi. Anche tu mi hai visto fin da piccolo muovere i primi passi tra microscopi ed esperimenti fatti in casa. È per me un onore averti come guida morale e di vita, sapendoti sempre pronto per ascoltare le mie lagne e per condividere i tuoi spericolati viaggi all'insegna dell'arte sacra italiana. Grazie davvero Erry.

E giunge ora il momento più delicato: ringraziare la mia Federica, con la quale da 8 anni condivido ogni sentimento. Amore, grazie davvero! Mi hai supportato nei momenti critici, spronandomi a continuare senza abbassare mai la testa. Tuo è anche il merito di sopportazione quando il mio carattere fa le bizze... Ma per fortuna sei una bilancia che sa moderare un impavido e scalpitante sagittario come me. Anche questo traguardo l'abbiamo raggiunto insieme. Ne mancano ancora, è vero, ma uno già sai qual è: TI AMO! Ovviamente un grazie va anche alla famiglia di Federica - Maurizio, Lusia e Davide - per avermi sostenuto durante questo percorso.

Un doveroso ringraziamento va poi agli altri componenti della mia famiglia: siete tanti e non vi elencherò qui uno ad uno, ma a tutti voi è rivolto un grosso grazie.

Non mi resta poi che concludere ringraziando i miei amici più stretti. In primis i nostri due sposini Nicolò e Rachele: già sapete quanto tenga a voi, siete speciali e vi voglio davvero un mondo di bene. Gli amici di una vita: Taccio, Pozz, Nicòlo, Alessia, Michela, che seppur saltuariamente si sono sorbiti le mie "pillole" di scienza e di noia durante aperitivi, cene e viaggi! Grazie davvero a tutti.

Dulcis in fundo, un ringraziamento me lo prendo anche io: bravo l'Ema per non aver mai mollato e per aver sempre tenuto a mente che se ...

Insisti e persisti,

Raggiungi e conquisti.

Pavia, Febbraio 2022

Emanuele Casali

Chapter 5

APPENDIX I - Experimental / Computational procedures and additional data

5.1 Chapter 1

General methods

The practical work was performed by the aid of the following instruments.

For the characterisation of compounds:

- Brucker NMR AV 300 MHz spectrometer
- Brucker NMR AV 200 MHz spectrometer
- "Thermo scientific" LTQ-XL with HESI (Heated Electrospray Ionization source)
- "Thermo scientific" Focus GC-DSQ II
- Brucker ALPHA II FTIR Spectrometer equipped with QuickSnap^{TM} universal sampling module.

Cromathographic techniques:

- Silica gel Sigma-Aldrich High-purity grade (9385), pore size 60Å, 230-400 mesh

- Silica gel on TLC glass plates Sigma-Aldrich, silica gel matrix with fluorescent indicator

- ESI-MS thermo LTQ

- MPLC Isolera One Biotage Flash Cromatography for chromatographic purifications of raw materials of more than 500 mg

- Fluorescence lamp 254-366 nm,

- $KMnO_4$ (solution in acetone), Vanilline (solution in H_2SO_4-EtOH) and Phosphomolibdic Acid (solution in EtOH), for the stain detection on TLC plates.

All preparations involving anhydrous conditions and inert atmosphere, were carried out under atmosphere of argon, into dried reactors dried in oven at 120°C for one night. Most of the solvents used were dried by distillation with an appropriate drying agent under an argon atmosphere.

In particular: the tetrahydrofuran from sodium and using benzophenone as indicator for H_2O; dichloromethane was freshly distilled from calcium hydride and toluene from sodium.

The IR spectra were reported using the wave numbers expressed in cm^{-1}. The NMR spectra were tabulated bringing the chemical shift (δ) in ppm and the coupling constants (J) in Hz. The multiplicity of the signals are abbreviated thus: s (singlet), d (doublet), t (triplet), q (quartet), m (multiplet), br (broadened signal). For the ^{13}C-NMR, the number of carbon atom bound to any hydrogen atoms was determined by DEPT experiments.

Glossary

AcOEt.....Ethylacetate

Brine.....Saturated Acqueous solution of NaCl

DCM.....Dichloromethane

DIBAL-H.....Diisobutylaluminium hydride

DMAP.....4-Dimethylaminopyridine

DMF.....*N*,*N*'-Dimethylformamide

DMS.....Dimethylsulphide

EDCI.....1-Ethyl-3-(3-dimethylaminopropyl)carbodiimide hydrochloride

Et_2O.....Diethyl Ether

MeOH.....Methanol

MTBE.....Methyl-*tert*-Butyl Ether

Py.....Pyridine

Rochelle solution.....Sodium potassium tartrate saturated solution

TBAF.....Tetrabutyl ammonium fluoride

TBS.....*t*-Butyl dimethylsilyl

THF.....Tetrahydrofurane

Synthetic procedures for the (E,E)-*meso*-diol 1

Synthesis of compound 3

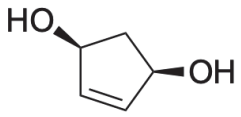

3

Chemical Formula: C_5H

Exact Mass: 100.05

In a photochemical reactor equipped with a magnetic stirring bar was filled with freshly distilled cyclopentadiene (1 Equiv., 6.61 g, 100 mmol) and solubilized in methanol (0.1M). Thiourea (1.2 Equiv., 9.134 g, 120 mmol) was then added followed by the photosensitizer Rose Bengal (0.0014 Equiv., 136.31 mg, 0.14 mmol). The so obtained mixture was cooled down to 0°C and the oxygen is bubbled inside for at least 10 minutes, by maintaining a constant stirring. The mercury vapor lamp (253.7 nm) was then turned on and maintained operative for 3.5 h at 0°C. After that time, the lamp can be turned off and the mixture was left reaching room temperature under continuous stirring for 20 hours. Thus, the reaction mixture was filtered over a silica gel pad and the filtrate was evaporated to dryness with the aid of the rotary evaporation. The so obtained residue was then recovered with THF and the precipitate was filtered off. After the evaporation of the remaining solvent, the raw product was purified from the unreacted cyclopentadiene and the photosensitizer through a silica gel column [9:1, DCM/MeOH] to afford the corresponding diol derivative **3** (isolated yield = 30%).

The spectroscopic data collected in our synthesis match perfectly with those reported in literature.[1]

Synthesis of compound 4

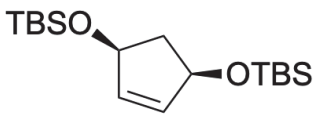

4

Chemical Formula: $C_{17}H_{36}O_2Si_2$

Exact Mass: 328.23

In a two-necked round bottom flask, imidazole (8 Equiv., 2.72 g, 39.95 mmol) and DMAP (0.1 Equiv., 61 mg, 0.5 mmol) were solubilized in dry DCM (9 mL) under Ar atmosphere. A solution of diol **3** (1 Equiv., 500 mg, 5 mmol) in dry DMF (500 μL) was added dropwise via syringe under continuous stirring. The mixture was cooled to 0°C, then TBSCl (2.6 Equiv., 2.00 g, 13.0 mmol) was quickly added. The stirring was maintained for 5 minutes at 0°C and then the temperature was spontaneously raised to room temperature and the solution was kept under vigorous stirring. Reaction was monitored via TLC, (95:5, DCM/MeOH). After completion, it was quenched with water (9 mL) and diluted with diethyl ether (20 mL). The aqueous layer was extracted one time with 30 mL of diethyl ether and the combined organic layers were washed with water (20 mL) and brine (20 mL), then dried on Na_2SO_4 and filtered. The solvent was removed under reduced pressure and the resulting crude oil was purified by flash chromatography on silica gel [gradient of Hex/Et_2O: (99:1) then (95:5)] to afford the corresponding protected derivative **4** (isolated yield = 98%).

MS (HESI): 329.27 ($M+H^+$); 351.22 ($M+Na^+$)

^{1}H-NMR ($CDCl_3$): 300 MHz δ (ppm)= 5.68 (s, 2H), 4.10 (m, 2H), 2.00-1.50 (m, 2H), 0.91 (s, 18H), 0.1 (s, 12H).

^{13}C-NMR ($CDCl_3$): 75 MHz δ (ppm)= 131.9, 65.9, 28.6, 25.8, 18.1, -4.7.

IR (neat): (cm^{-1})= 2956, 2912, 2878, 1370, 1238, 1080, 1040, 1007, 824, 742.

Synthesis of compound 5

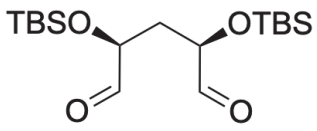

5

Chemical Formula: $C_{17}H_{36}O_4Si_2$

Exact Mass: 360.22

In a two-necked round bottom flask, alkene **4** (1 Equiv., 4.90 g, 15 mmol) was solubilized in dry DCM (125 mL). The solution was cooled to -78°C and a O_3/O_2 mixture was bubbled in it under stirring until the color became blue. The excess of ozone was eliminated through oxygen bubbling in the solution that was kept at -78°C. The mixture became colorless, then Ar or N_2 was bubbled in order to remove the oxygen. Under vigorous stirring, at -78°C, a solution of pyridine (3 drops) in dimethyl sulfide (8 Equiv., 11 mL, 126.72 mmol) was added dropwise to the mixture and the temperature was slowly raised to -32°C. After 2 hours, the temperature was spontaneously increased at room temperature, then the solvent was removed under reduced pressure.

The so obtained crude oil was directly used in the next step of the reaction without no further purification.

Synthesis of compound 6

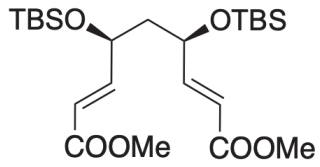

6

Chemical Formula: $C_{23}H_{44}O_6Si_2$

Exact Mass: 472.27

The crude oil from the previous step was directly dissolved in dry THF (10 mL) under Ar atmosphere and subsequently it was transferred via cannula into a round bottom flask containing a THF solution (65 mL) of methyl(triphenylphosphoranyliden) acetate (6 Equiv., 15.030 g, 45 mmol) that was kept under vigorous stirring.

After 30 minutes, the temperature was raised at 50°C and the mixture was stirred for 20 hours. The reaction was monitored by TLC (9:1, Hex/AcOEt). It was quenched through addition of NH_4Cl saturated aqueous solution (60 mL) and diluted with H_2O (100 mL). Phases were separated, then the aqueous one was extracted with Et_2O (3 x 100 mL). The combined organic layers were washed with water (2 x 250 mL) and Brine (250 mL), dried on Na_2SO_4 and filtered. The solvent was removed under reduced pressure and the resulting crude material was filtered on a silica gel pad (45 g) by washing with 8:2 Hex/AcOEt. Finally, the raw compound was purified by flash chromatography on silica gel [gradient of Hex/AcOEt: (96:4) then (9:1)] to afford the corresponding methyl-ester derivative **6** (isolated yield = 75%).

MS (HESI): 473.30 ($M+H^+$)

^{1}H-NMR ($CDCl_3$): 300 MHz δ (ppm)= 7.10-6.90 (dd, J_1=15.6, J_2=5.1, 2H), 6.10-5.95 (dd, J_1=15.6, $J2$=1.5, 2H), 4.90-4.40 (m, 2H), 3.76 (s, 6H), 1.95-1.50 (m, 2H), 0.90 (s, 18H), 0.1 (d, J=8Hz, 12H).

^{13}C-NMR ($CDCl_3$): 75 MHz δ (ppm)= 166.9, 150.5, 119.7, 68.3, 52.6, 45.5, 28.8, 18.1, -4.7.

IR (neat): (cm^{-1})= 2955, 2879, 1731, 1300, 1277, 1166, 1128, 1007, 980, 729.

Synthesis of compound 7

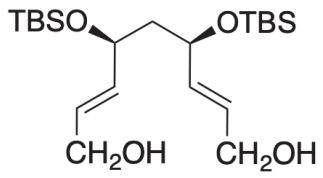

7

Chemical Formula: $C_{21}H_{44}O_4Si_2$

Exact Mass: 416.28

In a two-necked round bottom flask equipped with a pressure equalizing funnel, ester **6** (1 Equiv., 3.0 g, 6.63 mmol), was dissolved in dry THF (50 mL) under Ar atmosphere. The funnel was charged with DIBAL-H (4.7 Equiv., 31.5 mL, 31.5 mmol, 1M solution in Hex) and the reaction mixture was cooled down to -78°C. The DIBAL-H solution was thus added to the ester solution dropwise and under vigorous stirring. The reaction was constantly monitored by TLC (7:3, Hex/EtOAc) and it was completed after 1.5 hours. The mixture was then quenched through dilution with Et_2O (50 mL) and subsequently with saturated Rochelle salt solution (80 mL) and water (50 mL): these two additions were slowly operated to the -78°C solution and only after that the temperature was increased to r.t. The so obtained double phases system was kept under vigorous stirring overnight, until two clear layers were obtained. After separation, the aqueous phase was extracted with Et_2O (3 x 150 mL). The combined organic layers were washed with water (100 mL) and Brine (100 mL), then dried over Na_2SO4, filtered and the solvent was removed under reduced pressure. Finally, the raw compound was purified by flash chromatography on silica gel [7:3, Hex/AcOEt] to afford the corresponding diol derivative **7** (isolated yield = 92%).

MS (HESI): 417.26 ($M+H^+$)

^{1}H-NMR ($CDCl_3$): 300 MHz δ (ppm)= 5.80-5.60 (m, 4H), 4.25-4.20 (m, 2H), 4.20-4.10 (d, J=4.4, 4H), 1.95-1.60 (m, 3H), 1.60-1.55 (m, 1H), 0.90 (s, 18H), 0.1 (d, J=8Hz, 12H).

^{13}C-NMR ($CDCl_3$): 75 MHz δ (ppm)= 134.7, 129.2, 70.0, 63.0, 47.1, 28.8, 18.1, -4.7.

IR (neat): (cm^{-1})= 3340, 2955, 2913, 2877, 1459, 1415, 1239, 1088, 1005, 972, 739.

Synthesis of compound 8

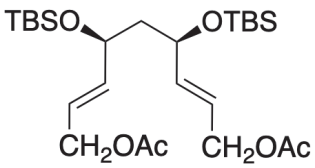

8

Chemical Formula: $C_{25}H_{48}O_6Si_2$

Exact Mass: 500.30

In a two-necked round bottom flask, under Ar atmosphere, diol **7** (1 Equiv., 2.10 g, 6.25 mmol) was dissolved in dry DCM (25 mL). The so obtained mixture was kept to 0°C and pyridine (2.8 Equiv., 1.4 mL, 17.3 mmol) was subsequently added dropwise followed by acetic anhydride (2.4 Equiv., 1.35 mL, 14.3 mmol). Finally, DMAP (0.15 Equiv., 113 mg, 0.95 mmol) was added. After the additions were completed, the temperature was raised to r.t. and the reaction was kept under continuous stirring overnight. The reaction was monitored by TLC (8:2, Hex/AcOEt). Quenching was operated by the addition of saturated $NaHCO_3$ solution (35 mL) and when bubbling due to acetic anhydride decomposition stopped, the phases were separated. The aqueous one was extracted with Et_2O (3 x 80 mL). The combined organic layers were washed with water (80 mL), saturated solution of $CuSO_4$ (3 x 80 mL, to eliminate pyridine residues), again water (80 mL) and finally with Brine (100 mL). After drying on Na_2SO_4 and removal of the solvent at reduce pressure, the resulting crude oil was purified by flash chromatography [gradient of Hex/AcOEt: (95:5) then (9:1)] to afford the corresponding acetylated derivative **8** (isolated yield = 98%).

MS (HESI): 501.32 ($M+H^+$)

^{1}H-NMR ($CDCl_3$): 300 MHz δ (ppm)= 5.85-5.65 (m, 4H), 4.65-4.50 (d, J=5.3, 4H), 4.30-4.15 (m, 2H), 2.07 (s, 6H), 1.90-1.75 (dt, J_1= 13.5, J2=6.8, 1H), 1.65-1.50 (dt, J_1= 13.5, J_2=6.3, 1H), 0.90 (s, 18H) 0.1 (d, J=8Hz, 12H).

^{13}C-NMR ($CDCl_3$): 75 MHz δ (ppm)= 170.7, 137.6, 123.9, 69.6, 64.3, 46.6, 20.09, 28.4, 18.3, -4.3.

IR (neat): (cm^{-1})= 2955, 2914, 2878, 1745, 1366, 1237, 1085, 1006, 971, 745.

Synthesis of compound 1

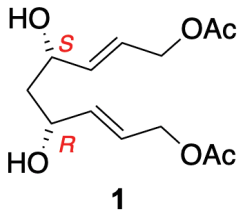

1

Chemical Formula: $C_{13}H_{20}O_6$

Exact Mass: 272.13

The TBS protected substrate **8** (1 Equiv., 2.85g, 5.78 mmol) was transferred in a Teflon flask equipped with magnetic stirrer and subsequently dissolved in MeCN HPLC grade (45 mL). After a few minutes, an aqueous solution of HF 48% p/p (30 Equiv., 6.3 mL, 173.4 mmol, 27.6M), was slowly added to the reaction mixture. The flask was tightly closed in order to prevent the escape of HF vapors. The reaction was monitored by TLC (9:1, Hex/iPrOH) and it was quenched through addition of solid $NaHCO_3$ (30 Equiv., 14.65 g, 173.4 mmol) till the bubbling due to CO2 release stopped. The resulting mixture was filtered on a Celite pad and concentrated. Finally, the crude was purified by flash chromatography on silica [4:6, Hex/EtOAc] to afford the corresponding (E,E)-*meso*-diol **1** (isolated yield = 91%).

The spectroscopic data collected in our synthesis match perfectly those reported in literature and those of the previous synthesis reported in the preexisting thesis work in our laboratory.[2],[3]

Synthesis of compound 1 (through ring-opening cross-metathesis)

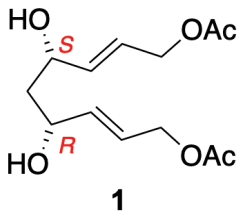

1

Chemical Formula: $C_{13}H_{20}O_6$

Exact Mass: 272.13

The commercially available (Z)-2-buten-1,4-diyl diacetate (11 Equiv., 11868 mg, 69 mmol) and **3** (1 Equiv., 600 mg, 6 mmol), were transferred in a round bottom flask under Ar atmosphere. The 2nd generation Grubbs catalyst (0.11 Equiv., 600 mg, 0.706 mmol) was added and the reaction mixture was kept under vigorous stirring at 40°C. The reaction was monitored by TLC (7:3, Hex/AcOEt) and after 36 hours the temperature was lowered at r.t. The mixture was thus diluted with DCM (15 mL) and air was bubbled inside for 10 minutes. DCM was removed at reduced pressure and the crude material was purified by liquid chromatography on silica gel [3:7, Hex/AcOEt] to afford the corresponding (E,E)-*meso*-diol **1** (isolated yield = 55%).

The spectroscopic data collected in our synthesis match perfectly those reported in literature and those of the previous synthesis reported in the preexisting thesis work in our laboratory.[2],[3]

Synthetic procedures for the (Z,Z)-*meso*-diol 14

Synthesis of compound 15

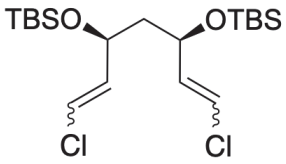

15

Chemical Formula: $C_{19}H_{38}Cl_2O_2Si_2$

Exact Mass: 424.18

In a two-necked round bottom flask, a suspension of the chloromethyltriphenylphosphonium chloride salt (6 Equiv., 9.4 g, 24 mmol) is prepared in dry THF (0.1 M) and then cooled down to -78°C, followed by the addition of potassium *tert*-butoxide (6 Equiv., 2.7 g, 24 mmol). The so obtained mixture was stirred for additional 45 minutes. Meanwhile, in another pre-dried flask, the compound **5** (obtained with the same procedure described above) was solubilized in dry THF and then added via cannula to the previous stirred mixture. Once the additions finished, the mixture was kept for an additional 1.5 h at -78°C and then increased to -20°C for additional 16 hours. TLC control was operated by using 9:1, DCM/MeOH as eluent mixture. The reaction is quenched by the addition, at -20°C, of a saturated solution of NH4Cl (60 mL) and H_2O (120mL). After reaching r.t. the phases are then separated and the aqueous one extracted with ethyl ether (3 x 120 mL). The combined organic extracts are washed with water (1 x 120 mL) and Brine (200 mL), dried over Na_2SO_4, filtered and the solvent removed under reduced pressure. The reaction crude was then filtered quickly on silica gel (100g, eluent 95:5, Hex/Et_2O).

The crude product, dissolved in DCM, is treated at 0°C with 850μL of tBuOOH 5.5M in nonane to remove the excess of PPh_3 which is difficult to separate by chromatography. The transformation of the phosphine into the respective phosphine oxide is completed in about 30 minutes and is verified by TLC using pure hexane as eluent. Excess oxidant is removed by adding a 1:1 $Na_2S_2O_3$/$NaHCO_3$ solution (60

mL). The two phases are separated, then the aqueous one is extracted with hexane (2 x 60 mL). The combined organic phases are washed with water (120 mL) and brine (120 mL), dried over Na_2SO_4 and filtered. The crude material was purified by liquid chromatography on silica gel [95:5, Hex/MTBE] to afford the corresponding diene **15** (isolated yield = 76%).

MS (HESI): 425.21 ($M+H^+$)
^{1}H-NMR ($CDCl_3$): 300 MHz δ (ppm)= 6.18-5.77 (m, 4H), 4.85-4.69 (m, 1H), 4.34-4.17 (m, 1H), 1.94-1.65 (m, 2H), 0.90 (s, 18H), 0.07 (m, 12H).
^{13}C-NMR ($CDCl_3$): 75 MHz δ (ppm)= 135.5, 118.9, 116.9, 68.5, 65.2, 45.4, 25.7, -3.7, -4.6.

Synthesis of compound 16

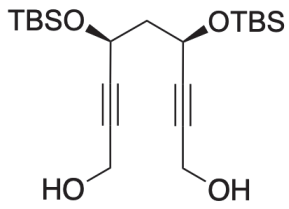

16

Chemical Formula: $C_{21}H_{40}O_4Si_2$
Exact Mass: 412.25

The diasteromeric mixture of olefins **14** (1 Equiv., 1.69 g, 3.97 mmol) is placed in a two-necked flask equipped with a desiccant valve under an atmosphere of Ar, dissolved in anhydrous THF (7 mL) and cooled to -78°C. Under stirring, a solution of 2.5M BuLi in hexane (4.4 Equiv., 7 mL, 17.47 mmol) is added dropwise: the solution takes on a brown color. After the additions, the reaction was left 30 minutes at -78°C and then allowed to rise spontaneously up to r.t.. This temperature was maintained for 30', during which the color of the solution changed from brown to yellow. The disappearance of the starting material was confirmed by TLC (pure hexane eluent). The temperature is brought again to -78°C and the paraformaldehyde (4 Equiv., 500

mg, 15.88 mmol) was added; the cooling bath was removed and the reaction was left at r.t. for 16h under continuous stirring. The TLC control (8:2, Hex/AcOEt) shows the disappearance of the starting material and of the dialkyne intermediate and the appearance of a brown spot at R_f = 0.25. The reaction is quenched by adding a solution of saturated NH_4Cl (20 mL), diluted with water (80 mL) and ethyl ether (80mL). The phases are separated and the aqueous phase is extracted 3 times with 80 mL of ethyl ether. The combined organic phases are washed with 50 mL of water and finally with 50 mL of Brine, dried on Na_2SO_4, filtered and concentrated. The resulting crude oil was purified by flash chromatography [gradient of Hex/AcOEt: (8:2) then (7:3)] to afford the corresponding diol derivative **16** (isolated yield = 56%).

MS (HESI): 413.27 ($M+H^+$)
^{1}H-NMR ($CDCl_3$): 300 MHz δ (ppm)= 4.67-4.52 (t, 2H), 4.31 (s, 4H), 2.23-2-08 (m, 1H), 2.08-1.93 (m, 1H), 1.65 (bs, 2H), 0.9 (s, 18H), 0.1 (m, 12H).
^{13}C-NMR ($CDCl_3$): 75 MHz δ (ppm)= 86.4, 82.8, 60.1, 51.0, 46.8, 25.6, 18.1, -4.6, -5.2.

Synthesis of compound 17

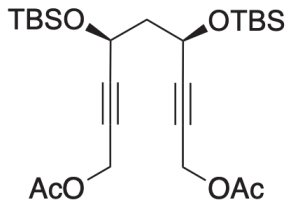

17

Chemical Formula: $C_{25}H_{44}O_6Si_2$
Exact Mass: 496.27

The propargyl diol **16** (1 Equiv., 1.34 g, 3.25 mmol) was dissolved in anhydrous DCM (32.5 mL) in a two-necked flask fitted with a desiccant valve under an Ar atmosphere. Pyridine (4 Equiv., 1054 μL, 13 mmol) and then acetic anhydride (3 Equiv., 921?L, 9.75 mmol) were added under stirring. Finally, DMAP was

added (0.15 Equiv., 60 mg, 0.4875 mmol). The reaction, controlled by TLC (8:2 Hex/AcOEt), was completed in about 1 hour and was quenched by adding a saturated solution of $NaHCO_3$ (30mL). After the complete decomposition of the acetic anhydride, the phases were separated and the aqueous phase extracted with ethyl ether (3 x 60mL). The combined organic phases were washed with water (60 mL), saturated aqueous $CuSO_4$ (3 x 60mL, to remove pyridine residues), water (60 mL) and finally Brine (100mL). After drying with Na_2SO_4 and concentration with the rotary evaporator, the resulting raw product was purified by flash chromatography [gradient of Hex/AcOEt: (95:5) then (9:1)] to afford the corresponding diacetylated derivative **17** (isolated yield = 92%).

MS (HESI): 497.25 ($M+H^+$)
^{1}H-NMR ($CDCl_3$): 300 MHz δ (ppm)= 4.71 (m, 4H), 4.60-4.50 (m, 2H), 2.23-1.90 (m, 2H), 2.10 (s, 6H), 0.91 (s, 18H), 0.15-0.12 (m, 12H).
^{13}C-NMR ($CDCl_3$): 75 MHz δ (ppm)= 170.0, 87.2, 78.6, 60.0, 52.1, 46.3, 25.6, 20.6, 18.0, -4.8, -5.4.

Synthesis of compound 18

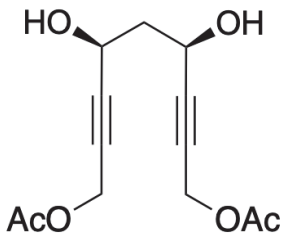

18

Chemical Formula: $C_{13}H_{16}O_6$
Exact Mass: 268.09

The product **17** to be deprotected (1 Equiv., 165 mg, 0.329 mmol) was transferred in a two-necked flask equipped with a magnetic stirring bar and under Ar atmosphere. Anhydrous THF (0.05 M) was added and the resulting mixture was

cooled down to 0°C, followed by the addition of TBAF (3 Equiv., 0.98 mL, 0.98 mmol, 1M) in THF. The so obtained reaction mixture was stirred vigorously for 3 hours at 0°C. The reaction was monitored by TLC (9:1, Hex/iPrOH) and followed until the disappearance of the starting material and the intermediate (due to the mono-deprotection). Once the reaction is complete, phosphate buffer (5 mL) and Brine (10 mL) were added. The mixture was diluted with AcOEt (25 mL), separated with the aid of a separatory funnel and then the aqueous phase is extracted three times with AcOEt (20 mL). After drying with Na_2SO_4 and concentration with the rotary evaporator, the raw product was purified by flash chromatography [1:1, Hex/AcOEt] to afford the corresponding diol derivative **18** (isolated yield = 37%).

MS (HESI): 291.07 ($M+H^+$)
^{1}H-NMR ($CDCl_3$): 300 MHz δ (ppm)= 4.72-4.67 (m, 6H), 2.75 (bs, 2H), 2.23-1.90 (m, 2H), 2.12 (s, 6H).
^{13}C-NMR ($CDCl_3$): 75 MHz δ (ppm)= 170.3, 86.4, 79.5, 60.4, 52.1, 44.2, 20.6.

Synthesis of compound 14

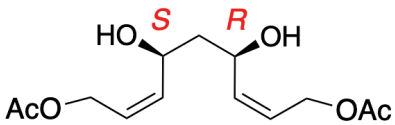

14

Chemical Formula: $C_{13}H_{20}O_6$
Exact Mass: 272.13

A solution of quinoline (35% w/w vs. alkyne, 52 μL, 0.44 mol) in AcOEt (5 mL) was prepared in a 100 mL flask. Lindlar catalyst (15% w/w vs. alkyne, 25 mg) was added to this solution. The flask was equipped with magnetic stirrer, desiccant-free valve and 3-way valve. The internal atmosphere was saturated with H_2 while the Lindlar suspension was stirred. Separately, a solution of **18** (1 Equiv., 163.5 mg, 0.61 mmol) in AcOEt (5 mL) was prepared. Once ready, the latter solution was cannulated in the previously prepared mixture by using additional 2 mL of AcOEt for

washing the cannula. For the entire duration of the reaction, the static atmosphere of H_2 was maintained by means of a balloon. The reaction was monitored by TLC (8:2, Hex/iPrOH) and was completed in about 3 h. The reaction was then filtered on a Celite pad and concentrated on the rotary evaporator. The resulting crude oil was purified by flash chromatography [gradient of Hex/AcOEt: (8:2) > (6:4) > (4:6)] to afford the corresponding (Z,Z)-*meso*-diol **14** (isolated yield = 99%).

MS (HESI): 273.15 ($M+H^+$)

^{1}H-NMR ($CDCl_3$): 300 MHz δ (ppm)= 5.70-5.50 (m, 4H), 4.90-4.50 (m, 4H), 3.31 (bs, 2H), 1.85-1.6 (m, 1H), 1.6-1.4 (m, 1H).

^{13}C-NMR ($CDCl_3$): 75 MHz δ (ppm)= 171.3, 136.4, 124.7, 66.9, 60.3, 42.7, 20.9.

Synthetic procedures for the preparation of the ligands

Synthesis of ligand (S,S)-L1 [(S,S)-DACH-Ph Trost Ligand]

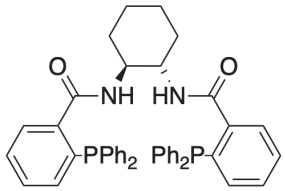

(S,S)-**L1** [DACH-Ph]

Chemical Formula: $C_{44}H_{42}N_2O_2P_2$

Exact Mass: 692.27

In a round bottom flask, under Ar atmosphere, enantiopure 1,2-cyclohexanediamine **9** (1 Equiv., 250 mg, 1.22 mmol), the 2-(diphenylphosphino)benzoic acid (2.2 Equiv., 818 mg, 2.7 mmol), DCC (2.2 Equiv., 550 mg, 2.7 mmol), DMAP (0.09 Equiv., 24 mg, 0.196 mmol) were added and then dissolved in dry DCM (0.2 M). The mixture was stirred for 16 hours at room temperature and was monitored by TLC (1:6:4, DCM/Hex/AcOEt). After 16 hours it was quenched by filtrating away the dicyclohexylurea on a cielite pad and removing the solvent at reduced pressure. The crude oil was diluted again in DCM and washed firstly with HCl 1.2 M (25 mL), then with a saturated aqueous solution $NaHCO_3$ (25 mL) and then water (30 mL). The collected organic phases were dried over Mg_2SO_4 and then evaporated to dryness. The raw product was purified by flash chromatography [gradient of Hex/AcOEt: 7:3 then 1:1] to afford the corresponding (S,S)-**L1** ligand (isolated yield = 62%).

The spectroscopic data collected in our synthesis match perfectly those reported in literature.[4]

Synthesis of ligand (R,R)-L2 [(R,R)-ANDEN-Ph Trost Ligand]

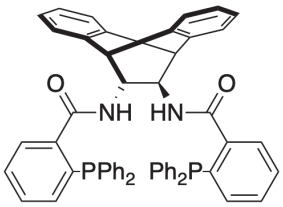

(R,R)-**L2** [ANDEN-Ph]

Chemical Formula: $C_{54}H_{48}N_2O_2P_2$

Exact Mass: 818.32

In a round bottom flask, under Ar atmosphere, enantiopure (11R,12R)-11,12-diamino-9,10-dihydro-9,10-ethanoanthracene **10** (1 Equiv., 250 mg, 1.06 mmol) and the 2-(diphenylphosphino)benzoic acid (2.2 Equiv., 714 mg, 2.33 mmol) were dissolved in dry DCM (0.2 M). Temperature was lowered at 0°C and the DCC (2.2 Equiv., 480 mg, 2.33 mmol) was added portion wise. The temperature was kept to 0°C fot additional 30 minutes and then increased to room temperature for 20 hours. The mixture was monitored by TLC (7:3, Hex/AcOEt). After completion the reaction mixture was quenched by filtrating away the dicyclohexylurea on a cielite pad and removing the solvent at reduced pressure. The residue was diluted again in DCM and washed with a saturated solution of $NaHCO_3$ (25 mL) and then washed with water (30 mL). The aqueous phase was then extracted several times with DCM until the yellowish color of the aqueous phase disappeared. The collected organic phases were then evaporated and purified by flash chromatography [95:5 Hex/iPrOH] to afford the corresponding (R,R)-**L2** ligand (isolated yield = 53%).

The spectroscopic data collected in our synthesis match perfectly those reported in literature.[5]

Synthesis of ligand (S,S)-L1-Me [(S,S)-DACH-Me-Ph Trost Ligand]

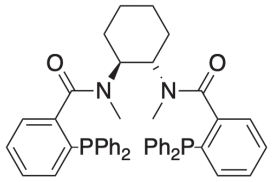

(S,S)-**L1**-Me [DACH-Me-Ph]

Chemical Formula: $C_{46}H_{46}N_2O_2P_2$

Exact Mass: 720.30

In a round bottom flask, under Ar atmosphere, enantiopure (1S,2S)-*N*,*N*'-dimethylcyclohexane-1,2-diamine **13** (1 Equiv., 100 mg, 0.70 mmol), the 2-(diphenylphosphino)-benzoic acid (2 Equiv., 429 mg, 1.40 mmol), EDCI (2 Equiv., 269 mg, 1.40 mmol), DMAP (1 Equiv., 86 mg, 0.70 mmol) were added and then dissolved in dry DCM (0.2 M). The mixture was stirred for 16 hours at room temperature and was monitored by TLC (1:6:4, DCM/Hex/AcOEt). After 16 hours it was quenched removing the solvent at reduced pressure. The raw product was purified by flash chromatography [gradient of Hex/AcOEt: 7:3 then 1:1] to afford the corresponding (S,S)-**L1**-Me ligand (isolated yield = 61%).

The spectroscopic data collected in our synthesis match perfectly those reported in literature.[6]

General procedure for the Tsuj-Trost AAA cyclization

Ligand (8 mol%) and $Pd_2(dba)_3 \cdot CHCl_3$ (3 mol%) were dissolved in dry solvent (toluene, 0.02 M) under Argon atmosphere and the mixture was stirred for 45 minutes at room temperature, till the formation of the chiral ligand was completed. The solution switch from violet/red to yellow/orange (depending on the ligand involved). Meanwhile in another flask, the *meso*-diol (**1** or **14**, 1 Equiv.) was dissolved in dry solvent (toluene, 0.1 M) under Argon atmosphere and the catalyst containing solution previously prepared was cannulated. The mixture was stirred till the reaction was completed and checked by TLC (1:1, Hex/AcOEt). The reaction was thus quenched by addition of silica and filtrated on a silica pad by washing with AcOEt. The resulting crude material is purified by liquid chromatography on silica gel to give the pure cyclized product [gradient of Hex/AcOEt: (8:2) > (7:3 - removes dba residues) > (1:1)]. *d.r.* ST:AC was determined by HPLC. Enantiomeric excess was determined by chiral HPLC, on Chiralpak AS-H column with 80:20 Heptane:iPrOH isocratic eluent mixture.

The spectroscopic data collected in our synthesis match perfectly those reported in literature.[7]

General procedure for the cyclization with Hex_4NCl additive

Ligand (8 mol%) and $Pd_2(dba)_3{\cdot}CHCl_3$ (3 mol%) were dissolved in dry solvent (DCM, 0.02 M) under Argon atmosphere and the mixture was stirred for 45 minutes at room temperature, till the formation of the chiral ligand was completed. The solution switch from violet/red to yellow/orange (depending on the ligand involved). Meanwhile in another flask, the *meso*-diol (**1** or **14**, 1 Equiv.) was dissolved in dry solvent (DCM, 0.1 M) under Argon atmosphere and the Hex_4NCl (30 mol%) was added. Thus, the catalyst containing solution previously prepared was cannulated. The mixture was stirred till the reaction was completed and checked by TLC (1:1, Hex/AcOEt). The reaction was thus quenched by addition of silica and filtrated on a silica pad by washing with AcOEt. The resulting crude material is purified by liquid chromatography on silica gel to give the pure cyclized product [gradient of Hex/AcOEt: (8:2) > (7:3 - removes dba residues) > (1:1)]. *d.r.* ST:AC was determined by HPLC. Enantiomeric excess was determined by chiral HPLC, on Chiralpak AS-H column with 80:20 Heptane:iPrOH isocratic eluent mixture.

The spectroscopic data collected in our synthesis match perfectly those reported in literature.[7]

General reduction procedure for the stereochemical correlation

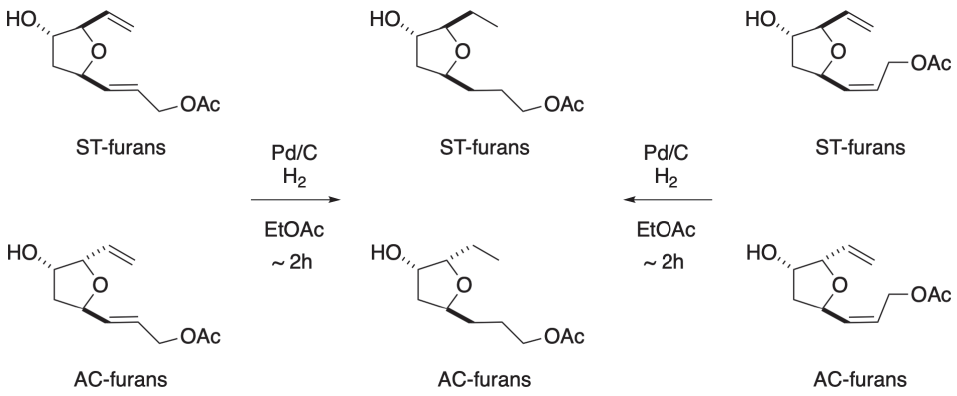

The substrate to be hydrogenated (1 Equiv., 17.8 mg, 0.083 mmol) was placed in an Erlenmeyer flask of suitable size, equipped with magnetic stirrer bar and dissolved in ethyl acetate (2 mL, 0.01-0.05M). Then, Pd/C 10% (2 mg, 5% w/w with respect to the substrate) was added. After the completion of the additions, a static atmosphere of H_2 was realized in the flask and was maintained for the next hours at atmospheric pressure through the aid of a balloon. The conversion was monitored by TLC (6:4, Hex/AcOEt) and by looking specifically not at the change in the R_f of the product (which remains more or less similar to that of the starting material), but to the change in the color of the vanillin stain from brown to black once developed. The reaction completed in 2.5 h with quantitative conversion. The solvent was removed and the product rapidly purified with a chromatographic column [gradient of Hex/AcOEt: 1:1 then 2:8] to afford the corresponding reduced product ready to be directly injected in the HPLC to obtain the results of both *d.r.* and enantiomeric excess by using the Chiralpak IA-3 column with 90:10 Heptane:iPrOH as eluent mixture.

Since no other spots besides the one of the product were detected in TLC, we decided not to run NMR analysis, but a simple mass spectroscopy to verify the outcome of the hydrogenation.

MS (HESI): 217.17 ($M+H^+$)

HPLC chromatograms

Hex_4NCl + (R,R)-L1 [(E,E)-*meso*-diol 1] in DCM

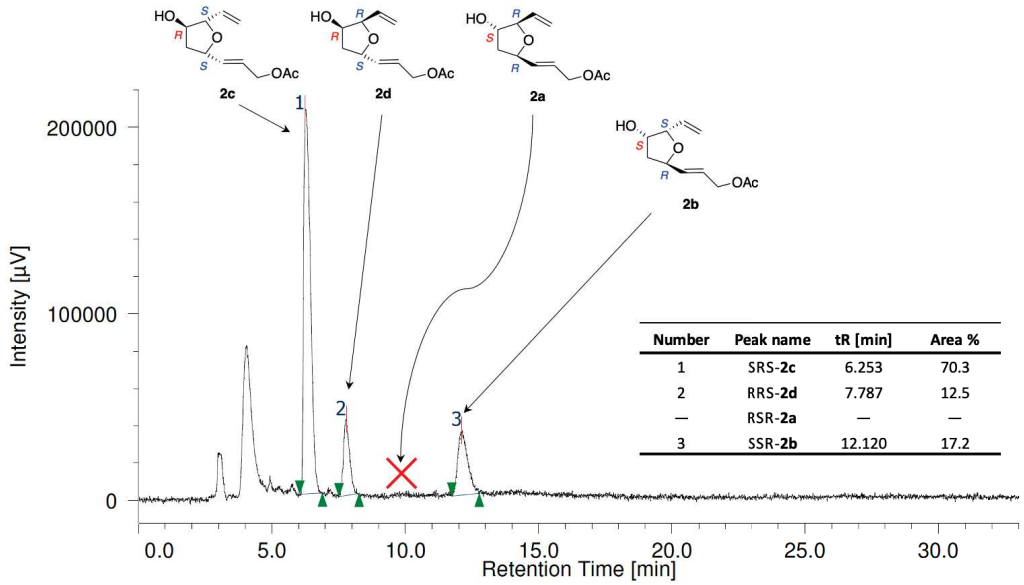

Number	Peak name	tR [min]	Area %
1	SRS-**2c**	6.253	70.3
2	RRS-**2d**	7.787	12.5
—	RSR-**2a**	—	—
3	SSR-**2b**	12.120	17.2

Chiralpak AS-H column, 80:20 Heptane:iPrOH isocratic eluent mixture, 1mL/min

Hex_4NCl + (S,S)-L2 [(E,E)-*meso*-diol 1] in DCM

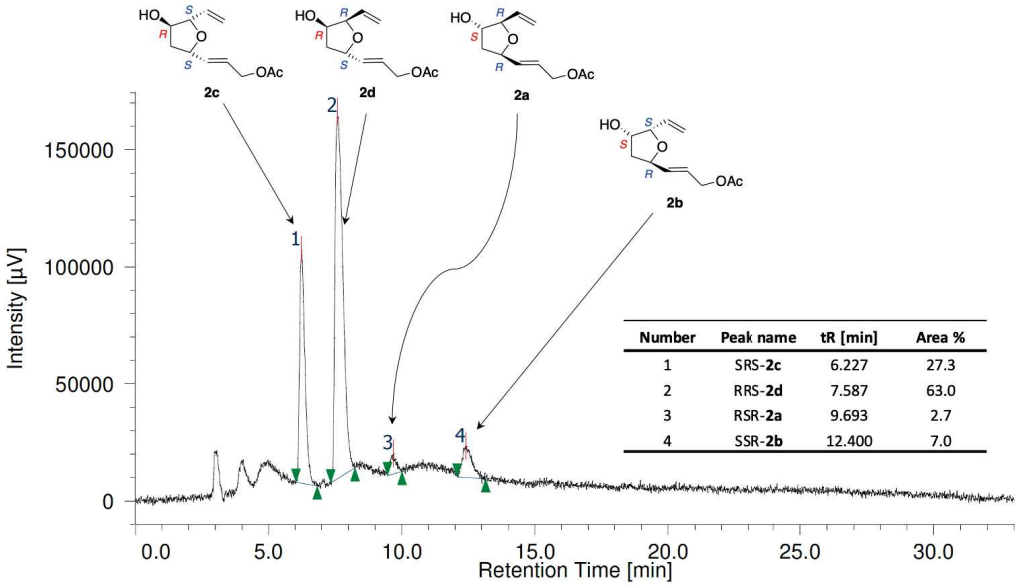

Number	Peak name	tR [min]	Area %
1	SRS-**2c**	6.227	27.3
2	RRS-**2d**	7.587	63.0
3	RSR-**2a**	9.693	2.7
4	SSR-**2b**	12.400	7.0

Chiralpak AS-H column, 80:20 Heptane:iPrOH isocratic eluent mixture, 1mL/min

Correlation chromatogram: reduction of cyclized product from 1 and (S,S)-L1

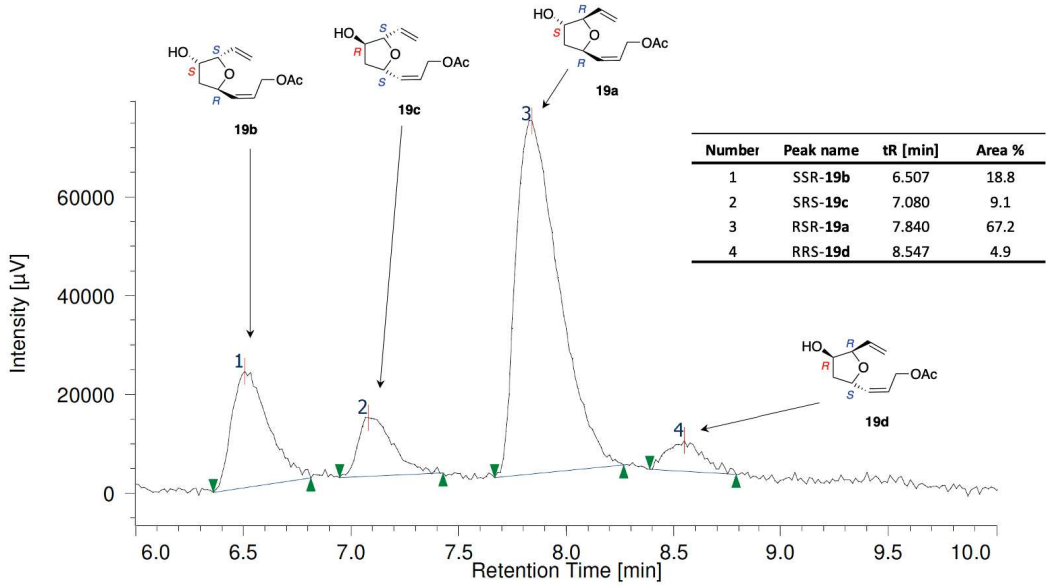

Number	Peak name	tR [min]	Area %
1	SSR-**19b**	6.507	18.8
2	SRS-**19c**	7.080	9.1
3	RSR-**19a**	7.840	67.2
4	RRS-**19d**	8.547	4.9

Chiralpak IA-3 column, 90:10 Heptane:iPrOH isocratic eluent mixture, 1mL/min

Correlation chromatogram: reduction of cyclized product from 1 and (R,R)-L2

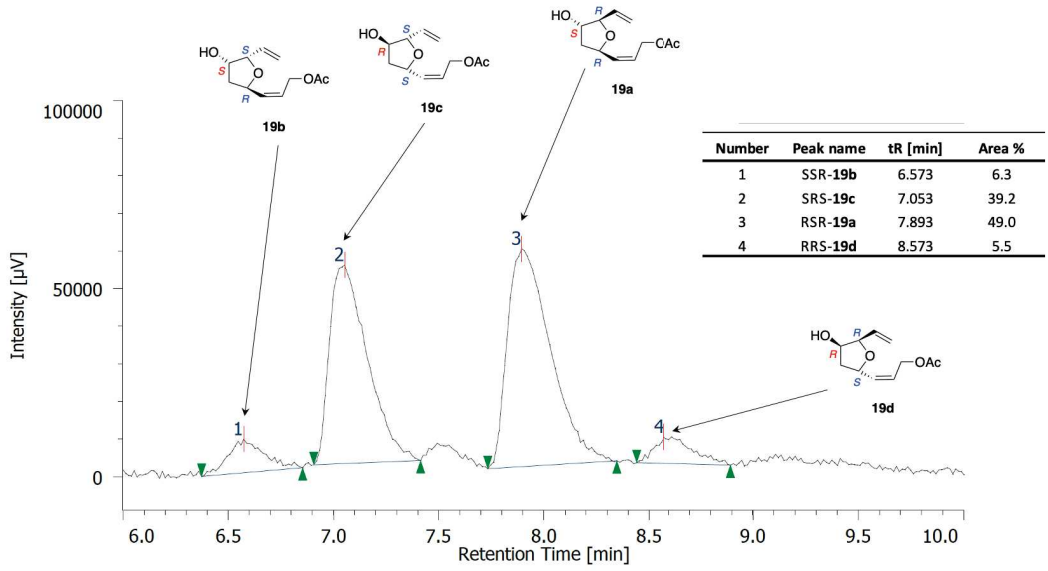

Number	Peak name	tR [min]	Area %
1	SSR-**19b**	6.573	6.3
2	SRS-**19c**	7.053	39.2
3	RSR-**19a**	7.893	49.0
4	RRS-**19d**	8.573	5.5

Chiralpak IA-3 column, 90:10 Heptane:iPrOH isocratic eluent mixture, 1mL/min

(S,S)-L1 [(Z,Z)-*meso*-diol 14] in toluene after reduction

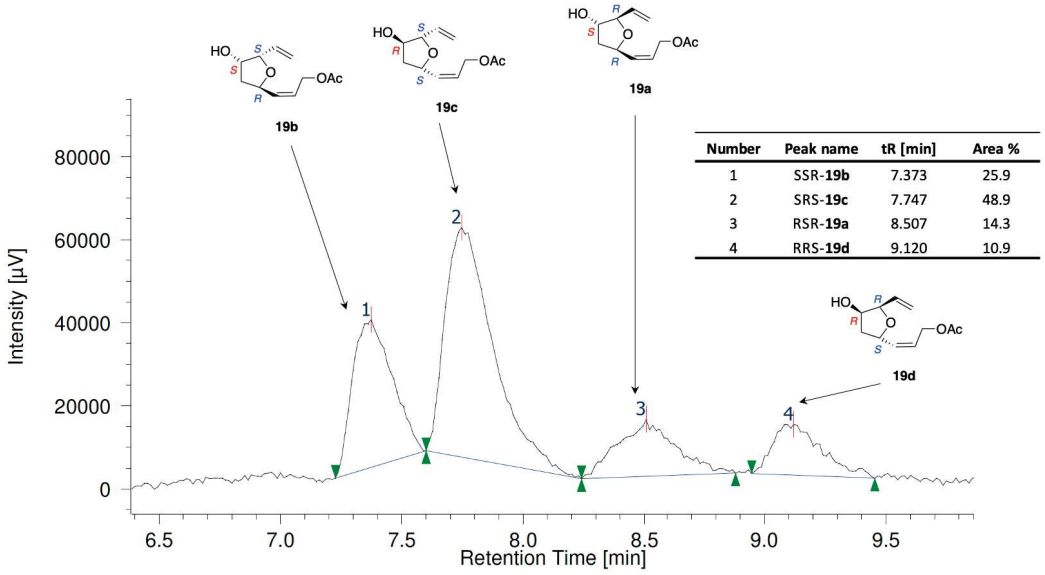

Number	Peak name	tR [min]	Area %
1	SSR-**19b**	7.373	25.9
2	SRS-**19c**	7.747	48.9
3	RSR-**19a**	8.507	14.3
4	RRS-**19d**	9.120	10.9

Chiralpak IA-3 column, 90:10 Heptane:iPrOH isocratic eluent mixture, 1mL/min

(R,R)-L2 [(Z,Z)-*meso*-diol 14] in toluene after reduction

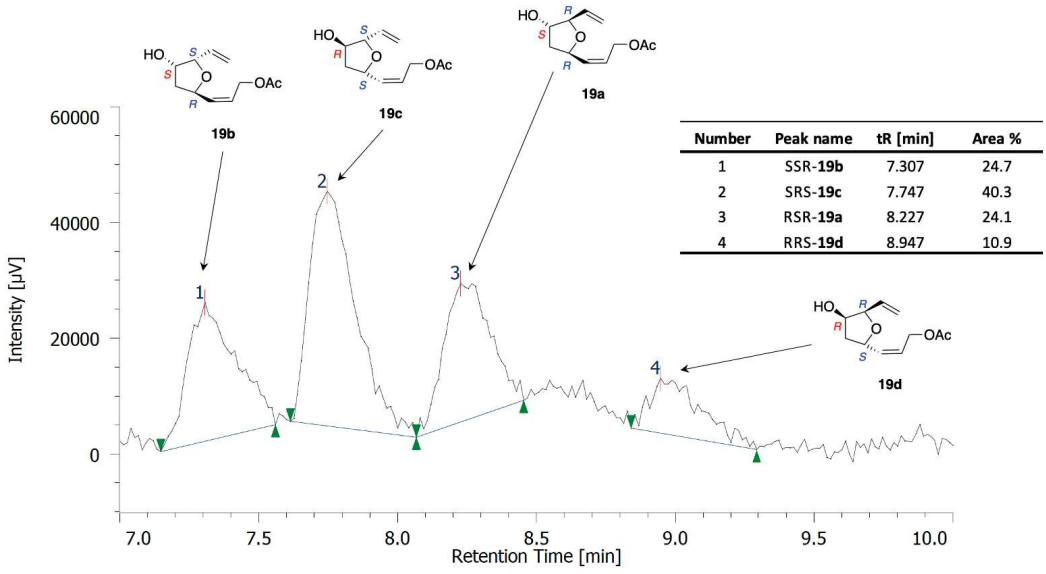

Number	Peak name	tR [min]	Area %
1	SSR-**19b**	7.307	24.7
2	SRS-**19c**	7.747	40.3
3	RSR-**19a**	8.227	24.1
4	RRS-**19d**	8.947	10.9

Chiralpak IA-3 column, 90:10 Heptane:iPrOH isocratic eluent mixture, 1mL/min

Hex_4NCl + (S,S)-L1 [(Z,Z)-*meso*-diol 14] in DCM after reduction

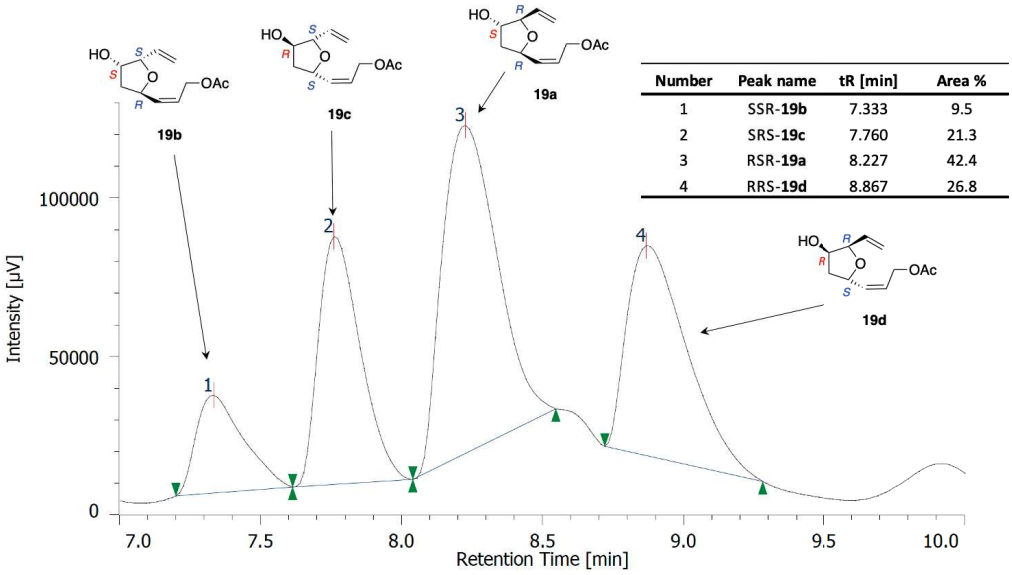

Number	Peak name	tR [min]	Area %
1	SSR-**19b**	7.333	9.5
2	SRS-**19c**	7.760	21.3
3	RSR-**19a**	8.227	42.4
4	RRS-**19d**	8.867	26.8

Chiralpak IA-3 column, 90:10 Heptane:iPrOH isocratic eluent mixture, 1mL/min

Hex_4NCl + (R,R)-L2 [(Z,Z)-*meso*-diol 14] in DCM after reduction

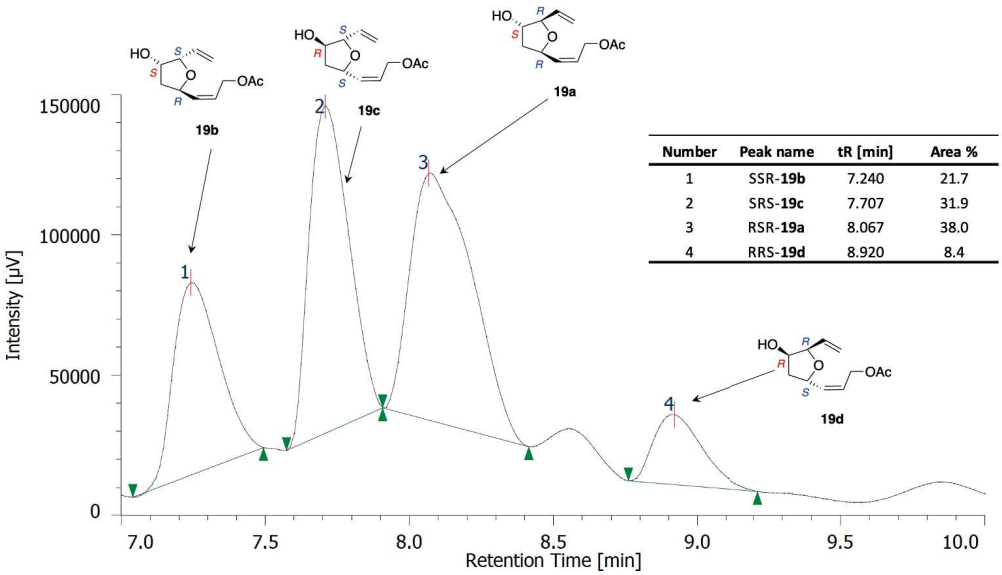

Number	Peak name	tR [min]	Area %
1	SSR-**19b**	7.240	21.7
2	SRS-**19c**	7.707	31.9
3	RSR-**19a**	8.067	38.0
4	RRS-**19d**	8.920	8.4

Chiralpak IA-3 column, 90:10 Heptane:iPrOH isocratic eluent mixture, 1mL/min

Computational details

All structures were optimized with the Gaussian 09 program package,[8] using the B3LYP functional at the 6-31G(d) level for all the atoms, but for Palladium the effective core potential LanL2DZ was used. All the optimizations were performed in vacuo. Conformational analysis was performed manually: due to the extreme high degrees of freedom of the molecules and complexes under examination we focused our attention on the most realistic conformational changes. All data reported, are referred to this level of theory and the discussions are based on the values of (E) and activation (E_{att}) relative energies in kcal/mol.

References

[1] Menard, F.; Perez, D.; Sustac Roman, D.; Chapman, T. M.; Lautens, M., Ligand-Controlled Selectivity in the Desymmetrization of meso Cyclopenten-1,4-diols via Rhodium(I)-Catalyzed Addition of Arylboronic Acids, *J. Org. Chem.*, **2010**, *75*, 4056-4068.

[2] Jiang, L.; Burke, S. D., A Novel Route to the F-Ring of Halichondrin B. Diastereoselection in Pd(0)-Mediated *meso* and C_2 Diol Desymmetrization, *Org. Lett.*, **2002**, *4*, 3411-3414.

[3] PhD Thesis of: Matteo Valli, Davide Sbarbada and Mattia Fredditori.

[4] Fuchs, S.; Berl, V.; Lepoittevin, J.-P., A Highly Stereoselective Divergent Synthesis of Bicyclic Models of Photoreactive Sesquiterpene Lactones, *Eur. J. Org. Chem.*, **2007**, 1145-1152.

[5] Trost, B. M.; Van Vranken, D. L.; Bingel, C., A modular approach for ligand design for asymmetric allylic alkylations via enantioselective palladium-catalyzed ionizations, *J. Am. Chem. Soc.*, **1992**, *114*, 9327-9343.

[6] Huang, D.; Liu, X.; Li, L.; Cai, Y.; Liu, W.; Shi, Y., Enantioselective Bromoaminocyclization of Allyl N-Tosylcarbamates Catalyzed by a Chiral Phosphine?$Sc(OTf)_3$ Complex, *J. Am. Chem. Soc.*, **2013**, *135*, 8101-8104.

[7] Valli, M.; Bruno, P.; Sbarbada, D.; Porta, A.; Vidari, G.; Zanoni, G., Stereodivergent Strategy for Neurofuran Synthesis via Palladium-Catalyzed Asymmetric Allylic Cyclization: Total Synthesis of 7-*epi*-ST-^{8}-10-Neurofuran, *J. Org. Chem.*, **2013**, *78*, 5556-5567.

[8] Frisch, M. J.; Trucks, G. W.; Schlegel, H. B.; Scuseria, G. E.; Robb, M. A.; Cheeseman, J. R.; Scalmani, G.; Barone, V.; Mennucci, B.; Petersson, G. A.; Nakatsuji, H.; Caricato, M.; Li, X.; Hratchian, H. P.; Izmaylov, A. F.; Bloino, J.; Zheng, G.; Sonnenberg, J. L.;

Hada, M.; Ehara, M.; Toyota, K.; Fukuda, R.; Hasegawa, J.; Ishida, M.; Nakajima, T.; Honda, Y.; Kitao, O.; Nakai, H.; Vreven, T.; Montgomery, J. A., Jr.; Peralta, J. E.; Ogliaro, F.; Bearpark, M.; Heyd, J. J.; Brothers, E.; Kudin, K. N.; Staroverov, V. N.; Keith, T.; Kobayashi, R.; Normand, J.; Raghavachari, K.; Rendell, A.; Burant, J. C.; Iyengar, S. S.; Tomasi, J.; Cossi, M.; Rega, N.; Millam, J. M.; Klene, M.; Knox, J. E.; Cross, J. B.; Bakken, V.; Adamo, C.; Jaramillo, J.; Gomperts, R.; Stratmann, R. E.; Yazyev, O.; Austin, A. J.; Cammi, R.; Pomelli, C.; Ochterski, J. W.; Martin, R. L.; Morokuma, K.; Zakrzewski, V. G.; Voth, G. A.; Salvador, P.; Dannenberg, J. J.; Dapprich, S.; Daniels, A. D.; Farkas, O.; Foresman, J. B.; Ortiz, J. V.; Cioslowski, J.; Fox, D. J. Gaussian 09, Revision B.01; Gaussian, Inc., Wallingford, CT, **2010**.

5.2 Chapter 2

Systems under study

The enantioselective Strecker synthesis of α-aminoacids

The experimental data reported in Schemes 1 and 2 was recovered from five different papers published from 1998 to 2013 by Jacobsen and co-workers.[1] Here are reported the structures of catalysts and substrates obtained from papers.

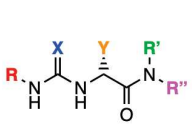

1J R = A; X = S; Y = *t*-Bu; R' = Me; R'' = Me
2J R = A; X = S; Y = *t*-Bu; R' = Me; R'' = Bn
3J R = A; X = S; Y = *t*-Bu; R' = Me; R'' = (*S*)-1-phenylethyl
4J R = A; X = S; Y = *t*-Bu; R' = Me; R'' = (*R*)-1-phenylethyl
5J R = A; X = S; Y = *t*-Bu; R' = Me; R'' = 1,1-bisphenylmethyl
6J R = A; X = O; Y = *t*-Bu; R' = Me; R'' = 1,1-bisphenylmethyl
7J R = A; X = S; Y = *t*-Bu; R' = Me; R'' = *i*-Pr
8J R = Ph; X = S; Y = Me; R' = Me; R'' = 1,1-bisphenylmethyl
9J R = B; X = O; Y = *t*-Bu; R' = H; R'' = Bn

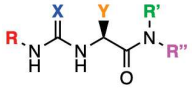

10J R = Ph; X = S; Y = *t*-Bu; R' = H; R'' = 1,1-bisphenylmethyl
11J R = Ph; X = S; Y = *t*-Bu; R' = Me; R'' = 1,1-bisphenylmethyl
12J R = Cy; X = S; Y = *t*-Bu; R' = Me; R'' = 1,1-bisphenylmethyl
13J R = C; X = S; Y = *t*-Bu; R' = H; R'' = Bn
14J R = B; X = S; Y = *t*-Bu; R' = H; R'' = Bn

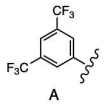

A

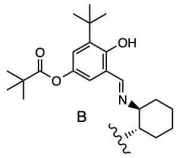

B

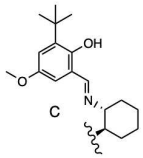

C

Scheme 1: *Representatives of the catalysts tested data set.*

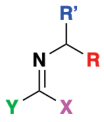

1J-s R = Ph; R' = Ph; X = H; Y = *t*-Bu
2J-s R = Ph; R' = Ph; X = H; Y = Et_2MeC
3J-s R = Ph; R' = Ph; X = H; Y = $PhMe_2C$
4J-s R = Ph; R' = Ph; X = H; Y = (1-methyl)cyclohexyl
5J-s R = Ph; R' = Ph; X = H; Y = 1-adamantly
6J-s R = Ph; R' = Ph; X = H; Y = cyclohexyl
7J-s R = Ph; R' = Ph; X = H; Y = *p*-$OMeC_6H_4$
8J-s R = Ph; R' = Ph; X = H; Y = *p*-MeC_6H_4
9J-s R = Ph; R' = Ph; X = H; Y = C_6H_5
10J-s R = Ph; R' = Ph; X = H; Y = *p*-ClC_6H_4
11J-s R = Ph; R' = Ph; X = H; Y = *p*-$CF_3C_6H_4$
12J-s R = Ph; R' = Ph; X = H; Y = *p*-CNC_6H_4
13J-s R = Ph; R' = Ph; X = H; Y = *p*-BrC_6H_4
14J-s R = Ph; R' = Ph; X = H; Y = *o*-$OMeC_6H_4$
15J-s R = Ph; R' = Ph; X = H; Y = *o*-BrC_6H_4
16J-s R = Ph; R' = Ph; X = H; Y = *m*-BrC_6H_4
17J-s R = Ph; R' = Ph; X = H; Y = 2-furyl
18J-s R = Ph; R' = Ph; X = H; Y = 3-furyl
19J-s R = Ph; R' = Ph; X = H; Y = 2-thiophenyl
20J-s R = Ph; R' = Ph; X = H; Y = 1-cyclohexenyl
21J-s R = Ph; R' = Ph; X = H; Y = (*E*)-1-methyl-pent-1-enyl
22J-s R = Ph; R' = Ph; X = H; Y = (*E*)-cinnamyl
23J-s R = Ph; R' = Ph; X = H; Y = (*E*)-hexenyl
24J-s R = vinyl; R' = H; X = Me; Y = C_6H_5
25J-s R = vinyl; R' = H; X = Et; Y = C_6H_5
26J-s R = vinyl; R' = H; X = Me; Y = napthalen-2-yl
27J-s R = vinyl; R' = H; X = Me; Y = 4-phenylpropan-1-yl
28J-s R = Ph; R' = H; X = Me; Y = C_6H_5
29J-s R = Ph; R' = H; X = Me; Y = *p*-MeC_6H_4
30J-s R = Ph; R' = H; X = Me; Y = *p*-BrC_6H_4
31J-s R = Ph; R' = H; X = Me; Y = *p*-$NO_2C_6H_4$
32J-s R = Ph; R' = H; X = Me; Y = *p*-$OMeC_6H_4$
33J-s R = Ph; R' = H; X = Me; Y = *p*-$CF_3C_6H_4$
34J-s R = Ph; R' = H; X = Me; Y = *m*-BrC_6H_4
35J-s R = Ph; R' = H; X = Me; Y = *o*-BrC_6H_4
36J-s R = Ph; R' = H; X = Me; Y = *t*-Bu
37J-s R = *p*-$OMeC_6H_4$; R' = H; X = Me; Y = C_6H_5
38J-s R = *p*-$CF_3C_6H_4$; R' = H; X = Me; Y = C_6H_5
39J-s R = *p*-*t*-BuC_6H_4; R' = H; X = Me; Y = C_6H_5
40J-s R = *p*-BrC_6H_4; R' = H; X = Me; Y = C_6H_5
41J-s R = vinyl; R' = H; X = H; Y = C_6H_5
42J-s R = vinyl; R' = H; X = H; Y = *p*-$OMeC_6H_4$
43J-s R = vinyl; R' = H; X = H; Y = *p*-BrC_6H_4
44J-s R = vinyl; R' = H; X = H; Y = napthalen-2-yl
45J-s R = vinyl; R' = H; X = H; Y = cyclohexyl
46J-s R = vinyl; R' = H; X = H; Y = *t*-Bu
47J-s R = vinyl; R' = H; X = H; Y = *m*-$OMeC_6H_4$
48J-s R = vinyl; R' = H; X = H; Y = *o*-$OMeC_6H_4$
49J-s R = vinyl; R' = H; X = H; Y = *p*-MeC_6H_4
50J-s R = vinyl; R' = H; X = H; Y = *m*-MeC_6H_4
51J-s R = vinyl; R' = H; X = H; Y = *o*-MeC_6H_4
52J-s R = vinyl; R' = H; X = H; Y = *m*-BrC_6H_4
53J-s R = vinyl; R' = H; X = H; Y = *o*-BrC_6H_4
54J-s R = vinyl; R' = H; X = H; Y = *p*-*t*-BuC_6H_4
55J-s R = Ph; R' = H; X = H; Y = *t*-Bu
56J-s R = Ph; R' = H; X = H; Y = cyclohexyl
57J-s R = Ph; R' = H; X = H; Y = 1-cyclohexenyl
58J-s R = Ph; R' = H; X = H; Y = $(CH_3)_3CCH_2$
59J-s R = Ph; R' = H; X = H; Y = $CH_3(CH_2)_4$
60J-s R = Ph; R' = H; X = H; Y = *i*-Pr
61J-s R = Ph; R' = H; X = H; Y = cyclopropyl
62J-s R = Ph; R' = H; X = H; Y = cyclooctyl
63J-s 3,4-dihydroisoquinoline

Scheme 2: *Representatives of the substrates tested data set.*

Additionally, in accordance with a paper published by List and co-workers we prepared a set of catalysts that should not give any enantioselection.[1e] This helped

us in increasing the number of data available in the region close to $\Delta\Delta G^{\ddagger}=0$, which were found to be underpopulated due to absence of low scoring data in the published literature.

In Scheme 3 the structures of those catalysts are reported.

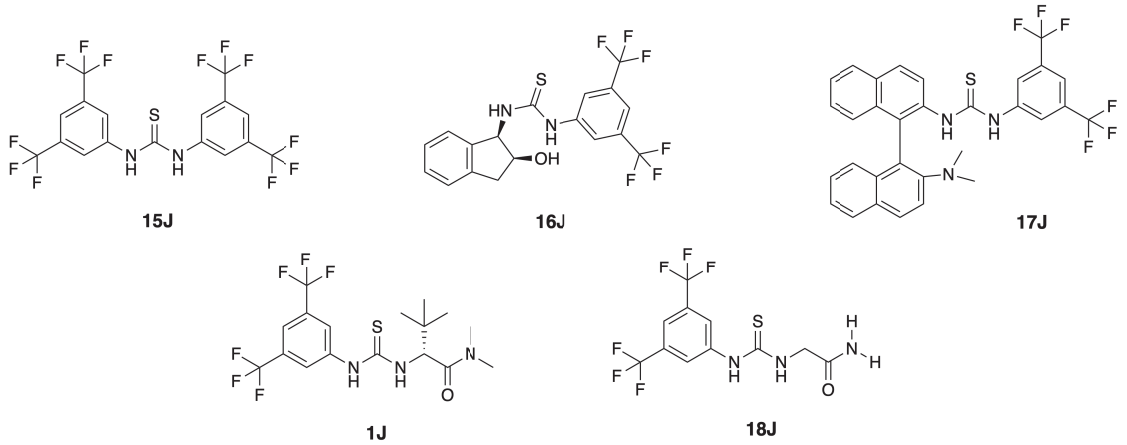

Scheme 3: *Structures of low to 0 scoring ee catalysts.*

The Pictet-Spengler cyclizations of hydroxylactams

The experimental data reported in Schemes 4 and 5 was recovered from two different papers published in 2007 and 2008 by Jacobsen and co-workers.[2]

Here are reported the structures of catalysts and substrates obtained from papers.

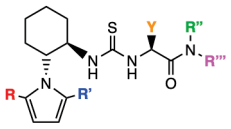

1JP R = Ph; R' = Me; Y = *t*-Bu; R'' = *i*-Bu; R''' = *i*-Bu
2JP R = Ph; R' = Me; Y = *t*-Bu; R'' = Me; R''' = *n*-pentyl
3JP R = Ph; R' = Me; Y = *t*-Bu; R'' = Me; R''' = cyclohexyl
4JP R = Ph; R' = Me; Y = *t*-Bu; R'' = H; R''' = *n*-Bu
5JP R = Ph; R' = Me; Y = *t*-Bu; R'' = H; R''' = *n*-pentyl
6JP R = Ph; R' = Me; Y = *t*-Bu; R'' = H; R''' = *n*-hexyl
7JP R = Ph; R' = Me; Y = *t*-Bu; R'' = H; R''' = *n*-heptyl
8JP R = Ph; R' = Me; Y = *t*-Bu; R'' = H; R''' = *i*-Bu
9JP R = Ph; R' = Me; Y = *t*-Bu; R'' = H; R''' = *t*-Bu
10JP R = Ph; R' = Me; Y = *t*-Bu; R'' = Me; R''' = *n*-Bu
11JP R = Ph; R' = Me; Y = *t*-Bu; R'' = Me; R''' = *n*-hexyl
12JP R = Ph; R' = Me; Y = *t*-Bu; R'' = Me; R''' = *i*-Bu
13JP R = Ph; R' = Me; Y = *t*-Bu; R'' = Me; R''' = *t*-Bu
14JP R = Ph; R' = Me; Y = *t*-Bu; R'' = Et; R''' = *n*-Bu
15JP R = Ph; R' = Me; Y = *t*-Bu; R'' = *n*-pentyl; R''' = *n*-pentyl
16JP R = Ph; R' = Me; Y = *t*-Bu; R'' = H; R''' = Bn
17JP R = Ph; R' = Me; Y = *t*-Bu; R'' = Me; R''' = Bn
18JP R = Ph; R' = Me; Y = *t*-Bu; R'' = H; R''' = 1,1-bisphenylmethyl
19JP R = Ph; R' = Me; Y = *t*-Bu; R'' = Me; R''' = 1,1-bisphenylmethyl
20JP R = Ph; R' = H; Y = *t*-Bu; R'' = *i*-Bu; R''' = *i*-Bu
21JP R = Ph; R' = Et; Y = *t*-Bu; R'' = *i*-Bu; R''' = *i*-Bu
22JP R = 2-furyl; R' = Me; Y = *t*-Bu; R'' = *i*-Bu; R''' = *i*-Bu
23JP R = *p*-methoxyphenyl; R' = Me; Y = *t*-Bu; R'' = *i*-Bu; R''' = *i*-Bu
24JP R = *p*-fluorophenyl; R' = Me; Y = *t*-Bu; R'' = *i*-Bu; R''' = *i*-Bu
25JP R = *o*-chlorophenyl; R' = Me; Y = *t*-Bu; R'' = *i*-Bu; R''' = *i*-Bu
26JP R = 2-naphtyl; R' = Me; Y = *t*-Bu; R'' = *i*-Bu; R''' = *i*-Bu

27JP R = 1-naphtyl; R' = Me; Y = *t*-Bu; R'' = *i*-Bu; R''' = *i*-Bu
28JP R = 2-naphtyl; R' = Me; Y = *t*-Bu; R'' = Me; R''' = *n*-pentyl
29JP R = 1-naphtyl; R' = Me; Y = *t*-Bu; R'' = Me; R''' = *n*-pentyl
30JP R = *p*-methoxyphenyl; R' = Me; Y = *t*-Bu; R'' = Me; R''' = *n*-pentyl
31JP R = *p*-fluorophenyl; R' = Me; Y = *t*-Bu; R'' = Me; R''' = *n*-pentyl
32JP R = Me; R' = Me; Y = *t*-Bu; R'' = Me; R''' = *n*-pentyl
33JP R = Ph; R' = Ph; Y = *t*-Bu; R'' = Me; R''' = *n*-pentyl
34JP R = Ph; R' = H; Y = *i*-Pr; R'' = Me; R''' = *n*-pentyl

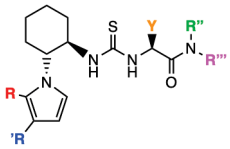

35JP R = *t*-Bu; R' = COOMe; Y = *t*-Bu; R'' = *i*-Bu; R''' = *i*-Bu
36JP R = *t*-Bu; R' = COO*t*-Bu; Y = *t*-Bu; R'' = *i*-Bu; R''' = *i*-Bu

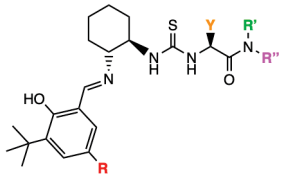

37JP R = *t*-Bu; Y = *t*-Bu; R' = Me; R'' = Bn
38JP R = *t*-Bu; Y = *t*-Bu; R' = Bn; R'' = Bn
39JP R = OPiv; Y = *t*-Bu; R' = Me; R'' = Me

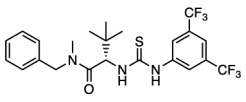

40JP

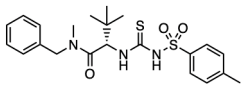

41JP

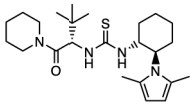

42JP

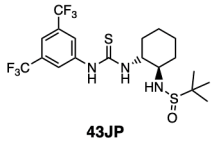

43JP

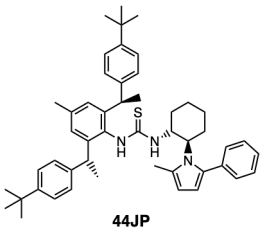

44JP

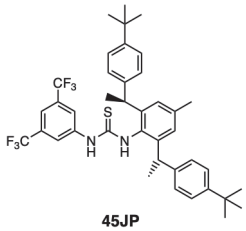

45JP

Scheme 4: *Representatives of the catalysts tested data set.*

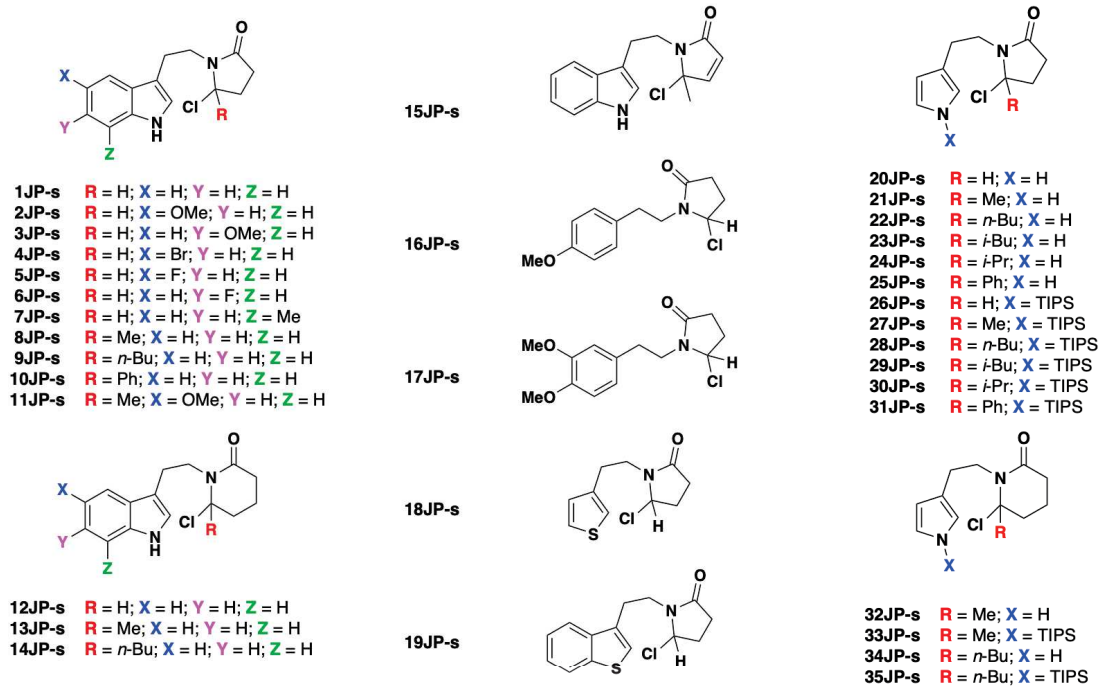

Scheme 5: *Representatives of the substrates tested data set.*

Computational details

All the quantomechanical calculations were operated by the usage of *ORCA v4.1 package*,[4] using the PBE functional at the def2-SVP level for all the atoms. Both in single point and optimisations, D3BJ dispersions were used.[4] Moreover, RI approximations and an automatically generated auxiliary basis set ('AutoAux' Keyword) was involved to decrease the amount of calculation cost.[4] When required, the role of solvent was modelled by using the SMD polarizable continuum solvation model.[4]

Conformational studies were carried out using the opensource *SIMAN* tool associated with the *xTB* software, by specifying the solvents involved in the reaction as well as possible charges already present in the starting materials.[3] The level of theory of these semiempirical calculations relies on the extended tight binding (*xTB (GFN2-xTB)*) approach.[3]

All the other scripts to extract the conformations, sampling them on RMSD and then respect with the energy, can be found on the GitHub account of the group:

https://github.com/duartegroup.

References

[1] a) Vachal, P., Jacobsen, E. N., Enantioselective Catalytic Addition of HCN to Ketoimines. Catalytic Synthesis of Quaternary Amino Acids, *Org. Lett.*, **2000**, *6*, 867-870; b) Zuend, S. J., Jacobsen, E. N., Mechanism of Amido-Thiourea Catalyzed Enantioselectiv Imine Hydrocyanation: Transition State Stabilization via Multiple Non-Covalent Interactions, *J. Am. Chem. Soc.*, **2009**, *131*, 15358-15374; c) Sigman, M. S., Jacobsen, E. N., Schiff Base Catalysts for the Asymmetric Strecker Reaction Identified and Optimized from Parallel Synthetic Libraries, *J. Am. Chem. Soc.*, **1998**, *120*, 4901-4902; d) Sigman, M. S.; Zuend, S. J.; Jacobsen, E. N., A General Catalyst for the Asymmetric Strecker Reaction, *Angew. Chem. Int. Ed.*, **2000**, *39*, 1279-1281; e) Pan, S. C.; List, B., The Catalytic Acylcyanation of Imines, *Chem. Asian J.*, **2008**, *3*, 430-437; f) Brak, K., Jacobsen, E. N., Asymmetric Ion-Pairing Catalysis., *Angew. Chem. Int. Ed.*, **2013**, *52*, 534-561; g) Zuend, S. J., Coughlin, M. P., Lalonde, M. P., Jacobsen, E. N., Scaleable catalytic asymmetric Strecker syntheses of unnatural ?-amino acids, *Nature*, **2009**, *461*, 968-971.

[2] a) Raheem, I. T.; Thiara, P. S.; Peterson, E. A.; Jacobsen, E. N., Enantioselective Pictet-Spengler-Type Cyclizations of Hydroxylactams: H-Bond Donor Catalysis by Anion Binding, *J. Am. Chem. Soc.*, **2007**, *129*, 13404-13405; b) Raheem, I. T.; Thiara, P. S.; Jacobsen, E. N., Regio- and Enantioselective Catalytic Cyclisation of Pyrroles onto N-Acyliminium Ions, *Org. Lett.*, **2008**, *10*, 1577-1580.

[3] a) Grimme, S.; Neese, F., Fully Automated Quantum-Chemistry-Based Computation of Spin-Spin-Coupled Nuclear Magnetic Resonance Spectra, *Angew. Chem. Int. Ed.*, **2017**, *56*, 14763-14769; b) Bannwarth, C.; Ehlert, S.; Grimme, S., GFN2-xTB-An Accurate and Broadly Parametrized Self-Consistent Tight-Binding Quantum Chemical Method with Multipole Electrostatics and Density-Dependent Dispersion Contributions, *J. Chem. Theory Comput.*, **2019**, *15*, 1652-1671; c) Pracht, P.; Bohle, F.; Grimme, S., Automated exploration of the low-energy chemical space with fast quantum chemical methods, *Phys. Chem. Chem. Phys.*, **2020**, *22*, 7169-7192.

[4] a) Neese, F.; Wennmohs, F.; Becker, U.; Riplinger, C., The ORCA quantum chemistry program package, *J. Chem. Phys.*, **2020**, *152*, 224108; b) for the PBE functional see: (i) Perdew, J. P.; Burke, K.; Ernzerhof, M., Generalized gradient approximation made simple, *Phys. Rev. Lett.*, **1996**, *77*, 3865-3868; (ii) Perdew, J. P.; Burke, K.; Ernzerhof, M., Errata: Generalized gradient approximation made simple, *Phys. Rev. Lett.*, **1997**, *78*, 1396; c) for the D3BJ empirical dispersions see: Grimme, S.; Ehrlich, S.; Goerigk, L., Effect of the damping

function in dispersion corrected density functional theory, *J. Comp. Chem.*, **2011**, *32*, 1456-1465; d) for the def2-SVP basis set see: (i) Weigend, F.; Ahlrichs, R., Balanced basis sets of split valence, triple zeta valence and quadruple zeta valence quality for H to Rn: Design and assessment of accuracy, *Phys. Chem. Chem. Phys.*, **2005**, *7*, 3297-305; (ii) Weigend, F., Accurate Coulomb-fitting basis sets for H to Rn, *Phys. Chem. Chem. Phys.*, **2006**, *8*, 1057-65; e) for the RI and AutoAux approximatons please refer to the Orca manual 4.1.0 or the Orca Input Library (https://sites.google.com/site/orcainputlibrary/).

5.3 Chapter 3

General methods

The practical work was performed by the aid of the following instruments.

For the characterisation of compounds:

- Brucker NMR AV 200, 300, 400, 500 and 700 MHz spectrometer
- "Thermo scientific" LTQ-XL with HESI (Heated Electrospray Ionization source)
- "Thermo scientific" Focus GC-DSQ II
- Brucker ALPHA II FTIR Spectrometer equipped with QuickSnap^{TM} universal sampling module.

Cromathographic techniques:

- Silica gel Sigma-Aldrich High-purity grade (9385), pore size 60Å, 230-400 mesh
- Silica gel on TLC glass plates Sigma-Aldrich, silica gel matrix with fluorescent indicator
- ESI-MS thermo LTQ
- MPLC Isolera One Biotage Flash Cromatography for chromatographic purifications of raw materials of more than 500 mg
- Fluorescence lamp 254-366 nm,
- $KMnO_4$ (solution in acetone), Vanilline (solution in H_2SO_4-EtOH) and Phosphomolibdic Acid (solution in EtOH), for the stain detection on TLC plates.

All preparations involving anhydrous conditions and inert atmosphere, were carried out under atmosphere of argon, into dried reactors dried in oven at 120°C for one night. Most of the solvents used were dried by distillation with an appropriate drying agent under an argon atmosphere.

In particular: the toluene was distilled from sodium metal; tetrahydrofuran from sodium and using benzophenone as indicator for H_2O; acetonitrile by azeotrope distillation with water under reduced pressure; other solvents were used as well as commercially available; chloroform and methanol dried over activated molecular sieves (4Å).

The IR spectra were reported using the wave numbers expressed in cm^{-1}. The NMR spectra were tabulated bringing the chemical shift (δ) in ppm and the coupling constants (J) in Hz. The multiplicity of the signals are abbreviated thus: s (singlet), d (doublet), t (triplet), q (quartet), m (multiplet), br (broadened signal). For the ^{13}C-NMR, the number of carbon atom bound to any hydrogen atoms was determined by DEPT experiments.

Glossary

AcOEt.....Ethylacetate

bdt-H_2.....Benzenedithiol

-(bdt).....Benzenedithiolate (ligand)

Brine .....Saturated Acqueous solution of NaCl

t-BuLi.....*tert*-Butyl Litium

Cp.....Cyclopentadienyl

Cp*.....Pentamethyl cyclopentadienyl

DCE.....Dichloroethane

DCM .....Dichloromethane

DIPEA.....*N*,*N*-Diisopropylethylamine

DMPU.....1,3-Dimethyl-3,4,5,6-tetrahydro-2(1H)-pyrimidinone

EDCI.....1-Ethyl-3-(3-dimethylaminopropyl)carbodiimide hydrochloride

Et_3N.....Triethyl amine

Et_2O.....Diethyl Ether

HOBt.....*N*-Hydroxybenzotriazole

MeOH.....Methanol

MTBE.....Methyl-*tert*-Butyl Ether

NHS.....*N*-Hydroxysuccinimide

PEG.....Poliethylene glycol

TBDMS-Cl.....*tert*-Butyldimethylsilyl chloride

TEG.....Triethylene glycol

THF.....Tetrahydrofurane

Synthetic procedures

Synthesis of compound 1

red

Chemical Formula: $C_{15}H_{20}Cl_2Ti$

Exact Mass: 318.04

In a two-necked round bottom flask under Ar atmosphere and equipped with a magnetic stir-bar, (pentamethylcyclopentadienyl)titanium(IV) Trichloride (300 mg, 1.04 mmol) was added and dissolved in dry THF (300 μL). Then, the solution was cooled to 0°C and CpNa (5 Equiv., 5.18 mmol) was added dropwise. The resulting mixture was covered with an alu foil and allowed to warm to room temperature. The solution turned from red-orange to purple. The course of the reaction was monitored with TLC (pure DCM) to observe the disappearance of the starting material. After the solution had been stirred for 3h, a solution of HCl in dioxane 4M was added (5 Equiv., 5.18 mmol) in order to quench the remained CpNa. Then, the solvent was evaporated to dryness. The crude obtained was then purified form cyclopentadiene by flash chromatography [gradient of DCM/Hexane: (1:1)>(1:0); $R_{f,\ product}$: 0.67 in (1:0)]. The so treated product was further purified from the starting material with extraction in $CHCl_3$ followed by concentration and precipitation in Hexane at -20°C. This procedure let us to obtain the red-purple crystals of the product **1** with an isolated yield of 82%.

The spectroscopic data collected in our synthesis match perfectly with those reported in literature.[1]

Synthesis of compound 2

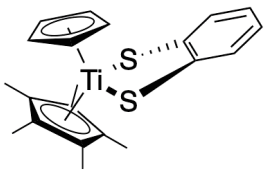

dark-green

Chemical Formula: $C_{21}H_{24}S_2Ti$

Exact Mass: 388.08

In a two-necked round bottom flask under Ar atmosphere and equipped with a magnetic stir-bar, compound **1** (1 Equiv., 132 mg, 0.41 mmol) was added and dissolved in dry THF (resulting solution 0.5 M). Then 1,2-benzenedithiole (1.2 Equiv., 0.49 mmol) and Et_3N (2.2 Equiv., 0.90 mmol) were added by using a gastight syringe. The reaction mixture was stirred for 6h at 30°C, checked through TLC (DCM/Hexane 1:1) in order to observe the complete conversion of starting material (the colour of the resulting solution turned from red to a dark-green). The resulting reaction mixture was evaporated and purified through a silica gel column [gradient of DCM/Hexane: (4:6)>(1:1)>(1:0); $R_{f,\ product}$: 0.58 in (1:1)] to afford the corresponding dithiolic derivative **2** with an isolated yield of 80%.

MS (HESI): 389.09 (M); 323.05 (M-Cp); 411.15 ($M+Na^+$)

^{1}H-NMR (CD_3CN): 300 MHz δ (ppm)= 7.30 (2H, m), 7.05 (2H, m), 5.63 (3H, s), 5.47 (2H, s), 2.18 (15H, s).

^{13}C-NMR (CD_3CN): 75 MHz δ (ppm)= 153.8, 129.7, 125.2, 123.7, 112.9, 54.3, 12.1.

IR (neat): (cm^{-1})= 2359.9, 1427.7, 1017.5, 816.0, 739.8, 465.9, 430.4, 413.1.

General procedure for (bdt)-Cl, Br and I exchange

Synthesis of compounds 1(bis), 3 and 4

In a two-necked round bottom flask under Ar atmosphere and equipped with a magnetic stir-bar, methanol dry (2.5 Equiv., 4.13 mg, 0.13 mmol) and the respective acetyl-halide (2.5 Equiv., 0.13 mmol) were added to dry $CHCl_3$ (resulting solution 0.4 M) by maintaining the temperature near to 0°C. Then the temperature was allowed to rise to room temperature. Meanwhile, in another two-necked round bottom flask under Ar atmosphere and equipped with a magnetic stir-bar, compound **2** (1 Equiv., 20 mg, 0.05 mmol) was added and dissolved in dry $CHCl_3$ (resulting solution 0.5 M). After five minutes, in order to form the HX *in situ*, the solution of the first flask was transferred *via cannula* into the solution of **2**. The color of the solution changed within seconds: with HCl **1** the solution turned to the previous red colour, while using HBr **4** and HI **5** the colors were dark-brown and brown/violet respectively. The reaction mixture was then treated by adding Hexane in order to promote the precipitation of the Titanocene-dihalide compound. The so obtained precipitate was then washed with Hexane in a Buckner funnel in order to purify the final product from the 1,2-benzenedithiol. Thus, it was dried under vacuum and then stored.

- Compound 1(bis)

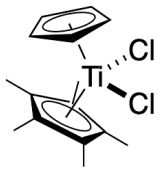

red

Chemical Formula: $C_{15}H_{20}Cl_2Ti$

Exact Mass: 318.04

Isolated yield: 96%

The spectroscopic data collected in our synthesis match perfectly with those reported in the synthesis of compound (**1**) which is the same found in literature.[1]

- Compound 4

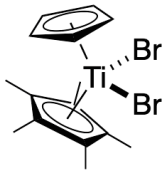

dark-brown

Chemical Formula: $C_{15}H_{20}Br_2Ti$

Exact Mass: 405.94

Isolated yield: 71%

The spectroscopic data collected in our synthesis match perfectly with those reported in literature.[2]

- Compound 5

brown/violet

Chemical Formula: $C_{15}H_{20}I_2Ti$

Exact Mass: 501.91

Isolated yield: 84%

MS (HESI): 525.02 ($M+Na^+$)

^{1}H-NMR (CD_3CN): 300 MHz δ (ppm)= 6.28 (5H, s), 2.01 (15H, s).

^{13}C-NMR (CD_3CN): 75 MHz δ (ppm)= 1127.8, 116.9, 54.3, 11.7.

IR (neat): (cm^{-1})= 1617.8, 821.4, 553.1, 464.1, 451.9, 436.6, 427.5, 419.4, 411.3.

- Compound 3

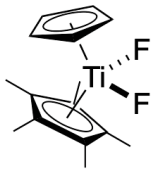

light-orange

Chemical Formula: $C_{15}H_{20}F_2Ti$

Exact Mass: 286.10

In a Teflon vial equipped with a magnetic stir-bar, methanol dry (1188 mg, 37.07 mmol) and benzoylfluoride (2300 mg, 18.54 mmol) were added. Then the temperature was brought to 60°C and the so prepared solution was let under stirring overnight in order to obtain a 2.3 M solution of in situ prepared HF. The day after, in another two-necked round bottom flask under Ar atmosphere and equipped with a magnetic stir-bar, compound **2** (1 Equiv., 25 mg, 0.06 mmol) was added and dissolved in dry $CHCl_3$ (resulting solution 0.5 M). By the use of a gastight syringe, the solution of HF was picked up (2.5 Equiv., 65 μL) and transferred in the second flask. The color of the solution changed within 5 minutes, turning from dark-green to a light-orange color. The reaction mixture was then concentrated and the crude oil obtained was treated by adding Hexane in order to promote the precipitation of the Titanocene-difluoride compound. The so obtained precipitate was then washed with Hexane in a Buckner funnel in order to purify the final product **3** from the 1,2-benzenedithiol, with an isolated yield of 81%.

The spectroscopic data collected in our synthesis match perfectly with those reported in literature.[2]

- Compound 3 with XeF_2

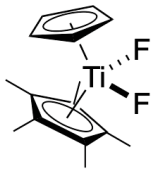

light-orange

Chemical Formula: $C_{15}H_{20}F_2Ti$

Exact Mass: 286.10

In a two-necked round bottom flask under Ar atmosphere and equipped with a magnetic stir-bar, compound **2** (29 mg, 0.075 mmol) was added and dissolved in dry $CHCl_3$ (resulting solution 0.1 M). Meanwhile, in a Teflon vial equipped with a magnetic stir-bar under Ar atmosphere and equipped with a magnetic stir-bar, crystals of Xenon difluoride [XeF_2] (1 Equiv., 0.075 mmol) were added. Thus, the solution contained in the first flask was slowly added in to the vial by using a cannula and maintaining continuous stirring. The color of the solution changed within seconds, turning from dark-green to a light-orange color. The reaction mixture was then poured in a single-necked round bottom flask, concentrated by using a water pump and the crude oil obtained was treated by adding Hexane in order to promote the precipitation of the Titanocene-difluoride compound. The so obtained precipitate was then washed with Hexane in a Buckner funnel in order to purify the final product **3** from the 1,2-benzenedithiol, with an isolated yield of 67%.

The spectroscopic data collected in our synthesis match perfectly with those reported in literature.[2]

Synthesis of compound 6

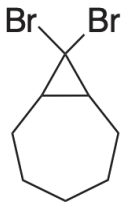

Chemical Formula: $C_8H_{12}Br_2$

Exact Mass: 265.93

In a two-necked round bottom flask under Ar atmosphere and equipped with a magnetic stir-bar, cycloheptene (1.0 Equiv., 500 mg, 5.20 mmol) was added and dissolved in dry pentane (0.1 M). The reaction mixture was cooled to 0°C and Bromoform (0.466 mL, 5.2 mmol) was added in 6 h. then allowing the reaction mixture to warm to room temperature and react overnight. The reaction was monitored with TLC (Hexane as eluent). The reaction was quenched with H_2O and HCl_{conc}. until neutralization checked with pH indicator strip. Pentane (15 mL) was added and layers were separated in a separatory funnel. The aqueous layer was extracted three times with pentane (3x20 mL). Combined organic layers were washed with brine (20 mL), dried over Na_2SO_4, filtered and concentrated under vacuum obtaining the crude product. This crude was purified by flash chromatography (pure pentane as eluent) to afford the product **6** with an isolated yield of 68%.

The spectroscopic data collected in our synthesis match perfectly with those reported in literature.[3]

Synthesis of compound 7

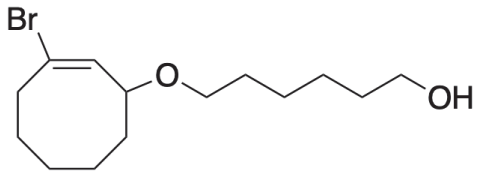

Chemical Formula: $C_{14}H_{25}BrO_2$

Exact Mass: 304.10

In a two-necked round bottom flask under Ar atmosphere and equipped with a magnetic stir-bar, compound **6** (1.5g, 5,61mmol) was added and dissolved in dry acetone (30 mL); thus, 1,6-hexandiol (20 Equiv., 112 mmol) and $AgClO_4$ (3 Equiv., 16.8 mmol) were added in the reaction mixture at 0°C. The resulting mixture was covered with an alu foil and allowed to warm to room temperature. Reaction was monitored with TLC (Hexane as eluent) and was completed in 18 hours. Silver salts were filtered off on celite and the liquid phase was quenched with HCl (1N, 2mL). The so precipitated silver salts were filtered again and layers were separated in a separatory funnel. The aqueous layer was extracted three times with AcOEt (3x30 mL). Combined organic layers were washed with HCl (1x5mL), H_2O (1x10mL), Brine (1x10mL), dried over Na_2SO_4, filtered and concentrated under vacuum obtaining the crude product. This crude was purified by flash chromatography (2:8 AcOEt/Hexane, $Rf_{product}$: 0.17) affording the product **7** with an isolated yield of 62%.

MS (HESI): 305.30 ($M+H^+$), 327.30 ($M+Na^+$)

^{1}H-NMR ($CDCl_3$): 500 MHz δ (ppm)= 6.14 (dd, J = 11.7, 4.1 Hz, 1H), 3.80 (dd, J = 10.3, 4.9 Hz, 1H), 3.59 (t, J = 6.7 Hz, 2H), 3.48 (dt, J = 9.1, 6.8 Hz, 1H), 3.24 (dt, J = 9.2, 6.5 Hz, 1H), 2.71 (qd, J = 11.9, 5.5 Hz, 1H), 2.25 (dddd, J = 11.4, 5.5, 4.1, 1.7 Hz, 1H), 2.05 - 1.78 (m, 5H), 1.74 - 1.16 (m, 11H), 0.84 - 0.71 (m, 1H).

^{13}C-NMR ($CDCl_3$): 126 MHz δ (ppm)= 133.7, 131.1, 85.0, 68.9, 62.8, 39.6, 36.5, 33.3, 32.7, 29.6, 28.2, 26.4, 26.1, 25.6.

Synthesis of compound 8

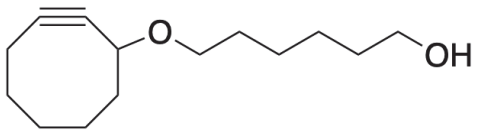

Chemical Formula: $C_{14}H_{24}O_2$

Exact Mass: 224.18

In a two-necked round bottom flask under Ar atmosphere and equipped with a magnetic stir-bar, compound **7** (460mg, 1.52mmol) was added and dissolved in dry DMSO (15 mL). The reaction mixture was heated at 80°C and DBU (10 Equiv., 15.2 mmol) was added dropwise. The solution was stirred for 18 h at 80°C. Reaction was monitored with TLC to observe the complete conversion of the starting material. The reaction mixture was quenched with a saturated solution of NH_4Cl and layers were separated in a separatory funnel and the aqueous layer was extracted three times with Et_2O (3x30 mL). The combined organic layers were dried over Na_2SO_4, filtered and concentrated under vacuum obtaining the crude product. This crude was purified by flash chromatography (3:7 AcOEt/Hexane, $Rf_{product}$: 0.35) to afford the product **8** with an isolated yield of 95%.

MS (HESI): 225.36 ($M+H^+$), 247.36 ($M+Na^+$)

^{1}H-NMR ($CDCl_3$): 500 MHz δ (ppm)= 4.08 (ddt, J = 7.3, 5.2, 2.2 Hz, 1H), 3.53 (t, J = 6.7 Hz, 2H), 3.47 (dt, J = 9.2, 6.8 Hz, 1H), 3.23 (dt, J = 9.2, 6.6 Hz, 1H), 2.33 (s, 1H), 2.24 - 1.99 (m, 4H), 1.92 - 1.81 (m, 2H), 1.75 (dddd, J = 15.0, 9.3, 8.1, 4.1 Hz, 2H), 1.62 (dtt, J = 17.6, 9.3, 1.7 Hz, 1H), 1.58 - 1.41 (m, 4H), 1.41 - 1.21 (m, 5H).

^{13}C-NMR ($CDCl_3$): 126 MHz δ (ppm)= 134.2, 99.5, 93.1, 72.3, 69.3, 62.5, 42.3, 34.2, 32.6, 29.7, 29.5, 26.3, 25.9, 25.5, 20.6.

Synthesis of compound 9

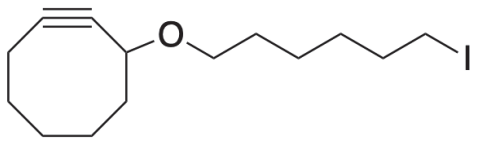

Chemical Formula: $C_{14}H_{23}OI$

Exact Mass: 334.08

In a two-necked round bottom flask under Ar atmosphere and equipped with a magnetic stir-bar, compound **8** (1.0 Equiv., 200 mg, 0.9mmol) was added and dissolved in dry THF (2.5 mL). Then, imidazole (1.2 Equiv., 73 mg, 1.08 mmol) and PPh_3 (1.3 Equiv., 306mg, 1.17 mmol) were added to the reaction vessel. The reaction was cooled to 0°C and I_2 (1.1 Equiv., 251mg, 0.99 mmol) was added in 3 portions; the resulting mixture was covered with an alu foil and allowed to warm to room temperature. Reaction was monitored with TLC (8:2 Hexane:EtOAc as eluents) and was completed in 4 hours. The reaction mixture was quenched with a saturated solution of di $Na_2S_2O_3$ (5mL) and diluted with Et_2O (5mL). Layers were separated in a separatory funnel and the aqueous layer was extracted three times with Et_2O(3x25mL). The combined organic layers were washed with brine (10mL), dried over Na_2SO_4, filtered and concentrated under vacuum obtaining the crude product. This crude was purified by flash chromatography (98:2 Hexane:MTBE as eluents, $Rf_{product}$: 0.33) to afford the product **9** with an isolated yield of 70%.

MS (HESI): 335.56 ($M+H^+$), 347.56 ($M+Na^+$)

^{1}H-NMR ($CDCl_3$): 500 MHz δ (ppm)= 4.15 (ddt, J = 7.3, 5.3, 2.2 Hz, 1H), 3.55 (dt, J = 9.3, 6.7 Hz, 1H), 3.31 (dt, J = 9.2, 6.5 Hz, 1H), 3.20 (t, J = 7.0 Hz, 2H), 2.27 (dddd, J = 16.1, 8.0, 6.1, 2.0 Hz, 1H), 2.22 - 2.07 (m, 2H), 2.00 - 1.90 (m, 2H), 1.88 - 1.78 (m, 4H), 1.75 - 1.54 (m, 5H), 1.50 - 1.32 (m, 4H), 0.94 - 0.81 (m, 1H).

^{13}C-NMR ($CDCl_3$): 126 MHz δ (ppm)= 99.6, 93.2, 72.4, 69.2, 42.4, 34.3, 33.5, 30.3, 29.8, 29.4, 26.4, 25.2, 20.7, 7.1.

Synthesis of compound 10

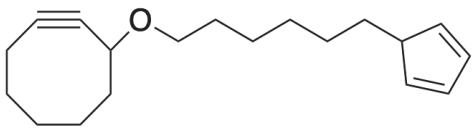

Chemical Formula: $C_{19}H_{28}O$

Exact Mass: 272.21

In a two-necked round bottom flask under Ar atmosphere and equipped with a magnetic stir-bar, compound **9** (300 mg, 0.90 mmol) was added and dissolved in dry THF (3.5 mL). Then, DMPU (2 Equiv., 1.80 mmol) was added to the reaction vessel. The reaction was cooled to -78°C and CpNa (2 Equiv., 1.80 mmol) in THF (1 mL) was cannulated. The resulting mixture was covered with an alu foil and allowed to warm to -30°C. Reaction was monitored with TLC after the complete conversion of the starting material. The reaction mixture was quenched with a saturated solution of NH_4Cl and H_2O (2 mL). Layers were separated in a separatory funnel and the aqueous layer was extracted three times with a mixture of MTBE/Hexane 1:1 (3x20 mL). Combined organic layers were dried over Na_2SO_4, filtered and concentrated under vacuum obtaining the crude product. This crude was purified by flash chromatography [2:98 AcOEt/Hexane, $Rf_{product}$: 0.37] to afford the product **10** with an isolated yield of 92%.

MS (HESI): 273.24 ($M+H^+$)

^{1}H-NMR ($CDCl_3$): 500 MHz δ (ppm)= 6.46 - 6.34 (m, 1H), 6.24 - 6.18 (m, 1H), 6.12 (p, J = 1.5 Hz, 1H), 5.97 (p, J = 1.6 Hz, 1H), 4.13 (ddt, J = 7.3, 4.8, 2.2 Hz, 1H), 3.54 (dt, J = 9.2, 6.8 Hz, 1H), 3.28 (dt, J = 9.2, 6.6 Hz, 1H), 2.92 (h, J = 1.6 Hz, 1H), 2.85 (q, J = 1.5 Hz, 1H), 2.44 - 2.29 (m, 2H), 2.29 - 2.03 (m, 3H), 2.01 - 1.74 (m, 4H), 1.74 - 1.48 (m, 5H), 1.48 - 1.28 (m, 5H).

^{13}C-NMR ($CDCl_3$): 126 MHz δ (ppm)= 149.9, 147.2, 134.8, 133.5, 132.4, 130.2, 126.2, 125.6, 99.3, 93.4, 72.3, 69.4, 43.2, 42.4, 41.2, 34.3, 30.7, 29.8, 29.6, 28.8, 26.4, 26.1, 20.7. (the higher number is due to the Cp-H shift)

IR (neat): (cm^{-1})= 3221.6, 3194.4, 3065.3, 3024.9, 2958.2, 2295.6, 1501.1, 1367.5, 1147.3, 1122.5, 984.3, 910.8, 774.4, 726.4, 552.5, 461.8.

Synthesis of compound 11

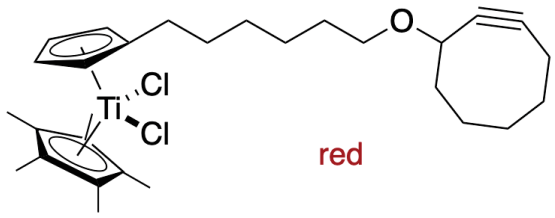

Chemical Formula: $C_{29}H_{42}OCl_2Ti$

Exact Mass: 524.21

In a two-necked round bottom flask under Ar atmosphere and equipped with a magnetic stir-bar, compound **10** (205 mg, 0.75 mmol) was added and dissolved in dry THF (2.5 mL). The reaction was cooled to -78°C and *t*-BuLi (1.1 Equiv., 0.83 mmol) was added dropwise. The reaction mixture was stirred for 1 h to obtain a deep yellow solution (anion formation). $TiCp^*Cl_3$ (0.9 Equiv., 0.68 mmol), solubilized in THF (0.8 mL), was cannulated (-78°C) into the reaction vessel and the solution was stirred for 2 h at -30°C. Reaction was monitored with TLC (AcOEt/Hexane 15:85) to observe the disappearance of the starting material and the product formation. Then, the solvent was evaporated under vacuum obtaining the crude product. This crude was purified by flash chromatography [AcOEt/Hexane (15:85) $R_{f,\ product}$: 0.45] to afford the product **11** with an isolated yield of 47%.

MS (HESI): 525.34 ($M+H^+$)

^{1}H-NMR ($CDCl_3$): 400 MHz δ (ppm)= 6.09 - 5.98 (m, 2H), 5.40 - 5.31 (m, 2H), 4.15 (ddt, J = 7.3, 5.2, 2.2 Hz, 1H), 3.52 (dt, J = 9.2, 6.7 Hz, 1H), 3.29 (dt, J = 9.2, 6.6 Hz, 1H), 2.65 (7, 2H), 2.34 - 2.07 (m, 2H), 2.05 (s, 15H), 1.99 - 1.77 (m, 4H), 1.77 - 1.28 (m, 12H).

^{13}C-NMR ($CDCl_3$): 101 MHz δ (ppm)= 138.9, 129.4, 122.1, 115.7, 99.2, 93.3, 72.3, 69.2, 42.4, 34.3, 30.6, 30.3, 29.8, 29.6, 29.3, 26.4, 25.9, 20.6, 13.2.

IR (neat): (cm^{-1})= 3099.2, 3046.1, 2936.0, 2854.3, 2206.4, 1726.9, 1651.6, 1496.9, 1448.8, 1376.5, 1337.3, 1266.7, 1225.3, 1138.9, 1096.1, 1022.6, 962.7, 893.0, 821.8, 773.1, 735.5, 702.5, 617.3, 543.7, 461.5, 453.7, 445.2, 437.1, 423.5, 419.0, 411.4.

Synthesis of compound 12

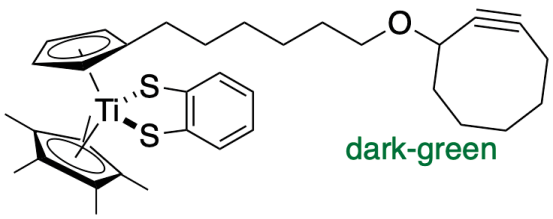

Chemical Formula: $C_{35}H_{46}OS_2Ti$

Exact Mass: 594.25

In a two-necked round bottom flask under Ar atmosphere and equipped with a magnetic stir-bar, compound **11** (1 Equiv., 85 mg, 0.16 mmol) was added and dissolved in dry THF (resulting solution 0.5 M). Then Et_3N (2.2 Equiv., 50 μL, 0.36 mmol) and 1,2 benzendithiole (1.2 Equiv., 23 μL, 0.19 mmol) were added inside the flask. The reaction mixture was stirred for 6h and was checked with TLC (DCM/Hexane 1:1) to observe the disappearance of the starting material and it is remarkable that the colour of the resulting solution turned from red to a dark green. Then, the solvent was evaporated under vacuum obtaining the crude product. This crude was purified by flash chromatography [gradient of DCM/Hexane: (4:6)>(1:1)>(1:0); $R_{f,\ product}$: 0.43 in (1:1)] to afford the corresponding dithiolic product **12** with an isolated yield of 56%.

MS (HESI): 595.61 ($M+H^+$); 617.39 ($M+Na^+$)

^{1}H-NMR ($CDCl_3$): 300 MHz δ (ppm)= 7.42 (2H, dd, J =5.85 Hz, J =3.42 Hz), 7.05 (2H, dd, J =6.85 Hz, J =3.42 Hz), 5.62-5.60 (2H, m), 5.35-5.32 (2H, m), 4.14-4.10 (1H, m), 3.54-3.46 (1H, m), 3.30-3.25 (1H, m), 2.65 (2H, t, J =7.55), 2.25-2.07 (2H, m), 2.06 (15H, s), 2.00-1.75 (4H, m), 1.64-1.53 (6H, m), 1.48-1.39 (6H, m).

^{13}C-NMR ($CDCl_3$): 75 MHz δ (ppm)= 153.4, 132.1, 130.0, 128.0, 127.4, 127.2, 127.0, 124.3, 123.7, 112.6, 111.8, 99.4, 93.2, 79.5, 72.2, 69.9, 69.3, 42.3, 35.9, 34.4, 34.2, 30.6, 30.2, 30.1, 29.7, 29.4, 29.0, 29.0, 26.6, 26.3, 25.8, 25.8, 24.0, 20.6, 12.9.
IR (neat): (cm^{-1})= 3038.0, 2926.4, 2853.9, 1739.7, 1451.3, 1428.8, 1376.5, 1264.4, 1095.6, 1020.9, 808.9, 744.2, 662.6, 459.3, 440.1, 431.7, 423.3, 413.9.

Synthesis of compound 14

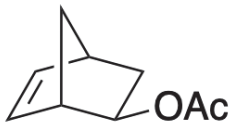

Chemical Formula: $C_9H_{12}O_2$
Exact Mass: 152.08

In a dry pressure tube equipped with a magnetic stir-bar, freshly distilled 2,5-norbornadiene **13** (9060 mg, 98.33 mmol) was added together with acetic acid (0.55 Equiv., 54.08 mmol). Then, the pressure tube was cooled at -78°C and treated with Ar. Thus, it was rapidly sealed. The reaction was then stirred at 188°C for 24h and was checked with TLC [AcOEt/Hexane (2:8); $R_{f,\ product}$: 0.67] to observe the product formation. Thereafter, the reaction mixture was cooled and then poured in an Erlenmeyer flask to be treated with powdered calcium carbonate ($CaCO_3$): this procedure is fundamental in order to switch-off the acidity of the solution. The so obtained mixture was then extracted three times with Pentane. Combined organic layers were washed with brine and then dried over Na_2SO_4, filtered and concentrated under vacuum obtaining the crude product. This crude was purified by flash chromatography [gradient of Et_2O/Pentane: (0:1)>(1:9)] to afford the corresponding product **14** with an isolated yield of 15%.

The spectroscopic data collected in our synthesis match perfectly with those reported in literature.[4]

Synthesis of compound 15

Chemical Formula: $C_7H_{10}O$

Exact Mass: 110.07

In a one-necked round bottom flask equipped with a magnetic stir-bar, a water solution of KOH (3.5 Equiv., 322 mg, 5.74 mmol) was prepared. Meanwhile, in another flask, a solution of compound **14** (1 Equiv., 250 mg, 1.64 mmol) was prepared by adding methanol (resulting solution 2.1 M). Then, this second solution was slowly added to the first flask under continuous stirring. Once the addition was completed, the reaction was heated to reflux for 4h. The reaction mixture was then concentrated under vacuum in order to eliminate the methanol. Thus, the resulting aqueous phase was acidified with H_2SO_4 in order to protonate the acetate ion. Furthermore, the aqueous layer was extracted three times with Et_2O. Combined organic layers were washed firstly with water, then with brine and finally dried over Na_2SO_4. The dried organic phase was then filtered and concentrated under vacuum obtaining the crude product. This crude was purified by flash chromatography [4:6 Et_2O/Pentane; $R_{f,\ product}$: 0.23] to afford the corresponding soft-white crystals product **15** with an isolated yield of 90%.

The spectroscopic data collected in our synthesis match perfectly with those reported in literature.[4]

Synthesis of compound 16

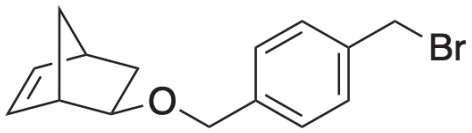

Chemical Formula: $C_{15}H_{17}BrO$

Exact Mass: 292.05

In a two-necked round bottom flask under Ar atmosphere and equipped with a magnetic stir-bar, compound **15** (307 mg, 2.78 mmol) was added and dissolved in dry THF (resulting solution 0.5 M). Then, well cleaned Sodium metal (1.5 Equiv., 4.17 mmol) was added to the reaction vessel. The reaction was then stirred and heated at reflux of THF for 12h. The reaction mixture was then cooled down to room temperature. Meanwhile, in another two-necked round bottom flask under Ar atmosphere and equipped with a magnetic stir-bar, α,α'-dibromo-*p*-xylene (1.1 Equiv., 3.06 mmol) was added and dissolved in dry THF (resulting solution 0.53 M). Thus, the solution contained in the first flask is slowly added in to the second one by using a cannula and maintaining continuous stirring. The new solution has to be heated at reflux of THF for other 12h. Thereafter, the solution is cooled, poured in a separatory funnel with Et_2O and washed several times with: 1) water; 2) NaOH 1.0M; 3) HCl 1.0M; 4) brine. Combined organic layers were then dried over Na_2SO_4, filtered and concentrated under vacuum obtaining the crude product. This crude was purified by flash chromatography [3:7 DCM/Hexane] to afford the corresponding clear oil product **16** with an isolated yield of 20%.

The spectroscopic data collected in our synthesis match perfectly with those reported in literature.[5]

Synthesis of compound 17

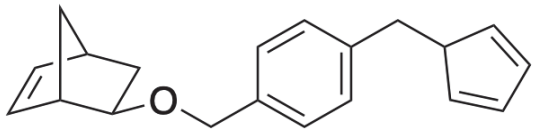

Chemical Formula: $C_{20}H_{22}O$

Exact Mass: 278.17

In a two-necked round bottom flask under Ar atmosphere and equipped with a magnetic stir-bar, compound **16** (150 mg, 0.51 mmol) was added and dissolved in dry THF (5.1 mL). Then, DMPU (2 Equiv., 1.02 mmol) was added to the reaction vessel. The reaction was cooled to -78°C and CpNa (2 Equiv., 1.02 mmol) in THF (0.5 mL) was added. The resulting mixture was covered with an alu foil and allowed to warm to -30°C. Reaction was monitored with TLC after the complete conversion of the starting material. The reaction mixture was quenched with a saturated solution of NH_4Cl and H_2O (2 mL). Layers were separated in a separatory funnel and the aqueous layer was extracted three times with a mixture of MTBE/Hexane 1:1 (3x20 mL). Combined organic layers were dried over Na_2SO_4, filtered and concentrated under vacuum obtaining the crude product. This crude was purified by flash chromatography [5:95 MTBE/Hexane, $R_{f,\ product}$: 0.50] to afford the product **17** with an isolated yield of 70%.

MS (HESI): 301.27 ($M+Na^+$)

^{1}H-NMR ($CDCl_3$): 300 MHz δ (ppm)= 7.29 (2H, d, J =6.06 Hz), 7.21 (2H, d, J =6.78 Hz), 6.42 (2H, s), 6.30-6.28 (1H, m), 6.23-6.20 (2H, m), 6.04-6.03 (1H, m), 5.96-5.93 (2H, m), 4.52 (2H, m), 3.73 (1H, d, J =9.46 Hz), 3.62 (1H, m), 2.98 (1H, d, J =8.28 Hz), 2.85 (1H, d, J =11.77 Hz), 1.78 (1H, d, J =8 Hz), 1.62-1.56(2H, m), 1.48-1.44 (1H, m).

^{13}C-NMR ($CDCl_3$): 75 MHz δ (ppm)= 140.6, 134.4, 133.9, 133.1, 132.2, 131.3, 128.7, 127.6, 79.9, 79.9, 70.9, 46.4, 45.9, 43.0, 41.2, 40.3, 37.0, 36.0, 34.4.

IR (neat): (cm^{-1})= 3059.1, 2972.1, 2938.8, 2892.7, 2866.9, 2359.8, 2340.4, 1640.8, 1513.0, 1432.1, 1362.7, 1342.1, 1100.5, 1077.8.

Synthesis of compound 18

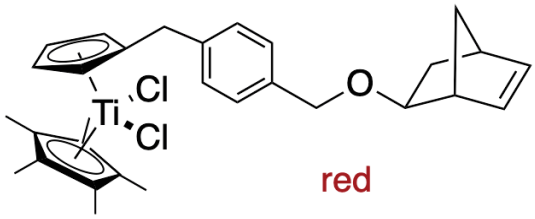

Chemical Formula: $C_{30}H_{36}OCl_2Ti$

Exact Mass: 530.16

In a two-necked round bottom flask under Ar atmosphere and equipped with a magnetic stir-bar, compound **17** (150 mg, 0.54 mmol) was added and dissolved in dry THF (1.8 mL). The reaction was cooled to -78°C and *t*-BuLi (1.1 Equiv., 0.60 mmol) was added dropwise. The reaction mixture was stirred for 1 h to obtain a deep yellow solution (anion formation). TiCp*Cl_3 (0.9 Equiv., 0.49 mmol), solubilized in THF (0.6 mL), was cannulated (-78°C) into the reaction vessel and the solution was stirred for 2 h at -30°C. Reaction was monitored with TLC (MTBE/Hexane 2:8) to observe the product formation. Then, the solvent was evaporated under vacuum obtaining the crude product. This crude was purified by flash chromatography [2:8 MTBE/Hexane; $R_{f,\ product}$: 0.33] to afford the product **18** with an isolated yield of 48%.

MS (HESI): 553.32 ($M+Na^+$)

^{1}H-NMR ($CDCl_3$): 300 MHz δ (ppm)= 7.29-7.21 (4H, m), 6.19 (1H, m), 6.12 (2H, m), 6.00 (2H, m), 5.94 (1H, m), 4.51-4.49 (2H, m), 4.06 (2H, s), 3.60 (1H, d, J=6.06 Hz), 2.95 (1H, s), 2.83 (1H, s), 2.07 (15H, s), 1.77-1.75 (1H, m), 1.58-1.55 (2H, m), 1.47-1.42 (1H, m).

^{13}C-NMR ($CDCl_3$): 75 MHz δ (ppm)= 140.6, 139.6, 136.7, 136.5, 133.1, 129.6, 128.9, 127.8, 123.1, 115.1, 79.9, 70.9, 46.4, 45.9, 40.3, 36.5, 34.4, 13.4.

IR (neat): (cm^{-1})= 3056.6, 2971.1, 2937.9, 2908.6, 2864.8, 2360.2, 1706.7, 1613.8, 1493.6, 1434.6, 1342.7, 1078.7, 820.8, 709.2.

Synthesis of compound 19

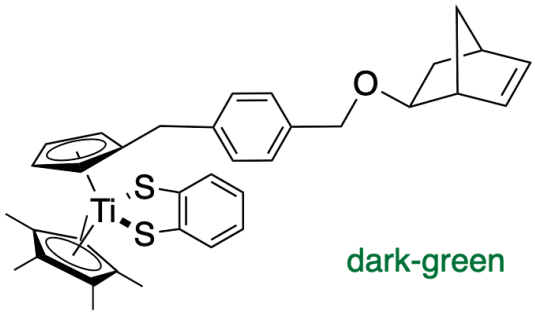

Chemical Formula: $C_{36}H_{40}OS_2Ti$

Exact Mass: 600.20

In a two-necked round bottom flask under Ar atmosphere and equipped with a magnetic stir-bar, compound **18** (1 Equiv., 50 mg) was added and dissolved in dry THF (resulting solution 0.5 M). Then Et_3N (2.2 Equiv., 0.21 mmol) and 1,2 benzendithiole (1.2 Equiv., 0.12 mmol) were added inside the flask. The reaction mixture was stirred for 6h and was checked with TLC (MTBE/Hexane 2:8) to observe the product formation. It was observed the complete conversion of starting material and it is remarkable that the colour of the resulting solution turned from red to dark-green. Then, the solvent was evaporated under vacuum obtaining the crude product. This crude was purified by flash chromatography [gradient of DCM/Hexane: (1:9)>(3:7)>(1:1); $R_{f,\ product}$: 0.39 in (1:1)] to afford the corresponding dithiolic product **19** with an isolated yield of 53%.

MS (HESI): 623.32 ($M+Na^+$)

^{1}H-NMR ($CDCl_3$): 300 MHz δ (ppm)= 7.46-7.43 (2H, m), 7.20 (2H, d, J =7.94 Hz), 7.10-7.07 (2H, m), 7.02 (2H, d, J =7.90 Hz), 6.20-6.18 (1H, m), 5.93-5.90 (1H, m), 5.64 (2H, m), 5.29 (2H, m), 4.47-4.45 (2H, m), 3.57 (1H, d, J=6.18 Hz), 3.52 (2H, s), 2.93 (1H, s), 2.82 (1H, s), 2.05 (15H, s), 1.75-1.72 (1H, m), 1.58-1.53 (2H, m), 1.44-1.39 (1H, m).

^{13}C-NMR ($CDCl_3$): 75 MHz δ (ppm)= 153.3, 140.6, 140.1, 136.5, 133.1, 131.0, 130.0, 128.5, 127.6, 124.5, 123.9, 112.7, 111.4, 79.8, 70.8, 46.3, 45.9, 40.3, 36.2, 34.3, 13.0.

IR (neat): (cm^{-1})= 2972.0, 2861.4, 2359.1, 2071.6, 1649.6, 1428.7, 1376.7, 1076.2, 807.8.

Synthesis of compound 20

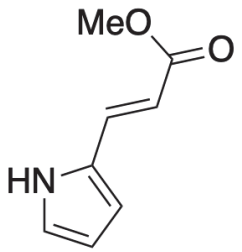

Chemical Formula: $C_8H_9NO_2$

Exact Mass: 151.06

In a two-necked round bottom flask under Ar atmosphere and equipped with a magnetic stir-bar, Pyrrole-2-carboxaldehyde (1000 mg, 10.52 mmol) was added and dissolved in dry THF (resulting solution 0.5 M). Then, Methyl-(triphenylphosphoranylidene)acetate (4200 mg, 12.62 mmol) was added. The reaction mixture was stirred at 60°C for 20 hours and was checked with TLC (AcOEt/Hexane 2:8) to observe the disappearance of the starting material. Then, the solvent was evaporated under vacuum obtaining the crude product. This crude was purified by flash chromatography [1) AcOEt/Hexane: (2:8); 2)DCM/Hexane: (98:2)] to afford the corresponding product **20** with an isolated yield of 65%.

The spectroscopic data collected in our synthesis match perfectly with those reported in literature.[6]

Synthesis of compound 21

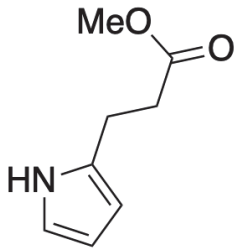

Chemical Formula: $C_8H_{11}NO_2$

Exact Mass: 153.08

In a two-necked round bottom flask under Ar atmosphere and equipped with a magnetic stir-bar, compound **20** (1030 mg, 6.81 mmol) was added and dissolved in a mixture of MeOH/THF 5:1 (resulting solution 0.2 M). Then, Pd/C powder (105 mg, $10\%_{w/w}$) was added, followed by replacement of the Argon with Hydrogen atmosphere. The reaction mixture was stirred for 20 hours at room temperature. Then, the Pd/C was filtered off on a Celite pad and washed with MeOH. The combined organic phases were dried and concentrated in vacuo to afford the corresponding reduced product **21** with an isolated yield of 99% which required no further purification.

The spectroscopic data collected in our synthesis match perfectly with those reported in literature.[7]

Synthesis of compound 22

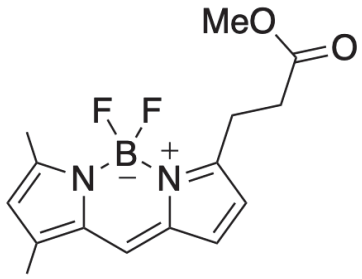

Chemical Formula: $C_{15}H_{17}BF_2N_2O_2$

Exact Mass: 306.14

In a two-necked round bottom flask under Ar atmosphere and equipped with a magnetic stir-bar, 3,5-dimethyl-1H-pyrrole-2-carbaldehyde (1.1 Equiv., 920 mg, 7.48 mmol) and compound **21** (1 Equiv., 1043 mg, 6.8 mmol) were added and dissolved in dry DCM (resulting solution 0.11 M). The mixture was cooled to 0°C in an ice-bath and DCM diluted (1.45 M) $POCl_3$ (1.1 Equiv., 7.48 mmol, 687 μL) was added dropwise. The reaction was stirred for 30 minutes at 0°C and then for 6 hours at room temperature. The so obtained black solution was cooled again to 0°C and DIPEA (6.2 Equiv., 42.2 mmol, 7.35 mL) was added dropwise, followed by BF_3 (6 Equiv., 40.8 mmol, 5.04 mL). The mixture was then stirred for 14 hours at room temperature. The reaction was then quenched with water, filtered on Celite and washed with DCM. The aqueous layer was extracted with DCM (3x20mL). Then, the combined organic phases were dried on Na_2SO_4 and concentrated in vacuo to afford the crude product. The crude obtained was then purified by flash chromatography [isocratic gradient of 100% DCM; $R_{f,\ product}$: 0.46] to afford the corresponding product **22** with an isolated yield of 46%.

The spectroscopic data collected in our synthesis match perfectly with those reported in literature.[8]

Synthesis of compound 23

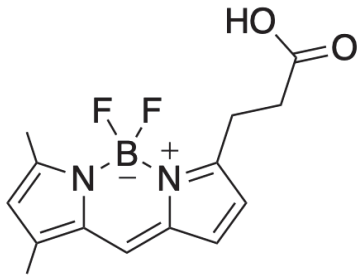

Chemical Formula: $C_{14}H_{15}BF_2N_2O_2$

Exact Mass: 292.09

In a two-necked round bottom flask equipped with a magnetic stir-bar, compound **22** (1 Equiv., 400 mg, 1.31 mmol) was added and dissolved in a mixture of H_2O/THF (4:6). Concentrated 12M HCl (24 mL) was then added to the solution to hydrolyze the methyl ester to the carboxylic acid. The reaction was thus stirred for 36 hours at room temperature. The reaction was then diluted with DCM (50 mL), and separated in a separatory funnel. The aqueous layer was extracted for three times with DCM. Then, the combined organic phases were washed with brine, dried on Na_2SO_4 and concentrated in vacuo to afford the crude product. The crude obtained was then quickly purified by flash chromatography [MeOH/DCM: 1:9 ; $R_{f,\ product}$: 0.53] to afford the corresponding product **23** with an isolated yield of 58%.

The spectroscopic data collected in our synthesis match perfectly with those reported in literature.[8]

Synthesis of compound 24

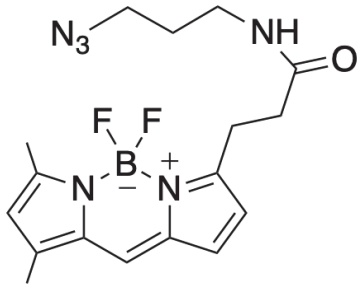

Chemical Formula: $C_{17}H_{21}BF_2N_6O$

Exact Mass: 374.18

In a two-necked round bottom flask under Ar atmosphere and equipped with a magnetic stir-bar, compound **23** (1 Equiv., 206 mg, 0.704 mmol) was added and dissolved in toluene (resulting solution 0.03 M). Then, *N*-hydroxysuccinimide (2 Equiv., 162 mg, 1.41 mmol), dicyclohexylcarbodiimide (2 Equiv., 291 mg, 1.41 mmol) and Et_3N (2 Equiv., 200 μL) were added. The reaction was stirred overnight at room temperature. Thus, the reaction mixture was filtered on Celite bed in order to remove the dicyclohexylurea byproduct of the carboxylic acid activation. The combined organic phases were concentrated in vacuo to afford the crude product. The crude obtained was then quickly purified by flash chromatography [gradient of AcOEt/Hexane (4 minutes): (1:1)>(1:0); followed by gradient of MeOH/DCM (6 minutes): (0:1)>(5:95); $R_{f,\ product}$: 0.8 in MeOH/DCM (5:95)] to afford the corresponding activated product **S24** with an isolated yield of 55%. The so obtained product was directly involved in the next step of the reaction.

In a two-necked round bottom flask under Ar atmosphere and equipped with a magnetic stir-bar, the ester **S24** (1 Equiv., 70 mg, 0.18 mmol) was added and dissolved in DCE (resulting solution 0.1 M). Then, DIPEA (6 Equiv., 1.08 mmol, 185 μL) and 3-azidopropanamine (3 Equiv., 54.1 mg, 0.54 mmol) were added. The reaction was stirred for 5 hours at room temperature and was monitored with TLC (MeOH/DCM 5:95) to observe the product formation ($R_{f,\ product}$: 0.7). The reaction mixture was then diluted with DCM (50 mL), washed with aqueous saturated solution of $NaHCO_3$ and then with 1.0 M HCl. The aqueous layer was thus extracted for

three times with DCM. Then, the combined organic phases were washed with brine, dried on Na_2SO_4 and concentrated in vacuo to afford the crude product. The crude obtained was then quickly purified by flash chromatography [1:99 MeOH/DCM] to afford the corresponding product **24** with an isolated yield of 85%.

The spectroscopic data collected in our synthesis match perfectly with those reported in literature.[8],[9]

Synthesis of compound 25

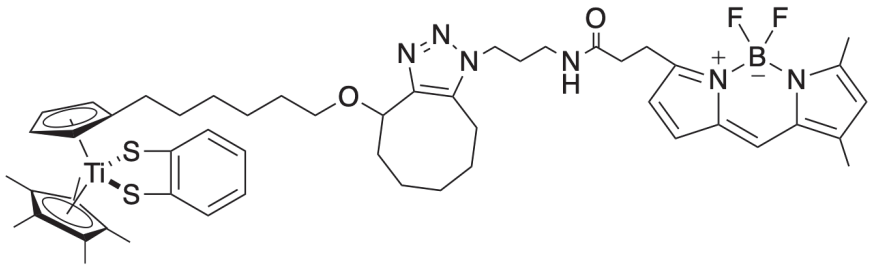

Chemical Formula: $C_{52}H_{67}BF_2N_6O_2S_2Ti$

Exact Mass: 968.43

In a two-necked round bottom flask under Ar atmosphere and equipped with a magnetic stir-bar, compound **12** (25 mg, 0.042 mmol) was added and dissolved in dry acetonitrile (resulting solution 0.01 M). Then compound **24** (1 Equiv., 0.042 mmol) was added inside the flask. The reaction mixture was stirred at 30°C for 48 hours and was checked with TLC (AcOEt/Hexane 1:1) to observe the product formation. Then, the solvent was evaporated under vacuum obtaining the crude product. This crude was purified by flash chromatography [gradient of AcOEt/Hexane: (1:1)>(1:0); $R_{f,\ product}$: 0.08 in (1:1)] to afford the corresponding clicked product **25** with an isolated yield of 38% and a percentage of conversion after 48 hours of 67%.

MS (HESI): 969.44 ($M+H^+$)

^{1}H-NMR (CD_2Cl_2): 300 MHz δ (ppm)= 7.37 (2H, dd, J =5.93 Hz, J =3.4 Hz), 7.17 (1H, s), 7.05 (2H, dd, J =6.03 Hz, J =3.53 Hz), 6.95 (1H, d, J =3.91 Hz), 6.32 (1H, d, J =3.91 Hz), 6.19 (1H, s), 6.00 (1H, m), 5.64-5.61 (2H, m), 5.36-5.35

(2H, m), 4.74-4.71 (1H, m), 4.59-4.55 (1H, m), 4.34 (1H, m), 4.21 (1H, m), 3.30-3.25 (5H, m), 2.65 (2H, t, J =7.55 Hz), 2.61 (2H, t, J =7.69 Hz), 2.57 (3H, s), 2.30 (3H, s), 2.28-2.11 (2H, m), 2.04 (15H, s), 2.00-1.75 (4H, m), 1.74-1.71 (2H, m), 1.64-1.53 (6H, m), 1.48-1.39 (6H, m).

^{13}C-NMR (CD_2Cl_2): 75 MHz δ (ppm)= 172.3, 154.6, 134.3, 134.0, 133.0, 132.9, 130.7, 128.9, 125.3, 124.6, 124.3, 121.2, 117.7, 113.5, 112.6, 75.0, 72.5, 69.4, 69.3, 54.2, 53.8, 53.5, 45.8, 37.4, 37.3, 36.4, 36.2, 31.5, 31.4, 31.0, 30.1, 30.7, 30.5, 29.9, 29.8, 27.9, 26.8, 26.7, 26.3, 25.4, 21.6, 13.5, 11.9.

IR (neat): (cm^{-1})= 3041.2, 2928.1, 2856.0, 2095.5, 1669.6, 1605.8, 1528.7, 1488.1, 1439.9, 1376.3, 1321.9, 1305.9, 1264.3, 1250.6, 1174.4, 1134.6, 1085.9, 1064.7, 998.4, 973.5, 901.7, 850.3, 811.1, 737.3, 701.6, 669.8, 590.0, 483.3, 463.2, 449.6, 438.0, 430.6, 425.8, 415.6, 407.8.

Synthesis of compound 26

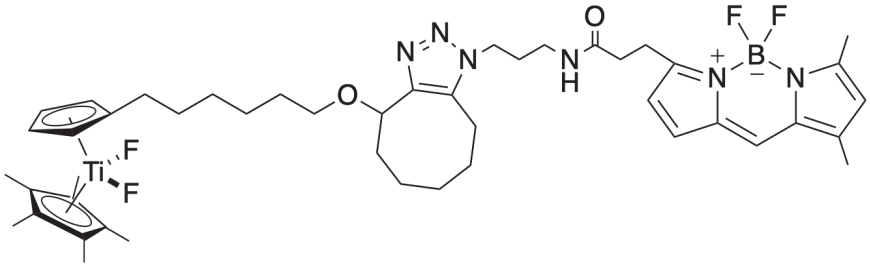

Chemical Formula: $C_{46}H_{63}BF_4N_6O_2Ti$

Exact Mass: 866.45

In a two-necked round bottom flask under Ar atmosphere and equipped with a magnetic stir-bar, compound **25** (6 mg, 0.0062 mmol) was added and dissolved in dry $CHCl_3$ (resulting solution 0.1 M). Meanwhile, in a Teflon vial equipped with a magnetic stir-bar under Ar atmosphere and equipped with a magnetic stir-bar, crystals of Xenon difluoride [XeF_2] (1 Equiv., 1.05 mg, 0.0062 mmol) were added. Thus, the solution contained in the first flask was slowly added in to the vial by using a cannula and maintaining continuous stirring. The color of the solution changed within seconds, turning from dark-green to a light-orange color. The reaction mixture

was then poured in a single-necked round bottom flask, concentrated by using a water pump and the crude oil obtained was treated by adding Hexane in order to promote the precipitation of the Titanocene-difluoride compound. The so obtained precipitate was then washed with Hexane in a Buckner funnel in order to purify the final product **26** from the 1,2-benzenedithiol, with an isolated yield of 93%.

MS (HESI): 889.55 ($M+Na^+$)

^{1}H-NMR (CD_2Cl_2): 300 MHz δ (ppm)= 7.17 (1H, s), 6.95 (1H, d, J =3.91 Hz), 6.32 (1H, d, J =3.91 Hz), 6.19 (1H, s), 6.04 (1H, m), 6.02 (2H, s), 5.73 (2H, s), 4.74-4.71 (1H, m), 4.59-4.55 (1H, m), 4.34 (1H, m), 4.21 (1H, m), 3.30-3.25 (5H, m), 2.65 (2H, t, J =7.55), 2.61 (2H, t, J =7.69 Hz), 2.57 (3H, s), 2.30 (3H, s), 1.96 (15H, s), 1.75-1.35 (12H, m), 1.34-1.29 (6H, m).

^{13}C-NMR (CD_2Cl_2): 75 MHz δ (ppm)= 145.0, 131.0, 129.4, 129.0, 128.9, 127.4, 124.7, 117.8, 117.3, 116.0, 115.9, 72.5, 69.3, 54.9, 54.2, 53.9, 53.5, 47.0, 46.9, 45.8, 37.4, 36.5, 36.2, 30.8, 30.7, 30.2, 30.1, 29.8, 27.9, 26.8, 26.4, 25.4, 21.6, 20.7, 13.1, 12.3, 11.9, 9.2.

IR (neat): (cm^{-1})= 2927.9, 2956.4, 2358.5, 1651.5, 1605.3, 1437.6, 1250.1, 1174.2, 1134.1, 1085.9, 750.1, 669.4, 573.9, 494.5, 470.9, 459.7, 448.4, 439.5, 430.7, 424.8, 414.4, 405.3.

Synthesis of compound 27

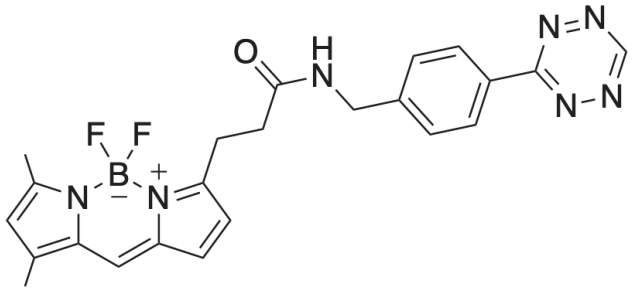

Chemical Formula: $C_{23}H_{22}BF_2N_7O$

Exact Mass: 461.19

In a two-necked round bottom flask under Ar atmosphere and equipped with a magnetic stir-bar, compound **23** (1 Equiv., 16 mg, 0.033 mmol) was added and dissolved in DCM dry (resulting solution 0.03 M). The resulting solution was cooled down to 0°C and [4-(1,2,4,5-tetrazin-3-yl)phenyl]methanamine hydrochloride (1.6 Equiv., 10 mg, 0.053 mmol) was added, followed by EDCI (1.56 Equiv., 7 mg, 0.034 mmol), HOBt (1.5 Equiv., 5 mg, 0.036 mmol) and Et_3N (2.1 Equiv., 10.5 μL, 0.070 mmol). The solution was then allowed to reach room temperature and the stirring was maintained for 3-4 hours. After a TLC control (DCM/MeOH, 9:1) the solvent was removed with rotatory evaporation and the crude obtained was quickly purified by flash chromatography [1:9 MeOH/DCM; $Rf_{product}$: 0.83] to afford the corresponding ready-to-click product **27** with an isolated yield of 83%.

MS (HESI): 462.20 ($M+H^+$), 484.17 ($M+Na^+$)

^{1}H-NMR ($CDCl_3$): 300 MHz δ (ppm)= 10.22 (d, J = 0.9 Hz, 1H), 8.50 (d, J = 8.2 Hz, 2H), 7.36 (d, J = 8.1 Hz, 3H), 7.12 (s, 1H), 6.92 (d, J = 4.1 Hz, 1H), 6.33 (d, J = 4.1 Hz, 1H), 6.29 (s, 1H), 6.10 (s, 1H), 4.53 (d, J = 5.9 Hz, 2H), 3.34 (t, J = 7.3 Hz, 3H), 2.80 (t, J = 7.3 Hz, 3H), 2.55 (s, 4H), 2.26 (s, 4H).

^{13}C-NMR ($CDCl_3$): 75 MHz δ (ppm)= 171.6, 166.2, 160.5, 157.6, 156.6, 144.1, 143.9, 133.2, 132.0, 131.9, 131.8, 130.25, 128.3, 123.7, 120.4, 117.5, 77.1, 43.9, 35.8, 29.6, 24.7, 14.8, 11.2.

Synthesis of compound 28

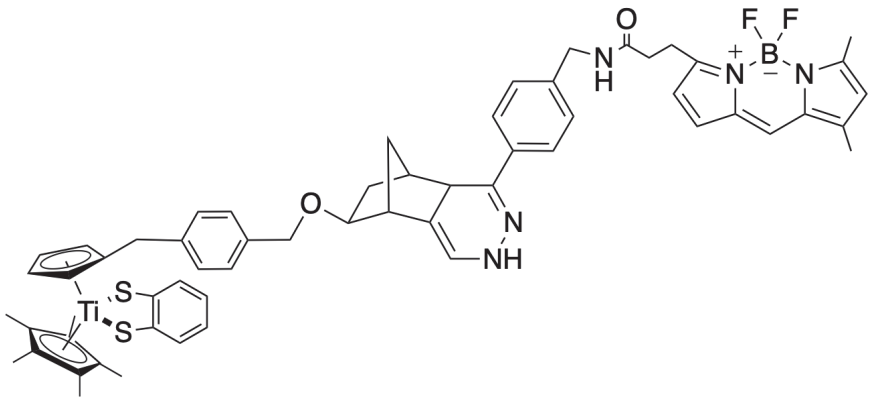

Chemical Formula: $C_{59}H_{62}BF_2N_5O_2S_2Ti$

Exact Mass: 1033.39

In a two-necked round bottom flask under Ar atmosphere and equipped with a magnetic stir-bar, compound **27** (1 Equiv., 5 mg, 0.010 mmol) was added. Simultaneously, **19** (1.6 Equiv., 10 mg, 0.017 mmol) was solubilized in THF dry (resulting solution 0.1 M) and then added under stirring to the previous flask. The resulting solution was left under continuous stirring at room temperature for 48 hours. TLC control (DCM/MeOH, 98:2) was performed showing the disappearance of the starting material and the presence of a red/green spot which was fluorescent under 366 nm UV lamp. Thus, the solvent was evaporated and the crude obtained was quickly purified by flash chromatography [gradient of MeOH/DCM: (0:1)¿(1:9); $Rf_{product}$: 0.24 in (2:98)] to afford the corresponding click-product **28** with an isolated yield of 92% and with a percentage of conversion after 48 hours of 80%.

MS (HESI): 1034.38 ($M+H^+$)

^{1}H-NMR (CD_2Cl_2): 300 MHz δ (ppm)= 7.85 - 6.83 (m, 12H), 6.66 (d, J = 6.7 Hz, 1H), 6.29 (s, 2H), 6.15 (s, 1H), 5.63 (q, J = 3.0 Hz, 2H), 5.37 (s, 1H), 5.28 (dd, J = 5.6, 2.7 Hz, 2H), 4.55 - 4.25 (m, 6H), 3.50 (t, J = 5.7 Hz, 2H), 3.28 (s, 3H), 2.68 (s, 4H), 2.55 (s, 4H), 2.25 (dd, J = 7.5, 3.1 Hz, 4H), 2.07 - 2.00 (m, 18H).

^{13}C-NMR (CD_2Cl_2): 75 MHz δ (ppm)= 172.5, 154.5, 144.8, 141.4, 141.2, 137.3, 136.6, 135.9, 134.1, 132.8, 132.7, 132.5, 131.9, 130.8, 129.3, 129.2, 128.9, 128.6, 128.5,

128.1, 127.2, 127.1, 126.9, 126.0, 125.5, 124.5, 121.7, 121.2, 117.8, 117.0, 114.8, 114.5, 113.6, 113.3, 112.2, 111.9, 70.9, 43.8, 43.2, 37.1, 36.2, 32.7, 30.5, 30.1, 25.4, 23.5, 15.5, 14.8, 13.6, 11.9.

Synthesis of compound 29

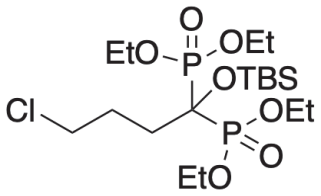

Chemical Formula: $C_{18}H_{41}ClO_7P_2Si$

Exact Mass: 494.18

In a two-necked round bottom flask under Ar atmosphere and equipped with a magnetic stir-bar, 4-chlorobuthyrryl chloride (1 Equiv., 1000 mg, 7.09 mmol) was added. The solution was then cooled down to 0°C and $P(OEt)_3$ (1 Equiv., 7.09 mmol, 1320 μL) was added dropwise and under continuous stirring. The resulting mixture was allowed to reach room temperature and stirred additional 15 minutes after which, anhydrous DCM (15 mL) was added via cannula. Diethyl phosphite (1.1 Equiv., 7.80 mmol, 1006 μL), DMAP (1 Equiv., 7.09 mmol, 867 mg) e TBDMS-Cl (1.1 Equiv., 7.80 mmol, 1176 mg) were then added sequentially and the so obtained mixture was left under stirring overnight at room temperature. The reaction was checked through TLC [Hexane/AcOEt (4:6)] and after completion was quenched with a solution of HCl 0.1 M. The solvent was then evaporated and the crude product was purified though flash chromatography [gradient of AcOEt/Hexane: (6:4)¿(1:0); $Rf_{product}$: 0.22 in (6:4)] to afford the corresponding product **29** with an isolated yield of 32%.

The spectroscopic data collected in our synthesis match perfectly those reported in literature.[10]

Synthesis of compound 30

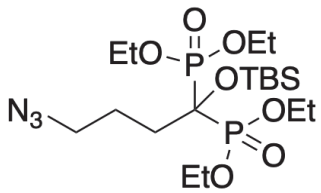

Chemical Formula: $C_{18}H_{41}N_3O_7P_2Si$

Exact Mass: 501.22

In a two-necked round bottom flask under Ar atmosphere and equipped with a magnetic stir-bar, compound **29** (1 Equiv., 500 mg, 1.01 mmol) was added and solubilized in DMF dry (5.05 mL). Sodium azide (2 Equiv., 131 mg, 2.02 mmol) was added under stirring and the so obtained mixture was heated up to 80°C for 2 h. Once the reaction completed, water and DCM were added and separated in a separatory funnel. The organic layer was washed for two times with water, dried on Na_2SO_4 and concentrated in vacuo to afford the crude product. The crude obtained was then quickly purified by flash chromatography [pure AcOEt, $Rf_{product}$: 0.30] to afford the corresponding product **30** with an isolated yield of 84%.

The spectroscopic data collected in our synthesis match perfectly those reported in literature.[10]

Synthesis of compound 31

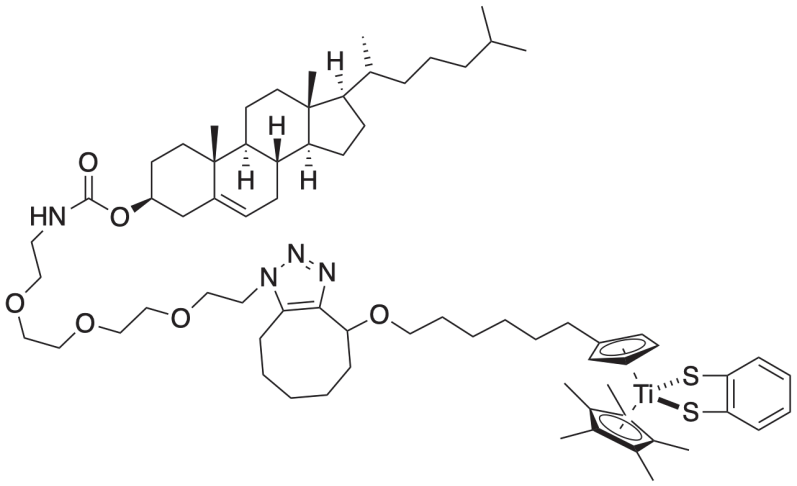

Chemical Formula: $C_{71}H_{108}N_4O_6S_2Ti$

Exact Mass: 1224.72

In a two-necked round bottom flask under Ar atmosphere and equipped with a magnetic stir-bar, compound **12** (1 Equiv., 30 mg, 0.050 mmol) was added and dissolved in dry DCM (resulting solution 0.025 M). Then cholesteryl-TEG-azide (1 Equiv., 31 mg, 0.05 mmol) was added inside the flask followed by a small drop of dry DMSO to increase the dissolution. The reaction mixture was stirred at 30°C for 48 hours and was checked with TLC (AcOEt pure) to observe the product formation. Then, the solvent was evaporated under vacuum obtaining the crude product. This crude was purified by flash chromatography [pure AcOEt; $Rf_{product}$: 0.12] to afford the corresponding clicked product **31** with an isolated yield of 52%.

MS (HESI): 1225.73 ($M+H^+$), 1247.71 ($M+Na^+$)

^{1}H-NMR (CD_2Cl_2): 400 MHz δ (ppm)= 7.30 - 7.20 (m, 2H), 6.94 (dd, J = 5.9, 3.4 Hz, 2H), 5.51 (t, J = 2.6 Hz, 2H), 5.33 - 5.17 (m, 10H), 5.11 (s, 1H), 4.70 - 4.58 (m, 1H), 4.48 - 4.22 (m, 3H), 3.86 - 3.73 (m, 2H), 3.53 - 3.36 (m, 11H), 3.32 - 3.10 (m, 5H), 2.97 (tdd, J = 14.4, 9.1, 5.4 Hz, 1H), 2.76 - 2.54 (m, 1H), 2.31 - 0.50 (m, 65H).

^{13}C-NMR (CD_2Cl_2): 101 MHz δ (ppm)= 155.9, 153.8, 150.5, 140.1, 134.5, 132.2, 129.9, 124.5, 124.5, 123.5, 122.3, 117.1, 112.7, 111.7, 74.3, 74.1, 71.6, 70.7, 70.6, 70.4,

70.2, 70.0, 69.9, 68.5, 66.6, 56.7, 56.2, 50.1, 48.4, 47.5, 47.1, 43.9, 42.3, 40.7, 39.8, 39.5, 38.6, 37.0, 36.6, 36.2, 35.8, 35.7, 31.9, 30.7, 30.7, 30.3, 29.8, 29.7, 29.2, 29.1, 28.6, 28.2, 28.0, 27.0, 26.0, 25.9, 25.6, 24.6, 24.3, 23.8, 22.8, 22.6, 22.5, 22.3, 21.0, 20.9, 19.9, 19.1, 18.5, 12.8, 11.6.

Synthesis of compound 32

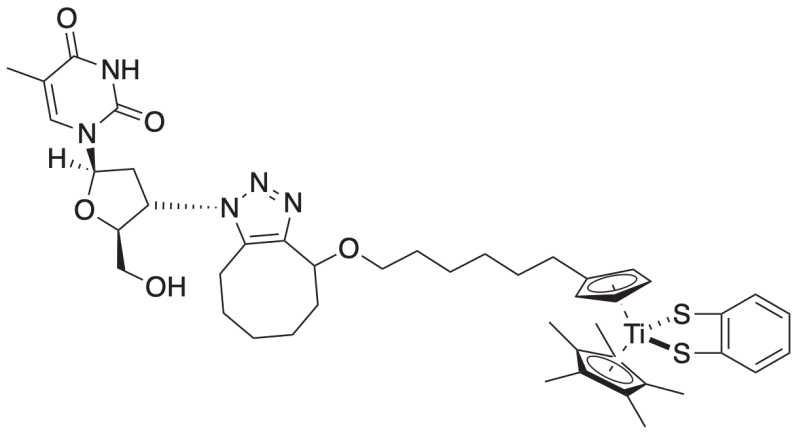

Chemical Formula: $C_{45}H_{59}N_5O_5S_2Ti$

Exact Mass: 861.34

In a two-necked round bottom flask under Ar atmosphere and equipped with a magnetic stir-bar, compound **12** (1 Equiv., 30 mg, 0.050 mmol) was added and dissolved in dry DCM (3.75 mL). Then 1-[(2R,4S,5S)-4-azido-5-(hydroxymethyl)oxolan-2-yl]-5-methyl-1,2,3,4-tetrahydropyrimidine-2,4-dione (1 Equiv., 13 mg, 0.05 mmol) was solubilized in dry DMSO (1.25 mL) and added in the flask under stirring. The reaction mixture was stirred at 30°C for 48 hours and was checked with TLC (AcOEt pure) to observe the product formation. Then, the solvent was evaporated under vacuum obtaining the crude product. This crude was purified by flash chromatography [pure AcOEt; $Rf_{product}$: 0.35] to afford the corresponding clicked product **32** with an isolated yield of 62%.

MS (HESI): 862.37 ($M+H^+$)

^{1}H-NMR (CD_2Cl_2): 700 MHz δ (ppm)= 8.16 (s, 1H), 7.37 (dtt, J = 6.9, 4.5, 2.3 Hz, 2H), 7.05 (dt, J = 6.0, 3.1 Hz, 2H), 6.28 (t, J = 6.6 Hz, 1H), 5.63 (t, J = 2.5

Hz, 2H), 5.55 - 5.46 (m, 1H), 5.34 (dt, J = 8.6, 2.4 Hz, 1H), 4.68 (dd, J = 9.2, 3.2 Hz, 1H), 4.59 (dt, J = 4.9, 2.3 Hz, 1H), 4.03 - 3.95 (m, 1H), 3.68 (dd, J = 12.6, 6.1 Hz, 1H), 3.53 (dt, J = 8.8, 6.8 Hz, 1H), 3.46 (dt, J = 8.9, 6.4 Hz, 1H), 3.11 (dt, J = 14.7, 6.1 Hz, 1H), 3.03 - 2.93 (m, 1H), 2.93 - 2.77 (m, 2H), 2.16 (dd, J = 8.8, 6.5 Hz, 2H), 2.05 (d, J = 1.6 Hz, 15H), 1.94 (dd, J = 12.4, 1.4 Hz, 3H), 1.76 (s, 1H), 1.70 - 1.60 (m, 6H), 1.53 - 1.47 (m, 2H), 1.31 (d, J = 9.9 Hz, 10H).

^{13}C-NMR (CD_2Cl_2): 176 MHz δ (ppm)= 162.9, 153.8, 150.2, 144.2, 138.0, 133.9, 132.2, 129.9, 124.6, 124.5, 123.5, 112.8, 112.7, 111.8, 110.9, 89.6, 85.2, 71.4, 68.7, 62.1, 57.2, 53.7, 38.1, 31.9, 30.6, 30.2, 30.2, 30.0, 29.8, 29.7, 29.5, 29.3, 29.1, 29.1, 28.2, 27.2, 25.9, 25.5, 24.7, 24.2, 23.3, 22.7, 13.9, 12.8, 12.2.

Synthesis of compound 33

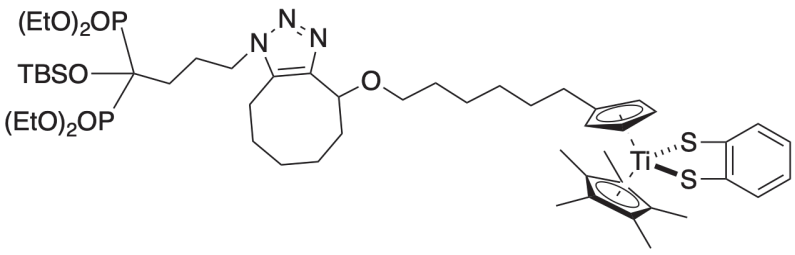

Chemical Formula: $C_{53}H_{87}N_3O_8P_2S_2SiTi$

Exact Mass: 1095.47

In a two-necked round bottom flask under Ar atmosphere and equipped with a magnetic stir-bar, compound **12** (1 Equiv., 0.185 mmol, 110 mg) was added. Subsequently, a solution of product **30** (1 Equiv., 0.185 mmol, 93 mg) in DCM dry (1.9 mL) was added. The so obtained mixture was then stirred at 30°C for 48 hours and was checked with TLC (AcOEt pure) to observe the product formation. Then, the solvent was evaporated under vacuum obtaining the crude product which was purified by flash chromatography [pure AcOEt] to afford the corresponding clicked product **33** with an isolated yield of 28% and with a percentage of conversion after 48 hours of 30%.

MS (HESI): 1096.51 ($M+H^+$), 1118.50 ($M+Na^+$)

^{1}H-NMR (CD_2Cl_2): 300 MHz δ (ppm)= 7.37 (dd, J = 5.9, 3.4 Hz, 2H), 7.05 (dd, J = 6.0, 3.4 Hz, 2H), 5.62 (t, J = 2.6 Hz, 2H), 5.35 (dt, J = 5.4, 1.9 Hz, 4H), 4.71 (ddd, J = 28.7, 7.0, 3.4 Hz, 1H), 4.34 (td, J = 6.8, 3.5 Hz, 1H), 4.28 - 4.04 (m, 11H), 3.53 - 3.22 (m, 2H), 3.21 - 2.58 (m, 3H), 2.33 - 2.10 (m, 4H), 2.05 (s, 16H), 1.93 - 1.46 (m, 4H), 1.38 - 1.28 (m, 19H), 0.91 (s, 10H), 0.18 (d, J- = 3.5 Hz, 6H).
^{13}C-NMR (CD_2Cl_2): 75 MHz δ (ppm)= 154.6, 146.1, 145.2, 134.1, 133.7, 133.0, 130.8, 125.4, 124.4, 113.6, 112.7, 80.5, 78.4, 76.4, 75.1, 72.5, 69.4, 63.7, 63.6, 52.8, 49.7, 48.7, 36.5, 34.1, 34.0, 32.7, 31.6, 31.6, 31.1, 30.7, 30.7, 30.5, 30.1, 29.9, 29.4, 28.0, 26.9, 26.5, 26.5, 25.9, 25.7, 25.5, 25.1, 24.6, 23.6, 21.7, 20.9, 19.7, 17.2, 17.1, 17.1, 13.6, -1.9.

Synthesis of compound 34

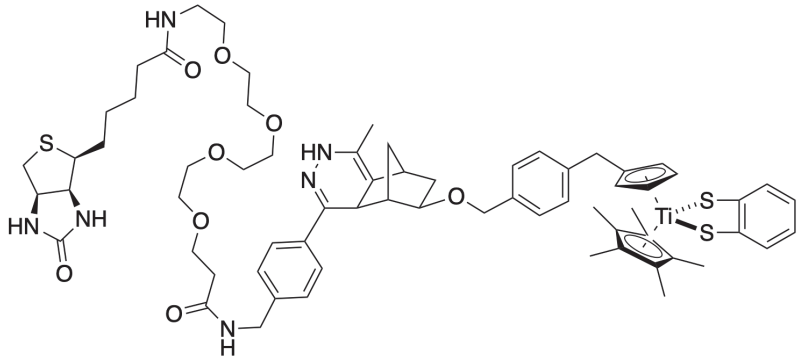

Chemical Formula: $C_{67}H_{86}N_6O_8S_3Ti$

Exact Mass: 1246.51

In a two-necked round bottom flask under Ar atmosphere and equipped with a magnetic stir-bar, compound **19** (1 Equiv., 22 mg, 0.037 mmol) was added and dissolved in dry DCM (resulting solution 0.05 M). Then cholesteryl-TEG-azide (1 Equiv., 25 mg, 0.037 mmol) was added inside the flask followed by a small drop of dry DMSO to increase the dissolution. The reaction mixture was stirred at 30°C for 48 hours and was checked with TLC (DCM/MeOH, 9:1) to observe the product formation. Then, the solvent was evaporated under vacuum obtaining the crude product which was purified by flash chromatography [gradient of MeOH/DCM: (0:1)

> (1:9); $Rf_{product}$: 0.35 in (1:9)] to afford the corresponding click-product **34** with an isolated yield of 54%.

MS (HESI): 1246.56 ($M+H^+$), 1269.53 ($M+Na^+$)

^{1}H-NMR (CD_2Cl_2): 400 MHz δ (ppm)= 11.02 (s, 1H), 8.46 - 6.39 (m, 9H), 6.36 - 4.69 (m, 6H), 4.43 (q, J = 41.8, 34.0 Hz, 4H), 4.02 - 3.06 (m, 19H), 3.06 - 2.89 (m, 3H), 2.89 - 0.45 (m, 44H).

^{13}C-NMR (CD_2Cl_2): 101 MHz δ (ppm)= 173.0, 171.4, 167.0, 153.7, 130.0, 128.6, 128.5, 128.5, 128.5, 127.9, 127.9, 127.8, 127.7, 127.7, 127.7, 127.6, 127.5, 127.4, 124.8, 123.7, 112.8, 111.4, 70.8, 70.4, 70.3, 70.2, 70.0, 69.8, 67.3, 57.2, 56.8, 54.4, 46.5, 42.7, 42.6, 41.9, 39.2, 36.9, 36.3, 35.3, 29.7, 26.8, 25.3, 24.8, 18.3, 17.1, 12.8, 12.5, 11.8.

Synthesis of compound 35

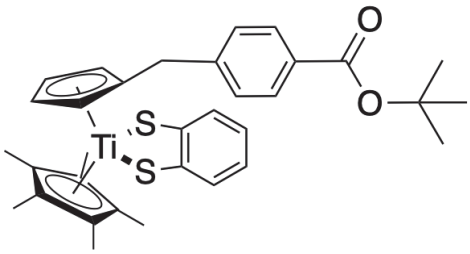

Chemical Formula: $C_{33}H_{38}S_2O_2Ti$

Exact Mass: 578.18

In a two-necked round bottom flask under Ar atmosphere and equipped with a magnetic stir-bar, compound **39** (1 Equiv., 250 mg) was added and dissolved in dry THF (resulting solution 0.5 M). Then Et_3N (2.2 Equiv., 0.95 mmol) and 1,2 benzendithiole (1.2 Equiv., 0.52 mmol) were added inside the flask. The reaction mixture was stirred for 6h and was checked with TLC (AcOEt/Hexane 3:7) to observe the product formation. It was observed the complete conversion of starting material and it is remarkable that the color of the resulting solution turned from red to dark-green. Then, the solvent was evaporated under vacuum obtaining the crude product. This crude was purified by flash chromatography [gradient of DCM/Hexane: (1:9)

> (4:6) > (1:1) > (1:0)] to afford the corresponding dithiolic product **35** with an isolated yield of 70%.

MS (HESI): 579.24 ($M+H^+$), 601.24 ($M+Na^+$)

^{1}H-NMR (CD_2Cl_2): 300 MHz δ (ppm)= 7.85 (dd, J = 8.4, 1.7 Hz, 2H), 7.43 (dd, J = 5.9, 3.4 Hz, 2H), 7.11 (td, J = 6.1, 2.7 Hz, 4H), 5.67 (t, J = 2.6 Hz, 2H), 5.29 (t, J = 2.6 Hz, 2H), 3.60 (s, 2H), 2.07 (d, J = 1.3 Hz, 15H), 1.59 (d, J = 1.3 Hz, 9H).

^{13}C-NMR (CD_2Cl_2): 75 MHz δ (ppm)= 166.2, 154.5, 146.8, 131.1, 130.8, 130.1, 129.2, 125.6, 124.6, 113.6, 112.1, 81.4, 37.3, 30.2, 28.7, 13.6.

Synthesis of compound 36

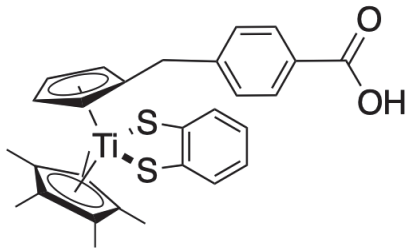

Chemical Formula: $C_{29}H_{30}S_2O_2Ti$

Exact Mass: 521.11

In a two-necked round bottom flask under Ar atmosphere and equipped with a magnetic stir-bar, compound **35** (1.0 Equiv., 60 mg, 0.10 mmol) was added and dissolved in DCM dry (1.5 mL). The resulting solution was cooled to 0°C and TFA (30 Equiv., 3.13 mmol, 239 μL) was added. Then the temperature was increased to 4°C and left under stirring overnight. The proceeding of the reaction was checked by TLC [AcOEt:Hexane 7:3]: at the completion, the reaction mixture was evaporated to dryness. Then DCM was added together with 1 Equiv. of 1,2 benzendithiole and 2 Equiv. of Et_3N. The solution was evaporated and resolubilized in DCM and re-evaporated for 5 times until the green color was persistent. The so obtainied crude was purified by liquid chromatography [gradient of AcOEt/Hexane: (3:7) > (1:1) > (1:0)] to afford the product **36** with an isolated yield of 56%.

MS (HESI): 522.44 ($M+H^+$)

^{1}H-NMR (CD_2Cl_2): 400 MHz δ (ppm)= 7.84 (d, J = 8.3 Hz, 2H), 7.31 (dd, J = 5.9, 3.4 Hz, 2H), 7.07 (d, J = 8.1 Hz, 2H), 6.98 (dd, J = 5.9, 3.4 Hz, 2H), 5.56 (t, J = 2.6 Hz, 2H), 5.16 (t, J = 2.6 Hz, 2H), 3.50 (s, 2H), 1.94 (s, 15H). The acidic proton signal was not detected.

^{13}C-NMR (CD_2Cl_2): 101 MHz δ (ppm)= 153.6, 147.7, 130.1, 130.1, 128.8, 124.9, 123.8, 112.8, 111.1, 36.6, 12.8, 12.2.

Synthesis of compound 37

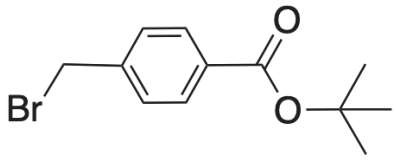

Chemical Formula: $C_{12}H_{15}BrO_2$

Exact Mass: 270.03

In a two-necked round bottom flask under Ar atmosphere and equipped with a magnetic stir-bar, 4-(bromomethyl)benzoic acid (1.0 Equiv., 1120 mg, 5.05 mmol) was added and dissolved in a mixture of ciclohexane (9 mL), CH_2Cl_2 (5mL) and THF (10 mL). A solution of *tert*-butyl 2,2,2-trichloroacetimidate (2.0 Equiv. 10.1 mmol, 3.3 M in ciclohexane) was added via cannula and then catalytic BF_3Et_2O was added. The reaction mixture was stirred at room temperature for 18 h. The reaction mixture was quenched with 1g of $NaHCO_3$, filtered and concentrated under vacuum obtaining the crude product. This crude was purified by liquid chromatography (9:1 AcOEt:Hexane as eluent, $Rf_{product}$: 0.47) to afford the product **37** with an isolated yield of 79%.

The spectroscopic data collected in our synthesis match perfectly those reported in literature.[11]

Synthesis of compound 38

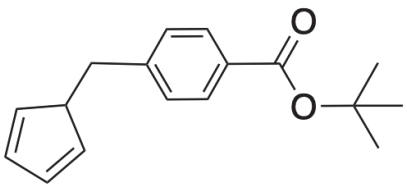

Chemical Formula: $C_{17}H_{20}O_2$

Exact Mass: 256.15

In a two-necked round bottom flask under Ar atmosphere and equipped with a magnetic stir-bar, 4.8 mL of a solution of CpNa 0.8 M in THF was added. The reaction mixture was cooled to -78°C and compound **37** (1.1 Equiv., 1168 mg, 4.3 mmol) dissolved in dry THF (9 mL) was added via cannula. The resulting mixture was covered with an alu foil and allowed to warm to room temperature and react for 2 h. Reaction was monitored with TLC (AcOEt:Hexane 2:8) to observe the complete conversion of the starting material. The reaction mixture was quenched with a satured solution NH_4Cl then Hexane (5 mL was added). Layers were separated in a separatory funnel and the aqueous layer was extracted three times with Et_2O (3x30 mL). Combined organic layers were dried over Na_2SO_4, filtered and concentrated under vacuum obtaining the crude product. This crude was purified by flash chromatography (2:98 AcOEt:Hexane as eluent) to afford the product **38** with an isolated yield of 76%.

MS (HESI): 257.45 ($M+H^+$)

^{1}H-NMR ($CDCl_3$): 400 MHz δ (ppm)= 7.89 - 7.78 (m, 2H), 7.21 - 7.07 (m, 2H), 6.31 (tq, J = 5.3, 1.7 Hz, 1H), 6.27 (dq, J = 5.1, 1.5 Hz, 0.5H), 6.17 (dq, J = 5.5, 1.5 Hz, 0.5H), 6.06 (p, J = 1.4 Hz, 0.5H), 5.94 - 5.87 (m, 0.5H), 3.75 - 3.59 (m, 2H), 2.88 (h, J = 1.6 Hz, 1H), 2.73 (q, J = 1.5 Hz, 1H), 1.49 (d, J- = 1.2 Hz, 9H).

^{13}C-NMR ($CDCl_3$): 101 MHz δ (ppm)= 165.8, 147.3, 145.8, 145.1, 145.1, 134.3, 132.3, 131.7, 129.9, 129.6, 128.7, 128.6, 128.5, 127.9, 80.7, 43.1, 41.4, 37.4, 36.4, 28.2, 28.1.

Synthesis of compound 39

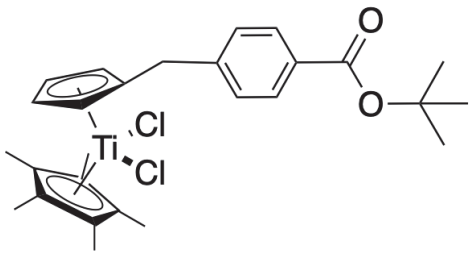

Chemical Formula: $C_{27}H_{34}Cl_2O_2Ti$

Exact Mass: 508.14

In a two-necked round bottom flask under Ar atmosphere and equipped with a magnetic stir-bar, compound **38** (1.0 Equiv., 152 mg, 0.593 mmol) was added and dissolved in dry THF (1 mL). The reaction mixture was cooled to -78°C and *t*-BuLi (1.05 Equiv. 0.37 mL, 1.7 M) was added dropwise. The reaction mixture was stirred for 1h at room temperature. A solution 0.85 M of Cp*$TiCl_3$ (0.77 Equiv. 136 mg) in THF was added via cannula and reaction mixture was stirred for 16h at -30°C. The solvent was evaporated by vacuum obtaining the crude product. This crude was purified by liquid chromatography (gradient 1:9 to 2:8 AcOEt:Hexane as eluent) to afford the product **39** with an isolated yield of 62%.

MS (HESI): 509.87 ($M+H^+$), 531.87 ($M+Na^+$)

^{1}H-NMR (CD_2Cl_2): 400 MHz δ (ppm)= 7.78 (d, J = 8.3 Hz, 2H), 7.19 (d, J = 8.4 Hz, 2H), 5.97 (t, J = 2.7 Hz, 2H), 5.92 (d, J = 2.7 Hz, 2H), 3.97 (s, 2H), 1.94 (s, 15H), 1.47 (s, 9H).

^{13}C-NMR (CD_2Cl_2): 101 MHz δ (ppm)= 170.8, 165.4, 145.5, 135.1, 130.2, 129.9, 129.7, 129.5, 128.8, 123.3, 122.5, 115.8, 115.1, 80.6, 60.2, 41.5, 36.8, 29.4, 27.9, 20.8, 14.0, 13.3.

Synthesis of compound 40

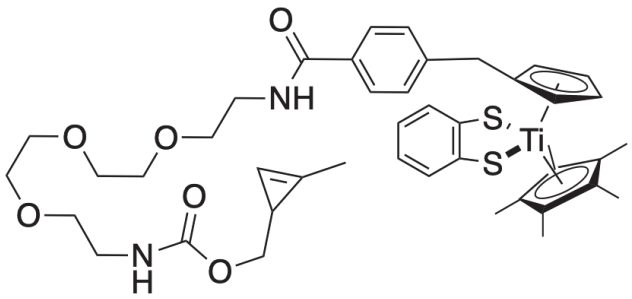

Chemical Formula: $C_{43}H_{54}N_2O_6S_2Ti$

Exact Mass: 806.29

In a two-necked round bottom flask under Ar atmosphere and equipped with a magnetic stir-bar, compound **36** (1 Equiv., 11 mg, 0.021 mmol) was added and dissolved in DCM dry (resulting solution 0.03 M). The resulting solution was cooled down to 0°C and methylcyclopropene-PEG3-amine hydrochloride (1.6 Equiv., 10 mg, 0.033 mmol) was added, followed by EDCI (1.6 Equiv., 6.4 mg, 0.033 mmol), HOBt (1.5 Equiv., 4.4 mg, 0.032 mmol) and Et_3N (2 Equiv., 6 μL, 0.066 mmol). The solution was then allowed to reach room temperature and the stirring was maintained for 3-4 hours. After a TLC control (DCM/MeOH, 97:3) to check the formation of the product, the solvent was removed with rotatory evaporation and the crude obtained was quickly purified by flash chromatography [3:97 MeOH/DCM; $Rf_{product}$: 0.60] to afford the corresponding clicked product **40** with an isolated yield of 59%.

MS (HESI): 829.39 ($M+Na^+$)

^{1}H-NMR (CD_2Cl_2): 400 MHz δ (ppm)= 7.89 - 6.42 (m, 12H), 5.63 - 4.64 (m, 6H), 3.86 - 3.10 (m, 13H), 2.14 (m, 1H), 1.94 (s, 15H), 1.82 - 0.14 (m, 5H).-

^{13}C-NMR (CD_2Cl_2): 101 MHz δ (ppm)= 153.7, 147.3, 130.4, 130.1, 128.8, 128.7, 127.0, 124.9, 124.8, 123.8, 123.8, 112.8, 111.3, 111.2, 70.4, 70.3, 70.2, 70.2, 70.0, 70.0, 69.7, 69.7, 39.7, 36.6, 36.4, 12.8.

Synthesis of compound 41

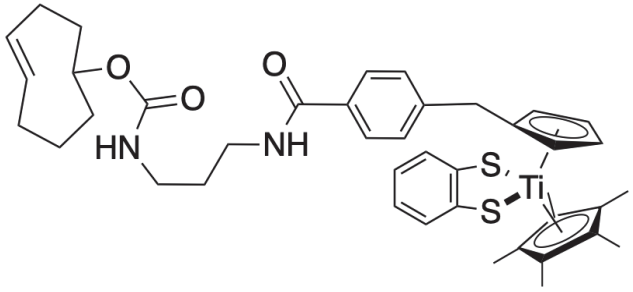

Chemical Formula: $C_{41}H_{50}N_2O_3S_2Ti$

Exact Mass: 730.27

In a two-necked round bottom flask under Ar atmosphere and equipped with a magnetic stir-bar, compound **36** (1 Equiv., 13 mg, 0.024 mmol) was added and dissolved in DCM dry (resulting solution 0.03 M). The resulting solution was cooled down to 0°C and *trans*-cyclooctene-amine hydrochloride (1.6 Equiv., 10 mg, 0.038 mmol) was added, followed by EDCI (1.6 Equiv., 7 mg, 0.037 mmol), HOBt (1.5 Equiv., 5 mg, 0.036 mmol) and Et_3N (2 Equiv., 8 μL, 0.048 mmol). The solution was then allowed to reach room temperature and the stirring was maintained for 3-4 hours. After a reverse phase TLC control (MeCN/MeOH, 8:2) to check the formation of the product, the solvent was removed with rotatory evaporation and the crude obtained was quickly purified by reverse phase flash chromatography [2:8 MeOH/MeCN; $Rf_{product}$: 0.48] to afford the corresponding clicked product **41** with an isolated yield of 98%.

MS (HESI): 731.33 ($M+H^+$), 753.42 ($M+Na^+$)

^{1}H-NMR (CD_2Cl_2): 300 MHz δ (ppm)= 7.68 (d, J = 8.0 Hz, 2H), 7.42 (dd, J = 5.9, 3.4 Hz, 2H), 7.20 - 7.05 (m, 4H), 5.78 - 5.45 (m, 3H), 5.41 - 5.32 (m, 4H), 5.12 (s, 1H), 4.33 (d, J = 8.8 Hz, 1H), 3.59 (s, 2H), 3.46 (d, J = 9.6 Hz, 2H), 3.23 (s, 3H), 2.35 (d, J = 4.4 Hz, 4H), 2.04 (d, J- = 15.7 Hz, 17H), 1.76 - 1.57 (m, 2H), 1.34 - 1.23 (m, 3H).

^{13}C-NMR (CD_2Cl_2): 75 MHz δ (ppm)= 167.6, 154.4, 145.6, 135.7, 133.6, 133.3, 131.2, 130.8, 130.5, 130.5, 130.4, 129.5, 127.7, 125.6, 124.5, 113.6, 111.9, 81.3, 76.8,

61.0, 44.4, 41.8, 39.4, 38.1, 37.2, 36.7, 34.9, 34.7, 33.3, 32.4, 31.7, 30.9, 26.3, 25.6, 23.4, 23.1, 14.8, 14.6, 13.6, 2.5.

Synthesis of compound 42

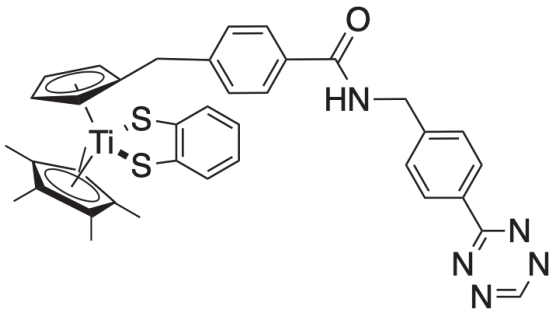

Chemical Formula: $C_{38}H_{37}N_5OS_2Ti$

Exact Mass: 691.19

In a two-necked round bottom flask under Ar atmosphere and equipped with a magnetic stir-bar, compound **36** (1 Equiv., 13 mg, 0.024 mmol) was added and dissolved in DCM dry (resulting solution 0.03 M). The resulting solution was cooled down to 0°C and [4-(1,2,4,5-tetrazin-3-yl)phenyl]methanamine hydrochloride (1.6 Equiv., 8 mg, 0.039 mmol) was added, followed by EDCI (1.6 Equiv., 8 mg, 0.039 mmol), HOBt (1.5 Equiv., 5 mg, 0.037 mmol) and Et_3N (2 Equiv., 8 μL, 0.048 mmol). The solution was then allowed to reach room temperature and the stirring was maintained for 3-4 hours. After a TLC control (DCM/EtOAc, 9:1) to check the formation of the product, the solvent was removed with rotatory evaporation and the crude obtained was quickly purified by flash chromatography [1:9 EtOAc/DCM; $Rf_{product}$: 0.57] to afford the corresponding clicked product **42** with an isolated yield of 88%.

MS (HESI): 692.23 ($M+H^+$)

^{1}H-NMR (CD_2Cl_2): 300 MHz δ (ppm)= 10.25 (s, 1H), 8.61 (d, J = 8.3 Hz, 2H), 7.70 (d, J = 8.2 Hz, 2H), 7.61 (d, J = 8.3 Hz, 2H), 7.43 (dd, J = 5.9, 3.4 Hz, 2H), 7.17 (d, J = 8.2 Hz, 2H), 7.09 (dd, J = 5.9, 3.4 Hz, 2H), 6.63 (t, J = 4.1 Hz, 1H),

5.67 (t, J = 2.5 Hz, 2H), 5.29 (t, J = 2.5 Hz, 2H), 4.75 (d, J = 5.9 Hz, 2H), 3.60 (s, 2H), 2.06 (s, 15H).

^{13}C-NMR (CD_2Cl_2): 75 MHz δ (ppm)= 167.7, 167.1, 158.7, 154.4, 146.0, 145.0, 132.8, 131.6, 131.1, 130.8, 129.6, 129.2, 129.1, 127.8, 125.6, 124.5, 113.5, 111.9, 44.2, 37.2, 13.6.

Synthesis of compound 43

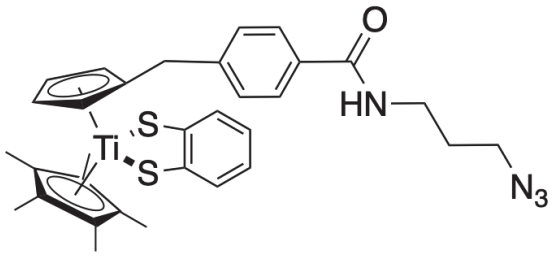

Chemical Formula: $C_{32}H_{36}N_4OS_2Ti$

Exact Mass: 604.18

In a two-necked round bottom flask under Ar atmosphere and equipped with a magnetic stir-bar, compound **36** (1 Equiv., 50 mg, 0.096 mmol) was added and dissolved in DCM dry (resulting solution 0.03 M). The resulting solution was cooled down to 0°C and 3-azidopropanamine (1.6 Equiv., 16 mg, 0.154 mmol) was added, followed by EDCI (1.6 Equiv., 29 mg, 0.150 mmol), HOBt (1.5 Equiv., 20 mg, 0.144 mmol) and Et_3N (1 Equiv., 16 μL, 0.096 mmol). The solution was then allowed to reach room temperature and the stirring was maintained for 3-4 hours. After a TLC control (DCM/EtOAc, 9:1) to check the formation of the product, the solvent was removed with rotatory evaporation and the crude obtained was quickly purified by flash chromatography [1:9 EtOAc/DCM; $Rf_{product}$: 0.5] to afford the corresponding clicked product **43** with an isolated yield of 51%.

MS (HESI): 605.31 ($M+H^+$), 627.30 ($M+Na^+$)

^{1}H-NMR (CD_2Cl_2): 300 MHz δ (ppm)= 7.62 (d, J = 8.2 Hz, 2H), 7.42 (dd, J = 5.9, 3.4 Hz, 2H), 7.18 - 7.03 (m, 4H), 6.37 (s, 1H), 5.67 (t, J = 2.6 Hz, 2H), 5.28 (t,

J = 2.6 Hz, 2H), 3.58 (s, 2H), 3.55 - 3.36 (m, 4H), 2.06 (s, 15H), 1.88 (t, J = 6.7 Hz, 2H).

^{13}C-NMR (CD_2Cl_2): 75 MHz δ (ppm)= 167.7, 154.4, 145.7, 133.2, 131.1, 130.8, 129.5, 127.6, 125.6, 124.5, 113.5, 111.9, 50.3, 38.3, 37.2, 29.6, 13.6.

Synthesis of compound 44-(*endo*) and 45-(*exo*)

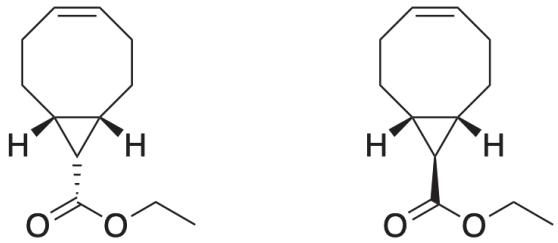

44-*endo* **45-*exo***

Chemical Formula: $C_{12}H_{18}O_2$

Exact Mass: 194.13

In a two-necked round bottom flask under Ar atmosphere and equipped with a magnetic stir-bar, 1,5-cyclooctadyene (8.0 Equiv., 7580 mg, 70.08 mmol) was added and cooled to 0°C. In a second round bottom flask ethyl diazoacetate (1.0 Equiv., 8.76 mmol, 922 μL), $Rh_2(OAc)_4$ (0.045 Equiv., 0.39 mmol, 174 mg) were added under Ar atmosphere and solubilized in DCM dry (5.15 mL). The resulting mixture was transferred dropwise in the first balloon by assuring a continuous stirring. Once the addition was completed, the resulting mixture was left under stirring at room temperature for 72 h. The reaction was followed with TLC [Hexane:AcOEt (95:5)]. The reaction was then filtered through a silica gel pad and evaporated to dryness. This crude was purified by liquid chromatography (gradient 1:99 to 2:98 AcOEt:Hexane as eluent, $Rf_{endo} = 0.65$, $Rf_{exo} = 0.5$) to afford the products **44-*endo*** and **45-*exo*** with isolated yields of 30% and 45%, respectively.

The spectroscopic data collected in our synthesis match perfectly those reported in literature.[12]

Synthesis of compound 46

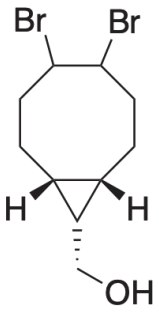

Chemical Formula: $C_{10}H_{16}Br_2O$

Exact Mass: 309.95

In a two-necked round bottom flask under Ar atmosphere and equipped with a magnetic stir-bar, compound **44** (1.0 Equiv., 377 mg, 1.94 mmol) was dissolved in dry Et_2O (6.5 mL) and a suspension of $LiAlH_4$ (1.03 Equiv., 1.99 mmol, 76 mg) in Et_2O (6.5 mL) was added dropwise at 0°C. The so obtained mixture was stirred at room temperature for 15 minutes and then was cooled again to 0°C. Water was added until a white precipitating solid was formed. The mixture was then dried over Na_2SO_4, filtrated and evaporated till dryness by obtaining the alcohol-derivative. This compound was then directly involved in the next step without further purifications. Specifically, it was placed in a new round bottom flask under Ar atmosphere and equipped with a magnetic stir-bar and a solution of bromine (1.3 Equiv., 2.52 mmol, 130 μL) in DCM dry (2 mL) was added dropwise until the solution color was a persistent yellow. The reaction was then quenched with an aqueous solution of $Na_2S_2O_3$ (10%) and transferred in a separating funnel where it was extracted three times with DCM. Combined organic layers were dried over Na_2SO_4, filtered and concentrated under vacuum obtaining the crude dibromide-product which was directly involved in the next step without further purifications.

Synthesis of compound 47

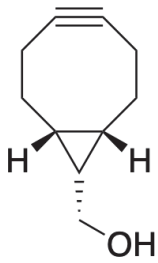

Chemical Formula: $C_{10}H_{14}O$

Exact Mass: 150.10

The unpurified product **46** was placed in a new round bottom flask under Ar atmosphere and equipped with a magnetic stir-bar and solubilized in THF dry (20 mL). Potassium *tert*-butoxide (1M solution in THF) was added dropwise and the resulting mixture was refluxed for 2 h at 75°C. The reaction mixture was then quenched by the addition of a saturated solution of NH_4Cl (50 mL) and it was extracted three times with DCM. The combined organic layers were dried over Na_2SO_4, filtered and concentrated under vacuum obtaining the crude cyclooctyne-product which was purified though flash chromatography [AcOEt:Hexane (2:8)]. The purified product **47** was obtained with an isolated yield of 28%.

The spectroscopic data collected in our synthesis match perfectly those reported in literature.[12]

Synthesis of compound 48

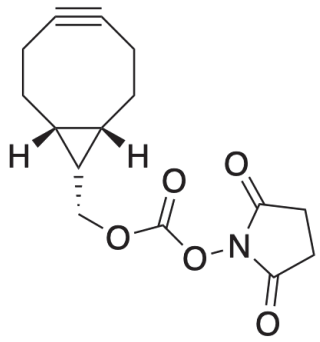

Chemical Formula: $C_{15}H_{17}NO_5$

Exact Mass: 291.11

In a two-necked round bottom flask under Ar atmosphere and equipped with a magnetic stir-bar, compound **47** (1.0 Equiv. 0.53 mmol, 80 mg) and *N,N'*-Disuccinimidyl carbonate (2.0 Equiv., 1.06 mmol, 273 mg) were added and dissolved in MeCN dry (15 mL). Triethylamine (3.0 Equiv., 1.60 mmol, 225 μL) was then added dropwise and the so obtained mixture was left under stirring at room temperature overnight. The reaction was checked through TLC [AcOEt:Hexane (3:7)] and the workup was operated by evaporating the reaction mixture to dryness. The residue was purified by flash chromatography [AcOEt:Hexane (3:7)] and the purified product **48** was obtained with an isolated yield of 98%.

The spectroscopic data collected in our synthesis match perfectly those reported in literature.[12]

Synthesis of compound 49

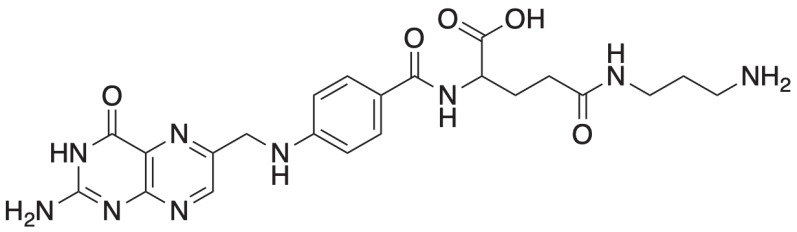

Chemical Formula: $C_{22}H_{27}N_9O_5$

Exact Mass: 497.21

In a two-necked round bottom flask under Ar atmosphere and equipped with a magnetic stir-bar, folic acid (1 Equiv., 1.34 mmol, 640 mg) was added and solubilized in dry DMSO (25 mL) by increasing the temperature to 38°C (30 minutes are required). Subsequently, DCC (2 Equiv., 2.86 mmol, 522 mg) was added and left for 2 hours at room temperature. NHS (2 Equiv., 2.86 mmol, 308 mg) and DMAP (0.5 Equiv., 0.67 mmol) were added and the resulting mixture was left overnight at 40°C under continuous stirring. The resulting DCU precipitate was filtered away and the filtrate concentrated under vacuum. Thus, the NHS-activated product was precipitated by dropwise addition of the product concentrated solution into a pre-cooled solution of Acetone/Et_2O (3:7) and followed by filtration. The purification of the precipitate was achieved through washing with the mixture Acetone/Et_2O (3:7) solution and then pure Et_2O. The so obtained filtered product was dried under vacuum and readily involved in the next step of the reaction.

In a new two-necked round bottom flask under Ar atmosphere and equipped with a magnetic stir-bar, 1,3-propanediamine (2 Equiv., 2.68 mmol, 176 μL) and Et_3N (2 Equiv., 2.68 mmol, 376 μL) were dissolved in 5 mL of DMSO. The previously obtained NHS-activated folic acid was added and the so obtained mixture was left under stirring at room temperature overnight. After that, a mixture of 20% of Acetone in Et_2O was added, followed by the rapid formation of a yellow precipitate, which was carefully washed with Acetone/Et_2O (1:1), centrifuged and dried under vacuum overnight to obtain the product **49** with an isolated yield of 73%.

The spectroscopic data collected in our synthesis match perfectly those reported in literature.[13]

Synthesis of compound 50

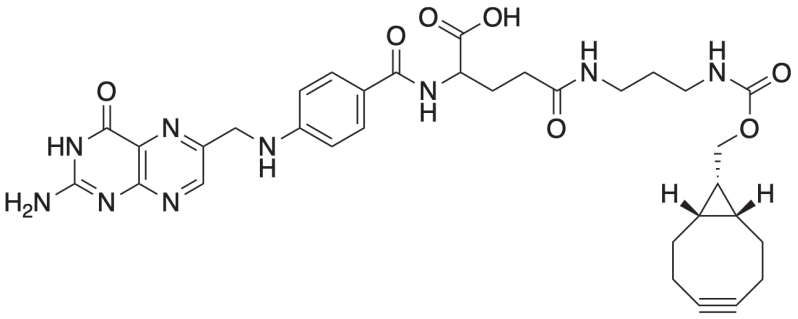

Chemical Formula: $C_{33}H_{39}N_9O_7$

Exact Mass: 673.30

In a two-necked round bottom flask under Ar atmosphere and equipped with a magnetic stir-bar, compound **49** (1 Equiv. 0.280 mmol, 139 mg) and product **48** (1.4 Equiv., 0.392 mmol, 75 mg) were added and followed by DIPEA (4 Equiv., 1.12 mmol, 192 μL) and solubilize in dry DMSO (2.8 mL). The resulting mixture was stirred for 30 minutes until obtaining a clear solution. Thus, the solution was poured in a mixture of 20% of Acetone in Et_2O, with the concomitant formation of a yellow precipitate, which was carefully washed with Acetone/Et_2O (1:1), centrifuged and dried under vacuum overnight to obtain the product **50** with an isolated yield of 73%.

MS (HESI): 674.35 ($M+H^+$), 696.28 ($M+Na^+$)

^{1}H-NMR (DMSO): 300 MHz δ (ppm)= 8.64 (s, 1H), 8.29 (s, 1H), 8.18 - 7.65 (m, 6H), 7.06 (m, 3H), 6.76 - 6.63 (m, 4H), 4.49 (d, J = 4.9 Hz, 1H), 4.34 (d, J = 6.6 Hz, 2H), 4.02 (d, J = 7.8 Hz, 3H), 3.05 - 2.70 (m, 3H), 2.22 - 1.85 (m, 8H), 1.51 (m, 4H), 1.25 (m, 1H), 0.85 (t, J = 9.2 Hz, 2H).

^{13}C-NMR (DMSO): 75 MHz δ (ppm)= 171.7, 166.1, 166.0, 156.4, 153.8, 150.7, 149.2, 148.4, 129.0, 128.6, 127.9, 123.2, 121.5, 118.3, 111.9, 111.1, 109.7, 98.9, 61.3, 53.3, 45.9, 38.0, 37.8, 36.2, 32.1, 31.1, 29.7, 29.5, 28.6, 27.7, 20.8, 19.5, 17.6.

Synthesis of compound 51

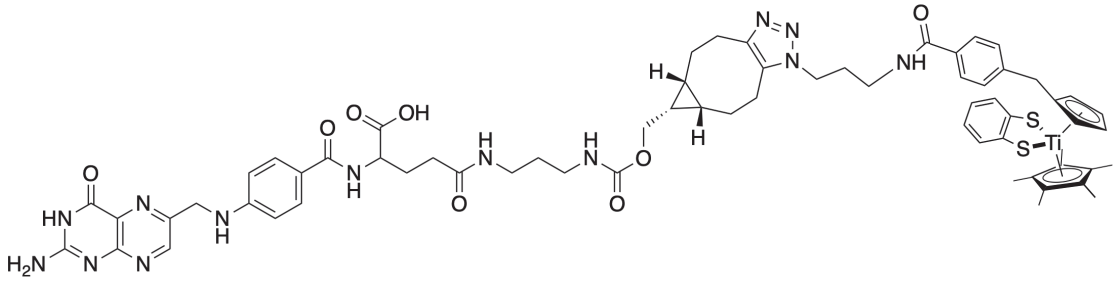

Chemical Formula: $C_{65}H_{75}N_{13}O_8S_2Ti$

Exact Mass: 1277.48

In a two-necked round bottom flask under Ar atmosphere and equipped with a magnetic stir-bar, compound **50** (1 Equiv., 0.024 mmol, 17 mg) was added and solubilized in dry DMSO (240 μL), followed by the addition of product **43** (2 Equiv., 0.048 mmol, 29 mg). The so obtained mixture was then stirred at room temperature for 48 hours. Thus, it was quenched by pouring it in a mixture of 20% of Acetone in Et_2O. A brown precipitate was observed: it was filtered and washed with Acetone/Et_2O (1:1), centrifuged and dried under vacuum overnight to obtain the product **51** with an isolated yield of 69%.

MS (HESI): 1278.52 ($M+H^+$)

^{1}H-NMR (DMSO): 300 MHz δ (ppm)= 8.64 (s, 1H), 8.37 (m, 1H), 8.00 (d, J = 8.0 Hz, 1H), 7.83 - 7.78 (m, 2H), 7.67 (d, J = 7.9 Hz, 3H), 7.43 - 7.32 (m, 2H), 7.10 - 7.04 (m, 4H), 6.92 (m, 1H), 6.41 (d, J = 8.0 Hz, 1H), 5.70 (s, 2H), 5.36 (s, 2H), 4.49 - 4.47 (m, 2H), 4.28 - 4.24 (m, 3H), 4.04 - 4.01 (m, 2H), 3.46 (s, 2H), 3.27 - 3.24 (m, 3H), 3.03 - 2.95 (m, 9H), 2.75 - 2.69 (m, 3H), 2.09 (s, 4H), 1.99 (s, 15H), 1.51 (m, 6H), 1.25 - 0.90 (m, 6H).

^{13}C-NMR (DMSO): 75 MHz δ (ppm)= 171.8, 171.7, 166.1, 156.4, 153.8, 153.3, 150.7, 148.5, 144.2, 143.4, 134.3, 132.8, 132.2, 130.1, 129.6, 129.0, 128.5, 128.4, 128.2, 128.1, 127.9, 127.2, 124.7, 123.6, 121.5, 113.1, 111.6, 111.1, 82.1, 61.3, 45.9, 45.2, 40.9, 38.0, 37.9, 37.8, 36.7, 36.2, 35.8, 32.1, 30.7, 29.4, 25.4, 22.1, 21.8, 21.2, 19.1, 18.6, 17.3, 12.7.

Synthesis of compound 52

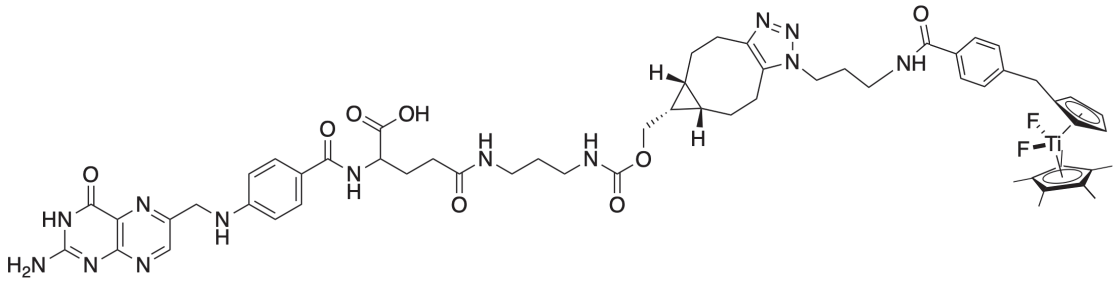

Chemical Formula: $C_{59}H_{71}F_2N_{13}O_8Ti$

Exact Mass: 1175.50

In a Teflon vial equipped with a magnetic stir-bar under Ar atmosphere and equipped with a magnetic stir-bar, product **51** (1 Equiv., 0.018 mmol, 23 mg) was added and solubilized in DMSO (180 μL). Crystals of Xenon difluoride [XeF_2] (1 Equiv., 0.018 mmol, 5 mg) were added. Suddenly, the color of the solution changed, turning from dark-brown to a yellowish-orange color. The reaction mixture was stirred for other 15 minutes at room temperature before to be poured in a mixture of 20% of Acetone in Et_2O, with the formation of a precipitate. It was then carefully washed with Acetone/Et_2O (1:1), centrifuged and dried under vacuum overnight to obtain the product **52** with a quantitative yield.

MS (HESI): 1176.51 ($M+H^+$)

Computational details

All structures were optimized with the Gaussian 09 program package,[14] using the B3LYP functional at the 6-31G(d) level for all the atoms, but for Titanium and Xenon, for which the effective core potential LanL2DZ was used. All the optimizations were performed in vacuo. With the optimized geometries, single-point energy calculations in THF or cloroform were performed using PCM continuum solvent model and differentiated basis sets: 6-311+G(d,p) for C, H and F, and 6-311+G(2df,p) for S and Cl. For Ti and Xe LanL2DZ was maintained. In the reaction with XeF_2 both restricted and unrestricted calculations were performed. Frequency calculations were performed for each species in order to confirm the effective minimum or transition state nature of the optimized structures. Intrinsic reaction coordinate (IRC) calculations were performed to connect the transition states with the corresponding reactants and products. For the open-shell structures the stability of the wavefunction was always checked, optimizing it when found unstable.

All data reported, are referred to this level of theory and the discussions are based on the values of (E) and activation (E_{att}) relative energies in kcal/mol, summed with the zero-point correction to energy of each species.

References

[1] Chen, J.; Kai, Y.; Kasai, N. Steric effect of allyl substituent on the molecular structures of allyltitanium complexes. *Journal of Organometallic Chemistry*, **1991**, *407*, 191-205.

[2] Gassman, P. G.; Campbell, W. H.; Macomber, D. W. An unusual relationship between ^{49}Ti chemical shift and Ti(2p3/2) binding energy. The use of ^{49}Ti NMR in evaluating the electronic effect of methyl substitution on the cyclopentadienyl ligand. *Organometallics*, **1984**, *3*, 385-387.

[3] Neef, A. B.; Schultz, C., Selective Fluorescence Labeling of Lipids in Living Cells. *Angew. Chem. Int. Ed.*, **2009**, *48*, 1498-1500.

[4] Posner, G. H.; Ting, J. S.; Lentz, M., A mechanistic and synthetic study of organocopper substitution reactions with some homo allylic and cyclopropylcarbinyl substrates application to isoprenoid synthesis. *Tetrahedron*, **1976**, *32*, 2281-2287.

[5] Watson, K. J.; Nguyen, S. T.; Mirkin, C. A., The synthesis and ring-opening metathesis polymerisation of an amphiphilic redox-active norbornene. *Journal of Organometallic Chemistry*, **2000**, *606*, 79-83.

[6] Greene, L. E.; Lincoln, R.; Cosa, G., Rate of Lipid Peroxyl Radical Production during Cellular Homeostasis Unraveled via Fluorescence Imaging. *J. Am. Chem. Soc.*, **2017**, *139*, 15801-15811.

[7] Hansen, A. M.; Sewell, A. L.; Pedersen, R. H.; Long, D.; Gadegaard, N.; Marqueza, R., Tunable BODIPY derivatives amenable to 'click' and peptide chemistry, *Tetrahedron*, **2013**, *69*, 8527-8533.

[8] Sorkin, M. R.; Walker, J. A.; Brown, J. S.; Alabi, C. A., Versatile Platform for the Synthesis of Orthogonally Cleavable Heteromultifunctional Cross-Linkers, *Bioconjugate Chem.*, **2017**, *28*, 907-912.

[9] Willems, L. I.; Li, N.; Florea, B. I.; Ruben, M; van der Marel, G. A.; Overkleeft, H. S., Triple Bioorthogonal Ligation Strategy for Simultaneous Labeling of Multiple Enzymatic Activities. *Angew. Chem., Int. Ed.*, **2012**, *51*, 4431-4434.

[10] P. Vachal, J. J. Hale, Z. Lu, E. C. Streckfuss, S. G. Mills, M. MacCoss, D. H. Yin, K. Algayer, K. Manser, F. Kesisoglou, S. Ghosh, L. L. Alani, Synthesis and Study of Alendronate Derivatives as Potential Prodrugs of Alendronate Sodium for the Treatment of Low Bone Density and Osteoporosis. *J. Med. Chem.*, **2006**, *49*, 3060-3063.

[11] Tayama, E.; Kimura, H., Asymmetric Sommelet-Hauser Rearrangement of *N*-Benzylic Ammonium Salts, *Angew. Chem. Int. Ed.*, **2007**, *46*, 8869-8871.

[12] DeForest, C.; Tirrell, D., *Nature Materials*, NMAT4219, Method S1.

[13] Pinhassi, R. I.; Assaraf, Y. G.; Farber, S.; Stark, M.; Ickowicz, D.; Drori, S.; Domb, A. J.; Livney, Y. D., Arabinogalactan-Folic Acid-Drug Conjugate for Targeted Delivery and Target-Activated Release of Anticancer Drugs to Folate Receptor-Overexpressing Cells, *Biomacromolecules*, **2010**, *11*, 294-303.

[14] Frisch, M. J.; Trucks, G. W.; Schlegel, H. B.; Scuseria, G. E.; Robb, M. A.; Cheeseman, J. R.; Scalmani, G.; Barone, V.; Mennucci, B.; Petersson, G. A.; Nakatsuji, H.; Caricato, M.; Li, X.; Hratchian, H. P.; Izmaylov, A. F.; Bloino, J.; Zheng, G.; Sonnenberg, J. L.; Hada, M.; Ehara, M.; Toyota, K.; Fukuda, R.; Hasegawa, J.; Ishida, M.; Nakajima, T.; Honda, Y.; Kitao, O.; Nakai, H.; Vreven, T.; Montgomery, J. A., Jr.; Peralta, J. E.; Ogliaro, F.; Bearpark, M.; Heyd, J. J.; Brothers, E.; Kudin, K. N.; Staroverov, V. N.; Keith, T.; Kobayashi, R.; Normand, J.; Raghavachari, K.; Rendell, A.; Burant, J. C.; Iyengar, S. S.; Tomasi, J.; Cossi, M.; Rega, N.; Millam, J. M.; Klene, M.; Knox, J. E.; Cross, J. B.; Bakken, V.; Adamo, C.; Jaramillo, J.; Gomperts, R.; Stratmann, R. E.; Yazyev, O.; Austin, A. J.;

Cammi, R.; Pomelli, C.; Ochterski, J. W.; Martin, R. L.; Morokuma, K.; Zakrzewski, V. G.; Voth, G. A.; Salvador, P.; Dannenberg, J. J.; Dapprich, S.; Daniels, A. D.; Farkas, O.; Foresman, J. B.; Ortiz, J. V.; Cioslowski, J.; Fox, D. J. *Gaussian 09, Revision B.01*; Gaussian, Inc., Wallingford, CT, **2010**.

5.4 Chapter 4

Computational details

All structures were optimized with the Gaussian 09 program package,[1] using the UB3LYP functional at the 6-31G(d) level for all the atoms, but for iron, for which the effective core potential LanL2DZ was used. All the optimization were performed in toluene solvent, using the SMD solvation model. With the optimized geometries, single-point energy calculations in toluene were performed using the all-electron def2-TZVP basis set for all atoms. Dispersion corrections were computed with the Grimme's D3 method. After optimizations, frequency analyses were performed at the UB3LYP/6-31G(d) level (LanL2DZ for iron) to define the optimized structures as minima or transition states. The zero-point energy so determined was added to the def2-TZVP single-point energy to give the electronic energy as reported throughout the manuscript whereas addition of the free energy correction to the single-point energy gives the free energy values. Intrinsic reaction coordinate (IRC) calculations were performed to connect the transition states with the corresponding reactants and products. For the open-shell structures the stability of the wavefunction was always checked, optimizing it when found unstable. For all the species containing iron, the various spin states were investigated.

References

[1] Frisch, M. J.; Trucks, G. W.; Schlegel, H. B.; Scuseria, G. E.; Robb, M. A.; Cheeseman, J. R.; Scalmani, G.; Barone, V.; Mennucci, B.; Petersson, G. A.; Nakatsuji, H.; Caricato, M.; Li, X.; Hratchian, H. P.; Izmaylov, A. F.; Bloino, J.; Zheng, G.; Sonnenberg, J. L.; Hada, M.; Ehara, M.; Toyota, K.; Fukuda, R.; Hasegawa, J.; Ishida, M.; Nakajima, T.; Honda, Y.; Kitao, O.; Nakai, H.; Vreven, T.; Montgomery, J. A., Jr.; Peralta, J. E.; Ogliaro,

F.; Bearpark, M.; Heyd, J. J.; Brothers, E.; Kudin, K. N.; Staroverov, V. N.; Keith, T.; Kobayashi, R.; Normand, J.; Raghavachari, K.; Rendell, A.; Burant, J. C.; Iyengar, S. S.; Tomasi, J.; Cossi, M.; Rega, N.; Millam, J. M.; Klene, M.; Knox, J. E.; Cross, J. B.; Bakken, V.; Adamo, C.; Jaramillo, J.; Gomperts, R.; Stratmann, R. E.; Yazyev, O.; Austin, A. J.; Cammi, R.; Pomelli, C.; Ochterski, J. W.; Martin, R. L.; Morokuma, K.; Zakrzewski, V. G.; Voth, G. A.; Salvador, P.; Dannenberg, J. J.; Dapprich, S.; Daniels, A. D.; Farkas, O.; Foresman, J. B.; Ortiz, J. V.; Cioslowski, J.; Fox, D. J. *Gaussian 09, Revision B.01*; Gaussian, Inc., Wallingford, CT, **2010**.

Chapter 6

APPENDIX II - Cartesian Coordinates and absolute energies

6.1 Chapter 1

(R,R)-ANDEN-Ph [(R,R)-L2] Trost Ligand investigation

Reagents Pro-S-A
b3lyp/6-31g(d) & LanL2DZ,
el. energy = -3883.368902 a.u.

C 1.78662400 2.51818200 -0.55399700
C 2.37904400 1.31644300 0.16344500
O 0.38027700 2.71187100 -0.34255700
C 2.51115300 3.85611000 -0.22439900
C 2.15879600 0.98055900 1.50402900
H 3.32010400 1.01459700 -0.28114900
C 3.18118400 0.19006400 2.27503100
H 1.45919400 1.55360700 2.10723700
H 3.69512300 -0.53881300 1.64765700
H 2.74266500 -0.30640100 3.14182800
H 2.03050200 4.29763500 0.65836700
C 4.01334500 3.75479900 0.08106000
H 2.33720000 4.55120100 -1.05542400
O 4.66838100 2.99413800 -0.94336800
H 5.26696200 2.36970000 -0.49821500
H 0.18412100 2.72416300 0.61655100
H 1.88109100 2.33485700 -1.62634800
H 4.10762100 3.24048000 1.04443300
C 6.32177000 2.13660600 2.94355200
H 6.05416200 2.22077500 3.99804000
H 7.32094500 1.70470900 2.83813600
H 6.34780400 3.13713400 2.49679200
C 5.33309300 1.28481500 2.17683000
O 4.22722800 1.04149200 2.88802000
O 5.53382700 0.88759400 1.03768500
N -1.74054000 1.23478900 -1.64081500
C -2.91293100 1.03919800 -0.80024300
C -2.78250800 1.84693700 0.52068900
N -2.33255900 1.00711300 1.62543900
C -1.40724000 0.29818200 -2.56742100
C -1.29952700 1.35839800 2.43099700
O -0.69808100 2.43613600 2.31000800
O -2.09985900 -0.69416700 -2.80612800
C -0.16808400 0.61389200 -3.37736800
C -0.95124200 0.42582500 3.56810300
C 1.01463200 -0.16196700 -3.33369300
C 2.06257800 0.18702200 -4.20009200
C 1.95244900 1.26028200 -5.08702100
C 0.78743700 2.02210700 -5.11734700
C -0.26409800 1.69601500 -4.26052600
C -0.97024300 1.03404400 4.83118900
C -0.64941500 0.32056100 5.98333000
C -0.27930000 -1.01791400 5.87259300
C -0.23025700 -1.62619300 4.61736900
C -0.56418600 -0.93246400 3.44111400
P 1.26824500 -1.44119300 -2.00140200
P -0.34243300 -1.74419400 1.76602300
C 3.00746500 -2.03257600 -2.31311600
C 0.34907600 -2.93981900 -2.59363600
C -2.08259500 -2.26600300 1.38027900
C 0.44005300 -3.37528300 2.19507500
C -0.27991100 -4.50109100 2.62693000
C 0.37568500 -5.70376600 2.89921600

C 1.75991900 -5.80237500 2.74403200
C 2.48656800 -4.69286800 2.30754500
C 1.83028900 -3.49260700 2.02970700
C -0.33895700 -3.00839400 -3.81218000
C -0.97231400 -4.19179900 -4.20099200
C -0.92561000 -5.32014300 -3.38147400
C -0.24489600 -5.26016100 -2.16265400
C 0.38337900 -4.07852200 -1.77076500
C 3.31773500 -2.91877100 -3.35981400
C 4.63165600 -3.33744800 -3.57236000
C 5.65970500 -2.88172300 -2.74266800
C 5.36499800 -2.00571600 -1.69779400
C 4.04869600 -1.58958900 -1.48491100
C -2.41362800 -2.52139800 0.04033500
C -3.69486200 -2.95596700 -0.30472400
C -4.66787900 -3.12890800 0.68097200
C -4.35643800 -2.86303600 2.01601300
C -3.07245600 -2.43687500 2.36570800
H -1.00297200 1.86998600 -1.31942600
H -2.99098100 -0.02761300 -0.57729200
H -2.02535900 2.62145800 0.41442800
H -2.81333200 0.13144000 1.79565500
H 2.98786700 -0.37658200 -4.17483800
H 2.78503100 1.50122300 -5.74245100
H 0.69590200 2.86711800 -5.79423700
H -1.17662400 2.28579700 -4.26909700
H -1.23385900 2.08537200 4.89414200
H -0.67819400 0.80983400 6.95283400
H -0.01795400 -1.59213500 6.75759000
H 0.08214400 -2.66232900 4.55237100
H -1.35747700 -4.44505600 2.74416400
H -0.19875300 -6.56582300 3.22861800
H 2.26740600 -6.74046200 2.95281600
H 3.56239900 -4.76292400 2.17040000
H 2.39189000 -2.63985400 1.65839300
H -0.39869000 -2.13573200 -4.45188800
H -1.50526400 -4.22670600 -5.14776800
H -1.41894200 -6.23914700 -3.68751100
H -0.20579100 -6.13075800 -1.51311200
H 0.90630000 -4.04315100 -0.81831600
H 2.52952000 -3.28601900 -4.00960300
H 4.85158400 -4.02294800 -4.38693100
H 6.68224200 -3.21012200 -2.91045600
H 6.15088300 -1.63788000 -1.04364400
H 3.83095900 -0.91233700 -0.66879000
H -1.68098100 -2.35829000 -0.74139800
H -3.92789400 -3.13510700 -1.35008900
H -5.66874800 -3.45341900 0.41059400
H -5.11191300 -2.98439900 2.78790600
H -2.84141500 -2.24013400 3.40902200
Pd 1.04144800 -0.48897300 0.23647400
C -4.25882500 1.43691500 -1.51161300
H -4.31321000 0.94235600 -2.48361900
C -4.13682300 2.59062100 0.80789100
H -4.09065400 3.08510200 1.78212200
C -6.18530100 1.25829900 1.70227200
C -7.19515000 0.32685500 1.43090500
C -7.27986700 -0.27128600 0.17240900
C -6.35299300 0.04941200 -0.82710200
C -5.35399600 0.98173900 -0.56212300
C -5.27164300 1.58795200 0.70460800
H -6.12213100 1.72988700 2.68048500
H -7.91832000 0.07440200 2.20203000
H -8.06996900 -0.98847000 -0.03481600
H -6.41445000 -0.42118100 -1.80541300
C -4.31585700 4.96449500 -0.24456000
C -4.40942100 5.73257200 -1.41153000
C -4.45225300 5.11171600 -2.66105200
C -4.40434100 3.71577800 -2.75845400
C -4.32039700 2.95009800 -1.59902200
C -4.27713800 3.57675200 -0.34150900
H -4.27428700 5.44790800 0.72879800
H -4.44641600 6.81645400 -1.34231400
H -4.52343200 5.71368300 -3.56314800
H -4.43835100 3.23138600 -3.73160900
C 4.65318100 5.11677600 0.19363700
C 4.99972500 5.71400600 1.33752500
H 4.81822000 5.62334000 -0.75867900
H 4.81954100 5.18982400 2.27921300
C 5.60995900 7.08272200 1.45365700
H 4.97161100 7.75493800 2.04350100
H 6.58219200 7.04644100 1.96421100
H 5.76121200 7.53819400 0.46916400

Reagents Pro-S-B
b3lyp/6-31g(d) & LanL2DZ,
el. energy = -3883.363760 a.u.

C 1.45927100 2.43716600 -1.52631600
C 2.14037600 1.74903800 -0.34618400
O 0.07196600 2.69104800 -1.29680800
C 2.13438600 3.74253300 -2.01668100
C 1.66334700 1.80846100 0.96602900
H 3.19945500 1.54633000 -0.51241900
C 2.53799400 1.60774600 2.17134300
H 0.72314800 2.31126800 1.15711800
H 3.26699300 0.81054000 2.02277700
H 1.93402000 1.38615200 3.05397500
H 1.54074900 4.06697000 -2.87998900
C 2.22218200 4.91688800 -1.00323900
H 3.14091600 3.52035300 -2.39398700
O 1.06707300 4.91276300 -0.13628200
H 1.32883100 4.73853200 0.78907300
H 0.04568900 3.50615800 -0.74830300
H 1.49274200 1.75342900 -2.37816200
H 2.16188300 5.85189100 -1.57627000
C 3.92103000 4.83064300 3.51904800
H 4.94477100 4.54766600 3.26666500
H 3.72420600 5.86496600 3.23020600
H 3.79992500 4.75055500 4.60611800
C 2.90759000 3.92346000 2.85442200
O 3.43404300 2.72935600 2.56070000
O 1.75362500 4.24989900 2.63624100

N -1.73759000 0.50948900 -1.91664400
C -2.86990600 0.30912100 -1.02223800
C -2.82880700 1.31665300 0.15881700
N -2.33895700 0.68530900 1.37673800
C -1.22959100 -0.53106800 -2.62277500
C -1.65187700 1.41265100 2.30114900
O -1.50542700 2.63053100 2.18841300
O -1.71980500 -1.66397800 -2.61386000
C -0.05662400 -0.20152800 -3.52126800
C -1.10698900 0.69494600 3.51659000
C 1.23964900 -0.74188100 -3.33707200
C 2.22159000 -0.43094300 -4.29069200
C 1.93997800 0.37476100 -5.39681800
C 0.66350400 0.90447600 -5.56616400
C -0.32567500 0.61562900 -4.62557800
C -1.29932100 1.40015600 4.71433900
C -0.83745000 0.90947400 5.93177700
C -0.14619800 -0.30014700 5.95792200
C 0.07880600 -0.99818000 4.77111500
C -0.39065600 -0.53023400 3.52996200
P 1.67611700 -1.62474600 -1.75157000
P 0.05116400 -1.46208000 1.96211200
C 3.50826800 -1.92169600 -1.90196700
C 1.09485900 -3.36756000 -2.01753300
C -1.50109200 -2.45061800 1.69311800
C 1.21830300 -2.76865500 2.59039300
C 0.80803500 -4.03050800 3.04880600
C 1.74726100 -4.97722200 3.46636100
C 3.11035600 -4.67860300 3.43670100
C 3.53233500 -3.42781500 2.97988200
C 2.59457500 -2.48659900 2.55424600
C 0.43643700 -3.80683500 -3.17364300
C 0.05507600 -5.14497600 -3.30422600
C 0.32593000 -6.05937500 -2.28590000
C 0.97972800 -5.62941200 -1.12828600
C 1.35813000 -4.29433000 -0.99431700
C 4.04747900 -2.84864500 -2.81149900
C 5.42470200 -3.05857500 -2.88294300
C 6.28800200 -2.35534400 -2.03837700
C 5.76508200 -1.44495500 -1.11983900
C 4.38548600 -1.23268100 -1.05263500
C -1.77227200 -2.93388400 0.40345000
C -2.91198300 -3.70190200 0.15602800
C -3.79998900 -3.99531900 1.19192700
C -3.54660900 -3.51397300 2.47836600
C -2.40706200 -2.74621400 2.72899400
H -1.18186000 1.36376900 -1.82356900
H -2.80927200 -0.71508500 -0.64852700
H -2.12732900 2.12322100 -0.05591700
H -2.56491800 -0.28389700 1.55755700
H 3.22856200 -0.81188400 -4.16644600
H 2.72509800 0.59038800 -6.11680500
H 0.43661600 1.54124800 -6.41682000
H -1.32412300 1.02810600 -4.74098000
H -1.81036200 2.35582700 4.66219500
H -1.00752600 1.47129800 6.84606600
H 0.22880100 -0.70176800 6.89581600
H 0.63789600 -1.92579800 4.81344300
H -0.24718500 -4.28142000 3.07514800
H 1.40980100 -5.95044000 3.81376400
H 3.83926000 -5.41716600 3.75972900
H 4.59186600 -3.18857000 2.94224900
H 2.92799800 -1.52711200 2.16950500
H 0.20039800 -3.10513100 -3.96482700
H -0.45849000 -5.46878700 -4.20591400
H 0.02669700 -7.09911900 -2.39063000
H 1.19170700 -6.33040400 -0.32520800
H 1.86436200 -3.97309300 -0.08805800
H 3.38683100 -3.41523000 -3.46113600
H 5.82352200 -3.77765500 -3.59386600
H 7.36043400 -2.52395500 -2.09165800
H 6.42806900 -0.90216800 -0.45071900
H 3.97323900 -0.53909000 -0.32639800
H -1.11191100 -2.69347200 -0.42078500
H -3.10361400 -4.04929300 -0.85467500
H -4.69209500 -4.58463400 0.99753300
H -4.23791500 -3.72988300 3.28885900
H -2.22334700 -2.37708700 3.73366500
Pd 1.16123500 -0.23149500 0.17758500
C -4.25760000 0.42961500 -1.75499900
H -4.26698300 -0.22974700 -2.62629000
C -4.24483600 1.98066900 0.32385600
H -4.23718000 2.64133200 1.19384600
C -6.13474800 0.62106200 1.48516100
C -7.02722300 -0.45554400 1.41386600
C -7.04547700 -1.28071000 0.28794800
C -6.17095700 -1.03980200 -0.77868900
C -5.29032100 0.03639100 -0.71323100
C -5.27206200 0.86846000 0.42055500
H -6.11872800 1.26407800 2.36221200
H -7.70865200 -0.64756400 2.23866900
H -7.74205000 -2.11364500 0.23709800
H -6.18083800 -1.68547300 -1.65377000
C -4.64379200 4.10369200 -1.12645600
C -4.81668200 4.64067300 -2.40785800
C -4.81408000 3.80686600 -3.52746900
C -4.63710200 2.42591800 -3.37869600
C -4.47306900 1.88954400 -2.10457000
C -4.47942000 2.72947200 -0.97708200
H -4.63577900 4.75355700 -0.25468500
H -4.95121100 5.71220700 -2.52974900
H -4.94903200 4.23047000 -4.51935900
H -4.63395300 1.77503800 -4.25033800
C 3.53374800 4.92845600 -0.26210300
C 4.38912500 5.95537700 -0.29906700
H 3.80298400 4.02076700 0.27703200
H 4.10509100 6.85108900 -0.85512000
C 5.74276700 5.98918500 0.35113100
H 5.81787000 6.81336600 1.07347600
H 5.96335300 5.05323900 0.87513700
H 6.53306800 6.15469000 -0.39381900

Reagents Pro-R-A
b3lyp/6-31g(d) & LanL2DZ,
el. energy = -3883.368069 a.u.

C 1.70283400 2.40569600 0.68298700
C 2.22327600 1.01130400 0.96783200
C 2.68072300 3.50680300 1.16251800
C 1.78812600 0.32622200 2.10789900
H 3.22011600 0.82042600 0.58761100
C 2.68593400 -0.62079200 2.85533800
H 0.99657000 0.76516100 2.71158600
H 3.48708700 -1.01694800 2.22687100
H 2.13495400 -1.44030700 3.31894900
H 2.94429200 3.30582200 2.21023500
C 3.96350500 3.69917200 0.32942200
H 2.14165100 4.46291200 1.15334900
O 4.74032600 2.50286100 0.19506700
H 4.91989800 2.14310300 1.08413300
C 4.80938000 1.48818600 5.09958100
H 4.84969200 0.75936700 5.91399500
H 5.78635900 1.95133400 4.95409600
H 4.08222000 2.25757000 5.38394100
C 4.36332800 0.82961600 3.81282400
O 3.30302800 0.03921500 4.01900300
O 4.89896600 1.00613000 2.73158900
N -1.23826300 1.61996800 -1.64720100
C -2.50824400 1.48650500 -0.94782000
C -2.38860800 1.92276400 0.53915700
N -2.33205600 0.77211200 1.43263700
C -0.92001100 0.77740000 -2.66318800
C -1.66123800 0.84291100 2.61478600
O -1.12963700 1.88967400 2.99654900
O -1.68550700 -0.08433900 -3.10127900
C 0.43164900 1.02709800 -3.29883100
C -1.61066600 -0.38805100 3.49305400
C 1.52603300 0.13989100 -3.16564900
C 2.71037400 0.44747500 -3.85614400
C 2.81297900 1.58520600 -4.65961800
C 1.72919900 2.45120800 -4.78416600
C 0.54669100 2.16903400 -4.10043900
C -1.85374300 -0.11567100 4.84800700
C -1.80539200 -1.11643800 5.81374400
C -1.48130800 -2.41538900 5.42871300
C -1.21264000 -2.69687900 4.08894700
C -1.27450700 -1.70736300 3.09117400
P 1.44806500 -1.28797600 -1.96792400
P -0.80347400 -2.13903300 1.32877700
C 3.17188500 -1.98588000 -2.05173200
C 0.54489300 -2.60823100 -2.91012100
C -2.48241100 -2.36901300 0.56540600
C -0.20685700 -3.89192300 1.48261700
C -1.04754800 -5.01493700 1.42667700
C -0.51775500 -6.30493000 1.51045300
C 0.85812000 -6.49387400 1.65380900
C 1.70582300 -5.38502800 1.70507100
C 1.17755800 -4.09667500 1.61182900
C 0.02520900 -2.43559200 -4.19972600
C -0.62759700 -3.48878000 -4.84620100
C -0.76702000 -4.72625300 -4.21735500
C -0.25170100 -4.90806200 -2.93136900
C 0.39481100 -3.85689200 -2.28265900
C 3.58951400 -2.83155900 -3.09413200
C 4.89215200 -3.33102200 -3.12671600
C 5.80034800 -2.99532100 -2.11970500
C 5.39826300 -2.15694100 -1.07937100
C 4.09334600 -1.66030600 -1.04564600
C -2.60114300 -2.26571700 -0.82964100
C -3.83825800 -2.43830100 -1.45386800
C -4.97688800 -2.71052100 -0.69396100
C -4.87475600 -2.80847800 0.69544100
C -3.63785600 -2.63988900 1.32237200
H -0.47939000 2.18127400 -1.25383800
H -2.79306400 0.43406100 -1.01058500
H -1.45822800 2.46935800 0.69842400
H -2.88092400 -0.04971500 1.21349900
H 3.57078400 -0.20470200 -3.76063200
H 3.74492300 1.79195000 -5.17869900
H 1.80266800 3.34416000 -5.39866500
H -0.30176600 2.84316300 -4.17877200
H -2.06884100 0.90986300 5.12984300
H -2.00653100 -0.87992800 6.85486400
H -1.42794900 -3.21265900 6.16551600
H -0.94465200 -3.71100200 3.81570600
H -2.11898900 -4.88633900 1.31090100
H -1.18355400 -7.16279500 1.46113000
H 1.26807500 -7.49842300 1.71627300
H 2.77952700 -5.52159700 1.80325700
H 1.84250100 -3.23717400 1.61479100
H 0.11022200 -1.47693500 -4.69730800
H -1.02862200 -3.33573300 -5.84487100
H -1.27574300 -5.54275300 -4.72337400
H -0.35720500 -5.86508300 -2.42728200
H 0.78816700 -4.01111900 -1.28181500
H 2.89406200 -3.10369900 -3.88154100
H 5.19658500 -3.98453500 -3.94029000
H 6.81428400 -3.38593900 -2.14659800
H 6.09641200 -1.88557300 -0.29202600
H 3.78292400 -1.01446000 -0.23290100
H -1.73601000 -2.02436800 -1.43482600
H -3.90201600 -2.33527100 -2.53285600
H -5.94187700 -2.83259900 -1.17844000
H -5.75813200 -3.01056200 1.29554800
H -3.57407800 -2.71586900 2.40380200
Pd 0.89262200 -0.69551400 0.34882100
C -3.66608000 2.30465400 -1.63114300
H -3.71621100 2.04411900 -2.69110100
C -3.56033100 2.91282300 0.88697000
H -3.51097600 3.17563500 1.94627000
C -5.92249700 1.91944900 1.33852800
C -7.05747000 1.29120800 0.81144700
C -7.12134600 0.97885400 -0.54770000
C -6.05046800 1.28857600 -1.39500300
C -4.92570100 1.92199900 -0.87389700

C -4.86166300 2.23826600 0.49492700
H -5.87174800 2.16363800 2.39719800
H -7.89217900 1.04853300 1.46394900
H -8.00618900 0.49381500 -0.95170600
H -6.09665600 1.03968300 -2.45258900
C -3.10035700 5.42085200 0.37257400
C -2.90176300 6.40735000 -0.60086400
C -2.94629000 6.07769200 -1.95671500
C -3.19112100 4.75795300 -2.35504500
C -3.39821900 3.77780400 -1.38856100
C -3.35367300 4.11062000 -0.02359300
H -3.05823300 5.67469300 1.42916100
H -2.71009200 7.43328900 -0.29795800
H -2.79004700 6.84808400 -2.70727000
H -3.22584900 4.50026400 -3.41122600
H 3.66795600 3.95715000 -0.69331200
O 1.36347100 2.63660600 -0.70148900
H 1.91915900 2.05308900 -1.24275200
H 0.77001500 2.54466300 1.23855700
C 4.80425800 4.81866700 0.89473200
C 5.05710200 5.97584300 0.27908500
H 5.22594700 4.63246400 1.88609300
H 4.63205900 6.14331600 -0.71270100
C 5.89075000 7.09488000 0.83630200
H 6.28699600 6.84674300 1.82699100
H 6.74049900 7.32331200 0.17836700
H 5.30708100 8.02149800 0.92703800

Reagents Pro-R-B
b3lyp/6-31g(d) & LanL2DZ,
el. energy = -3883.361072 a.u.

C 1.45923100 2.60838200 -0.81296500
C 2.23550700 1.46124700 -0.19043300
C 2.36908600 3.80805400 -1.14484700
C 2.11927500 1.22932200 1.18687900
H 3.16617700 1.20148300 -0.69981200
C 3.22204400 0.63660500 2.02263900
H 1.40445400 1.83028400 1.73882700
H 3.68829600 -0.22751300 1.54802500
H 2.84919600 0.35301400 3.01029400
H 1.74337300 4.58938400 -1.59362400
C 3.10177300 4.38045300 0.08163500
H 3.11127900 3.51198600 -1.90022400
O 2.12830000 4.75767800 1.05728000
H 2.33636700 4.32198900 1.90186100
C 5.50598000 3.41768200 3.09555700
H 6.37848200 2.79289900 2.89666900
H 5.51057600 4.27063700 2.40661700
H 5.54577400 3.81603800 4.11276500
C 4.21071300 2.65540000 2.91653500
O 4.39041200 1.51655100 2.23308200
O 3.13169100 3.05015300 3.32381700
N -1.77256700 0.74246800 -1.92588100
C -2.84924200 0.76965300 -0.94620500
C -2.50811600 1.72295600 0.23273700
N -2.09718900 0.98042500 1.41724500
C -1.54518600 -0.35913200 -2.68195200
C -1.23385700 1.53406400 2.31496500
O -0.82991500 2.69182400 2.19253700
O -2.24842800 -1.37188100 -2.65342000
C -0.39370500 -0.22696400 -3.66002800
C -0.80943700 0.70900800 3.50991000
C 0.85219700 -0.87732400 -3.49534100
C 1.81985800 -0.70937100 -4.50112000
C 1.56752500 0.06156300 -5.63790000
C 0.33550700 0.69309500 -5.79194700
C -0.63501500 0.54752200 -4.80117100
C -0.82624900 1.42316000 4.71713700
C -0.43361400 0.83635800 5.91640700
C 0.01040400 -0.48406200 5.91334700
C 0.06039400 -1.19839900 4.71589800
C -0.34564000 -0.63193700 3.49436900
P 1.25012500 -1.77938700 -1.91018200
P -0.14252800 -1.60629700 1.90903900
C 3.01930600 -2.30383200 -2.16519400
C 0.43739500 -3.43678900 -2.12159300
C -1.86717600 -2.25023500 1.65877200
C 0.74968600 -3.13508100 2.47484500
C 0.10161300 -4.28209000 2.96017900
C 0.83580600 -5.41090400 3.33227900
C 2.22797300 -5.41224300 3.22815300
C 2.88469800 -4.27883600 2.74338100
C 2.15016500 -3.15463500 2.36378500
C -0.37665100 -3.78106000 -3.20858200
C -0.93871600 -5.05819200 -3.29404500
C -0.69426000 -6.00603400 -2.30044300
C 0.11607800 -5.67122600 -1.21231300
C 0.67392900 -4.39698400 -1.12222400
C 3.37198200 -3.34310600 -3.04431200
C 4.70655500 -3.71423800 -3.20996700
C 5.71343300 -3.05945300 -2.49554500
C 5.37664100 -2.03321100 -1.61282900
C 4.03944900 -1.66221900 -1.44933300
C -2.23896600 -2.68056100 0.37539100
C -3.51878700 -3.18405800 0.13482600
C -4.44926700 -3.26058300 1.17242100
C -4.09510200 -2.83053700 2.45301800
C -2.81408400 -2.32934900 2.69714800
H -1.04156700 1.45836900 -1.91555600
H -2.97649300 -0.25276700 -0.58364100
H -1.66127100 2.35994100 -0.02746400
H -2.52609200 0.08505100 1.61301700
H 2.78839500 -1.18442200 -4.39620900
H 2.33898500 0.16767700 -6.39590900
H 0.13192300 1.30270800 -6.66783700
H -1.59389900 1.04833200 -4.90134100
H -1.14048700 2.46117800 4.68876200
H -0.46236300 1.40975900 6.83865100
H 0.32880700 -0.96154000 6.83643500
H 0.43008800 -2.21729900 4.73365100
H -0.98013700 -4.30013300 3.04418400
H 0.31600400 -6.29091700 3.70241000

H 2.79685700 -6.29234100 3.51602800
H 3.96740200 -4.27275600 2.64885800
H 2.66205200 -2.28628300 1.95943500
H -0.59466600 -3.05229100 -3.97952800
H -1.57155900 -5.30673100 -4.14210100
H -1.13386800 -6.99765300 -2.37026600
H 0.31058200 -6.39766300 -0.42777600
H 1.29953500 -4.15075800 -0.26877000
H 2.59929500 -3.86834300 -3.59746900
H 4.95954700 -4.51970200 -3.89457400
H 6.75211100 -3.35298400 -2.62285700
H 6.15102100 -1.52248800 -1.04616200
H 3.77479900 -0.87557100 -0.75138000
H -1.54019000 -2.60332000 -0.44836100
H -3.78270900 -3.49132400 -0.87247500
H -5.44969400 -3.64037600 0.98341300
H -4.81671500 -2.87777000 3.26436400
H -2.55471400 -1.99724400 3.69811900
Pd 1.06601600 -0.43741300 0.14343100
C -4.23096600 1.19608800 -1.56900600
H -4.44889000 0.56496900 -2.43406200
C -3.72579400 2.68246700 0.49519500
H -3.50848000 3.31437700 1.35925500
C -5.77206400 1.75028900 1.80389200
C -6.87793100 0.89138900 1.80659200
C -7.15921000 0.10279100 0.68942500
C -6.33637600 0.16156900 -0.44194200
C -5.24245300 1.02257200 -0.44941900
C -4.96015700 1.81895200 0.67493100
H -5.55194800 2.36514400 2.67359400
H -7.52030800 0.84109900 2.68196400
H -8.02068500 -0.56003600 0.69630200
H -6.55064800 -0.45732500 -1.31013300
C -3.75796900 4.85830500 -0.92950100
C -3.90893100 5.43616000 -2.19575600
C -4.17583000 4.63593000 -3.30813200
C -4.29315200 3.24785800 -3.16743100
C -4.15064900 2.67250500 -1.90782800
C -3.88670500 3.47958900 -0.78755100
H -3.54025500 5.47949300 -0.06407400
H -3.81542000 6.51265500 -2.31160200
H -4.29182100 5.09115800 -4.28827500
H -4.49951500 2.62314300 -4.03374300
H 3.76050100 3.59482800 0.47380400
H 0.69987500 2.94444200 -0.10419500
O 0.72833700 2.24347300 -2.00537200
H 1.26115700 1.60315900 -2.50340800
C 3.94340500 5.58150400 -0.27553100
C 5.27487000 5.58471100 -0.38756400
H 3.37799000 6.49784200 -0.45195900
H 5.81932500 4.65460000 -0.20634600
C 6.11269100 6.77432800 -0.76568100
H 6.85253800 7.00769800 0.01235300
H 6.67810800 6.58779300 -1.68929800
H 5.49448100 7.66472200 -0.92251800

TS Pro-S-A
b3lyp/6-31g(d) & LanL2DZ,
el. energy = -3883.333112 a.u.
im. frequency -102.56

C -1.75852800 2.65792500 0.10184600
C -2.26326200 1.36585200 -0.48973100
O -0.34659400 2.87052100 -0.08135300
C -2.55211800 3.87882600 -0.44254400
C -1.94438500 0.95295300 -1.80958900
H -3.24782600 1.07889400 -0.13871300
C -2.47312000 -0.25383800 -2.26330500
H -1.21112100 1.47302500 -2.41880300
H -3.30360200 -0.72439300 -1.75680800
H -2.17839400 -0.66095700 -3.22467600
H -2.10730800 4.18246400 -1.40010500
C -4.06077700 3.63534800 -0.67172100
H -2.39758000 4.71108000 0.25560300
O -4.62906800 2.96458300 0.45159900
H -5.09293000 2.16914800 0.08702700
H -0.11451000 2.77651900 -1.02503400
H -1.89705200 2.61507200 1.18315400
H -4.16533400 3.00433900 -1.56398100
C -6.99439400 1.21118700 -2.42370400
H -7.23278600 1.07647200 -3.48157100
H -7.76986200 0.74326900 -1.80653700
H -6.99923500 2.28178100 -2.18385100
C -5.62028300 0.61272300 -2.07854800
O -4.93625400 0.14245800 -3.01914800
O -5.28658100 0.65293800 -0.84446200
N 1.75407700 1.55628100 1.46330200
C 2.96546900 1.20698600 0.73604400
C 2.90169400 1.73916200 -0.71975700
N 2.48350300 0.69943300 -1.65382100
C 1.31990100 0.76155500 2.47637900
C 1.49674200 0.90894400 -2.56095200
O 0.90879400 1.99574100 -2.65730400
O 1.94647400 -0.22248000 2.87691900
C 0.05042700 1.22496100 3.15236000
C 1.18845900 -0.20555000 -3.53813700
C -1.14935500 0.47554300 3.15572400
C -2.23912900 0.97461000 3.88613500
C -2.14937000 2.16932800 4.60366000
C -0.96567900 2.90207600 4.59251200
C 0.12535900 2.42840200 3.86356100
C 1.27877200 0.19021300 -4.88085900
C 1.01430300 -0.69755500 -5.92052000
C 0.63056200 -2.00198900 -5.61998600
C 0.50838100 -2.40202300 -4.28862400
C 0.78154900 -1.52819000 -3.22203100
P -1.38083300 -0.99669500 2.04420300
P 0.45431400 -2.10024600 -1.47045600
C -3.13335700 -1.51835900 2.35845400
C -0.49522200 -2.40988100 2.84631100
C 2.15718300 -2.49299400 -0.86684300
C -0.30677100 -3.77361100 -1.68311800
C 0.44482100 -4.95775400 -1.74941100

C -0.19210800 -6.19331600 -1.88370900
C -1.58468900 -6.26376800 -1.95540700
C -2.34226900 -5.09262000 -1.88614600
C -1.70860800 -3.85772300 -1.74346300
C 0.17105200 -2.31794900 4.07484500
C 0.76252500 -3.45075800 4.64029500
C 0.69274100 -4.68367800 3.99043400
C 0.02728000 -4.78383200 2.76594800
C -0.56115300 -3.65469600 2.19795300
C -3.46972400 -2.25575000 3.51009600
C -4.79385400 -2.61429800 3.75861500
C -5.80469800 -2.24440500 2.86571800
C -5.48169500 -1.51658400 1.72184300
C -4.15420600 -1.16184500 1.46719200
C 2.40230500 -2.50217400 0.51410400
C 3.66879400 -2.82448400 1.00624300
C 4.70783700 -3.13138800 0.12691900
C 4.47825700 -3.11603200 -1.25096500
C 3.21127200 -2.80176700 -1.74756700
H 1.07608800 2.19237000 1.03483400
H 3.04046700 0.11717700 0.73021000
H 2.14800200 2.52001700 -0.80140500
H 2.98295700 -0.18215100 -1.65712500
H -3.17885900 0.43559200 3.88408700
H -3.01340700 2.52677400 5.15646400
H -0.89034000 3.83904200 5.13715400
H 1.05270200 2.99379400 3.83984800
H 1.55306300 1.21793300 -5.09724800
H 1.09594200 -0.36708900 -6.95189600
H 0.41129800 -2.70959400 -6.41471700
H 0.18126100 -3.41353000 -4.07692500
H 1.52765900 -4.92016000 -1.69047800
H 0.40323600 -7.10137600 -1.93008700
H -2.07758800 -7.22664800 -2.05835500
H -3.42666200 -5.13672000 -1.93333200
H -2.30622400 -2.95419700 -1.67087400
H 0.24780200 -1.36417900 4.58230400
H 1.27961500 -3.36433600 5.59229700
H 1.15374900 -5.56197700 4.43470600
H -0.03336200 -5.73829500 2.25009600
H -1.07865100 -3.74430400 1.24661100
H -2.69870400 -2.55206600 4.21397300
H -5.03528500 -3.18411900 4.65235600
H -6.83610900 -2.52336100 3.06573900
H -6.23980200 -1.19829100 1.01307700
H -3.95928900 -0.59884900 0.56459000
H 1.61794600 -2.23805400 1.21186000
H 3.83616900 -2.80956800 2.07877700
H 5.69665500 -3.36648300 0.50977400
H 5.28504700 -3.34482200 -1.94190300
H 3.04407100 -2.79822000 -2.82090000
Pd -1.05249200 -0.50767400 -0.34963000
C 4.28236900 1.73408100 1.41689900
H 4.29001500 1.44166900 2.46938800
C 4.27452200 2.40663100 -1.08873000
H 4.27674400 2.70026800 -2.14205000
C 6.34146000 0.91330900 -1.61029200
C 7.32673800 0.05029700 -1.11491700
C 7.35118100 -0.28495400 0.23999700
C 6.38725900 0.23245200 1.11432600
C 5.41174000 1.09627000 0.62524300
C 5.39086000 1.43922000 -0.73903200
H 6.32696900 1.18209000 -2.66423200
H 8.07919100 -0.35267000 -1.78770300
H 8.12419900 -0.94771200 0.62034300
H 6.40319200 -0.03231000 2.16883100
C 4.42800700 4.94151200 -0.51787300
C 4.47681000 5.92489900 0.47757700
C 4.46152400 5.56344700 1.82571700
C 4.39820700 4.21431300 2.19492300
C 4.35721900 3.23475400 1.20677700
C 4.37481700 3.60029100 -0.15054300
H 4.43211200 5.22346500 -1.56820500
H 4.52460400 6.97365000 0.19737100
H 4.49854700 6.33188000 2.59321400
H 4.38612000 3.93234600 3.24524000
C -4.78577800 4.93551600 -0.91886600
C -5.29919400 5.31604000 -2.09161700
H -4.88423800 5.58108700 -0.04381600
H -5.19890200 4.64695300 -2.94892100
C -6.02340400 6.60831800 -2.34544100
H -5.51670200 7.20715000 -3.11524600
H -7.04358600 6.42771300 -2.71118700
H -6.09257700 7.21537800 -1.43603700

TS Pro-S-B
b3lyp/6-31g(d) & LanL2DZ,
el. energy = -3883.333018 a.u.
im. frequency -17.15

C -0.01733500 3.23723200 -1.23818500
C 0.63427400 2.70035600 0.01916200
O -1.36098900 2.78469000 -1.38011900
C 0.03538200 4.78321100 -1.34472800
C -0.11485200 2.21677100 1.09596200
H 1.65191200 3.03864500 0.20284100
C 0.51271200 1.65386300 2.21456800
H -1.19152300 2.13250300 1.00792800
H 1.52438000 1.94960200 2.48246100
H -0.08721900 1.23635000 3.00985200
H -0.44422100 5.01720900 -2.30379500
C -0.69285600 5.55829900 -0.21194300
H 1.07670800 5.12060500 -1.41155200
O -1.90266200 4.86479900 0.09374800
H -2.01760300 4.72174500 1.10434500
H -1.88310600 3.44449800 -0.83966500
H 0.53819300 2.85368400 -2.09779700
H -0.94690900 6.54497400 -0.63485100
C -2.35904500 3.58016600 4.81872600
H -1.68129800 3.64746600 5.67507900
H -3.23785400 4.21229200 4.97836200
H -2.70616500 2.54274400 4.72825800
C -1.64119800 3.96070900 3.51398000

O -0.38644800 3.82773700 3.47882400
O -2.39833300 4.33970900 2.56903600
N -1.57729800 -0.02552300 -2.09065300
C -2.46014600 -0.97331700 -1.42178200
C -2.90911200 -0.44553200 -0.03066900
N -2.16652800 -1.09783800 1.04840100
C -0.52975400 -0.46610800 -2.82517700
C -2.09396000 -0.50806300 2.27643500
O -2.65685900 0.55984400 2.51322000
O -0.27169000 -1.66149200 -3.00841200
C 0.31551400 0.59876200 -3.48352200
C -1.31701500 -1.19352800 3.37976600
C 1.67305000 0.80806900 -3.14351300
C 2.40056200 1.75867400 -3.87565700
C 1.81412400 2.47345200 -4.92275500
C 0.47577600 2.26443300 -5.24640900
C -0.26716700 1.33168300 -4.52269700
C -1.98862100 -1.21003500 4.61198400
C -1.39475100 -1.72838800 5.75821200
C -0.08987900 -2.21237600 5.69060600
C 0.60230600 -2.17683400 4.48048600
C 0.01104400 -1.68054400 3.30485700
P 2.39812200 -0.00316400 -1.63523900
P 1.00601500 -1.67972100 1.72670500
C 4.03866200 0.83129400 -1.39647300
C 2.98957100 -1.66141400 -2.21126300
C 0.41621200 -3.25423600 0.95145400
C 2.71725900 -2.07162500 2.30899500
C 3.28063000 -3.35447500 2.23928400
C 4.59085600 -3.57607000 2.67273800
C 5.35117800 -2.52420300 3.18510900
C 4.79888100 -1.24263100 3.25883500
C 3.49599600 -1.01689400 2.81645400
C 2.70004100 -2.18417100 -3.47819000
C 3.20355100 -3.43205200 -3.85559300
C 3.99851800 -4.16889600 -2.97753800
C 4.29104200 -3.65322000 -1.71233400
C 3.79042700 -2.40937200 -1.33137400
C 5.11109200 0.60112500 -2.27751400
C 6.34052300 1.22890700 -2.08054000
C 6.52554500 2.08851900 -0.99432100
C 5.47613000 2.31159200 -0.10335800
C 4.24368800 1.68436700 -0.30314700
C 0.38775300 -3.37244200 -0.44468400
C -0.04534300 -4.55438700 -1.05057700
C -0.45123000 -5.63479700 -0.26795800
C -0.43233200 -5.52757800 1.12563400
C -0.00770600 -4.34604300 1.73373500
H -1.65386300 0.97961100 -1.89220800
H -1.88935200 -1.89761800 -1.31185900
H -2.69033400 0.62003900 0.05009300
H -1.85975700 -2.05471900 0.92983300
H 3.43353600 1.96230800 -3.61948000
H 2.40546000 3.20113500 -5.47155200
H 0.00737800 2.82781700 -6.04832000
H -1.31486800 1.16830200 -4.75741600
H -2.98560500 -0.78456300 4.65429400
H -1.94014800 -1.73580500 6.69741300
H 0.39906800 -2.60736000 6.57689700
H 1.62366100 -2.53894700 4.45438200
H 2.70174000 -4.18242000 1.84422600
H 5.01385700 -4.57530100 2.61108800
H 6.36886300 -2.69971500 3.52273600
H 5.38371000 -0.41709700 3.65488000
H 3.07796600 -0.01556000 2.86827400
H 2.06503300 -1.63565400 -4.16234700
H 2.96982000 -3.82523900 -4.84138200
H 4.38810800 -5.13867500 -3.27553600
H 4.90870500 -4.21738000 -1.01874900
H 4.03429900 -2.01861600 -0.34770700
H 4.98717100 -0.07759700 -3.11589300
H 7.15666800 1.04133100 -2.77307900
H 7.48524800 2.57430100 -0.84061200
H 5.61267700 2.96948000 0.75057200
H 3.43912900 1.84512400 0.40619400
H 0.67618300 -2.54311300 -1.07526500
H -0.07152300 -4.60746200 -2.13441500
H -0.79332000 -6.55304700 -0.73766400
H -0.75754200 -6.36104700 1.74248000
H -0.01154900 -4.27363800 2.81656000
Pd 1.04425000 0.37850300 0.42765100
C -3.73430500 -1.32788700 -2.27375500
H -3.42700500 -1.64401700 -3.27415500
C -4.46830300 -0.59448900 0.10325800
H -4.77866200 -0.27471400 1.09975800
C -5.45105600 -2.94220600 0.64149300
C -5.70443400 -4.24507300 0.19538900
C -5.32137800 -4.63625000 -1.08888600
C -4.67883800 -3.72981200 -1.94104700
C -4.43591100 -2.43135400 -1.50179900
C -4.82214300 -2.03617900 -0.20844000
H -5.75133300 -2.63577200 1.64086200
H -6.20418400 -4.95275300 0.85166800
H -5.52363400 -5.64790800 -1.43089600
H -4.37678800 -4.03489300 -2.94035700
C -5.83720300 1.41324000 -0.82317900
C -6.25084900 2.13946400 -1.94623600
C -5.85853900 1.74377900 -3.22626300
C -5.04246800 0.61949500 -3.39904300
C -4.63465000 -0.10666100 -2.28350900
C -5.03802000 0.28663700 -0.99593600
H -6.13055200 1.72970600 0.17445200
H -6.87537100 3.01911900 -1.81782900
H -6.18327300 2.31360000 -4.09285000
H -4.73223700 0.31330100 -4.39580800
C 0.16359900 5.78706800 1.01271300
C 0.87163200 6.90227300 1.21717200
H 0.15400700 5.00834900 1.77875900
H 0.83786000 7.70810400 0.47829300
C 1.71996900 7.15055200 2.43405200
H 1.41753800 8.07492300 2.94578900
H 1.62835100 6.32359600 3.14579300

H 2.78202900 7.27239700 2.17369500

TS Pro-R-A
b3lyp/6-31g(d) & LanL2DZ,
el. energy = -3883.327896 a.u.
im. frequency -119.54

C -1.77136500 2.45024400 -0.84989100
C -2.05388500 0.98506400 -1.09808800
C -2.90224800 3.31255200 -1.48363500
C -1.56904200 0.37246300 -2.27149800
H -2.99867500 0.62371200 -0.71759600
C -1.92262600 -0.95236100 -2.53622500
H -0.85715900 0.88402600 -2.91371100
H -2.74327100 -1.42946000 -2.02105600
H -1.49604900 -1.47551300 -3.38577600
H -3.21276600 2.85157900 -2.42914700
C -4.12699900 3.50652300 -0.55595400
H -2.50171800 4.30418100 -1.72926500
O -4.46382300 2.31118000 0.15193300
H -4.79056800 1.63182800 -0.49446000
C -6.27662200 0.58639200 -3.53381500
H -6.58225900 -0.02764700 -4.38555900
H -7.11041300 0.70964000 -2.83605100
H -6.00851400 1.57884500 -3.92082400
C -5.05443100 -0.02746800 -2.82837900
O -4.27544600 -0.70913500 -3.53967600
O -4.92212300 0.22573900 -1.58477500
N 1.04528300 1.86873800 1.55622100
C 2.35732200 1.80349700 0.92951600
C 2.28341200 2.07108700 -0.59846300
N 2.35760200 0.82869500 -1.36318000
C 0.74029500 1.04849000 2.59420700
C 1.83283400 0.76324900 -2.61928700
O 1.28724200 1.74101500 -3.13861000
O 1.54199300 0.25328500 3.09093300
C -0.65226800 1.21634300 3.15471300
C 1.96147000 -0.52509900 -3.40450500
C -1.66645100 0.25073400 2.97396300
C -2.91163400 0.47391100 3.58203500
C -3.14654900 1.61155800 4.35682200
C -2.13816800 2.55646000 4.53281100
C -0.89709100 2.35573500 3.92847800
C 2.29783300 -0.31489900 -4.75111600
C 2.42577500 -1.37175900 -5.64718900
C 2.19039400 -2.67092500 -5.20413200
C 1.82994500 -2.89629700 -3.87548900
C 1.71117400 -1.84603000 -2.94806800
P -1.41050500 -1.20224700 1.84204200
P 1.14589200 -2.23844200 -1.21000000
C -3.07943000 -2.01608300 1.81522100
C -0.46371100 -2.42876500 2.85789000
C 2.75564200 -2.24246900 -0.29447700
C 0.69103500 -4.03039100 -1.29080300
C 1.60403500 -5.07124700 -1.05879400
C 1.18515700 -6.40297700 -1.10505200
C -0.14705100 -6.71340600 -1.38529300
C -1.06463000 -5.68549000 -1.61331900
C -0.64999400 -4.35435700 -1.55822000
C -0.01037400 -2.17683500 4.15923500
C 0.67361800 -3.16614600 4.87100700
C 0.90956000 -4.41545200 4.29650700
C 0.45811400 -4.67609100 3.00018200
C -0.22091600 -3.68950600 2.28676100
C -3.46644200 -2.92690600 2.81605000
C -4.73795700 -3.50069000 2.79832100
C -5.64618600 -3.17349600 1.78754400
C -5.27507500 -2.26692500 0.79526500
C -4.00015700 -1.69681900 0.80654200
C 2.75823100 -1.97748900 1.08365400
C 3.95405700 -1.98541400 1.80492700
C 5.16132100 -2.25706800 1.16015500
C 5.17240900 -2.51614200 -0.21267200
C 3.97977300 -2.50677400 -0.93812300
H 0.27980700 2.41165800 1.15328100
H 2.73293800 0.79569200 1.11830000
H 1.32448700 2.52259800 -0.85440200
H 2.95671000 0.08371800 -1.02951900
H -3.71418700 -0.24033900 3.44093500
H -4.12253400 1.75756500 4.81084400
H -2.31556700 3.44876200 5.12665600
H -0.10666900 3.09157400 4.04827200
H 2.44287200 0.70736900 -5.08376000
H 2.69390100 -1.17858000 -6.68189400
H 2.27452100 -3.51178100 -5.88718200
H 1.63042800 -3.91288000 -3.55684800
H 2.64186400 -4.84586400 -0.83584200
H 1.90292300 -7.19774600 -0.91963400
H -0.47019900 -7.75029900 -1.41858000
H -2.10554400 -5.91550600 -1.82252900
H -1.37516500 -3.56023100 -1.70796900
H -0.17284100 -1.20781900 4.61471000
H 1.02147700 -2.95442900 5.87866600
H 1.44159500 -5.18168000 4.85433500
H 0.63625200 -5.64402100 2.53968400
H -0.57247900 -3.90629500 1.28253000
H -2.77716900 -3.18856600 3.61160800
H -5.01839600 -4.20358000 3.57875000
H -6.63654900 -3.62150300 1.77897300
H -5.95958600 -1.97855100 0.00346800
H -3.76818200 -0.99609500 0.01578900
H 1.83668000 -1.74158500 1.60003900
H 3.92852200 -1.75825300 2.86610900
H 6.09262500 -2.25443600 1.71985600
H 6.11003400 -2.71851600 -0.72332600
H 4.00247400 -2.70240600 -2.00595200
Pd -0.67770100 -0.74645600 -0.52294300
C 3.39748200 2.79336900 1.57372400
H 3.40663300 2.65425100 2.65762300
C 3.39169100 3.11301200 -0.99895900
H 3.38297900 3.25478300 -2.08187600
C 5.85029900 2.28899000 -1.21678100
C 6.99956700 1.82389700 -0.56590200

C 7.00785400 1.66707700 0.82128900
C 5.86726100 1.97223500 1.57395800
C 4.72765000 2.44452500 0.92882300
C 4.71870700 2.60278400 -0.46847700
H 5.84323800 2.41213900 -2.29738700
H 7.88874800 1.58684700 -1.14418300
H 7.90403800 1.30880300 1.32109400
H 5.87133400 1.84537200 2.65400500
C 2.69052100 5.60967600 -0.79532000
C 2.35023500 6.67318500 0.04919400
C 2.34195100 6.49825700 1.43418300
C 2.67434500 5.25766600 1.99149900
C 3.02099800 4.20152000 1.15352200
C 3.03099900 4.37904800 -0.24093600
H 2.68993900 5.74282800 -1.87452300
H 2.08984300 7.63819300 -0.37715100
H 2.07580700 7.32783800 2.08375400
H 2.66744900 5.12071100 3.07045200
H -3.84383700 4.22418500 0.22270600
O -1.59713400 2.76391800 0.53412900
H -2.41687400 2.47169300 0.97775700
H -0.82560000 2.72149300 -1.33058400
C -5.30401200 4.05795600 -1.31903800
C -5.80578200 5.28527900 -1.16250400
H -5.75027900 3.37555900 -2.04519200
H -5.34684900 5.94826300 -0.42573400
C -6.97070300 5.85171700 -1.92363100
H -7.37979100 5.12359500 -2.63214500
H -7.77876800 6.15619500 -1.24432700
H -6.68108400 6.74905800 -2.48800600

INT Pro-S-A
b3lyp/6-31g(d) & LanL2DZ,
el. energy = -3883.347071 a.u.

C -1.72573900 2.99203100 -0.02856500
C -1.85140700 1.75555700 -0.87909700
O -0.35400000 3.40990600 0.15281100
C -2.55575100 4.16852100 -0.59730400
C -0.94768800 1.43817400 -1.90211100
H -2.85891400 1.34156800 -0.96704700
C -1.12847100 0.23552600 -2.60598400
H -0.02057000 1.99202600 -2.02731600
H -2.12694700 -0.21426600 -2.68270000
H -0.38989300 -0.05246200 -3.34393600
H -2.01274800 4.60995200 -1.44829700
C -3.97192800 3.79285600 -1.08889000
H -2.61512700 4.93934800 0.18158300
O -4.61339000 2.97933700 -0.11185200
H -4.92808100 2.18175500 -0.59633600
H -0.12788300 4.01960300 -0.56696300
H -2.09778300 2.77246100 0.97249800
H -3.87340200 3.22381400 -2.02250600
C -6.18351800 -0.21172400 -3.26518700
H -6.17573700 -0.97423500 -4.04792700
H -6.99583400 -0.42972700 -2.56034200
H -6.40074300 0.76863300 -3.70390300
C -4.84156300 -0.16665000 -2.51788900
O -3.98308500 -1.04364100 -2.78473800
O -4.70725800 0.76899800 -1.66300300
N 1.73102200 1.63825500 1.33222700
C 2.98433200 1.19197000 0.74098600
C 2.96741600 1.32979800 -0.80460200
N 2.70933500 0.04930000 -1.45667300
C 1.26387500 1.06073000 2.46713200
C 2.20937000 0.02092400 -2.72206800
O 2.02344600 1.05978200 -3.36130500
O 1.86555200 0.16505400 3.06623900
C -0.02374200 1.64011500 3.00863800
C 1.90849100 -1.31262300 -3.37178300
C -1.27214600 0.98198200 2.93193100
C -2.38071100 1.59650400 3.53736600
C -2.26129700 2.81296900 4.21191300
C -1.02581100 3.45111400 4.28575000
C 0.08379000 2.86313400 3.68037100
C 2.40902900 -1.41912300 -4.67871900
C 2.15277200 -2.53492600 -5.46946600
C 1.34647700 -3.55352000 -4.96701200
C 0.81903400 -3.45116600 -3.67975000
C 1.09434100 -2.34991800 -2.85066200
P -1.50655500 -0.56714800 1.92538300
P 0.35832400 -2.32853200 -1.13137900
C -3.31344800 -0.92242900 2.06529900
C -0.84888700 -1.94088400 2.98104300
C 1.81526500 -2.93567800 -0.16116100
C -0.84963100 -3.72185300 -1.15087500
C -0.52954800 -5.02975400 -0.75062000
C -1.50586500 -6.02825900 -0.76704100
C -2.80554300 -5.73460700 -1.18742400
C -3.12896200 -4.43634500 -1.58625600
C -2.16278800 -3.42895600 -1.56175800
C -0.20615100 -1.74087600 4.20881100
C 0.21355700 -2.83635400 4.96923900
C -0.00740000 -4.13700700 4.51688300
C -0.65465000 -4.34342500 3.29572700
C -1.07311800 -3.25439200 2.53372500
C -3.85577800 -1.42751700 3.26374400
C -5.22436800 -1.66266500 3.37308100
C -6.07099900 -1.39895400 2.29083100
C -5.53957700 -0.90464000 1.10194200
C -4.16552400 -0.67289400 0.98424800
C 2.04441400 -2.43645100 1.12824400
C 3.14114300 -2.86755400 1.87856100
C 4.02241900 -3.80960100 1.34892000
C 3.81019200 -4.31141000 0.06162900
C 2.72114600 -3.87434400 -0.69282100
H 1.13461700 2.32019800 0.85981000
H 3.10589100 0.14563800 1.02889900
H 2.15575600 1.99369100 -1.10825800
H 2.95055600 -0.81244400 -0.98412500
H -3.35585400 1.12979400 3.47100500
H -3.14070300 3.25986900 4.66687200
H -0.92439600 4.40238800 4.80060300

H 1.05110100 3.35617700 3.72180000
H 2.99102600 -0.59182100 -5.07138300
H 2.56128100 -2.59568600 -6.47412200
H 1.11315300 -4.42383200 -5.57417500
H 0.17305200 -4.24212300 -3.31670600
H 0.47499300 -5.27098200 -0.41800900
H -1.24828500 -7.03573500 -0.45033300
H -3.56245000 -6.51454900 -1.19838800
H -4.13296700 -4.18457000 -1.91439400
H -2.46487800 -2.42757700 -1.86173100
H -0.01016400 -0.73814100 4.56611100
H 0.71333900 -2.66565700 5.91911300
H 0.31966100 -4.98561200 5.11202600
H -0.83623800 -5.35151200 2.93321400
H -1.58709200 -3.43027300 1.59349500
H -3.20956600 -1.63764900 4.11030300
H -5.62981200 -2.05242400 4.30329500
H -7.13909900 -1.58045400 2.37987300
H -6.17512300 -0.68053700 0.25137700
H -3.79722900 -0.29949500 0.03569100
H 1.38002700 -1.69838400 1.55533300
H 3.29487500 -2.44816000 2.86774200
H 4.87830200 -4.14496200 1.92851200
H 4.49912900 -5.03728600 -0.36212300
H 2.58358200 -4.25822700 -1.69882800
Pd -0.82021900 -0.31295700 -0.45934900
C 4.23887700 1.95337500 1.31029900
H 4.21713800 1.92043300 2.40234300
C 4.30040000 2.01615500 -1.28046100
H 4.32079600 2.05073200 -2.37141700
C 6.47734600 0.59557900 -1.37214800
C 7.47985400 -0.07231900 -0.65853400
C 7.45673100 -0.09169700 0.73728300
C 6.43013000 0.55507700 1.43602300
C 5.43890800 1.22788300 0.72711900
C 5.46149700 1.24754600 -0.67844600
H 6.49460700 0.61123600 -2.45944200
H 8.27979700 -0.57590000 -1.19483300
H 8.23879900 -0.61030400 1.28548300
H 6.40832900 0.53606100 2.52311000
C 4.23502300 4.61648900 -1.32636300
C 4.16814500 5.80722500 -0.59234500
C 4.12216200 5.77335600 0.80265800
C 4.14308100 4.54828100 1.48052500
C 4.21793500 3.36393700 0.75258400
C 4.26672800 3.39869900 -0.65221400
H 4.26548700 4.64137300 -2.41310200
H 4.15269300 6.76131000 -1.11245300
H 4.07086900 6.70121900 1.36609000
H 4.10800900 4.52170500 2.56729900
C -4.78829100 5.03298200 -1.35879600
C -5.16131700 5.45608900 -2.56890700
H -5.08334300 5.59285300 -0.46907300
H -4.86829400 4.86921100 -3.44202800
C -5.97453100 6.68909600 -2.84594000
H -5.43059200 7.39067800 -3.49378800
H -6.90827200 6.44043500 -3.36881300
H -6.23429700 7.21472500 -1.92059200

INT Pro-S-B
b3lyp/6-31g(d) & LanL2DZ,
el. energy = -3883.333175 a.u.

C -0.37155900 3.23147300 -1.13799100
C 0.32969600 2.78072100 0.12775900
O -1.62657300 2.58416400 -1.31490200
C -0.54977600 4.76886200 -1.25055600
C -0.35703500 2.18221300 1.18837800
H 1.29822600 3.23778500 0.32120300
C 0.34320300 1.62551500 2.27048300
H -1.41206400 1.96238400 1.08234100
H 1.30585700 2.04316700 2.56309200
H -0.21411800 1.13440500 3.05602300
H -0.99143200 4.92823400 -2.24265700
C -1.46810200 5.42741700 -0.18369800
H 0.42945500 5.26285300 -1.24819500
O -2.58641400 4.56797200 0.02859300
H -2.80607800 4.43705200 1.03288600
H -2.26634200 3.18039400 -0.82164200
H 0.25916300 2.94165200 -1.98314900
H -1.82211500 6.37070000 -0.63441700
C -3.24957900 3.15720500 4.63001200
H -2.64316500 3.36320400 5.51787900
H -4.24339900 3.60130000 4.73676100
H -3.36498300 2.06941100 4.54233300
C -2.54704000 3.66463300 3.36199100
O -1.28773500 3.60670600 3.33668000
O -3.31082100 4.06631300 2.43054500
N -1.49075300 -0.17515400 -2.14640000
C -2.25063400 -1.24009000 -1.50346400
C -2.79639300 -0.78775200 -0.11895300
N -1.99979300 -1.35036700 0.97237400
C -0.34941700 -0.45462100 -2.81719000
C -2.04133700 -0.77543400 2.20990400
O -2.74056900 0.20943500 2.44083800
O 0.09640600 -1.59725900 -2.97562000
C 0.36494400 0.72188500 -3.43752600
C -1.21305800 -1.37360800 3.32796000
C 1.68209300 1.08211200 -3.06628600
C 2.30485400 2.12755700 -3.76453100
C 1.65580400 2.79116800 -4.80861200
C 0.35688000 2.43409500 -5.16192300
C -0.28348000 1.40466900 -4.47187200
C -1.90215600 -1.46924400 4.54659500
C -1.27617600 -1.91880300 5.70501700
C 0.07632200 -2.25043300 5.66420800
C 0.78383100 -2.13515400 4.46774500
C 0.16329100 -1.70857400 3.28022900
P 2.46599700 0.33206400 -1.55577800
P 1.18541900 -1.58894100 1.72529600
C 3.97671600 1.36492700 -1.24666400
C 3.28483200 -1.22046800 -2.14546900
C 0.76352100 -3.19571600 0.90794500

C 2.91883300 -1.84130800 2.32299300
C 3.55989800 -3.08952400 2.32383800
C 4.88395700 -3.20459400 2.75561200
C 5.58256800 -2.07921900 3.19539800
C 4.95327400 -0.83187600 3.19938500
C 3.63500200 -0.71357100 2.75950100
C 3.11232300 -1.73656900 -3.43641200
C 3.78647100 -2.89734000 -3.82469500
C 4.63474700 -3.55398600 -2.93274500
C 4.80953300 -3.04553100 -1.64320700
C 4.14011900 -1.88720600 -1.25174200
C 5.09312900 1.30849200 -2.10077500
C 6.22223400 2.08645800 -1.84661600
C 6.26306600 2.92379400 -0.72832800
C 5.17145300 2.97321600 0.13804400
C 4.03877200 2.19711000 -0.12037400
C 0.84863800 -3.31078600 -0.48632400
C 0.55424100 -4.52095500 -1.11861000
C 0.17571800 -5.63244100 -0.36604700
C 0.08318700 -5.52901200 1.02450900
C 0.36998300 -4.32012800 1.65948000
H -1.71202100 0.80707600 -1.94133100
H -1.56276300 -2.08008600 -1.38688000
H -2.71632000 0.29613300 -0.02522000
H -1.60310400 -2.27552100 0.86576000
H 3.30198400 2.44594800 -3.48448600
H 2.16636700 3.59500000 -5.33168600
H -0.16053700 2.95611500 -5.96173100
H -1.30016000 1.12365900 -4.73031300
H -2.94168500 -1.16001800 4.56871500
H -1.83617000 -1.99008800 6.63287200
H 0.58950500 -2.58830000 6.56035700
H 1.83991300 -2.37946300 4.46238400
H 3.03136400 -3.97349400 1.98325300
H 5.36741500 -4.17789100 2.74764400
H 6.61225800 -2.17170400 3.52961200
H 5.49005600 0.05071000 3.53591600
H 3.15800800 0.26214900 2.74972800
H 2.43845900 -1.25135400 -4.13147700
H 3.64357400 -3.28654300 -4.82924600
H 5.15645600 -4.45679000 -3.23905500
H 5.46658100 -3.54846800 -0.93890800
H 4.29324100 -1.49947700 -0.24871800
H 5.08312600 0.64769200 -2.96235400
H 7.07377500 2.03360100 -2.51962300
H 7.14496700 3.52702900 -0.53084000
H 5.19767600 3.61224800 1.01654800
H 3.20041100 2.22267800 0.56767700
H 1.11457900 -2.45905400 -1.09641900
H 0.61086800 -4.57358800 -2.20138600
H -0.05869800 -6.57251600 -0.85805900
H -0.22059800 -6.38718600 1.61788600
H 0.28459200 -4.25307900 2.73925200
Pd 1.03757800 0.50213200 0.48894300
C -3.44844800 -1.75608200 -2.38366000
H -3.08168500 -2.02476300 -3.37802900
C -4.32586700 -1.13772300 -0.02250500
H -4.69898000 -0.86654300 0.96683000
C -4.99659700 -3.59904700 0.49017700
C -5.05979800 -4.92272200 0.03732200
C -4.59900700 -5.25326300 -1.23834100
C -4.06824800 -4.26417500 -2.07531300
C -4.01388900 -2.94648000 -1.62930300
C -4.47884700 -2.61219300 -0.34477600
H -5.35662500 -3.34059300 1.48338500
H -5.47231200 -5.69451300 0.68193200
H -4.65358300 -6.28184500 -1.58534900
H -3.70526700 -4.52119900 -3.06786800
C -5.92417700 0.67880700 -0.97627400
C -6.40403500 1.34963500 -2.10737200
C -5.93516100 1.01435000 -3.37888200
C -4.97513900 0.00736700 -3.53486000
C -4.50112100 -0.66410800 -2.41140900
C -4.98090700 -0.33303700 -1.13261200
H -6.27771600 0.95077200 0.01490500
H -7.14049600 2.13985300 -1.99151300
H -6.31220400 1.54081800 -4.25168200
H -4.60446500 -0.25087600 -4.52451800
C -0.74894700 5.77123900 1.10021300
C -0.23988300 6.98055900 1.35536200
H -0.69692400 4.98581500 1.85737200
H -0.34903000 7.77983000 0.61661600
C 0.47564100 7.34691100 2.62647700
H -0.01082900 8.19681500 3.12548000
H 0.48441100 6.50415800 3.32543100
H 1.51549900 7.65168500 2.43594100

INT Pro-R-A
b3lyp/6-31g(d) & LanL2DZ,
el. energy = -3883.342090 a.u.

C -1.67024200 2.72324600 -1.40180700
C -1.73018300 1.25865600 -1.80450600
C -2.96497300 3.46383400 -1.82083600
C -0.73755100 0.72271900 -2.62416200
H -2.69147100 0.75295400 -1.75412100
C -0.75360700 -0.65333000 -2.93542100
H 0.14422700 1.30961000 -2.87516300
H -1.72261200 -1.15715000 -2.97086800
H 0.06242100 -1.06888500 -3.51611700
H -3.33222100 3.03012700 -2.75874900
C -4.08081100 3.39669300 -0.74800000
H -2.73579100 4.51857200 -2.01706800
O -4.10478200 2.11421900 -0.10921200
H -4.41033000 1.45604100 -0.79324300
C -5.56409400 -0.57739100 -4.16423000
H -5.47705800 -1.59537800 -4.55298600
H -6.60724300 -0.35649900 -3.91501000
H -5.26670000 0.12580400 -4.95263600
C -4.66504900 -0.36979900 -2.93615100
O -3.77563400 -1.23500200 -2.70220300
O -4.88201500 0.68392400 -2.26287400
N 1.17900400 1.84624500 1.18161700

C 2.55703200 1.69648900 0.73059800
C 2.66084600 1.60440700 -0.81579100
N 2.81362100 0.21620200 -1.25532200
C 0.84440600 1.52327500 2.45775400
C 2.59659300 -0.12590700 -2.55333600
O 2.35568600 0.72387400 -3.41502700
O 1.64949400 1.05925100 3.27065100
C -0.58128700 1.84906200 2.84797700
C 2.66024300 -1.58276500 -2.96031000
C -1.70796200 1.05866300 2.52640000
C -2.97646000 1.53064600 2.90370100
C -3.12618000 2.72366800 3.61187000
C -2.00531300 3.46785100 3.97210500
C -0.74059900 3.02691500 3.58760100
C 3.39619000 -1.80839500 -4.13355400
C 3.46888900 -3.06939200 -4.71732000
C 2.76089200 -4.12523900 -4.14729800
C 2.00378600 -3.91278800 -2.99495400
C 1.94719000 -2.65576600 -2.36855700
P -1.55613900 -0.56126800 1.61905900
P 0.94325700 -2.47373400 -0.80201900
C -3.27596100 -1.23583000 1.57893500
C -0.84891300 -1.69943800 2.91395300
C 2.31107800 -2.62140000 0.44280600
C -0.00583800 -4.05365600 -0.69166600
C 0.48296100 -5.20913100 -0.06114200
C -0.30232400 -6.36184900 0.00657900
C -1.58196700 -6.37576900 -0.55267800
C -2.07882500 -5.22938100 -1.17600400
C -1.30050700 -4.07262500 -1.24070000
C -0.31964200 -1.27202600 4.13867300
C 0.15991900 -2.20389200 5.06490100
C 0.11356600 -3.56873700 4.78581000
C -0.41919200 -4.00385800 3.56951900
C -0.89678100 -3.07870000 2.64378400
C -3.92422400 -1.60490100 2.77482400
C -5.20998600 -2.13706400 2.74394100
C -5.86280000 -2.32312000 1.51983200
C -5.22186900 -1.97223400 0.33484700
C -3.93301200 -1.42777800 0.35952400
C 2.28249200 -1.85143200 1.61326200
C 3.31331000 -1.93310700 2.55255200
C 4.38807400 -2.79445800 2.33434800
C 4.43516500 -3.56322700 1.16802500
C 3.41221200 -3.47213000 0.22388500
H 0.45851000 2.28455400 0.60225700
H 2.93289200 0.77866500 1.18852400
H 1.73913000 1.97449600 -1.27100200
H 3.14185700 -0.47768900 -0.59638800
H -3.86114800 0.97447800 2.62395700
H -4.12300400 3.06383700 3.87724400
H -2.11167400 4.39202700 4.53329000
H 0.14103400 3.60696900 3.84568500
H 3.89606600 -0.96205300 -4.59304100
H 4.05528400 -3.21870800 -5.61932700
H 2.78443100 -5.11330000 -4.59867000
H 1.44414500 -4.74262300 -2.57850500
H 1.46945800 -5.20966600 0.39008400
H 0.08723400 -7.24785600 0.50103800
H -2.19220700 -7.27292600 -0.49435000
H -3.07762500 -5.22262300 -1.60221700
H -1.71754400 -3.18265600 -1.70315800
H -0.25757300 -0.21858100 4.37858800
H 0.56708700 -1.85192800 6.00909000
H 0.48495200 -4.28910600 5.50994500
H -0.46817400 -5.06452200 3.33858600
H -1.32662600 -3.43657000 1.71374100
H -3.42139900 -1.47983700 3.72904700
H -5.70055700 -2.41280400 3.67394400
H -6.86540500 -2.74282200 1.49759200
H -5.70533700 -2.11175900 -0.62679100
H -3.48001700 -1.17597200 -0.59579100
H 1.46019100 -1.17653200 1.80103100
H 3.26222800 -1.30742600 3.43774000
H 5.19335200 -2.85902800 3.06103900
H 5.27605800 -4.22665900 0.98441700
H 3.47868500 -4.05507200 -0.68910600
Pd -0.58167300 -0.59333600 -0.74287300
C 3.50224000 2.84951200 1.23966600
H 3.37543700 2.96713300 2.31789000
C 3.81570400 2.54917600 -1.31547500
H 3.93943000 2.42791800 -2.39252900
C 6.28185400 1.77354200 -1.03269500
C 7.34252700 1.51351900 -0.15639900
C 7.17970100 1.69209800 1.21876500
C 5.95422600 2.13143100 1.73420800
C 4.90302900 2.40090900 0.86218500
C 5.06595700 2.22041000 -0.52234800
H 6.40774200 1.63502100 -2.10405400
H 8.29673500 1.17300800 -0.54980300
H 8.00731600 1.48982100 1.89354800
H 5.82439400 2.26480500 2.80561600
C 3.08694900 4.99827300 -1.80233600
C 2.63791700 6.21916700 -1.28444800
C 2.45528400 6.37673000 0.09068900
C 2.72014800 5.31579100 0.96489600
C 3.17512900 4.10404700 0.45247000
C 3.36055100 3.94675000 -0.93192600
H 3.22315200 4.87189100 -2.87377100
H 2.42903600 7.04636600 -1.95749000
H 2.10419300 7.32636100 0.48542600
H 2.57503900 5.43775200 2.03578300
H -3.83302700 4.10980500 0.04723600
O -1.38038500 2.89868400 -0.01115100
H -2.14534500 2.50215400 0.45295200
H -0.81754800 3.18028700 -1.91843100
C -5.42321200 3.75046300 -1.33386600
C -6.09820500 4.86961500 -1.06046700
H -5.82375800 3.00792500 -2.02532300
H -5.66930300 5.58645400 -0.35608800
C -7.42961200 5.24230800 -1.64998200
H -7.79325600 4.46856400 -2.33436600

H -8.18672700 5.38660700 -0.86658000
H -7.37140000 6.18830400 -2.20665000

RSR-INT
b3lyp/6-31g(d) & LanL2DZ,
el. energy = -3883.353763 a.u.

C 2.33025900 1.65340300 -0.99597500
C 1.25460800 1.38141400 -1.83590100
H 3.14095200 0.93191200 -0.92551100
C 1.14620000 0.10206100 -2.45746100
H 0.45946700 2.11731800 -1.93495800
H 2.05469400 -0.43277300 -2.72138900
H 0.30234000 -0.09161200 -3.11530200
C 6.99159600 -0.50877100 0.55024900
H 7.69463700 -0.65220800 -0.27664800
H 6.58679300 -1.49538800 0.81027400
H 7.51536500 -0.10438600 1.42013500
C 5.84385100 0.41343000 0.11884000
O 5.35473800 0.20414900 -1.03586700
O 5.46391800 1.28532200 0.94791500
C 2.54035200 2.94527200 -0.25404900
H 1.56314300 3.37985100 -0.01943100
C 3.27585300 3.98223300 -1.15089900
H 3.38692000 4.89544900 -0.55334800
H 2.64537200 4.22379700 -2.01750400
C 4.64546500 3.49763600 -1.65266700
H 5.27476400 3.25978800 -0.78567800
O 4.43816900 2.32910800 -2.44809100
H 4.87541600 1.56195400 -1.99289100
O 3.19419900 2.73547300 0.97708000
H 4.06012000 2.25354700 0.84624100
N -2.93631200 -0.53332200 -1.78629100
C -3.64909400 0.18224200 -0.73633300
C -3.12446300 1.64199000 -0.60178500
N -2.24314000 1.80171600 0.54644400
C -2.42302100 -1.78142700 -1.58980000
C -1.24594900 2.73622200 0.52220100
O -1.04115000 3.43341500 -0.47425300
O -2.60040000 -2.41507600 -0.55078700
C -1.63747000 -2.35905600 -2.73447900
C -0.44432900 2.95211800 1.78291500
C -0.34515200 -2.90604400 -2.53563200
C 0.30125000 -3.47072400 -3.64428400
C -0.30823800 -3.51938700 -4.90169400
C -1.58072100 -2.98677700 -5.08364900
C -2.23708300 -2.40412300 -3.99839500
C -0.39144500 4.29489900 2.18942400
C 0.32285000 4.68190700 3.31822400
C 1.02448800 3.72062100 4.04276400
C 1.00694200 2.38961000 3.63109800
C 0.27437100 1.97224800 2.50747900
P 0.57220500 -2.67439500 -0.92238300
P 0.31907300 0.17252700 2.01617500
C 2.27361100 -3.31863300 -1.26468900
C -0.02837900 -4.00137300 0.21438500
C -1.21898500 -0.44737300 2.84733400
C 1.68300800 -0.53438700 3.03783000
C 1.46481300 -1.44727300 4.08114800
C 2.55020500 -1.99148300 4.77438900
C 3.85553900 -1.62354300 4.44224800
C 4.07782400 -0.70945500 3.40885100
C 3.00011500 -0.17684600 2.70272900
C -0.99225000 -4.95229800 -0.14330600
C -1.34334500 -5.96707200 0.74974200
C -0.74024400 -6.04014800 2.00648400
C 0.21925900 -5.09237900 2.37000700
C 0.57437400 -4.07922900 1.48004800
C 2.49720000 -4.69247800 -1.48051700
C 3.77988900 -5.16412500 -1.75416400
C 4.86063900 -4.27696200 -1.80725800
C 4.65674300 -2.91890000 -1.56866100
C 3.37038100 -2.44743800 -1.29109200
C -1.87933700 -1.56899100 2.32739200
C -3.02416900 -2.07399500 2.94917200
C -3.52494600 -1.46420700 4.09929000
C -2.87633500 -0.34453800 4.62702300
C -1.73264100 0.16212200 4.00812400
H -2.72674300 -0.05028000 -2.64937300
H -3.45760800 -0.37906000 0.17968600
H -2.51846100 1.90524200 -1.47060100
H -2.48107600 1.35178000 1.42180200
H 1.30175800 -3.87183400 -3.53507800
H 0.22291300 -3.97048400 -5.73514100
H -2.06156000 -3.02003700 -6.05707900
H -3.23671700 -1.99624300 -4.12493200
H -0.91481200 5.03418000 1.59138800
H 0.34402100 5.72590600 3.61759300
H 1.60354200 4.00330400 4.91739000
H 1.59233200 1.66488200 4.18451500
H 0.45557900 -1.73546700 4.35674000
H 2.37016600 -2.69815200 5.58076800
H 4.69512100 -2.04517600 4.98892500
H 5.07923900 -0.39142400 3.13573500
H 3.19339400 0.54619100 1.91816900
H -1.47988500 -4.89518800 -1.10966200
H -2.09212400 -6.69974700 0.46027400
H -1.01646500 -6.83066700 2.69920500
H 0.69399600 -5.13772500 3.34627900
H 1.32455600 -3.35039300 1.77482600
H 1.66946500 -5.39400700 -1.42938900
H 3.93634100 -6.22677600 -1.92131600
H 5.85837300 -4.65003700 -2.02361600
H 5.46641900 -2.19603400 -1.58952800
H 3.25059100 -1.39259300 -1.07676000
H -1.52273600 -2.04329800 1.42391500
H -3.52087800 -2.93820600 2.51818900
H -4.41865500 -1.85252900 4.58055400
H -3.26117200 0.13917000 5.52092400
H -1.24020600 1.03228000 4.43012300
Pd 0.73020600 -0.30802300 -0.38616700
C -5.20391200 0.21139500 -0.95762300
H -5.57443900 -0.80629100 -1.10699500

C -4.34569800 2.63265300 -0.59213700
H -3.98589100 3.65399000 -0.44757500
C -5.70261100 2.89667500 1.61224600
C -6.58967400 2.31570600 2.52653000
C -7.06157600 1.01775200 2.32275500
C -6.65076600 0.28409100 1.20339100
C -5.77543500 0.86425200 0.28948700
C -5.30097500 2.17196700 0.49317300
H -5.33478700 3.90767000 1.77084300
H -6.91243800 2.87955700 3.39759700
H -7.75131800 0.57344900 3.03531400
H -7.01401100 -0.72894200 1.04709600
C -5.17153300 3.39282400 -2.94008000
C -5.79020300 3.03641800 -4.14466500
C -6.24334300 1.73127100 -4.34566700
C -6.08313600 0.76619700 -3.34358200
C -5.47671500 1.12188000 -2.14147600
C -5.02178100 2.43708000 -1.93875000
H -4.81196000 4.40738000 -2.78659700
H -5.91664000 3.78063300 -4.92620100
H -6.72370100 1.46226800 -5.28257900
H -6.43789700 -0.25042700 -3.49819500
C 5.32935100 4.55371000 -2.48438900
H 4.86777000 4.74758800 -3.45471800
C 6.41866900 5.23164800 -2.11584100
H 6.86953200 5.01166300 -1.14606600
C 7.09887200 6.29251500 -2.93500300
H 7.12019200 7.25583400 -2.40613400
H 8.14476700 6.02680600 -3.14257300
H 6.59211700 6.44503700 -3.89436600

SSR-INT
b3lyp/6-31g(d) & LanL2DZ,
el. energy = -3883.351696 a.u.

C -2.11414500 2.68182800 -0.09420800
C -1.15738900 2.41279500 1.04689200
O -2.85489900 1.54913700 -0.49194000
C -3.00670100 3.92450600 0.16173000
C -1.19038100 1.26173700 1.83969900
H -0.57125100 3.26294600 1.38382800
C -0.16662800 0.97994700 2.75988900
H -1.95003200 0.51039400 1.64851500
H 0.43334500 1.79020900 3.17552400
H -0.23847200 0.08723300 3.36958100
H -3.56476700 4.11831700 -0.76195000
C -3.96833000 3.76724700 1.34695800
H -2.35659300 4.79327600 0.34157800
O -3.19409200 3.49316900 2.50462400
H -3.54978800 2.63034800 2.87488500
H -3.40894100 1.15709300 0.26777600
H -1.50159500 2.95759800 -0.95906900
H -4.64328100 2.92632100 1.13745900
C -5.14301800 -1.00027700 3.08113900
H -5.91630200 -1.36303100 2.39569700
H -4.39801100 -1.79491500 3.20089400
H -5.58222500 -0.77239500 4.05545500
C -4.44699900 0.22990700 2.49451200
O -4.13521600 0.15457100 1.25872300
O -4.21969900 1.18909500 3.27332000
N -1.35163700 -0.49552300 -1.82849000
C -1.29602800 -1.91338900 -1.49100900
C -1.79964200 -2.19678800 -0.04708500
N -0.65476700 -2.43532800 0.83972000
C -0.40225700 0.03656500 -2.62882600
C -0.75910100 -2.28403600 2.18865000
O -1.81048700 -1.95499000 2.73555100
O 0.51609500 -0.61700800 -3.14193700
C -0.52310400 1.51006900 -2.93626000
C 0.45925200 -2.54051000 3.05605900
C 0.44442800 2.44942600 -2.50919500
C 0.31319000 3.77982000 -2.93651700
C -0.73537800 4.17256400 -3.77120100
C -1.68905100 3.24235200 -4.17827800
C -1.58023800 1.91745800 -3.75641600
C 0.17259100 -3.29554000 4.20445000
C 1.14151800 -3.55862100 5.16719500
C 2.42090800 -3.02991300 5.00856400
C 2.71682800 -2.25549000 3.88742900
C 1.75972900 -2.00280500 2.88775600
P 1.72315300 1.96506600 -1.24996700
P 2.26005300 -0.98060500 1.40819700
C 2.46839200 3.57412800 -0.70132000
C 3.14510200 1.28787400 -2.22335100
C 2.65656400 -2.31716900 0.19066400
C 3.91331200 -0.30567100 1.89230700
C 5.12866200 -0.91710600 1.54925000
C 6.34333200 -0.33334800 1.91872500
C 6.36073800 0.86328900 2.63706200
C 5.15600100 1.47995000 2.98412900
C 3.94297100 0.90334800 2.60820900
C 3.07242600 1.00240300 -3.59282200
C 4.19482200 0.51567500 -4.26858200
C 5.39543500 0.30894000 -3.58894000
C 5.47335900 0.58925500 -2.22234400
C 4.35658300 1.07460900 -1.54404000
C 3.32509500 4.30913900 -1.54074100
C 3.87733600 5.51585100 -1.11202900
C 3.59397300 6.00504200 0.16596900
C 2.75971900 5.27770100 1.01451800
C 2.20452000 4.07055100 0.58276000
C 2.49847600 -2.07251100 -1.17997900
C 2.79844800 -3.06181100 -2.11926200
C 3.26571600 -4.30690600 -1.70026500
C 3.42383300 -4.56495200 -0.33572000
C 3.11683900 -3.58217800 0.60571500
H -2.00920100 0.14595600 -1.35764100
H -0.24663500 -2.20145600 -1.58040800
H -2.35087300 -1.34527300 0.35871000
H 0.15976200 -2.90014200 0.45836800
H 1.02307500 4.52784800 -2.60346300
H -0.80930000 5.20961900 -4.08656200
H -2.51833600 3.54411100 -4.81161800

H -2.32381400 1.18542600 -4.05690100
H -0.84253000 -3.65507900 4.33499400
H 0.89306600 -4.15501600 6.04039300
H 3.18937100 -3.20835600 5.75580600
H 3.71337400 -1.84031600 3.79070200
H 5.13063800 -1.84524300 0.98770900
H 7.27646500 -0.81751600 1.64308100
H 7.30672200 1.31562700 2.92171100
H 5.15991600 2.41371500 3.53959400
H 3.00982600 1.39660800 2.86578200
H 2.14006100 1.13123700 -4.12779900
H 4.12459700 0.29824200 -5.33104400
H 6.26531400 -0.06942100 -4.11928800
H 6.40186700 0.43033300 -1.68079400
H 4.43392200 1.29682400 -0.48378400
H 3.56668700 3.93321400 -2.53023400
H 4.53399300 6.07194900 -1.77569900
H 4.02725400 6.94426500 0.49882000
H 2.53981500 5.64485200 2.01336700
H 1.57078900 3.50030200 1.25357600
H 2.11411300 -1.12505700 -1.53021300
H 2.64549900 -2.84712600 -3.17217400
H 3.49361200 -5.07977900 -2.42928400
H 3.77628200 -5.53669800 -0.00043900
H 3.23038100 -3.80398300 1.66204100
Pd 0.78267100 0.85740000 0.77560700
C -2.08459900 -2.82072900 -2.50586400
H -1.76766000 -2.58647700 -3.52547500
C -2.81729200 -3.39550000 -0.08596900
H -3.13732100 -3.63215600 0.93076400
C -1.86944900 -5.81344300 -0.25814600
C -1.22148600 -6.77280100 -1.04620000
C -0.83651000 -6.46643800 -2.35268200
C -1.09369500 -5.19718800 -2.88529500
C -1.74804600 -4.24678100 -2.10644100
C -2.13662600 -4.55448300 -0.78991100
H -2.17105700 -6.05158100 0.75939600
H -1.02036500 -7.76020300 -0.63864600
H -0.33645500 -7.21588200 -2.96084400
H -0.79028500 -4.95609100 -3.90159700
C -5.28637500 -2.73432900 -0.56880600
C -6.21914300 -2.25996700 -1.49732300
C -5.82570900 -1.95477900 -2.80152500
C -4.49166500 -2.11783700 -3.19165800
C -3.56553400 -2.59937200 -2.27063700
C -3.96372800 -2.91427200 -0.96103100
H -5.58795100 -2.95043700 0.45192400
H -7.25369300 -2.11938300 -1.19637700
H -6.55602600 -1.58311400 -3.51557800
H -4.18076400 -1.87515600 -4.20556500
C -4.79133000 5.01652400 1.55149600
H -4.23373200 5.88017400 1.92039400
C -6.10357500 5.11707800 1.32803400
H -6.64384700 4.23554400 0.97719600
C -6.92687500 6.35825100 1.53044700
H -7.73072300 6.18866500 2.26027300
H -6.31403500 7.19199600 1.89086000
H -7.41406800 6.67454400 0.59713300

SRS-INT
b3lyp/6-31g(d) & LanL2DZ,
el. energy = -3883.341794 a.u.

C 3.46655200 2.10267900 -0.61037200
C 2.88808800 1.38513100 0.58303600
C 3.77453800 3.58154100 -0.26034600
C 1.60413300 1.58574900 1.08880200
H 3.52609900 0.63612700 1.04304800
C 1.09116600 0.80168200 2.15246500
H 0.99003200 2.38604500 0.67845800
H 1.79335500 0.22704300 2.75648300
H 0.21231300 1.15111400 2.67873100
H 2.84549600 4.09537800 0.02502600
C 4.77331300 3.64446700 0.89952500
H 4.17073700 4.07544700 -1.15480200
O 4.22761900 2.83386000 1.93454700
H 4.98169300 2.23984000 2.28173100
C 7.44606000 -0.69646800 2.37260000
H 7.02734900 -1.70479900 2.46951400
H 8.21309700 -0.74131300 1.59000900
H 7.90931000 -0.39644200 3.31522300
C 6.34868100 0.28850700 1.95493000
O 5.67842700 -0.02005500 0.91811700
O 6.20179400 1.31883100 2.66402700
N -1.79116300 1.64148100 -1.60357500
C -3.05802300 1.40150000 -0.92549900
C -3.00538000 1.86406700 0.55836100
N -2.80328900 0.74123500 1.46817900
C -1.23945600 0.70941000 -2.43503600
C -2.23564700 0.96205000 2.68732600
O -1.94476200 2.10289000 3.05497800
O -1.80459500 -0.35345200 -2.69021100
C 0.08031500 1.07192900 -3.06109600
C -1.96214000 -0.20241900 3.61595800
C 1.20066800 0.20254200 -3.00958200
C 2.36667800 0.59486600 -3.68265100
C 2.42455600 1.78759900 -4.41008900
C 1.31736100 2.62830600 -4.46442200
C 0.15264600 2.26919500 -3.78329700
C -2.28498700 0.07886300 4.95308500
C -2.02963700 -0.82949000 5.97523800
C -1.40632300 -2.03682800 5.67015000
C -1.05747800 -2.32405400 4.35057100
C -1.33088100 -1.43362900 3.29711500
P 1.24875600 -1.27975400 -1.87557800
P -0.80676500 -1.91471100 1.56746100
C 2.95445600 -1.96221300 -2.08793600
C 0.30226800 -2.62553500 -2.72501400
C -2.43987100 -2.43766400 0.85915000
C 0.08474200 -3.51954600 1.80657300
C -0.55564400 -4.76885700 1.79964500
C 0.18450000 -5.94335300 1.95460800
C 1.56949700 -5.88695400 2.12175400

C 2.21703500 -4.64945500 2.12807000
C 1.48084200 -3.47568800 1.96491100
C -0.23910300 -2.50361500 -4.01097000
C -0.87142900 -3.59177100 -4.61650300
C -0.97062200 -4.81250800 -3.94674300
C -0.43005100 -4.94310700 -2.66566000
C 0.20321900 -3.85797600 -2.05963000
C 3.30235800 -2.72316800 -3.22104200
C 4.59580400 -3.22026400 -3.36706200
C 5.56289200 -2.96488900 -2.38918700
C 5.23048300 -2.21270600 -1.26451800
C 3.93074100 -1.72225400 -1.11435000
C -2.62912500 -2.41288500 -0.52981600
C -3.84032500 -2.82697200 -1.08922800
C -4.87843500 -3.27060000 -0.26983800
C -4.70388900 -3.29569200 1.11615300
C -3.49578700 -2.88151400 1.67962200
H -1.27358700 2.48608000 -1.40221800
H -3.22048500 0.32426200 -0.98595700
H -2.14938400 2.52473100 0.71555200
H -3.18439100 -0.16807500 1.23969500
H 3.25686800 -0.01839300 -3.61520400
H 3.34624500 2.05704500 -4.91746700
H 1.35461100 3.55809100 -5.02495700
H -0.72196300 2.91326700 -3.83009500
H -2.72486600 1.04495900 5.17618200
H -2.29865800 -0.58680500 6.99921000
H -1.18076100 -2.75603200 6.45274800
H -0.55961700 -3.26299300 4.13940600
H -1.63078600 -4.83021800 1.66677600
H -0.32472200 -6.90341200 1.94242200
H 2.14259500 -6.80261000 2.23870000
H 3.29541200 -4.59451700 2.24595300
H 1.99525900 -2.51823100 1.94500800
H -0.18155000 -1.55746100 -4.53645100
H -1.28734100 -3.48181200 -5.61466900
H -1.46358100 -5.65727600 -4.42068600
H -0.49911900 -5.88878000 -2.13476000
H 0.62817700 -3.97713300 -1.06662400
H 2.56298600 -2.93231900 -3.98747300
H 4.84840800 -3.80691800 -4.24678700
H 6.57267100 -3.34888100 -2.51080700
H 5.95835400 -1.95681600 -0.50197100
H 3.70256700 -1.13972700 -0.23204700
H -1.85018700 -2.04589000 -1.18328400
H -3.96257500 -2.78691900 -2.16737900
H -5.82288300 -3.58585800 -0.70493700
H -5.50934300 -3.63299900 1.76297500
H -3.37762400 -2.90255000 2.75828000
Pd 0.75032700 -0.44713500 0.43266000
C -4.27931300 2.08937000 -1.63661400
H -4.28437600 1.82085100 -2.69633300
C -4.28578600 2.71961900 0.87979100
H -4.28237900 2.99318200 1.93666800
C -6.53709400 1.48408600 1.29462200
C -7.58725600 0.73398500 0.75166000
C -7.59186800 0.40818800 -0.60588900
C -6.54526900 0.82675600 -1.43640800
C -5.50601700 1.58097300 -0.89890300
C -5.50067900 1.90977100 0.46795200
H -6.53347800 1.73872400 2.35188600
H -8.40318300 0.40678000 1.39060100
H -8.41143500 -0.17187200 -1.02170500
H -6.54567600 0.56884400 -2.49289900
C -4.06318400 5.25814200 0.35220500
C -3.93829000 6.25264300 -0.62560200
C -3.92213100 5.91277100 -1.97962400
C -4.03109700 4.57305800 -2.37225300
C -4.16436000 3.58402400 -1.40105100
C -4.18247600 3.92681200 -0.03732800
H -4.06724800 5.52220200 1.40686500
H -3.85239000 7.29385600 -0.32704600
H -3.82590800 6.69012600 -2.73284800
H -4.02115700 4.30712900 -3.42699000
H 5.72792600 3.22151200 0.55885800
H 2.71115600 2.11702100 -1.40751000
O 4.59679400 1.43969500 -1.12725800
H 5.08581700 1.00124700 -0.38064400
C 4.99506200 5.05403600 1.38657600
H 4.13400600 5.51616400 1.87326000
C 6.13800900 5.73237500 1.26205700
H 6.98934100 5.24041400 0.78765300
C 6.36775400 7.14017000 1.73488400
H 5.47076200 7.55690800 2.20606000
H 7.18680000 7.18489100 2.46584600
H 6.65304600 7.80103600 0.90423700

RRS-INT
b3lyp/6-31g(d) & LanL2DZ,
el. energy = -3883.335975 a.u.

C 1.31372300 2.35880300 1.03328600
C 1.96614300 1.47758800 1.88992400
H 0.23057100 2.41566000 1.11770200
C 1.19234400 0.53412400 2.62079900
H 3.05187500 1.50225600 1.94341300
H 0.16309900 0.77928900 2.86832800
H 1.69257900 -0.12068300 3.33094000
C 5.97538800 3.29580800 3.71666300
H 5.78173500 3.81473900 4.65838900
H 6.80098200 3.79051400 3.19099100
H 6.29837400 2.26796600 3.91932400
C 4.72876100 3.28645500 2.82063600
O 3.71620300 3.91194000 3.22375800
O 4.84225200 2.63309900 1.72986000
C 1.95818800 3.31647900 0.05762600
H 1.30249000 3.33052100 -0.82330200
C 2.06726100 4.78293200 0.59611200
H 2.09116400 5.45504400 -0.26951600
H 3.03969500 4.84051500 1.09233700
C 1.02607700 5.25568000 1.62475800
O 1.02555800 4.37694500 2.73927500
H 1.97342400 4.19743300 2.97130900

O 3.21699600 2.89289700 -0.39418500
H 3.84802200 2.88486800 0.38784700
N -2.08966400 1.05406700 -1.80864600
C -3.09610600 0.23723800 -1.14410400
C -3.17526700 0.52886400 0.38786500
N -2.56135900 -0.53639800 1.17477700
C -0.92567900 0.50504700 -2.27036400
C -2.12673300 -0.26967200 2.44015500
O -2.22319500 0.86045300 2.92175200
O -0.70766700 -0.70501700 -2.19223100
C 0.08573400 1.42518100 -2.87683400
C -1.56020100 -1.39025000 3.28803100
C 1.46716200 1.11487200 -2.77539100
C 2.38261100 2.01121500 -3.34332900
C 1.95706400 3.14937300 -4.03152900
C 0.59793000 3.42659500 -4.15966200
C -0.33064300 2.56704000 -3.57562900
C -2.06263300 -1.39162000 4.59903200
C -1.62233300 -2.30766300 5.54934900
C -0.63737100 -3.22880400 5.20111500
C -0.10960200 -3.22565100 3.91018200
C -0.55441900 -2.32331900 2.92831100
P 2.08149300 -0.32474400 -1.75684000
P 0.25308400 -2.35814600 1.24596600
C 3.92789900 -0.15599400 -1.76440600
C 1.95331200 -1.81132100 -2.85915500
C -0.99263900 -3.33435700 0.27347800
C 1.64096500 -3.56680100 1.43336700
C 1.47167700 -4.95395900 1.29438400
C 2.56219500 -5.81587200 1.42562900
C 3.83382600 -5.30623000 1.69707200
C 4.01383300 -3.92828400 1.83474500
C 2.92590000 -3.06465500 1.69833800
C 1.34156500 -1.79745100 -4.11878100
C 1.31030100 -2.95195000 -4.90463900
C 1.88745900 -4.13636300 -4.44277300
C 2.50235900 -4.15931300 -3.18887200
C 2.53791000 -3.00528500 -2.40527800
C 4.70306800 -0.45014900 -2.90184800
C 6.08949800 -0.30182800 -2.87068400
C 6.72438400 0.14339500 -1.70665300
C 5.96813100 0.43103100 -0.57103900
C 4.58156200 0.27044100 -0.60188900
C -0.81741500 -3.48164700 -1.11114000
C -1.71305800 -4.24327400 -1.86199800
C -2.80558100 -4.85913800 -1.24830200
C -2.99230600 -4.71951400 0.12728100
C -2.08906300 -3.96999300 0.88604500
H -2.17577500 2.06008400 -1.75189500
H -2.77986900 -0.79312600 -1.31267300
H -2.61382200 1.43567000 0.62056400
H -2.62858300 -1.49341000 0.85077100
H 3.44441600 1.83484300 -3.22961500
H 2.69612200 3.81954000 -4.46117600
H 0.26053100 4.30390600 -4.70409900
H -1.39267900 2.76794100 -3.68930800
H -2.79752100 -0.63866900 4.86316500
H -2.03397400 -2.28909700 6.55435600
H -0.26821300 -3.94527000 5.92983500
H 0.66882900 -3.93894900 3.66585000
H 0.48993900 -5.36377000 1.07899800
H 2.41661200 -6.88689800 1.31232200
H 4.68141800 -5.97913300 1.79469900
H 5.00066000 -3.52141800 2.03667500
H 3.07528700 -1.99136300 1.78252900
H 0.88068200 -0.88783600 -4.48742600
H 0.83461200 -2.92211700 -5.88169400
H 1.86202600 -5.03304300 -5.05640600
H 2.95646000 -5.07409400 -2.81753500
H 3.02774700 -3.03584600 -1.43559000
H 4.22601100 -0.79751400 -3.81347100
H 6.67401800 -0.53092800 -3.75824800
H 7.80409700 0.26906100 -1.69108500
H 6.42463500 0.81795100 0.33473400
H 4.00845700 0.51211700 0.28103500
H 0.00764400 -2.99455600 -1.61015400
H -1.55495800 -4.34153000 -2.93213400
H -3.50798600 -5.44230800 -1.83774000
H -3.83818100 -5.19396700 0.61712500
H -2.23998000 -3.88979000 1.95754600
Pd 1.20323800 -0.22012400 0.59735800
C -4.51846900 0.42832800 -1.77595500
H -4.46840200 0.26836500 -2.85650400
C -4.67156500 0.80483600 0.78773700
H -4.73500100 0.97436300 1.86442400
C -6.24992900 -1.23914400 1.10202800
C -6.94204200 -2.29745700 0.50070500
C -6.86667900 -2.49447400 -0.87940000
C -6.09764400 -1.63611000 -1.67435400
C -5.41677500 -0.57843600 -1.07783100
C -5.49266100 -0.37868900 0.31158500
H -6.30828000 -1.08495800 2.17692400
H -7.54253200 -2.96592000 1.11197700
H -7.40849700 -3.31586900 -1.34063000
H -6.03617400 -1.79146500 -2.74902000
C -5.46406400 3.26395400 0.48674400
C -5.77555700 4.30283700 -0.39959900
C -5.68916500 4.10362500 -1.77895900
C -5.29003200 2.86185900 -2.28901100
C -4.98940800 1.82528100 -1.40847600
C -5.07833900 2.02552300 -0.01912100
H -5.52224400 3.42234600 1.56065300
H -6.08512100 5.26850000 -0.00972100
H -5.93300300 4.91420300 -2.46027800
H -5.22417400 2.70489600 -3.36343400
H 1.33884700 6.26875600 1.93447200
C -0.38099200 5.35408800 1.09043400
H -0.92221600 4.41148500 0.98927400
C -0.98206700 6.49434600 0.74266100
H -0.43922400 7.43243500 0.87563400
C -2.36947000 6.61199600 0.17783400
H -2.35801900 7.06517300 -0.82376900

H -2.86132800 5.63600400 0.10201000
H -2.99884400 7.25890000 0.80470300

SSR-TS
b3lyp/6-31g(d) & LanL2DZ,
el. energy = -3883.349415 a.u.
im. frequency -150.58

C 2.45122300 -2.57526400 -0.27320300
C 1.63511400 -2.46708900 0.99728700
O 3.05815500 -1.36352500 -0.66052100
C 3.45250400 -3.73740100 -0.14367900
C 1.30646400 -1.23819400 1.60089600
H 1.09642500 -3.35831300 1.30076000
C 0.32836200 -1.06874600 2.59713000
H 1.91447700 -0.38226200 1.33628600
H -0.12715600 -1.94181900 3.06715700
H 0.35866700 -0.17681500 3.21171000
H 4.08730100 -3.77909100 -1.03418500
C 4.27035500 -3.53706000 1.13917900
H 2.89662900 -4.68387300 -0.08077800
O 3.31462000 -3.17311900 2.13993800
H 3.68165200 -2.29386200 2.60486300
H 3.62633900 -0.98197300 0.08633400
H 1.75331900 -2.83941200 -1.07554600
H 4.97248600 -2.70655200 0.99072200
C 5.09510000 1.12690800 3.09832600
H 5.84338700 1.60961700 2.46226400
H 4.26354100 1.82624100 3.24001000
H 5.52344700 0.88584500 4.07440500
C 4.54572300 -0.12308500 2.41759100
O 4.39793500 -0.07324300 1.16151400
O 4.25956300 -1.09944800 3.17603000
N 1.29181900 0.63114800 -1.91104400
C 1.13553000 2.03071400 -1.53186500
C 1.64447800 2.31341300 -0.08930900
N 0.51524900 2.44948100 0.83485300
C 0.31941000 0.01984000 -2.62915800
C 0.68359200 2.26670300 2.17323100
O 1.78309700 1.99553000 2.65733700
O -0.69943400 0.59169500 -3.03473600
C 0.54728700 -1.42957300 -2.97911200
C -0.50261100 2.42745300 3.10611600
C -0.35513300 -2.43879700 -2.56729900
C -0.13830800 -3.74742700 -3.02470300
C 0.92960300 -4.05237700 -3.87262000
C 1.81729400 -3.05283500 -4.26464000
C 1.62442800 -1.74703900 -3.81292800
C -0.18807800 3.14529200 4.27150000
C -1.11862100 3.33661000 5.28746200
C -2.38702000 2.77350500 5.16354100
C -2.70936100 2.03626300 4.02485700
C -1.79306700 1.85377400 2.97304900
P -1.64993700 -2.05578600 -1.28482400
P -2.31573700 0.85025400 1.48769000
C -2.22822500 -3.73420400 -0.73544900
C -3.13407700 -1.50646900 -2.24519700
C -2.78684800 2.20588600 0.31314400
C -3.94474900 0.13560400 2.00084600
C -5.18030900 0.74052700 1.72435500
C -6.37360700 0.12059500 2.10462400
C -6.34955200 -1.10594100 2.77030200
C -5.12464000 -1.71672500 3.05140500
C -3.93326900 -1.10482300 2.66205700
C -3.11661100 -1.27690500 -3.62680200
C -4.27879500 -0.87010900 -4.28752900
C -5.46717100 -0.68835200 -3.57940600
C -5.49107500 -0.91141100 -2.20027000
C -4.33275600 -1.31461000 -1.53736800
C -3.09940700 -4.51793600 -1.51226100
C -3.51069900 -5.77590100 -1.07007800
C -3.06639800 -6.26993800 0.15886600
C -2.21134600 -5.49736800 0.94547300
C -1.79907100 -4.23925900 0.50065700
C -2.73863600 1.96456500 -1.06769700
C -3.09669700 2.96244200 -1.97709600
C -3.50965000 4.21380100 -1.51996900
C -3.55828800 4.46830100 -0.14696000
C -3.19685000 3.47552000 0.76481300
H 2.03350500 0.04880800 -1.50238600
H 0.06536500 2.23744100 -1.59739300
H 2.25912100 1.48872900 0.27643600
H -0.35314200 2.83760900 0.48880300
H -0.79937300 -4.54588500 -2.70744100
H 1.06829200 -5.07478700 -4.21353900
H 2.65891700 -3.28506300 -4.91105400
H 2.31503700 -0.96087600 -4.10308000
H 0.81945600 3.53469700 4.37060200
H -0.84846000 3.90516100 6.17278000
H -3.12629500 2.89721400 5.95039400
H -3.69652400 1.59393300 3.95442500
H -5.21523700 1.69401500 1.20769700
H -7.32252500 0.60028100 1.87924100
H -7.27889700 -1.58634500 3.06402200
H -5.09630100 -2.67426200 3.56430200
H -2.98411100 -1.59500600 2.86235000
H -2.19563000 -1.39338000 -4.18524800
H -4.25012500 -0.69419800 -5.35968300
H -6.36874400 -0.37161100 -4.09716700
H -6.40878400 -0.76758000 -1.63637000
H -4.36457900 -1.48258200 -0.46428200
H -3.46279600 -4.14149800 -2.46358600
H -4.18280700 -6.36850200 -1.68511500
H -3.39043300 -7.24844700 0.50301800
H -1.86718800 -5.86914500 1.90704300
H -1.14733700 -3.63257100 1.12221100
H -2.39409600 1.01282100 -1.44816500
H -3.03087100 2.75193100 -3.04008800
H -3.78049100 4.99303400 -2.22728600
H -3.86952000 5.44364100 0.21762100
H -3.22965900 3.69274500 1.82768600
Pd -0.80598800 -0.89130600 0.75061900
C 1.84158300 3.01872200 -2.53272200

H 1.52390200 2.79138600 -3.55378600
C 2.58106200 3.57663900 -0.11143700
H 2.90181800 3.80651600 0.90657000
C 1.47608100 5.93116900 -0.20116200
C 0.75247000 6.86610700 -0.95160500
C 0.36305300 6.56928800 -2.25900300
C 0.69193100 5.33409800 -2.83053800
C 1.42038900 4.40827600 -2.08868500
C 1.81334400 4.70643800 -0.77157400
H 1.78044900 6.16183300 0.81724900
H 0.49536900 7.82728200 -0.51396200
H -0.19636200 7.29995200 -2.83756200
H 0.38507200 5.10009100 -3.84742900
C 5.07706700 3.08202500 -0.64923100
C 6.02137500 2.69044300 -1.60466400
C 5.62528400 2.39964300 -2.91122600
C 4.27727000 2.49123800 -3.27672700
C 3.33853000 2.88854700 -2.32866400
C 3.73971500 3.19305300 -1.01702100
H 5.38218300 3.28762100 0.37296300
H 7.06735300 2.60450000 -1.32338800
H 6.36483100 2.09426100 -3.64688300
H 3.96537000 2.25762400 -4.29243300
C 5.02356600 -4.77068800 1.55698300
H 4.40349400 -5.62903500 1.82267700
C 6.35420000 -4.86014400 1.61766500
H 6.94911700 -3.98129200 1.36259000
C 7.12429200 -6.08518800 2.02133600
H 7.75726300 -5.88388400 2.89636500
H 6.45626100 -6.91693000 2.27039400
H 7.79666900 -6.41772500 1.21826200

RSR-TS
b3lyp/6-31g(d) & LanL2DZ,
el. energy = -3883.348815 a.u.
im. frequency -80.60

C 2.53416400 1.84903600 -0.44460200
C 1.39097000 1.66874000 -1.25445700
H 3.27839200 1.06010800 -0.42286100
C 1.32313700 0.58184900 -2.16545000
H 0.59994800 2.41325200 -1.21921900
H 2.24401200 0.09632200 -2.48208400
H 0.52833000 0.56222400 -2.90726900
C 7.52851100 0.13171100 -0.00064300
H 8.06496700 -0.02981600 -0.93960900
H 7.38772200 -0.81441600 0.53012700
H 8.15032500 0.77805200 0.63184200
C 6.18826800 0.82995500 -0.25038200
O 6.14324600 1.61165700 -1.24384200
O 5.24587400 0.59257700 0.56521600
C 2.63874900 2.87188600 0.66131300
H 1.66839900 2.95872600 1.16112300
C 2.95962900 4.25225600 0.04846300
H 3.11457100 4.98072100 0.85123200
H 2.10598900 4.58865800 -0.55485200
C 4.20266400 4.10356100 -0.83179900
H 5.07978200 3.94751100 -0.19146700
O 3.97578900 2.91517400 -1.60699100
H 4.83462500 2.33826500 -1.51979700
O 3.58790000 2.48805300 1.63619100
H 4.26878200 1.89508900 1.22437500
N -2.78364600 -0.22377100 -1.93646800
C -3.56495900 0.27238300 -0.81146200
C -3.05283200 1.66804900 -0.34410800
N -2.26762900 1.58713300 0.88116500
C -2.27726700 -1.49066700 -1.96955900
C -1.30019600 2.51686200 1.13540000
O -1.05864100 3.42896400 0.34133300
O -2.52320300 -2.32587400 -1.10041300
C -1.40430700 -1.81171300 -3.15324000
C -0.56980800 2.45381900 2.45653100
C -0.11620700 -2.37996900 -2.98283600
C 0.62837900 -2.66332700 -4.13606800
C 0.11644600 -2.42692800 -5.41569000
C -1.15566500 -1.88483500 -5.57154700
C -1.90720100 -1.57302800 -4.43735000
C -0.55152900 3.67563900 3.14831300
C 0.12665000 3.81516000 4.35494400
C 0.83205100 2.72906400 4.87011900
C 0.84551800 1.51861900 4.17907000
C 0.14188300 1.34525000 2.97475400
P 0.64681000 -2.50662600 -1.28321300
P 0.21866900 -0.30297700 2.10318000
C 2.39150000 -3.06260200 -1.56903800
C -0.03076200 -4.06585800 -0.55233100
C -1.30894900 -1.10771300 2.78273600
C 1.60624200 -1.18134400 2.95097800
C 1.41866800 -2.27464900 3.81050700
C 2.52280100 -2.95874300 4.32866800
C 3.81929500 -2.56085400 3.99675400
C 4.01360500 -1.46849100 3.14716800
C 2.91578800 -0.78595600 2.62624200
C -0.89130500 -4.93358000 -1.23694800
C -1.31010100 -6.12518500 -0.64175300
C -0.87780900 -6.46193900 0.64210800
C -0.02261500 -5.59967900 1.33168400
C 0.39788700 -4.40878000 0.73957500
C 2.68465200 -4.32042700 -2.12877000
C 4.00601500 -4.73396300 -2.28938200
C 5.05597600 -3.90975900 -1.87200000
C 4.77740500 -2.67549600 -1.28727700
C 3.45338400 -2.25475500 -1.13838100
C -2.00984200 -2.02585100 1.98718600
C -3.15442100 -2.66221400 2.47573000
C -3.61287400 -2.39033000 3.76459100
C -2.92496600 -1.47441800 4.56550200
C -1.78375900 -0.83544200 4.07975900
H -2.50026000 0.42926600 -2.65429400
H -3.44177100 -0.46781200 -0.01915500
H -2.37978900 2.08917500 -1.09356600
H -2.53113100 0.92663900 1.60143000
H 1.63100700 -3.06313700 -4.04195200

H 0.72220700 -2.66491900 -6.28569400
H -1.56157600 -1.69981700 -6.56197300
H -2.90407000 -1.15328900 -4.54630300
H -1.06849900 4.52280200 2.70893000
H 0.12019800 4.76844300 4.87575700
H 1.38678600 2.82268900 5.79954600
H 1.42716100 0.69449800 4.57655000
H 0.41684800 -2.59769400 4.07509700
H 2.36469200 -3.80503300 4.99260100
H 4.67325400 -3.10095100 4.39743200
H 5.00794800 -1.13880400 2.86135200
H 3.09527000 0.07149400 1.98790900
H -1.24660200 -4.67695500 -2.22893100
H -1.97800700 -6.78941200 -1.18421700
H -1.20591200 -7.39000800 1.10283800
H 0.31844000 -5.85027900 2.33257200
H 1.06566900 -3.74851100 1.28678900
H 1.87785300 -4.98476400 -2.42565700
H 4.21603300 -5.70577600 -2.72862600
H 6.08522700 -4.23788900 -1.99078500
H 5.57660300 -2.03207100 -0.93390400
H 3.25606400 -1.30348200 -0.65556800
H -1.68414800 -2.23652900 0.97655400
H -3.68172900 -3.36396300 1.83605300
H -4.50464700 -2.88249500 4.14378500
H -3.27851500 -1.25270300 5.56908700
H -1.26400800 -0.12174100 4.71129600
Pd 0.69963200 -0.29024800 -0.30199800
C -5.09985800 0.36920500 -1.13489200
H -5.45659900 -0.59276800 -1.51260600
C -4.27203400 2.65595800 -0.23220800
H -3.92286700 3.62197400 0.13931000
C -5.79659700 2.49992900 1.87043400
C -6.75260600 1.76389400 2.58077100
C -7.20708700 0.53906500 2.08868300
C -6.70955100 0.03477700 0.88110000
C -5.76601800 0.77073100 0.16982500
C -5.30873300 2.00482600 0.66397500
H -5.44186200 3.45357500 2.25428700
H -7.14221100 2.14965700 3.51901900
H -7.94996000 -0.02687700 2.64428500
H -7.05909500 -0.92185000 0.49990100
C -4.91453400 3.87936600 -2.43710500
C -5.44124900 3.77898400 -3.73059000
C -5.87946000 2.54705100 -4.21998400
C -5.79579000 1.39983200 -3.42120000
C -5.28107400 1.50025500 -2.13115400
C -4.84173800 2.74165000 -1.63767900
H -4.56664100 4.83744300 -2.05861900
H -5.50780300 4.66530300 -4.35566100
H -6.28812600 2.47698700 -5.22450500
H -6.13822600 0.43978100 -3.80104500
C 4.43731500 5.27954700 -1.73938300
H 3.65483500 5.46220900 -2.47801500
C 5.50793400 6.07514500 -1.68449400
H 6.28222900 5.85978300 -0.94580700
C 5.75283200 7.26294600 -2.57091000
H 5.85449700 8.18616500 -1.98359600
H 6.68693900 7.14782700 -3.13760700
H 4.93670600 7.40557200 -3.28754600

SRS-TS
b3lyp/6-31g(d) & LanL2DZ,
el. energy = -3883.341745 a.u.
im. frequency -9.98

C 3.52876400 2.10225100 -0.66883700
C 2.93947700 1.41148100 0.53574900
C 3.84258600 3.58306200 -0.33660500
C 1.64176100 1.61334100 1.01121800
H 3.55967700 0.65094800 1.00013200
C 1.11461100 0.86193900 2.09193100
H 1.03927200 2.41094900 0.57904400
H 1.80754300 0.29841300 2.71679500
H 0.23667400 1.23494200 2.60376200
H 2.91323300 4.11058400 -0.07890600
C 4.81225600 3.64140600 0.84779200
H 4.26645000 4.06134700 -1.22658200
O 4.23277500 2.82647400 1.86324400
H 4.97615300 2.22562200 2.23357700
C 7.42843000 -0.69916500 2.41184600
H 7.01092200 -1.70896100 2.49733400
H 8.22033000 -0.74274700 1.65444700
H 7.85951000 -0.39497400 3.36824800
C 6.34127500 0.27933700 1.95615500
O 5.70729200 -0.03206000 0.89873700
O 6.16538600 1.31037000 2.65975300
N -1.83676300 1.62207200 -1.61359200
C -3.09148300 1.37301300 -0.91628400
C -3.02732000 1.85623200 0.56051500
N -2.79474000 0.74946900 1.48247600
C -1.28201100 0.68642900 -2.43921100
C -2.21009400 0.99533600 2.68887100
O -1.92878800 2.14534700 3.03497000
O -1.83664000 -0.38616000 -2.67591600
C 0.02773100 1.05668000 -3.08179100
C -1.90681400 -0.15152200 3.63015900
C 1.15569700 0.19679900 -3.03594500
C 2.31239800 0.59552700 -3.72141000
C 2.35400100 1.78517100 -4.45515300
C 1.23922300 2.61625500 -4.50389900
C 0.08367500 2.25072400 -3.81066900
C -2.20699800 0.14836300 4.96856700
C -1.92443400 -0.74110700 6.00010300
C -1.29648000 -1.94790000 5.70254700
C -0.97001100 -2.25332200 4.38135400
C -1.27091700 -1.38244500 3.31905700
P 1.22423400 -1.27927700 -1.89475900
P -0.77214800 -1.88489400 1.58799700
C 2.93252100 -1.95203000 -2.11885800
C 0.27928900 -2.63500400 -2.72994000
C -2.41267500 -2.43099300 0.91428800
C 0.13396300 -3.48071200 1.83505100

C -0.49873600 -4.73376400 1.86231900
C 0.25150500 -5.90124900 2.02138100
C 1.63927400 -5.83412100 2.15879300
C 2.27925500 -4.59299300 2.13097000
C 1.53273800 -3.42634900 1.96352300
C -0.26358600 -2.52601000 -4.01649100
C -0.89356600 -3.62098900 -4.61180400
C -0.98936100 -4.83582500 -3.93078000
C -0.44831200 -4.95324700 -2.64867300
C 0.18276800 -3.86109400 -2.05282200
C 3.28027200 -2.70628200 -3.25642000
C 4.57489600 -3.19868300 -3.40771700
C 5.54327500 -2.94573700 -2.43040900
C 5.21125400 -2.20092400 -1.30073500
C 3.91029700 -1.71499300 -1.14598600
C -2.62407600 -2.42838800 -0.47179600
C -3.84122100 -2.85865600 -1.00557500
C -4.86339900 -3.29621100 -0.16316100
C -4.66677700 -3.29927500 1.22005000
C -3.45250800 -2.86920000 1.75787900
H -1.32558400 2.47326800 -1.42430300
H -3.23934200 0.29289600 -0.96006500
H -2.18075200 2.53321400 0.69782100
H -3.16718600 -0.16787800 1.27287000
H 3.20778700 -0.01110000 -3.65989700
H 3.26854000 2.05935400 -4.97295200
H 1.26346300 3.54321600 -5.06981000
H -0.79677100 2.88709500 -3.85319700
H -2.65119800 1.11411000 5.18440600
H -2.17626200 -0.48419200 7.02498600
H -1.04999400 -2.65253200 6.49207400
H -0.46808600 -3.19136400 4.17583800
H -1.57608500 -4.80369400 1.75341900
H -0.25204300 -6.86427800 2.03577100
H 2.22022100 -6.74440200 2.27905000
H 3.35950600 -4.52992100 2.22523900
H 2.04040800 -2.46629500 1.91637300
H -0.20861800 -1.58429400 -4.55038500
H -1.31067200 -3.52112000 -5.61054100
H -1.48055800 -5.68608600 -4.39667300
H -0.51550500 -5.89408600 -2.10900900
H 0.60705800 -3.96945200 -1.05821200
H 2.53945100 -2.91441300 -4.02185000
H 4.82746400 -3.78017000 -4.29088200
H 6.55385700 -3.32624800 -2.55620200
H 5.94033000 -1.94777200 -0.53822700
H 3.67966300 -1.13935000 -0.25952900
H -1.85776700 -2.06611300 -1.14275500
H -3.98105000 -2.83568700 -2.08211300
H -5.81259400 -3.62376000 -0.57840000
H -5.45975000 -3.63175300 1.88456600
H -3.31667600 -2.87302500 2.83470100
Pd 0.75113200 -0.42220400 0.40803500
C -4.33176000 2.03304100 -1.62095800
H -4.34539300 1.75101000 -2.67707100
C -4.31772900 2.69456900 0.88738900
H -4.30584400 2.98117100 1.94076600
C -6.54369000 1.42811400 1.34520600
C -7.58804700 0.65453000 0.82444900
C -7.60372900 0.31163300 -0.52878600
C -6.57426600 0.73671400 -1.37719900
C -5.54114200 1.51445400 -0.86191300
C -5.52433800 1.86008000 0.50073800
H -6.53148800 1.69595100 2.39914200
H -8.39074300 0.32226800 1.47738900
H -8.41870000 -0.28674900 -0.92732600
H -6.58323800 0.46572200 -2.43037200
C -4.14354400 5.22949600 0.32612800
C -4.04636500 6.21371800 -0.66511400
C -4.04049600 5.85735300 -2.01495600
C -4.13228500 4.51126600 -2.38984000
C -4.23806900 3.53223900 -1.40515600
C -4.24561800 3.89167100 -0.04563900
H -4.13954600 5.50649600 1.37747300
H -3.97402000 7.25981900 -0.38032500
H -3.96575200 6.62672100 -2.77875700
H -4.13019000 4.23252400 -3.44130400
H 5.77364600 3.21435600 0.53280000
H 2.77753100 2.10578900 -1.47013000
O 4.66013700 1.42695300 -1.16661700
H 5.13407300 0.98536000 -0.41273600
C 5.02615100 5.04606300 1.35016400
H 4.15206300 5.51252900 1.80845100
C 6.17819400 5.71550900 1.26896300
H 7.04142700 5.21872400 0.82199000
C 6.40257000 7.11908800 1.75630800
H 5.49317200 7.54132100 2.19779300
H 7.19588300 7.15324500 2.51562500
H 6.72245600 7.78106600 0.93932800

RRS-TS
b3lyp/6-31g(d) & LanL2DZ,
el. energy = -3883.335529 a.u.
im. frequency -67.06

C 1.40929000 2.46947400 1.05265000
C 2.13539000 1.46718400 1.71483200
H 0.33826400 2.48582800 1.23196700
C 1.45282900 0.56032700 2.56948900
H 3.21866400 1.48728900 1.65340300
H 0.46134100 0.82555100 2.92376800
H 2.03263800 -0.06559000 3.24537300
C 6.36277300 3.71280700 3.05239700
H 6.32696000 4.42377400 3.88087100
H 7.13675000 4.01327400 2.33715600
H 6.64651500 2.72428700 3.43322900
C 5.00763600 3.61765100 2.34193900
O 4.05627100 4.29003800 2.82756500
O 4.96748500 2.85961300 1.32326800
C 1.91622200 3.32895200 -0.08985000
H 1.17744400 3.19708100 -0.89351800
C 1.97068000 4.84954800 0.27860000
H 1.66643900 5.45996100 -0.57847400

H 3.02501900 5.05999100 0.47965200
C 1.18225900 5.20691800 1.55048600
O 1.44928900 4.18716700 2.51093000
H 2.45614600 4.17346500 2.65255200
O 3.14133400 2.90424400 -0.61913300
H 3.84152900 2.97912100 0.09705200
N -1.99774200 0.93220000 -2.00718900
C -3.04923800 0.23899800 -1.27822200
C -3.14644600 0.72078900 0.20434600
N -2.59433200 -0.25272500 1.13671600
C -0.84646700 0.29258700 -2.38184300
C -2.00458000 0.16493300 2.29376700
O -1.86694000 1.36140700 2.55619400
O -0.68040000 -0.91098300 -2.18449500
C 0.20996300 1.11946100 -3.04381300
C -1.58724000 -0.87957900 3.30787400
C 1.57821200 0.78010800 -2.88097900
C 2.53076200 1.59696200 -3.50613400
C 2.15634500 2.67958700 -4.30374100
C 0.80946500 2.98138000 -4.49078300
C -0.15599100 2.20415400 -3.85432300
C -2.08968900 -0.63563600 4.59514900
C -1.77722500 -1.46643500 5.66739000
C -0.92469900 -2.54888300 5.46321500
C -0.39542200 -2.78752300 4.19477500
C -0.71149200 -1.97340100 3.09369900
P 2.13902800 -0.59045500 -1.73893600
P 0.11203200 -2.29106600 1.44771400
C 3.99341700 -0.46781600 -1.80003300
C 1.93402700 -2.15445900 -2.71335600
C -1.21566800 -3.23651100 0.55699900
C 1.34387400 -3.62507300 1.81674200
C 1.00587800 -4.98691500 1.87603300
C 1.98371000 -5.94862400 2.13735900
C 3.31098200 -5.56531700 2.34233600
C 3.65933000 -4.21451300 2.28152200
C 2.68346200 -3.25230000 2.01598500
C 1.42425400 -2.19901800 -4.01717100
C 1.33441400 -3.41172000 -4.70422000
C 1.75325000 -4.59822000 -4.09892200
C 2.26587500 -4.56408900 -2.80034900
C 2.35552700 -3.35207700 -2.11372400
C 4.75629800 -1.02717600 -2.84205800
C 6.14521400 -0.89289700 -2.85314100
C 6.79582000 -0.19377200 -1.83180600
C 6.05089500 0.36694200 -0.79453800
C 4.66286300 0.21886100 -0.77824800
C -1.04519100 -3.52012900 -0.80660400
C -2.00426400 -4.25627500 -1.50312700
C -3.15746400 -4.70569000 -0.85685100
C -3.34142900 -4.42692500 0.49805000
C -2.37419300 -3.70581400 1.20395000
H -2.03492400 1.94161400 -2.05038600
H -2.77189300 -0.81549700 -1.31044400
H -2.54995500 1.62394300 0.33809700
H -2.80001600 -1.23560300 1.00374800
H 3.58413800 1.39751200 -3.35733400
H 2.92495200 3.28585700 -4.77457200
H 0.50999600 3.81318500 -5.12210200
H -1.20886200 2.42079000 -4.01479900
H -2.72023700 0.23511800 4.74336500
H -2.18377200 -1.25887700 6.65306300
H -0.65763400 -3.20422200 6.28782700
H 0.28378700 -3.62189600 4.06371000
H -0.02081900 -5.29950100 1.71288000
H 1.70710300 -6.99896500 2.17690000
H 4.07085700 -6.31619800 2.54146800
H 4.69079800 -3.90732200 2.43046000
H 2.96135400 -2.20352600 1.94720900
H 1.08936000 -1.28652400 -4.49887200
H 0.93645900 -3.42651300 -5.71580900
H 1.68360900 -5.54087600 -4.63540900
H 2.59562100 -5.48009700 -2.31732600
H 2.75809800 -3.34243100 -1.10411400
H 4.26935100 -1.56837700 -3.64697200
H 6.71934100 -1.33260000 -3.66504700
H 7.87733600 -0.08452000 -1.85116800
H 6.51759900 0.94510600 -0.00259200
H 4.09980400 0.67602300 0.01983400
H -0.17540100 -3.15265300 -1.33293200
H -1.84889600 -4.46313000 -2.55821600
H -3.90914200 -5.26738100 -1.40495600
H -4.23534700 -4.77001800 1.01173000
H -2.52472800 -3.51729400 2.26243900
Pd 1.29549900 -0.34556300 0.62725100
C -4.45053900 0.40536800 -1.96284000
H -4.38670200 0.11363200 -3.01462700
C -4.63818500 1.09843200 0.53170900
H -4.71973100 1.39855600 1.57927200
C -6.29798100 -0.83596800 1.05612000
C -7.01708400 -1.93563500 0.57206500
C -6.92394600 -2.30145100 -0.77196700
C -6.10950400 -1.57323600 -1.64753400
C -5.40115300 -0.47462800 -1.16888300
C -5.49536800 -0.10468700 0.18430200
H -6.37066800 -0.55014500 2.10288300
H -7.65279800 -2.50357600 1.24613400
H -7.48712600 -3.15383600 -1.14244800
H -6.03304200 -1.86111500 -2.69344300
C -5.34165000 3.52608400 -0.08361500
C -5.59926500 4.45858600 -1.09639400
C -5.48979200 4.09017300 -2.43855900
C -5.12195500 2.78389200 -2.78441300
C -4.87436000 1.85287000 -1.77821700
C -4.98478900 2.22448100 -0.42625800
H -5.42289400 3.81412100 0.96168400
H -5.88542400 5.47338000 -0.83420300
H -5.69205800 4.81860000 -3.21909900
H -5.03968600 2.49529600 -3.82998000
H 1.56218200 6.17037100 1.92325900
C -0.30692800 5.32485900 1.35719500
H -0.85271400 4.39509100 1.18994600

C -0.97645300 6.47971800 1.37016600
H -0.42589500 7.40279000 1.56268300
C -2.45386500 6.62927900 1.14172200
H -2.66084700 7.28951700 0.28783400
H -2.93120100 5.66297300 0.94516600
H -2.94609000 7.08185900 2.01360100

SSR-Product
b3lyp/6-31g(d) & LanL2DZ,
el. energy = -3883.382357 a.u.

C -2.46059400 2.71322100 -0.52381300
C -1.83511600 2.78028600 0.88333800
O -3.05559800 1.45816500 -0.83359300
C -3.48934000 3.84933100 -0.46379300
C -1.24885700 1.50591000 1.40670200
H -1.11295100 3.60421400 0.92778800
C -0.38046900 1.40363900 2.48097000
H -1.83584200 0.62409300 1.16956100
H 0.06880700 2.29456300 2.92053100
H -0.39539000 0.52432800 3.11530400
H -4.26228800 3.74487100 -1.22934000
C -4.05435200 3.75405900 0.96399100
H -2.98648700 4.81382200 -0.61018000
O -2.97167800 3.16400000 1.74838400
H -3.62194500 1.92051800 2.70447400
H -3.65024300 1.17082400 -0.10367100
H -1.70891400 2.88457800 -1.29235800
H -4.89682800 3.05113900 0.98850500
C -5.16199600 -0.88639300 3.20031800
H -5.88719000 -1.41301700 2.57739500
H -4.32641400 -1.55734000 3.42751400
H -5.61790600 -0.56744100 4.14106100
C -4.59534100 0.28816100 2.44642600
O -4.60688500 0.36573300 1.22002700
O -4.07224000 1.20788000 3.24634000
N -1.24751600 -0.64414000 -2.00349200
C -1.15517400 -2.02533100 -1.55022600
C -1.74430900 -2.21405800 -0.12369800
N -0.68266700 -2.36244400 0.86960800
C -0.23071700 -0.10271000 -2.72274300
C -0.90852700 -2.06718800 2.17733600
O -2.02050200 -1.69878400 2.57002000
O 0.76208500 -0.74006300 -3.08549100
C -0.39917000 1.34167100 -3.12571300
C 0.21183800 -2.25050900 3.18015600
C 0.50033300 2.34284100 -2.68940000
C 0.32830600 3.64297400 -3.18919800
C -0.69208600 3.94732200 -4.09434300
C -1.57682300 2.95455900 -4.50963000
C -1.42723000 1.65627100 -4.02059600
C -0.22016600 -2.84023000 4.37961100
C 0.64961300 -3.06084500 5.44214100
C 1.97919900 -2.66152400 5.32393300
C 2.41834800 -2.05209000 4.14917000
C 1.56407200 -1.83697000 3.05194400
P 1.71821200 1.95602300 -1.32744700
P 2.22026600 -0.94430500 1.54044600
C 2.33477600 3.64151700 -0.83119500
C 3.21736600 1.34251100 -2.23441900
C 2.64003100 -2.39606100 0.45663300
C 3.88622300 -0.35930600 2.10921900
C 5.08146200 -1.06883400 1.91728400
C 6.30321300 -0.52626900 2.32581900
C 6.34820300 0.72729800 2.93758500
C 5.16426700 1.44364200 3.13312500
C 3.94636900 0.90913100 2.71343400
C 3.25671000 1.11498600 -3.61620100
C 4.42664800 0.65047800 -4.22352100
C 5.57006500 0.40871000 -3.46143300
C 5.53881100 0.62904600 -2.08189700
C 4.37116500 1.08764700 -1.47351900
C 3.24838600 4.37674900 -1.60606000
C 3.68432000 5.63580000 -1.19018100
C 3.22212700 6.17895200 0.01123300
C 2.32485400 5.45401600 0.79656500
C 1.88816600 4.19487700 0.37790900
C 2.68378400 -2.20365100 -0.93381000
C 2.99912800 -3.26153000 -1.78961900
C 3.27331700 -4.52749200 -1.27099200
C 3.22687900 -4.73476700 0.10968200
C 2.91140400 -3.67970200 0.96786100
H -1.96575200 -0.01849200 -1.62941700
H -0.09132300 -2.27173800 -1.55427800
H -2.32557700 -1.33809700 0.16881100
H 0.19518300 -2.78297500 0.59229600
H 0.99053700 4.43636900 -2.86131200
H -0.79423900 4.96386200 -4.46540800
H -2.38004100 3.18530300 -5.20397800
H -2.11406700 0.87386900 -4.33058200
H -1.26724800 -3.11103000 4.46287300
H 0.28880400 -3.52773000 6.35439000
H 2.67715700 -2.81492800 6.14293700
H 3.45270200 -1.73377700 4.08521300
H 5.06363600 -2.04475500 1.44288000
H 7.22015500 -1.08752400 2.16450100
H 7.29937400 1.14746800 3.25361300
H 5.19020100 2.42457600 3.60042300
H 3.03026200 1.48110700 2.83876500
H 2.37169200 1.28092200 -4.21930600
H 4.43925900 0.47617400 -5.29649900
H 6.47807000 0.04696700 -3.93709300
H 6.41989700 0.43802700 -1.47491200
H 4.35823300 1.24856600 -0.39881900
H 3.62609900 3.96030400 -2.53513300
H 4.39040100 6.19029600 -1.80307700
H 3.56640800 7.15750800 0.33579700
H 1.96890000 5.86329700 1.73874600
H 1.20830400 3.61621500 0.99699700
H 2.44906700 -1.23623300 -1.36011900
H 3.01031000 -3.08605400 -2.86117900
H 3.51059100 -5.35253800 -1.93748300
H 3.43059600 -5.71979600 0.52169700

H 2.87359700 -3.85834100 2.03815300
Pd 0.85623500 0.87124200 0.68279200
C -1.85669900 -3.03279700 -2.53508100
H -1.47802200 -2.87242200 -3.54779000
C -2.74564100 -3.42787300 -0.13289500
H -3.12639200 -3.58912700 0.87778400
C -1.76688500 -5.83708800 -0.04898600
C -1.05847000 -6.84534800 -0.71383600
C -0.58691300 -6.63578700 -2.01098100
C -0.81846000 -5.41601000 -2.65819200
C -1.53221200 -4.41707900 -2.00189900
C -2.00655800 -4.62722400 -0.69509300
H -2.13281100 -5.99898200 0.96239500
H -0.87590900 -7.79459900 -0.21682600
H -0.03832500 -7.42244200 -2.52248400
H -0.44686000 -5.24978000 -3.66664200
C -5.18552100 -2.85185200 -0.82674800
C -6.06028900 -2.46416100 -1.84830200
C -5.58241400 -2.25356700 -3.14283100
C -4.22294200 -2.42512000 -3.43010300
C -3.35372800 -2.81905600 -2.41663300
C -3.83664900 -3.03779400 -1.11487100
H -5.55475700 -3.00416500 0.18427600
H -7.11540200 -2.32281400 -1.62989500
H -6.26703700 -1.95176200 -3.93121700
H -3.84844800 -2.25704600 -4.43744800
C -4.46221700 5.05866500 1.57519300
H -3.67510500 5.81098900 1.64958300
C -5.69663700 5.33374500 2.00474800
H -6.46103500 4.55825700 1.92687500
C -6.13930100 6.64101700 2.59548900
H -6.53631700 6.50104000 3.60996700
H -5.31436400 7.35934000 2.64894000
H -6.94644900 7.09238600 2.00247700

RSR-Product
b3lyp/6-31g(d) & LanL2DZ,
el. energy = -3883.381139 a.u.

C -2.93305400 -1.90402800 -0.23054700
C -1.58813100 -1.54780800 -0.80749500
H -3.62146400 -1.05872500 -0.33622600
C -1.49616900 -0.67112000 -1.88964700
H -0.79579400 -2.27166600 -0.63460800
H -2.39039600 -0.21483300 -2.31022800
H -0.64681400 -0.71388000 -2.56780600
C -8.08811600 -1.73922100 -1.53966700
H -8.03756200 -0.88408100 -2.22165800
H -8.73454200 -1.50703700 -0.69273900
H -8.50404800 -2.57943000 -2.10613600
C -6.70218100 -2.09125000 -1.04926900
O -5.86043900 -2.33680700 -2.04641600
O -6.40606800 -2.14500100 0.13832800
C -2.95687200 -2.41925800 1.21999000
H -2.12677500 -2.01520300 1.79747500
C -2.81920800 -3.93820000 1.03785400
H -3.17601800 -4.48363300 1.91537000
H -1.76763200 -4.19663000 0.86273100
C -3.65975600 -4.22106500 -0.21247300
H -4.71959400 -4.31580800 0.06005000
O -3.51293500 -3.01019700 -1.01933000
H -4.95441600 -2.59261000 -1.68004100
O -4.13753200 -2.03759900 1.90868000
H -4.90561300 -2.13879800 1.31056200
N 2.49308200 0.12264900 -2.02748600
C 3.33954100 -0.34244100 -0.93765100
C 2.84739500 -1.71423000 -0.38677700
N 2.18300900 -1.57992000 0.90296400
C 2.06667100 1.41705000 -2.11233500
C 1.22830200 -2.47439100 1.28332800
O 0.93380700 -3.44261300 0.57552800
O 2.45021800 2.29345500 -1.33954500
C 1.12125000 1.71765600 -3.24495600
C 0.58886700 -2.30493400 2.64150000
C -0.11135800 2.37915200 -3.01680800
C -0.91020700 2.66624500 -4.13264400
C -0.50744900 2.33343200 -5.42955000
C 0.70808500 1.68941500 -5.64121500
C 1.51501800 1.38030100 -4.54502200
C 0.55718900 -3.48947900 3.39450800
C -0.01953100 -3.53135700 4.65999300
C -0.60027600 -2.37642000 5.18014400
C -0.60087200 -1.20070800 4.43015600
C -0.01205700 -1.12862300 3.15448400
P -0.73871600 2.62946900 -1.27254600
P -0.11611000 0.47129300 2.17713900
C -2.48107200 3.23337500 -1.51760200
C 0.03722600 4.22408700 -0.72823600
C 1.50092200 1.24582600 2.67931500
C -1.36108600 1.44550500 3.14858900
C -1.01947300 2.57928300 3.90115900
C -2.00783600 3.33163400 4.54356900
C -3.34762100 2.95553700 4.45298600
C -3.69707200 1.82323500 3.71158300
C -2.71745400 1.07917500 3.05471700
C 0.87546700 5.00522300 -1.53460300
C 1.39231500 6.21224100 -1.05835200
C 1.07871100 6.65490700 0.22770700
C 0.24800300 5.88007400 1.04057600
C -0.26496800 4.67206100 0.56798500
C -2.77730200 4.51740100 -2.00816800
C -4.10001000 4.93731900 -2.15075300
C -5.14979100 4.08691900 -1.79312000
C -4.86904200 2.81720800 -1.28822000
C -3.54435300 2.39547100 -1.15081300
C 2.09981900 2.17255000 1.81200500
C 3.30370700 2.79503500 2.15227500
C 3.92940100 2.49859800 3.36331600
C 3.34713600 1.57387900 4.23416400
C 2.14426000 0.95155600 3.89672800
H 2.08488200 -0.55950900 -2.65153400
H 3.27730300 0.42730000 -0.16619600
H 2.10280100 -2.14503100 -1.06018600

H 2.46970700 -0.84721800 1.53935500
H -1.87030500 3.14930400 -3.99266700
H -1.15241200 2.57773000 -6.26942100
H 1.02873700 1.42660600 -6.64540100
H 2.47109800 0.88553900 -4.69705200
H 0.98780000 -4.38477900 2.95770200
H -0.02498700 -4.45849300 5.22628800
H -1.06500000 -2.38672400 6.16242800
H -1.08316300 -0.32151000 4.84197300
H 0.01919400 2.88061800 3.98851100
H -1.72391500 4.20909700 5.11928400
H -4.11495100 3.53851900 4.95560800
H -4.73669800 1.51555700 3.63816200
H -3.02083300 0.20468900 2.48506800
H 1.13648000 4.66755900 -2.53181600
H 2.04270100 6.80595100 -1.69589100
H 1.48161500 7.59499500 0.59570000
H 0.00158400 6.21199700 2.04583600
H -0.90456900 4.07468800 1.21319900
H -1.97031300 5.19605900 -2.26895400
H -4.31080500 5.93292300 -2.53287500
H -6.17962700 4.41841100 -1.89804900
H -5.67808500 2.15486300 -0.99155600
H -3.32251000 1.41602600 -0.73701900
H 1.64213000 2.39893900 0.85767400
H 3.74712500 3.50206500 1.45722600
H 4.86873600 2.97798000 3.62659400
H 3.83002300 1.33278600 5.17772100
H 1.70716900 0.23538100 4.58535200
Pd -0.79240200 0.46297200 -0.13870100
C 4.84866900 -0.46802800 -1.35944500
H 5.18886300 0.48049800 -1.78322600
C 4.05612600 -2.72051500 -0.34700900
H 3.72032800 -3.67160400 0.07194400
C 5.73155900 -2.54339000 1.63538400
C 6.74436500 -1.80551800 2.25983000
C 7.17582600 -0.59660400 1.71088000
C 6.59934200 -0.11100100 0.53113300
C 5.59954400 -0.84952600 -0.09583000
C 5.16441400 -2.06673600 0.45655900
H 5.39295300 -3.48357700 2.06438300
H 7.19572600 -2.17671400 3.17611700
H 7.96226700 -0.02845800 2.20053000
H 6.93051800 0.83347700 0.10580700
C 4.52029500 -4.00245800 -2.56318700
C 4.95701700 -3.94027800 -3.89206800
C 5.38054700 -2.72739800 -4.43871900
C 5.37092800 -1.56165200 -3.66272900
C 4.94533400 -1.62405700 -2.33836800
C 4.52157000 -2.84644100 -1.78707200
H 4.18423500 -4.94552700 -2.13887700
H 4.96529500 -4.84125400 -4.49958300
H 5.71967500 -2.68647000 -5.47044400
H 5.70104000 -0.61622400 -4.08747500
C -3.22967000 -5.40461700 -1.02134400
H -2.20031300 -5.37774100 -1.38096000
C -4.01170800 -6.45344300 -1.29023600
H -5.03953500 -6.44765900 -0.92193600
C -3.59452200 -7.66973600 -2.06570900
H -3.68716900 -8.58041400 -1.45808300
H -4.23339900 -7.81485300 -2.94746800
H -2.55651800 -7.59313900 -2.40620900

RRS-Product
b3lyp/6-31g(d) & LanL2DZ,
el. energy = -3883.376402 a.u.

C 1.56043900 2.59660200 0.86896200
C 2.21068100 1.29448400 1.24066700
H 0.48628900 2.54533400 1.08257300
C 1.70132900 0.56064200 2.31293100
H 3.24889800 1.17408500 0.94698500
H 0.82212900 0.91373400 2.84405400
H 2.34408700 -0.11976200 2.86838000
C 6.83721500 3.23080500 2.56491800
H 6.97614700 3.99692200 3.33396600
H 7.59385000 3.33358900 1.78635800
H 6.94292000 2.25600300 3.05405600
C 5.45718700 3.34205700 1.96057100
O 4.50118300 3.37311900 2.87894600
O 5.25864900 3.39063200 0.75083400
C 1.78380600 3.16854700 -0.53808500
H 1.12806500 2.68759600 -1.26876100
C 1.42614700 4.64908400 -0.32332600
H 0.33738100 4.77446100 -0.30450600
H 1.84027400 5.27954100 -1.11433200
C 2.02049000 4.95585600 1.06236300
O 2.11386100 3.66263000 1.73388300
H 3.59614400 3.41648700 2.43776900
O 3.10028500 3.00628400 -1.03011400
H 3.75499500 3.24600900 -0.33928200
N -1.70820900 0.92521100 -2.03009400
C -2.87926000 0.49658600 -1.28182600
C -2.91313900 1.13636400 0.13979800
N -2.53994200 0.18733000 1.17811300
C -0.86832300 0.03818600 -2.64426700
C -1.90582600 0.61619400 2.30834100
O -1.62969800 1.80506200 2.48302800
O -1.08362300 -1.17114200 -2.67124600
C 0.32178300 0.63819600 -3.34060400
C -1.61590900 -0.39595900 3.39412000
C 1.62801400 0.13342500 -3.12898800
C 2.66295400 0.65862500 -3.91523800
C 2.42764800 1.64912700 -4.87222100
C 1.14256400 2.15041700 -5.05901200
C 0.09477100 1.64157100 -4.29097300
C -2.00160400 0.03355200 4.67320500
C -1.78733800 -0.75406800 5.80030200
C -1.15174400 -1.98559400 5.65697500
C -0.73790400 -2.41194600 4.39460100
C -0.95892100 -1.64243300 3.23874900
P 1.96504800 -1.08495300 -1.74843500
P -0.28273400 -2.21825400 1.58932700

C 3.82588700 -1.10006700 -1.65220100
C 1.64589700 -2.72566300 -2.55362700
C -1.80099400 -3.02152200 0.87178800
C 0.73438600 -3.69990800 2.06494100
C 0.23071100 -5.00901700 2.12678300
C 1.06822900 -6.07905800 2.45287200
C 2.41881600 -5.85830700 2.72732700
C 2.93263500 -4.56067100 2.66653300
C 2.09990400 -3.49316600 2.33000800
C 1.53919700 -2.89437400 -3.94139600
C 1.32983100 -4.16110400 -4.48853200
C 1.23341700 -5.28075500 -3.65934900
C 1.34424100 -5.12547900 -2.27664200
C 1.54176600 -3.85601000 -1.72898500
C 4.58685900 -2.26453500 -1.83836700
C 5.97200000 -2.24850000 -1.64723800
C 6.62131100 -1.07085700 -1.27724000
C 5.87533200 0.09811100 -1.10334800
C 4.49227300 0.08294000 -1.28282000
C -1.84228200 -3.24457200 -0.51340000
C -2.94777500 -3.86412900 -1.10020000
C -4.03222800 -4.26142100 -0.31599500
C -4.00761100 -4.03702500 1.06205000
C -2.89991600 -3.42458100 1.65354600
H -1.44328300 1.90024900 -2.00202600
H -2.79697200 -0.58917200 -1.21065100
H -2.18034300 1.94246600 0.20515800
H -2.86529000 -0.76944500 1.11584500
H 3.67611800 0.30172900 -3.77145500
H 3.25627700 2.02886500 -5.46367800
H 0.95148000 2.92405600 -5.79755000
H -0.91827300 2.00398300 -4.44727200
H -2.46330900 1.01124800 4.76645900
H -2.10221500 -0.40258300 6.77892000
H -0.96602000 -2.61467600 6.52365600
H -0.22537300 -3.36333900 4.30897900
H -0.81686600 -5.19857500 1.91643000
H 0.66140400 -7.08643800 2.49161300
H 3.06852700 -6.69221400 2.97975100
H 3.98490700 -4.37910300 2.86876000
H 2.50892100 -2.48944900 2.25245400
H 1.61127700 -2.03428000 -4.59920000
H 1.24222000 -4.27243300 -5.56645900
H 1.07130300 -6.26629300 -4.08839100
H 1.26830200 -5.98714900 -1.61854400
H 1.62046500 -3.74488900 -0.65139000
H 4.10725800 -3.19155100 -2.13196700
H 6.54125800 -3.16312300 -1.79472600
H 7.69850100 -1.06250600 -1.13008300
H 6.35816700 1.02956500 -0.81849200
H 3.93417300 1.00605900 -1.16027400
H -1.02778800 -2.90714700 -1.14162800
H -2.95950200 -4.01864800 -2.17545500
H -4.89611100 -4.73458000 -0.77537500
H -4.85009100 -4.33662900 1.68005000
H -2.89074300 -3.26330900 2.72725900
Pd 1.14099600 -0.57371600 0.50805800
C -4.22360200 0.82790100 -2.02570800
H -4.19098400 0.42303600 -3.04068900
C -4.32506600 1.78846700 0.38199300
H -4.36680600 2.20128500 1.39271200
C -6.30237900 0.22940700 1.03697900
C -7.19594500 -0.77163600 0.63729100
C -7.14892100 -1.27964100 -0.66215500
C -6.20660400 -0.79430800 -1.57674700
C -5.32360200 0.20716900 -1.18274200
C -5.37135900 0.72028500 0.12535400
H -6.33750400 0.62458300 2.04955600
H -7.92984100 -1.15272600 1.34250200
H -7.84666200 -2.05514100 -0.96690400
H -6.16559500 -1.19414300 -2.58722500
C -4.59190600 4.22642000 -0.48753700
C -4.67004600 5.08218300 -1.59321700
C -4.60464200 4.56717100 -2.88922300
C -4.46167600 3.18925500 -3.09470500
C -4.39491900 2.33595400 -1.99612500
C -4.46028000 2.85528100 -0.69059600
H -4.63475200 4.62793200 0.52208100
H -4.78106000 6.15231200 -1.44001700
H -4.66597100 5.23689200 -3.74291800
H -4.41232100 2.78665000 -4.10403000
H 3.05580700 5.31174000 0.95075500
C 1.26771100 5.91583100 1.94399600
H 1.52754800 5.84864900 3.00091900
C 0.38215900 6.83092100 1.54225000
H 0.13132100 6.90587000 0.48363100
C -0.31427400 7.80490200 2.45012200
H -1.40541200 7.69466600 2.38714700
H -0.01866400 7.66210800 3.49482200
H -0.08698500 8.84290300 2.17063700

SRS-Product
b3lyp/6-31g(d) & LanL2DZ,
el. energy = -3883.372963 a.u.

C 3.89381400 2.01977300 -1.12553100
C 3.41134400 1.63807400 0.28520300
C 4.00057400 3.55099200 -1.02423900
C 1.91710700 1.62933400 0.48348000
H 3.85482700 0.69475800 0.60973200
C 1.34273700 1.22183900 1.69123200
H 1.37016600 2.35427200 -0.12093400
H 1.97184400 0.78214700 2.46534900
H 0.43232700 1.68692600 2.05285000
H 3.00894300 4.01836800 -1.07950300
C 4.60345200 3.75045800 0.37008000
H 4.62910900 3.96350400 -1.81726200
O 4.01911900 2.67018100 1.15759000
H 5.11584300 2.00582800 2.18410600
C 7.65825600 0.14504500 2.99524900
H 8.31320800 -0.48582600 2.39348900
H 8.24685100 0.91224600 3.50928400
H 7.16514900 -0.45460000 3.76765300

C 6.62087700 0.80140900 2.11366200
O 6.55944800 0.61979300 0.90255700
O 5.79771700 1.58437200 2.79909500
N -2.08944500 1.37317500 -1.76410200
C -3.24240700 1.10753600 -0.91608700
C -3.08073300 1.76123400 0.48582600
N -2.69809200 0.78498300 1.49719400
C -1.50917000 0.38844400 -2.51188800
C -2.01911100 1.19756500 2.60514500
O -1.78041700 2.39372600 2.79260600
O -1.97134000 -0.74976700 -2.57202300
C -0.29247100 0.79403200 -3.30032300
C -1.59129800 0.17895600 3.63793900
C 0.90935800 0.04240300 -3.25270100
C 1.97150000 0.46378300 -4.06678900
C 1.85505000 1.57118500 -4.91260700
C 0.66822800 2.29675200 -4.95592100
C -0.39834500 1.90560900 -4.14498200
C -1.77514800 0.62990600 4.95528300
C -1.40494800 -0.14156400 6.05162400
C -0.81157600 -1.38326600 5.83616600
C -0.59947800 -1.83469700 4.53385700
C -0.98210900 -1.08248100 3.40809700
P 1.15615100 -1.29043500 -1.96434500
P -0.59193700 -1.74528600 1.69721100
C 2.90995000 -1.84656500 -2.22248500
C 0.31972100 -2.79554000 -2.66092600
C -2.24947200 -2.45707000 1.23879300
C 0.39291500 -3.27525200 2.07272000
C -0.16543100 -4.55747100 2.19044500
C 0.64909500 -5.66936400 2.42224400
C 2.03054600 -5.51695400 2.54669900
C 2.59814600 -4.24529100 2.43220500
C 1.78750800 -3.13670800 2.18890400
C -0.26265300 -2.85681000 -3.93353900
C -0.81011000 -4.05200600 -4.40479500
C -0.78348900 -5.20116200 -3.61236400
C -0.20663100 -5.14895700 -2.34169600
C 0.33899100 -3.95476500 -1.86954800
C 3.33041000 -2.52900000 -3.37902800
C 4.65406400 -2.94435800 -3.51459100
C 5.57929800 -2.69241600 -2.49639600
C 5.17218500 -2.03234200 -1.33865700
C 3.84342800 -1.62215400 -1.20439100
C -2.54452500 -2.64080800 -0.12123100
C -3.76464300 -3.19487200 -0.51620400
C -4.70998900 -3.56814300 0.43991000
C -4.43251100 -3.38299000 1.79640900
C -3.21301000 -2.83172100 2.19488700
H -1.62033700 2.26517900 -1.68953100
H -3.29686900 0.02120500 -0.82866700
H -2.27486600 2.49888400 0.46822200
H -3.01051200 -0.17393900 1.41355700
H 2.91570900 -0.06724100 -4.03157700
H 2.70046600 1.86234800 -5.53009800
H 0.56796900 3.15813100 -5.61040200
H -1.33517800 2.45607200 -4.17923800
H -2.20471900 1.61586500 5.09681100
H -1.56745300 0.22945400 7.05972900
H -0.50542800 -2.00271900 6.67519600
H -0.12117000 -2.79664200 4.39174900
H -1.23786300 -4.69370200 2.09775900
H 0.19955800 -6.65564700 2.50520300
H 2.66229700 -6.38311500 2.72484400
H 3.67392100 -4.11764700 2.51837300
H 2.23395400 -2.15243100 2.07370100
H -0.30421500 -1.96821500 -4.55398800
H -1.26037800 -4.08219000 -5.39391800
H -1.21054000 -6.12999400 -3.98178600
H -0.18238100 -6.03562700 -1.71353400
H 0.78496000 -3.92685500 -0.87863800
H 2.61957000 -2.74584000 -4.17120700
H 4.96386900 -3.46874400 -4.41508700
H 6.61223100 -3.01157000 -2.60881200
H 5.88386500 -1.81120600 -0.54818900
H 3.51555300 -1.12539500 -0.29798700
H -1.83681100 -2.32931600 -0.87884400
H -3.97039500 -3.31894000 -1.57542900
H -5.66228600 -3.99184100 0.13203600
H -5.16597100 -3.66433300 2.54763900
H -3.01205500 -2.69466200 3.25299700
Pd 0.79248000 -0.33314700 0.25880800
C -4.59454700 1.59009900 -1.55707100
H -4.68699600 1.18180600 -2.56693900
C -4.39203300 2.55461800 0.84202900
H -4.30105100 2.96816200 1.84833300
C -6.47077900 1.22742900 1.66781700
C -7.50399600 0.33780700 1.34955400
C -7.62107500 -0.17146200 0.05494800
C -6.70607000 0.20242200 -0.93652200
C -5.68472800 1.09486500 -0.62300600
C -5.56609500 1.60809600 0.68042600
H -6.37805100 1.62345200 2.67636700
H -8.21785900 0.04399100 2.11458300
H -8.42614000 -0.86057500 -0.18622600
H -6.79362800 -0.19749400 -1.94406100
C -4.45759400 5.00740100 -0.02401200
C -4.52911500 5.86701100 -1.12706500
C -4.62885200 5.34854400 -2.41949600
C -4.65772700 3.96347500 -2.62434500
C -4.59554000 3.10763300 -1.52755400
C -4.49759200 3.63035700 -0.22555600
H -4.37125900 5.41015900 0.98223800
H -4.50605400 6.94275700 -0.97469800
H -4.68503400 6.02159100 -3.27100100
H -4.73618100 3.55863800 -3.63098300
H 5.69006400 3.59205700 0.32573600
H 3.17460700 1.71311100 -1.88895900
O 5.14106200 1.44157800 -1.46668600
H 5.63717200 1.23033800 -0.65185300
C 4.30256900 5.05896200 1.03076300
H 3.24425700 5.27689500 1.18004900

C 5.23320400 5.93558400 1.41729200
H 6.28447800 5.68288900 1.26539100
C 4.95925100 7.26778400 2.05311300
H 3.88542400 7.43975700 2.18146100
H 5.43645700 7.33949300 3.03982000
H 5.36630400 8.08907100 1.44744700

(S,S)-DACH-Ph [(S,S)-L1] Trost Ligand investigation

Reagents Pro-R-A
b3lyp/6-31g(d) & LanL2DZ,
el. energy = -3501.108346 a.u.

C 2.59354300 -0.79444300 -1.52154100
C 2.36320700 -0.19902500 -0.14061100
O 1.60813900 -1.74384100 -1.95457200
C 3.99436000 -1.45402100 -1.68517400
C 2.03177500 -0.92045600 1.01411700
H 2.92525400 0.71876900 -0.01176500
C 2.40396000 -0.40360200 2.37727700
H 1.84070500 -1.98925600 0.95634200
H 2.34913500 0.68392600 2.43209700
H 1.79032600 -0.84877200 3.16184800
H 3.91560300 -2.50488700 -1.37741000
C 5.13786800 -0.82939900 -0.87203400
H 4.24438300 -1.45917800 -2.75363400
O 5.15921700 0.59061200 -1.07158500
H 5.27137100 1.00110400 -0.19663800
H 1.49105400 -2.44914800 -1.28499800
H 2.51624000 0.02389400 -2.24011800
H 4.93700700 -1.05443300 0.18168600
C 6.10764200 -0.44846200 3.00060700
H 5.99027600 -1.29965600 3.67312300
H 6.62130300 0.37059900 3.51225800
H 6.72928800 -0.74333900 2.14755900
C 4.77518700 0.05162600 2.48490800
O 3.77666200 -0.78403500 2.78805900
O 4.65009900 1.09380900 1.85708900
N -1.05464800 -1.14640300 -2.77559400
C -2.06403000 -2.20171300 -2.75696100
C -1.63654500 -3.39338600 -1.87298000
N -1.52576700 -3.03748300 -0.45503600
C -1.39026400 0.14673300 -3.00449400
C -0.44643500 -3.32714700 0.31069700
O 0.62450400 -3.72994000 -0.16959800
O -2.55375900 0.55928000 -3.03574500
C -0.23738600 1.05952800 -3.38460600
C -0.62386500 -3.26469000 1.81397900
C 0.23051100 2.13932900 -2.60030400
C 1.21809600 2.97571300 -3.14440500
C 1.73219000 2.76315300 -4.42493600
C 1.27298600 1.69329700 -5.18862200
C 0.29370300 0.85006800 -4.66366900
C -0.16463900 -4.41122400 2.47806900
C -0.26398800 -4.53787300 3.86182600
C -0.81300800 -3.49460900 4.60343100
C -1.24838600 -2.33609000 3.95756400
C -1.16969200 -2.18951500 2.56201000
P -0.26688400 2.29019500 -0.81631700
P -1.58316500 -0.55253300 1.75757200
C 0.75044200 3.72253500 -0.20262500
C -1.93573800 3.09938600 -0.85078500
C -3.29203000 -0.88281800 1.10339000
C -1.93308600 0.55870900 3.20251500
C -3.17248300 0.63516300 3.85809900
C -3.36085600 1.52142500 4.92101400
C -2.31593000 2.34444200 5.34576300
C -1.08087700 2.28386700 4.69689200
C -0.89484600 1.40336300 3.63012000
C -2.59568900 3.47659400 -2.02785600
C -3.84277900 4.10469300 -1.96877600
C -4.44356500 4.36729300 -0.73733000
C -3.79380300 3.99299400 0.44198500
C -2.55285000 3.35986500 0.38518700
C 0.40801200 5.05700900 -0.48294200
C 1.19717500 6.10773500 -0.01359200
C 2.34073200 5.84518900 0.74538300
C 2.68954300 4.52542200 1.03365000
C 1.89725200 3.47458600 0.56582900
C -3.74046300 -0.13392000 0.00432300
C -5.01185300 -0.34859000 -0.53214700
C -5.85193600 -1.31942700 0.01697800
C -5.41477600 -2.07925700 1.10516200
C -4.14391800 -1.86403100 1.64535400
H -0.06681100 -1.37394100 -2.61327600
H -2.98326600 -1.76626600 -2.34926300
H -0.64126400 -3.73121100 -2.17649300
H -2.38581300 -2.77843600 0.01381100
H 1.60515700 3.79959800 -2.55587600
H 2.49708100 3.42990200 -4.81381300
H 1.67345800 1.50976700 -6.18192600
H -0.07233700 0.01299200 -5.25194400
H 0.28204600 -5.20307600 1.88545600
H 0.09368800 -5.43873000 4.35249400
H -0.89506100 -3.57005300 5.68456500
H -1.64723300 -1.52373100 4.55498800
H -3.99856000 0.00926900 3.53595700
H -4.32825500 1.57047500 5.41431300
H -2.46627600 3.03528800 6.17114300
H -0.26547600 2.93004900 5.01099700
H 0.05528800 1.37847300 3.10356600
H -2.15080400 3.26127600 -2.99200800
H -4.34374100 4.38589500 -2.89153800
H -5.41325700 4.85675200 -0.69514600
H -4.25448100 4.18800900 1.40694400
H -2.06019800 3.06850200 1.30933800

H -0.48033300 5.27627200 -1.06722000
H 0.91630700 7.13324200 -0.23999900
H 2.95310100 6.66566200 1.11067100
H 3.57607000 4.30235800 1.62117700
H 2.17442800 2.45377100 0.79949800
H -3.09164500 0.60086800 -0.45636000
H -5.32523600 0.23473200 -1.39267000
H -6.83859600 -1.49135700 -0.40531100
H -6.06027100 -2.84104200 1.53505000
H -3.81256600 -2.46662100 2.48672600
Pd 0.23235500 0.23950900 0.38831000
C 6.47634800 -1.41770300 -1.24575200
C 7.15576900 -2.30904700 -0.51827400
H 6.87973200 -1.06777000 -2.19740600
H 6.72859800 -2.64777600 0.42877600
C 8.47512200 -2.91979900 -0.89947400
H 8.39700200 -4.01192100 -0.99155800
H 9.24244000 -2.72420600 -0.13778500
H 8.83823200 -2.52564900 -1.85473300
C -2.63313200 -4.56863300 -1.99658500
C -2.34336200 -2.66497200 -4.20624000
H -2.25497500 -5.40556400 -1.39754700
H -3.58892600 -4.26270900 -1.54449100
H -1.39154300 -2.98112700 -4.65734400
H -2.69349600 -1.79501100 -4.77272800
C -2.88128500 -5.00252300 -3.44587300
H -3.61733600 -5.81584400 -3.46691800
H -1.95241500 -5.40801000 -3.87239000
C -3.35464000 -3.81346400 -4.28893600
H -4.33378100 -3.47153400 -3.92290500
H -3.49797700 -4.11265500 -5.33463100

Reagents Pro-S-A
b3lyp/6-31g(d) & LanL2DZ,
el. energy = -3501.105152 a.u.

C -2.78889600 1.21454200 -0.45903300
C -2.22996500 0.45388500 0.72679600
C -4.27932000 1.58894700 -0.26513600
C -1.48851300 1.13592100 1.69879100
H -2.81034600 -0.41265200 1.02178600
C -1.52254600 0.73401600 3.14706700
H -1.23954600 2.18104700 1.52783500
H -1.80511400 -0.31325100 3.27851700
H -0.58106400 0.93414300 3.66063600
H -4.38842400 2.09278200 0.70545600
C -5.29892200 0.43767000 -0.37194300
H -4.54336100 2.32854600 -1.03212400
O -5.04724300 -0.63385800 0.54498500
H -4.96960700 -0.26684200 1.44565600
C -4.61068100 2.27013100 4.59747300
H -4.16214400 2.48508500 5.57131500
H -5.62436900 1.88596800 4.72036900
H -4.64721400 3.21178100 4.03732700
C -3.77748800 1.26632300 3.83149900
O -2.47469400 1.56378000 3.90679300
O -4.23969200 0.31826200 3.21948700
N 0.04915500 0.76325900 -2.92793900
C 0.89298800 1.88278500 -3.34613200
C 0.73342500 3.12117600 -2.44004100
N 1.19303200 2.87874100 -1.06973700
C 0.41405800 -0.52117000 -3.17103700
C 0.56514900 3.44472000 -0.00065600
O -0.52828200 4.00713400 -0.10817500
O 1.54640500 -0.86145500 -3.52297900
C -0.71234000 -1.54022300 -3.12263800
C 1.27934900 3.45813600 1.34013900
C -0.91104100 -2.47630100 -2.08205800
C -1.94431300 -3.41838900 -2.22470800
C -2.75361500 -3.44787800 -3.36138800
C -2.54798800 -2.52510800 -4.38470300
C -1.53168700 -1.57904400 -4.25848100
C 1.13971500 4.68233600 2.01329800
C 1.71019000 4.90072100 3.26404100
C 2.42009000 3.87112200 3.87659700
C 2.54942900 2.64045500 3.23232100
C 1.99639800 2.40160700 1.96169700
P 0.05779100 -2.34079400 -0.50070000
P 2.09762100 0.68920700 1.21742400
C -0.70330200 -3.65569700 0.57173700
C 1.67376800 -3.16039100 -0.90269600
C 3.50032700 0.91509900 0.01564500
C 2.88741900 -0.31760900 2.56259000
C 4.27227300 -0.40670100 2.77564100
C 4.78471100 -1.21615500 3.79224000
C 3.92345400 -1.94783500 4.61229800
C 2.54426000 -1.87473600 4.40526000
C 2.03279700 -1.07274800 3.38396500
C 1.99581600 -3.68328200 -2.16242200
C 3.23460400 -4.29370700 -2.37893000
C 4.16350300 -4.39471900 -1.34327700
C 3.85102600 -3.87708300 -0.08340300
C 2.61922400 -3.26155700 0.13300100
C -0.36613500 -5.01497700 0.45301100
C -0.96860500 -5.97092400 1.27214000
C -1.91820600 -5.58651900 2.22196000
C -2.26088800 -4.23989400 2.35000100
C -1.65367300 -3.28316800 1.53380800
C 3.54926200 0.09430400 -1.12168500
C 4.57907800 0.23037200 -2.05547700
C 5.57417300 1.19110900 -1.86763600
C 5.53239200 2.02258100 -0.74523900
C 4.50223900 1.88929400 0.18844700
H -0.90593500 0.92055600 -2.59590500
H 1.92803000 1.52820600 -3.29226400
H -0.32665600 3.37869000 -2.35721900
H 2.14435500 2.55050500 -0.95566900
H -2.12617800 -4.13561800 -1.43258900
H -3.54486700 -4.18862300 -3.43811200
H -3.17650900 -2.53282000 -5.27092700
H -1.36926400 -0.85089300 -5.04864000
H 0.55603200 5.46018700 1.53295500
H 1.59023700 5.86172800 3.75649300

H 2.86817300 4.01470700 4.85641200
H 3.08916000 1.84520600 3.73386100
H 4.95683300 0.14949900 2.14325900
H 5.85996300 -1.27605200 3.94015000
H 4.32495300 -2.57858500 5.40099600
H 1.86620400 -2.45174100 5.02850500
H 0.96210000 -1.04587000 3.19815200
H 1.29343900 -3.60106800 -2.98348600
H 3.47005100 -4.68861300 -3.36386900
H 5.12572400 -4.86992300 -1.51600100
H 4.56752200 -3.94472900 0.73099100
H 2.39156300 -2.85853800 1.11597100
H 0.37139700 -5.32802000 -0.27918700
H -0.69455700 -7.01762700 1.16736100
H -2.38627300 -6.33276100 2.85868400
H -2.99989700 -3.92896000 3.08357800
H -1.91519700 -2.23667000 1.64023500
H 2.77242000 -0.63816700 -1.30022200
H 4.57930200 -0.40770100 -2.93389600
H 6.37297000 1.30112400 -2.59657500
H 6.29859100 2.77927200 -0.59654400
H 4.47380200 2.55042000 1.04983400
Pd -0.07420000 -0.15347000 0.57217100
H -5.19738000 -0.01341100 -1.36500500
H -2.23154100 2.15099300 -0.56201300
O -2.62848100 0.53531600 -1.72368300
H -2.57994700 -0.41747600 -1.54426500
C -6.70812100 0.95535900 -0.20982400
C -7.64383900 0.94680800 -1.16193200
H -6.94879900 1.35795700 0.77771900
H -7.38875000 0.53574300 -2.14085100
C -9.04720700 1.46134100 -1.00815000
H -9.78439700 0.66973300 -1.20081500
H -9.25875900 2.26722000 -1.72462100
H -9.22448400 1.85064000 0.00037300
C 1.49673100 4.33853600 -3.01291900
H 2.57605500 4.13458600 -2.94587100
H 1.29554400 5.19883200 -2.36431600
C 0.56877000 2.22899300 -4.81935700
H 0.76008000 1.33439100 -5.42304600
H -0.50750600 2.44259000 -4.89532000
C 1.13398000 4.65490500 -4.46818300
H 1.72628500 5.50810300 -4.82173700
H 0.07873600 4.95830900 -4.52743900
C 1.36257000 3.42589800 -5.35419100
H 2.43459200 3.18077200 -5.37208900
H 1.07130200 3.63364500 -6.39137800

Reagents Pro-R-B
b3lyp/6-31g(d) & LanL2DZ,
el. energy = -3501.102078 a.u.

C 2.24700000 1.00469300 -1.97236900
C 2.20731200 1.12623900 -0.44981900
O 1.81631000 -0.27022400 -2.44601400
C 3.60133800 1.36730400 -2.63306700
C 2.36888900 0.04013600 0.41575600
H 2.42731100 2.13102100 -0.08590700
C 2.81301700 0.18425700 1.84350400
H 2.49151400 -0.94969400 -0.00410300
H 2.41360600 1.08699500 2.30787800
H 2.51854800 -0.68763900 2.43228500
H 3.43785900 1.23994500 -3.71015500
C 4.84317700 0.53273300 -2.21578800
H 3.81843700 2.43156800 -2.47260500
O 4.45119300 -0.82630100 -1.94125300
H 4.64908700 -1.06487500 -1.01705900
H 2.53303500 -0.90879100 -2.24662100
H 1.52439600 1.71748800 -2.38077600
H 5.51548800 0.48800200 -3.08421700
C 6.50220900 -0.39970100 2.24507200
H 6.63764300 0.60635200 2.64533500
H 7.23177300 -0.59890500 1.45651000
H 6.67135000 -1.12632500 3.04827800
C 5.10735100 -0.61005600 1.69490900
O 4.26948500 0.36129000 2.07813500
O 4.79832100 -1.56182700 0.99898500
N -0.99060600 -0.82149100 -2.85108200
C -1.50024800 -2.18566600 -2.98180500
C -0.48446400 -3.22480500 -2.46437100
N -0.24415700 -3.09459600 -1.02774600
C -1.83229000 0.23304000 -2.72860000
C 1.00724000 -3.10140500 -0.49097600
O 2.02415000 -3.04691800 -1.18528500
O -3.04791300 0.12447700 -2.53881300
C -1.22725900 1.59778800 -3.00823400
C 1.12109200 -3.29582100 1.01083200
C -1.12126300 2.64254600 -2.05944600
C -0.67085300 3.89641500 -2.50251300
C -0.33935200 4.12530300 -3.83976300
C -0.43897700 3.09085800 -4.76639700
C -0.88009800 1.83659400 -4.34417400
C 2.13334800 -4.19956100 1.36637000
C 2.37825500 -4.53872600 2.69426200
C 1.61256900 -3.95181100 3.69826000
C 0.62466400 -3.02418500 3.36439700
C 0.35198700 -2.67248600 2.03002800
P -1.31525800 2.28209900 -0.24675600
P -0.83581200 -1.26973800 1.67197600
C -0.88610200 3.89923700 0.56975700
C -3.14587800 2.28632700 0.04967700
C -2.37006600 -2.19017600 1.16399700
C -1.31558200 -0.66869600 3.36492100
C -2.31052600 -1.26139300 4.15910600
C -2.63420000 -0.73016800 5.40955300
C -1.97076100 0.40169600 5.88731400
C -0.98472600 1.00577100 5.10454000
C -0.66584500 0.47783300 3.85237700
C -4.09739000 2.56480300 -0.94070100
C -5.45879300 2.58517300 -0.62657800
C -5.88637900 2.33086800 0.67708600
C -4.94505200 2.04711800 1.67005400
C -3.58635800 2.01977600 1.35738600

C -1.75334600 5.00551400 0.55670200
C -1.39675800 6.19780200 1.18766300
C -0.17146900 6.30418000 1.85092200
C 0.69318700 5.20970200 1.88224900
C 0.33552300 4.01729800 1.24807400
C -3.30752800 -1.53652400 0.34917800
C -4.47332600 -2.18890500 -0.05798500
C -4.71746700 -3.50586100 0.33666200
C -3.78882800 -4.17125300 1.14082700
C -2.62339300 -3.51942300 1.55259900
H 0.02111800 -0.65759600 -2.83085200
H -2.41608800 -2.25049800 -2.38391000
H 0.48490300 -3.05513900 -2.94259000
H -1.03206600 -3.26938900 -0.41705600
H -0.56526900 4.70841000 -1.79209300
H 0.00188000 5.11022900 -4.14768200
H -0.17379600 3.25233400 -5.80771700
H -0.96204800 1.02247400 -5.05884600
H 2.73651100 -4.62158600 0.56998300
H 3.16603700 -5.24595400 2.93824600
H 1.78567400 -4.19927600 4.74252300
H 0.06172200 -2.55573500 4.16370500
H -2.84220900 -2.13662300 3.80022800
H -3.40981500 -1.20067600 6.00845800
H -2.22689000 0.81538900 6.85914800
H -0.47104800 1.89438300 5.46203800
H 0.07897600 0.96560400 3.22879800
H -3.78165800 2.74367400 -1.96186000
H -6.18471200 2.79730000 -1.40736200
H -6.94627600 2.34759200 0.91781500
H -5.26722100 1.83987200 2.68723000
H -2.86400800 1.78824500 2.13625400
H -2.71486400 4.93334700 0.05723900
H -2.07985200 7.04309700 1.16569900
H 0.10250100 7.23242300 2.34558300
H 1.64442300 5.27947800 2.40394400
H 0.99889200 3.15886300 1.28343300
H -3.12306300 -0.52586600 0.00589200
H -5.17393900 -1.66391600 -0.70042400
H -5.62124000 -4.01542700 0.01272800
H -3.96801600 -5.19842000 1.44838400
H -1.90520300 -4.04980000 2.17200200
Pd 0.18487200 0.50181900 0.38015500
C 5.60910000 1.18327600 -1.09285200
C 6.88876400 1.55716400 -1.19659900
H 5.05476700 1.40035000 -0.18051300
H 7.42215100 1.33877500 -2.12405100
C 7.67588400 2.28488100 -0.14399100
H 8.56187800 1.71157700 0.16156600
H 7.07241000 2.48348800 0.74789600
H 8.04435200 3.24739400 -0.52459400
C -0.95423200 -4.66603300 -2.76431200
H -0.17052600 -5.35767400 -2.43345000
H -1.84316100 -4.87790500 -2.15054400
C -1.86266400 -2.45318100 -4.46124600
H -2.62504400 -1.72421100 -4.75823700
H -0.97210200 -2.25661700 -5.07588000
C -1.29745500 -4.89602300 -4.24094500
H -1.65197200 -5.92457100 -4.38403700
H -0.38830400 -4.78926200 -4.85018700
C -2.34869500 -3.88496700 -4.71244500
H -3.29091300 -4.05672400 -4.17161100
H -2.56973200 -4.02399500 -5.77816500

Reagents Pro-S-B
b3lyp/6-31g(d) & LanL2DZ,
el. energy = -3501.098388 a.u.

C -2.75258600 0.33889000 1.45958700
C -2.31961300 0.73129100 0.05742700
C -4.20098200 0.77428300 1.75865000
C -2.23004100 -0.26271000 -0.92818400
H -2.57512200 1.75126600 -0.23939700
C -2.47987100 0.00540700 -2.38867800
H -2.39274200 -1.29026400 -0.62168900
H -1.98392800 0.91287400 -2.73587500
H -2.16285700 -0.84237100 -3.00181700
H -4.43466900 0.47333600 2.78746200
C -5.24321200 0.16535800 0.80314300
H -4.27326800 1.87072200 1.71729000
O -5.14941700 -1.25958900 0.86117300
H -4.94100100 -1.60564600 -0.02352800
C -6.17523000 -0.26355400 -2.99619000
H -6.15002800 0.63178100 -3.61978500
H -6.78478500 -0.06572400 -2.10658700
H -6.64118100 -1.09170900 -3.53675900
C -4.79083700 -0.68349700 -2.55160200
O -3.88766000 0.28962000 -2.73684300
O -4.53926600 -1.76955100 -2.05816400
N 0.67282200 -0.39922200 3.03875000
C 1.08144700 -1.75816900 3.39260000
C 0.17015800 -2.82618100 2.75409200
N 0.26555300 -2.83942100 1.29166000
C 1.56460200 0.61869700 2.97235200
C -0.81977200 -3.14848200 0.52234200
O -1.95606300 -3.20446300 0.99522100
O 2.78983800 0.47099900 2.97642300
C 0.96240000 2.01447200 3.03761600
C -0.59807200 -3.51801800 -0.93384000
C 0.83201800 2.89677900 1.94037200
C 0.32924400 4.18735700 2.18308800
C -0.02344300 4.60543300 3.46719800
C 0.11604900 3.73274300 4.54419900
C 0.60529700 2.44636700 4.32198100
C -1.40078200 -4.59228000 -1.34827200
C -1.34863300 -5.08665300 -2.64828100
C -0.49377000 -4.48847900 -3.57061900
C 0.29151600 -3.40215400 -3.18373200
C 0.26498900 -2.89455000 -1.87262200
P 1.15504300 2.29956300 0.20766100
P 1.23464600 -1.35447200 -1.45923100
C 0.71361900 3.77652100 -0.83504900
C 3.00293200 2.36615300 0.05186800

C 2.72210100 -2.09025300 -0.61744000
C 1.93407100 -0.83488600 -3.10013200
C 3.16023200 -1.28812100 -3.61163100
C 3.63711600 -0.81828800 -4.83795000
C 2.89672000 0.10794500 -5.57442800
C 1.67711300 0.57035700 -5.07476300
C 1.20611100 0.10877300 -3.84512800
C 3.86496100 2.74894800 1.08814800
C 5.24699300 2.78245800 0.88098300
C 5.78380100 2.43985000 -0.36008500
C 4.93158000 2.05614000 -1.39905400
C 3.55365500 2.01538200 -1.19296800
C 1.55717100 4.89565100 -0.94349000
C 1.19592100 5.98571200 -1.73598800
C -0.01239800 5.97617200 -2.43730500
C -0.85714500 4.86972300 -2.34156700
C -0.49397200 3.77871100 -1.54815500
C 3.41832500 -1.32003300 0.32634200
C 4.53486000 -1.83847800 0.98629900
C 4.97230500 -3.13545800 0.71280400
C 4.28340000 -3.91734100 -0.21834700
C 3.16459800 -3.40186200 -0.87638200
H -0.31973000 -0.15640900 2.96724100
H 2.10436700 -1.88544100 3.02238600
H -0.87480100 -2.59531700 2.98226500
H 1.18997500 -2.95996800 0.89641900
H 0.20808300 4.87745300 1.35589300
H -0.40792200 5.61052800 3.61851600
H -0.16089800 4.04336900 5.54777500
H 0.70844600 1.75593400 5.15468300
H -2.08356200 -5.02214200 -0.62359900
H -1.97977200 -5.92227400 -2.93735500
H -0.44004200 -4.85351800 -4.59303500
H 0.93291600 -2.93430900 -3.92219800
H 3.75118600 -2.00510200 -3.05152300
H 4.59091400 -1.17764300 -5.21581700
H 3.27074100 0.47284700 -6.52733400
H 1.09768500 1.29937000 -5.63511300
H 0.27298800 0.49417800 -3.44431700
H 3.46732000 3.00052800 2.06409200
H 5.90215800 3.07538900 1.69727300
H 6.85907800 2.46623700 -0.51674600
H 5.33730800 1.77963400 -2.36859600
H 2.90196200 1.70669900 -2.00550800
H 2.50214800 4.91315300 -0.40931600
H 1.86167000 6.84188600 -1.80843200
H -0.29012500 6.82430800 -3.05761500
H -1.79684400 4.85024400 -2.88762600
H -1.14437200 2.91257700 -1.48408100
H 3.08172900 -0.32146700 0.57262900
H 5.03977300 -1.22414800 1.72538700
H 5.83772300 -3.54150700 1.23013900
H 4.61167500 -4.93173400 -0.43031800
H 2.62994500 -4.02457000 -1.58786900
Pd -0.15450300 0.35297600 -0.43009100
H -5.02590400 0.52951600 -0.20927000
H -2.69412700 -0.74723400 1.55630800
O -1.89953500 0.85922700 2.50576100
H -1.54157000 1.71069900 2.20856100
C -6.64702800 0.57887600 1.17298600
C -7.37947200 1.49185700 0.52869100
H -7.05522100 0.06899800 2.04703500
H -6.95059800 1.98972900 -0.34450800
C -8.76819000 1.92049200 0.91349400
H -9.48090900 1.75488200 0.09385600
H -8.80481600 2.99345700 1.14805200
H -9.12728700 1.37090300 1.79015600
C 0.49418700 -4.23953600 3.29169300
H -0.22654400 -4.93981800 2.85451700
H 1.48878400 -4.53263200 2.92269600
C 1.09498200 -1.88971000 4.93452900
H 0.10052300 -1.61064100 5.31222300
H 1.80474200 -1.15284300 5.32809100
C 0.47974600 -4.32602800 4.82195800
H 0.74231500 -5.34293500 5.13947000
H -0.53753500 -4.13392800 5.19238300
C 1.44511900 -3.29933800 5.42382600
H 1.41469400 -3.33174000 6.52011700
H 2.47557100 -3.54859000 5.13065600

TS Pro-R-A
b3lyp/6-31g(d) & LanL2DZ,
el. energy = -3501.073492 a.u.
im. frequency -95.94

C 2.46017000 -1.77353900 -0.94155700
C 2.24461800 -0.73769000 0.13335800
O 1.37922100 -2.71049400 -1.09557600
C 3.79350900 -2.54499000 -0.72102700
C 1.78907900 -1.06250400 1.43673600
H 2.93933900 0.09231600 0.07640600
C 1.65234100 -0.02940400 2.36238900
H 1.43416400 -2.05660400 1.69143700
H 2.12267600 0.92974000 2.19891700
H 1.21387900 -0.21306300 3.33730300
H 3.59925500 -3.37994900 -0.03418700
C 4.95613200 -1.70985300 -0.14032800
H 4.08156200 -2.98802100 -1.68262600
O 5.07118100 -0.47079300 -0.83823200
H 5.06976900 0.23459400 -0.14320500
H 1.12283300 -3.08598800 -0.23059500
H 2.51925500 -1.25666900 -1.90045500
H 4.73085900 -1.51390700 0.91610800
C 6.27892600 0.90379400 2.83156900
H 6.44392200 0.70513900 3.89337000
H 6.68440600 1.88776700 2.57020300
H 6.82743300 0.16378600 2.23543300
C 4.78372300 0.84220500 2.47624200
O 3.98606200 0.48308900 3.37561000
O 4.48007400 1.15795800 1.27461200
N -1.17694600 -2.01471700 -2.22465200
C -2.37412700 -2.81026200 -1.96742200
C -2.26670900 -3.60926800 -0.65239100

N -2.15200400 -2.74931200 0.53043400
C -1.23898900 -0.86726500 -2.94390400
C -1.15891500 -2.87845800 1.44407600
O -0.15829600 -3.58219600 1.24255900
O -2.29558900 -0.30416700 -3.24588800
C 0.08685100 -0.37313200 -3.49241000
C -1.37178800 -2.23106000 2.79963900
C 0.74341600 0.80851100 -3.08049100
C 1.90892100 1.19712200 -3.76005000
C 2.41310500 0.45001100 -4.82588300
C 1.76338300 -0.71465600 -5.22613100
C 0.60842900 -1.11892400 -4.55703300
C -1.15846600 -3.11353100 3.86908800
C -1.33537100 -2.71261600 5.19137900
C -1.71611200 -1.40080500 5.46107800
C -1.90114700 -0.50155100 4.40983300
C -1.73591300 -0.88510300 3.06825200
P 0.23560900 1.69953300 -1.53815800
P -1.80841000 0.41726900 1.73262900
C 1.47506500 3.06625300 -1.36876400
C -1.26867500 2.68274600 -1.97476400
C -3.48156100 0.13241400 0.99545900
C -2.00368800 2.00815300 2.65356600
C -3.24908800 2.57314500 2.97108400
C -3.32046000 3.79606300 3.64199800
C -2.15296900 4.46905100 4.00653000
C -0.90867900 3.91838800 3.69152200
C -0.83471200 2.70170700 3.01299300
C -1.84110100 2.70142900 -3.25316000
C -2.94865400 3.51260200 -3.51601100
C -3.49237500 4.31357900 -2.51161200
C -2.92547200 4.30200100 -1.23418500
C -1.82337100 3.49139800 -0.96742500
C 1.37558600 4.23569100 -2.14632400
C 2.33552000 5.24073100 -2.03410800
C 3.40817100 5.09656200 -1.14810300
C 3.51353500 3.94302600 -0.37268900
C 2.54885400 2.93776400 -0.47771100
C -3.68843500 0.42128200 -0.36063800
C -4.93544600 0.20215900 -0.95057700
C -5.98996900 -0.31083100 -0.19327300
C -5.79430300 -0.60927500 1.15841700
C -4.54815000 -0.39212000 1.75087800
H -0.25419000 -2.35493800 -1.93105600
H -3.21245400 -2.10969700 -1.89268300
H -1.35320200 -4.21116600 -0.67010800
H -2.98000000 -2.23046500 0.79868200
H 2.44218200 2.08513700 -3.44231200
H 3.31958000 0.77648600 -5.32746100
H 2.15325800 -1.31131600 -6.04608200
H 0.09678300 -2.02788700 -4.86126900
H -0.84192600 -4.12642700 3.64241700
H -1.16637700 -3.41802800 5.99973400
H -1.85449700 -1.06538500 6.48515100
H -2.16156400 0.52534300 4.64111200
H -4.16625500 2.06663400 2.68936000
H -4.29201300 4.22271100 3.87694400
H -2.21209800 5.42099900 4.52706000
H 0.00607500 4.43744900 3.96328300
H 0.13645300 2.29105800 2.75371100
H -1.44265900 2.07078900 -4.03836200
H -3.38465200 3.51393900 -4.51148500
H -4.35297200 4.94348100 -2.72110000
H -3.34060100 4.92165200 -0.44388700
H -1.38803600 3.49533000 0.02840400
H 0.54942000 4.36233000 -2.83886900
H 2.24494600 6.13801000 -2.64107900
H 4.15584200 5.88154800 -1.06789600
H 4.33989000 3.78859300 0.31414200
H 2.67344600 2.06309100 0.14651600
H -2.87612300 0.79221100 -0.97175600
H -5.06071900 0.41656200 -2.00729600
H -6.95865100 -0.48668900 -0.65347500
H -6.60936500 -1.01364800 1.75288200
H -4.40389600 -0.63685700 2.79954200
Pd 0.26168700 0.26136300 0.44204600
C 6.25751200 -2.46999200 -0.21842800
C 6.91204200 -2.98044500 0.82798700
H 6.66527400 -2.58153100 -1.22512100
H 6.49084300 -2.84483000 1.82640700
C 8.20747400 -3.73928100 0.75623600
H 8.09968500 -4.75534800 1.16120000
H 8.99060600 -3.24776300 1.34977600
H 8.56676800 -3.82287400 -0.27533800
C -3.48511500 -4.54011100 -0.46560400
C -2.63190900 -3.75790000 -3.16175500
H -3.34162500 -5.11973200 0.45397000
H -4.38027900 -3.91783900 -0.31216800
H -1.73756300 -4.38016500 -3.31108300
H -2.74788500 -3.14254400 -4.06093600
C -3.71656400 -5.46902500 -1.66399000
H -4.60898000 -6.08219800 -1.48865000
H -2.87005100 -6.16441200 -1.75593300
C -3.85550600 -4.65878200 -2.95785100
H -4.76405000 -4.04117700 -2.90764900
H -3.97761600 -5.32578100 -3.81995600

TS Pro-R-B
b3lyp/6-31g(d) & LanL2DZ,
el. energy = -3501.070645 a.u.
im. frequency -12.10

C -2.56936800 2.15284200 0.97495500
C -2.07110600 1.52463200 -0.31106900
O -2.86375200 1.17615700 1.97002500
C -3.79819000 3.07649800 0.76725800
C -2.29995800 0.18119600 -0.62043800
H -1.87035500 2.21814200 -1.12543900
C -1.76594800 -0.38533200 -1.78607400
H -2.74771100 -0.47238300 0.11904600
H -1.57223800 0.24112100 -2.65419900
H -1.91391600 -1.43661000 -1.98569300
H -4.02078800 3.47956500 1.76353600

C -5.07206400 2.38448400 0.20662900
H -3.52817300 3.92486600 0.12671800
O -5.19023400 1.10211000 0.82283400
H -5.37323400 0.35571900 0.13552600
H -3.79811600 0.89741400 1.73867100
H -1.77473700 2.78750800 1.37672100
H -5.92158200 3.01118200 0.52688100
C -5.45453000 -2.66845500 -2.29431700
H -5.32490700 -2.75247900 -3.37749100
H -6.47486000 -2.94472400 -2.01096900
H -4.77095100 -3.37272200 -1.80288100
C -5.11553900 -1.25182400 -1.80411100
O -4.35684100 -0.54920400 -2.52624400
O -5.60967200 -0.93736900 -0.67769800
N -0.54079300 -0.25361100 2.95256600
C -0.51750600 -1.62856300 3.45626200
C -1.23763900 -2.62432500 2.52481700
N -0.58647400 -2.75202400 1.21093100
C 0.53277200 0.55913600 3.07964000
C -1.34150900 -3.13660700 0.13396400
O -2.57013200 -3.12788800 0.17301800
O 1.66798700 0.17089800 3.38327000
C 0.27511900 2.04544200 2.93400500
C -0.65739300 -3.65493500 -1.11917300
C 0.78084900 2.83393100 1.87549100
C 0.58883700 4.22336700 1.92670100
C -0.07347400 4.82600500 2.99796400
C -0.57531500 4.04238100 4.03438900
C -0.40110800 2.65952900 3.99488600
C -1.29442300 -4.78848200 -1.65148200
C -0.85434800 -5.39325600 -2.82436100
C 0.22794500 -4.84663300 -3.50998900
C 0.85602500 -3.70603200 -3.01231900
C 0.44080400 -3.09403800 -1.81581300
P 1.48655900 2.01912700 0.36601400
P 1.34411600 -1.57814400 -1.22632500
C 1.62558800 3.37563100 -0.88968800
C 3.27842500 1.75630100 0.74645000
C 2.54405900 -2.34935300 -0.04503200
C 2.36317400 -1.08535400 -2.68771800
C 3.74575500 -1.30397900 -2.77750900
C 4.46115700 -0.86197300 -3.89451600
C 3.80675900 -0.20388500 -4.93580500
C 2.42912200 0.01814400 -4.85613400
C 1.71554300 -0.41040100 -3.73804600
C 3.82391600 1.93465300 2.02440000
C 5.19161600 1.74103200 2.23766300
C 6.02611500 1.37005000 1.18341800
C 5.48760800 1.18826600 -0.09314900
C 4.12410300 1.37798400 -0.31037500
C 2.59184900 4.39064500 -0.77009700
C 2.68164300 5.40157900 -1.72645000
C 1.81683800 5.40992700 -2.82423400
C 0.86633700 4.39884600 -2.96388400
C 0.77441000 3.38802800 -2.00379800
C 2.82263100 -1.72420800 1.17690400
C 3.70949100 -2.30427700 2.08839300
C 4.33335600 -3.51329600 1.78469900
C 4.05799500 -4.15104200 0.57053100
C 3.16398600 -3.58084000 -0.33467600
H -1.43665400 0.16639400 2.66933600
H 0.53856200 -1.90580300 3.53913600
H -2.24790600 -2.25897600 2.31955200
H 0.40395400 -2.96744400 1.20800000
H 0.94219500 4.84719900 1.11404400
H -0.20556400 5.90433700 3.00922000
H -1.10696800 4.49895900 4.86433900
H -0.79645200 2.04081100 4.79515900
H -2.16330900 -5.17339800 -1.12938000
H -1.36563000 -6.27211400 -3.20621900
H 0.57961800 -5.29348400 -4.43587500
H 1.68069900 -3.28030900 -3.57269000
H 4.27020200 -1.81319200 -1.97624200
H 5.53240400 -1.03738000 -3.94786900
H 4.36487500 0.13676900 -5.80350300
H 1.91023800 0.53030800 -5.66168300
H 0.64686800 -0.22374800 -3.68161600
H 3.18513600 2.19748000 2.85820500
H 5.60081300 1.88264500 3.23438800
H 7.08933000 1.22284700 1.35358000
H 6.12785000 0.89934600 -0.92239800
H 3.72192500 1.24035200 -1.30980600
H 3.28091100 4.38622600 0.06900700
H 3.43143000 6.18047700 -1.61681400
H 1.89027200 6.19682000 -3.56994200
H 0.19724400 4.39040100 -3.81995600
H 0.04740600 2.59205200 -2.12795900
H 2.34116000 -0.79491700 1.44732400
H 3.89205000 -1.79917200 3.03173200
H 5.02335100 -3.96640300 2.49164900
H 4.53131300 -5.09980600 0.33202900
H 2.94198000 -4.09935300 -1.26226200
Pd -0.03056900 0.28188100 -0.53050200
C -5.10355000 2.30078200 -1.30253400
C -5.70968000 3.20524300 -2.07799900
H -4.64444900 1.42177500 -1.76070600
H -6.22201100 4.05611000 -1.61953700
C -5.76289900 3.12688100 -3.57914700
H -6.80098600 3.14103900 -3.93968300
H -5.29310600 2.20445500 -3.93569700
H -5.25758500 3.98254000 -4.05148200
C -1.34327100 -4.02383900 3.17439100
H -1.91343200 -4.66774600 2.49624700
H -0.33151700 -4.45072600 3.25167800
C -1.14768700 -1.64398300 4.86986700
H -0.56429600 -0.96781000 5.50613000
H -2.16033100 -1.22119800 4.80131000
C -1.98803700 -3.99597600 4.56429200
H -2.01347500 -5.00968900 4.98267900
H -3.03244600 -3.66483700 4.47791400
C -1.22250900 -3.04400800 5.48890400
H -0.20589800 -3.43027100 5.65371300

H -1.70083200 -2.98884500 6.47453500

TS Pro-S-A
b3lyp/6-31g(d) & LanL2DZ,
el. energy = -3501.065696 a.u.
im. frequency -132.87

C 2.62374300 1.84898300 -0.39959800
C 2.08044700 0.55584400 -0.96519600
C 4.05620200 2.09632000 -0.95427900
C 1.35883000 0.57663300 -2.18097000
H 2.69503700 -0.31667900 -0.79418900
C 0.97096000 -0.63571200 -2.75074600
H 1.03978800 1.51563700 -2.62620100
H 1.38331500 -1.57512100 -2.41542700
H 0.34328000 -0.65319900 -3.63593200
H 4.08951400 1.77352900 -2.00218900
C 5.16930200 1.38818100 -0.14183500
H 4.26484000 3.17367900 -0.94673800
O 4.78728200 0.07439600 0.27399900
H 4.71297300 -0.51144500 -0.52356100
C 5.47115000 -1.54430900 -3.84474600
H 5.39683100 -1.99422600 -4.83861300
H 6.18911900 -2.09573000 -3.23016500
H 5.85053600 -0.52119400 -3.97083600
C 4.09254200 -1.49128500 -3.16295200
O 3.09130400 -1.42675400 -3.91911900
O 4.08434200 -1.49415500 -1.88704900
N -0.14673900 2.27351900 2.00766700
C -1.11054000 3.35105900 1.78384800
C -1.15415400 3.81881800 0.31602400
N -1.61728700 2.76640500 -0.60016500
C -0.35137900 1.34209900 2.97413000
C -1.21190300 2.77499500 -1.90517400
O -0.27117100 3.48002000 -2.28019400
O -1.43084800 1.16634600 3.54527300
C 0.88850800 0.58068800 3.40600600
C -1.98070000 1.96351800 -2.93499800
C 1.26486600 -0.69013000 2.92312800
C 2.41746000 -1.29247700 3.45402100
C 3.17346200 -0.66532800 4.44463400
C 2.78640100 0.58267400 4.92873400
C 1.64844500 1.19667600 4.40824100
C -2.09786900 2.63461700 -4.16340900
C -2.75893200 2.06937500 -5.24997600
C -3.30359900 0.79379600 -5.12820000
C -3.17782400 0.10102300 -3.92407000
C -2.52806300 0.65916500 -2.80949200
P 0.32483900 -1.50840900 1.54961800
P -2.32219000 -0.37787500 -1.27407700
C 1.28897700 -3.06043100 1.22857300
C -1.17582600 -2.21038900 2.38326900
C -3.67934400 0.29153500 -0.20431400
C -2.92832800 -2.05084700 -1.77480700
C -4.25493600 -2.47741400 -1.60830300
C -4.63428000 -3.77002100 -1.97842300
C -3.69734800 -4.65113400 -2.52109900
C -2.37341500 -4.23789900 -2.68792900
C -1.99039700 -2.95080000 -2.31012700
C -1.51412400 -1.95873700 3.71956500
C -2.66193100 -2.53053800 4.27688600
C -3.48055200 -3.36206000 3.51339100
C -3.14822800 -3.62262100 2.18115200
C -2.00765000 -3.05003100 1.62111400
C 1.10732700 -4.21363900 2.01482800
C 1.86868200 -5.35833200 1.77855400
C 2.82717500 -5.37111100 0.76105400
C 3.02014700 -4.23111300 -0.01816300
C 2.25296400 -3.08643900 0.21041700
C -3.51131900 0.30446300 1.18827900
C -4.50587000 0.82390900 2.02028500
C -5.68408100 1.33088500 1.47075200
C -5.86217300 1.32825100 0.08414400
C -4.86572400 0.81913600 -0.75001800
H 0.80541400 2.33966300 1.63838000
H -2.08902200 2.94788300 2.06543000
H -0.14315000 4.07767500 -0.01121200
H -2.49704800 2.31971100 -0.36880300
H 2.73454800 -2.25957400 3.08246600
H 4.06402500 -1.15397800 4.82944700
H 3.36855500 1.08128800 5.69872600
H 1.34445400 2.17358600 4.77481100
H -1.64005900 3.61380200 -4.24861600
H -2.83526700 2.61822700 -6.18422900
H -3.81614400 0.32803400 -5.96550200
H -3.58553500 -0.90115600 -3.85491600
H -4.99387300 -1.80665600 -1.18282400
H -5.66465000 -4.08675700 -1.83976200
H -3.99486100 -5.65649000 -2.80639800
H -1.63448100 -4.91858100 -3.10133300
H -0.95365700 -2.64625500 -2.41902800
H -0.90269400 -1.30229200 4.32573300
H -2.91081500 -2.32129600 5.31388600
H -4.37115000 -3.80508000 3.95139300
H -3.77634600 -4.26846200 1.57365800
H -1.75749100 -3.27090500 0.58780100
H 0.37253500 -4.22037500 2.81291500
H 1.71306100 -6.24080700 2.39399600
H 3.41980600 -6.26467900 0.58239800
H 3.76547100 -4.20159000 -0.80704900
H 2.44505600 -2.22901800 -0.42080700
H -2.59831100 -0.06817300 1.63342700
H -4.33493600 0.84078800 3.09191600
H -6.45751700 1.73790100 2.11674700
H -6.77340300 1.73037800 -0.35078700
H -5.00759100 0.84023300 -1.82648800
Pd 0.00944500 -0.23808700 -0.56980900
H 5.30819600 1.94732300 0.79060700
H 1.98152100 2.67912400 -0.71282500
O 2.61307300 1.88284700 1.03197500
H 3.11828100 1.09772500 1.31914700
C 6.47133200 1.37776200 -0.90079500
C 7.56528400 2.05759200 -0.54922700

H 6.48182700 0.75684100 -1.79889900
H 7.53432000 2.66699400 0.35666000
C 8.86625700 2.05992300 -1.30076300
H 9.69050800 1.70257300 -0.66823800
H 9.13823500 3.07357900 -1.62650300
H 8.81852100 1.42023500 -2.18845100
C -2.05821900 5.06272200 0.15019500
H -3.10001600 4.76279100 0.33900200
H -2.00206900 5.38427700 -0.89565000
C -0.77520900 4.53084400 2.72783900
H -0.81680900 4.15774000 3.75758600
H 0.26397900 4.83904800 2.54156600
C -1.68481900 6.21263000 1.09261700
H -2.37648800 7.05139900 0.94615000
H -0.68168700 6.58496600 0.83983000
C -1.70309000 5.73761000 2.54910000
H -2.72900600 5.45962800 2.83138100
H -1.39917200 6.54505500 3.22657400

INT Pro-R-A
b3lyp/6-31g(d) & LanL2DZ,
el. energy = -3501.080295 a.u.

C 2.48236900 -2.05288700 -0.25415200
C 2.26997300 -0.82429600 0.59894700
O 1.33058900 -2.91835100 -0.32555000
C 3.71003600 -2.86497000 0.22854900
C 1.63566000 -0.93145500 1.86076200
H 2.99666700 -0.01272900 0.46986000
C 1.34217200 0.23872600 2.56427900
H 1.18668000 -1.86530100 2.18895500
H 1.96012000 1.13459100 2.41269400
H 0.73938000 0.17884600 3.46597300
H 3.44212600 -3.40140500 1.15022800
C 4.97557300 -2.02212400 0.49789100
H 3.91472200 -3.62525800 -0.53588500
O 5.20565100 -1.13930600 -0.59493700
H 5.22272900 -0.23426300 -0.20313800
H 1.02979700 -3.16340400 0.56923200
H 2.66381900 -1.73976300 -1.28216200
H 4.80995700 -1.43149700 1.40893400
C 5.93535800 2.39038000 2.26558500
H 5.82018600 3.11351500 3.07706400
H 6.51948100 2.83954100 1.45354300
H 6.50659900 1.52601000 2.62448400
C 4.57185200 1.92567100 1.73022400
O 3.53208800 2.41140300 2.25110400
O 4.59789600 1.08462300 0.77883700
N -1.11845400 -2.41866000 -1.76320000
C -2.37366200 -3.10140900 -1.45870500
C -2.42087000 -3.59719400 -0.00025600
N -2.35299800 -2.50439700 0.97601600
C -1.04633200 -1.53529000 -2.78884100
C -1.45964100 -2.48238100 1.99519800
O -0.50094000 -3.26538400 2.05392000
O -2.03781700 -1.10332500 -3.38472100
C 0.35966200 -1.20731000 -3.26035600
C -1.74901000 -1.54289300 3.15310300
C 1.06076300 -0.01197100 -2.98481000
C 2.33875300 0.15830500 -3.54267600
C 2.90581000 -0.81140700 -4.37007200
C 2.20377000 -1.98072500 -4.65164600
C 0.94053500 -2.17198300 -4.09372600
C -1.72362100 -2.18791100 4.39890200
C -1.99590600 -1.50334600 5.58129800
C -2.28089200 -0.14139900 5.53104000
C -2.27786200 0.52282300 4.30347900
C -2.01743500 -0.14934100 3.09775800
P 0.44041400 1.21594300 -1.74810900
P -1.86096700 0.84458300 1.52479300
C 1.63818000 2.62040100 -1.78181600
C -0.99951300 2.07442100 -2.53897800
C -3.47669700 0.48578700 0.69587500
C -1.99704500 2.60780600 2.05771800
C -3.21579900 3.29981400 2.14720800
C -3.23972700 4.64290900 2.52827300
C -2.05059500 5.31154300 2.82550300
C -0.83257500 4.63501600 2.73238400
C -0.80347600 3.29529900 2.34347500
C -1.45763700 1.80044800 -3.83340200
C -2.50285600 2.54937300 -4.38258100
C -3.09581200 3.57825200 -3.65163400
C -2.63914200 3.86196100 -2.36130300
C -1.59918400 3.11664500 -1.80975800
C 1.76745100 3.41516700 -2.93846400
C 2.62222900 4.51364800 -2.94490800
C 3.34339500 4.84811900 -1.79224300
C 3.21188400 4.07298300 -0.64346200
C 2.36792000 2.95728400 -0.63722400
C -3.53324000 0.38444600 -0.70099900
C -4.73863300 0.09833100 -1.34617300
C -5.90375300 -0.09278600 -0.60179700
C -5.85912700 -0.00638400 0.79288600
C -4.65430600 0.27601400 1.44004000
H -0.24616600 -2.68819900 -1.29497400
H -3.17839500 -2.37469700 -1.61339300
H -1.54585900 -4.22392400 0.19617100
H -3.15515100 -1.88845000 1.03296700
H 2.90929300 1.05064400 -3.31393200
H 3.89996800 -0.65232600 -4.77715600
H 2.63792600 -2.74650800 -5.28828500
H 0.39151000 -3.08700000 -4.29924300
H -1.47866500 -3.24482200 4.42354000
H -1.97496000 -2.03052200 6.53069800
H -2.49059700 0.41328900 6.44138600
H -2.46599100 1.59068800 4.28618200
H -4.14824100 2.79844900 1.91045700
H -4.19028700 5.16630600 2.58811200
H -2.07218800 6.35750200 3.11912400
H 0.10028200 5.14732600 2.94914700
H 0.15416200 2.79141500 2.25127800
H -1.02351600 0.99264100 -4.40841300
H -2.85009100 2.32200800 -5.38694500

H -3.90710600 4.15840000 -4.08351000
H -3.09028300 4.66406200 -1.78337800
H -1.24439900 3.35740600 -0.81092200
H 1.19247100 3.18020600 -3.82948500
H 2.71795500 5.11581000 -3.84480600
H 4.00241400 5.71272400 -1.79683400
H 3.75525400 4.30873900 0.26582400
H 2.31579300 2.37211200 0.27404800
H -2.63721600 0.50202700 -1.29470400
H -4.74399900 0.00943000 -2.42806100
H -6.84158000 -0.31859000 -1.10225100
H -6.76032200 -0.16340000 1.37964600
H -4.62979900 0.32394600 2.52510400
Pd 0.30167300 0.31883900 0.54037200
C 6.17564000 -2.91264500 0.71003900
C 6.79236900 -3.10399100 1.87856700
H 6.53902000 -3.41680300 -0.18776100
H 6.41986600 -2.57655300 2.75949300
C 7.98483100 -3.99211400 2.09855900
H 7.76847600 -4.78044500 2.83338700
H 8.83845300 -3.42335000 2.49269500
H 8.30178600 -4.47574500 1.16802800
C -3.70312300 -4.41630200 0.26678600
C -2.58518200 -4.27543700 -2.44252700
H -3.66858000 -4.78897000 1.29742500
H -4.56920100 -3.73956500 0.20333100
H -1.72163600 -4.95242900 -2.36909400
H -2.58803900 -3.86501600 -3.45799200
C -3.89327200 -5.57147000 -0.72404500
H -4.83358900 -6.09281300 -0.50645000
H -3.08774200 -6.30724800 -0.58782300
C -3.87515600 -5.05602000 -2.16744400
H -4.74422200 -4.40323100 -2.33525100
H -3.96796800 -5.88857100 -2.87543700

INT Pro-S-A
b3lyp/6-31g(d) & LanL2DZ,
el. energy = -3501.079807 a.u.

C 2.53153600 1.99773800 -1.65250700
C 1.82990600 0.67875400 -1.93111900
C 4.01978900 1.93733600 -2.07734600
C 0.67445200 0.65958500 -2.71217900
H 2.40811700 -0.23704700 -1.83720400
C -0.00597500 -0.55796900 -2.91986700
H 0.19640500 1.59253800 -3.00662300
H 0.58174200 -1.47897700 -2.90693900
H -0.93813500 -0.55313400 -3.47289400
H 4.10711500 1.30523800 -2.96916800
C 4.94754300 1.39236700 -0.96276100
H 4.36314300 2.94193200 -2.35420200
O 4.31551200 0.32710900 -0.24390800
H 4.23918800 -0.44220100 -0.87443300
C 4.17842800 -3.04071800 -4.03909000
H 3.54816400 -3.85677900 -4.40179000
H 5.15775600 -3.42898700 -3.73863900
H 4.35437500 -2.33432700 -4.85994700
C 3.51880600 -2.30186800 -2.86482500
O 2.31900100 -2.57993400 -2.58816800
O 4.24731900 -1.44702100 -2.27312600
N -0.38541900 2.81133600 0.86471500
C -1.49350000 3.68504800 0.45395500
C -1.93679300 3.48485100 -1.00857700
N -2.46587900 2.13522400 -1.26580600
C -0.20992000 2.54659500 2.19223100
C -2.55917800 1.68188700 -2.54879600
O -2.04411000 2.29717800 -3.48622600
O -1.08699900 2.72209100 3.04160300
C 1.19025100 2.12956900 2.59881600
C -3.34839400 0.42137600 -2.85897700
C 1.78606500 0.86873800 2.37584000
C 3.12784000 0.69015500 2.75426300
C 3.84916400 1.71116400 3.37315300
C 3.23552800 2.93188000 3.64524500
C 1.91265600 3.13307000 3.25850400
C -4.12459000 0.54161300 -4.02348500
C -4.85845400 -0.52699800 -4.52912600
C -4.79513300 -1.76198300 -3.88814900
C -4.01313200 -1.90733100 -2.74251000
C -3.29345700 -0.83088000 -2.19618400
P 0.84444000 -0.53692100 1.60945300
P -2.30371600 -1.11194600 -0.64340800
C 1.99746300 -1.97647300 1.67245400
C -0.31566200 -1.04722900 2.97514400
C -3.51304200 -0.43804500 0.59160200
C -2.29831400 -2.94450500 -0.42333000
C -3.28377000 -3.64513700 0.29050400
C -3.19861700 -5.03134800 0.43588700
C -2.13121200 -5.73361300 -0.12760200
C -1.14237200 -5.04427200 -0.83238000
C -1.21871400 -3.65795200 -0.97473900
C -0.55279800 -0.29805900 4.13531400
C -1.41780000 -0.77965800 5.12314200
C -2.05227100 -2.01140100 4.97049600
C -1.81768400 -2.76713600 3.81900100
C -0.95745800 -2.29035500 2.83211500
C 2.41457200 -2.50573600 2.91009800
C 3.26309000 -3.60832100 2.95384000
C 3.69564600 -4.20780300 1.76516600
C 3.27482000 -3.69703500 0.54019900
C 2.42882800 -2.58372200 0.48896300
C -3.06149300 0.37645500 1.63817300
C -3.95772100 0.93628900 2.55247100
C -5.32326800 0.68048900 2.43301800
C -5.79074900 -0.12247000 1.38817200
C -4.89730500 -0.66776700 0.46650000
H 0.46141100 2.76569500 0.28963000
H -2.33005200 3.44376800 1.11815800
H -1.07226500 3.60662000 -1.66958900
H -3.03496100 1.70710500 -0.54534900
H 3.62394900 -0.24781200 2.54329700
H 4.88827800 1.54334100 3.64122000
H 3.78339400 3.72850900 4.14086700

H 1.42778200 4.08560600 3.45214900
H -4.11954400 1.49523800 -4.53985500
H -5.45613300 -0.39876200 -5.42701100
H -5.34142400 -2.61653800 -4.27790000
H -3.95771100 -2.88063200 -2.26805000
H -4.11044600 -3.11192000 0.74732600
H -3.96646300 -5.56030400 0.99432400
H -2.06538700 -6.81176600 -0.00941800
H -0.29941300 -5.57700300 -1.26249000
H -0.42217100 -3.13771300 -1.49898600
H -0.08533300 0.66787700 4.27853800
H -1.58812900 -0.18330300 6.01560000
H -2.72130500 -2.38261100 5.74236500
H -2.29987100 -3.73191400 3.68684800
H -0.77043200 -2.90114900 1.95455500
H 2.07242200 -2.05794400 3.83841600
H 3.58227100 -4.00406000 3.91462900
H 4.35521300 -5.07122900 1.80164900
H 3.59305200 -4.14827800 -0.39422100
H 2.12813000 -2.22683700 -0.49277400
H -2.00765700 0.58922100 1.74070000
H -3.56808000 1.57424700 3.33918700
H -6.02467900 1.11304500 3.14147000
H -6.85513500 -0.31356500 1.28026100
H -5.28156800 -1.25769700 -0.35974300
Pd -0.05705400 -0.25591400 -0.73659600
H 5.09799100 2.18927500 -0.22452200
H 2.02726800 2.77600700 -2.23846800
O 2.38275300 2.42429600 -0.29333000
H 2.82550700 1.72897100 0.23359100
C 6.28328900 0.97175600 -1.51910000
C 7.43458700 1.60574600 -1.28351500
H 6.24995200 0.08373700 -2.15165500
H 7.42920600 2.48648500 -0.63679300
C 8.77192500 1.20710600 -1.84173900
H 9.49238700 0.99539400 -1.03928200
H 9.20902200 2.01151100 -2.45007400
H 8.69164600 0.31333400 -2.46948000
C -3.00610100 4.53059700 -1.40682300
H -3.91768600 4.32870200 -0.82481100
H -3.25193200 4.37208400 -2.46102100
C -1.08451100 5.15792400 0.70208800
H -0.83611600 5.26003800 1.76401300
H -0.16360700 5.36055200 0.13618100
C -2.55922100 5.97572300 -1.16441300
H -3.36401500 6.66519700 -1.44769900
H -1.70239000 6.21061600 -1.81218800
C -2.16292800 6.17050200 0.30191800
H -3.04774800 6.03878500 0.94158500
H -1.79807100 7.19001100 0.47748200

INT Pro-R-B
b3lyp/6-31g(d) & LanL2DZ,
el. energy = -3501.070724 a.u.

C -2.55261300 2.16996700 0.85466100
C -2.04039500 1.55706300 -0.43436500
O -2.85877400 1.18083700 1.83222700
C -3.77043000 3.11212100 0.66339200
C -2.27636400 0.22026900 -0.77225100
H -1.80724200 2.26105900 -1.23109600
C -1.66355300 -0.34641000 -1.90070400
H -2.75744000 -0.43401400 -0.05515900
H -1.42665600 0.28248800 -2.75812400
H -1.82847800 -1.39246500 -2.11731200
H -3.96931000 3.52052600 1.66255500
C -5.06797200 2.44419500 0.12919400
H -3.49731900 3.95473400 0.01662000
O -5.20716700 1.17776500 0.76886300
H -5.48868900 0.42069300 0.11525400
H -3.80790900 0.93350600 1.61324900
H -1.75407600 2.79291600 1.26849600
H -5.89577500 3.10063900 0.44902500
C -5.61417900 -2.64089100 -2.17761800
H -5.53023900 -2.70060700 -3.26744700
H -6.61726100 -2.93575800 -1.85632100
H -4.89302200 -3.34382000 -1.74128400
C -5.26483100 -1.23025100 -1.68120000
O -4.39689700 -0.58603500 -2.32949200
O -5.86402900 -0.85317700 -0.62652200
N -0.59743100 -0.26455000 2.87841200
C -0.61451900 -1.64416300 3.36995300
C -1.33295800 -2.61289300 2.40938000
N -0.64657700 -2.74096300 1.11357900
C 0.47294200 0.53827800 3.07236800
C -1.37225300 -3.11917400 0.01509900
O -2.60153600 -3.11552900 0.02452800
O 1.58703800 0.14086700 3.43607100
C 0.23317000 2.02846100 2.92540300
C -0.65464300 -3.61660700 -1.22865700
C 0.76847600 2.81981200 1.88385200
C 0.58808300 4.21095500 1.94047400
C -0.09363400 4.81216600 2.99992800
C -0.62600100 4.02574100 4.01898900
C -0.46167600 2.64202000 3.97459800
C -1.29600800 -4.71885100 -1.81767200
C -0.82792300 -5.29781600 -2.99307600
C 0.28958400 -4.75608500 -3.62343700
C 0.92560400 -3.64637200 -3.06835200
C 0.48152800 -3.06204600 -1.86893400
P 1.50328600 2.01243700 0.38480300
P 1.39181700 -1.58173700 -1.20496300
C 1.69949900 3.38339300 -0.84829900
C 3.27912100 1.71670600 0.81347800
C 2.48715500 -2.39965700 0.04506700
C 2.52894800 -1.10600700 -2.58271300
C 3.88317300 -1.46893400 -2.63229400
C 4.69262100 -1.03966600 -3.68784600
C 4.16130200 -0.24893300 -4.70731400
C 2.81345500 0.11761900 -4.66756000
C 2.00670600 -0.30049400 -3.60996900
C 3.79036100 1.88077900 2.10745100
C 5.14730700 1.66010200 2.35966700

C 6.00474700 1.27648300 1.32861300
C 5.50052200 1.10956300 0.03607800
C 4.14779700 1.32618100 -0.22017600
C 2.68379700 4.37571400 -0.69064200
C 2.81601000 5.39974400 -1.62800900
C 1.97644400 5.44422800 -2.74432300
C 1.00827400 4.45603000 -2.92137200
C 0.87403300 3.43217400 -1.98034800
C 2.77413100 -1.75403200 1.25449800
C 3.58472000 -2.36577200 2.21435500
C 4.12425100 -3.62852600 1.97271400
C 3.83941800 -4.28697700 0.77216300
C 3.02052400 -3.68383500 -0.18206400
H -1.47548300 0.16790200 2.55827800
H 0.43254900 -1.94619900 3.47725700
H -2.32827100 -2.22094100 2.18080400
H 0.34263600 -2.95898500 1.13826300
H 0.96676500 4.83693200 1.14096400
H -0.21670000 5.89149300 3.01570000
H -1.17329000 4.48117200 4.83936000
H -0.87992700 2.02156500 4.76183400
H -2.19077600 -5.09922900 -1.33779800
H -1.34442500 -6.15295600 -3.41922300
H 0.66411600 -5.18282500 -4.54986100
H 1.78073600 -3.22513800 -3.58473300
H 4.31275900 -2.07999600 -1.84590600
H 5.74046800 -1.32710500 -3.71032000
H 4.79292700 0.08336000 -5.52651200
H 2.39131700 0.73530500 -5.45538400
H 0.96355200 0.00110100 -3.57871700
H 3.13267400 2.15241500 2.92354000
H 5.52980100 1.79010100 3.36848700
H 7.05938100 1.10749400 1.52920300
H 6.15843900 0.80999800 -0.77524100
H 3.77170600 1.19904700 -1.23111400
H 3.35305100 4.34372100 0.16374000
H 3.57910300 6.16076900 -1.48871700
H 2.08284400 6.24151600 -3.47485000
H 0.35780700 4.47620100 -3.79153900
H 0.13240100 2.65519700 -2.13279200
H 2.35328000 -0.78431100 1.47826500
H 3.77139200 -1.84434700 3.14783400
H 4.75376600 -4.10690600 2.71834100
H 4.24549500 -5.27690000 0.58189100
H 2.78848800 -4.21683100 -1.09885500
Pd 0.00209500 0.29877000 -0.58350000
C -5.11694900 2.34314800 -1.37861300
C -5.69949100 3.26065300 -2.15684600
H -4.68606400 1.44280300 -1.82199400
H -6.18169800 4.12957600 -1.69947800
C -5.76620100 3.18100100 -3.65726100
H -6.80668500 3.20782300 -4.01026100
H -5.31026100 2.25373200 -4.01938300
H -5.25370000 4.02977900 -4.13417700
C -1.48924300 -4.01607100 3.04040400
H -2.05571300 -4.63872000 2.33989400
H -0.49002200 -4.46708600 3.14045100
C -1.28166700 -1.65966900 4.76636900
H -0.69915000 -1.00460000 5.42507900
H -2.28175100 -1.21209100 4.67543100
C -2.17048800 -3.98701600 4.41268500
H -2.23163200 -5.00418700 4.81884000
H -3.20394000 -3.62956900 4.30240500
C -1.40693800 -3.06391100 5.36778000
H -0.40497900 -3.47722100 5.55555500
H -1.91013800 -3.00698600 6.34085900

TS Pro-R-A-new
b3lyp/6-31g(d) & LanL2DZ,
el. energy = -3501.075482 a.u.
im. frequency -26.58

C -2.55900900 -1.50742500 -2.02195700
C -1.89137200 -0.21119700 -1.63095000
C -3.88298800 -1.29061400 -2.77556400
C -1.06898200 0.48623400 -2.53465000
H -2.35035000 0.35668100 -0.82526800
C -0.38833300 1.63002900 -2.10255400
H -0.84072800 0.03708600 -3.49867900
H -3.68160800 -0.72496000 -3.69459800
C -4.97468900 -0.57899100 -1.94552600
H -4.25410700 -2.27986600 -3.06914500
C -3.56635700 5.07712500 -1.39052200
H -3.79043100 5.43325900 -2.39893800
H -3.34315900 5.93087900 -0.73958600
H -4.45003500 4.58016900 -0.97295800
C -2.37970800 4.09993400 -1.39706600
O -1.84812300 3.81964200 -2.49205400
O -2.04676000 3.64393200 -0.24561300
N -0.07675600 2.80997900 1.34925200
C -0.70826600 2.65723000 2.65848100
C -1.99497800 1.80787600 2.57282100
N -1.71395400 0.39202100 2.24840900
C 1.25423000 2.74673600 1.17101500
C -2.66476300 -0.37672100 1.66439900
O -3.68489000 0.12718200 1.16816900
O 2.06250700 2.32138300 2.01254900
C 1.77622800 3.30970900 -0.13408200
C -2.54882400 -1.88817100 1.69453600
C 2.54924800 2.55472100 -1.04730600
C 3.11058900 3.21073800 -2.15248500
C 2.92015800 4.57943100 -2.35673100
C 2.13843700 5.31193400 -1.46842400
C 1.57050100 4.67386500 -0.36574700
C -3.74654600 -2.50570500 2.09579600
C -3.87415400 -3.88854700 2.16107400
C -2.79559600 -4.68838700 1.79369700
C -1.60699100 -4.09451700 1.37331900
C -1.44873600 -2.69753900 1.31825900
P 2.59425200 0.70196100 -0.93030600
P 0.20447100 -2.00129600 0.80059400
C 3.32363300 0.14661600 -2.54141100
C 3.98808900 0.28472000 0.21013200

C 0.97955300 -1.79486100 2.47224100
C 1.08803700 -3.46844000 0.08940900
C 2.29962200 -3.93192600 0.62357900
C 2.99027600 -4.98316400 0.01267900
C 2.48058000 -5.59011100 -1.13435500
C 1.27022000 -5.14185400 -1.66971300
C 0.58243900 -4.08881500 -1.06789000
C 4.67463100 1.24913500 0.95905400
C 5.74206500 0.87185900 1.77802500
C 6.13439900 -0.46445000 1.85850600
C 5.45403200 -1.43080400 1.11318100
C 4.38807900 -1.05924800 0.29518000
C 4.69720000 0.27991000 -2.81287800
C 5.22316200 -0.14079200 -4.03414200
C 4.38995500 -0.71088000 -5.00038500
C 3.02834900 -0.86088700 -4.73778500
C 2.50124200 -0.43598400 -3.51597100
C 1.66258100 -0.61518200 2.78892300
C 2.23133100 -0.43975000 4.05483100
C 2.13143800 -1.44645900 5.01264300
C 1.45091200 -2.63059200 4.70682400
C 0.87246700 -2.80266800 3.45118700
H -0.70108700 3.18756700 0.59897300
H 0.01880400 2.17555500 3.32193400
H -2.60336700 2.19778800 1.75227300
H -0.97718200 -0.06864400 2.77082000
H 3.68583000 2.64946600 -2.87958100
H 3.36752300 5.05983400 -3.22242500
H 1.96024100 6.37051700 -1.63342300
H 0.95327400 5.23572500 0.32848600
H -4.58996600 -1.87193700 2.34674400
H -4.81292600 -4.33205400 2.47913600
H -2.87364900 -5.77167700 1.82277900
H -0.78678300 -4.73616600 1.07436300
H 2.71064900 -3.47518400 1.51701300
H 3.92692800 -5.32817100 0.44268500
H 3.01780000 -6.40805000 -1.60631700
H 0.85597400 -5.61225100 -2.55721700
H -0.36527100 -3.77412400 -1.49439000
H 4.36214200 2.28494900 0.92694000
H 6.26562800 1.62997000 2.35432700
H 6.96580500 -0.75245100 2.49645900
H 5.75477300 -2.47403700 1.16526200
H 3.87474300 -1.81926400 -0.28685300
H 5.35827300 0.70891100 -2.06608000
H 6.28621500 -0.02727000 -4.22902400
H 4.80277000 -1.04172300 -5.94952900
H 2.37401900 -1.31224500 -5.47863200
H 1.44442000 -0.56794200 -3.30869900
H 1.75327100 0.19091600 2.07330800
H 2.74480600 0.49246400 4.26865200
H 2.57348100 -1.31302800 5.99655300
H 1.36256600 -3.41764500 5.45107100
H 0.33355600 -3.71986900 3.23562900
Pd 0.26832100 -0.15684000 -0.80687200
C -6.24203200 -0.45552700 -2.75864500
C -7.43954300 -0.89798300 -2.37216100
H -6.12681300 0.03384300 -3.72763400
H -7.51336500 -1.37717400 -1.39773500
C -8.70156800 -0.78093100 -3.17882800
H -9.46943900 -0.21109200 -2.63704000
H -9.13630600 -1.76898500 -3.38594900
H -8.52586900 -0.28158800 -4.13831100
C -2.80171200 1.85042800 3.89048900
H -2.22700300 1.32951400 4.67190900
H -3.72749900 1.28381500 3.74151400
C -1.03406700 4.07528100 3.18820800
H -0.08819500 4.62038200 3.29353300
H -1.61722000 4.58594500 2.41005000
C -3.11015700 3.27670100 4.35902000
H -3.66110200 3.24389700 5.30735600
H -3.76539700 3.76935600 3.62755400
C -1.81388500 4.07952500 4.50661600
H -1.19920100 3.64114900 5.30707000
H -2.02917800 5.11260000 4.80690400
H 0.33417000 2.11716200 -2.74564500
H -0.75989700 2.20450300 -1.25981100
H -4.62151100 0.44003700 -1.71571400
H -2.78950400 -2.08059800 -1.11676000
O -1.71494500 -2.28190200 -2.88911700
H -0.80785900 -2.18033400 -2.55657700
O -5.21553900 -1.28631200 -0.73679400
H -4.77087300 -0.80002000 -0.01413600

TS Pro-S-A-new
b3lyp/6-31g(d) & LanL2DZ,
el. energy = -3501.077905 a.u.
im. frequency -93.01

C -3.15701000 -0.97693800 -1.05014900
C -2.12231400 0.12238100 -0.97060300
C -4.43825400 -0.47924000 -1.76022200
C -1.41194900 0.56291300 -2.10455700
H -2.31013400 0.86131200 -0.19384300
C -0.55174600 1.66279800 -2.00727200
H -1.45181500 -0.00999600 -3.02987700
H -0.57746200 2.31681700 -1.14895200
H 0.12317100 1.92043000 -2.81066400
H -4.88498800 0.34062700 -1.18319000
C -5.49618000 -1.59230100 -1.95065600
H -4.16241700 -0.07172100 -2.74106300
O -5.99143200 -2.06595400 -0.71225400
H -5.22547200 -2.07261900 -0.10576100
C -2.76048900 5.63837800 -2.11993500
H -2.18197900 6.56722100 -2.05118100
H -3.55058900 5.69542600 -1.36246900
H -3.20818300 5.55971400 -3.11322600
C -1.84620000 4.44038800 -1.82080500
O -1.70899600 3.58259700 -2.73260600
O -1.31136600 4.42891600 -0.66754400
N 0.53880400 3.37043600 1.00606000
C 0.03289400 3.55341400 2.36146100
C -1.25562000 2.74459200 2.62948800

N -0.98280700 1.29571200 2.68766400
C 1.66718600 2.70662500 0.68797900
C -1.95550100 0.38268900 2.47255700
O -3.03598800 0.67856100 1.93623800
O 2.28216200 1.95131700 1.45738600
C 2.21416300 3.02442000 -0.68678700
C -1.79187800 -1.00563500 3.05345800
C 2.71318200 2.03584100 -1.56755600
C 3.27468900 2.44987300 -2.78420800
C 3.36266600 3.80094800 -3.12547600
C 2.86854700 4.76940800 -2.25720400
C 2.29364300 4.37584600 -1.05009100
C -2.57908200 -1.20293000 4.20344200
C -2.65082100 -2.44214600 4.82726500
C -1.94271400 -3.51877500 4.29116000
C -1.16614600 -3.33332500 3.15287400
C -1.07095200 -2.08382800 2.51099100
P 2.46780300 0.22641300 -1.20917300
P 0.10782500 -1.93997100 1.07153500
C 2.76986500 -0.60335200 -2.84471400
C 4.01383900 -0.27044100 -0.31669900
C 1.67137000 -2.22600300 2.02476100
C -0.17460900 -3.49593000 0.11757100
C 0.88693100 -4.08723200 -0.58866900
C 0.66658800 -5.19338500 -1.41015900
C -0.61915300 -5.72050500 -1.54799000
C -1.68257500 -5.13012300 -0.86300300
C -1.46747100 -4.02406200 -0.03770400
C 4.85256200 0.66226600 0.30769400
C 6.02893000 0.24501700 0.93476200
C 6.38017500 -1.10494000 0.95280800
C 5.54540600 -2.04280500 0.34086300
C 4.37273500 -1.62807900 -0.28775400
C 4.05699800 -0.74139200 -3.39641400
C 4.24084400 -1.36894900 -4.62833900
C 3.14424000 -1.87878400 -5.32871300
C 1.86438700 -1.76127600 -4.78719700
C 1.68095800 -1.13048600 -3.55410500
C 2.33460400 -1.09591300 2.52655900
C 3.42629400 -1.24243700 3.38488300
C 3.87936600 -2.51365400 3.73762600
C 3.23786200 -3.64355100 3.22518500
C 2.13767700 -3.50264600 2.37898000
H -0.02894700 3.81509400 0.25639400
H 0.81747500 3.21992300 3.05237800
H -1.93951400 2.90765300 1.79222200
H -0.15262100 0.99602700 3.18504400
H 3.63539600 1.71309900 -3.49159000
H 3.80643100 4.08615900 -4.07541000
H 2.91825700 5.82298300 -2.51661500
H 1.89647700 5.12361400 -0.37208900
H -3.15137900 -0.36671000 4.59466700
H -3.26230500 -2.56891300 5.71606400
H -1.99403700 -4.49938700 4.75603700
H -0.62382300 -4.18085700 2.74896400
H 1.89292500 -3.69103800 -0.49081200
H 1.50191600 -5.64209300 -1.94124200
H -0.79076500 -6.58227700 -2.18728500
H -2.68841300 -5.52765500 -0.96937100
H -2.30718200 -3.55821300 0.46716400
H 4.58183900 1.71031200 0.32044700
H 6.67174400 0.98277300 1.40795000
H 7.29744200 -1.42569800 1.43960500
H 5.80586300 -3.09764600 0.35197500
H 3.74601800 -2.36571800 -0.78037600
H 4.92023900 -0.36379200 -2.85738200
H 5.24247700 -1.46286200 -5.03954700
H 3.28959700 -2.37058000 -6.28680600
H 1.00648700 -2.16520000 -5.31797500
H 0.68567900 -1.05819400 -3.12671400
H 2.02569600 -0.09688200 2.23135300
H 3.93155900 -0.35639800 3.75793700
H 4.73309000 -2.62571000 4.40084000
H 3.58937000 -4.63814100 3.48790200
H 1.64829100 -4.39189700 1.99471400
Pd 0.09313200 -0.19102000 -0.58875500
H -4.99699900 -2.41849900 -2.49953500
H -2.75580800 -1.82861400 -1.61482300
O -3.47210800 -1.50008800 0.24911500
H -3.52283900 -0.74671500 0.88306600
C -6.63701700 -1.10254000 -2.80574800
C -7.90592200 -1.01037500 -2.40358800
H -6.36233900 -0.80901600 -3.82064900
H -8.14276900 -1.31727600 -1.38694000
C -9.04215200 -0.51913700 -3.25448200
H -9.82014800 -1.28772600 -3.36346300
H -8.70555400 -0.23423700 -4.25776200
H -9.53021800 0.35474500 -2.80086100
C -1.94582100 3.16041600 3.94874400
H -1.30777500 2.84968100 4.79013900
H -2.88438200 2.60088600 4.03386300
C -0.22272400 5.06953400 2.54138500
H 0.73791100 5.58743000 2.43182300
H -0.85701700 5.39731600 1.70691200
C -2.20105900 4.66794900 4.04217400
H -2.67227300 4.90477500 5.00419000
H -2.90836300 4.97249300 3.25844500
C -0.88667400 5.43631300 3.87238300
H -0.21272900 5.19835900 4.70901800
H -1.06219700 6.51848500 3.90938000

TS Pro-S-B-new
b3lyp/6-31g(d) & LanL2DZ,
el. energy = -3501.066887 a.u.
im. frequency -258.20

C 0.26857400 0.68373000 -2.65802500
C -0.92405500 1.15817100 -2.03149800
C -2.02547900 0.35334900 -1.84607200
H -0.92600300 2.17624700 -1.65604400
H -2.02322200 -0.63574300 -2.30594600
C 0.88071400 4.38560900 -4.83763100
H 0.07551300 5.07833100 -4.56372300

H 0.70467500 4.03484700 -5.85713600
H 1.82460900 4.93619800 -4.78025400
C 0.89059500 3.22053900 -3.84057300
O 1.40968400 3.43114200 -2.71209800
O 0.33827000 2.14651100 -4.24628700
N 2.35547500 2.37685300 -0.28498400
C 2.25646100 3.30260100 0.84224100
C 0.80666000 3.76136800 1.11223900
N -0.07261300 2.67104200 1.57543800
C 3.14537600 1.27910100 -0.23389100
C -1.37902800 2.64408700 1.22366000
O -1.81808800 3.39934400 0.33767900
O 3.61708100 0.80783100 0.80858300
C 3.53303000 0.66936200 -1.56503100
C -2.36990100 1.76966000 1.96767000
C 3.25318400 -0.67492300 -1.90839200
C 3.78486500 -1.18238700 -3.10248400
C 4.58113400 -0.39374100 -3.93615300
C 4.83731100 0.93285600 -3.60140200
C 4.30847400 1.45815500 -2.42217200
C -3.55264400 2.45568800 2.29476800
C -4.61472000 1.82021200 2.93087800
C -4.51634500 0.46293300 3.22864500
C -3.35638000 -0.23657200 2.89625900
C -2.26253300 0.38973100 2.27370000
P 2.00186800 -1.64014300 -0.93196400
P -0.76275300 -0.61209600 1.80756400
C 1.63789400 -3.11440000 -2.00197500
C 2.94995500 -2.45991300 0.42903600
C 0.35003200 -0.19604900 3.23334500
C -1.28852200 -2.35260500 2.15604600
C -1.06887000 -3.01121000 3.37538600
C -1.46213600 -4.34167800 3.54268600
C -2.08279400 -5.02984900 2.49888000
C -2.30338500 -4.38496900 1.27905600
C -1.90073100 -3.06069500 1.10713200
C 4.30529500 -2.20720700 0.67915500
C 4.96568600 -2.87243400 1.71567900
C 4.28407500 -3.79403200 2.51118200
C 2.93160900 -4.04902300 2.26954300
C 2.26867500 -3.38559700 1.23810700
C 2.51835400 -4.20719300 -2.08530800
C 2.22305100 -5.29823800 -2.90339600
C 1.04154700 -5.31989300 -3.64845700
C 0.15538100 -4.24513800 -3.56883400
C 0.45179000 -3.15382300 -2.74940900
C 1.73804300 -0.19367400 3.03499500
C 2.60598900 0.11136000 4.08687900
C 2.09912400 0.41621500 5.35001400
C 0.71665000 0.42742900 5.55828000
C -0.15301900 0.12877000 4.50890400
H 2.01819400 2.71332900 -1.20329500
H 2.64529000 2.77409400 1.71904500
H 0.37274000 4.11354400 0.17320600
H 0.22684300 2.13193000 2.38020600
H 3.56505900 -2.20139600 -3.39974200
H 4.98165300 -0.81725000 -4.85316000
H 5.43540200 1.56155700 -4.25491100
H 4.49151200 2.49564700 -2.16025600
H -3.63022900 3.50295100 2.02347500
H -5.51429000 2.37825900 3.17313300
H -5.33860200 -0.05727800 3.71242700
H -3.30196200 -1.29563600 3.12167500
H -0.58477200 -2.49022300 4.19493400
H -1.28142000 -4.83913800 4.49202000
H -2.38667100 -6.06463700 2.63167800
H -2.77794600 -4.91564600 0.45811600
H -2.04905800 -2.56956900 0.14843000
H 4.84016300 -1.47696200 0.08398400
H 6.01677900 -2.66531200 1.89897500
H 4.80150700 -4.30915400 3.31631200
H 2.38871900 -4.76109800 2.88533500
H 1.21735400 -3.59545200 1.06109000
H 3.43634200 -4.20692500 -1.50573600
H 2.91642600 -6.13349900 -2.95609700
H 0.81195000 -6.17170700 -4.28296400
H -0.76894700 -4.25469100 -4.14038200
H -0.24743200 -2.32625200 -2.67945800
H 2.15429000 -0.39457700 2.05728900
H 3.67529400 0.11894900 3.89907100
H 2.77390900 0.65620400 6.16761400
H 0.31301300 0.67464300 6.53674600
H -1.22440500 0.15371000 4.68314000
Pd -0.02922500 -0.36924900 -0.52478700
C 0.75465200 4.90117500 2.15560300
H -0.28888800 5.21903900 2.26276900
H 1.06851400 4.49961500 3.13126400
C 3.15892800 4.52224700 0.53143900
H 4.18627700 4.15661500 0.41564000
H 2.85337800 4.92452600 -0.44465500
C 1.64833300 6.09125500 1.78895800
H 1.58574700 6.85660600 2.57246100
H 1.27987700 6.55473200 0.86309400
C 3.09475000 5.62857500 1.58960300
H 3.49522700 5.25529900 2.54374300
H 3.73329200 6.46824300 1.28840600
C -3.37722900 0.81879800 -1.32579300
H -3.49199100 0.49920500 -0.27792100
O -3.54319000 2.22698000 -1.42474300
H -3.00075300 2.68557900 -0.74184300
C -4.51059600 0.15924300 -2.13312100
H -4.44077900 0.48085700 -3.18057300
H -4.37065700 -0.92903200 -2.10686600
C -5.91979100 0.49453200 -1.59293800
H -5.93717600 0.22432300 -0.51930900
C -6.97435900 -0.31007300 -2.30611400
C -7.69042400 -1.29109100 -1.75254800
H -7.13115600 -0.03846900 -3.35116900
H -7.52826300 -1.52693600 -0.69850400
C -8.72969500 -2.11377600 -2.46032600
H -9.71142100 -2.01519300 -1.97698900
H -8.83651600 -1.81107800 -3.50750100

H -8.47713600 -3.18322400 -2.44020100
O -6.22981700 1.86875000 -1.76753500
H -5.39354100 2.35172200 -1.61230400

6.2 Chapter 3

HCl
b3lyp/6-311+g(d,p) & 6-311+g(2df,p),
el. energy = -460.836453 a.u.
H 0.00000000 0.00000000 -1.21215200
Cl 0.00000000 0.00000000 0.07130300

2
b3lyp/6-311+g(d,p) & 6-311+g(2df,p) & LanL2DZ,
el. energy = -1669.551876 a.u.
C -1.91705400 -1.30940000 -1.03190500
C -1.52538000 -1.82155100 0.23758900
C -2.05737600 -0.95927100 1.24279200
C -2.79843900 0.06988100 0.59147000
C -2.69953800 -0.13952600 -0.81492900
Ti -0.47434100 0.37243800 -0.01533100
C 0.98962100 2.32501100 -0.41907700
C -0.11753100 2.41687300 -1.30325900
C 0.50915000 2.43318100 0.89963700
C -1.27813300 2.59021900 -0.52509800
C -0.89815600 2.56885900 0.84576500
S 1.05399300 -0.67769600 -1.58027300
C 2.55285000 -0.37110600 -0.70209300
C 2.55446000 -0.30408100 0.71624400
C 3.77083900 -0.25192000 -1.39293900
C 3.77314600 -0.11621400 1.39062300
C 4.96606100 -0.08103300 -0.70762500
H 3.76341700 -0.29739500 -2.47607600
C 4.96728600 -0.01205200 0.69039200
H 3.76797400 -0.05858500 2.47322400
H 5.89631500 0.00149800 -1.25859700
H 5.89811600 0.12568100 1.22913200
S 1.05913200 -0.54000200 1.61984600
H 1.10368400 2.38548700 1.79670800
H 2.01771100 2.18905600 -0.70846300
H -1.55394200 2.69380300 1.69254700
H -2.27636300 2.72465900 -0.90555800
H -0.07089900 2.36003600 -2.37971500
C -3.71794300 1.03855200 1.27703100
H -4.71893200 0.59998800 1.36675600
H -3.38203800 1.27626600 2.28759000
H -3.82686000 1.97748100 0.73155400
C -2.00726700 -1.20061000 2.72440800
H -2.08617700 -0.27220600 3.29303600
H -2.83823000 -1.84668500 3.03154500
H -1.08067900 -1.69186300 3.02450800
C -0.82326800 -3.12626800 0.45555000
H -0.40348900 -3.19812100 1.45785800
H -1.52843800 -3.95576800 0.32088600
H -0.00390500 -3.25830000 -0.25303400
C -1.74036500 -2.00193800 -2.35036100
H -0.82175400 -2.58841800 -2.37996500
H -2.58009100 -2.68544500 -2.52629600
H -1.71125700 -1.29696600 -3.18333600
C -3.47797800 0.56603400 -1.89014900
H -2.85309900 0.85414300 -2.73964300
H -4.26240100 -0.09420900 -2.27727600
H -3.97307100 1.46357700 -1.51765800

TS1$_{HCl}$
b3lyp/6-311+g(d,p) & 6-311+g(2df,p) & LanL2DZ,
el. energy = -2130.371656 a.u.
im. frequency -81.14
C 1.87748700 -1.81927600 -0.55881000
C 1.47423200 -1.01260400 -1.67461700
C 2.02035900 0.28321000 -1.50245000
C 2.78296900 0.28749500 -0.28870300
C 2.72524000 -1.02481200 0.26368400
Ti 0.50161700 -0.05378400 0.37451100
C -0.60634600 -0.72147700 2.43059100
C 0.79392200 -0.78386800 2.59729500
C -0.95920400 0.62858000 2.20907300
H -1.27857900 -1.56217100 2.43600800
C 1.30105100 0.54979200 2.52757800
H 1.36068100 -1.67638100 2.80610400
C 0.21710400 1.41597600 2.30338700
H -1.95721800 0.99904700 2.03801200
H 2.32669400 0.85621100 2.64933100
H 0.28399600 2.47988200 2.14888200
S -1.19895200 -1.72426400 -0.37852000
C -2.73422700 -0.86558300 -0.19913200
C -2.79302900 0.49911200 -0.52546300
C -3.91669800 -1.50959600 0.18532800
C -3.99114500 1.20596400 -0.47499000
C -5.11729600 -0.80439600 0.24583600
H -3.88713800 -2.56293400 0.43899800
C -5.15790400 0.55104000 -0.07938200
H -4.01790900 2.25586700 -0.74396400
H -6.02307300 -1.31551500 0.55195200
H -6.09168200 1.09866700 -0.03101200
S -1.25240200 1.23449800 -1.06617900
H 1.21820300 1.14488800 -2.46745200
H 0.24025600 -0.14573100 -3.35325300

H -1.30743600 2.45349600 -0.48167400
Cl 0.83049500 3.36964900 -0.09284600
C 0.79824800 -1.48782100 -2.92514800
H 0.06411600 -0.76813700 -3.29089900
H 1.55090900 -1.62024400 -3.71209000
H 0.28549600 -2.43720200 -2.78320600
C 1.67541100 -3.30143200 -0.42219200
H 0.75362200 -3.63473000 -0.89811600
H 2.50636400 -3.83734900 -0.89631000
H 1.63642300 -3.61522000 0.62254900
C 3.60883900 -1.55103900 1.35610000
H 3.22533900 -2.47574600 1.78935100
H 4.59639300 -1.77916500 0.93818000
H 3.76495000 -0.83496600 2.16398900
C 3.70263600 1.39205400 0.14249900
H 4.07806000 1.23896400 1.15568000
H 4.57394900 1.42369600 -0.52291400
H 3.20441800 2.36208800 0.10054900
C 2.02045200 1.36481200 -2.53957300
H 2.04300100 2.35509800 -2.08750800
H 2.90332800 1.24438600 -3.18054700
H 1.14036500 1.31104400 -3.18246600

INT1$_{\mathbf{HCl}}$

b3lyp/6-311+g(d,p) & 6-311+g(2df,p) & LanL2DZ,

el. energy = -2130.379311 a.u.

C -1.65302700 1.82114400 -0.56346700
C -1.39072700 0.96362900 -1.68497600
C -2.19804400 -0.18701800 -1.55098000
C -2.92398800 -0.08550300 -0.31928000
C -2.62053100 1.18526100 0.25376800
Ti -0.59972600 -0.23392500 0.36012300
C 0.75442900 -0.06867800 2.37945900
C -0.45330600 0.65163200 2.55192100
C 0.43491600 -1.43059400 2.23666500
C -1.51401500 -0.29569000 2.60047700
C -0.97128200 -1.57147600 2.39440700
S 1.29884200 1.61556800 -0.06188500
C 2.85819000 0.79987400 -0.05219500
C 2.95414600 -0.51081500 -0.54151800
C 4.03597700 1.42713300 0.38188100
C 4.17275200 -1.18076900 -0.61310800
C 5.25768600 0.76130100 0.31931800
H 3.98206200 2.43784300 0.76971100
C 5.33192100 -0.54247200 -0.17314500
H 4.22253300 -2.18781700 -1.01246700
H 6.15653600 1.26168800 0.66234100
H 6.28304500 -1.05970700 -0.21800900
S 1.41175400 -1.19985900 -1.11854400
H 1.60125500 -2.47040200 -0.72485000
Cl -1.01539500 -2.70306100 -0.30822500
C -1.27264900 3.26828200 -0.44352700
H -2.11136200 3.88954900 -0.78274700
H -1.04697500 3.55723100 0.58488900
H -0.40639300 3.51785900 -1.05305800
C -3.37772900 1.88258100 1.34659500
H -2.72725700 2.35677400 2.08534400
H -3.98899800 2.67885900 0.90610500
H -4.05976700 1.21268200 1.87019500
C -4.00580400 -1.02661600 0.12237100
H -4.25345300 -0.90101100 1.17804700
H -4.92378400 -0.84834800 -0.45036000
H -3.70970000 -2.06527800 -0.03003400
C -2.42121700 -1.20186100 -2.63019300
H -2.90525000 -2.09918000 -2.25234900
H -3.06282600 -0.76065700 -3.40385000
H -1.48926900 -1.50872200 -3.10705500
C -0.59170400 1.32485600 -2.90007000
H -0.24096900 0.43705300 -3.42884600
H -1.21250100 1.90005300 -3.59816100
H 0.28029700 1.92594100 -2.64224500
H -0.53178700 1.71960200 2.67845000
H -2.55307400 -0.08179100 2.77962800
H -1.52285300 -2.49285700 2.32744700
H 1.12967900 -2.23400400 2.05045200
H 1.74098400 0.35646400 2.32900200

TS2$_{\mathbf{HCl}}$

b3lyp/6-311+g(d,p) & 6-311+g(2df,p) & LanL2DZ,

el. energy = -2130.377530 a.u.

im. frequency -88.74

C -2.98175400 -0.20423400 -0.19610200
C -2.71029500 1.12871200 0.22610600
C -1.80444800 1.71306500 -0.69803900
C -1.56953500 0.75821900 -1.74402400
C -2.30309300 -0.40975500 -1.44141200
Ti -0.62022600 -0.18241500 0.36893800
C 0.82240900 0.46082600 2.23223200
C -0.45941500 1.03635700 2.38452700
C 0.68703200 -0.93903700 2.31167600
C -1.37956500 -0.02207400 2.64446000
C -0.67230500 -1.23218700 2.59909400
Cl -0.95016100 -2.66469400 0.07181000
C 2.81286500 0.76566800 -0.28068900
C 3.08203600 -0.59279500 -0.52561100
C 4.36284100 -1.11448400 -0.35439100
C 5.39684800 -0.28451500 0.07975400
C 5.14614100 1.06443800 0.32671400
C 3.86497200 1.58469200 0.15001000
H 4.55854400 -2.15931900 -0.56799000
H 6.39191300 -0.69169100 0.21710100
H 5.94735200 1.71383500 0.66155400
H 3.66848400 2.63280900 0.34504100
S 1.68010400 -1.53502100 -1.08613900
H 1.98256500 -2.69513600 -0.47415900
S 1.19859200 1.41144700 -0.59791400
C -0.88259600 1.00529100 -3.05428100
H -1.63655800 1.17184300 -3.83394500
H -0.22922400 1.87435300 -3.01987100
H -0.27428100 0.15201900 -3.36025000

C -2.51512700 -1.54867200 -2.39049600
H -3.23292100 -1.24180800 -3.16226700
H -1.59230100 -1.84103100 -2.89355000
H -2.90748500 -2.42936200 -1.88765700
C -3.99683200 -1.13588300 0.39660500
H -4.95585200 -1.03358300 -0.12528600
H -3.67448000 -2.17436000 0.31387700
H -4.17809300 -0.92763900 1.45263900
C -3.45660100 1.89889900 1.27626700
H -4.16406000 2.57647700 0.78408500
H -4.04057800 1.25081400 1.92983600
H -2.80853900 2.51867000 1.89907600
C -1.44852200 3.17120200 -0.72141400
H -2.28743200 3.74632700 -1.13354600
H -1.24472000 3.56064900 0.27810700
H -0.57224000 3.37312600 -1.33450600
H -1.09377800 -2.21566000 2.71170000
H 1.47662000 -1.66339900 2.19143000
H 1.73770100 0.99745000 2.05799900
H -0.67398000 2.09259500 2.36928600
H -2.42840900 0.07975200 2.86283300

INT2$_{HCl}$

b3lyp/6-311+g(d,p) & 6-311+g(2df,p) & LanL2DZ,

el. energy = -2130.404697 a.u.

C -3.05929600 0.71536100 0.11979700
C -3.10940600 -0.69883200 -0.00853600
C -2.30824200 -1.26556700 1.02917300
C -1.83550500 -0.19623100 1.84554400
C -2.26458900 1.02605200 1.26731100
Ti -0.79791500 -0.02539400 -0.40577300
C 0.50375000 -1.82559600 -1.35139500
C -0.85111800 -2.07067400 -1.63478200
C 0.89104800 -0.64324300 -2.03972100
C -1.31235500 -1.03614900 -2.50069500
C -0.21932900 -0.18681000 -2.77569600
Cl -0.60011100 2.22833100 -1.11022900
C 2.68596900 -0.37276400 0.61911000
C 3.54422900 0.63891400 0.13820200
C 4.86752900 0.31812200 -0.19702400
C 5.35031600 -0.97640200 -0.04639300
C 4.51682000 -1.97626700 0.45366500
C 3.20291600 -1.66610000 0.78674600
H 5.52705400 1.09285000 -0.57173700
H 6.37810000 -1.19842100 -0.31049400
H 4.88829900 -2.98508200 0.59210000
H 2.55654000 -2.42989000 1.20423700
S 2.91331400 2.29181700 -0.01133600
H 4.08000100 2.83044500 -0.41518900
S 1.03783700 -0.01285200 1.19009800
C -1.23044800 -0.35641000 3.20647100
H -0.58019500 0.47665900 3.47281400
H -2.03812200 -0.40105400 3.94821000
H -0.64439200 -1.27151300 3.29082000
C -2.21323500 -2.71849900 1.39983400
H -1.19318100 -3.01079700 1.66175200
H -2.84363100 -2.92899900 2.27172800
H -2.55496800 -3.37181100 0.59609900
C -4.04677300 -1.45538100 -0.90364100
H -3.64176600 -2.41166900 -1.23826500
H -4.97183800 -1.67445300 -0.35718600
H -4.32725600 -0.87936200 -1.78650300
C -3.85229300 1.69964300 -0.68691700
H -4.02365500 1.35030400 -1.70694700
H -4.83280400 1.86255600 -0.22311700
H -3.34291300 2.66008300 -0.75263800
C -2.06959400 2.38634400 1.86310500
H -2.04614300 3.15826300 1.09477300
H -2.88791000 2.61689800 2.55622600
H -1.13213800 2.44886600 2.41793600
H -1.42481300 -2.90877200 -1.27676700
H 1.13694900 -2.42230200 -0.71695300
H 1.86346900 -0.17961300 -2.00938900
H -0.25062500 0.70423700 -3.37901300
H -2.29882200 -0.95090000 -2.92672300

TS3$_{HCl}$

b3lyp/6-311+g(d,p) & 6-311+g(2df,p) & LanL2DZ,

el. energy = -2130.400327 a.u.

im. frequency -239.37

C -3.15683400 -0.46242600 0.14204900
C -2.44460500 -0.67175000 1.36059800
C -1.85646300 0.57069400 1.73869000
C -2.13216900 1.52093400 0.72016100
C -2.94025800 0.88255200 -0.26938600
Ti -0.77858500 -0.22952900 -0.34854200
C 0.31445400 -2.38286300 -0.51562800
C -1.06088000 -2.56833000 -0.74421200
C 0.83409100 -1.59125400 -1.57387900
C -1.39932400 -1.89299800 -1.95315900
C -0.21843800 -1.32512400 -2.47287700
Cl -0.26771900 1.56200400 -1.81135200
C 2.64520700 -0.24225400 0.70353000
C 3.48488900 0.67596100 0.03755200
C 4.78355300 0.29403900 -0.32201500
C 5.26786300 -0.97635900 -0.03065900
C 4.46383600 -1.86931600 0.67673900
C 3.17743700 -1.49668500 1.04796700
H 5.42043400 1.01778500 -0.81687000
H 6.27403000 -1.25331100 -0.32391300
H 4.84073900 -2.84895700 0.94920200
H 2.56666900 -2.18148300 1.62372300
S 2.96734400 2.37146900 -0.24295500
H 2.95670100 2.31958200 -1.58720700
S 1.00160000 0.18816700 1.24662500
C -3.59292500 1.56001000 -1.43757300
H -2.96381000 2.35405800 -1.83740500
H -3.79664900 0.86322300 -2.25272500
H -4.54918600 2.00121300 -1.13153900
C -1.77299200 2.97405000 0.77111800

H -1.74406300 3.41310000 -0.22503000
H -2.51066500 3.52502300 1.36725200
H -0.79087000 3.12658700 1.22158500
C -1.29327600 0.87791600 3.09255300
H -0.60323700 1.72098000 3.07032400
H -2.11912400 1.13786900 3.76683200
H -0.76286700 0.02803300 3.52268900
C -2.52108600 -1.87913200 2.25095100
H -1.54546000 -2.14369200 2.66580400
H -3.19155900 -1.68589900 3.09663100
H -2.91262400 -2.75234400 1.72744100
C -4.16721900 -1.39985000 -0.45185400
H -3.86518700 -2.44692500 -0.39802500
H -5.11106700 -1.31078500 0.09899500
H -4.38355100 -1.16376800 -1.49441200
H -0.14899700 -0.72406100 -3.36337800
H 1.85435200 -1.25963000 -1.67553100
H 0.86965100 -2.76759200 0.32206000
H -1.72645700 -3.14691000 -0.12607900
H -2.36936400 -1.86758100 -2.42222300

INT3$_{\mathbf{HCl}}$

b3lyp/6-311+g(d,p) & 6-311+g(2df,p) & LanL2DZ,

el. energy = -2130.408871 a.u.

C -3.08423600 -0.77700500 -0.12574100
C -2.26198800 -1.44395600 0.83127300
C -1.84585400 -0.47672100 1.79573000
C -2.33192600 0.79111600 1.38846800
C -3.09417000 0.60824400 0.19178500
Ti -0.79850300 0.04892900 -0.39204300
C 0.57328700 -1.48938400 -1.64786300
C -0.77550100 -1.74893200 -1.95049300
C 0.88911800 -0.18886600 -2.12514000
C -1.30213600 -0.60696800 -2.62273700
C -0.25787800 0.33163000 -2.75760900
Cl -0.62649700 2.41510700 -0.66761800
C 2.68223100 -0.44397200 0.58109200
C 3.54629200 0.60336300 0.19131300
C 4.87615500 0.30501100 -0.14625500
C 5.36074200 -0.99473500 -0.09346200
C 4.51743400 -2.03281200 0.30278500
C 3.19899200 -1.74926700 0.63795000
H 5.53345100 1.11238600 -0.45077500
H 6.39308500 -1.19439900 -0.35737400
H 4.88409000 -3.05130900 0.35918000
H 2.54570100 -2.54686300 0.97362400
S 3.08692000 2.31249200 0.12053600
H 1.76005100 2.14230000 0.28731700
S 1.02544200 -0.17842100 1.18383400
C -3.91378200 1.66265200 -0.49111500
H -3.44229100 2.64184900 -0.41604000
H -4.05532800 1.44866400 -1.55226400
H -4.90751400 1.72619100 -0.03163100
C -2.22852800 2.05870400 2.17976600
H -2.25116400 2.93622700 1.53507000
H -3.06680800 2.12942000 2.88368900
H -1.30392300 2.10008800 2.75769800
C -1.24329400 -0.79314000 3.13026700
H -0.63716300 0.02641500 3.51635100
H -2.05228400 -0.97810900 3.84825600
H -0.61156600 -1.68055900 3.09788700
C -2.09545700 -2.92825200 0.98895800
H -1.07034800 -3.19876300 1.25247400
H -2.74581800 -3.30153100 1.78881300
H -2.36394300 -3.47034400 0.08127500
C -3.98015400 -1.44497700 -1.12743900
H -3.51842300 -2.30605200 -1.61349300
H -4.88043200 -1.81036700 -0.61939800
H -4.31158500 -0.75579200 -1.90510400
H -0.34370300 1.31084100 -3.19742800
H 1.84061200 0.30944200 -2.03258000
H 1.24938800 -2.15511100 -1.13854400
H -1.30125900 -2.66377900 -1.73405500
H -2.29920100 -0.49962600 -3.01763400

TS4$_{\mathbf{HCl}}$

b3lyp/6-311+g(d,p) & 6-311+g(2df,p) & LanL2DZ,

el. energy = -2591.224279 a.u.

im. frequency -94.74

C -3.33590000 0.18144800 -0.21819000
C -2.91299000 -0.57983700 0.90464300
C -2.07007300 0.25771900 1.70439600
C -1.95760200 1.51641300 1.05773700
C -2.71673100 1.46235800 -0.15440000
Ti -0.90139000 -0.12933400 -0.41063800
C 0.07170100 -1.98846600 -1.61420400
C -1.34365300 -2.05913100 -1.69649100
C 0.49423100 -0.82630600 -2.28091700
C -1.77979900 -0.96464700 -2.48995500
C -0.65455700 -0.19591900 -2.83428200
Cl 0.22033000 1.98301400 -1.08164900
Cl -0.35699400 -2.66621700 1.32099900
C 2.87265900 -0.33257100 0.48498600
C 3.80852100 0.65840700 0.13329600
C 5.04291700 0.25693600 -0.39535600
C 5.35490900 -1.08789100 -0.55801100
C 4.42252000 -2.06303900 -0.20858400
C 3.18583200 -1.68547200 0.30247200
H 5.75849000 1.01958500 -0.67910200
H 6.31990900 -1.37070600 -0.96260600
H 4.65349100 -3.11505100 -0.32901000
H 2.46074600 -2.43962000 0.58596500
S 3.58778200 2.40236900 0.42593000
H 2.31833100 2.49656800 -0.02521100
S 1.31797100 0.11053000 1.25784900
H 1.04673500 -1.12356600 1.77325500
C -1.32792700 2.73876800 1.65162300
H -1.06684700 3.47028300 0.88965800
H -2.03264800 3.20676500 2.35000400
H -0.42012000 2.50284000 2.20885700

C -1.61012200 -0.04683700 3.09809600
H -0.73616400 0.54258900 3.38103100
H -2.41109300 0.20703700 3.80349200
H -1.36762500 -1.10151100 3.21923500
C -3.52446700 -1.88139700 1.32879700
H -2.86075400 -2.44724600 1.97763200
H -4.46160200 -1.68240400 1.86490300
H -3.76853800 -2.51744100 0.47590200
C -4.47757600 -0.19544400 -1.11532400
H -4.48570100 -1.25790300 -1.36477000
H -5.41875400 0.01497600 -0.59312400
H -4.49164400 0.38148600 -2.04087300
C -3.01747800 2.61949700 -1.05933900
H -3.88647500 3.17251600 -0.68252500
H -2.17618500 3.30760100 -1.12181400
H -3.25241300 2.29277200 -2.07429800
H -0.66120500 0.72577500 -3.39102000
H -2.78920400 -0.76452700 -2.80166000
H -1.95546000 -2.83379800 -1.26368900
H 0.69325600 -2.67951900 -1.07440000
H 1.50682400 -0.46163100 -2.34716400

1

b3lyp/6-311+g(d,p) & 6-311+g(2df,p) & LanL2DZ,

el. energy = -1562.515549 a.u.

C 2.02800900 1.35839100 0.93509800
C 2.70877600 0.12434100 1.02716800
C 2.95466800 -0.34260900 -0.27903300
C 2.47565400 0.63357000 -1.19051900
C 1.90551200 1.68353500 -0.44702800
H 1.71927500 1.97123600 1.76626300
H 2.93210000 -0.40474600 1.93808500
H 3.39182100 -1.29243200 -0.54169800
H 2.49934500 0.55663000 -2.26543900
H 1.48174800 2.58513400 -0.85589800
Ti 0.52390700 -0.22173200 -0.02629300
C -1.86832600 -0.59268000 0.30670300
C -1.43525800 0.36446600 1.28048700
C -1.74134700 -0.00049500 -0.97355400
C -1.03281000 1.53866800 0.59198800
C -1.17450100 1.29643700 -0.81124500
Cl 0.61455700 -1.65090900 -1.89227800
Cl 0.66587800 -1.96837500 1.55055600
C -1.55614000 0.21245700 2.76703600
H -2.55459900 0.52454200 3.09628300
H -1.40532000 -0.82177700 3.07427000
H -0.82636100 0.82288500 3.30210800
C -2.50702200 -1.91702900 0.59109000
H -2.15336600 -2.33862900 1.53097400
H -3.59616100 -1.80468900 0.65387600
H -2.28962500 -2.64210300 -0.19505800
C -0.76505500 2.87173200 1.22641800
H -1.69268700 3.45587900 1.25028500
H -0.42377000 2.77458000 2.25794100
H -0.02938100 3.46582400 0.68144900
C -1.04867100 2.30623400 -1.91676300
H -2.04300300 2.61835300 -2.25628900
H -0.52547900 3.20739200 -1.59488600
H -0.52418100 1.90268200 -2.78639700
C -2.27358800 -0.55342100 -2.25704400
H -3.30783700 -0.21245600 -2.39352000
H -1.69242400 -0.22154100 -3.11762500
H -2.27285300 -1.64241200 -2.26180100

bdt-H_2

b3lyp/6-311+g(d,p) & 6-311+g(2df,p),

el. energy = -1028.748567 a.u.

C 0.00916900 0.70346600 0.00401900
C 0.01049500 -0.70394000 0.01410300
C -1.20601100 -1.39362700 0.01042500
C -2.41596600 -0.70806900 -0.00654800
C -2.41668200 0.68560900 0.00270700
C -1.21433400 1.38405400 0.01238500
H -1.19252400 -2.47706000 0.03237900
H -3.34913300 -1.25868700 -0.01154100
H -3.35197400 1.23341300 0.00042800
H -1.22572900 2.46798800 0.01058700
S 1.51394700 -1.66318800 -0.04762500
H 2.20107600 -0.96087600 0.87537800
S 1.56550900 1.56309300 -0.03192100
H 1.04695700 2.79179300 0.14295700

HF

b3lyp/6-311+g(d,p),

el. energy = -460.836453 a.u.

F 0.00000000 0.00000000 0.09222200
H 0.00000000 0.00000000 -0.82999700

$TS1_{HF}$

b3lyp/6-311+g(d,p) & 6-311+g(2df,p) & LanL2DZ,

el. energy = -1769.989584 a.u.

im. frequency -90.44

C 2.67864600 -0.78381600 0.96810200
C 2.13600000 -1.72446700 0.04785400
C 2.12398100 -1.10903300 -1.24829700
C 2.65880900 0.20660100 -1.11627500
C 2.98326500 0.41156700 0.25646000
Ti 0.54126300 0.10468400 0.20795500
C -1.50692200 3.25832300 -0.39700900
C -0.28805300 3.55573300 0.27874400
C -1.27584900 2.20309300 -1.25613900
H -2.46224000 3.73504600 -0.20975800
C 0.71684900 2.71250000 -0.19263800
H -0.16423000 4.31783100 1.04165900
C 0.12086800 1.80455600 -1.16230100
H -2.00957000 1.71075400 -1.88330900
H 1.76954400 2.84605600 0.00394000
H 0.62552500 1.49803100 -2.07275800
S -1.49462500 0.66909600 1.55343900
C -2.81947100 -0.08685900 0.64784200

C -2.54657000 -0.97082800 -0.41396200
C -4.15148100 0.21282400 0.96639800
C -3.60641000 -1.54403600 -1.13364900
C -5.19793900 -0.36400400 0.24871300
H -4.35798400 0.89981000 1.78193500
C -4.92614700 -1.24292400 -0.80434000
H -3.38442100 -2.22329200 -1.95194000
H -6.22533000 -0.12628900 0.51113900
H -5.73923700 -1.69037100 -1.36931600
S -0.87731000 -1.41488400 -0.82637300
C 1.80854300 -3.15644100 0.36932000
H 1.13991100 -3.59812600 -0.37250900
H 2.72783900 -3.75822500 0.39561800
H 1.32179200 -3.24005200 1.34439000
C 3.08802500 -1.04282200 2.39131000
H 2.62468500 -1.94429600 2.79234600
H 4.17903900 -1.17145200 2.43682200
H 2.82910000 -0.21443300 3.05792200
C 3.75190700 1.56395400 0.84505900
H 3.29451900 1.94732700 1.76398500
H 4.76813100 1.23742700 1.10538100
H 3.85081200 2.39612600 0.14331300
C 3.03315400 1.12166300 -2.24751500
H 2.83164500 2.17369900 -2.02397500
H 4.10657600 1.03142700 -2.46327400
H 2.49863900 0.86999900 -3.16818300
C 1.82278300 -1.79442400 -2.55211400
H 1.34985700 -1.11983700 -3.27209500
H 2.75416000 -2.16405700 -3.00342400
H 1.15665900 -2.64962700 -2.42050400
F 0.38481900 -1.09213800 2.47008500
H -0.52955900 -0.69161400 2.42039800

INT1$_{\mathbf{HF}}$

b3lyp/6-311+g(d,p) & 6-311+g(2df,p) & LanL2DZ,

el. energy = -1770.061621 a.u.

C 2.19530000 1.48254600 0.79229300
C 1.90985900 0.46092600 1.73762700
C 2.46179700 -0.76094800 1.24890400
C 3.15470800 -0.47340000 0.03658300
C 2.96127100 0.90594000 -0.26227300
Ti 0.78533500 -0.09936300 -0.39448900
C -0.89533600 -1.19567500 -1.77891600
C 0.18479100 -0.88683700 -2.62532500
C -0.44458600 -2.14196800 -0.81631000
H -1.88981400 -0.78631800 -1.84723000
C 1.31992000 -1.58954400 -2.16855500
H 0.17207500 -0.15385700 -3.41630300
C 0.91873300 -2.38939200 -1.05564400
H -1.04379600 -2.58039800 -0.03515500
H 2.29713300 -1.57225900 -2.62267200
H 1.54026300 -3.07533800 -0.50372000
S -2.82564700 2.18768400 -0.88221700
C -3.41405800 0.69018000 -0.13390900
C -2.64288700 -0.15032800 0.70092700
C -4.75570800 0.36301900 -0.38405800
C -3.25656300 -1.28533900 1.25565100
C -5.34160700 -0.76383500 0.17824600
H -5.33991200 1.00693600 -1.03255300
C -4.58733500 -1.59763400 1.00321200
H -2.67091200 -1.91458500 1.91620300
H -6.38112000 -0.98988100 -0.03072400
H -5.03168100 -2.47910600 1.45116500
S -0.98693900 0.24397600 1.22367400
C 1.36681300 0.66147400 3.11953700
H 0.85216800 -0.22497500 3.49079200
H 2.20016200 0.87790600 3.79939200
H 0.66604100 1.49415900 3.17378400
C 1.83059500 2.93109200 0.89389600
H 1.08169800 3.10561900 1.66686800
H 2.71188600 3.53594000 1.13681800
H 1.42353700 3.29211000 -0.05261400
C 3.52096900 1.66958100 -1.42503100
H 2.76144200 2.32312500 -1.85834100
H 4.36227500 2.29580300 -1.10665500
H 3.88445700 1.00896800 -2.21411800
C 4.11893400 -1.39372700 -0.65261700
H 4.32875900 -1.08071600 -1.67607600
H 5.07343800 -1.38766500 -0.11341300
H 3.77586100 -2.42939800 -0.67967200
C 2.51115400 -2.04568500 2.02607900
H 2.82362100 -2.88811800 1.40725900
H 3.23185900 -1.96800700 2.84877900
H 1.54295100 -2.29423400 2.46717200
F 0.46165700 1.47442500 -1.37016600
H -1.50385800 1.95122300 -0.76396900

TS2$_{\mathbf{HF}}$

b3lyp/6-311+g(d,p) & 6-311+g(2df,p) & LanL2DZ,

el. energy = -1870.529145 a.u.

im. frequency -489.63

C 2.10759200 1.45774000 0.97824000
C 2.16849000 0.23968700 1.69999900
C 2.87283100 -0.71634500 0.90133000
C 3.28743000 -0.06336300 -0.29290600
C 2.78245500 1.26825600 -0.26526800
Ti 0.84105900 -0.17708100 -0.30940500
C -0.80261000 -1.20424600 -1.82099300
C 0.05968600 -0.42395500 -2.62160000
C -0.04173500 -2.26803600 -1.27206400
H -1.85880200 -1.04023100 -1.67650600
C 1.36216000 -0.94371100 -2.50372300
H -0.21206400 0.48126700 -3.13873500
C 1.29625500 -2.10003400 -1.66168900
H -0.40957800 -3.02496100 -0.60068700
H 2.23634100 -0.57223200 -3.01245500
H 2.11443800 -2.75068700 -1.39786700
S -3.02518400 2.31990800 -0.63209400
C -3.59475600 0.71512700 -0.11701100
C -2.86648600 -0.14727900 0.73002800

C -4.86480000 0.32250800 -0.56255000
C -3.42968700 -1.38196900 1.08464700
C -5.41588000 -0.89692500 -0.18642200
H -5.41472800 0.98450000 -1.22207500
C -4.69030200 -1.75902700 0.63467800
H -2.87212900 -2.04184500 1.73891400
H -6.40030000 -1.17603900 -0.54434100
H -5.10341000 -2.71687900 0.92952100
S -1.30415600 0.33938900 1.43330100
C 1.73789800 0.02595300 3.11884700
H 1.44434500 -1.00788500 3.29625100
H 2.57199800 0.26121400 3.79102200
H 0.90193900 0.66811100 3.39992400
C 1.51754100 2.75232300 1.44119300
H 0.84958200 2.61428500 2.29149400
H 2.31196700 3.44328000 1.74699300
H 0.94721600 3.22594400 0.64081100
C 3.00210200 2.34241500 -1.28531600
H 2.07264600 2.87974700 -1.48026900
H 3.74381000 3.06592200 -0.92791400
H 3.36474100 1.94130700 -2.23313600
C 4.28822700 -0.60111700 -1.27254400
H 4.29745700 -0.03644300 -2.20522600
H 5.29186500 -0.52082900 -0.83924400
H 4.12923400 -1.65325600 -1.51352500
C 3.28751100 -2.08312800 1.35850500
H 3.69434100 -2.67936500 0.54005600
H 4.07080700 -2.00816200 2.12217400
H 2.44731400 -2.62733600 1.79116600
F 0.19365700 1.50729700 -0.93079500
H -1.69994600 2.05244300 -0.63332900
F 0.29873600 -1.79385800 1.26975600
H -0.56801600 -1.04502400 1.56164200

3
b3lyp/6-311+g(d,p) & LanL2DZ,
el. energy = -841.817932 a.u.
C 2.29804100 0.12417900 1.16491800
C 2.72557900 -1.03382200 0.47769600
C 2.84519100 -0.71756400 -0.88922100
C 2.53421000 0.65695100 -1.05126700
C 2.19942400 1.18070200 0.21269000
H 2.11899400 0.20212200 2.22555800
H 2.83156400 -2.01724100 0.90715600
H 3.06742800 -1.41176800 -1.68463000
H 2.49719600 1.18775300 -1.99021900
H 1.93942700 2.20499800 0.42187600
Ti 0.48583000 -0.42008800 -0.30566500
C -1.90037600 -0.56137200 -0.08858500
C -1.37838200 -0.37884500 1.22976400
C -1.66558900 0.62720900 -0.82589900
C -0.78170000 0.90554300 1.29043900
C -0.93201200 1.52082700 0.00076000
C -1.50166700 -1.38156600 2.33578400
H -2.54328600 -1.45968700 2.66703000
H -1.18128500 -2.36832800 1.99508900
H -0.89979800 -1.11210700 3.20522800
C -2.61591700 -1.78430000 -0.57476000
H -2.07180200 -2.68775100 -0.29108800
H -3.62297700 -1.84618600 -0.14600900
H -2.71335800 -1.78212100 -1.66122000
C -0.29392200 1.59259500 2.53271900
H -1.10094000 2.19470600 2.96642300
H 0.02252800 0.88038100 3.29615200
H 0.54154900 2.26851000 2.34145800
C -0.62121200 2.95166500 -0.34221800
H -1.53987700 3.54967600 -0.33952200
H 0.05551500 3.40837000 0.38113800
H -0.17123500 3.05506900 -1.33244300
C -2.11523700 0.88108400 -2.23050500
H -3.19042100 0.70264700 -2.32639500
H -1.92000800 1.91097000 -2.53374800
H -1.59298300 0.21965900 -2.92701300
F 0.34420000 -2.21657600 0.15511300
F 0.32323600 -0.60091600 -2.14445400

XeF_2
b3lyp/6-31g(d) & LanL2DZ,
el. energy = -214.943797 a.u.
Xe 0.00000000 0.00000000 0.00009800
F 0.00000000 0.00000000 -2.04444500
F 0.00000000 0.00000000 2.04385900

$^{1cs}2$
b3lyp/6-31g(d) & LanL2DZ,
el. energy = -1669.255677 a.u.
C -1.93652800 -1.29014400 -1.04554900
C -1.53983500 -1.83083900 0.21301100
C -2.05455900 -0.97944400 1.23917000
C -2.78828000 0.07245800 0.61185200
C -2.70505900 -0.11414300 -0.80131800
Ti -0.47378100 0.37165000 -0.01525000
C 0.98155500 2.30683900 -0.48330100
C -0.17759300 2.41666400 -1.30031800
C 0.58081800 2.40722600 0.86371500
C -1.28836700 2.60082700 -0.45132900
C -0.82932500 2.55682200 0.89508400
S 1.04468000 -0.68808400 -1.58829100
C 2.54840900 -0.38223500 -0.70331800
C 2.54722600 -0.31572300 0.71782000
C 3.76781800 -0.24606300 -1.39327600
C 3.76371300 -0.11355900 1.39626700
C 4.96151300 -0.06321200 -0.70335800
H 3.76273000 -0.29033200 -2.47877600
C 4.95960400 0.00425800 0.69666200
H 3.75518700 -0.05727300 2.48121600
H 5.89413800 0.03024000 -1.25352600
H 5.89031400 0.15172600 1.23807500
S 1.04476400 -0.56323200 1.62056500
H 1.22821100 2.33537900 1.72484200
H 1.98971100 2.15066200 -0.83513500
H -1.43765700 2.66183700 1.78290700

H -2.30919500 2.74121900 -0.77171400
H -0.19727700 2.35939000 -2.38043700
C -3.68146400 1.04639500 1.32873300
H -4.68864300 0.62069200 1.43820500
H -3.31760900 1.26977500 2.33584000
H -3.79050300 1.99490100 0.79497500
C -1.98903500 -1.24099700 2.71891100
H -2.02637100 -0.31442300 3.29981300
H -2.83830700 -1.86265300 3.03484200
H -1.07275200 -1.76762300 2.99827300
C -0.82044800 -3.13358900 0.39923100
H -0.42615000 -3.23701800 1.41171700
H -1.50552200 -3.97238200 0.21079200
H 0.02226000 -3.21742400 -0.29280200
C -1.76801400 -1.95482700 -2.38178200
H -0.85607100 -2.55522000 -2.42366800
H -2.61909400 -2.62241800 -2.57825700
H -1.72620400 -1.22703300 -3.19788100
C -3.47595800 0.62436400 -1.86281300
H -2.84158500 0.94127200 -2.69832300
H -4.25640500 -0.02576500 -2.28042900
H -3.97824400 1.51075300 -1.46599600

^{1os}2

b3lyp/6-31g(d) & LanL2DZ,
el. energy = -1669.255677 a.u.

C 2.05443900 -0.97965400 1.23908500
C 1.53965900 -1.83074400 0.21274100
C 1.93645300 -1.28984400 -1.04571000
C 2.70505000 -0.11397200 -0.80121300
C 2.78820700 0.07235600 0.61202200
Ti 0.47366900 0.37159000 -0.01492500
C -0.58058700 2.40722700 0.86372400
C 0.82960700 2.55665200 0.89520200
C -0.98120300 2.30678700 -0.48331300
C 1.28872600 2.60060200 -0.45117000
C 0.17801300 2.41641200 -1.30024600
S -1.04511400 -0.56358700 1.62058200
C -2.54741300 -0.31583000 0.71781100
C -2.54847000 -0.38211900 -0.70332100
C -3.76396200 -0.11362800 1.39615100
C -3.76776900 -0.24561600 -1.39341700
C -4.95975800 0.00443800 0.69643300
H -3.75556300 -0.05754600 2.48111100
C -4.96152300 -0.06276000 -0.70360500
H -3.76256000 -0.28962900 -2.47892300
H -5.89049800 0.15190100 1.23779600
H -5.89406500 0.03090600 -1.25387600
S -1.04466000 -0.68781500 -1.58832800
H 1.43781600 2.66206800 1.78305200
H -1.22800800 2.33544600 1.72484200
H -1.98931600 2.15051800 -0.83522500
H 0.19781400 2.35876500 -2.38034100
H 2.30958600 2.74089400 -0.77150100
C 0.82031900 -3.13358400 0.39851600
H 1.50591500 -3.97229500 0.21161400
H 0.42434900 -3.23660800 1.41038900
H -0.02124700 -3.21793900 -0.29484600
C 1.76839100 -1.95460200 -2.38194700
H 2.61871900 -2.62348500 -2.57726400
H 0.85562900 -2.55371600 -2.42470200
H 1.72857600 -1.22690800 -3.19822500
C 3.47627100 0.62461200 -1.86242400
H 4.25580400 -0.02602000 -2.28094600
H 2.84192900 0.94299900 -2.69739700
H 3.97970900 1.51007100 -1.46496800
C 3.68155800 1.04603800 1.32902600
H 4.68931100 0.62110200 1.43618800
H 3.78890900 1.99550900 0.79663500
H 3.31920400 1.26740200 2.33713300
C 1.98861500 -1.24121000 2.71882600
H 2.83931300 -1.86057200 3.03544700
H 2.02304300 -0.31451200 3.29972300
H 1.07354500 -1.77026100 2.99752100

^{3os}2

b3lyp/6-31g(d) & LanL2DZ,
el. energy = -1669.235139 a.u.

C 1.63241400 -1.26413800 1.33596100
C 0.79142800 -1.89181600 0.35756700
C 1.39184400 -1.69937300 -0.92791200
C 2.57652500 -0.94311500 -0.75211700
C 2.73473600 -0.68533000 0.65197500
Ti 0.71372500 0.49036300 -0.04413800
C 0.56361700 2.81958400 0.73593700
C 1.92423600 2.44972600 0.72623900
C 0.07981700 2.76257000 -0.59802000
C 2.29745400 2.19913100 -0.62732700
C 1.16119000 2.38826400 -1.44438200
S -1.23199600 0.41455700 1.60922200
C -2.67951200 0.15769000 0.70034000
C -2.67200700 0.01389800 -0.72992000
C -3.92310800 0.08949800 1.38569900
C -3.90843000 -0.19068500 -1.40096000
C -5.10406900 -0.11155800 0.70340000
H -3.92043500 0.20030400 2.46591600
C -5.09671100 -0.25312700 -0.70458500
H -3.89449400 -0.29714600 -2.48154700
H -6.04334400 -0.16086500 1.24751200
H -6.03036700 -0.41047300 -1.23772100
S -1.21368000 0.08541300 -1.65694400
H 2.57408000 2.38898900 1.58895900
H -0.02333600 3.06842700 1.60899300
H -0.93257500 2.97191600 -0.91330000
H 1.11446700 2.26462200 -2.51876700
H 3.28403400 1.92705100 -0.97270300
C -0.38485500 -2.78636000 0.63407100
H -0.08234100 -3.84171000 0.57858800
H -0.79983600 -2.61192600 1.62921400
H -1.19087900 -2.63673800 -0.09089900
C 0.95955700 -2.34127700 -2.21652400
H 1.52795900 -3.26725700 -2.38688100

H -0.10223400 -2.59748300 -2.20830300
H 1.13272600 -1.68963800 -3.07946800
C 3.58072100 -0.65929800 -1.83699000
H 4.09392300 -1.58346200 -2.13701700
H 3.11286000 -0.24543900 -2.73747000
H 4.35354900 0.04169300 -1.50890700
C 3.95490500 -0.09733000 1.30464000
H 4.72182800 -0.87241700 1.44347200
H 4.41061200 0.69929400 0.70849000
H 3.73137800 0.31250500 2.29423600
C 1.47001400 -1.34585100 2.82955200
H 2.00141200 -2.21975200 3.23229400
H 1.87192200 -0.46011100 3.33289400
H 0.41934700 -1.43451000 3.11715500

^{1cs}Adduct$_{XeF2}$
b3lyp/6-31g(d) & LanL2DZ,
el. energy = -1884.214910 a.u.
C -3.13172000 -1.37716200 -0.93864700
C -2.04821600 -1.16281600 -1.84389800
C -0.93383200 -1.92491500 -1.38145300
C -1.33311200 -2.62791000 -0.20536400
C -2.69249300 -2.28590500 0.07030800
Ti -1.38894000 -0.27801500 0.35456500
C -1.44225000 0.97649600 2.46536400
C -2.09497200 -0.27069500 2.66307700
C -0.09032000 0.72019800 2.17258200
C -1.11862100 -1.28996500 2.54089100
C 0.11273600 -0.68922900 2.19200100
C 0.84307700 3.57260200 -0.38217300
C -0.12683800 2.55455600 -0.43401700
C 0.49084800 4.87856700 -0.05625800
C -1.48101900 2.87251400 -0.13802200
C -0.84216300 5.19111600 0.23952500
H 1.25330600 5.65257600 -0.03016100
C -1.81395000 4.19622800 0.20421300
H -1.12054500 6.20935600 0.49798300
H -2.84893800 4.43282000 0.43491300
S 0.31473000 0.90775800 -0.91935600
H -3.14261000 -0.40812500 2.89720300
H -1.91167100 1.94802900 2.49547200
H 0.65316100 1.46762800 1.93965100
H 1.03171700 -1.20914200 1.95512900
H -1.28854300 -2.34754500 2.66566100
C -2.11697000 -0.37885900 -3.12003900
H -2.50381200 -1.01202800 -3.93136300
H -2.77464200 0.48742700 -3.01765100
H -1.13272000 -0.00905900 -3.41517300
C 0.37386700 -2.12216500 -2.09613300
H 0.32094200 -3.01447800 -2.73628000
H 0.61388700 -1.27107800 -2.73918700
H 1.19662900 -2.26694200 -1.39030200
C -0.50872400 -3.70445800 0.44741900
H -0.45570200 -4.57948000 -0.21530800
H 0.51945800 -3.38102800 0.63862900
H -0.94397800 -4.04804600 1.38966400
C -3.60013900 -2.92585700 1.08443700
H -4.21540300 -3.69792800 0.60233500
H -3.04894200 -3.41375100 1.89218200
H -4.28817300 -2.20426700 1.53644300
C -4.54504100 -0.90153200 -1.12608800
H -5.10956400 -1.62508000 -1.73103800
H -5.06929600 -0.79179600 -0.17194500
H -4.58550900 0.06215700 -1.64001400
F 2.51143000 -2.10852300 0.52391900
F 5.13519100 0.86826200 -0.50337200
Xe 3.81697100 -0.58316300 -0.00641800
H 1.87690300 3.32730700 -0.60987000
S -2.74011600 1.63331000 -0.27452700

^{1os}Adduct$_{XeF2}$
b3lyp/6-31g(d) & LanL2DZ,
el. energy = -1884.214915 a.u.
C -3.12914700 -1.38207100 -0.94045000
C -2.04518200 -1.16555500 -1.84467600
C -0.92975100 -1.92538000 -1.38112300
C -1.32873900 -2.62918300 -0.20542700
C -2.68908100 -2.28995700 0.06891900
Ti -1.38994900 -0.27929500 0.35446400
C -1.45131100 0.97426900 2.46554300
C -2.09898100 -0.27577900 2.66173800
C -0.09789600 0.72386800 2.17447700
C -1.11802600 -1.29083700 2.54056600
C 0.11116900 -0.68469300 2.19372300
C 0.83697800 3.57502500 -0.37978300
C -0.13099100 2.55518500 -0.43289400
C 0.48189400 4.88043700 -0.05474100
C -1.48619400 2.87085300 -0.13915200
C -0.85212200 5.19067300 0.23892500
H 1.24292700 5.65581400 -0.02765100
C -1.82205200 4.19402600 0.20228500
H -1.13273300 6.20845900 0.49675400
H -2.85783100 4.42879900 0.43128600
S 0.31445000 0.90897800 -0.91672100
H -3.14627200 -0.41784100 2.89462700
H -1.92501700 1.94373700 2.49533700
H 0.64272700 1.47448900 1.94271200
H 1.03242000 -1.20068500 1.95714300
H -1.28354700 -2.34920400 2.66461600
C -2.11405000 -0.38153400 -3.12078300
H -2.49901600 -1.01522100 -3.93259800
H -2.77326800 0.48363300 -3.01894200
H -1.13011500 -0.01005400 -3.41487600
C 0.37905900 -2.12021900 -2.09440100
H 0.32850700 -3.01266000 -2.73455500
H 0.61829800 -1.26871400 -2.73718500
H 1.20118200 -2.26344800 -1.38752200
C -0.50280000 -3.70410000 0.44808500
H -0.44560500 -4.57816000 -0.21555600
H 0.52399000 -3.37796300 0.64219900
H -0.93944900 -4.05007800 1.38881500
C -3.59630600 -2.93183000 1.08219200

H -4.20780000 -3.70686200 0.60002900
H -3.04491200 -3.41648800 1.89176400
H -4.28785700 -2.21210300 1.53177900
C -4.54318000 -0.90905600 -1.12920600
H -5.10590000 -1.63373800 -1.73447500
H -5.06843200 -0.80004300 -0.17552900
H -4.58495400 0.05445000 -1.64337600
F 2.51284400 -2.10149000 0.52942400
F 5.14033200 0.86853900 -0.50764800
Xe 3.82013100 -0.57938200 -0.00586500
H 1.87160700 3.33155800 -0.60577700
S -2.74291700 1.62946900 -0.27761700

^{3os}Adduct$_{XeF2}$
b3lyp/6-31g(d) & LanL2DZ,
el. energy = -1884.193319 a.u.
C -3.16946100 -1.07185100 -1.14705000
C -2.08843800 -0.44636000 -1.85426300
C -0.95300400 -1.31558400 -1.78032100
C -1.31537400 -2.45242200 -1.01787500
C -2.69426600 -2.31023300 -0.63828500
Ti -1.47715000 -0.51801200 0.48188900
C -1.98748700 -0.24151100 2.87930300
C -2.34670300 -1.55176100 2.50321400
C -0.58581900 -0.09696000 2.69447000
C -1.15456200 -2.23433700 2.11838400
C -0.06800000 -1.33895300 2.23155500
C 0.79771000 3.72154800 -0.29074400
C -0.10285100 2.65276200 -0.03526300
C 0.37194800 5.03350000 -0.28555200
C -1.47982000 2.96495200 0.23323400
C -0.98337900 5.34026500 -0.02136500
H 1.07971200 5.83374300 -0.48423700
C -1.88428600 4.32791900 0.23210200
H -1.31404800 6.37527800 -0.01766100
H -2.92638900 4.55380800 0.43738800
S 0.48385100 1.02419500 -0.05100900
H -3.34432400 -1.96970200 2.52420400
H -2.66227100 0.53262800 3.21723500
H -0.01730900 0.80420300 2.87636800
H 0.95489200 -1.54660900 1.94829400
H -1.08770100 -3.26566000 1.80525100
C -2.17787900 0.78343700 -2.71473300
H -2.25237700 0.50248600 -3.77484500
H -3.05533100 1.38573800 -2.46892900
H -1.29684400 1.42344200 -2.60512100
C 0.34497800 -1.16005000 -2.52226000
H 0.33769100 -1.78338900 -3.42857500
H 0.51258800 -0.12536700 -2.83133600
H 1.19343100 -1.47333000 -1.90727700
C -0.43948300 -3.66181200 -0.82809100
H -0.32374400 -4.20216300 -1.77837600
H 0.56364100 -3.38629800 -0.48503900
H -0.86459600 -4.37025600 -0.11093800
C -3.54504900 -3.37367000 -0.00116200
H -3.92569100 -4.06434900 -0.76684800
H -2.99322200 -3.97678600 0.72628300
H -4.41532500 -2.94945700 0.50874400
C -4.59333700 -0.58753900 -1.09622300
H -5.16978800 -0.97959100 -1.94619200
H -5.10180700 -0.91093200 -0.18180400
H -4.65143900 0.50362300 -1.13132000
F 2.33313900 -1.81272900 0.11764500
F 5.62413900 0.61562100 -0.12442700
Xe 3.97943500 -0.56226000 -0.00561200
H 1.83757900 3.48222000 -0.49296800
S -2.65620600 1.74149200 0.56199600

^{1cs}TS1$_{XeF2}$
b3lyp/6-31g(d) & LanL2DZ,
el. energy = -1884.201569 a.u.
im. frequency -166.07
C 2.75650700 -1.79303900 0.82097600
C 1.82206600 -1.34727700 1.81032700
C 0.56829900 -1.95503700 1.53406300
C 0.71729000 -2.77733700 0.36706100
C 2.08015600 -2.69916300 -0.04428900
Ti 1.01020900 -0.50637100 -0.37918300
C 1.30661100 0.76378500 -2.45180900
C 1.97471700 -0.48167000 -2.59741200
C -0.07149000 0.50889000 -2.30739400
C 0.98830800 -1.49907300 -2.60866500
C -0.27133700 -0.89551000 -2.41157200
C -0.11829500 3.95334600 0.46866000
C 0.54925500 2.71328100 0.42870400
C 0.55727900 5.13356800 0.18303000
C 1.93031300 2.68021300 0.09185800
C 1.91805400 5.09921300 -0.15782600
H 0.02798300 6.08188900 0.21953300
C 2.59425500 3.88550300 -0.20641300
H 2.44611700 6.02085300 -0.38758200
H 3.64763600 3.85363000 -0.47035200
S -0.29164700 1.22368100 0.83578500
H 3.04353100 -0.61764600 -2.69472400
H 1.77754300 1.73364100 -2.41568400
H -0.83623000 1.25345600 -2.14177700
H -1.20980200 -1.41479100 -2.30875500
H 1.16315300 -2.55568800 -2.73756800
C 2.11570600 -0.50774000 3.01772600
H 2.10892400 -1.13417800 3.92097700
H 3.08942600 -0.02061500 2.94607100
H 1.36212800 0.27563100 3.14166800
C -0.61641700 -1.89179600 2.45377600
H -0.42484900 -2.50635500 3.34470500
H -0.80147700 -0.86845500 2.79674200
H -1.52128400 -2.25794500 1.97106800
C -0.32259800 -3.72088300 -0.16928000
H -0.37414800 -4.63021600 0.44535100
H -1.30415100 -3.24472200 -0.16776700
H -0.10055800 -4.03386900 -1.19419900
C 2.78181400 -3.57893800 -1.04219200
H 3.44877200 -4.27267600 -0.51264900

H 2.08257200 -4.18901400 -1.61964200
H 3.40418900 -3.01406300 -1.74522300
C 4.24302800 -1.57372200 0.82979900
H 4.73970700 -2.40609300 1.34864200
H 4.65511400 -1.52561400 -0.18300600
H 4.51891400 -0.65045200 1.34324200
F -1.60480300 -1.04661500 -0.08076400
F -5.61478900 0.59190500 0.06865900
Xe -3.63515500 -0.12645000 0.01747600
H -1.17292800 3.97463200 0.72883400
S 2.80781800 1.15818600 0.15325100

^{1os}TS1$_{XeF2}$
b3lyp/6-31g(d) & LanL2DZ,
el. energy = -1884.206542 a.u.
im. frequency -269.25
C -2.71389900 -2.22832800 -0.76535700
C -1.94918500 -1.56722600 -1.77858400
C -0.57027600 -1.82543000 -1.52828200
C -0.47616500 -2.65481300 -0.36889200
C -1.80405300 -2.92122100 0.08853000
Ti -1.37286300 -0.56738200 0.38726900
C -2.00670700 0.32468100 2.56865300
C -1.86650600 -1.08261500 2.66079600
C -0.74396400 0.87007500 2.24736200
C -0.49095700 -1.39254600 2.45275200
C 0.19809800 -0.19412600 2.17983000
C -0.72621400 3.90362000 -0.47243100
C -1.24392000 2.58977500 -0.43648800
C -1.53322400 4.99588500 -0.19116400
C -2.61736900 2.39719300 -0.09870500
C -2.88382100 4.80345600 0.14548100
H -1.11807600 5.99929500 -0.22769200
C -3.41491700 3.52128100 0.19367500
H -3.51545000 5.65807900 0.37234500
H -4.45831600 3.36911400 0.45435600
S -0.20832700 1.23416200 -0.84963500
H -2.65422400 -1.78534000 2.89574200
H -2.92785300 0.87672100 2.68104600
H -0.53103900 1.91471200 2.07698800
H 1.22413500 -0.12047500 1.84773800
H -0.04742400 -2.37572600 2.48463200
C -2.48104500 -0.84222500 -2.97987700
H -2.35980100 -1.46662700 -3.87604700
H -3.54052700 -0.60290700 -2.87482100
H -1.94345600 0.09575000 -3.14625200
C 0.58123600 -1.46263100 -2.42235200
H 0.85745200 -2.33001900 -3.03926900
H 0.32311500 -0.64298300 -3.09691700
H 1.45054200 -1.16443000 -1.83103800
C 0.80320300 -3.29171800 0.10005600
H 1.15001800 -4.01822400 -0.64804900
H 1.58791200 -2.53847900 0.22626500
H 0.67414600 -3.83888700 1.03838500
C -2.19949600 -3.93448700 1.12533600
H -2.28017200 -4.92734900 0.66154700
H -1.46998900 -4.01925400 1.93539600
H -3.17294000 -3.70874900 1.57050900
C -4.21325000 -2.33665400 -0.72007600
H -4.54989800 -3.20486700 -1.30339900
H -4.58397100 -2.46471400 0.30145800
H -4.69809000 -1.45079700 -1.13813600
F 2.23647200 -0.48117500 0.06107100
F 6.49851300 0.80929400 -0.06660700
Xe 4.41927100 0.18123400 -0.01795400
H 0.32058600 4.04428000 -0.72588700
S -3.33383500 0.79164300 -0.15918200

^{3os}TS1$_{XeF2}$
b3lyp/6-31g(d) & LanL2DZ,
el. energy = -1884.190559 a.u.
im. frequency -343.17
C -3.00459600 -1.33045100 -1.16202200
C -1.99348400 -0.58986500 -1.86187400
C -0.77052700 -1.32578100 -1.77738800
C -1.01098300 -2.49803300 -1.01336600
C -2.40138700 -2.51195300 -0.65321800
Ti -1.38120400 -0.61667700 0.47624800
C -2.03187100 -0.38973500 2.82973500
C -2.22544400 -1.72997600 2.43771800
C -0.64549400 -0.09330300 2.72150800
C -0.94532800 -2.27879900 2.12319700
C 0.02953000 -1.27341000 2.30514400
C 0.36806400 3.85737200 -0.25480200
C -0.40538900 2.68906500 -0.01428900
C -0.21242900 5.10779600 -0.26577500
C -1.81441300 2.83445500 0.22013600
C -1.60123100 5.24915800 -0.03396500
H 0.39783400 5.98734200 -0.45142900
C -2.38132700 4.13737800 0.20391500
H -2.05342000 6.23706200 -0.04261200
H -3.44733500 4.23829100 0.38422800
S 0.38008200 1.14874700 -0.00457100
H -3.17107900 -2.25415000 2.41028100
H -2.80430800 0.30360400 3.13088400
H -0.18734800 0.86335500 2.92967700
H 1.07772800 -1.36266800 2.06019000
H -0.74683200 -3.29567700 1.81865100
C -2.21184700 0.62087100 -2.72500400
H -2.25315800 0.32684400 -3.78320100
H -3.14901000 1.12704200 -2.48393500
H -1.40340300 1.35070600 -2.61938200
C 0.50565700 -1.02601700 -2.51046200
H 0.57422900 -1.65145100 -3.41249100
H 0.55648100 0.01965900 -2.82390100
H 1.36879700 -1.23617900 -1.87561800
C -0.01347900 -3.60875800 -0.82213900
H 0.15243400 -4.13525800 -1.77275100
H 0.95080100 -3.21984300 -0.48049600
H -0.36301700 -4.35597000 -0.10336400
C -3.13986000 -3.66931800 -0.04194600
H -3.42029600 -4.38929600 -0.82345900

H -2.53940500 -4.21420000 0.69223100
H -4.06508700 -3.35202300 0.44819200
C -4.47395600 -1.00835100 -1.12569300
H -4.99425700 -1.47935500 -1.97153700
H -4.94929400 -1.37084500 -0.20820300
H -4.65457400 0.06809900 -1.18254800
F 2.12724800 -1.40356100 0.17495600
F 5.85655900 0.72875500 -0.16781300
Xe 4.03378100 -0.31971900 0.00430900
H 1.43372100 3.74243700 -0.42977300
S -2.83779200 1.47521500 0.52578700

^{1cs}INT1$_{XeF2}$
b3lyp/6-31g(d) & LanL2DZ,
el. energy = -1884.252902 a.u.

C -3.34834800 0.76785700 0.17674900
C -2.53744300 1.30442600 -0.87598500
C -2.36454500 0.28692200 -1.85757700
C -3.08901000 -0.86329800 -1.43758500
C -3.72467700 -0.55788700 -0.20142400
Ti -1.28270900 -0.54870200 0.20575800
C -1.16212100 -0.93054900 2.67564400
C -2.25158800 -1.64846900 2.16840300
C 0.03095900 -1.46833300 2.09876300
C -1.74952100 -2.63310400 1.26265300
C -0.33625700 -2.54955000 1.27904700
C 2.43049500 2.83699400 -1.01867100
C 1.41853600 2.05846200 -0.39044100
C 2.81049800 4.05485400 -0.50004600
C 0.77344500 2.55924400 0.79264600
C 2.18559500 4.54315400 0.67312700
H 3.58618900 4.63931800 -0.98591400
C 1.19392500 3.81782000 1.30083900
H 2.48780900 5.50368900 1.08204400
H 0.71733000 4.19889100 2.19870800
S 0.98413500 0.52576400 -1.02680900
H -3.28392200 -1.49461800 2.44037900
H -1.21380400 -0.11478500 3.38188100
H 1.03308600 -1.10366400 2.27459500
H 0.33048100 -3.12992500 0.65911500
H -2.33239500 -3.34862900 0.69866500
C -2.14887900 2.74402000 -1.05115800
H -2.82787200 3.21477700 -1.77593200
H -2.21747600 3.30247200 -0.11665800
H -1.13144400 2.85533300 -1.43461700
C -1.65003400 0.39787300 -3.17051500
H -2.37105500 0.37059100 -3.99910800
H -1.08195300 1.32764700 -3.25180500
H -0.95630600 -0.43805700 -3.30430500
C -3.21846900 -2.12990500 -2.22800600
H -3.76416500 -1.95027700 -3.16390800
H -2.22844200 -2.51970600 -2.48404900
H -3.75939600 -2.90312600 -1.67422800
C -4.81776500 -1.38192800 0.41981700
H -5.70556200 -1.34402200 -0.22552000
H -4.55052200 -2.43740000 0.53180800
H -5.11956900 -0.99896900 1.39783400
C -3.91227600 1.54379300 1.33423800
H -4.84775700 2.04399000 1.04673900
H -4.13892400 0.89809000 2.18866600
H -3.21497300 2.31031000 1.68128500
F -0.57879900 -1.65253900 -1.11720600
F 5.04770600 -2.72986400 0.41923400
Xe 3.26371300 -1.32760000 -0.21243600
H 2.90090700 2.44544200 -1.91570300
S -0.46828700 1.68434300 1.60640600

^{1os}INT1$_{XeF2}$
b3lyp/6-31g(d) & LanL2DZ,
el. energy = -1884.282666 a.u.

C -2.62692500 -2.01678500 -0.85143000
C -2.04176800 -1.07513300 -1.76134100
C -0.68673400 -1.45252600 -1.96617100
C -0.43740100 -2.64441500 -1.22585400
C -1.63681100 -3.00344300 -0.55445200
Ti -0.86893400 -0.84859100 0.41820700
C -1.93951000 -0.81536900 2.69772200
C -1.59281000 -2.13473600 2.37352600
C -0.73714600 -0.04578300 2.77298400
C -0.16964000 -2.20220600 2.26179300
C 0.34592600 -0.92073600 2.56229900
C -0.94155800 4.11838500 -0.43545800
C -1.27635000 2.77012700 -0.13210500
C -1.89217800 5.11508100 -0.38506300
C -2.63568800 2.46346200 0.22590300
C -3.22924300 4.81253900 -0.02541100
H -1.61628600 6.13935800 -0.62050200
C -3.59058600 3.51780500 0.27482100
H -3.97075400 5.60579100 0.01251400
H -4.61256500 3.27681800 0.55107200
S -0.06564500 1.54850700 -0.19126600
H -2.28396000 -2.95678900 2.26742000
H -2.93989400 -0.44703900 2.86850100
H -0.67492800 1.01592500 2.96798600
H 1.38368400 -0.63068200 2.49581000
H 0.41618200 -3.07810500 2.01765400
C -2.74472900 0.00204200 -2.53829100
H -2.79397400 -0.28440900 -3.59775900
H -3.76526500 0.16284900 -2.18776400
H -2.21595900 0.95816200 -2.47971600
C 0.30705500 -0.78502900 -2.86727000
H 0.47587400 -1.38801500 -3.77028500
H -0.03075900 0.20578800 -3.18059300
H 1.26693700 -0.66736600 -2.35580900
C 0.85267200 -3.40636200 -1.23332800
H 1.06304800 -3.80794100 -2.23352500
H 1.68110600 -2.74875300 -0.95297000
H 0.83099800 -4.25003800 -0.53686800
C -1.88628000 -4.32580500 0.11631900
H -1.93358000 -5.11702800 -0.64415100
H -1.09524600 -4.60684400 0.81914800
H -2.83916600 -4.34189900 0.65184900

C -4.08241600 -2.12804500 -0.48628100
H -4.57806100 -2.88578900 -1.10935200
H -4.22493600 -2.42452300 0.55902500
H -4.61137500 -1.18352100 -0.62840400
F 0.97173100 -0.83227000 0.07269400
F 6.88436400 0.45345500 -0.02557300
Xe 4.29815800 0.51235500 0.01717300
H 0.08468200 4.34643500 -0.70715000
S -3.11259900 0.85526700 0.58529300

^{3os}INT1$_{XeF2}$
b3lyp/6-31g(d) & LanL2DZ,
el. energy = -1884.282762 a.u.
C -2.89133800 -1.69990600 -0.84758500
C -2.14115200 -0.89582600 -1.77007300
C -0.87056600 -1.50605300 -1.94473900
C -0.83333200 -2.69613500 -1.16024300
C -2.08772900 -2.82783600 -0.50388100
Ti -0.95832000 -0.80760000 0.41522700
C -1.93244800 -0.50375700 2.72326500
C -1.90409800 -1.86805400 2.39863000
C -0.58590900 -0.02635700 2.76038500
C -0.53433500 -2.25816600 2.26122000
C 0.26486500 -1.12665100 2.53893900
C -0.29175000 4.11316300 -0.42899200
C -0.82628100 2.82694300 -0.14486600
C -1.08158300 5.24098000 -0.36274000
C -2.21575700 2.72339200 0.21123700
C -2.44951100 5.13789100 -0.00737000
H -0.65393200 6.21549900 -0.58206200
C -3.00213900 3.90788300 0.27392100
H -3.06312100 6.03311700 0.04315600
H -4.04920400 3.81931200 0.54720800
S 0.18482900 1.43605700 -0.22330400
H -2.76595000 -2.51285000 2.31626000
H -2.81711900 0.08217900 2.92054200
H -0.27995500 0.99402000 2.94559800
H 1.33954900 -1.08188100 2.44821700
H -0.16693500 -3.24747200 2.02455600
C -2.64036700 0.26799800 -2.57962600
H -2.73460600 -0.03034600 -3.63267700
H -3.61819700 0.61443200 -2.24155400
H -1.95217900 1.11775300 -2.53802400
C 0.23151400 -1.04292400 -2.84760000
H 0.30852700 -1.69359200 -3.72969200
H 0.06690600 -0.02007900 -3.19534900
H 1.18994600 -1.07074400 -2.32137400
C 0.30928500 -3.66555700 -1.12687800
H 0.45051500 -4.13555400 -2.10929000
H 1.23708700 -3.14777100 -0.86491300
H 0.14382000 -4.46685100 -0.40012200
C -2.57088500 -4.06298000 0.20311400
H -2.77566100 -4.84951200 -0.53601600
H -1.83722100 -4.47037000 0.90581200
H -3.50259000 -3.88760300 0.74736700
C -4.35124800 -1.55785900 -0.51215200
H -4.95062100 -2.25972200 -1.10891700
H -4.55737800 -1.77114100 0.54269000
H -4.72000300 -0.55078200 -0.71501900
F 0.86286500 -1.06490700 0.05283200
F 6.82211700 -0.01467800 0.09456100
Xe 4.24456600 0.19549700 -0.02365100
H 0.75756400 4.18801700 -0.69792200
S -2.92914300 1.20003500 0.55101300

6
b3lyp/6-31g(d),
el. energy = -1027.397613 a.u.
C 0.05756800 0.69921400 -0.00006300
C 0.05756900 -0.69921400 0.00006600
C 1.23672500 -1.43175900 0.00024300
C 2.43143300 -0.70076900 0.00016900
C 2.43143200 0.70077000 -0.00004900
C 1.23672400 1.43176000 -0.00016900
H 1.24079800 -2.51762600 0.00022900
H 3.37806400 -1.23359800 0.00021200
H 3.37806300 1.23360000 -0.00001500
H 1.24079700 2.51762700 -0.00014800
S -1.68582500 -1.08216800 -0.00043700
S -1.68582700 1.08216700 0.00034600

Xe
b3lyp/LanL2DZ,
el. energy = -15.469884 a.u.
Xe 0.00000000 0.00000000 0.00000000

3
b3lyp/6-31g(d) & LanL2DZ,
el. energy = -841.584471 a.u.
C 2.30564600 0.09000600 1.15822900
C 2.72711400 -1.05773000 0.44771700
C 2.84178600 -0.71654000 -0.91596900
C 2.53615400 0.66346700 -1.05117200
C 2.20688800 1.16555300 0.22479400
H 2.12369600 0.14797100 2.22241200
H 2.82566200 -2.05286100 0.85859400
H 3.05126300 -1.40015500 -1.72761000
H 2.49404100 1.21320900 -1.98217300
H 1.94377800 2.18769100 0.45363800
Ti 0.47920800 -0.42467900 -0.32575700
C -1.91752100 -0.54912500 -0.07357200
C -1.37262200 -0.39025400 1.24016700
C -1.68940600 0.65129300 -0.79616900
C -0.76916400 0.89255300 1.31210200
C -0.93531200 1.52801600 0.03270200
C -1.47147400 -1.41965600 2.32750400
H -2.51046800 -1.52827000 2.66570900
H -1.13305200 -2.39491100 1.96321900
H -0.86697000 -1.15671800 3.20066000
C -2.63245300 -1.77084400 -0.57145200
H -2.05375000 -2.67239000 -0.34541600
H -3.61868900 -1.87483100 -0.09909400

H -2.78044100 -1.73114200 -1.65429100
C -0.25200100 1.55745900 2.55696100
H -1.04130700 2.17311800 3.00990500
H 0.06045700 0.82882700 3.31036400
H 0.59737700 2.21954800 2.36239900
C -0.59591900 2.95560500 -0.30721600
H -1.50754000 3.56656300 -0.35326700
H 0.05341600 3.41095500 0.44577700
H -0.09654600 3.04734600 -1.27812300
C -2.13780600 0.92316300 -2.20031000
H -1.96497600 1.96644400 -2.48096600
H -1.59255500 0.28801400 -2.90740500
H -3.20925000 0.71989700 -2.31203200
F 0.32375900 -2.19380300 0.07357400
F 0.30066600 -0.55654900 -2.12819000

bdt-H$^-$
b3lyp/6-311+g(d,p) & 6-311+g(2df,p)
el. energy = -1028.216501 a.u.
H 2.22762700 -0.40029800 0.00007800
S 1.53256300 -1.61694600 -0.00009200
C 0.01357100 -0.70132200 -0.00003000
C 0.06305200 0.73053900 0.00002900
C -1.20850200 -1.37779500 -0.00003700
C -1.18557900 1.39263200 0.00008300
C -2.42036200 -0.68602800 0.00001800
H -1.20898100 -2.46403100 -0.00008300
C -2.39892400 0.71113300 0.00007800
H -1.17641600 2.47739300 0.00012700
H -3.35979900 -1.23024200 0.00001500
H -3.32963200 1.27260700 0.00012200
S 1.57166600 1.61254700 0.00002300

Et_3N
b3lyp/6-311+g(d,p)
el. energy = -292.501518 a.u.
N 0.00005600 0.00014300 0.01279600
C -0.74182900 1.19359000 0.43732800
H -0.06596800 2.04929100 0.37677600
H -1.04103400 1.11354600 1.49964800
C -0.66261800 -1.23897700 0.43757900
H -1.74160300 -1.08129500 0.37747000
H -0.44327600 -1.45809900 1.49980100
C 1.40445900 0.04601200 0.43779600
H 1.80738600 -0.96731300 0.37859600
H 1.48435200 0.34637800 1.49979900
C 2.27230500 0.95757800 -0.43018000
H 1.94180900 1.99878800 -0.39750300
H 3.30995100 0.93275700 -0.08384900
H 2.24546900 0.62904200 -1.47189000
C -1.96593300 1.48822500 -0.42997500
H -2.70256400 0.68163200 -0.39528200
H -2.46273400 2.39995300 -0.08469800
H -1.66884500 1.62737700 -1.47217900
C -0.30641100 -2.44648900 -0.42991000
H 0.76051500 -2.68091200 -0.39633500
H -0.84702700 -3.33264000 -0.08387800
H -0.57666000 -2.25913900 -1.47187100

Et_3NH^+
b3lyp/6-311+g(d,p)
el. energy = -292.887912 a.u.
N 0.00009700 -0.00002700 0.01333700
C -0.30855700 1.42451100 0.45575000
H 0.62901200 1.97644100 0.41022900
H -0.61194900 1.35496000 1.50161500
C -1.07923200 -0.97931600 0.45605400
H -2.02581100 -0.44296200 0.41104700
H -0.86708000 -1.20761400 1.50184600
C 1.38789800 -0.44503900 0.45610300
H 1.39707300 -1.53301600 0.41071100
H 1.47941100 -0.14761800 1.50202700
C 2.49493400 0.13521900 -0.41070000
H 2.53819400 1.22522500 -0.37600400
H 3.45392100 -0.23825400 -0.04643300
H 2.39772200 -0.18188400 -1.45289800
C -1.36466200 2.09250300 -0.41128300
H -2.33031300 1.58518900 -0.37587100
H -1.52045800 3.10996500 -0.04752700
H -1.04167400 2.16626800 -1.45357400
C -1.13048300 -2.22780800 -0.41109400
H -0.20868900 -2.81101700 -0.37562800
H -1.93425900 -2.87097000 -0.04762000
H -1.35546200 -1.98461300 -1.45339800
H 0.00029600 -0.00033400 -1.01085300

Et_3NHCl
b3lyp/6-311+g(d,p) & 6-311+g(2df,p)
el. energy = -753.362130 a.u.
N -0.55824300 0.00215100 0.00216300
C -0.99273500 0.63273100 -1.28951200
H -0.61853800 1.65427900 -1.26635200
H -2.08768500 0.67076300 -1.28994800
C -0.99631400 -1.43026200 0.10644000
H -0.63349900 -1.92238100 -0.79372400
H -2.09160100 -1.44593600 0.08559500
C -0.98200100 0.81004700 1.19487700
H -0.61193200 0.27540300 2.06743900
H -2.07702000 0.80309400 1.22996400
C -0.42343300 2.22995800 1.21379100
H -0.89266200 2.88262300 0.47571000
H -0.61496600 2.66209800 2.19889300
H 0.65619100 2.21842200 1.04987500
C -0.44943900 -0.06277000 -2.53431500
H -0.92438400 -1.02642600 -2.72587200
H -0.64740000 0.57518600 -3.39900000
H 0.63056500 -0.20302100 -2.45356200
C -0.44216300 -2.16242400 1.32519700
H -0.90486500 -1.84399300 2.26083100
H -0.64623300 -3.22940700 1.20785200
H 0.63932000 -2.02712200 1.39377600
H 0.56529200 -0.00269500 -0.00226100

Cl 2.34609500 -0.00938900 -0.00901300

TS1$_{rev}$

b3lyp/6-311+g(d,p) & 6-311+g(2df,p) & LanL2DZ,

el. energy = -2590.704972 a.u.

im. frequency -57.60

C 2.77304500 1.38640800 -0.79143500
C 2.13930300 1.88791600 0.38814600
C 2.43016500 1.01082600 1.45455400
C 3.30269200 -0.01239700 0.96007300
C 3.53424800 0.23942700 -0.41249000
Ti 1.10662600 -0.31833500 -0.20844400
C -0.37488300 -1.70893600 -1.62482500
C 0.50950500 -1.01387800 -2.49218100
C 0.39417800 -2.58068500 -0.83451500
H -1.43952200 -1.56025600 -1.54475900
C 1.82067600 -1.43662700 -2.21355700
H 0.22716500 -0.25284000 -3.19923000
C 1.76071800 -2.39172800 -1.15844000
H 0.01270800 -3.20851600 -0.04907200
H 2.70487400 -1.10427200 -2.72832400
H 2.59281500 -2.90332400 -0.70030000
Cl 0.90686300 -1.62865600 1.87454100
Cl -0.39863400 1.38979900 -1.09983300
S -1.92803500 -0.37749900 1.39344300
C -3.30522100 0.37819700 0.62019800
C -4.36393800 -0.38225300 0.03479300
C -3.42343000 1.78186300 0.54439800
C -5.45297800 0.25312800 -0.56662300
C -4.50784500 2.40876900 -0.06098500
H -2.62637000 2.37593500 0.97443600
C -5.53300800 1.64430200 -0.62050100
H -6.24744300 -0.34951300 -0.99631100
H -4.55102600 3.49341900 -0.09775000
H -6.38614200 2.12047000 -1.09368200
S -4.30842200 -2.15634100 0.08315500
H -3.11367700 -2.08967100 0.78921800
C 4.05000500 -1.01692100 1.78321500
H 3.46857200 -1.33588400 2.64650400
H 4.29484700 -1.91230100 1.20685100
H 4.99559900 -0.58410600 2.13844400
C 4.61007500 -0.42830900 -1.22092300
H 5.59305400 -0.13228500 -0.83389100
H 4.56625900 -1.51945200 -1.17329600
H 4.58019700 -0.13298800 -2.27072600
C 2.81182900 2.08408700 -2.11909300
H 3.54929500 2.89744100 -2.11543500
H 3.08251800 1.40269400 -2.92959600
H 1.83559100 2.50834600 -2.36036000
C 1.45603600 3.21163900 0.54402100
H 2.15763400 3.92871300 0.99278400
H 1.11700400 3.61041600 -0.40985400
H 0.58406800 3.13952500 1.19537100
C 2.03568300 1.23728400 2.88308000
H 2.67875700 2.00375900 3.33641300
H 1.00005100 1.57421100 2.96318500
H 2.11968600 0.32319000 3.46809600

INT1$_{rev}$

b3lyp/6-311+g(d,p) & 6-311+g(2df,p) & LanL2DZ,

el. energy = -2130.408871 a.u.

C -3.08423600 -0.77700500 -0.12574100
C -2.26198800 -1.44395600 0.83127300
C -1.84585400 -0.47672100 1.79573000
C -2.33192600 0.79111600 1.38846800
C -3.09417000 0.60824400 0.19178500
Ti -0.79850300 0.04892900 -0.39204300
C 0.57328700 -1.48938400 -1.64786300
C -0.77550100 -1.74893200 -1.95049300
C 0.88911800 -0.18886600 -2.12514000
C -1.30213600 -0.60696800 -2.62273700
C -0.25787800 0.33163000 -2.75760900
Cl -0.62649700 2.41510700 -0.66761800
C 2.68223100 -0.44397200 0.58109200
C 3.54629200 0.60336300 0.19131300
C 4.87615500 0.30501100 -0.14625500
C 5.36074200 -0.99473500 -0.09346200
C 4.51743400 -2.03281200 0.30278500
C 3.19899200 -1.74926700 0.63795000
H 5.53345100 1.11238600 -0.45077500
H 6.39308500 -1.19439900 -0.35737400
H 4.88409000 -3.05130900 0.35918000
H 2.54570100 -2.54686300 0.97362400
S 3.08692000 2.31249200 0.12053600
H 1.76005100 2.14230000 0.28731700
S 1.02544200 -0.17842100 1.18383400
C -3.91378200 1.66265200 -0.49111500
H -3.44229100 2.64184900 -0.41604000
H -4.05532800 1.44866400 -1.55226400
H -4.90751400 1.72619100 -0.03163100
C -2.22852800 2.05870400 2.17976600
H -2.25116400 2.93622700 1.53507000
H -3.06680800 2.12942000 2.88368900
H -1.30392300 2.10008800 2.75769800
C -1.24329400 -0.79314000 3.13026700
H -0.63716300 0.02641500 3.51635100
H -2.05228400 -0.97810900 3.84825600
H -0.61156600 -1.68055900 3.09788700
C -2.09545700 -2.92825200 0.98895800
H -1.07034800 -3.19876300 1.25247400
H -2.74581800 -3.30153100 1.78881300
H -2.36394300 -3.47034400 0.08127500
C -3.98015400 -1.44497700 -1.12743900
H -3.51842300 -2.30605200 -1.61349300
H -4.88043200 -1.81036700 -0.61939800
H -4.31158500 -0.75579200 -1.90510400
H -0.34370300 1.31084100 -3.19742800
H 1.84061200 0.30944200 -2.03258000
H 1.24938800 -2.15511100 -1.13854400
H -1.30125900 -2.66377900 -1.73405500

H -2.29920100 -0.49962600 -3.01763400

INT1$_{anion}$

b3lyp/6-311+g(d,p) & 6-311+g(2df,p) & LanL2DZ,

el. energy = -2129.856637 a.u.

C 0.20046500 -1.49453900 2.34616300
C -0.94592500 -0.80950900 1.90283900
C -0.67292400 0.58662200 1.98139200
C 0.64235300 0.74906300 2.45681500
C 1.20406200 -0.54399800 2.65026600
H 0.31982100 -2.56412000 2.35947200
H -1.84944900 -1.27456100 1.53268400
H -1.35871900 1.37321400 1.71152000
H 1.12963500 1.69106700 2.64301400
H 2.19984100 -0.76560700 3.00177500
Ti 0.81275400 -0.29621100 0.31956600
C 2.32121500 0.04902700 -1.62720800
C 3.16705100 -0.21917500 -0.50064100
C 1.68468800 1.29447100 -1.40733200
C 3.02042900 0.84304500 0.41990400
C 2.06194400 1.76280000 -0.11646000
Cl 1.17208500 -2.61420200 -0.22195900
S -1.04936100 -0.02945300 -1.10561700
C -2.66531500 0.42824400 -0.49476800
C -3.67687800 -0.55888400 -0.29095900
C -2.94553100 1.79451400 -0.35040000
C -4.94641400 -0.05594300 0.11624700
C -4.20233500 2.24488900 0.04390200
H -2.15889000 2.51215600 -0.56213600
C -5.20543000 1.29442300 0.28125300
H -5.73016000 -0.78509400 0.29036200
H -4.39807500 3.30673300 0.15128000
H -6.19709900 1.61573800 0.58937500
S -3.41122400 -2.25367800 -0.51642300
C 1.73834500 3.13279500 0.41261800
H 2.07843400 3.26607700 1.44124200
H 2.23382400 3.90495500 -0.18946400
H 0.66580300 3.34309700 0.38728800
C 0.91961100 2.08735800 -2.42183600
H 0.22581000 2.78543800 -1.95155100
H 1.62134400 2.66701200 -3.03773100
H 0.33177200 1.44913600 -3.08085800
C 2.26607500 -0.76345100 -2.88609100
H 1.35071600 -0.56766900 -3.44729500
H 3.11761400 -0.52894400 -3.53866500
H 2.28887700 -1.83145500 -2.66379300
C 4.16706900 -1.33280700 -0.41629600
H 3.76514100 -2.25556300 -0.83449200
H 5.07699600 -1.06801500 -0.97156800
H 4.45920900 -1.54371300 0.61476100
C 3.87493000 1.06965200 1.63364200
H 4.26352100 0.13277600 2.03745400
H 4.74061700 1.69382100 1.37637200
H 3.34183300 1.58009300 2.43813600

TS2$_{rev}$

b3lyp/6-311+g(d,p) & 6-311+g(2df,p) & LanL2DZ,

el. energy = -2129.843658 a.u.

im. frequency -90.60

C 0.25535300 -1.74481300 2.23443100
C -0.94897600 -1.03521400 2.03826200
C -0.68492000 0.33823300 2.25499800
C 0.68710600 0.48033800 2.54997600
C 1.27646700 -0.81908800 2.53167600
H 0.38431100 -2.80373100 2.09555700
H -1.88518600 -1.46502100 1.72493600
H -1.40459200 1.13557300 2.17992000
H 1.17956600 1.40738200 2.78874500
H 2.30878600 -1.06419300 2.72514800
Ti 0.64670100 -0.27324900 0.29227000
C 2.40124500 -0.03410700 -1.51585300
C 3.07521400 -0.14506600 -0.26060300
C 1.68766500 1.18309600 -1.52661200
C 2.79379600 1.02820700 0.48741500
C 1.89217100 1.83153700 -0.26568700
Cl 1.06645300 -2.57812400 -0.48201200
S -1.11217100 1.13679500 -0.63991400
C -2.78137700 0.69405300 -0.25298100
C -3.26614900 -0.62476300 -0.51761500
C -3.65269800 1.70346600 0.17920400
C -4.66530900 -0.81473200 -0.38674600
C -5.01926000 1.47106900 0.32706400
H -3.24533800 2.68902400 0.38315500
C -5.51991900 0.19887400 0.02689900
H -5.06156500 -1.79953200 -0.60978400
H -5.67853300 2.26618900 0.66009100
H -6.58323300 -0.00459100 0.12414000
S -2.18517300 -1.90736900 -0.93556200
C 1.46188700 3.22838900 0.07659100
H 1.37763800 3.37727300 1.15583800
H 2.18727800 3.96234900 -0.30042600
H 0.48711400 3.45651000 -0.35508400
C 1.05469900 1.77854300 -2.74918100
H 0.35244200 2.57373200 -2.50438200
H 1.83827400 2.20011300 -3.39466600
H 0.50863300 1.02942700 -3.32473700
C 2.57422900 -0.92923500 -2.70545100
H 1.62213500 -1.13123100 -3.19986000
H 3.24287300 -0.45262600 -3.43593600
H 2.99888800 -1.89072100 -2.42339200
C 4.08048200 -1.19949800 0.09683400
H 3.69874300 -2.19529700 -0.13752900
H 5.01477900 -1.04750600 -0.45962600
H 4.32886800 -1.17679000 1.16061700
C 3.54108000 1.46556000 1.71480100
H 3.63551000 0.67901900 2.46651800
H 4.55956500 1.76437600 1.43603200
H 3.07669800 2.32995900 2.19207300

6.3 Chapter 4

Reaction coordinates: General Mechanism

EDA
b3lyp/def2tzvp,
el. energy = -416.139030 a.u.

C -1.29467600 -0.79862400 -0.00014000
C -0.22256600 0.19182300 -0.00009600
O -0.37873000 1.40038100 -0.00012800
O 0.97500100 -0.43261200 -0.00009800
C 2.13708400 0.43239500 0.00010200
H 2.09874000 1.07564600 0.88507900
H 2.09886600 1.07605800 -0.88454500
N -3.58771700 0.04076400 0.00021400
N -2.52370100 -0.35971300 0.00002300
C 3.36554300 -0.45434600 0.00008000
H 3.39122100 -1.09423100 -0.88845300
H 4.26693000 0.16904600 -0.00059900
H 3.39197600 -1.09335300 0.88922400
H -1.15028500 -1.87016400 -0.00023600

^{1cs}FP^{-}
b3lyp/def2tzvp,
el. energy = -2367.955093 a.u.

C 1.72642300 2.48027200 -0.24833200
N 1.63992300 1.10837300 -0.22332700
H 3.44132000 3.92881300 -0.39376500
C 2.93333800 0.65167300 -0.32450600
C 3.85747100 1.76185900 -0.40438900
H 4.93379700 1.66717700 -0.49161500
C 3.10782600 2.89821300 -0.35363700
C 3.30765400 -0.68856600 -0.35520000
N 1.06759400 -1.67938300 -0.21413300
C 0.60594500 -2.97310300 -0.21196200
C 1.71025300 -3.90546400 -0.29997600
H 1.61003800 -4.98465200 -0.31814700
C 2.84729900 -3.15863000 -0.36587900
H 3.87388300 -3.49749100 -0.44493700
C 2.43604700 -1.77231400 -0.31165500
C 0.64294300 3.35288700 -0.21115600
H 0.86237100 4.41762100 -0.23176000
H -3.97356600 3.49676400 -0.22321200
C -2.94322900 3.16030800 -0.20701600
C -2.52558600 1.77454500 -0.17898700
H -1.71011200 4.98954500 -0.23601900
N -1.15499800 1.68514100 -0.17076600
C -0.69721400 2.97919200 -0.18982300
C -1.80653100 3.91008000 -0.21288600
C -0.73377100 -3.34664800 -0.17472500
H -0.95210700 -4.41185300 -0.17558500
H -5.03486900 -1.66379300 -0.21573800
C -3.95513500 -1.75916800 -0.20185300
C -3.20446000 -2.89544900 -0.19391800
H -3.53987100 -3.92619500 -0.20186800
C -1.81903800 -2.47539900 -0.17624600
N -1.73094200 -1.10637600 -0.17617100
C -3.02528100 -0.64921700 -0.18510800
C -3.39879700 0.69116200 -0.17817700
H -4.46367000 0.91112600 -0.18447600
H 4.36998700 -0.90663400 -0.43363900
Fe -0.04056300 -0.00123100 -0.02272700
O -0.16310800 -0.05493300 1.87074700
C 0.97364300 0.01429200 2.64210900
H 0.71278000 -0.17092200 3.70670100
H 1.75248200 -0.73846600 2.39110800
H 1.48720400 1.00299500 2.62860100

^{1os}FP^{-}
ub3lyp/def2tzvp,
el. energy = -2367.955395 a.u.

C 1.47492000 2.62751500 -0.26877700
N 1.52328000 1.25438800 -0.23749400
H 3.04427200 4.23444200 -0.40924700
C 2.85425100 0.92325400 -0.32926100
C 3.66757200 2.11858400 -0.40632900
H 4.74849800 2.12810400 -0.48609200
C 2.81133000 3.17664900 -0.36720500
C 3.35896500 -0.37358400 -0.35253400
N 1.22865100 -1.58265200 -0.23691400
C 0.89154600 -2.91214100 -0.23147300
C 2.08071100 -3.73318400 -0.30656800
H 2.08609000 -4.81700900 -0.32040000
C 3.14242800 -2.88014800 -0.36159700
H 4.19739200 -3.12005800 -0.42800400
C 2.59831600 -1.54019600 -0.31681400
C 0.31264400 3.39328900 -0.23636900
H 0.43064600 4.47400900 -0.25615800
H -4.30014800 3.09849500 -0.22202100
C -3.24252000 2.86108600 -0.21645000
C -2.69342600 1.52184600 -0.19613200
H -2.19015200 4.80032500 -0.24370100
N -1.32293300 1.56725400 -0.19845900
C -0.98876100 2.89676600 -0.21523300
C -2.18175400 3.71654900 -0.22719800
C -0.40905300 -3.40913200 -0.18361800
H -0.52596700 -4.49014600 -0.18492600
H -4.85258400 -2.14738400 -0.19118900
C -3.76880600 -2.13793200 -0.17994800
C -2.91206200 -3.19573300 -0.17502500
H -3.14678200 -4.25396600 -0.18218800
C -1.57210000 -2.64435000 -0.16550500
N -1.61884200 -1.27289900 -0.16080300
C -2.95073300 -0.94196200 -0.17084200
C -3.45481300 0.35535200 -0.17911900
H -4.53630400 0.46745200 -0.18055200

H 4.43846100 -0.48499800 -0.41863300
Fe -0.04204200 -0.00917900 -0.01479500
O -0.12578200 -0.05178200 1.91815200
C 0.98757500 0.20411300 2.68025900
H 0.76849500 0.03303700 3.75863500
H 1.86533400 -0.44430000 2.45396500
H 1.36363800 1.25243000 2.62006600

^{3}FP^{-}
ub3lyp/def2tzvp,
el. energy = -2367.961485 a.u.
C -1.21740500 -2.76937000 -0.27917200
N -1.39762800 -1.40782400 -0.26768300
H -2.62624700 -4.51726600 -0.39486800
C -2.75231700 -1.20323700 -0.35977700
C -3.44846800 -2.47001000 -0.42144000
H -4.52349600 -2.58355600 -0.49832300
C -2.49374200 -3.44166200 -0.37038800
C -3.37425600 0.04221800 -0.39182800
N -1.36122000 1.44198400 -0.26438400
C -1.14741900 2.79874600 -0.27564300
C -2.40683400 3.50267100 -0.36537900
H -2.51258300 4.58125600 -0.38915200
C -3.38534600 2.55525000 -0.41675700
H -4.45726600 2.69522000 -0.49337500
C -2.72081400 1.27126000 -0.35673300
C 0.01396900 -3.41857300 -0.23156500
H 0.00090300 -4.50538800 -0.24936200
H 4.57699000 -2.69423600 -0.20449100
C 3.50216500 -2.55565600 -0.19604100
C 2.83360300 -1.27199900 -0.17634900
H 2.63135300 -4.58231700 -0.22927200
N 1.47258200 -1.44331400 -0.17253700
C 1.26048400 -2.79997900 -0.19878800
C 2.52374100 -3.50384200 -0.21052700
C 0.09943000 3.41736400 -0.23064500
H 0.11332400 4.50417100 -0.24734600
H 4.64341900 2.58057600 -0.20853500
C 3.56551800 2.46832500 -0.20018600
C 2.61080700 3.44066800 -0.21378500
H 2.74499800 4.51617100 -0.23183200
C 1.33070200 2.76828400 -0.20141100
N 1.50934300 1.40685100 -0.17676200
C 2.86541200 1.20182700 -0.17997700
C 3.48871900 -0.04331100 -0.17161400
H 4.57535800 -0.05754600 -0.17234500
H -4.45874300 0.05628800 -0.46147200
Fe 0.04743300 -0.00035500 0.01627800
O 0.04842500 -0.00110900 2.02413100
C -1.07719000 0.01064600 2.80295500
H -0.83517400 0.00867700 3.89323100
H -1.73093400 0.90378900 2.65498900
H -1.74866700 -0.86935100 2.65574400

^{5}FP^{-}
ub3lyp/def2tzvp,
el. energy = -2367.975132 a.u.
N -1.52823000 1.33341900 -0.30945700
Fe 0.03590700 -0.00044300 0.39483500
C -3.36406900 -0.29320500 -0.46693100
C 0.35148200 -3.42084300 -0.32559700
C -0.95277000 -2.90648300 -0.36306100
C -2.15981700 -3.70038800 -0.51302600
C -3.20451900 -2.82243100 -0.55532100
C -2.63574400 -1.49129900 -0.43067600
N -1.27801000 -1.58089100 -0.30603700
H -2.19275200 -4.78157100 -0.58810300
H -4.25941000 -3.04523000 -0.67037800
C -3.63905100 2.22471000 -0.56083600
C -1.43503200 2.69509100 -0.37116000
C -2.76102000 3.26958100 -0.52188000
H -4.71655800 2.26219200 -0.67601600
H -2.98008900 4.32860200 -0.60037200
C 2.88223300 -3.26791400 -0.32155000
C 2.96451900 -1.00969300 -0.23796000
C 3.76083100 -2.22341700 -0.29783500
H 3.10595000 -4.32747400 -0.37574500
H 4.84395800 -2.26123100 -0.32875100
C -0.23674400 3.42340300 -0.34088100
C 3.47872200 0.29510300 -0.23454200
C 3.32681700 2.82493200 -0.31744500
C 1.06711800 2.90870900 -0.29561300
C 2.28246700 3.70343700 -0.34703700
H 4.38753700 3.04738100 -0.35000900
H 2.32149100 4.78525400 -0.40832700
C 2.74933300 1.49302800 -0.24774800
C -2.85041300 1.01157000 -0.43385200
C 1.54871800 -2.69194800 -0.27662000
N 1.63755800 -1.33038100 -0.21711100
N 1.38679000 1.58290400 -0.22816200
O 0.03038700 -0.00341700 2.29568000
C -1.05461400 -0.01451000 3.14621900
H -1.69885000 -0.91303000 3.03360100
H -0.73719700 -0.00367700 4.21123000
H -1.72550100 0.86276400 3.02279400
H -4.44317900 -0.38573800 -0.56925600
H 0.44539900 -4.50343600 -0.37654600
H 4.56246900 0.38802100 -0.25261800
H -0.32739000 4.50607900 -0.39716500

^{1cs}FP^{-}-EDA
b3lyp/def2tzvp,
el. energy = -2784.108251 a.u.
C -0.56170400 3.07264600 -0.38664900
N -0.72982600 1.76904300 -0.78558000
H -1.83663200 4.92186500 -0.53017600
C -1.96583000 1.71760900 -1.37892200
C -2.59435000 3.02209900 -1.35787500
H -3.57418200 3.24526400 -1.76442100
C -1.72192200 3.86424100 -0.73790600
C -2.55444900 0.57034900 -1.90370300
N -0.74584900 -1.01542500 -1.40882700

C -0.61328200 -2.37473300 -1.56660500
C -1.80450000 -2.93316900 -2.16796200
H -1.94989000 -3.98335000 -2.39317100
C -2.66201000 -1.89486800 -2.37377500
H -3.65671900 -1.91654200 -2.80399100
C -1.99498700 -0.70406800 -1.89174300
C 0.55923300 3.56822200 0.27267700
H 0.55783100 4.62442800 0.53099900
H 4.68782100 2.35308200 1.95175400
C 3.71093100 2.34007800 1.48222700
C 3.09221800 1.17250700 0.89090300
H 2.93911100 4.40198900 1.63414300
N 1.85481000 1.48700300 0.38719500
C 1.68052200 2.82694600 0.63489600
C 2.83169900 3.36869800 1.32466600
C 0.50325900 -3.11964000 -1.19718400
H 0.47073900 -4.18975000 -1.38626500
H 4.65541900 -2.78159600 0.79877600
C 3.68459900 -2.55673600 0.37245300
C 2.78794000 -3.41207700 -0.19123200
H 2.87169200 -4.48418100 -0.32668000
C 1.64702900 -2.61412200 -0.58781500
N 1.85103000 -1.29207100 -0.27176500
C 3.08825200 -1.23794700 0.32361300
C 3.67378700 -0.09188200 0.85239100
H 4.66039300 -0.19848400 1.29636900
C -0.68282800 -0.36525700 2.48128100
C -1.97158900 -1.04377500 2.49832100
O -2.16846400 -2.18803300 2.87481500
O -2.93255100 -0.20845000 2.04373100
C -4.25570400 -0.76757700 1.91091600
H -4.50688200 -1.31821600 2.82267400
H -4.25177600 -1.47730600 1.07605200
N 1.25436900 -1.63946200 3.24932200
N 0.35988500 -1.04248800 2.88365800
H -3.54617000 0.67347900 -2.33718200
Fe 0.62578300 0.26782100 -0.66685000
C -5.21248400 0.38216200 1.66070700
H -4.93402700 0.93274100 0.75629600
H -6.23026900 -0.00496800 1.53198300
H -5.21402500 1.08230900 2.50346100
H -0.50648900 0.62583400 2.08561100
O 1.48540300 0.78916600 -2.27939100
C 1.45543000 -0.05225700 -3.36807700
H 2.13499300 0.33726500 -4.15667200
H 1.79923200 -1.08871800 -3.16142200
H 0.45786400 -0.15085900 -3.85494200

^{1os}FP^{-}-EDA
ub3lyp/def2tzvp,
el. energy = -2784.110044 a.u.

C -0.44550000 3.13791300 -0.19014600
N -0.66026100 1.86614200 -0.65913600
H -1.65318100 5.03705400 -0.24130400
C -1.88995400 1.88972200 -1.26398000
C -2.47267500 3.21174800 -1.17196700
H -3.44076100 3.49304900 -1.57046800
C -1.57355300 3.98861400 -0.50450600
C -2.50601200 0.79561900 -1.86864000
N -0.73940900 -0.87139100 -1.49725300
C -0.64219000 -2.21769200 -1.75800800
C -1.84511800 -2.69451500 -2.40762500
H -2.01789200 -3.71950200 -2.71472300
C -2.67479800 -1.62193400 -2.52874900
H -3.66851500 -1.58393300 -2.96013800
C -1.97840100 -0.48979300 -1.95310400
C 0.69051500 3.55089400 0.50239200
H 0.72818500 4.58967400 0.82116900
H 4.73228400 2.07207700 2.18278500
C 3.76754500 2.12665300 1.69164600
C 3.11681200 1.02074800 1.01905100
H 3.07648100 4.20556500 1.94992500
N 1.90810900 1.41863000 0.50407400
C 1.77866700 2.74631300 0.82953400
C 2.93511500 3.19796400 1.57620800
C 0.44402900 -3.02392200 -1.43067000
H 0.38400900 -4.07320300 -1.70821700
H 4.54057500 -2.98067400 0.70943000
C 3.59062800 -2.69128100 0.27513300
C 2.68904300 -3.47079200 -0.38544100
H 2.74788800 -4.53037100 -0.60553900
C 1.58666900 -2.60801500 -0.75138500
N 1.81946500 -1.32511800 -0.32182900
C 3.03642900 -1.35497600 0.31125900
C 3.64660500 -0.26354700 0.92583800
H 4.61520500 -0.43451900 1.38907900
C -0.77764000 -0.60359800 2.47916000
C -2.09971200 -1.21246100 2.43261300
O -2.36587500 -2.35785900 2.76077900
O -3.00261600 -0.31377800 1.97879200
C -4.34738000 -0.80321300 1.79498000
H -4.65618700 -1.35034400 2.69089000
H -4.35102500 -1.50349300 0.95212300
N 1.06533300 -2.02393300 3.22121800
N 0.21562100 -1.35807800 2.86688900
H -3.49241200 0.95589600 -2.29706900
Fe 0.66610600 0.31853300 -0.65821700
C -5.23835700 0.39457000 1.52872500
H -4.90389200 0.93999500 0.64046800
H -6.26883100 0.05856900 1.36281100
H -5.23348800 1.08520800 2.37923800
H -0.53651400 0.38815700 2.12197700
O 1.58024100 0.94328200 -2.24784800
C 1.59123400 0.17882800 -3.38978700
H 2.26859900 0.62755900 -4.15097800
H 1.96028900 -0.86212800 -3.24705100
H 0.60243000 0.08350700 -3.89749100

^{3}FP^{-}-EDA
ub3lyp/def2tzvp,
el. energy = -2784.114743 a.u.

C -1.81283900 -0.93906300 -2.18947300

N -1.06701400 -1.31366800 -1.10386400
H -3.69231900 -1.74083000 -3.12652400
C -1.67846000 -2.42175700 -0.58189400
C -2.86182600 -2.74429500 -1.34214300
H -3.52613300 -3.57580100 -1.13729700
C -2.94490600 -1.81986400 -2.34564500
C -1.21123900 -3.14540100 0.51680800
N 0.81435800 -1.83009200 0.99348700
C 1.72534000 -1.85221800 2.02605500
C 1.43816100 -2.95067600 2.92755900
H 2.01171200 -3.18386000 3.81713000
C 0.32777900 -3.57115500 2.44838900
H -0.20154100 -4.42196800 2.86132200
C -0.06888900 -2.85478000 1.25222800
C -1.50884600 0.12962900 -3.03534200
H -2.18851600 0.31717500 -3.86237000
H 1.37483000 3.68463800 -3.61050000
C 0.90244000 2.77674400 -3.25398700
C 1.34639100 2.01181500 -2.10469700
H -0.81310700 2.42177400 -4.59132700
N 0.53599900 0.91611300 -1.91833300
C -0.42669300 0.98970800 -2.89784900
C -0.19468500 2.14335800 -3.74593300
C 2.73877100 -0.92467900 2.23400900
H 3.38579000 -1.08149900 3.09298800
H 4.53515500 2.99206200 0.54948800
C 3.91844300 2.11517900 0.70871000
C 4.01767600 1.17783000 1.69838700
H 4.73148200 1.13317400 2.51261000
C 2.97207500 0.21287900 1.45884100
N 2.24047800 0.56973300 0.35659700
C 2.81424800 1.71572600 -0.12938100
C 2.40316300 2.38551200 -1.28360600
H 2.94846000 3.28549300 -1.55606600
C -1.12066300 2.02923800 1.38258500
C -2.46379000 2.11511400 1.93467300
O -2.80291100 2.79199500 2.89360700
O -3.30072700 1.32529700 1.22417100
C -4.67113600 1.29343900 1.67104900
H -5.08956000 2.30500700 1.61819200
H -4.69790800 0.97693600 2.71948300
N 0.62956900 3.31166200 2.50360100
N -0.17856200 2.70970800 1.97678100
H -1.80348100 -3.99850700 0.83823700
Fe 0.78582600 -0.56734500 -0.57916300
C -5.41893800 0.32700300 0.77328700
H -4.98287300 -0.67567500 0.82764500
H -6.46826300 0.26918800 1.08616300
H -5.38664800 0.65519300 -0.27101000
H -0.83332300 1.41497200 0.53794700
O 1.91877000 -1.58082400 -1.84273200
C 2.55136500 -2.76789500 -1.56335500
H 2.90347100 -3.27687200 -2.49064100
H 3.46344700 -2.65636000 -0.93004300
H 1.91536600 -3.51754200 -1.04109500

^{5}FP^{-}-EDA
ub3lyp/def2tzvp,
el. energy = -2784.130894 a.u.

C 1.34963500 0.80352200 2.42175600
N 0.87028800 -0.22757800 1.66056000
H 3.12810800 0.99491200 3.79979700
C 1.71283800 -1.29005700 1.84559700
C 2.76853200 -0.92176700 2.77031900
H 3.57370500 -1.57269200 3.09189000
C 2.54286600 0.37661800 3.12848600
C 1.58692600 -2.53649600 1.21595600
N -0.41552600 -2.12508100 -0.14635900
C -1.09969500 -2.82982000 -1.09637700
C -0.49041900 -4.13701700 -1.26993600
H -0.82913100 -4.89902400 -1.96283600
C 0.57327000 -4.19035700 -0.41592800
H 1.27524100 -5.00436500 -0.27416400
C 0.61513200 -2.91543000 0.27855500
C 0.78828400 2.08689000 2.48167100
H 1.28512400 2.80205000 3.13349200
H -2.51726000 4.82623400 0.72654800
C -1.89124900 3.97275000 0.96114400
C -2.03395100 2.64517100 0.38967800
H -0.41721400 4.71968800 2.42120200
N -1.07621800 1.81604500 0.90295000
C -0.32329200 2.55895100 1.76917300
C -0.82989200 3.91907300 1.81769500
C -2.19807400 -2.34879500 -1.82340500
H -2.63870300 -3.03424600 -2.54401300
H -4.82716600 1.38805600 -2.62658000
C -4.09086400 0.70273500 -2.22229200
C -3.86637300 -0.59578300 -2.57646700
H -4.38445900 -1.18235300 -3.32671700
C -2.76560000 -1.06840800 -1.75414600
N -2.34811400 -0.06793100 -0.92327200
C -3.12689300 1.02411900 -1.18404800
C -2.99015600 2.27547300 -0.56675800
H -3.68566500 3.05007700 -0.88153700
C 1.53233400 1.00649700 -1.64752300
C 2.86595800 1.05049200 -2.22033400
O 3.16019700 1.44890700 -3.33799000
O 3.76599900 0.58018000 -1.32254500
C 5.13896400 0.56488900 -1.75573100
H 5.45682700 1.58907600 -1.98266300
H 5.21996600 -0.01840400 -2.67931300
N -0.30315700 1.80405200 -3.04764500
N 0.54568200 1.43014300 -2.39148300
H 2.34368400 -3.27952200 1.45758800
Fe -1.15642000 -0.35637400 0.87209300
C 5.96094800 -0.04200800 -0.63444500
H 5.63984100 -1.06779600 -0.42445300
H 7.01966000 -0.06166200 -0.91884400
H 5.86040100 0.54257200 0.28626500
H 1.28818800 0.65253700 -0.65223600
O -2.33670400 -0.89549200 2.25293200
C -2.30337200 -2.02988600 3.03670800

H -3.13029100 -2.03637900 3.77834500
H -2.40761100 -2.97236500 2.45732800
H -1.36811300 -2.13513000 3.62795200

^{1os}TS1^{-}
ub3lyp/def2tzvp,
el. energy = -2784.095122 a.u.
im. frequency -1120.47

C -1.91382400 -1.46693500 -1.42243100
N -0.63006300 -1.44838200 -0.93610600
H -3.31076000 -3.11734200 -2.04440100
C -0.23036100 -2.76221500 -0.86657300
C -1.29509100 -3.63264100 -1.30906100
H -1.23472600 -4.71422500 -1.34161300
C -2.33733500 -2.83108300 -1.66359300
C 1.02594600 -3.19609000 -0.46104000
N 2.04018300 -0.99221500 -0.08124400
C 3.29199600 -0.57819200 0.29740900
C 4.15249200 -1.72025300 0.51322300
H 5.18933500 -1.66225400 0.82271600
C 3.39730700 -2.83079600 0.27822900
H 3.68951800 -3.87214200 0.34572200
C 2.08237200 -2.36835900 -0.09394700
C -2.71590600 -0.34974500 -1.62839300
H -3.71133700 -0.51948900 -2.03045800
H -2.87102900 4.22802600 -1.01337600
C -2.54994600 3.19327800 -1.04585600
C -1.24832000 2.72027900 -0.63755300
H -4.25078800 2.05717100 -1.87938800
N -1.16335500 1.35995300 -0.80038900
C -2.36437300 0.96436900 -1.32208800
C -3.24333100 2.10245200 -1.48238700
C 3.67715600 0.74349100 0.50831900
H 4.70703300 0.92040900 0.80632300
H 2.06295700 5.07205200 0.62404500
C 2.15053500 3.99755900 0.51151200
C 3.25054700 3.21243000 0.69073100
H 4.25004400 3.50771700 0.98789900
C 2.83946300 1.85312200 0.41248300
N 1.51504100 1.81735100 0.06821400
C 1.07423600 3.12021900 0.11459900
C -0.21439600 3.54123400 -0.19166900
H -0.42283000 4.60516800 -0.11190100
C -0.24130000 0.07401500 1.84717700
C -1.45813300 -0.73688800 2.02562200
O -1.49552600 -1.92449700 2.30341600
O -2.57201800 0.03115000 1.88717100
C -3.82605500 -0.66550300 1.99376100
H -3.84375700 -1.23685900 2.92831600
H -3.91121100 -1.37844500 1.16667500
N 1.46934300 -1.32180600 2.90394700
N 0.81954700 -0.44077100 2.53933400
H 1.20128000 -4.26824000 -0.43891500
Fe 0.45961700 0.18305400 -0.50805500
C -4.93264100 0.37218500 1.95351600
H -4.89705400 0.94567800 1.02158900
H -5.90924700 -0.12232500 2.02146900
H -4.84472600 1.07367600 2.79092100
H -0.33070200 1.14938700 1.92389600
O 0.94102700 0.49161900 -2.27030900
C 1.38930200 -0.52327800 -3.10143100
H 1.66350600 -0.08347900 -4.07923900
H 2.28998200 -1.04381400 -2.72500400
H 0.62968300 -1.30109500 -3.30771000

^{3}TS1^{-}
ub3lyp/def2tzvp,
el. energy = -2784.096722 a.u.
im. frequency -426.84

C -2.37490100 0.06921400 -1.60289900
N -1.25483800 -0.61518600 -1.19870900
H -4.36459800 -0.57323800 -2.42119500
C -1.53676700 -1.95752200 -1.38307600
C -2.86972000 -2.11354900 -1.90733100
H -3.33376700 -3.06589500 -2.13518500
C -3.38642500 -0.86047300 -2.05379900
C -0.65679200 -2.99956600 -1.14879000
N 1.26542800 -1.65279500 -0.40977300
C 2.55094600 -1.96109700 -0.03718800
C 2.75884500 -3.38183900 -0.09939300
H 3.68530900 -3.88107800 0.15767600
C 1.57666200 -3.93790600 -0.51149400
H 1.34030500 -4.98429000 -0.66369300
C 0.65647900 -2.85682200 -0.70221700
C -2.54889100 1.44730100 -1.56119000
H -3.49404700 1.84398400 -1.92039000
H -0.49860200 5.35246100 -0.16680700
C -0.70925300 4.31490600 -0.39829300
C 0.19362200 3.22426600 -0.16345700
H -2.74098400 4.28781000 -1.27335900
N -0.38404600 2.03366600 -0.55533500
C -1.62065300 2.35826700 -1.04971300
C -1.83907800 3.77876100 -0.95481400
C 3.51539000 -1.04088100 0.38689700
H 4.49511400 -1.43100600 0.64595500
H 4.16429100 3.43388100 1.31586000
C 3.72937200 2.48619900 1.02052100
C 4.31054200 1.25396800 1.00748600
H 5.31878200 0.97900400 1.29337200
C 3.30985100 0.32395200 0.53166400
N 2.13334100 0.98559200 0.27793500
C 2.37801600 2.31757000 0.54738300
C 1.47494500 3.35321700 0.36728900
H 1.80636500 4.35444300 0.62973600
C -0.30193300 0.02300000 2.04584300
C -1.49473000 -0.75947100 2.31802600
O -1.53448200 -1.92983600 2.67191300
O -2.61932400 -0.00330600 2.12831200
C -3.86975900 -0.69621200 2.25562000
H -3.91985800 -1.18691700 3.23440800
H -3.93179700 -1.47769500 1.48949900
N 1.53454700 -1.34262400 2.86842800

N 0.87922200 -0.46786500 2.46186500
H -1.01162400 -4.00838100 -1.34046800
Fe 0.48449200 0.19621900 -0.60196400
C -4.97686500 0.32902800 2.08849000
H -4.90885100 0.81637400 1.11011000
H -5.95610600 -0.15890600 2.16616100
H -4.91593500 1.10247300 2.86264800
H -0.35300400 1.08856900 1.87923400
O 1.13754600 0.52340400 -2.24476800
C 1.24536600 -0.48698900 -3.20675600
H 1.41360600 -0.00184600 -4.18323500
H 2.09833900 -1.15907200 -3.01909600
H 0.33915300 -1.10390100 -3.29753100

^{5}TS1^{-}
ub3lyp/def2tzvp,
el. energy = -2784.079991 a.u.
im. frequency -221.19
C -0.50937700 3.06111500 -0.30168000
N -0.83720100 1.76122000 -0.57089800
H -1.69851300 4.97573000 -0.41159600
C -2.14465000 1.72729100 -0.96928200
C -2.67745400 3.07779800 -0.95865000
H -3.68990700 3.35034500 -1.23356900
C -1.67016000 3.90008500 -0.54247600
C -2.85896600 0.57486900 -1.33192300
N -1.14520300 -1.14717100 -0.97620900
C -1.04876200 -2.49517100 -1.16210900
C -2.32177100 -2.99559400 -1.64748300
H -2.53875900 -4.03223800 -1.87779500
C -3.15710500 -1.91882300 -1.75993000
H -4.18551600 -1.90676200 -2.10257400
C -2.39889700 -0.75272200 -1.34217400
C 0.75048900 3.51876800 0.12014800
H 0.83992600 4.59076300 0.27966600
H 5.12662300 2.19657900 0.97509100
C 4.06804300 2.20011300 0.74206300
C 3.27784700 1.02410200 0.41809600
H 3.46032200 4.31530700 0.86920700
N 1.98981600 1.40637700 0.19002700
C 1.91283800 2.75835900 0.32968900
C 3.22347000 3.27260400 0.69121500
C 0.11237900 -3.25612200 -0.95202400
H 0.02739900 -4.32313000 -1.14296800
H 4.63024500 -3.04940300 0.09853800
C 3.59303500 -2.79296300 -0.08293400
C 2.57085200 -3.62472700 -0.43152800
H 2.60629900 -4.69593700 -0.59196100
C 1.37932900 -2.79981600 -0.55720500
N 1.70184400 -1.50756700 -0.27099100
C 3.03506600 -1.45260000 0.00950300
C 3.75675200 -0.29293900 0.33289700
H 4.81540200 -0.43192000 0.53899200
C -0.06365400 0.01546700 1.76022100
C -1.28475600 -0.77016000 2.07422500
O -1.32900100 -1.93978400 2.41387600
O -2.40213200 0.00308500 1.96932400
C -3.65123600 -0.67559700 2.18454000
H -3.61438400 -1.20421100 3.14334700
H -3.79351200 -1.42593700 1.39902500
N 1.52072600 -1.47059800 2.78894800
N 1.05084600 -0.41324500 2.56259400
H -3.88822900 0.72981800 -1.64740200
Fe 0.44452000 0.12231700 -0.46303900
C -4.75418800 0.36675400 2.16591900
H -4.77456900 0.89764300 1.20875300
H -5.72730900 -0.11684100 2.31503300
H -4.61230000 1.10498700 2.96329500
H -0.20565900 1.08382200 1.88237600
O 1.05403500 0.24771900 -2.24957300
C 0.32113100 0.81763300 -3.27903500
H 0.87287600 0.68849200 -4.23111700
H -0.67068800 0.35011300 -3.42899700
H 0.15220200 1.90490800 -3.16012600

^{1os}INT1^{-}
ub3lyp/def2tzvp,
el. energy = -2784.103969 a.u.
C -2.12896400 -1.14494500 -1.41305800
N -0.85041900 -1.30820400 -0.94642100
H -3.72336400 -2.58219500 -2.08036000
C -0.61340700 -2.65792500 -0.93422300
C -1.78088800 -3.37307100 -1.39534900
H -1.85353200 -4.45121300 -1.47302600
C -2.71963000 -2.43379400 -1.69997400
C 0.58929300 -3.25841400 -0.57716500
N 1.86381800 -1.21508500 -0.11802900
C 3.16379800 -0.96528100 0.23098900
C 3.89225500 -2.20867700 0.35792400
H 4.93803800 -2.28557900 0.63037900
C 3.00842400 -3.20906800 0.09240400
H 3.17793600 -4.28000700 0.09667900
C 1.74339800 -2.57669300 -0.20840400
C -2.78555700 0.07168300 -1.57589600
H -3.79864900 0.04007100 -1.96755800
H -2.33843600 4.62013000 -0.90629900
C -2.15618300 3.55318500 -0.95597500
C -0.92142200 2.90743800 -0.56551900
H -3.99983400 2.65756700 -1.77501300
N -1.01837500 1.55508500 -0.74594500
C -2.26560600 1.32194200 -1.25484600
C -2.98968200 2.56799300 -1.39309900
C 3.71409500 0.29155000 0.46407300
H 4.76497900 0.33018200 0.73690400
H 2.68340500 4.78992200 0.68025800
C 2.62814500 3.71520200 0.55364100
C 3.61845000 2.79120800 0.69434500
H 4.65521100 2.94882500 0.96682800
C 3.02595600 1.50075800 0.41358200
N 1.70243900 1.64878600 0.10629400
C 1.43524200 2.98895800 0.17583500
C 0.20875900 3.58152000 -0.11027200

H 0.14043900 4.66145700 -0.01288800
C -0.17871900 0.11863600 1.69546000
C -1.38080000 -0.69434900 1.95669100
O -1.42970400 -1.87283800 2.26980800
O -2.51905300 0.06803600 1.84669100
C -3.75532800 -0.62952700 2.04763200
H -3.72397200 -1.16174300 3.00517600
H -3.88380700 -1.38176700 1.26161000
N 1.26690400 -1.29299100 2.97387500
N 0.95264600 -0.23437700 2.53439100
H 0.63611300 -4.34309000 -0.60649500
Fe 0.43507700 0.16443500 -0.44908300
C -4.87596700 0.39499500 2.02194100
H -4.89731900 0.92946100 1.06636300
H -5.84368200 -0.10258600 2.16166500
H -4.75175400 1.13365400 2.82203600
H -0.36653600 1.18186700 1.80751100
O 0.95619800 0.43978500 -2.20545100
C 1.35768600 -0.57898400 -3.06061000
H 1.53058000 -0.15192000 -4.06794800
H 2.30292100 -1.06484000 -2.75104900
H 0.60455800 -1.38090200 -3.18089700

^{3}INT1^{-}
ub3lyp/def2tzvp,
el. energy = -2784.102967 a.u.
C -0.94760800 2.89208800 -0.58008700
N -1.02931300 1.53816100 -0.75630300
H -2.38067300 4.58926200 -0.93169700
C -2.27233500 1.29082500 -1.26849200
C -3.00832500 2.52908100 -1.41377100
H -4.01787200 2.60698800 -1.79977400
C -2.18745600 3.52409000 -0.97722900
C -2.77851700 0.03453000 -1.58850400
N -0.83199300 -1.32425000 -0.94692800
C -0.58062800 -2.67168800 -0.93322300
C -1.73768200 -3.39910200 -1.40073600
H -1.79833800 -4.47793700 -1.47881600
C -2.68484000 -2.46982500 -1.71025500
H -3.68476700 -2.62904000 -2.09621300
C -2.10987700 -1.17489500 -1.42037200
C 0.17418700 3.57890600 -0.12374500
H 0.09500200 4.65843300 -0.03043400
H 4.62317500 2.99435000 0.97020800
C 3.58887100 2.82563800 0.69511200
C 3.01003100 1.52853400 0.41696900
H 2.63430600 4.81502800 0.67034500
N 1.68586500 1.66164000 0.10472400
C 1.40555600 2.99917700 0.16814500
C 2.59007400 3.73941300 0.54714500
C 0.62713700 -3.25938900 -0.57034900
H 0.68568900 -4.34350100 -0.59957700
H 4.96017500 -2.23677600 0.65046700
C 3.91441600 -2.17169400 0.37490900
C 3.04308200 -3.18279000 0.10782300
H 3.22385800 -4.25084700 0.11513100
C 1.77219000 -2.56431900 -0.19779200
N 1.87662800 -1.20171900 -0.10965700
C 3.17307800 -0.93649400 0.24325400
C 3.71003700 0.32654700 0.47348200
H 4.75985800 0.37557600 0.74856200
C -0.19098400 0.11898900 1.70926800
C -1.39283700 -0.69160200 1.97479000
O -1.44269100 -1.86410200 2.30986900
O -2.53297600 0.06460000 1.83603300
C -3.76928200 -0.63340000 2.03276600
H -3.74181400 -1.16482600 2.99067700
H -3.89384400 -1.38656600 1.24572700
N 1.25749600 -1.26969600 3.00437100
N 0.94588800 -0.21949700 2.53743300
H -3.78952500 -0.00849700 -1.98437600
Fe 0.43664900 0.16330600 -0.45214200
C -4.89097900 0.38987800 2.00104300
H -4.90804000 0.92455100 1.04547000
H -5.85896700 -0.10860000 2.13576800
H -4.77151300 1.12855700 2.80185800
H -0.37992900 1.18390400 1.80152000
O 0.96137400 0.43832400 -2.20327500
C 1.39315300 -0.57745200 -3.04805500
H 1.52114200 -0.16498700 -4.06600400
H 2.36771400 -1.00670500 -2.75115200
H 0.68104000 -1.41765200 -3.13104000

^{5}INT1^{-}
ub3lyp/def2tzvp,
el. energy = -2784.079520 a.u.
C -0.55048500 3.03750200 -0.35180900
N -0.85349100 1.72782200 -0.60565400
H -1.77352900 4.92751600 -0.48899300
C -2.15938400 1.66518000 -1.00644200
C -2.71642800 3.00511600 -1.01380600
H -3.73337500 3.25477500 -1.29368800
C -1.72537800 3.85107000 -0.60636000
C -2.85326300 0.49748300 -1.35829100
N -1.10679700 -1.18633200 -0.98801500
C -0.98652500 -2.53426400 -1.15744800
C -2.24835200 -3.06305000 -1.64188100
H -2.44529900 -4.10614100 -1.86045700
C -3.10342100 -2.00379200 -1.76576700
H -4.13179800 -2.01408100 -2.10842600
C -2.36790300 -0.82007100 -1.35778100
C 0.69776500 3.52589600 0.06856700
H 0.76590100 4.60161100 0.21194200
H 5.08829200 2.28923200 0.97278100
C 4.03137900 2.27286100 0.73305600
C 3.26109200 1.07923700 0.42574200
H 3.39029400 4.38035700 0.81823300
N 1.96973900 1.43741900 0.18284600
C 1.87095600 2.78969300 0.29802100
C 3.17120200 3.33101500 0.65780900
C 0.18352800 -3.27320700 -0.92549000
H 0.11947300 -4.34385800 -1.10301100

H 4.67860400 -2.97379600 0.19364400
C 3.64028600 -2.73777200 -0.00772500
C 2.63750000 -3.59129600 -0.36025300
H 2.69281600 -4.66385700 -0.50483100
C 1.43509900 -2.78902500 -0.51681600
N 1.73169000 -1.48718400 -0.24307300
C 3.05986100 -1.40627300 0.05699700
C 3.75993700 -0.23129600 0.37048900
H 4.81797400 -0.35109100 0.59073100
C -0.07935100 0.02218000 1.70749300
C -1.30185500 -0.75914000 2.01819400
O -1.36543100 -1.93436600 2.33373200
O -2.41524700 0.03377300 1.95771200
C -3.66291400 -0.62947100 2.21398200
H -3.60542700 -1.14884400 3.17722800
H -3.83809900 -1.38792300 1.44275100
N 1.39959000 -1.44323500 2.88421100
N 1.06200500 -0.36445000 2.52307800
H -3.88553200 0.63088200 -1.67344200
Fe 0.45132200 0.11705000 -0.44903400
C -4.75623700 0.42352800 2.21613200
H -4.80584200 0.93906700 1.25147700
H -5.72855700 -0.04659100 2.40795600
H -4.57809100 1.17358600 2.99499500
H -0.23599300 1.08931800 1.83071500
O 1.07179200 0.24109500 -2.20645000
C 0.32343700 0.75434200 -3.25862000
H 0.89027900 0.61034100 -4.19779500
H -0.64873600 0.24778200 -3.39611500
H 0.12093700 1.83743600 -3.17245700

^{1cs}TS2^{-}
b3lyp/def2tzvp,
el. energy = -2784.086946 a.u.
im. frequency -434.45

C -1.07963800 2.77827200 -0.63611500
N -1.09472500 1.41663000 -0.75412500
H -2.58643500 4.38998200 -1.09380600
C -2.31474800 1.08731000 -1.27418700
C -3.10712300 2.28283000 -1.48954900
H -4.10930000 2.29726100 -1.90242400
C -2.34258600 3.33390300 -1.08231700
C -2.75462400 -0.20947900 -1.53565700
N -0.74623200 -1.43884800 -0.83813600
C -0.41758400 -2.76440200 -0.78594400
C -1.53590300 -3.57817900 -1.21641900
H -1.53351200 -4.66094300 -1.26363200
C -2.53627100 -2.71695700 -1.55279600
H -3.52528600 -2.94755900 -1.93185800
C -2.03097600 -1.37970200 -1.31083200
C 0.00614100 3.53426500 -0.19473600
H -0.12897800 4.61189700 -0.14380100
H 4.50377500 3.26593100 0.83472100
C 3.47483000 3.02185000 0.59697100
C 2.97140500 1.68232700 0.36281700
H 2.39602400 4.94537800 0.53733000
N 1.63310600 1.71841100 0.08986800
C 1.27180700 3.03836000 0.11513000
C 2.41554800 3.86497800 0.45098700
C 0.83748000 -3.26157900 -0.43687700
H 0.96711900 -4.34071700 -0.45087300
H 5.17055000 -1.95611200 0.49336900
C 4.10566200 -1.95794800 0.29194800
C 3.28192700 -3.02442800 0.09836600
H 3.53288600 -4.07875500 0.09736700
C 1.95594800 -2.49048500 -0.13243500
N 1.97740600 -1.11827400 -0.06027900
C 3.28118700 -0.77162600 0.20040900
C 3.74787300 0.52523900 0.39900900
H 4.80669000 0.64252900 0.61552400
C -0.27282500 0.18558600 1.48830200
C -1.46327600 -0.59743400 1.96002400
O -1.45182200 -1.72383300 2.42381600
O -2.60151600 0.11895000 1.79341800
C -3.83528500 -0.57699800 2.06184600
H -3.77814400 -1.03963700 3.05248800
H -3.95806200 -1.37794400 1.32506400
N 1.80534100 -1.03508200 2.74061400
N 0.89061200 -0.39058400 2.64659600
H -3.75787600 -0.31946800 -1.94025800
Fe 0.44918700 0.13225600 -0.36218900
C -4.96110100 0.43662700 1.98013000
H -4.98876100 0.91158900 0.99425400
H -5.92304100 -0.06090900 2.15289400
H -4.83970000 1.22140600 2.73520900
H -0.32803600 1.21678900 1.84416800
O 0.97202500 0.43650400 -2.19954100
C 0.85359700 -0.51861700 -3.17985100
H 1.36440300 -0.17691800 -4.10701100
H 1.31349200 -1.50045400 -2.92744000
H -0.19350500 -0.74302600 -3.48703100

^{1os}TS2^{-}
ub3lyp/def2tzvp,
el. energy = -2784.095544 a.u.
im. frequency -457.50

C -0.14495500 3.17257800 -0.36781200
N -0.58876800 1.91266600 -0.65531000
H -1.07023700 5.21650100 -0.54439400
C -1.85763000 2.04990400 -1.14502600
C -2.23380300 3.44855000 -1.16805000
H -3.18811900 3.82731000 -1.51470200
C -1.17127300 4.14598300 -0.67917100
C -2.68311800 1.00565200 -1.55420300
N -1.17448700 -0.87966900 -1.09112400
C -1.28873000 -2.23846000 -1.21373500
C -2.59450300 -2.58400300 -1.72989100
H -2.93743700 -3.59442000 -1.91825900
C -3.26003400 -1.41080100 -1.92471600
H -4.26382700 -1.25936200 -2.30407800
C -2.36306000 -0.34982300 -1.51818900
C 1.11675300 3.48558900 0.13277700

H 1.33417100 4.53389300 0.31832400
H 5.21885500 1.62755100 1.16149900
C 4.18289100 1.76849900 0.87667900
C 3.28080600 0.70425500 0.48745700
H 3.80185600 3.93644500 1.02539100
N 2.04815000 1.21697200 0.19256900
C 2.13805900 2.56994500 0.37141500
C 3.47118500 2.92711600 0.81044800
C -0.28554100 -3.15697800 -0.91755800
H -0.51486400 -4.20964400 -1.05698200
H 4.14510100 -3.45555900 0.34939500
C 3.15754500 -3.08655500 0.09913700
C 2.05230900 -3.79670400 -0.25833100
H 1.94398000 -4.86933400 -0.36614800
C 0.99592900 -2.83400700 -0.48288600
N 1.45823500 -1.56471900 -0.25457100
C 2.77415100 -1.69086300 0.10201500
C 3.62750400 -0.64344100 0.44029500
H 4.64770000 -0.90301300 0.70921500
C -0.25646700 0.15276100 1.48939200
C -1.40425000 -0.67133200 1.90707800
O -1.42672300 -1.87334200 2.11959000
O -2.53686500 0.09923100 2.05262000
C -3.74084400 -0.61621100 2.36504700
H -3.63480400 -1.09939900 3.34450200
H -3.90023200 -1.40987200 1.62702800
N 1.26956800 -1.36928400 3.00971500
N 1.04704700 -0.30169100 2.66752400
H -3.67074000 1.27004600 -1.92286300
Fe 0.44135800 0.16243600 -0.45308100
C -4.88414000 0.38293300 2.36152500
H -4.98573300 0.85305400 1.37724800
H -5.82775600 -0.12184800 2.60268000
H -4.71937100 1.17398400 3.10199600
H -0.36964900 1.18749500 1.80926100
O 1.05370600 0.43045300 -2.20812100
C 1.06317300 -0.53832400 -3.19672000
H 1.56742300 -0.14166600 -4.09959700
H 1.60656700 -1.46135000 -2.91580800
H 0.05088200 -0.85239900 -3.51982100

^{3}TS2^{-}
ub3lyp/def2tzvp,
el. energy = -2784.091443 a.u.
im. frequency -437.04
C -1.14994600 2.77963500 -0.73620300
N -1.11362300 1.42128200 -0.88800500
H -2.70944500 4.34365900 -1.16801900
C -2.31612700 1.05925500 -1.42593600
C -3.14951300 2.22886800 -1.61735000
H -4.15055500 2.21472600 -2.03205600
C -2.42604300 3.29787000 -1.18416700
C -2.69954600 -0.24172400 -1.74069500
N -0.66051600 -1.41995900 -1.03287600
C -0.29624000 -2.73893800 -0.98858900
C -1.36714100 -3.56856900 -1.49205400
H -1.33163100 -4.64921000 -1.56100800
C -2.37958100 -2.72810000 -1.84397600
H -3.34813700 -2.97601100 -2.26206900
C -1.92887400 -1.38574700 -1.54770300
C -0.10589500 3.56150100 -0.24950400
H -0.27302200 4.63313700 -0.18362300
H 4.29301300 3.35537400 1.14674700
C 3.29701800 3.09826600 0.80601100
C 2.84335500 1.75400800 0.52074600
H 2.19344900 5.00414800 0.66479100
N 1.53858800 1.77532400 0.11277800
C 1.14832900 3.08695000 0.12646000
C 2.24210100 3.92617200 0.56573500
C 0.93270200 -3.22104200 -0.54714400
H 1.07962600 -4.29726800 -0.55511900
H 5.06596700 -1.83928900 0.98131000
C 4.04340500 -1.86209900 0.62369200
C 3.28022700 -2.94313600 0.30415900
H 3.54557300 -3.99285300 0.34306100
C 1.99253600 -2.43188100 -0.11397600
N 1.98150800 -1.06453100 -0.04347600
C 3.21814700 -0.69232100 0.40879800
C 3.63082800 0.61369200 0.65741100
H 4.64967200 0.75430400 1.00778200
C -0.32904900 0.13407400 1.47228200
C -1.47806500 -0.70463400 1.83099500
O -1.49793900 -1.91823200 1.97268300
O -2.61843700 0.05121800 2.02123400
C -3.81774900 -0.69113400 2.27790300
H -3.72882800 -1.21182000 3.24006600
H -3.94804400 -1.45847800 1.50676300
N 1.10956200 -1.34518200 3.16699100
N 0.97362700 -0.30078300 2.72261100
H -3.69208500 -0.37989100 -2.16092400
Fe 0.44287900 0.17606400 -0.48402700
C -4.97725200 0.28931600 2.28439700
H -5.05739800 0.80111800 1.31899000
H -5.91885100 -0.24087900 2.47424000
H -4.84873700 1.04954600 3.06333100
H -0.46301100 1.16706300 1.79145600
O 1.00742300 0.47143600 -2.23441300
C 1.70288800 -0.45352400 -2.99795800
H 1.76015000 -0.09727700 -4.04444500
H 2.74602500 -0.60580700 -2.66013800
H 1.22594100 -1.45093300 -3.02863400

^{5}TS2^{-}
ub3lyp/def2tzvp,
el. energy = -2784.070792 a.u.
im. frequency -442.21
C -0.89551500 2.90478400 -0.53783500
N -1.02070300 1.56194200 -0.75960400
H -2.34557200 4.61691300 -0.76999000
C -2.29547600 1.31755700 -1.18871300
C -3.01969200 2.57408300 -1.25272600
H -4.05173700 2.68239100 -1.56578700

C -2.15647200 3.55266200 -0.85053000
C -2.82144100 0.05744100 -1.51431700
N -0.87567400 -1.36873500 -1.06306500
C -0.58418400 -2.69648600 -1.15369300
C -1.75800500 -3.40442500 -1.63265400
H -1.81723300 -4.47408000 -1.79731900
C -2.73739900 -2.47069900 -1.82146200
H -3.74994700 -2.62937000 -2.17428100
C -2.16698400 -1.18437500 -1.46159500
C 0.26291400 3.55668000 -0.08450100
H 0.19186600 4.63654100 0.02210600
H 4.71207200 2.91371300 1.10331800
C 3.68154100 2.75528500 0.80693000
C 3.08357000 1.46323400 0.51311300
H 2.78211000 4.76793800 0.75681600
N 1.77581300 1.64684300 0.18032500
C 1.50409200 2.97978500 0.22961900
C 2.70410700 3.69368600 0.63424200
C 0.65493900 -3.27555200 -0.83969800
H 0.72705100 -4.35297700 -0.96634800
H 4.99924800 -2.39006200 0.54153200
C 3.95669800 -2.29017200 0.26265300
C 3.09002800 -3.27229500 -0.11606600
H 3.28384600 -4.33435700 -0.21117600
C 1.81368500 -2.62800700 -0.38483000
N 1.93373200 -1.29166300 -0.15176100
C 3.21625400 -1.03833400 0.23214800
C 3.74335300 0.22440700 0.54368100
H 4.79101600 0.24576200 0.83425700
C -0.21511600 0.05609800 1.49312600
C -1.38291100 -0.75267800 1.89808700
O -1.42429500 -1.95791500 2.08340100
O -2.49014400 0.03960600 2.09387500
C -3.70310300 -0.65141400 2.42929300
H -3.58795400 -1.13558700 3.40730400
H -3.89027200 -1.44254200 1.69525400
N 1.34057500 -1.48963300 2.98768000
N 1.08453100 -0.40917600 2.71625700
H -3.85576700 0.04296100 -1.84982700
Fe 0.46005500 0.13054500 -0.47437700
C -4.82509000 0.37136500 2.44419200
H -4.93284800 0.84282300 1.46131700
H -5.77472700 -0.11298100 2.70267600
H -4.63032100 1.15965000 3.18015300
H -0.32854800 1.09509000 1.79836800
O 1.15786800 0.27817000 -2.20516600
C 0.40252300 0.63239700 -3.31481700
H 1.01710900 0.50452000 -4.22615700
H -0.49813400 0.00667200 -3.45239300
H 0.06805700 1.68670400 -3.30360800

N_2
ub3lyp/def2tzvp,
el. energy = -109.567864 a.u.
N 0.00000000 0.00000000 0.55256300
N 0.00000000 0.00000000 -0.55256300

^{1cs}TC1^{-}
b3lyp/def2tzvp,
el. energy = -2674.539272 a.u.
C -1.03555300 2.65805200 -0.73897200
N -1.04441900 1.29212000 -0.80590200
H -2.55227100 4.24009200 -1.25565900
C -2.27199500 0.93412800 -1.28837300
C -3.07066700 2.11567300 -1.54665200
H -4.07927000 2.10699000 -1.94345800
C -2.30342700 3.18654700 -1.20224200
C -2.70283900 -0.37424100 -1.49775800
N -0.66665600 -1.53010500 -0.77336100
C -0.29097800 -2.84363200 -0.70185100
C -1.37398900 -3.69681000 -1.14638100
H -1.33252900 -4.77900000 -1.18745300
C -2.40353900 -2.87438700 -1.49066600
H -3.38143400 -3.14148400 -1.87433600
C -1.94770700 -1.51962500 -1.25456500
C 0.02885700 3.44520200 -0.30414000
H -0.11952300 4.52211100 -0.31490600
H 4.40778500 3.28194500 1.16728200
C 3.41145600 3.01504200 0.83423700
C 2.94024100 1.65867500 0.63011900
H 2.34248300 4.92160000 0.53584800
N 1.64349800 1.67017200 0.20274400
C 1.27290100 2.98248600 0.12005600
C 2.37418500 3.83835600 0.51728300
C 0.95417600 -3.30880100 -0.28216200
H 1.10232700 -4.38558700 -0.27997000
H 5.12697500 -1.95988800 1.17617000
C 4.09727700 -1.97338600 0.83804800
C 3.32200900 -3.04682700 0.52309400
H 3.58148000 -4.09868000 0.55183900
C 2.03135300 -2.52214600 0.11923100
N 2.03718000 -1.15729800 0.18948200
C 3.28006200 -0.79458600 0.62468800
C 3.70700500 0.51371900 0.84067100
H 4.72779400 0.65437500 1.18664600
C -0.04662900 -0.00712700 1.47118700
C -1.24383900 -0.60802500 2.08732000
O -1.23252200 -1.69927100 2.63927100
O -2.35916100 0.15283800 1.99189200
C -3.56324900 -0.41553700 2.54482200
H -3.37511400 -0.72994500 3.57710400
H -3.83060600 -1.30870000 1.96919300
H -3.70815900 -0.51293300 -1.88715100
Fe 0.47372200 0.06857500 -0.24826200
C -4.64788600 0.64273300 2.46953600
H -4.81314100 0.95971000 1.43460300
H -5.58897600 0.24081900 2.86418200
H -4.37715800 1.52576400 3.05902200
H 0.67072700 0.29855800 2.24663800
O 1.24004000 0.21620700 -2.03247500
C 0.59658700 -0.07496600 -3.21015200
H 1.26132500 0.12464500 -4.07983000

H 0.28365600 -1.13807600 -3.31492200
H -0.32010800 0.52920700 -3.39453100

^{1os}TC1^{-}
ub3lyp/def2tzvp,
el. energy = -2674.548627 a.u.
N -0.75760000 1.62041600 -0.91872000
Fe 0.41759800 0.04102300 -0.46106300
C -0.33136000 -0.14164900 1.31794700
C 0.65851000 3.41192900 -0.01025100
C 3.50715700 -0.36594800 1.01602200
C 3.02357000 0.93400900 0.89352600
C 3.73096100 2.11997900 1.33135400
C 2.92655000 3.18139400 1.04818500
C 1.72971900 2.64175700 0.43503500
N 1.81646100 1.28001000 0.35182400
H 4.71265500 2.11889800 1.79173700
H 3.11102500 4.23435000 1.22547900
C -1.56044000 3.77403200 -1.13012700
C -1.96147900 1.60071200 -1.56824200
C -2.47302700 2.94707100 -1.71047700
H -1.59054200 4.85322500 -1.03749400
H -3.41007300 3.20501000 -2.18967400
C 3.35729600 -2.86152400 0.73881600
C 1.32514000 -2.85756800 -0.23752400
C 2.41431500 -3.69746700 0.22197200
H 4.31578600 -3.11544300 1.17688900
H 2.43796300 -4.77809600 0.14631400
C -2.60781400 0.45682400 -2.02657200
C 0.16482700 -3.33395500 -0.84290500
C -2.05821800 -3.09223000 -1.98385900
C -2.13914200 -0.84355800 -1.87152000
C -2.83460200 -2.02779600 -2.32809800
H -2.24253700 -4.14616600 -2.15548700
H -3.79241600 -2.02545600 -2.83580200
C -0.88432900 -2.55561300 -1.32638800
C -0.48692000 2.93202500 -0.64193100
C 2.84232700 -1.51523300 0.59770900
N 1.61190500 -1.54373400 0.00264500
N -0.95960400 -1.19131600 -1.27279000
C -1.68895700 -0.12072400 1.83642700
O -2.73919200 0.06128300 1.22689100
O -1.71601400 -0.34535400 3.20792800
C -3.01379500 -0.35512000 3.80880500
H -3.64204500 -1.11233400 3.32275500
H -3.50249700 0.61446200 3.65231700
C -2.83875700 -0.65087400 5.28942400
H -3.81478000 -0.66661000 5.78928500
H -2.36040500 -1.62580000 5.44052300
H -2.21743200 0.11234200 5.77183100
O 1.37476400 0.17581500 -2.10149300
C 0.81346300 0.37421600 -3.34558700
H 0.22250600 1.30996900 -3.42860700
H 1.60609300 0.44151000 -4.11874100
H 0.13986000 -0.44543700 -3.67100400
H 0.39535100 -0.30648600 2.12064800
H 0.72978100 4.48700700 0.13160900
H 4.48478600 -0.49302000 1.47534100
H 0.07628200 -4.41041200 -0.96242500
H -3.56246000 0.58819300 -2.52861600

^{3}TC1^{-}
ub3lyp/def2tzvp,
el. energy = -2674.545836 a.u.
C -1.01488000 2.51461400 -1.46208900
N -0.97010300 1.15129300 -1.37814100
H -2.41964500 3.95768200 -2.46718300
C -2.03543800 0.68370300 -2.09334300
C -2.78737200 1.79003500 -2.64888000
H -3.67849400 1.68766100 -3.25690600
C -2.15709200 2.92875400 -2.25137700
C -2.36690100 -0.65550200 -2.27059800
N -0.55106700 -1.66285400 -0.96293700
C -0.22816200 -2.94904400 -0.62041600
C -1.18946800 -3.87111700 -1.18631500
H -1.16010500 -4.94745400 -1.06403300
C -2.08879200 -3.11875100 -1.87868800
H -2.95449500 -3.44925400 -2.44046800
C -1.68363700 -1.73758700 -1.72499700
C -0.08421900 3.39033500 -0.91031500
H -0.25039700 4.45372500 -1.05961300
H 3.90799600 3.50792900 1.41391400
C 3.00647000 3.17940500 0.91009500
C 2.60647600 1.79606500 0.74761900
H 1.98734100 5.01545100 0.23206100
N 1.42461600 1.72662700 0.06463700
C 1.05814300 3.01345800 -0.20968100
C 2.04243000 3.93647000 0.31706600
C 0.87543100 -3.32899500 0.13823700
H 1.00280000 -4.38918200 0.33910300
H 4.61179600 -1.63280500 2.26501200
C 3.68932800 -1.73355500 1.70516700
C 2.99683000 -2.86925900 1.40914500
H 3.23359200 -3.89256600 1.67554300
C 1.83932900 -2.46056200 0.64404500
N 1.83897700 -1.10113700 0.48098000
C 2.95245600 -0.63169500 1.12468800
C 3.32130300 0.70722300 1.24135600
H 4.24015600 0.92109900 1.78086800
C -0.48477300 0.14149100 1.27398800
C -1.86157500 0.01378600 1.66394600
O -2.84686800 -0.23198600 0.96580200
O -2.02817600 0.20585700 3.04077100
C -3.36802700 0.10299000 3.51923700
H -3.77530900 -0.88973800 3.28622800
H -4.00691200 0.83548000 3.00838800
H -3.25221000 -0.87439900 -2.86142700
Fe 0.43554300 0.02234000 -0.46478700
C -3.34586100 0.34788000 5.01937500
H -2.95198200 1.34497400 5.24760200
H -4.35963300 0.27583800 5.43252500
H -2.71498000 -0.39080300 5.52697300

H 0.16941800 0.34091700 2.12698600
O 1.41839500 0.04782600 -2.07972100
C 1.97985200 -1.06405200 -2.67793600
H 2.56039200 -0.76350200 -3.57324000
H 2.68151300 -1.61723400 -2.02229000
H 1.23016500 -1.80226800 -3.02815100

^{5}TC1^{-}
ub3lyp/def2tzvp,
el. energy = -2674.526215 a.u.
C 2.70949600 1.78041900 0.56859800
N 1.48907700 1.73866700 -0.03425700
H 4.06535700 3.50143000 1.12277000
C 1.10207200 3.01540200 -0.31012500
C 2.13795400 3.93053300 0.14278500
H 2.10046800 5.01007400 0.05161700
C 3.13126400 3.16746700 0.68564700
C -0.09684700 3.38345300 -0.94139700
N -1.12191700 1.18154000 -1.32729600
C -2.24262800 0.71727900 -1.94405700
C -3.00398500 1.84611600 -2.45420500
H -3.94372900 1.77374000 -2.98952700
C -2.30772600 2.97342300 -2.12789800
H -2.56615100 4.00354900 -2.34485400
C -1.11260800 2.54068400 -1.41986300
C 3.43012200 0.66122100 1.01530800
H 4.38510400 0.86452100 1.49436600
H 3.31140300 -3.96339800 1.46766000
C 3.06888100 -2.93815100 1.21262100
C 1.86548300 -2.50999100 0.52073900
H 4.75907200 -1.74300700 1.97132600
N 1.90269700 -1.15407500 0.36708600
C 3.05183700 -0.68920000 0.93579400
C 3.80155100 -1.81379400 1.46801900
C -2.59684700 -0.63375400 -2.06690200
H -3.53381800 -0.84165500 -2.57824200
H -1.35552900 -4.96819200 -0.94600900
C -1.37302300 -3.89137600 -1.06911200
C -2.32647900 -3.13066900 -1.68242900
H -3.24318100 -3.46459900 -2.15473200
C -1.89551200 -1.74707500 -1.58163000
N -0.70080700 -1.70322900 -0.92711600
C -0.34614100 -2.97883300 -0.59572400
C 0.82985400 -3.34792900 0.07627200
H 0.95646000 -4.41040900 0.27055400
C -0.36782100 0.16852400 1.28646200
C -1.70705500 0.05958700 1.79280100
O -2.75089800 -0.18360800 1.18808300
O -1.73923800 0.26804000 3.17377300
C -3.02857700 0.18024200 3.78023700
H -3.45767900 -0.81535300 3.60606000
H -3.71040500 0.90588000 3.31804000
H -0.24811000 4.44951000 -1.09481500
Fe 0.39600700 0.01072900 -0.51092600
C -2.86258600 0.45351600 5.26592900
H -2.44593700 1.45280600 5.43673400
H -3.83373600 0.39428000 5.77309700
H -2.18953400 -0.27866100 5.72658400
H 0.37369200 0.38614400 2.05634100
O 1.24786200 0.01627800 -2.19159100
C 1.73442300 -1.10854700 -2.83653500
H 2.34312700 -0.80491100 -3.71093300
H 2.38632300 -1.73951100 -2.20343100
H 0.93487300 -1.76846300 -3.22760100

^{1cs}TS3^{-}
b3lyp/def2tzvp,
el. energy = -2674.520740 a.u.
im. frequency -310.61
N 0.80332100 -1.52916500 -0.87241400
Fe -0.44301800 0.05213000 -0.41726900
C 0.61402400 -0.71469200 0.92737300
C -0.76129500 -3.38160200 -0.44358300
C -3.57957800 0.32888500 0.86932300
C -3.14254300 -0.96192600 0.58414200
C -3.91649900 -2.16625000 0.79820300
C -3.11569900 -3.20769300 0.43414200
C -1.86001700 -2.63064300 -0.00076900
N -1.90513400 -1.27046500 0.09282100
H -4.93183000 -2.19470000 1.17602000
H -3.33873300 -4.26828700 0.45074000
C 1.52035700 -3.64305500 -1.46728800
C 2.01525000 -1.43508800 -1.54944000
C 2.47103700 -2.75900600 -1.88865800
H 1.51415400 -4.72097000 -1.57907500
H 3.39596500 -2.97199800 -2.41157900
C -3.30476800 2.81316700 1.07690400
C -1.21252100 2.89291400 0.24327400
C -2.29740900 3.68133500 0.79093300
H -4.28205400 3.02607800 1.49437800
H -2.27498300 4.75707600 0.92036900
C 2.64222000 -0.25412400 -1.90035800
C -0.01604600 3.42469300 -0.22532500
C 2.21564000 3.27879400 -1.38025700
C 2.19273600 1.03629100 -1.60337200
C 2.94093400 2.24247700 -1.88664500
H 2.45021000 4.33678700 -1.38987500
H 3.90161800 2.27243800 -2.38732900
C 1.01743300 2.69938300 -0.81188800
C 0.45452700 -2.87915800 -0.87215800
C -2.83302000 1.49226800 0.71381600
N -1.55392000 1.56257100 0.21801100
N 1.02609000 1.33841500 -0.96327900
C 1.90126100 -0.40309200 1.55110700
O 2.96524900 -0.03237800 1.08423600
O 1.72644400 -0.53048500 2.91731100
C 2.81849200 -0.07887300 3.72873500
H 3.07702000 0.95197100 3.45968200
H 3.70222700 -0.69880500 3.53245200
C 2.38498400 -0.18015100 5.18028400
H 3.20088100 0.14048200 5.83962300
H 1.51484600 0.45680300 5.37375900

H 2.11876500 -1.21127100 5.43922700
O -1.25318700 0.01717700 -2.18178400
C -0.90831900 0.87717800 -3.19671100
H 0.13792000 0.77563800 -3.56346300
H -1.55075700 0.69264400 -4.08615500
H -1.04067600 1.95596600 -2.95177000
H 0.15215300 -1.57179700 1.41662600
H -0.88811700 -4.46050600 -0.48527500
H -4.58514300 0.43724600 1.26813800
H 0.10863600 4.50232100 -0.15450700
H 3.58873300 -0.33867900 -2.42778100

^{1os}TS3^{-}
ub3lyp/def2tzvp,
el. energy = -2674.525110 a.u.
im. frequency -453.25

N 0.85653800 -1.34801000 -1.01710800
Fe -0.48338900 0.06279000 -0.43420400
C 0.71152200 -0.72199500 0.85552700
C -0.53818100 -3.36268800 -0.73040000
C -3.55914200 -0.02275600 1.04649200
C -3.05082300 -1.24422600 0.59983500
C -3.72587100 -2.51574900 0.71785500
C -2.86766800 -3.45682300 0.22219300
C -1.68026600 -2.75070400 -0.19368100
N -1.81975400 -1.40988000 0.03275600
H -4.71767600 -2.65775500 1.13110000
H -3.01235900 -4.52829100 0.14520100
C 1.74378900 -3.34970300 -1.77505600
C 2.04138100 -1.10501400 -1.71717600
C 2.60506900 -2.36187300 -2.14680600
H 1.82899000 -4.41473000 -1.95617100
H 3.53813600 -2.45771900 -2.68947800
C -3.43371800 2.43298200 1.51871200
C -1.41436900 2.76549300 0.57324700
C -2.51270200 3.40217700 1.26865200
H -4.39193500 2.52448500 2.01669000
H -2.55797700 4.45668900 1.51465600
C 2.55046100 0.14254100 -2.01039800
C -0.30463100 3.44021100 0.08552200
C 1.85956700 3.57724600 -1.19590400
C 2.00858100 1.37011400 -1.61152300
C 2.64260100 2.64820900 -1.82062000
H 2.01053400 4.64779000 -1.12130600
H 3.57437400 2.79952100 -2.35296400
C 0.74376800 2.85792600 -0.62997000
C 0.62188500 -2.72481000 -1.11997700
C -2.89840500 1.19677200 0.98717800
N -1.66261400 1.41913800 0.42594300
N 0.84951100 1.52200800 -0.90458000
C 1.99303000 -0.36855000 1.45324200
O 2.96780600 0.19730600 0.98140600
O 1.97091300 -0.75171500 2.78463800
C 3.09185300 -0.32912400 3.57012800
H 3.25489600 0.74621500 3.43308900
H 3.99838100 -0.84115600 3.22239800
C 2.79212500 -0.66489800 5.02052200
H 3.63471800 -0.36967400 5.65780600
H 1.89669600 -0.13663900 5.36635600
H 2.62485000 -1.74041300 5.14877600
O -1.35018000 0.11616300 -2.12600200
C -1.15995900 1.10601800 -3.06874200
H -0.13613600 1.14476900 -3.49563700
H -1.84102600 0.93850900 -3.92947100
H -1.38135600 2.12953300 -2.69898000
H 0.30841000 -1.62980400 1.30131200
H -0.57493500 -4.44060100 -0.86692000
H -4.54459700 -0.03028700 1.50499600
H -0.25848800 4.51261200 0.25617500
H 3.48114000 0.17291200 -2.57084800

^{3}TS3^{-}
ub3lyp/def2tzvp,
el. energy = -2674.518246 a.u.
im. frequency -551.57

N -1.07487600 0.95112400 -1.19614800
Fe 0.53949600 -0.00538700 -0.46524100
C -0.92576400 0.56051500 0.76331500
C -0.25367700 3.27750600 -1.12258000
C 3.34241700 1.03806600 1.23421400
C 2.58804400 2.02617800 0.59000800
C 2.90816000 3.43287000 0.59182000
C 1.89395400 4.06668900 -0.07368700
C 0.96487700 3.04314700 -0.47234100
N 1.41630000 1.81048100 -0.07897700
H 3.78859800 3.86833200 1.04988200
H 1.77348800 5.12613400 -0.26752000
C -2.38977800 2.55942300 -2.22635400
C -2.11207600 0.33461800 -1.90194300
C -2.95026900 1.34875800 -2.49731600
H -2.72782300 3.53958600 -2.54120400
H -3.84045200 1.13851400 -3.07823400
C 3.78746400 -1.29634300 2.03544000
C 2.02836300 -2.25121100 0.99720800
C 3.17183600 -2.49602700 1.85059800
H 4.67872400 -1.07839900 2.61245200
H 3.45448200 -3.46686500 2.24069800
C -2.26704600 -1.02552000 -2.06667200
C 1.17522600 -3.23828000 0.52598800
C -0.78324300 -4.05887400 -0.82781000
C -1.45128800 -2.02534200 -1.52293800
C -1.73258000 -3.43443100 -1.59006600
H -0.67386000 -5.11657300 -0.61902200
H -2.56640000 -3.87612300 -2.12302000
C 0.08138600 -3.02406900 -0.31960500
C -1.18916800 2.32193200 -1.46351200
C 3.01949600 -0.31151300 1.30037500
N 1.95140400 -0.91462900 0.68554000
N -0.33224000 -1.79998600 -0.77126600
C -2.13947600 -0.01166400 1.31059300
O -2.82453600 -0.94731000 0.91242300
O -2.48021200 0.65806300 2.48272400

C -3.58233500 0.11014000 3.21087600
H -3.43281600 -0.96643300 3.35640800
H -4.50772500 0.23080900 2.63178900
C -3.66753000 0.84153200 4.53986000
H -4.50840200 0.45749500 5.13051300
H -2.74803200 0.70385900 5.11961600
H -3.81732800 1.91662400 4.38822000
O 1.50153300 -0.08336400 -2.07305700
C 2.09720100 -1.22452100 -2.58220500
H 1.37881800 -2.02879600 -2.83378700
H 2.63727800 -0.98190600 -3.51885300
H 2.84524200 -1.67210100 -1.89793600
H -0.75066600 1.56428600 1.14510100
H -0.48070200 4.30557500 -1.39319700
H 4.23901600 1.36070800 1.75658400
H 1.37420100 -4.26127400 0.83396500
H -3.12609100 -1.35291500 -2.64653200

^{5}TS3^{-}
ub3lyp/def2tzvp,
el. energy = -2674.504108 a.u.
im. frequency -319.89

N 1.08342200 -0.90920200 -1.29719900
Fe -0.54339100 0.08322400 -0.55537900
C 0.84323200 -0.65278400 0.81009200
C 0.10793400 -3.19967500 -1.34002400
C -3.36799000 -0.97189000 1.18434500
C -2.67596000 -1.99257200 0.51052700
C -3.03524100 -3.40380800 0.46362500
C -2.05438300 -4.03455800 -0.24980700
C -1.09579800 -3.00842400 -0.63455000
N -1.51948000 -1.80488700 -0.17353700
H -3.91386800 -3.84635100 0.91947300
H -1.97833100 -5.08983500 -0.48697900
C 2.21348100 -2.47177100 -2.53315200
C 2.13101600 -0.27951900 -1.94371500
C 2.85371400 -1.27463400 -2.70211700
H 2.46303100 -3.42599500 -2.98250200
H 3.72455500 -1.06993900 -3.31394500
C -3.75966300 1.37007500 2.05791300
C -1.94421200 2.30850600 1.08439400
C -3.09934800 2.55818400 1.92833900
H -4.66547300 1.16908400 2.61881500
H -3.36047900 3.51720400 2.36135300
C 2.40952500 1.09167900 -1.93634000
C -1.00916200 3.28369700 0.69503200
C 1.08629600 4.14115000 -0.49027700
C 1.68377300 2.11789500 -1.30738900
C 2.04315000 3.52609600 -1.24774500
H 1.02640100 5.18821300 -0.21522600
H 2.91796800 3.97348500 -1.70573700
C 0.13631800 3.10916300 -0.09911700
C 1.07794500 -2.24361300 -1.67075100
C -3.01247800 0.38452000 1.29528000
N -1.92948200 0.99019500 0.72205300
N 0.53116800 1.91919000 -0.62210400
C 2.10151100 -0.23929100 1.38152800
O 2.87416600 0.66033900 1.07012100
O 2.35139400 -1.01977200 2.51107700
C 3.45928900 -0.60570400 3.31374200
H 3.38107900 0.46542100 3.53593200
H 4.39574000 -0.75074600 2.75863200
C 3.44221400 -1.43502900 4.58636500
H 4.28610000 -1.15838900 5.23059600
H 2.51364100 -1.27222900 5.14506500
H 3.51975700 -2.50445900 4.35939000
O -1.47097800 0.33965600 -2.16624900
C -2.08375000 1.49029100 -2.62236700
H -1.38688300 2.34306200 -2.75061600
H -2.54649400 1.31803400 -3.61554800
H -2.89889800 1.84604000 -1.95952300
H 0.61001000 -1.69126500 1.02544000
H 0.30632400 -4.20870800 -1.69466500
H -4.27647400 -1.26666300 1.70526400
H -1.19413200 4.29130400 1.06128900
H 3.30004500 1.39213700 -2.48370800

^{1cs}BC^{-}
b3lyp/def2tzvp,
el. energy = -2674.539610 a.u.

N -0.91795600 1.96205300 0.15218300
Fe 0.38356400 0.02391600 -0.52514800
C -0.54831000 0.91032800 1.08194300
C 1.09998600 3.37589200 0.36076600
C 3.54957200 -0.83155200 0.14900000
C 3.26021500 0.52637700 0.28452000
C 4.20054300 1.54631300 0.68030400
C 3.49297600 2.71326500 0.74982100
C 2.12459900 2.39906000 0.40345900
N 2.01124200 1.06646500 0.10722100
H 5.25183300 1.38201700 0.88558400
H 3.85050900 3.70034700 1.02014600
C -1.18291500 4.17398200 -0.37201200
C -2.13507800 2.10778800 -0.53358600
C -2.31308300 3.51782700 -0.76862000
H -0.94386000 5.22066800 -0.51435100
H -3.16681800 3.93392900 -1.28925800
C 2.96450900 -3.24839900 -0.23029800
C 0.77971500 -2.89890200 -0.67813300
C 1.81713200 -3.90359000 -0.55244600
H 3.95146100 -3.66218300 -0.05910500
H 1.66736300 -4.96623900 -0.70368400
C -2.90399400 1.09491800 -1.06840200
C -0.53290500 -3.15293300 -1.05826100
C -2.89649900 -2.47207600 -1.61655300
C -2.58596300 -0.27082500 -1.20840400
C -3.54136300 -1.26836600 -1.63379700
H -3.29167600 -3.45278300 -1.85397500
H -4.57712000 -1.06500100 -1.88004000
C -1.54039700 -2.19998400 -1.20685300
C -0.24877600 3.20090300 0.12719100
C 2.63841400 -1.83811600 -0.14775600

N 1.29758800 -1.65120400 -0.40441600
N -1.36865900 -0.85448600 -0.98027700
C -1.57749900 0.23894800 1.86375800
O -2.79594400 0.27157000 1.75655600
O -0.96575500 -0.52533400 2.83435100
C -1.84148800 -1.29028200 3.66759400
H -2.43790000 -1.97197000 3.04974700
H -2.54187600 -0.62234100 4.18485200
C -0.97891000 -2.05655000 4.65546600
H -1.61061300 -2.66063900 5.31833100
H -0.28822500 -2.72657200 4.13152300
H -0.38723300 -1.37164700 5.27353200
O 0.84685900 0.49205900 -2.30277700
C 0.32549100 -0.14719400 -3.41070100
H -0.77128800 -0.02777000 -3.54035300
H 0.78647900 0.26386100 -4.33334900
H 0.52485100 -1.23922900 -3.43381200
H 0.27148700 1.23420900 1.71064300
H 1.43378200 4.40840000 0.43782100
H 4.57857900 -1.13769100 0.32205600
H -0.79638100 -4.18826400 -1.26100300
H -3.86863500 1.39993300 -1.46749100

^{1os}BC^{-}
ub3lyp/def2tzvp,
el. energy = -2674.549237 a.u.
N -0.37688600 1.96174900 -0.02586700
Fe 0.39809100 -0.00805600 -0.53714900
C -0.35465700 0.95787100 1.05083000
C 1.82850100 3.04883800 0.34755700
C 3.29655800 -1.59312100 0.23804900
C 3.32644500 -0.19080700 0.32195000
C 4.46367000 0.59489300 0.69917800
C 4.03476200 1.90282200 0.74592500
C 2.64789200 1.89175300 0.39664300
N 2.23437900 0.61220200 0.12155100
H 5.45019100 0.20209400 0.91600100
H 4.60490000 2.78810200 1.00370500
C -0.27631000 4.26751200 -0.26754800
C -1.57654100 2.43277000 -0.66554400
C -1.49587300 3.86558800 -0.72408300
H 0.12554700 5.27378800 -0.26678500
H -2.27059700 4.48631500 -1.15827300
C 2.17022700 -3.80967500 -0.02712200
C 0.12617400 -3.00738000 -0.55402500
C 0.90958500 -4.20641600 -0.34269000
H 3.03577400 -4.42503600 0.18937500
H 0.52597300 -5.21491600 -0.44465200
C -2.53636500 1.65980900 -1.24994400
C -1.18729400 -3.00183200 -0.97903900
C -3.30575500 -1.84212400 -1.70913100
C -2.54668100 0.25022300 -1.37676700
C -3.67266900 -0.51831800 -1.80838900
H -3.89746800 -2.72310700 -1.92905400
H -4.62812900 -0.10669300 -2.11190200
C -1.95450600 -1.85330500 -1.23868400
C 0.48827200 3.10856000 0.09164700
C 2.17609600 -2.36055600 -0.02491200
N 0.91349000 -1.89046200 -0.32843300
N -1.49943600 -0.57098300 -1.05642600
C -1.55558000 0.62105900 1.81868000
O -2.71597600 0.96481000 1.66377600
O -1.18474800 -0.21602800 2.84206100
C -2.25351000 -0.69456900 3.66968500
H -2.98760400 -1.22162500 3.04963200
H -2.76796900 0.15584200 4.13386000
C -1.64936800 -1.61462300 4.71490200
H -2.43670700 -2.00217900 5.37294900
H -1.14511100 -2.46436700 4.24189700
H -0.91660000 -1.08209500 5.33171000
O 0.95938300 0.29292600 -2.29088800
C 0.38322500 -0.30450500 -3.40195900
H -0.64124800 0.05151500 -3.62384800
H 0.99475700 -0.08210000 -4.29883000
H 0.33108300 -1.40812400 -3.32766100
H 0.48880000 1.13146900 1.70882900
H 2.33561300 4.00246900 0.47525400
H 4.22327700 -2.12312200 0.44168600
H -1.66412200 -3.96581800 -1.13637700
H -3.39863800 2.18903000 -1.64825400

^{3}BC^{-}
ub3lyp/def2tzvp,
el. energy = -2674.548077 a.u.
N 0.34687600 -1.99290100 -0.00059400
Fe -0.41910700 -0.01337900 -0.54087100
C 0.37938100 -0.96199800 1.04291500
C -1.86926300 -3.02520000 0.44824600
C -3.26980400 1.64591500 0.30826700
C -3.31488900 0.24144000 0.39869400
C -4.45643200 -0.52203600 0.80508500
C -4.05024100 -1.83765200 0.86280900
C -2.66952100 -1.85511500 0.49391400
N -2.24104200 -0.58518100 0.19146400
H -5.43357500 -0.11059700 1.03017300
H -4.63075400 -2.70789300 1.14674700
C 0.18276100 -4.29128000 -0.25321600
C 1.50622800 -2.48230500 -0.69322100
C 1.38811300 -3.91179400 -0.76317200
H -0.24601000 -5.28622400 -0.25014800
H 2.12421200 -4.54464600 -1.24448900
C -2.10660000 3.85221400 0.05819200
C -0.09522300 3.01119400 -0.53345400
C -0.84233700 4.22638500 -0.27479700
H -2.94960500 4.48426300 0.31283000
H -0.43483800 5.22762300 -0.35389700
C 2.45815700 -1.72149600 -1.31153500
C 1.21245600 2.97331700 -0.98318000
C 3.28398400 1.76608500 -1.77092400
C 2.48974400 -0.31425500 -1.44034800
C 3.61946100 0.43578500 -1.89204300
H 3.88996500 2.63597600 -1.99582500

H 4.55962000 0.00791500 -2.22023900
C 1.94270700 1.80414700 -1.26929800
C -0.53749400 -3.11565100 0.14951700
C -2.14677900 2.40319500 0.02409000
N -0.90731700 1.91644100 -0.32812700
N 1.46676400 0.52972000 -1.08871700
C 1.62164900 -0.63992500 1.75381700
O 2.75371600 -1.06342400 1.58766300
O 1.33429000 0.27946400 2.72934900
C 2.44242300 0.70596900 3.53343200
H 3.17356400 1.22508600 2.90254400
H 2.94323200 -0.16981800 3.96290600
C 1.89710500 1.61989700 4.61598000
H 2.71401800 1.96813800 5.25968400
H 1.40537500 2.49552900 4.17837000
H 1.16640700 1.09405600 5.24096700
O -1.00745100 -0.29741300 -2.28800900
C -0.59995500 0.45794700 -3.37759200
H 0.42986700 0.22921400 -3.71390700
H -1.26388200 0.26021600 -4.24227500
H -0.64190800 1.54817900 -3.19290400
H -0.44130100 -1.09796700 1.73828400
H -2.39123700 -3.96763100 0.59697100
H -4.18560700 2.18404600 0.53849900
H 1.71751100 3.92363600 -1.13474100
H 3.29652700 -2.26552100 -1.74017400

^{5}BC^{-}
ub3lyp/def2tzvp,
el. energy = -2674.561571 a.u.

N 0.82390300 -1.98562000 0.12127200
Fe -0.54477400 -0.05528800 -0.79749100
C 0.70810800 -1.00245000 1.13596900
C -1.29554900 -3.26255700 0.49488400
C -3.48312400 1.09890300 0.59723800
C -3.25785100 -0.28476000 0.73156600
C -4.20859000 -1.24166100 1.26479000
C -3.59132400 -2.46300000 1.24754400
C -2.26015100 -2.25093500 0.71589000
N -2.10036700 -0.93139200 0.40236100
H -5.20700800 -1.00545000 1.61506900
H -3.99178200 -3.41593500 1.57458400
C 0.77606600 -4.12863300 -0.67332300
C 1.91974700 -2.15421800 -0.73427200
C 1.91090400 -3.53639500 -1.14799900
H 0.40107600 -5.11602500 -0.91190200
H 2.63670200 -3.96039700 -1.83069700
C -2.83474100 3.51003200 0.10933600
C -0.74749300 3.02686200 -0.62740100
C -1.69713000 4.09694400 -0.36746200
H -3.75222600 3.99547100 0.42243200
H -1.50707900 5.15370900 -0.51754400
C 2.75181100 -1.15995200 -1.25362800
C 0.56545100 3.18812300 -1.09946600
C 2.91040700 2.42844400 -1.71883800
C 2.54044400 0.22879400 -1.33953700
C 3.52296300 1.20807000 -1.76411500
H 3.34081500 3.39874000 -1.93896000
H 4.55007400 0.98837000 -2.03247100
C 1.54212600 2.19348500 -1.28784800
C 0.02466700 -3.14605200 0.06736200
C -2.58796200 2.07776200 0.14314000
N -1.32615400 1.83073200 -0.31894000
N 1.35660400 0.85602000 -1.07868200
C 1.84415700 -0.46318000 1.80083400
O 3.04523100 -0.59142500 1.54935600
O 1.42816800 0.31248100 2.88012700
C 2.47482300 0.93480700 3.62075200
H 3.06852600 1.58056700 2.96172000
H 3.15737600 0.17442700 4.02309200
C 1.83387000 1.73865800 4.73989100
H 2.60651400 2.23679000 5.33880600
H 1.16351500 2.50508400 4.33514100
H 1.24877000 1.09112300 5.40332400
O -1.03549500 -0.64842700 -2.53271500
C -0.77011600 -0.03718200 -3.74280800
H 0.30068900 -0.07689600 -4.03496800
H -1.32893400 -0.52097200 -4.57144900
H -1.05615200 1.03575800 -3.76922200
H -0.20979000 -1.04582400 1.69413200
H -1.66678500 -4.28376100 0.55630900
H -4.46022400 1.45440600 0.91707600
H 0.87624900 4.20876700 -1.31179900
H 3.66358700 -1.52911000 -1.71913800

C_2H_2
b3lyp/def2tzvp,
el. energy = -78.628947 a.u.

C 0.66542400 -0.00001500 -0.00004500
H 1.23937600 0.92451900 0.00008100
H 1.23940700 -0.92444100 0.00034400
C -0.66546200 -0.00003300 -0.00015500
H -1.23934000 -0.92450900 0.00025700
H -1.23921200 0.92471700 0.00052000

^{1cs}TS4^{-}
b3lyp/def2tzvp,
el. energy = -2753.159784 a.u.
im. frequency -310.46

C -0.73763000 2.86304900 -0.76695600
N -0.89557400 1.50930800 -0.86876400
H -2.05499000 4.61772100 -1.27813900
C -2.13339100 1.30141400 -1.40872400
C -2.78882100 2.57193800 -1.65768600
H -3.77621500 2.68611400 -2.09009100
C -1.92601200 3.54188800 -1.24737000
C -2.70509100 0.05596500 -1.66119300
N -0.86517900 -1.37323400 -0.88532400
C -0.68994600 -2.72540700 -0.78978000
C -1.88165900 -3.41911400 -1.23212800
H -1.99974900 -4.49628800 -1.25403000
C -2.76904000 -2.46035500 -1.61857000

H -3.76702600 -2.58794500 -2.02200900
C -2.12209000 -1.18238700 -1.39358800
C 0.41447000 3.50460200 -0.31564300
H 0.39593600 4.59106100 -0.28129200
H 4.85924600 2.76117200 0.71395000
C 3.80802200 2.62767500 0.48583900
C 3.15833300 1.34722600 0.28098200
H 2.94773200 4.65720800 0.39266100
N 1.82978900 1.52812000 0.01344200
C 1.61705300 2.87839800 0.01279300
C 2.84695000 3.57980400 0.32810200
C 0.49051700 -3.35087300 -0.39296100
H 0.49528000 -4.43752200 -0.36956500
H 4.92806200 -2.51493800 0.59138700
C 3.87296700 -2.40292900 0.36981800
C 2.93588000 -3.37589800 0.19565400
H 3.06399600 -4.45140900 0.23691700
C 1.68523200 -2.70183100 -0.08878300
N 1.86440100 -1.34288300 -0.06273600
C 3.19104000 -1.13442400 0.20821500
C 3.79910000 0.11132600 0.36015100
H 4.86340700 0.11759500 0.58180600
C -0.31442600 0.25688600 1.36671600
C -1.52567500 -0.49163500 1.82458700
O -1.57853000 -1.63872200 2.23696500
O -2.64573200 0.28041800 1.71089500
C -3.89779900 -0.37625500 1.97748300
H -3.85607600 -0.84534600 2.96673900
H -4.04979400 -1.17251100 1.24034700
H -3.70504600 0.04881700 -2.08806000
Fe 0.48037300 0.07436300 -0.39590500
C -4.99491800 0.67026000 1.90375900
H -5.02471900 1.14005600 0.91526500
H -5.96946100 0.20424400 2.09406200
H -4.83908600 1.45694100 2.65067100
H -0.37803800 1.30056000 1.68233800
O 1.06368700 0.26498000 -2.23463000
C 0.90903600 -0.70044700 -3.20013200
H 1.50218600 -0.43461700 -4.10289800
H 1.25457700 -1.71495100 -2.90185000
H -0.13574100 -0.82929200 -3.56436000
C 0.51133500 0.21234300 3.89099400
H -0.29889800 -0.26493900 4.43543200
H 0.76826100 1.22754900 4.18551700
C 1.10189000 -0.38737300 2.81941800
H 1.97329200 0.05894300 2.35831500
H 0.93175400 -1.43733600 2.61227200

^{1os}TS4^{-}
ub3lyp/def2tzvp,
el. energy = -2753.172532 a.u.
im. frequency -432.83

C -0.79358900 2.81968100 -0.99711000
N -0.91208500 1.46018400 -1.05925800
H -2.15197100 4.51886100 -1.57433500
C -2.14063600 1.20070300 -1.59841400
C -2.82866600 2.44259200 -1.89019200
H -3.81762700 2.51435600 -2.32748600
C -1.99309100 3.44870700 -1.51163000
C -2.67112300 -0.06614000 -1.82767300
N -0.79670600 -1.42331000 -1.00042000
C -0.58375700 -2.76784100 -0.87566900
C -1.73537900 -3.50333800 -1.35390200
H -1.81904600 -4.58364400 -1.36313900
C -2.64254000 -2.57777500 -1.77078000
H -3.62648900 -2.74011000 -2.19497700
C -2.04510500 -1.27780500 -1.54096300
C 0.32284500 3.50912200 -0.53013300
H 0.27574200 4.59478900 -0.53647200
H 4.67967900 2.90772300 0.88736900
C 3.65676500 2.74183600 0.57016400
C 3.05207600 1.43965200 0.36995600
H 2.77090100 4.74567400 0.30924800
N 1.75271600 1.58075400 -0.03016800
C 1.51301400 2.92445700 -0.10295400
C 2.69795300 3.66472800 0.28165400
C 0.58310300 -3.35397700 -0.39238400
H 0.61629500 -4.43910100 -0.34760900
H 4.87108600 -2.35338100 1.00716100
C 3.84152400 -2.28104800 0.67670000
C 2.95838900 -3.28806300 0.42753600
H 3.11350000 -4.35748400 0.50768100
C 1.72383800 -2.66276300 0.00510500
N 1.86072500 -1.29911500 0.01385300
C 3.14344900 -1.03989700 0.41627300
C 3.70535100 0.22583600 0.57622800
H 4.74139900 0.26887900 0.90149800
C -0.39063100 0.27170900 1.31936400
C -1.55410600 -0.49489100 1.78382400
O -1.61803600 -1.68410700 2.06905600
O -2.67642200 0.30431400 1.88955300
C -3.89162400 -0.36550800 2.24571200
H -3.78881300 -0.81197200 3.24291700
H -4.08111300 -1.18504200 1.54286400
H -3.66688000 -0.11464600 -2.26042800
Fe 0.47278900 0.07330000 -0.49862500
C -5.01030600 0.66154400 2.21271900
H -5.11288700 1.09217200 1.21043500
H -5.96386000 0.19369600 2.48743900
H -4.81409500 1.47939800 2.91547300
H -0.50535700 1.32900800 1.56434400
O 1.14997600 0.18706400 -2.26811400
C 1.41163200 -0.89785000 -3.08277200
H 1.79630100 -0.54855900 -4.06233800
H 2.18098900 -1.58662300 -2.67681200
H 0.52215600 -1.52090800 -3.30617800
C 0.43075400 0.36205100 4.15531800
H -0.31683700 -0.16479600 4.74470600
H 0.64366300 1.38875200 4.44716200
C 0.96373700 -0.18348900 3.01921500
H 1.79276400 0.30904000 2.52515600
H 0.84803900 -1.24302500 2.81742400

^{3}TS4^{-}
ub3lyp/def2tzvp,
el. energy = -2753.166514 a.u.
im. frequency -397.00

C -1.14387100 2.64555400 -1.09186700
N -1.07957400 1.28066200 -1.12874000
H -2.70872300 4.13874500 -1.71466400
C -2.25547300 0.85216500 -1.67620400
C -3.09884700 1.98608100 -1.99842100
H -4.08306900 1.91828700 -2.44674600
C -2.40912900 3.10066200 -1.63158000
C -2.60593500 -0.47816600 -1.89044300
N -0.57119100 -1.55219800 -1.02474700
C -0.18341100 -2.85450300 -0.86391300
C -1.21938100 -3.74536900 -1.33749900
H -1.15958000 -4.82712100 -1.32139300
C -2.23574900 -2.95782300 -1.78511400
H -3.18508400 -3.25844800 -2.21254900
C -1.82136800 -1.58658100 -1.57961000
C -0.13797900 3.48674200 -0.62464700
H -0.32749300 4.55628000 -0.65577700
H 4.20014900 3.49007200 0.96647000
C 3.22285900 3.18512400 0.61114800
C 2.80565900 1.81238000 0.41590600
H 2.09232600 5.04917800 0.27048900
N 1.51761600 1.77313100 -0.04149100
C 1.10488200 3.07225400 -0.15170700
C 2.16374900 3.96788500 0.26274500
C 1.03725100 -3.27333000 -0.34227000
H 1.20927500 -4.34378000 -0.27245900
H 5.09181800 -1.68822100 1.20293000
C 4.07856900 -1.76078900 0.82572500
C 3.35024500 -2.88028500 0.56085200
H 3.64106300 -3.91802400 0.67346800
C 2.06236300 -2.43039300 0.07612600
N 2.01441900 -1.06247300 0.05877400
C 3.23237600 -0.62911100 0.50783000
C 3.60905900 0.70230600 0.67033100
H 4.61391200 0.89221700 1.03797800
C -0.41864100 0.20765200 1.32736200
C -1.58954800 -0.57821200 1.70776900
O -1.66668900 -1.79447100 1.84970900
O -2.70221800 0.21529400 1.93935700
C -3.91048700 -0.48222900 2.25766400
H -3.80139800 -0.99235300 3.22412000
H -4.09903000 -1.25656500 1.50503300
H -3.58120000 -0.67096700 -2.32934000
Fe 0.47078600 0.10307300 -0.54777000
C -5.03597900 0.53750800 2.29559700
H -5.14484200 1.03041500 1.32294000
H -5.98610900 0.04807200 2.54380300
H -4.84161000 1.31050400 3.04799600
H -0.52815800 1.25036200 1.63123400
O 1.13566800 0.27411200 -2.29858800
C 1.84484600 -0.70705600 -2.96962800
H 2.01172100 -0.39612700 -4.01968300
H 2.84733500 -0.90460700 -2.54031900
H 1.32059700 -1.68173000 -3.01094200
C 0.35307800 0.08503500 4.25796200
H -0.38067500 -0.50783300 4.80047400
H 0.53839400 1.08954600 4.63433600
C 0.90138200 -0.35258400 3.08620300
H 1.71251200 0.19949800 2.62573600
H 0.80135500 -1.39013800 2.78659800

^{5}TS4^{-}
ub3lyp/def2tzvp,
el. energy = -2753.148309 a.u.
im. frequency -381.76

C -0.44505100 3.01264900 -0.70872300
N -0.74780000 1.69901100 -0.92599400
H -1.62791400 4.90936600 -1.02690200
C -2.02187600 1.62912800 -1.41432500
C -2.55845900 2.97466600 -1.52526500
H -3.54897200 3.22263400 -1.88906700
C -1.58620200 3.82794600 -1.08904600
C -2.70086700 0.44817300 -1.75294800
N -0.99111700 -1.23093000 -1.21286300
C -0.88632200 -2.58735200 -1.27932800
C -2.12839500 -3.12898500 -1.80275800
H -2.33114600 -4.18160300 -1.96315700
C -2.95867800 -2.06999400 -2.03688700
H -3.96803400 -2.08817200 -2.43162600
C -2.22731000 -0.87174000 -1.66206000
C 0.77102400 3.49564000 -0.19852300
H 0.85621400 4.57599700 -0.10656400
H 5.02363100 2.24349500 1.20400400
C 3.99334300 2.22774400 0.86723000
C 3.22996200 1.02806300 0.56310900
H 3.39535700 4.34603800 0.74632200
N 1.97458000 1.38963000 0.17358800
C 1.89644500 2.74854800 0.18839100
C 3.16828500 3.29161300 0.63813500
C 0.24244000 -3.33465000 -0.90765000
H 0.16855200 -4.41125200 -1.04293300
H 4.60584200 -3.05657100 0.66662900
C 3.59685500 -2.81527800 0.35228000
C 2.62482500 -3.66953100 -0.07976500
H 2.68456000 -4.74616600 -0.19064300
C 1.45669600 -2.85809900 -0.38895100
N 1.74057500 -1.55321200 -0.12144400
C 3.02933300 -1.47561200 0.31207200
C 3.70945800 -0.29039500 0.63834600
H 4.74006200 -0.40578100 0.96631900
C -0.34242800 0.10725600 1.33347700
C -1.54318800 -0.65062000 1.70971300
O -1.66621100 -1.86572600 1.79390200
O -2.59436000 0.18011100 2.04132500
C -3.81823000 -0.47064700 2.40500300
H -3.65595800 -1.09264500 3.29415100

H -4.13325600 -1.13837800 1.59450700
H -3.71386500 0.56964400 -2.12951500
Fe 0.49265200 0.06430400 -0.53066700
C -4.85332700 0.60965000 2.66718900
H -5.01444000 1.22017100 1.77168200
H -5.81067200 0.15637500 2.95273200
H -4.53205600 1.27326200 3.47823200
H -0.42116700 1.15055000 1.64276600
O 1.32269700 0.09638700 -2.22872100
C 0.70080300 0.49376200 -3.40038500
H 1.35906000 0.27259000 -4.26398000
H -0.25569800 -0.02895300 -3.59407100
H 0.48531500 1.57970300 -3.44262400
C 0.35028300 -0.12203300 4.23808600
H -0.42271100 -0.70416100 4.73558300
H 0.54794300 0.86885100 4.64272500
C 0.93910400 -0.55446600 3.08588700
H 1.78093400 -0.01610000 2.66590000
H 0.81765000 -1.58107900 2.75799100

^{1os}INT2^{-}

ub3lyp/def2tzvp,
el. energy = -2753.205822 a.u.

C -1.00710000 2.74195900 -0.84272300
N -1.04185800 1.37839700 -0.91250400
H -2.47996800 4.35848600 -1.37710500
C -2.25834200 1.04840600 -1.43820800
C -3.02635200 2.24693900 -1.71072600
H -4.02255500 2.26026700 -2.13723700
C -2.25282100 3.30009500 -1.32851300
C -2.71976900 -0.24677900 -1.65819300
N -0.75320200 -1.48422400 -0.85982200
C -0.46338800 -2.81392300 -0.71499300
C -1.59321200 -3.61826000 -1.12491400
H -1.62292600 -4.70104500 -1.10157200
C -2.55931200 -2.75143200 -1.53703300
H -3.54733300 -2.97608800 -1.92142600
C -2.02392700 -1.41739900 -1.36328600
C 0.08388200 3.49951600 -0.42224700
H -0.03240900 4.57988700 -0.41389800
H 4.56894000 3.16567400 0.63146400
C 3.53552900 2.93725200 0.39857200
C 3.00177800 1.60155100 0.22735200
H 2.50354600 4.88206300 0.25448100
N 1.66498100 1.66203400 -0.05523900
C 1.33554800 2.98880200 -0.08777300
C 2.49786400 3.79924700 0.21236100
C 0.75981000 -3.32763900 -0.29316200
H 0.85263400 -4.40812200 -0.22777200
H 5.08723100 -2.06879400 0.71795600
C 4.03124600 -2.05967600 0.47468400
C 3.18617900 -3.11781400 0.32695100
H 3.40565800 -4.17493100 0.41793200
C 1.88855300 -2.56829000 0.00042300
N 1.94823300 -1.19967900 -0.02807600
C 3.24621500 -0.86439200 0.25334900
C 3.74720900 0.43179400 0.35712900
H 4.80324300 0.53811100 0.59018300
C -0.20015100 0.21189200 1.62350500
C -1.44553500 -0.52742500 1.88353400
O -1.55339200 -1.68937700 2.26247900
O -2.57078600 0.24232800 1.67809800
C -3.82579700 -0.41263600 1.87993400
H -3.82474300 -0.92285800 2.85003500
H -3.97063800 -1.18111700 1.11067000
H -3.71902700 -0.35505600 -2.07143000
Fe 0.45097700 0.08514800 -0.46338700
C -4.91758800 0.64233800 1.81370600
H -4.90734600 1.15750900 0.84717800
H -5.90220500 0.17681800 1.94774800
H -4.78432500 1.39468600 2.59971800
H -0.39434200 1.28465300 1.67051900
O 0.98442700 0.23056400 -2.26754600
C 1.35069800 -0.84397600 -3.06002000
H 1.65254500 -0.48082200 -4.06204400
H 2.21100900 -1.41797600 -2.66324400
H 0.53335600 -1.57309500 -3.22715200
C 0.53768600 0.23334200 4.03344700
H -0.19878400 -0.33120700 4.60175900
H 0.72884300 1.25373800 4.36383900
C 0.89877800 -0.18749800 2.64596600
H 1.84276700 0.27868100 2.35286300
H 1.03627400 -1.27308700 2.60513000

^{3}INT2^{-}

ub3lyp/def2tzvp,
el. energy = -2753.206292 a.u.

C -0.88313400 2.81381300 -0.79036300
N -0.98167200 1.45447200 -0.89114400
H -2.28099800 4.50849200 -1.27933400
C -2.21363700 1.19405600 -1.42060200
C -2.92604800 2.43305600 -1.66089200
H -3.92218700 2.50264200 -2.08198500
C -2.10354700 3.43979000 -1.25669300
C -2.73448400 -0.07208300 -1.67305800
N -0.83554800 -1.41755300 -0.88764400
C -0.61377500 -2.76278900 -0.75863400
C -1.77851700 -3.50348300 -1.18902700
H -1.86172600 -4.58373600 -1.18145100
C -2.69633700 -2.58371500 -1.59845600
H -3.69056500 -2.75366600 -1.99477100
C -2.09761900 -1.28065700 -1.39933600
C 0.24463500 3.51079000 -0.36357700
H 0.17903700 4.59502900 -0.33431300
H 4.72081800 2.93929100 0.62779400
C 3.67441400 2.76647200 0.40533600
C 3.07138600 1.46149200 0.22449400
H 2.74010800 4.76263300 0.30030400
N 1.73629300 1.59377300 -0.04059700
C 1.47407300 2.93477700 -0.05165200
C 2.67931100 3.68212200 0.24415000
C 0.57766600 -3.34249200 -0.33269200

H 0.61455600 -4.42679700 -0.27692600
H 4.96599200 -2.31768500 0.68361600
C 3.91101500 -2.25147000 0.44484300
C 3.01128300 -3.26322500 0.29271200
H 3.17557400 -4.33102800 0.37517400
C 1.74327300 -2.64479100 -0.02736200
N 1.87454800 -1.28149200 -0.04515800
C 3.18844500 -1.01543000 0.23356400
C 3.75557700 0.25330600 0.33886200
H 4.81747600 0.30369700 0.56399200
C -0.17912900 0.21590000 1.64142000
C -1.42755900 -0.52016800 1.90319600
O -1.53467200 -1.67640300 2.29915100
O -2.55181500 0.24324500 1.67547800
C -3.80703200 -0.40819100 1.89014900
H -3.80035300 -0.90927300 2.86483100
H -3.95763900 -1.18363500 1.12905100
H -3.73586100 -0.12281000 -2.09214000
Fe 0.44613800 0.08341000 -0.46811300
C -4.89803200 0.64727300 1.82137300
H -4.89587300 1.15222800 0.84951900
H -5.88183800 0.18401600 1.96842500
H -4.75745200 1.40756900 2.59838800
H -0.36730900 1.28979100 1.68015100
O 1.01064500 0.23117800 -2.26543000
C 1.33368300 -0.84852900 -3.06929400
H 1.61748500 -0.49046200 -4.07858700
H 2.19292300 -1.44028000 -2.69610500
H 0.49837200 -1.56179300 -3.21550400
C 0.54555000 0.24874100 4.03332900
H -0.19648200 -0.31218700 4.59769700
H 0.71536800 1.27882500 4.34516200
C 0.92184800 -0.18650000 2.65416600
H 1.86733100 0.27605500 2.36060800
H 1.05519000 -1.27252100 2.61980800

^{1os}TS5^{-}
ub3lyp/def2tzvp,
el. energy = -2753.197051 a.u.
im. frequency -906.74

C -0.95582400 2.72527100 -0.88741300
N -0.98722900 1.36066700 -0.93829300
H -2.42738600 4.33546300 -1.44770900
C -2.20008300 1.02563200 -1.47340800
C -2.96893600 2.21978900 -1.76336500
H -3.96173000 2.22777900 -2.19815100
C -2.19899500 3.27781100 -1.38641400
C -2.65588300 -0.27258500 -1.68687900
N -0.70351900 -1.49979200 -0.84296800
C -0.41506400 -2.82792600 -0.68891900
C -1.53652900 -3.63895900 -1.11190400
H -1.56421700 -4.72183500 -1.08264000
C -2.49791800 -2.77734700 -1.54606000
H -3.47864500 -3.00672700 -1.94620900
C -1.96623400 -1.44102400 -1.37140800
C 0.13393800 3.48605000 -0.46373700
H 0.01708200 4.56675800 -0.46472900
H 4.58094200 3.17146500 0.74327000
C 3.55875600 2.93736000 0.46937400
C 3.03808000 1.59919100 0.28091400
H 2.52615800 4.87817700 0.28166300
N 1.71236000 1.65036200 -0.05604000
C 1.37803900 2.98101400 -0.09991600
C 2.52520800 3.79512800 0.24070000
C 0.80545800 -3.33307800 -0.24215300
H 0.89862400 -4.41279900 -0.16059000
H 5.09872500 -2.07056100 0.89912400
C 4.05338500 -2.06094400 0.61287000
C 3.20906900 -3.11799200 0.45266500
H 3.42087900 -4.17393300 0.57296600
C 1.92695400 -2.57118500 0.06583300
N 1.99586700 -1.19874300 0.00654500
C 3.28383900 -0.86612000 0.33813500
C 3.78065800 0.43138000 0.44978200
H 4.82654300 0.54150700 0.72403200
C -0.34072800 0.24766700 1.79690500
C -1.59391700 -0.48914300 1.96988200
O -1.70832800 -1.64010900 2.37823000
O -2.69021600 0.26484400 1.64191100
C -3.95921400 -0.38987400 1.75375800
H -4.02257900 -0.90281900 2.71989600
H -4.04594900 -1.15295500 0.97127900
H -3.64876600 -0.38487000 -2.11515800
Fe 0.51815200 0.07575000 -0.50319000
C -5.04063500 0.66791800 1.61701900
H -4.96225500 1.18825400 0.65655900
H -6.03198700 0.20227300 1.68018300
H -4.96115000 1.41465200 2.41551100
H -0.44977500 1.31575400 1.65096000
O 1.00287800 0.19802700 -2.33681000
C 1.36746000 -0.89965000 -3.09262000
H 1.70080100 -0.56516200 -4.09622200
H 2.20974100 -1.48268600 -2.66667300
H 0.54349300 -1.62104200 -3.26990100
C 0.25038900 0.41917000 3.89992200
H -0.52493600 -0.09211700 4.46081600
H 0.39495300 1.47805800 4.09572400
C 0.81526300 -0.19705100 2.68466300
H 1.76585800 0.22968700 2.37052600
H 0.88739400 -1.28440700 2.72769800

^{3}TS5^{-}
ub3lyp/def2tzvp,
el. energy = -2753.204224 a.u.
im. frequency -534.58

C -0.70044900 2.88038200 -0.80564200
N -0.88212700 1.52858900 -0.91535700
H -1.99611000 4.66156900 -1.26896800
C -2.13485500 1.34994700 -1.43374600
C -2.77104900 2.63236400 -1.65807000
H -3.76521800 2.76757800 -2.06795000
C -1.88419600 3.58377600 -1.25532300

C -2.73405000 0.11941400 -1.68995200
N -0.92319400 -1.34430000 -0.91044700
C -0.78138600 -2.70270400 -0.79811400
C -1.98646200 -3.36900100 -1.24107200
H -2.13272000 -4.44257200 -1.24765700
C -2.84837200 -2.39170000 -1.63952800
H -3.84907000 -2.49857100 -2.04178700
C -2.17422900 -1.12857800 -1.42441100
C 0.47036000 3.50254000 -0.37789000
H 0.47243700 4.58867200 -0.34141000
H 4.88024800 2.65020400 0.71008400
C 3.83199700 2.54293900 0.45656600
C 3.15456700 1.27878300 0.25318000
H 3.02753400 4.59426000 0.33548100
N 1.83745100 1.49401200 -0.05258500
C 1.65971500 2.85043000 -0.05860900
C 2.90081300 3.51990800 0.27118300
C 0.37021000 -3.35612000 -0.36769100
H 0.34013200 -4.44125900 -0.32188500
H 4.78416500 -2.61724800 0.77747500
C 3.74363700 -2.48253000 0.50603100
C 2.78655500 -3.43451900 0.32120700
H 2.87939600 -4.51085100 0.40561300
C 1.57088700 -2.73495700 -0.03483700
N 1.78925800 -1.38176600 -0.04632900
C 3.10928700 -1.20202600 0.27497300
C 3.75374300 0.02837800 0.39514000
H 4.80924800 0.01054500 0.65364000
C -0.20237400 0.29176800 1.90186300
C -1.44759400 -0.46061800 2.06735800
O -1.54537400 -1.61410600 2.47299200
O -2.55167700 0.27794500 1.73183100
C -3.81406500 -0.38867500 1.85368000
H -3.86368500 -0.90217500 2.82026000
H -3.90077800 -1.15169100 1.07142100
H -3.73711200 0.13306800 -2.10837800
Fe 0.47245600 0.06949000 -0.54805000
C -4.90690600 0.65861600 1.72737800
H -4.84771000 1.17462300 0.76335400
H -5.89281300 0.18386800 1.80609300
H -4.82357900 1.40968900 2.52138300
H -0.31681400 1.35450300 1.72632100
O 1.06019400 0.16448300 -2.40575900
C 1.34090600 -0.95037000 -3.16547800
H 1.61206200 -0.65982800 -4.20365900
H 2.19685200 -1.55192600 -2.78902500
H 0.48955600 -1.65801500 -3.26478700
C 0.38274100 0.46643800 4.01828200
H -0.37086300 -0.06990700 4.58546800
H 0.49061900 1.53066700 4.20984000
C 0.94961400 -0.13048700 2.78580500
H 1.89531600 0.31178400 2.47440800
H 1.04591600 -1.21642200 2.83079200

^{5}FP-2^{-}
ub3lyp/def2tzvp,
el. energy = -5168.932869 a.u.

N 3.68769300 -2.12893400 0.57359500
Fe 4.51672000 -0.12563500 0.51200500
C 4.62183100 -2.97795100 -1.55812300
C 5.07782500 1.83003500 -2.38381600
C 5.13004000 0.42402100 -2.54130300
C 5.67778800 -0.25500200 -3.70224700
C 5.55533000 -1.59209400 -3.47207300
C 4.92721400 -1.73869100 -2.17084700
N 4.69684100 -0.50126300 -1.62979500
H 6.11198500 0.22333500 -4.56903700
H 5.87025700 -2.39968200 -4.11804100
C 3.59170200 -4.41312400 0.26589800
C 3.07146600 -2.70430900 1.65180600
C 3.01160400 -4.14464500 1.46849700
H 3.70560600 -5.37947300 -0.20511700
H 2.57707300 -4.85235200 2.16149200
C 4.49934900 3.95720600 -1.12173500
C 3.79806500 2.93126900 0.76445200
C 4.01527600 4.21705300 0.12418700
H 4.75360400 4.67543100 -1.88857800
H 3.80762200 5.18395300 0.56257200
C 2.53357900 -2.01671500 2.76767600
C 3.24975500 2.76763700 2.05853700
C 2.20480900 1.39959900 3.92116300
C 2.55316900 -0.61667600 2.95805500
C 1.97995100 0.07013000 4.10578900
H 1.91803700 2.21391100 4.57274200
H 1.47476600 -0.40278100 4.93654900
C 2.89561600 1.53493700 2.64887000
C 4.01563700 -3.13985900 -0.29174700
C 4.60366600 2.51147700 -1.24075900
N 4.16127400 1.92417200 -0.08547000
N 3.09533900 0.29881200 2.09784700
O 6.24274800 -0.15314400 1.29552200
C 7.27021400 -1.06238000 1.15437400
H 7.67975800 -1.11262200 0.12265300
H 8.13044400 -0.80704700 1.80868300
H 6.98706600 -2.10286500 1.42330000
C 1.87772700 -2.84725100 3.83823200
C 2.54454300 -3.08288300 5.04643900
C 0.58368200 -3.40417400 3.66105500
C 1.97162100 -3.85021400 6.06205900
H 3.53557300 -2.65757800 5.17825600
C 0.00583800 -4.17630300 4.68194900
C 0.70247000 -4.39528700 5.86997900
H 2.51448100 -4.02075100 6.98795000
H -0.97929200 -4.59313900 4.52733000
H 0.24030000 -4.99641700 6.64931500
C 4.93862600 -4.22509900 -2.32790100
C 4.25624100 -4.53671600 -3.51611300
C 5.92610300 -5.11700400 -1.87575800
C 4.55128200 -5.69985800 -4.22972100
H 3.48361700 -3.86216200 -3.87492400
C 6.22275100 -6.28014500 -2.58901900
H 6.46730100 -4.88753900 -0.96197800

C 5.53632600 -6.57624900 -3.76883700
H 4.00615700 -5.92299600 -5.14381700
H 6.99451800 -6.95300900 -2.22307500
H 5.76606400 -7.48239400 -4.32399900
C 5.56164000 2.66887200 -3.52827900
C 6.71038900 3.46845100 -3.39996700
C 4.87839700 2.68124200 -4.75636100
C 7.16010300 4.25412800 -4.46279700
H 7.25445500 3.46349700 -2.45961700
C 5.32731600 3.46626700 -5.82014200
H 3.98379800 2.07510600 -4.87011900
C 6.47049500 4.25602600 -5.67750400
H 8.05406700 4.86108400 -4.34148900
H 4.77973300 3.46358600 -6.75959200
H 6.82037100 4.86793900 -6.50524500
C 3.05704900 4.01209700 2.88550000
C 1.87421000 4.79002900 2.82626900
C 4.08419100 4.42083100 3.74465600
C 1.75456800 5.94477800 3.61870500
C 3.96776800 5.56692900 4.53209000
H 4.98836400 3.81991000 3.78623400
C 2.79850700 6.32365800 4.46144800
H 0.84336000 6.52234600 3.56577300
H 4.78112900 5.86138200 5.18981400
H 2.68767300 7.21989300 5.06713000
N 0.85751100 4.35662400 1.95071500
N -0.06750500 -3.15099600 2.43696300
C -0.39695500 4.88140400 1.75641700
O -0.83287700 5.86185600 2.36179900
C -1.22209600 -3.69659700 1.93131700
O -1.96568000 -4.43991100 2.57326800
C -1.53691400 -3.32985000 0.50382500
C -2.84034300 -3.58535100 0.05508000
C -0.59256600 -2.81414800 -0.39807500
C -3.22070000 -3.32654700 -1.26458600
H -3.55049500 -4.00230700 0.76248900
C -0.96366800 -2.54630500 -1.71428900
H 0.43985800 -2.64464200 -0.10909300
C -2.26665300 -2.79738800 -2.14273700
H -0.22764500 -2.14918400 -2.40773400
H -2.54550000 -2.58815000 -3.17258000
C -1.24727200 4.15661100 0.74955300
C -2.63345100 4.28518100 0.89147500
C -0.73601000 3.39380000 -0.31149300
C -3.52491200 3.65451600 0.01851700
H -3.00747500 4.89095900 1.71201400
C -1.61642900 2.77081500 -1.19493300
H 0.33450700 3.30513900 -0.47509200
C -2.99841600 2.89430900 -1.03174900
H -1.22245700 2.17992700 -2.01717800
H -3.66547800 2.38461000 -1.72012300
H 0.42564800 -2.49855500 1.84156200
H 1.06668500 3.48576500 1.47689600
C -5.01851500 3.86117700 0.25257500
H -5.25993600 4.90791500 0.02430900
H -5.20123700 3.75075200 1.32952300
C -5.99510200 2.98856500 -0.50837900
C -6.04079400 1.57611000 -0.29320600
C -6.89049600 3.54435300 -1.39651600
C -6.94078800 0.75630000 -0.96099000
C -7.85253600 2.76132100 -2.08533300
H -6.87170800 4.61765900 -1.57484300
C -7.88224700 1.34423400 -1.87039900
C -8.84957700 0.57726000 -2.58047600
C -9.73837700 1.17776600 -3.44644500
H -8.88466300 -0.49648300 -2.42869200
H -10.46997600 0.57151600 -3.97437100
C -9.70765700 2.57769800 -3.65342900
C -8.78214100 3.34852700 -2.98617200
H -10.41322900 3.03948500 -4.33904000
H -8.74699700 4.42483600 -3.13947900
C -6.89020800 -0.72460200 -0.73387200
C -7.82625700 -1.37598500 0.13761700
C -5.89646400 -1.47706800 -1.34341900
C -7.70464700 -2.78612600 0.36299400
C -5.75081100 -2.87834400 -1.10611100
C -6.65141800 -3.49822500 -0.26741200
H -6.55997500 -4.56554400 -0.07657800
C -4.62374600 -3.65994700 -1.75774100
H -4.81564400 -4.72650900 -1.58681500
H -4.64946600 -3.51489200 -2.84369200
C -8.87499300 -0.67671600 0.79970000
C -9.75715100 -1.33596900 1.62890900
H -8.97483300 0.39244600 0.64385500
H -10.55023700 -0.78082200 2.12312100
C -8.63088700 -3.43523000 1.22372200
C -9.63778500 -2.72981900 1.84388800
H -8.52468600 -4.50514200 1.38806700
H -10.33787500 -3.23835200 2.50144500
O -4.97398000 -0.86675000 -2.16637700
O -5.10534800 1.03148400 0.55442100
C -5.35062400 -0.76422600 -3.54053100
H -5.52053700 -1.75117900 -3.99238400
H -6.25505000 -0.15856700 -3.66761800
H -4.51698700 -0.27606000 -4.05192100
C -5.50951300 0.86148400 1.91511000
H -5.83097600 1.81002400 2.36593400
H -6.32208700 0.13208000 2.00588800
H -4.63080500 0.49183100 2.44849100

^{5}FP-2^{-}-EDA
ub3lyp/def2tzvp,
el. energy = -5585.089127 a.u.
N -3.08264100 2.40901000 1.18137400
Fe -4.31956000 0.63712500 1.10608600
C -2.98301600 -3.49416600 -3.45902000
C -4.38290800 3.83780400 -0.37172700
C -6.17142100 -0.53822500 -1.66347700
C -5.93330000 0.85402800 -1.59601900
C -6.62537600 1.84492700 -2.39912700
C -6.13210600 3.06192000 -2.03820000
C -5.12882400 2.82434900 -1.01688200

N -5.04379700 1.47963900 -0.76247000
H -7.40049000 1.64291200 -3.12485000
H -6.43386600 4.02767300 -2.41799900
C -2.61267600 4.66486400 1.24801700
C -2.09774400 2.63706100 2.10537800
C -1.80395900 4.05790300 2.16165500
H -2.65164500 5.71842700 1.01023200
H -1.07774700 4.53003000 2.80908400
C -5.74687000 -2.94773300 -0.98943700
C -4.29918100 -2.48045800 0.68234300
C -4.97714300 -3.54377000 -0.03753300
H -6.37190000 -3.43588600 -1.72384300
H -4.85383700 -4.60302000 0.13917600
C -1.43858100 1.65340200 2.87954400
C -3.35320100 -2.69524300 1.71183500
C -1.54883700 -1.93580600 3.32692600
C -1.69890700 0.26668200 2.83290800
C -1.00105400 -0.72911000 3.63069100
H -1.27003000 -2.90017700 3.72796600
H -0.19843100 -0.53115100 4.32694800
C -2.56936100 -1.69215300 2.32106300
C -3.42054300 3.62262700 0.63962300
C -5.55706300 -1.51377300 -0.84928700
N -4.67007600 -1.26933700 0.16569200
N -2.63560500 -0.35022400 2.04674700
C -2.23377900 -2.94458900 -2.33358500
O -1.75631900 -3.62920600 -1.43476900
O -2.13904700 -1.61758100 -2.45294000
C -1.47568000 -0.86580700 -1.39453600
H -2.10371100 0.01441400 -1.24626300
O -5.65850300 0.82145800 2.43642200
C -6.42446800 1.91207800 2.77707000
H -7.02288200 2.32259600 1.93353800
H -7.16049300 1.66477500 3.57273700
H -5.83244300 2.76807200 3.17289600
H -3.44953100 -2.90384900 -4.23543500
C -0.41011600 2.11844200 3.87468600
C -0.72236400 2.08190900 5.24003900
C 0.87896600 2.57345600 3.49033000
C 0.19418700 2.47349700 6.21586100
H -1.71097700 1.73633500 5.52931300
C 1.80386300 2.96385200 4.47336900
C 1.45754200 2.91242200 5.82270900
H -0.07862200 2.43394900 7.26691700
H 2.78536800 3.29346600 4.16463300
H 2.18839600 3.21913600 6.56694800
C -4.62070300 5.25375000 -0.80330200
C -4.28451500 5.68654800 -2.09760700
C -5.18595000 6.18834700 0.08166000
C -4.50568200 7.00679900 -2.49371500
H -3.83971700 4.98043600 -2.79342500
C -5.40693000 7.50890300 -0.31294500
H -5.46066300 5.86846700 1.08292800
C -5.06741300 7.92390600 -1.60263900
H -4.23280800 7.31933200 -3.49878200
H -5.85019400 8.21187400 0.38803900
H -5.23947600 8.95228200 -1.91038500
C -7.14034300 -1.02107200 -2.69912600
C -8.35135000 -1.63183700 -2.33009400
C -6.85889300 -0.88206400 -4.06961700
C -9.24934500 -2.08751900 -3.29704200
H -8.58908400 -1.73802900 -1.27529900
C -7.75638900 -1.33683300 -5.03730500
H -5.92367600 -0.41894600 -4.37285000
C -8.95569400 -1.94245900 -4.65500500
H -10.18247900 -2.55147500 -2.98709100
H -7.51491100 -1.22162700 -6.09129800
H -9.65527200 -2.29663700 -5.40793900
C -3.23231000 -4.09862600 2.23344400
C -2.08727500 -4.90690900 2.07176700
C -4.32520600 -4.63420200 2.94065900
C -2.05553900 -6.19510900 2.62955600
C -4.28923300 -5.91129100 3.49352600
H -5.20753700 -4.01381200 3.06899800
C -3.14230700 -6.69349100 3.33977300
H -1.16619700 -6.79921700 2.49629500
H -5.14655200 -6.28834100 4.04489100
H -3.09505400 -7.69310700 3.76406400
H -1.47980800 -1.45851500 -0.48089600
N -0.96406500 -4.45053700 1.32874800
N 1.17355900 2.64375000 2.11116500
C 0.32538600 -4.55041500 1.79549900
O 0.59364800 -4.94888100 2.93012900
C 2.34567300 3.00253200 1.49232600
O 3.40598500 3.19672800 2.09140100
C 2.27002200 3.15431900 -0.00387200
C 3.47752600 3.06424300 -0.71396400
C 1.08574000 3.44611100 -0.69345800
C 3.51979700 3.22637200 -2.09870500
H 4.38345000 2.86532400 -0.15352200
C 1.11808900 3.61675300 -2.07919800
H 0.14609800 3.58411300 -0.16704700
C 2.31966100 3.49952500 -2.77442900
H 0.20018300 3.84825900 -2.61280000
H 2.33119500 3.62924200 -3.85494200
C 1.42588800 -4.15529100 0.84847900
C 2.65637000 -3.79883200 1.41271300
C 1.30163800 -4.21462400 -0.54715700
C 3.76662700 -3.48911000 0.62009400
H 2.73667800 -3.78191200 2.49577000
C 2.40202200 -3.90590700 -1.34630600
H 0.36332800 -4.50604700 -1.00516800
C 3.62361200 -3.54570700 -0.77176000
H 2.31172400 -3.95625500 -2.42867900
H 4.46866200 -3.31172400 -1.41187400
H 0.40597100 2.37682100 1.50794900
H -1.15211500 -3.94561700 0.46305000
C -0.06710700 -0.49945500 -1.82313600
H -0.07191400 0.07882500 -2.75369700
H 0.40199300 0.11222100 -1.04510600
H 0.55048300 -1.39305300 -1.96397300
C 5.09074700 -3.16494400 1.31337500

H 5.45820900 -4.08345400 1.79082600
H 4.88282200 -2.46288700 2.12674400
C 6.19233600 -2.62281700 0.42839100
C 6.24931000 -1.23115800 0.10881100
C 7.14625200 -3.46134600 -0.10761400
C 7.21668400 -0.71169100 -0.74554100
C 8.16387100 -2.98627000 -0.97361700
H 7.12220200 -4.52267800 0.13204100
C 8.19578000 -1.59386000 -1.31464400
C 9.20013300 -1.14976400 -2.22196200
C 10.12723800 -2.02624500 -2.74373700
H 9.23199400 -0.10235900 -2.50212500
H 10.88473200 -1.66174000 -3.43285500
C 10.10245000 -3.39683200 -2.39043300
C 9.13792600 -3.86250700 -1.52551900
H 10.84111600 -4.07708400 -2.80612400
H 9.10195600 -4.91485700 -1.25260600
C 7.18982300 0.74775100 -1.08129800
C 8.17584900 1.65500700 -0.56354900
C 6.15926900 1.24938500 -1.86552400
C 8.07762000 3.05028800 -0.88025400
C 6.02524500 2.64344700 -2.14327400
C 6.98309100 3.50663300 -1.65895500
H 6.89764400 4.57241500 -1.86123100
C 4.81919200 3.15352000 -2.90064700
H 5.04908300 4.15775000 -3.28122200
H 4.63768300 2.52936700 -3.78340100
C 9.24915900 1.23211500 0.27130400
C 10.18001600 2.13123000 0.74562300
H 9.32877000 0.18361100 0.53712100
H 10.98909100 1.78288800 1.38241700
C 9.05677700 3.95015400 -0.37857400
C 10.08994000 3.50440000 0.41453900
H 8.96724600 5.00505400 -0.62797100
H 10.83054200 4.20314900 0.79439100
O 5.17951600 0.41617300 -2.35663100
O 5.27301900 -0.41890100 0.63314000
C 5.50267100 -0.25923900 -3.57202100
H 5.70478800 0.44963800 -4.38764900
H 6.37109800 -0.91706500 -3.45236000
H 4.62742300 -0.86108800 -3.82965500
C 5.63404800 0.29606200 1.82083300
H 5.83435100 -0.39094300 2.65486000
H 6.51679500 0.92435400 1.65803400
H 4.78374800 0.93359600 2.07089800
N -3.19242700 -4.78214300 -3.47682900
N -3.36106100 -5.90703800 -3.48182900

^{1os}INT1-2^{-}

ub3lyp/def2tzvp,
el. energy = -5585.073879 a.u.

N -3.62704700 2.16702200 0.50402400
Fe -3.96791300 0.17294600 0.34833200
C -2.09577000 -0.00051300 -0.83989700
C -4.68643700 2.95962500 -1.58784300
C -5.64985100 -1.81831500 -1.87244400
C -5.60795400 -0.44042300 -2.12917400
C -6.26404500 0.18578700 -3.25420900
C -5.97695900 1.51291900 -3.19114900
C -5.15183700 1.70714700 -2.01980300
N -4.94933900 0.50671700 -1.38495700
H -6.86518200 -0.32940300 -3.98967400
H -6.30439900 2.29456800 -3.86139600
C -3.55014100 4.44065900 0.10111500
C -2.99080200 2.79926000 1.54346000
C -2.95375000 4.22506000 1.30439400
H -3.69214000 5.38354600 -0.40647700
H -2.52321600 4.95892000 1.97110000
C -4.98187700 -3.87109800 -0.58968600
C -3.78948600 -2.80229800 0.99285500
C -4.23773800 -4.09676800 0.52207100
H -5.47648900 -4.59764000 -1.21817700
H -4.00711000 -5.04382700 0.98866500
C -2.42333000 2.18884500 2.67475200
C -3.04015300 -2.61808900 2.16253200
C -1.95292600 -1.16430300 3.89645100
C -2.40795400 0.80337400 2.89350400
C -1.78880300 0.17579600 4.04405100
H -1.62444900 -1.95344400 4.55776600
H -1.29513800 0.69950800 4.84999200
C -2.67063000 -1.36207900 2.65590400
C -3.98755200 3.15189900 -0.38674800
C -4.99050100 -2.43854800 -0.80451100
N -4.24682900 -1.81446400 0.16338300
N -2.92979100 -0.15360200 2.06259100
C -0.99050100 -0.53473200 -0.03309700
O -0.72656000 -1.71887500 0.14028600
O -0.22882700 0.46058700 0.51377100
C 0.94606000 0.04305300 1.24831800
H 1.13217300 0.85184500 1.95969400
O -5.51421700 0.24346800 1.36207100
C -6.49538700 1.21514200 1.20641300
H -6.91236800 1.26018300 0.18451800
H -7.33636000 0.98613700 1.88616900
H -6.14913300 2.23397700 1.46067200
H -1.95699600 1.04197700 -1.10863900
C -1.82117500 3.07153900 3.73261000
C -2.53069900 3.27846300 4.92297200
C -0.55601800 3.69705300 3.58064900
C -2.02713900 4.07569600 5.95076500
H -3.49968600 2.79864700 5.02978700
C -0.04685500 4.49658000 4.61901000
C -0.78151400 4.68102200 5.78898800
H -2.60148500 4.21973100 6.86192700
H 0.92174100 4.95851200 4.49452600
H -0.36735900 5.30431800 6.57779900
C -4.97744600 4.15429900 -2.44479900
C -4.36478400 4.30092700 -3.70087400
C -5.86794100 5.15435700 -2.01855600
C -4.63077200 5.41281200 -4.50252300
H -3.67202200 3.53761300 -4.04452800
C -6.13335600 6.26709900 -2.81886400

H -6.35924700 5.05165700 -1.05488500
C -5.51470500 6.40114700 -4.06392100
H -4.14175600 5.50776900 -5.46898200
H -6.82852900 7.02677500 -2.46980200
H -5.72088700 7.26775700 -4.68708600
C -6.39527100 -2.68971400 -2.84011200
C -7.65836500 -3.21225600 -2.52218900
C -5.83279100 -3.00163900 -4.08849800
C -8.34495000 -4.02091700 -3.43111300
H -8.10285000 -2.97903100 -1.55831800
C -6.51919800 -3.80948100 -4.99719100
H -4.84653100 -2.61631300 -4.33235700
C -7.77834700 -4.32003200 -4.67214300
H -9.32409900 -4.41417800 -3.16867800
H -6.06628400 -4.04384200 -5.95745500
H -8.31270500 -4.94923800 -5.37979800
C -2.72599100 -3.82856800 2.99539700
C -1.51299200 -4.55612400 2.89854000
C -3.70207500 -4.25369900 3.90900300
C -1.33439000 -5.68558200 3.72340200
C -3.51717800 -5.36864400 4.72331400
H -4.62479600 -3.68305200 3.96930600
C -2.32342000 -6.08144500 4.61955000
H -0.40894000 -6.23672400 3.66038100
H -4.29110400 -5.67125000 5.42363000
H -2.15043300 -6.95843200 5.23892800
H 0.71526000 -0.86622100 1.80689800
N -0.53596400 -4.16817100 1.95147100
N 0.13790000 3.50585000 2.36610500
C 0.76473500 -4.62698600 1.89400400
O 1.28056500 -5.32316000 2.77111600
C 1.33656900 4.05283300 1.96060000
O 2.07809500 4.70539000 2.69515900
C 1.69966900 3.80552300 0.52216400
C 3.05915500 3.84594500 0.17908000
C 0.74022300 3.60699600 -0.48128600
C 3.47714600 3.67017200 -1.14318100
H 3.78378300 4.02963200 0.96675500
C 1.14715500 3.42717100 -1.80177600
H -0.31989200 3.62871000 -0.25178200
C 2.50267000 3.45231000 -2.12721600
H 0.40309600 3.27326300 -2.57828800
H 2.80927700 3.31577100 -3.16168300
C 1.56643200 -4.26393000 0.67457800
C 2.96146600 -4.27160400 0.81982100
C 1.01150800 -4.01783700 -0.58767200
C 3.81426100 -4.02871400 -0.25787300
H 3.37203800 -4.48642900 1.80187500
C 1.85611700 -3.78238500 -1.67455900
H -0.06215900 -4.00201800 -0.73307300
C 3.24268100 -3.78505800 -1.51507900
H 1.42334100 -3.59080000 -2.65269400
H 3.88385700 -3.59360500 -2.37182700
H -0.32073000 2.88246600 1.71047800
H -0.78423900 -3.41004900 1.31337700
C 2.12860600 -0.15868800 0.31626900
H 2.34168200 0.75123100 -0.25289400
H 3.02610400 -0.42314900 0.88491500
H 1.93031400 -0.97219800 -0.38689600
C 5.32260500 -4.12242300 -0.05131700
H 5.65176200 -5.12753700 -0.34886300
H 5.52062400 -4.05071200 1.02379200
C 6.18348100 -3.12413800 -0.80183600
C 6.21297900 -1.74337700 -0.42520900
C 6.96753900 -3.53226500 -1.85883600
C 6.98590200 -0.81194900 -1.10430800
C 7.80002200 -2.63170400 -2.57225700
H 6.96133600 -4.57906400 -2.15626400
C 7.81508000 -1.25008100 -2.19339300
C 8.66102500 -0.36491400 -2.92058000
C 9.44358600 -0.82010700 -3.96027000
H 8.68606200 0.68433700 -2.64611100
H 10.08287000 -0.12461800 -4.49806700
C 9.42203100 -2.18504100 -4.33356700
C 8.61516800 -3.06829000 -3.65167400
H 10.04166300 -2.53143400 -5.15648700
H 8.58887900 -4.11950300 -3.92985300
C 6.96318300 0.63692700 -0.71260300
C 7.97909900 1.17374400 0.14860600
C 5.97894400 1.48258400 -1.20901800
C 7.94524400 2.56474100 0.48937300
C 5.95531200 2.87994000 -0.89907400
C 6.92270600 3.38245700 -0.05641700
H 6.92133500 4.44263400 0.18873800
C 4.94054800 3.81238400 -1.54026400
H 5.25854600 4.83835300 -1.31441200
H 5.00429900 3.71468400 -2.63019200
C 9.03080000 0.37727700 0.68486200
C 9.98717000 0.92439000 1.51348800
H 9.07217800 -0.67766600 0.43448900
H 10.78022900 0.29577000 1.91032600
C 8.94394900 3.09734400 1.34889500
C 9.94569000 2.29791100 1.85233000
H 8.90080300 4.15427900 1.60182600
H 10.70384200 2.71683000 2.50869800
O 4.95042300 0.98572700 -1.97789500
O 5.40119500 -1.34825400 0.61421000
C 5.17610200 0.89257100 -3.38533700
H 5.50378500 1.84974700 -3.81271200
H 5.92046400 0.12655300 -3.62593300
H 4.21743700 0.61100900 -3.82771300
C 5.99613800 -1.35466000 1.91456100
H 6.46470600 -2.32076800 2.14370400
H 6.74554800 -0.56260900 2.01817700
H 5.18333200 -1.17579300 2.62250200
N -2.35114700 -0.75153900 -2.05761500
N -2.20711300 -1.90952700 -2.28272000

^{1os}TS2-2^{-}
ub3lyp/def2tzvp,
el. energy = -5585.066729 a.u.
im. frequency -457.81

N -3.66709800 2.16814300 0.49015900
Fe -3.94287700 0.15898200 0.32490400
C -2.12223100 0.10565300 -0.62674800
C -4.69306900 2.92318700 -1.62986300
C -5.50914400 -1.88426900 -1.93923300
C -5.48733700 -0.50537400 -2.20297400
C -6.13602700 0.10441800 -3.34254300
C -5.89128600 1.43923800 -3.27016200
C -5.10123100 1.65630700 -2.07842800
N -4.87454300 0.45964600 -1.44270100
H -6.70950800 -0.42410000 -4.09027000
H -6.23049600 2.21206800 -3.94473300
C -3.61101300 4.43841900 0.06794400
C -3.04116400 2.81451200 1.52590100
C -3.01581800 4.23948900 1.27449100
H -3.76146800 5.37540500 -0.44822200
H -2.59591900 4.98332500 1.93696300
C -4.85275700 -3.91517800 -0.60958700
C -3.75629800 -2.80665700 1.01496100
C -4.15623400 -4.11475800 0.53776400
H -5.30256600 -4.65869300 -1.25172400
H -3.93113700 -5.05251400 1.02553900
C -2.47378600 2.21903100 2.66614500
C -3.06410400 -2.59678400 2.21529400
C -2.04092500 -1.11132000 3.96483800
C -2.46665200 0.83783000 2.91341500
C -1.87128600 0.23026900 4.08841400
H -1.72740900 -1.88866300 4.64724200
H -1.38971700 0.76734200 4.89287900
C -2.73241800 -1.33054700 2.71172400
C -4.02755200 3.13873900 -0.41270600
C -4.88189900 -2.48383400 -0.83817900
N -4.19343300 -1.83684700 0.15402700
N -2.98081000 -0.13356900 2.09487300
C -0.96705000 -0.43488400 0.09993000
O -0.73422800 -1.61698000 0.32543500
O -0.13221000 0.55741100 0.54207400
C 1.06769300 0.13507400 1.23459600
H 1.30563500 0.96073400 1.91014200
O -5.54639200 0.20873300 1.29332000
C -6.53512700 1.16261500 1.11509100
H -6.91767600 1.21745700 0.07778800
H -7.40253900 0.92002800 1.75845900
H -6.21896200 2.18753600 1.39169700
H -1.90919600 1.06908200 -1.08648100
C -1.86887600 3.11768100 3.70900500
C -2.58043900 3.34567700 4.89447200
C -0.60141700 3.73748600 3.54979100
C -2.07765100 4.15692000 5.91143800
H -3.55106600 2.87033700 5.00593400
C -0.09325300 4.55101700 4.57819600
C -0.82984400 4.75578300 5.74347300
H -2.65419500 4.31651200 6.81863900
H 0.87685500 5.00841300 4.44967100
H -0.41531500 5.38980900 6.52351700
C -5.00950700 4.11036500 -2.48782700
C -4.39495000 4.27768000 -3.74049000
C -5.93014300 5.08417100 -2.06423700
C -4.68841200 5.38328800 -4.54125700
H -3.67861700 3.53549800 -4.08227200
C -6.22340200 6.19042200 -2.86371300
H -6.42286700 4.96495700 -1.10325500
C -5.60276500 6.34482300 -4.10546700
H -4.19698500 5.49472600 -5.50479400
H -6.94207600 6.92889500 -2.51673100
H -5.83044800 7.20644900 -4.72807500
C -6.22813200 -2.77438100 -2.90829000
C -7.43728700 -3.39430600 -2.55333300
C -5.70696600 -3.01221600 -4.19086500
C -8.10730100 -4.22465400 -3.45425600
H -7.85245400 -3.21583500 -1.56520400
C -6.37642400 -3.84221200 -5.09227000
H -4.76556800 -2.54947900 -4.47326400
C -7.57948200 -4.45097600 -4.72748500
H -9.04425000 -4.69181800 -3.16084700
H -5.95299600 -4.01736100 -6.07832300
H -8.10051200 -5.09784100 -5.42906200
C -2.75290500 -3.79372900 3.06859300
C -1.53347500 -4.51316900 2.99006300
C -3.73153100 -4.21405000 3.98094100
C -1.34943600 -5.62856500 3.83210000
C -3.54235800 -5.31623300 4.81207100
H -4.65969600 -3.65095600 4.02667700
C -2.34175700 -6.01980800 4.72714900
H -0.41835900 -6.17170600 3.78265800
H -4.31866600 -5.61606000 5.51096800
H -2.16559700 -6.88584800 5.36089300
H 0.84299700 -0.75194000 1.83013400
N -0.55663300 -4.12734000 2.04192900
N 0.09724300 3.52960900 2.33976300
C 0.74018600 -4.59344400 1.97247500
O 1.25937200 -5.29999000 2.83931300
C 1.29782400 4.07353100 1.93458700
O 2.03669100 4.73251400 2.66636800
C 1.66868000 3.82056600 0.49860100
C 3.03074500 3.85187900 0.16358400
C 0.71341100 3.63370600 -0.51080400
C 3.45558400 3.67827100 -1.15694300
H 3.75195400 4.02784300 0.95617200
C 1.12666900 3.45939400 -1.83025300
H -0.34742000 3.65996200 -0.28495100
C 2.48437800 3.47500100 -2.14772000
H 0.38597200 3.31738600 -2.61231000
H 2.79569400 3.34323700 -3.18150100
C 1.53310500 -4.22781200 0.74741100
C 2.92964900 -4.24695200 0.87621500
C 0.96560500 -3.97218800 -0.50728300
C 3.77213200 -4.00676900 -0.21068200
H 3.34980500 -4.46942600 1.85252400
C 1.79915200 -3.73977200 -1.60330100
H -0.11003100 -3.95264900 -0.63916400
C 3.18762200 -3.75413700 -1.46007000

H 1.35687600 -3.54289100 -2.57617000
H 3.82005500 -3.56559100 -2.32391700
H -0.35182700 2.88857300 1.69365900
H -0.80202900 -3.35894000 1.41554000
C 2.19170700 -0.12231600 0.24835700
H 2.39513900 0.76613800 -0.35670100
H 3.11309300 -0.39558400 0.77204300
H 1.93346800 -0.94841500 -0.42045000
C 5.28238600 -4.11457200 -0.02295100
H 5.59800400 -5.12229100 -0.32625900
H 5.49409300 -4.04772900 1.04984500
C 6.14523000 -3.12357000 -0.78174500
C 6.18884600 -1.74259400 -0.40747300
C 6.91763500 -3.53852700 -1.84467100
C 6.95824900 -0.81596600 -1.09734200
C 7.75079500 -2.64465100 -2.56587500
H 6.90152100 -4.58555100 -2.14090700
C 7.77662800 -1.26195400 -2.19114200
C 8.62320800 -0.38388300 -2.92610800
C 9.39648400 -0.84666500 -3.96937100
H 8.65641600 0.66585500 -2.65422400
H 10.03696200 -0.15669700 -4.51280400
C 9.36395100 -2.21242500 -4.33894600
C 8.55607100 -3.08891400 -3.64955900
H 9.97628400 -2.56485400 -5.16475700
H 8.52167200 -4.14069000 -3.92472200
C 6.94051400 0.63492200 -0.71131300
C 7.95411000 1.17178700 0.15234700
C 5.96027800 1.48196700 -1.21373000
C 7.91886000 2.56280300 0.49315000
C 5.93367000 2.87896000 -0.90220300
C 6.89752400 3.38059400 -0.05487700
H 6.89471900 4.44040200 0.19183700
C 4.92204100 3.81261000 -1.54750000
H 5.24288000 4.83799300 -1.32292500
H 4.98911200 3.71262500 -2.63700300
C 9.00573900 0.37599400 0.68976800
C 9.96041900 0.92359600 1.52005000
H 9.04902500 -0.67866700 0.43833900
H 10.75375600 0.29564000 1.91737300
C 8.91549200 3.09569200 1.35492600
C 9.91697100 2.29684000 1.85976800
H 8.87117300 4.15250100 1.60814100
H 10.67361500 2.71607600 2.51765600
O 4.93699200 0.98588900 -1.99029700
O 5.39101100 -1.34029600 0.63985800
C 5.16957400 0.89957300 -3.39700100
H 5.50877500 1.85608300 -3.81667900
H 5.90753800 0.12764500 -3.63837900
H 4.21053100 0.63049800 -3.84648700
C 5.99310500 -1.36144700 1.93688400
H 6.44622700 -2.33610900 2.16037600
H 6.75656500 -0.58272400 2.03850600
H 5.18695800 -1.17098200 2.64940100
N -2.18740600 -0.86526500 -2.16275500
N -1.98584900 -1.98782600 -2.23338000

^{2}FP

ub3lyp/def2tzvp,
el. energy = -2367.868447 a.u.

C 1.69729900 2.48477000 -0.22847800
N 1.61862300 1.10979700 -0.24627600
H 3.39589200 3.94414300 -0.32787300
C 2.92015300 0.66640900 -0.34823500
C 3.83011000 1.78278000 -0.39563700
H 4.90596400 1.69657100 -0.48307400
C 3.07180400 2.91097400 -0.31670200
C 3.30932900 -0.66447100 -0.39032800
N 1.06692900 -1.65578600 -0.24606100
C 0.61371000 -2.95635300 -0.20665200
C 1.72072700 -3.87584300 -0.28400900
H 1.62493700 -4.95442500 -0.27967100
C 2.85328700 -3.12463400 -0.37240300
H 3.88032300 -3.45791200 -0.45349800
C 2.43972600 -1.74518500 -0.34245900
C 0.61421400 3.35088100 -0.17108300
H 0.82543300 4.41569800 -0.15483900
H -3.99311100 3.45640100 -0.21216900
C -2.96177400 3.12676500 -0.20058000
C -2.54164500 1.74732500 -0.21134200
H -1.73605700 4.95976500 -0.16028300
N -1.16785300 1.66187100 -0.20694400
C -0.71742000 2.96197500 -0.17459500
C -1.82932800 3.88101900 -0.17393600
C -0.71674500 -3.34583900 -0.14109300
H -0.92443800 -4.41120100 -0.11592900
H -5.01785800 -1.68921900 -0.19628100
C -3.93885300 -1.77863100 -0.18043400
C -3.18025800 -2.90765400 -0.14641700
H -3.50577900 -3.94028100 -0.12972000
C -1.80153800 -2.48115000 -0.14646800
N -1.72184800 -1.10887000 -0.18199700
C -3.02289000 -0.66368900 -0.19538500
C -3.41246200 0.66741900 -0.21106400
H -4.47703000 0.88030800 -0.21419900
H 4.37143400 -0.87637100 -0.46587100
Fe -0.04041700 0.00006000 0.00841000
O -0.11504000 0.01167100 1.78684000
C 1.04890700 -0.03769700 2.57148400
H 0.73735500 -0.26727700 3.60204300
H 1.75256100 -0.81994700 2.25410100
H 1.58246800 0.92471000 2.58772800

^{4}FP

ub3lyp/def2tzvp,
el. energy = -2367.875729 a.u.

C -1.15493400 -2.78919400 -0.29752400
N -1.35320500 -1.42632300 -0.28688700
H -2.53212700 -4.55322700 -0.39948900
C -2.71670900 -1.24553700 -0.35658000
C -3.38709700 -2.51962500 -0.41045300
H -4.46041200 -2.64796700 -0.47377700

C -2.41841700 -3.47676900 -0.37244400
C -3.36619400 -0.01913500 -0.37705000
N -1.36932700 1.41057600 -0.28563100
C -1.18639100 2.77572400 -0.29741700
C -2.45760700 3.44891100 -0.37307500
H -2.58366900 4.52396800 -0.40088200
C -3.41526200 2.48071700 -0.41034000
H -4.48995000 2.59679100 -0.47411500
C -2.73065100 1.21433200 -0.35577900
C 0.07800100 -3.42368500 -0.25561800
H 0.08538300 -4.50893700 -0.27081800
H 4.61068100 -2.59447100 -0.17988500
C 3.53405800 -2.47950700 -0.18597300
C 2.84582500 -1.21332000 -0.17193000
H 2.70372100 -4.52252600 -0.23803000
N 1.48472200 -1.40945500 -0.19264600
C 1.30307300 -2.77307600 -0.21827000
C 2.57669900 -3.44748400 -0.21539800
C 0.03930400 3.42427900 -0.25618600
H 0.03457500 4.50953700 -0.27223100
H 4.58109400 2.64592800 -0.18269400
C 3.50582700 2.51884300 -0.18786700
C 2.53765300 3.47598700 -0.21708900
H 2.65253800 4.55237400 -0.24053400
C 1.27157300 2.78757300 -0.21875600
N 1.46830100 1.42606800 -0.19222100
C 2.83170600 1.24507000 -0.17231800
C 3.48180800 0.01955400 -0.15336800
H 4.56702400 0.02570400 -0.13767200
H -4.45021000 -0.02509900 -0.43122900
Fe 0.04671000 0.00023300 0.07161000
O -0.00178400 -0.00444400 1.92729400
C -1.07297900 -0.00041500 2.81545400
H -0.70098600 -0.06133600 3.85196100
H -1.67633600 0.92089000 2.73874100
H -1.75066600 -0.85765000 2.66002300

^{6}FP
ub3lyp/def2tzvp,
el. energy = -2367.880187 a.u.

N -1.16353200 1.65371200 -0.27958900
Fe 0.03993000 0.00479400 0.23555200
C -3.34409600 0.52788700 -0.41260200
C -0.46676400 -3.38792700 -0.31946900
C -1.60178500 -2.57663900 -0.34729300
C -2.95929300 -3.05387100 -0.47013100
C -3.76740500 -1.95457100 -0.49892200
C -2.90930100 -0.79782500 -0.39296700
N -1.59868800 -1.20225800 -0.29378400
H -3.24445000 -4.09643500 -0.53864400
H -4.84549100 -1.91854400 -0.59534400
C -3.00559100 3.02661600 -0.45834500
C -0.75355600 2.96527500 -0.30668200
C -1.90492500 3.83151400 -0.41421100
H -4.04485300 3.31750600 -0.54922000
H -1.86360400 4.91263600 -0.46228100
C 2.01666000 -3.82196400 -0.30768900
C 2.63720800 -1.65266600 -0.23172400
C 3.11621800 -3.01555600 -0.27914600
H 1.97980200 -4.90335200 -0.35346300
H 4.15978400 -3.30457700 -0.29670400
C 0.57267900 3.39667000 -0.26772800
C 3.44832000 -0.51740300 -0.21100500
C 3.87891900 1.96633600 -0.23745700
C 1.70815100 2.58567300 -0.23401800
C 3.07092500 3.06537900 -0.25147600
H 4.96121100 1.93029400 -0.25131100
H 3.35966900 4.10877300 -0.27971000
C 3.01433200 0.80885300 -0.21130500
C -2.53384700 1.66338000 -0.37591500
C 0.85954200 -2.95612400 -0.27784900
N 1.26433300 -1.64517700 -0.22935500
N 1.70183800 1.21277100 -0.20700000
O 0.00303200 0.00146700 2.05416500
C -0.97947400 -0.09708000 3.04286100
H -1.63515900 -0.96656800 2.88124500
H -0.50401200 -0.21011800 4.02895800
H -1.60936300 0.80619300 3.07466100
H -4.41465700 0.69141200 -0.49485500
H -0.63136700 -4.46051900 -0.36518200
H 4.52185400 -0.68180400 -0.21527500
H 0.73904800 4.46963600 -0.29399500

^{2}FP-EDA
ub3lyp/def2tzvp,
el. energy = -2784.021704 a.u.

C 0.52270400 3.10267200 -0.04437000
N 0.72690700 1.85463700 0.50171500
H 1.78078700 4.95091700 -0.20539600
C 2.00426100 1.88115800 1.01787300
C 2.61081500 3.16929100 0.79566500
H 3.61288900 3.43956500 1.10456600
C 1.69010000 3.92842800 0.13942700
C 2.62552200 0.82277800 1.66532300
N 0.77998400 -0.78727500 1.48469800
C 0.61914500 -2.08631000 1.91512900
C 1.81181900 -2.54533300 2.58171600
H 1.93867400 -3.53533200 3.00147100
C 2.70079200 -1.51416500 2.55558100
H 3.70752700 -1.47979100 2.95283700
C 2.05008300 -0.42215000 1.87774200
C -0.62364200 3.51006900 -0.71297800
H -0.64856300 4.52867700 -1.08798200
H -4.72772000 2.02048900 -2.19180500
C -3.74888500 2.08265100 -1.73293200
C -3.10482300 1.00289100 -1.02711300
H -3.02619100 4.13172500 -2.11278200
N -1.86498900 1.39488600 -0.57460900
C -1.72841600 2.70881400 -0.96391500
C -2.89486800 3.14212500 -1.69307200
C -0.51352000 -2.86595800 1.72662900
H -0.49810100 -3.87392000 2.12931700

H -4.66508100 -2.86391100 -0.27737500
C -3.68782800 -2.57564700 0.08895300
C -2.80061900 -3.31070900 0.81196900
H -2.89580000 -4.33032600 1.16367900
C -1.64876100 -2.46963200 1.03485300
N -1.83029500 -1.23953000 0.44886900
C -3.07830600 -1.28549700 -0.12711800
C -3.67669500 -0.24477200 -0.82179700
H -4.66906900 -0.41557700 -1.22754700
C 0.54684400 -1.00260600 -2.50387700
C 1.86449600 -1.56988800 -2.23454100
O 2.10517600 -2.75711900 -2.09729400
O 2.78604800 -0.58477900 -2.17336300
C 4.14788400 -1.00988300 -1.93199500
H 4.40552600 -1.79709800 -2.64710300
H 4.21027000 -1.43675400 -0.92555000
N -1.29982100 -2.58515200 -2.73254300
N -0.45023400 -1.83916700 -2.62565500
H 3.63549600 0.97937600 2.03161800
Fe -0.62750400 0.37533100 0.65825200
C 5.03802500 0.20760500 -2.08563600
H 4.75603900 0.99306900 -1.37663300
H 6.08062100 -0.07163800 -1.89502300
H 4.97235100 0.61703700 -3.09949000
H 0.32914800 0.05026600 -2.61941800
O -1.45239800 0.91697600 2.13908000
C -0.75437600 1.52261800 3.19762700
H -1.42951000 1.53067500 4.06700800
H 0.15529700 0.97796700 3.48699900
H -0.48146800 2.56529000 2.97448400

^{4}FP-EDA
ub3lyp/def2tzvp,
el. energy = -2784.029255 a.u.
C 0.51411400 3.08712300 -0.07910200
N 0.69854000 1.84934400 0.49700300
H 1.77850600 4.93087800 -0.22096200
C 1.95418500 1.88051900 1.06123600
C 2.56663200 3.16603400 0.84283300
H 3.55507900 3.44284700 1.18771400
C 1.67369800 3.91393200 0.13576800
C 2.56528600 0.82741800 1.72792100
N 0.75396700 -0.81302000 1.47622500
C 0.61441400 -2.12979100 1.85391400
C 1.80449100 -2.58464800 2.52660800
H 1.94773600 -3.58614400 2.91225700
C 2.66685100 -1.53074600 2.55869700
H 3.66359600 -1.48695100 2.97953200
C 2.00520500 -0.43038900 1.90412400
C -0.60932400 3.48675800 -0.78935000
H -0.61832800 4.49637600 -1.18771700
H -4.70782700 1.99588400 -2.28469700
C -3.73397700 2.05963100 -1.81566000
C -3.11014700 0.99167100 -1.07634300
H -2.98459300 4.09026900 -2.24292300
N -1.87491200 1.38740400 -0.61757400
C -1.71619300 2.68771100 -1.04018100
C -2.86855400 3.11153600 -1.79447400
C -0.50291600 -2.92010500 1.62605400
H -0.47658500 -3.94280200 1.98820500
H -4.65343900 -2.88667700 -0.37805900
C -3.67986000 -2.59953800 -0.00135500
C -2.78319600 -3.35080600 0.69517100
H -2.86697800 -4.38351100 1.00926600
C -1.64171000 -2.50825300 0.94862600
N -1.84210600 -1.25891700 0.40881000
C -3.08601500 -1.29789300 -0.17663800
C -3.68654800 -0.25317300 -0.86484300
H -4.67408200 -0.42723800 -1.28019900
C 0.63312100 -0.96724600 -2.48284900
C 1.95519500 -1.52415900 -2.21667000
O 2.21309800 -2.71091000 -2.10854800
O 2.86140200 -0.52711800 -2.12067200
C 4.22615900 -0.93458800 -1.86843400
H 4.50947600 -1.69944800 -2.59801800
H 4.28106900 -1.38432700 -0.87140700
N -1.19947900 -2.55684000 -2.76579100
N -0.35520100 -1.80852000 -2.63143100
H 3.56245300 0.99399600 2.12306400
Fe -0.68792300 0.38414000 0.69971700
C 5.09615900 0.30202900 -1.97860000
H 4.78879600 1.06446300 -1.25518400
H 6.14077700 0.03728600 -1.77867300
H 5.03785500 0.73506800 -2.98301100
H 0.40248000 0.08691300 -2.54938000
O -1.48271900 0.95874000 2.27887500
C -0.93203400 1.46986100 3.45028900
H -1.70643700 1.53176200 4.23313900
H -0.11822200 0.83743500 3.84459600
H -0.52545900 2.48711300 3.31144800

^{6}FP-EDA
ub3lyp/def2tzvp,
el. energy = -2784.033194 a.u.
C 0.50747800 3.08118200 -0.12557300
N 0.69462700 1.85803300 0.47495800
H 1.78458900 4.92377300 -0.27226200
C 1.93679100 1.88868700 1.06208700
C 2.55071700 3.17561800 0.83129600
H 3.53362100 3.46494300 1.18241300
C 1.66711600 3.91259200 0.09731100
C 2.52633500 0.82959800 1.75366700
N 0.73283700 -0.83551800 1.52056700
C 0.59079800 -2.15388400 1.88160300
C 1.78318000 -2.60178000 2.56383400
H 1.93837700 -3.60337100 2.94517600
C 2.64027800 -1.54147100 2.60503800
H 3.63547100 -1.50145200 3.03040700
C 1.97712200 -0.43873200 1.94703700
C -0.61698700 3.45202600 -0.86427400
H -0.61898200 4.45466200 -1.28191900
H -4.66769100 1.91862000 -2.49421100

C -3.71583400 1.99288600 -1.98299200
C -3.11350500 0.93760700 -1.20156800
H -2.97173600 4.02185100 -2.41881400
N -1.90507400 1.36242700 -0.70463900
C -1.72869000 2.65429300 -1.13975500
C -2.86007300 3.05492300 -1.94397600
C -0.52464800 -2.94793700 1.61486500
H -0.49002300 -3.97425600 1.96812200
H -4.61330300 -3.00742200 -0.54922600
C -3.66482500 -2.69398400 -0.13112900
C -2.77902600 -3.43189000 0.59699300
H -2.85707700 -4.47045700 0.89352800
C -1.66305600 -2.56644500 0.90402200
N -1.88035600 -1.32219500 0.36564100
C -3.09374200 -1.37410400 -0.27563400
C -3.67037900 -0.32487800 -0.99211000
H -4.63610400 -0.51696800 -1.45050900
C 0.76265700 -0.94122600 -2.41827700
C 2.09000100 -1.49473000 -2.17650600
O 2.36234200 -2.68236300 -2.12393600
O 2.98501500 -0.49249000 -2.03481000
C 4.35206600 -0.89168000 -1.78669600
H 4.64771800 -1.63718500 -2.53114700
H 4.40724000 -1.36208200 -0.79888900
N -1.04825400 -2.53559600 -2.79717600
N -0.21442300 -1.78537200 -2.61448600
H 3.52039200 1.00031100 2.15684000
Fe -0.80712100 0.43039300 0.83692600
C 5.20965000 0.35622000 -1.86423500
H 4.88895700 1.09988600 -1.12717600
H 6.25568600 0.09856400 -1.66245300
H 5.15327700 0.81007800 -2.85950800
H 0.51430300 0.11092100 -2.40892300
O -1.59543500 1.02577700 2.36457400
C -1.15909000 1.65038500 3.53660400
H -1.96542600 1.63868400 4.28529300
H -0.28560000 1.14011600 3.97112900
H -0.88543300 2.70105700 3.35158500

^{2}TS2
ub3lyp/def2tzvp,
el. energy = -2783.983504 a.u.
im. frequency -297.87

C -0.52578500 3.02173300 -0.25938400
N -0.83874900 1.71708800 -0.55862700
H -1.68880500 4.93923200 -0.34775100
C -2.14530500 1.71711900 -0.98417000
C -2.67100400 3.06085700 -0.95716600
H -3.67628400 3.33586100 -1.25154100
C -1.67169200 3.86718000 -0.50059600
C -2.85815400 0.58875200 -1.37264100
N -1.09087300 -1.07943700 -0.99576200
C -1.02434200 -2.44373200 -1.13702900
C -2.29532700 -2.95375600 -1.59437400
H -2.50741000 -3.99863400 -1.78430000
C -3.12308600 -1.88102600 -1.74147600
H -4.15280600 -1.86504800 -2.07690000
C -2.36274000 -0.71236400 -1.36508600
C 0.71439400 3.47817000 0.17669300
H 0.80852700 4.54294000 0.36844100
H 5.08836200 2.17776200 0.88641900
C 4.02445700 2.17700800 0.68359000
C 3.25174500 1.00373000 0.34373200
H 3.36839900 4.27247600 0.89012000
N 1.93882100 1.34637200 0.15003900
C 1.85948500 2.70128000 0.33817900
C 3.15977100 3.22912800 0.68796900
C 0.10170000 -3.22840800 -0.91296700
H -0.00105800 -4.29770800 -1.07122200
H 4.61805500 -3.00827100 0.01436100
C 3.57577400 -2.75851000 -0.14085300
C 2.53903500 -3.58852900 -0.43790900
H 2.55296800 -4.66176300 -0.58194600
C 1.36043300 -2.75745400 -0.55253500
N 1.68016100 -1.44986300 -0.30405100
C 3.02903100 -1.42157300 -0.06320000
C 3.76946400 -0.28315300 0.24013600
H 4.83342500 -0.41088900 0.41521000
C -0.22891300 0.11874500 1.41679200
C -1.33128100 -0.73586800 1.98581700
O -1.20287800 -1.86152900 2.42005800
O -2.48478200 -0.05675000 1.92642500
C -3.68796800 -0.79171800 2.29043400
H -3.54070200 -1.22237600 3.28494800
H -3.82009400 -1.61111800 1.57764000
N 2.08610800 -1.10408200 2.98189300
N 1.18317400 -0.58648700 2.61108200
H -3.88482400 0.73088000 -1.69655800
Fe 0.43069300 0.13178100 -0.45946400
C -4.84335200 0.18637600 2.25815700
H -4.96195200 0.62135200 1.26064900
H -5.77042000 -0.33584800 2.52061400
H -4.69214200 0.99941800 2.97626000
H -0.16894100 1.09151000 1.90799500
O 1.01308100 0.31998400 -2.17444500
C 0.22432700 0.69730300 -3.26112400
H 0.84198300 0.65621000 -4.17296200
H -0.63673500 0.02647300 -3.41540700
H -0.16542500 1.72473700 -3.17227800

^{4}TS2
ub3lyp/def2tzvp,
el. energy = -2783.956276 a.u.
im. frequency -327.72

C -0.79930200 2.93238500 -0.42662800
N -0.99706300 1.58909600 -0.63677300
H -2.15635500 4.70919700 -0.67798600
C -2.28274900 1.41090600 -1.08299000
C -2.93230400 2.70232100 -1.15541300
H -3.95220400 2.86600200 -1.48194500
C -2.02297200 3.63637300 -0.74664200
C -2.86497400 0.18056500 -1.41401200

N -0.98601400 -1.33085700 -0.94024400
C -0.75243800 -2.67424100 -1.04437600
C -1.95733500 -3.32430900 -1.52052300
H -2.06207000 -4.38843700 -1.69397400
C -2.89203400 -2.34656900 -1.71219000
H -3.90697900 -2.45738200 -2.07446000
C -2.26829000 -1.08854100 -1.34982900
C 0.40094900 3.52723600 -0.01449500
H 0.38607100 4.60895600 0.08754200
H 4.88919300 2.70866600 0.86106100
C 3.83388300 2.58808200 0.64806600
C 3.17394600 1.32072100 0.39593200
H 3.00660100 4.63093000 0.66410900
N 1.84586000 1.54990400 0.17033300
C 1.63048700 2.89621300 0.23326200
C 2.88069600 3.56098300 0.55029000
C 0.46860300 -3.30673800 -0.77477700
H 0.49074700 -4.38400100 -0.91531300
H 4.94030900 -2.59873700 0.24574000
C 3.88164400 -2.45629100 0.06595300
C 2.94651200 -3.40117000 -0.23879700
H 3.09049700 -4.46798400 -0.35944000
C 1.67977500 -2.70872000 -0.39600700
N 1.86853300 -1.37769900 -0.15977900
C 3.19505600 -1.17751100 0.10290000
C 3.79243600 0.06271300 0.37166000
H 4.86091500 0.04788100 0.56898600
C -0.28272700 0.18147900 1.39846600
C -1.41267600 -0.64956600 1.95409800
O -1.29801500 -1.77221100 2.39907600
O -2.55600100 0.04292700 1.88352400
C -3.76883200 -0.67427900 2.25263400
H -3.62210500 -1.11079200 3.24452300
H -3.91551800 -1.48869500 1.53689000
N 1.96667900 -1.03953700 3.02081700
N 1.07901400 -0.49270000 2.65379000
H -3.89291300 0.21400500 -1.76490700
Fe 0.45740300 0.10554300 -0.46695200
C -4.91046200 0.32023700 2.23119800
H -5.03508400 0.75760100 1.23564600
H -5.84163700 -0.18931000 2.50372700
H -4.74090000 1.13095300 2.94778900
H -0.22591500 1.17379300 1.84579400
O 1.06838500 0.19620000 -2.17310700
C 0.31147100 0.66878900 -3.25171900
H 0.89445800 0.49670400 -4.17057800
H -0.64698500 0.13925200 -3.36429400
H 0.10321600 1.74810300 -3.18746000

^{6}TS2
ub3lyp/def2tzvp,
el. energy = -2783.967982 a.u.
im. frequency -384.47

C -1.53457200 2.28626600 -0.88974200
N -1.29192500 0.92993900 -0.80383600
H -3.31686100 3.44817300 -1.60394900
C -2.39472400 0.26814700 -1.30080200
C -3.38437400 1.24472600 -1.68129200
H -4.35016900 1.01274500 -2.11382500
C -2.85847500 2.48350700 -1.42354900
C -2.51221200 -1.12137300 -1.43186800
N -0.26090300 -1.82323700 -0.73932800
C 0.37944200 -3.01519200 -0.55433400
C -0.53197800 -4.09777100 -0.87230600
H -0.29054000 -5.15189200 -0.81171100
C -1.71364000 -3.52676400 -1.24574200
H -2.62803300 -4.02295400 -1.54708800
C -1.53614000 -2.09005600 -1.15151800
C -0.61696800 3.29397600 -0.56789100
H -0.97950900 4.31463900 -0.65320300
H 3.74177000 4.14558800 0.78239600
C 2.82749500 3.65048200 0.47882500
C 2.66219700 2.21663300 0.34406300
H 1.37585700 5.27484800 0.14337600
N 1.38366100 1.94981500 -0.05794400
C 0.72394900 3.14258600 -0.18146000
C 1.63053900 4.22213000 0.15479000
C 1.70679600 -3.16157600 -0.13068700
H 2.07417100 -4.18010000 -0.04091600
H 5.54587300 -0.87381900 1.11151500
C 4.53689700 -1.11440000 0.79973700
C 3.98979400 -2.34980000 0.60361400
H 4.46494300 -3.31561200 0.72386200
C 2.61694700 -2.14578900 0.19030200
N 2.35619100 -0.80121500 0.15544300
C 3.50309800 -0.14201800 0.51173100
C 3.64444500 1.24929000 0.59657900
H 4.61941500 1.61730100 0.90380600
C -0.59174600 0.32106900 1.36721900
C -1.79423100 -0.41434500 1.90929100
O -1.73720000 -1.50077400 2.45283600
O -2.93934800 0.26981200 1.72087200
C -4.15927600 -0.40679800 2.11891500
H -4.08937700 -0.65321600 3.18302500
H -4.23766800 -1.34547700 1.56131700
N 1.58569200 -0.49091600 3.21972200
N 0.61385000 -0.05912400 2.90363100
H -3.46526100 -1.48927600 -1.80218300
Fe 0.64457300 0.07128400 -0.63276300
C -5.31856600 0.52583700 1.83156400
H -5.37465700 0.77022100 0.76599200
H -6.25802500 0.04479700 2.12682100
H -5.22117300 1.46039600 2.39433000
H -0.63348800 1.37983100 1.63392700
O 1.10075800 0.16400400 -2.41548400
C 0.55220800 -0.14894200 -3.65430200
H 1.26351500 0.09599800 -4.45969600
H 0.31372100 -1.22255300 -3.73494200
H -0.37449700 0.41683500 -3.84744100

^{2}TC
ub3lyp/def2tzvp,

el. energy = -2674.429051 a.u.

C 2.47629100 2.15447200 0.59532200
N 1.21785100 1.86476500 0.13069400
H 3.50547900 4.06685000 1.15384700
C 0.54838000 3.06033700 0.04323100
C 1.41246100 4.13809500 0.45999400
H 1.12783400 5.18270900 0.47893600
C 2.60742800 3.57752000 0.79792100
C -0.75807200 3.22184500 -0.40402600
N -1.25339300 0.86433700 -0.89925400
C -2.34495600 0.21169400 -1.41279700
C -3.39001000 1.16157800 -1.71146400
H -4.35091600 0.90301100 -2.13893400
C -2.92074200 2.39070400 -1.35768700
H -3.41678900 3.35028300 -1.43357200
C -1.58412200 2.19778800 -0.85004000
C 3.47944100 1.22631400 0.85177100
H 4.43032700 1.60715100 1.21141600
H 4.37522300 -3.30128700 0.86759300
C 3.89290800 -2.33780600 0.76000500
C 2.53442000 -2.14626100 0.30666900
H 5.39459500 -0.83405000 1.35105800
N 2.23461700 -0.81082900 0.27831200
C 3.35753700 -0.14980000 0.70282800
C 4.40455400 -1.10003400 1.00206200
C -2.45487800 -1.16134000 -1.59849300
H -3.38121700 -1.53641700 -2.02239500
H -0.18708100 -5.13036900 -0.97049300
C -0.46132700 -4.08324500 -0.99695400
C -1.61514600 -3.51882300 -1.44536300
H -2.48770200 -4.00501100 -1.86347200
C -1.47815400 -2.09174800 -1.26717000
N -0.25539300 -1.80320200 -0.71784500
C 0.38750900 -3.00314000 -0.55096700
C 1.67650500 -3.17433800 -0.06430700
H 2.05141200 -4.19016500 0.01068400
C -0.09986900 -0.05448100 1.44155800
C -1.30752500 -0.67996600 2.01671700
O -1.23927900 -1.77581800 2.54601900
O -2.41618400 0.06081000 1.92323600
C -3.62855300 -0.51562500 2.48221000
H -3.42891700 -0.82398300 3.51272600
H -3.88202400 -1.40824000 1.90155900
H -1.15825700 4.23070500 -0.42394900
Fe 0.48449200 0.02820700 -0.31352000
C -4.71238900 0.53996700 2.40345300
H -4.87705200 0.85649900 1.36842500
H -5.65097900 0.13073400 2.79422700
H -4.44869000 1.42118700 2.99801600
H 0.56748500 0.35314200 2.20514100
O 1.17478200 0.12019700 -2.00868400
C 1.04670000 1.14492400 -2.94297700
H 1.58921100 0.86883300 -3.86026500
H -0.00552700 1.33089800 -3.21177800
H 1.46611600 2.09532300 -2.57416000

^{2}TS3

ub3lyp/def2tzvp,
el. energy = -2674.423794 a.u.
im. frequency -82.31

C 0.08988100 3.03931400 -0.17248000
N -0.43832400 1.79595100 -0.46062800
H -0.72397100 5.11950800 -0.33212300
C -1.71087300 2.01295900 -0.94872400
C -1.99339300 3.42466800 -0.95107200
H -2.92264800 3.86472500 -1.29108500
C -0.88597400 4.05705000 -0.46532700
C -2.56870600 1.02032000 -1.39977500
N -1.14643300 -0.93162700 -0.91870000
C -1.31889200 -2.28685000 -1.05340200
C -2.62181900 -2.56585600 -1.60628100
H -3.00323000 -3.55820500 -1.81241600
C -3.22626200 -1.36282700 -1.81830300
H -4.20814900 -1.16475200 -2.23008100
C -2.29999000 -0.34659800 -1.38000500
C 1.38371800 3.27646600 0.27298400
H 1.66580200 4.31062300 0.44576800
H 5.35777800 1.20589800 1.38943300
C 4.33937400 1.39832800 1.07561800
C 3.38635200 0.37781200 0.70468900
H 4.08886300 3.58900600 1.13399100
N 2.19558600 0.95355400 0.35046200
C 2.35928400 2.30603600 0.49729200
C 3.70238800 2.59477100 0.94719100
C -0.37497700 -3.25628400 -0.73467700
H -0.65843500 -4.29391200 -0.88219700
H 3.97244400 -3.82639600 0.70292900
C 3.02238300 -3.39773800 0.40929100
C 1.89059300 -4.03505100 0.00749000
H 1.71431800 -5.09809000 -0.09977800
C 0.91164400 -3.00651900 -0.27197100
N 1.44692600 -1.76967500 -0.03556500
C 2.73371000 -1.98018800 0.37951600
C 3.64315400 -0.98775000 0.72654900
H 4.63375700 -1.30468300 1.03820900
C -0.22051600 0.30570900 1.36514700
C -1.37490800 -0.29380700 2.05022700
O -1.09364400 -1.15103300 2.87401800
O -2.59441400 0.14776300 1.77001000
C -3.68930600 -0.48071800 2.50100900
H -3.49861800 -0.36806500 3.57231900
H -3.69444800 -1.54824500 2.26264600
H -3.53476300 1.33236000 -1.78469500
Fe 0.54227500 -0.00559600 -0.31506000
C -4.97230800 0.20244000 2.07727200
H -5.14928800 0.07773500 1.00438400
H -5.81500000 -0.24172400 2.61901300
H -4.94383400 1.27321900 2.30522200
H 0.24697200 1.07732400 1.98248100
O 1.22152000 -0.01311900 -2.01248900
C 0.75972300 0.75165600 -3.08323900
H 1.31965100 0.46966300 -3.98977200

H -0.31046800 0.58591800 -3.29110000
H 0.90644700 1.83320400 -2.92700900

^{2}BC
ub3lyp/def2tzvp,
el. energy = -2674.453351 a.u.
N -0.93460900 1.65632100 -0.20574200
Fe 0.58354400 -0.10142900 -0.37864000
C -0.56881700 0.83039200 0.95591700
C 0.83518100 3.37925900 0.03300700
C 3.68940800 -0.44007000 0.94747500
C 3.25187100 0.86485900 0.75279200
C 4.01366300 2.05200200 1.07709800
C 3.20084200 3.11258400 0.82385100
C 1.93929800 2.57304200 0.35311100
N 2.01086600 1.20613600 0.28343700
H 5.02545400 2.05280100 1.46257100
H 3.40835500 4.16713800 0.95724300
C -1.38875100 3.72220100 -1.08703400
C -2.08001900 1.55675400 -1.02261700
C -2.37835900 2.86744000 -1.50100500
H -1.25997200 4.76114200 -1.36187600
H -3.19783000 3.08847300 -2.17276500
C 3.41594900 -2.93534800 0.91623200
C 1.31228000 -2.94251300 0.10387100
C 2.41077300 -3.77287200 0.53533700
H 4.39963300 -3.19017900 1.28992500
H 2.40180300 -4.85563500 0.53289200
C -2.68463600 0.38852200 -1.45311300
C 0.11483700 -3.42871700 -0.41695700
C -2.18750800 -3.17227400 -1.40306600
C -2.20037200 -0.91788400 -1.33253300
C -2.95967100 -2.09404700 -1.70682200
H -2.41935500 -4.22321500 -1.52222900
H -3.95912100 -2.07647800 -2.12338600
C -0.94764300 -2.65372100 -0.86576200
C -0.43515400 2.97124700 -0.34087300
C 2.93535800 -1.58916500 0.72089800
N 1.64515900 -1.61830600 0.24821000
N -0.97601400 -1.28420300 -0.84579100
C -1.57318200 0.14772100 1.81023300
O -1.22657500 -0.51981000 2.77079500
O -2.86905000 0.35443200 1.49357800
C -3.83781900 -0.30823700 2.33902000
H -3.69412600 0.02750000 3.37106500
H -3.65389800 -1.38695100 2.31066600
C -5.21874300 0.04167200 1.82070400
H -5.97947800 -0.43347600 2.45072400
H -5.38592000 1.12424000 1.83968600
H -5.35570200 -0.31218000 0.79332400
O 1.08170800 -0.00920300 -2.13651800
C 2.35262700 0.28113800 -2.63384300
H 3.11016000 -0.45601400 -2.31343500
H 2.32533800 0.25357400 -3.73649200
H 2.71776900 1.27993600 -2.34106900
H 0.06662900 1.41387700 1.61320400
H 1.01874600 4.44953300 -0.00014100
H 4.69822300 -0.57783500 1.32481800
H 0.00563500 -4.50738100 -0.47692400
H -3.61943500 0.51138400 -1.99234100

^{4}BC
ub3lyp/def2tzvp,
el. energy = -2674.471301 a.u.
C 0.80690400 2.98363400 0.37027900
N 1.23114000 1.67352200 0.15206200
H 1.70185400 4.60197900 1.61541700
C 2.25931700 1.36907400 1.04050600
C 2.63763400 2.60828600 1.66142700
H 3.41680300 2.69418700 2.40755500
C 1.76417400 3.58344200 1.25542500
C 2.68144200 0.09285400 1.40436700
N 0.78899100 -1.36288700 0.69507500
C 0.57780900 -2.72328800 0.68835600
C 1.75146600 -3.38864300 1.20899500
H 1.85890600 -4.46158600 1.30879900
C 2.64631100 -2.41685500 1.54768800
H 3.63568000 -2.53705200 1.97169700
C 2.04629400 -1.14567400 1.20509600
C -0.43668100 3.49435000 -0.00427700
H -0.54071000 4.57157600 0.09604400
H -4.81575400 2.68173100 -1.26569600
C -3.78776500 2.54512200 -0.95385700
C -3.15857000 1.26211400 -0.71898700
H -2.95028000 4.57546900 -0.78465400
N -1.85348500 1.45855700 -0.33966900
C -1.62504900 2.81297700 -0.33989600
C -2.84741100 3.49993000 -0.70970000
C -0.58392000 -3.38353900 0.27214300
H -0.55676600 -4.46889300 0.31364500
H -4.88552100 -2.65088700 -1.32196700
C -3.87667500 -2.51897200 -0.95043700
C -2.96781100 -3.48455800 -0.62629300
H -3.08860900 -4.55948900 -0.68205100
C -1.76905500 -2.79618500 -0.18376700
N -1.96755100 -1.45027500 -0.24843300
C -3.23229500 -1.24095800 -0.70745600
C -3.79322800 0.02769400 -0.89518500
H -4.82562400 0.06377300 -1.23182200
C 0.70297300 0.86050600 -0.91051600
C 1.58173600 0.02519200 -1.77969700
O 1.11851800 -0.67032800 -2.66638400
O 2.90471300 0.15205400 -1.55618500
C 3.76914700 -0.65322800 -2.39302200
H 3.59402900 -0.38890800 -3.44065600
H 3.50094300 -1.70665400 -2.26365600
H 3.59482600 0.05767500 1.99229700
Fe -0.62782200 0.01427500 0.37466600
C 5.20002800 -0.37906700 -1.97444300
H 5.36330500 -0.65227100 -0.92657000
H 5.88359600 -0.97103000 -2.59387700
H 5.45299300 0.67933900 -2.10032400

H 0.10960700 1.47844800 -1.57499800
O -1.03480100 0.32077200 2.13230800
C -1.45905500 -0.60670100 3.08283800
H -1.73704300 -0.08232700 4.01258600
H -2.34461300 -1.17795300 2.75428100
H -0.67168700 -1.33571700 3.34395200

^{6}BC
ub3lyp/def2tzvp,
el. energy = -2674.463879 a.u.
N 0.43976400 -2.15438400 0.30722500
Fe -0.40400600 0.05625700 -0.60550200
C 0.42131800 -0.98153200 1.12602400
C -1.91322400 -2.87262100 0.70406200
C -3.16274700 1.83558600 0.30108400
C -3.23360800 0.45915100 0.57257300
C -4.38292600 -0.25105100 1.10182000
C -4.02068200 -1.56207300 1.21522500
C -2.64198900 -1.66729600 0.77146700
N -2.20944700 -0.42338900 0.38509600
H -5.33396600 0.20129900 1.35477700
H -4.62113300 -2.38854400 1.57560600
C -0.05442400 -4.28122800 -0.30308800
C 1.48633400 -2.60960900 -0.49025900
C 1.18968200 -3.98216500 -0.79590400
H -0.61827800 -5.19244900 -0.45429700
H 1.81823300 -4.61065300 -1.41320300
C -1.99952100 3.98463700 -0.38669100
C -0.02023300 3.02913400 -0.94074300
C -0.74581100 4.27644100 -0.84832800
H -2.80965700 4.67494500 -0.18631400
H -0.34030300 5.24991900 -1.09505300
C 2.50878000 -1.84384000 -1.06519000
C 1.30882100 2.87479500 -1.35807000
C 3.42000800 1.55892600 -1.89457300
C 2.59217600 -0.45650300 -1.27052200
C 3.74197000 0.23460000 -1.82276500
H 4.03877300 2.37692400 -2.24244000
H 4.67660700 -0.23856700 -2.09777300
C 2.05770300 1.68798100 -1.41272400
C -0.58258100 -3.10474600 0.32670800
C -2.06305400 2.55355500 -0.18857200
N -0.85164900 2.00972200 -0.54260900
N 1.59684900 0.45667000 -1.04145800
C 1.64262900 -0.57053700 1.82490800
O 2.76925200 -1.02929500 1.72123900
O 1.34395300 0.45693000 2.66973000
C 2.44274000 0.96882800 3.44794000
H 3.22285800 1.33383900 2.77106400
H 2.87396300 0.15514900 4.04183600
C 1.90303500 2.07885900 4.32964500
H 2.71388300 2.49736200 4.93710500
H 1.47326300 2.88607300 3.72666100
H 1.12701100 1.70318300 5.00565400
O -0.77318800 -0.93725100 -2.12397800
C -1.56642200 -0.52809500 -3.19955000
H -1.34547300 0.50410000 -3.52448800
H -1.40031100 -1.18841400 -4.06618600
H -2.64243900 -0.57361400 -2.95453700
H -0.42959300 -0.98259400 1.79209600
H -4.05589100 2.41560600 0.51630700
H 1.82042700 3.78120000 -1.66954200
H 3.32252100 -2.42474000 -1.49197800
H -2.50293200 -3.77327400 0.85718800

^{2}TS4
ub3lyp/def2tzvp,
el. energy = -2753.059195 a.u.
im. frequency -126.29
C -0.78641300 2.82607700 -0.65893800
N -0.94038700 1.46738300 -0.82169400
H -2.14569200 4.57595300 -1.00474600
C -2.21770100 1.27257900 -1.29315000
C -2.88589000 2.54320400 -1.43452200
H -3.89903900 2.66916800 -1.79591100
C -2.00442000 3.50264400 -1.03386600
C -2.78041400 0.03600400 -1.58214500
N -0.85888200 -1.37434700 -0.96820300
C -0.64259000 -2.72844300 -0.95283800
C -1.82906200 -3.42333100 -1.39156500
H -1.91802700 -4.49979900 -1.46917300
C -2.75821900 -2.47186700 -1.68680600
H -3.76752100 -2.60580700 -2.05588200
C -2.14475500 -1.19259900 -1.41778200
C 0.37798400 3.46073100 -0.24368900
H 0.35161700 4.54387800 -0.17127800
H 4.82319900 2.73774100 0.77614600
C 3.77735300 2.59675500 0.53289700
C 3.15194900 1.31481500 0.29918600
H 2.89220100 4.61595900 0.46749900
N 1.82225800 1.48571500 0.01431200
C 1.59001400 2.83496100 0.04290800
C 2.80720600 3.53981600 0.37977800
C 0.55014700 -3.35484600 -0.60947500
H 0.57051900 -4.43954500 -0.65364200
H 4.96260400 -2.52721600 0.46195900
C 3.90861800 -2.41579100 0.23924000
C 2.98603300 -3.38454500 -0.00808800
H 3.12489000 -4.45816600 -0.03674500
C 1.73079500 -2.70913000 -0.25920500
N 1.89276700 -1.35547400 -0.13892900
C 3.21411700 -1.14929000 0.15327800
C 3.80962000 0.09103100 0.36038000
H 4.87078900 0.10431800 0.59031800
C -0.32699300 0.23078900 1.24154500
C -1.47693900 -0.56688100 1.78789800
O -1.41403900 -1.71392900 2.18327500
O -2.60352600 0.17119500 1.79338400
C -3.82165100 -0.51384200 2.18761500
H -3.67945100 -0.92600700 3.19140600
H -3.98985200 -1.34845600 1.49990200
H -3.80026900 0.02410800 -1.95453100

Fe 0.49464200 0.04548200 -0.49354400
C -4.94893100 0.49768200 2.14433600
H -5.07064800 0.90927700 1.13707600
H -5.88807000 0.01343100 2.43517300
H -4.76205200 1.32628300 2.83584700
H -0.28639700 1.22889800 1.67503300
O 1.12735100 0.09613700 -2.20718400
C 0.39474300 0.43483600 -3.34386300
H 1.02570300 0.26956700 -4.23224300
H -0.51195700 -0.18057700 -3.46296100
H 0.08391800 1.49273600 -3.35070500
C 0.62307100 0.22419800 3.95353200
H -0.24939200 -0.18112700 4.46023100
H 0.87916400 1.25797200 4.17634300
C 1.34989600 -0.51371700 3.09896500
H 2.23784200 -0.11310300 2.62247200
H 1.11122800 -1.55322500 2.90258400

^{4}TS4
ub3lyp/def2tzvp,
el. energy = -2753.036780 a.u.
im. frequency -465.29

N -1.35772100 0.70507900 -0.91322400
Fe 0.66934000 0.02024100 -0.50400700
C -0.72631400 0.23778300 1.11014300
C -0.89904000 3.08932800 -0.68747400
C 3.51138300 1.48140400 0.74357100
C 2.42513500 2.29668000 0.40465800
C 2.43502700 3.73646500 0.51954900
C 1.20514300 4.18064600 0.13196600
C 0.42423900 3.01894300 -0.22566500
N 1.19414900 1.88819400 -0.05500600
H 3.28220900 4.32067600 0.85722000
H 0.84491800 5.20104600 0.08734700
C -2.98604700 2.08511200 -1.74385900
C -2.31324200 -0.06700800 -1.52726500
C -3.35112100 0.79620400 -2.03544800
H -3.50741100 2.99694400 -2.00902300
H -4.22424300 0.46407700 -2.58398000
C 4.69098100 -0.75761400 1.01526100
C 2.91556300 -1.98209700 0.34438200
C 4.29293900 -2.04457700 0.80037000
H 5.65866000 -0.40400000 1.35003500
H 4.87039900 -2.95263200 0.92479000
C -2.21224700 -1.45052100 -1.67310300
C 2.11869300 -3.06022100 -0.04907900
C 0.07078600 -4.14894400 -0.99830300
C -1.12913600 -2.26109800 -1.30864700
C -1.12689900 -3.69865600 -1.46391800
H 0.43162200 -5.16888600 -0.95041100
H -1.94844900 -4.27494500 -1.87107900
C 0.82162000 -2.99085900 -0.56569200
C -1.71775100 2.02302500 -1.06072200
C 3.55438600 0.08624900 0.69155100
N 2.50088900 -0.68757200 0.30922300
N 0.06670400 -1.86069100 -0.76306000
C -1.92088600 -0.61459800 1.49250200
O -1.88757200 -1.80385300 1.73945300
O -3.05667000 0.11731100 1.56004700
C -4.26575700 -0.60922200 1.88346000
H -4.14170500 -1.08276400 2.86334800
H -4.40724900 -1.40596200 1.14605900
C -5.41267500 0.38168200 1.87458700
H -6.34961300 -0.13517500 2.11193300
H -5.25915400 1.17093000 2.61865400
H -5.51730500 0.85095700 0.89068100
O 1.27811400 0.14652400 -2.21938600
C 1.05648600 1.13852300 -3.17260800
H 1.49924200 2.10694200 -2.88372100
H 1.52447100 0.83340500 -4.12308900
H -0.01465300 1.30661400 -3.37410200
C 0.56875700 -0.21731500 2.88355700
H 1.42915200 0.33537500 2.52704300
H 0.57676400 -1.28858500 2.71651100
C -0.34413900 0.35844300 3.70223700
H -0.90153600 1.27943000 1.36156700
H -0.30922100 1.41959900 3.93710100
H -1.15523300 -0.21311200 4.14506100
H -1.30842300 4.08861500 -0.80481800
H 4.40828800 1.99425300 1.07929400
H 2.55333200 -4.05298700 0.02475200
H -3.05212000 -1.95756200 -2.13949000

^{6}TS4
ub3lyp/def2tzvp,
el. energy = -2753.046289 a.u.
im. frequency -400.86

N 1.26872700 -0.63392200 -0.92673400
Fe -0.73888800 0.03899800 -0.57990800
C 0.78452100 -0.26140300 1.09995700
C 0.83821700 -3.06473900 -0.79197400
C -3.49406700 -1.51365000 0.79761800
C -2.44338500 -2.36761900 0.42958200
C -2.45442700 -3.81645700 0.51614700
C -1.23796300 -4.25001200 0.07376500
C -0.47234300 -3.06880200 -0.28121900
N -1.23512100 -1.95803000 -0.05468900
H -3.28689700 -4.41355500 0.86811300
H -0.88193700 -5.27011100 -0.00374300
C 2.87894500 -1.98296800 -1.83552100
C 2.22364800 0.16834400 -1.52996800
C 3.24535800 -0.68318600 -2.07827900
H 3.40085000 -2.88248600 -2.13862000
H 4.11739900 -0.33419200 -2.61785600
C -4.62238800 0.72705000 1.15769600
C -2.88752900 1.98886600 0.43575600
C -4.23542500 2.02239400 0.96485700
H -5.56895700 0.36460400 1.53949100
H -4.80504000 2.92320600 1.15791500
C 2.16230900 1.56304200 -1.63130200
C -2.12084500 3.10902600 0.08115600
C -0.06685200 4.29650400 -0.82706700

C 1.11404600 2.41167800 -1.24026000
C 1.12805400 3.86019900 -1.31962300
H -0.41257300 5.31779800 -0.72439000
H 1.95270800 4.45514800 -1.69242800
C -0.82637100 3.11742300 -0.45407800
C 1.62190000 -1.95748500 -1.13725900
C -3.51416000 -0.11229200 0.75081300
N -2.48325600 0.68585500 0.32729300
N -0.08070200 2.00519500 -0.72050800
C 2.03380300 0.51019600 1.48223900
O 2.06256900 1.68744700 1.78517300
O 3.14503300 -0.26623100 1.46738000
C 4.39078900 0.39231600 1.79253500
H 4.30828100 0.82972100 2.79341700
H 4.55559100 1.21250600 1.08574700
C 5.49312600 -0.64653500 1.72093700
H 6.45567500 -0.18319800 1.96618800
H 5.31418400 -1.46067700 2.43173600
H 5.56412000 -1.07610500 0.71596700
O -1.30455000 -0.15409500 -2.33243600
C -1.19482600 -1.06423400 -3.37573200
H -1.60558500 -2.05151400 -3.10399400
H -1.75196100 -0.70542900 -4.25709700
H -0.14749000 -1.21372400 -3.68906800
C -0.44712900 0.16945800 3.02769000
H -1.33468600 -0.33897100 2.66928900
H -0.41335100 1.24397300 2.88487600
C 0.47803700 -0.47167800 3.77383700
H 0.92120400 -1.31766000 1.32593600
H 0.41303900 -1.53939600 3.97012800
H 1.32892300 0.05150100 4.20203800
H 1.28547500 -4.03842200 -0.97224100
H -4.39630500 -1.99283500 1.16784900
H -2.58796700 4.07831300 0.23144600
H 3.02418600 2.04428400 -2.08536200

^{6}FP-2

ub3lyp/def2tzvp,
el. energy = -5168.831662 a.u.

N 3.71515700 -2.08402200 0.64905900
Fe 4.37930400 -0.10333300 0.42637000
C 4.75068800 -3.05059100 -1.39142300
C 5.07617500 1.71155100 -2.49705500
C 5.16354900 0.30709200 -2.56087900
C 5.75157500 -0.42285600 -3.65900900
C 5.68078200 -1.74599600 -3.34441400
C 5.03698500 -1.84149800 -2.05543900
N 4.74341600 -0.57754700 -1.59330800
H 6.17722700 0.02072900 -4.54718800
H 6.03596900 -2.58091800 -3.93028500
C 3.67617200 -4.38126800 0.46222100
C 3.05786800 -2.62172100 1.73434700
C 3.03332800 -4.06067100 1.61918500
H 3.83158700 -5.36661500 0.04789200
H 2.57897400 -4.73573000 2.32996400
C 4.49545000 3.87175500 -1.32452100
C 3.81624100 2.94049900 0.61484400
C 4.03706800 4.18660200 -0.08176900
H 4.74644900 4.55224700 -2.12488700
H 3.84580100 5.17028500 0.32311700
C 2.47809700 -1.90029600 2.79766500
C 3.29073000 2.84482900 1.91781000
C 2.22320800 1.55858800 3.80380600
C 2.51780700 -0.50024700 2.92182000
C 1.95363200 0.24327900 4.02659200
H 1.95417300 2.40332600 4.42203400
H 1.42457300 -0.18952900 4.86321600
C 2.92335100 1.64037000 2.54234100
C 4.10136400 -3.14298600 -0.14714800
C 4.59113100 2.43061400 -1.39071900
N 4.15290400 1.88790900 -0.20309700
N 3.09996900 0.37325500 2.02934100
O 6.03443200 -0.12057400 1.18116400
C 6.61044900 -0.70178300 2.31455700
H 6.48135200 -1.79537300 2.31994500
H 7.68977100 -0.48856000 2.33198700
H 6.17119900 -0.30024900 3.24141900
C 1.77143900 -2.68055900 3.87227000
C 2.38777500 -2.86454200 5.11623700
C 0.48406900 -3.23938200 3.65905500
C 1.76996400 -3.58700200 6.13700600
H 3.37369500 -2.43639100 5.27494800
C -0.13728700 -3.96554200 4.68850900
C 0.50787100 -4.13621700 5.91229800
H 2.27180400 -3.72003800 7.09118600
H -1.11626700 -4.38719500 4.51166400
H 0.01019300 -4.70190600 6.69560600
C 5.11928800 -4.33176100 -2.07683500
C 4.46844900 -4.72789600 -3.25669400
C 6.11750500 -5.16584200 -1.54746300
C 4.80666700 -5.92454200 -3.89044000
H 3.68719600 -4.09721200 -3.67151400
C 6.45751000 -6.36124300 -2.18353000
H 6.63203600 -4.87003300 -0.63740000
C 5.80310700 -6.74441800 -3.35626000
H 4.28673700 -6.21709200 -4.79884800
H 7.23628400 -6.99174100 -1.76267100
H 6.06648000 -7.67587000 -3.85015100
C 5.54749800 2.49470200 -3.68504500
C 6.70528100 3.28602000 -3.60733000
C 4.83934700 2.45595200 -4.89701100
C 7.14112700 4.02018800 -4.71166400
H 7.26689400 3.31717400 -2.67773600
C 5.27427400 3.19272400 -6.00009700
H 3.93827600 1.85310200 -4.96948300
C 6.42652800 3.97685000 -5.91088900
H 8.04215000 4.62301900 -4.63458000
H 4.70977400 3.15544000 -6.92810000
H 6.76505000 4.55020400 -6.76974500
C 3.12939000 4.12167600 2.69913700
C 1.94142600 4.89256600 2.66394500
C 4.20098900 4.56418400 3.48442900

C 1.86185300 6.07867100 3.41439300
C 4.12101400 5.74041700 4.22927000
H 5.10934300 3.96808600 3.50371900
C 2.94597000 6.49070300 4.18716200
H 0.94849300 6.65455900 3.38606900
H 4.96494000 6.06286300 4.83233600
H 2.86355200 7.41064500 4.76009200
N 0.88496400 4.43155400 1.85462600
N -0.12311100 -3.03409100 2.40438000
C -0.39399100 4.93142600 1.73138100
O -0.81591700 5.89108700 2.37376500
C -1.23994000 -3.63779100 1.86798200
O -1.96401600 -4.40728400 2.49672400
C -1.53055200 -3.29058900 0.43227300
C -2.82362800 -3.56117200 -0.03627900
C -0.57563800 -2.77036400 -0.45613000
C -3.18602500 -3.30771300 -1.36219700
H -3.54264300 -3.98052000 0.66050200
C -0.92799300 -2.51009200 -1.77891100
H 0.45115600 -2.59478200 -0.14849100
C -2.22308400 -2.77118600 -2.22583700
H -0.18606500 -2.11060300 -2.46504300
H -2.48907200 -2.56366600 -3.25927300
C -1.27025100 4.19839800 0.75552900
C -2.65178400 4.28036500 0.96196500
C -0.78285800 3.47049200 -0.34152800
C -3.56092800 3.63281400 0.11905400
H -3.00852400 4.86237300 1.80700000
C -1.68090600 2.83195200 -1.19459000
H 0.28147500 3.42807000 -0.55823400
C -3.05708100 2.90538500 -0.96500400
H -1.30796500 2.27166200 -2.04762400
H -3.73777400 2.38514500 -1.63098500
H 0.34828100 -2.36223300 1.81489200
H 1.07264600 3.56254200 1.37172100
C -5.04951700 3.77868700 0.42236300
H -5.32487300 4.83200600 0.28121500
H -5.18958000 3.58250400 1.49294100
C -6.02029800 2.93386000 -0.37548600
C -6.05612100 1.51437200 -0.21468000
C -6.90560400 3.51712800 -1.25563400
C -6.93747700 0.71324500 -0.92813800
C -7.84867000 2.75285300 -1.99006200
H -6.89285700 4.59648800 -1.39289500
C -7.86934500 1.32834700 -1.82956900
C -8.81912100 0.58114100 -2.58311500
C -9.69710300 1.20728000 -3.44185900
H -8.85055000 -0.49752800 -2.46986800
H -10.41589700 0.61628000 -4.00341700
C -9.67345500 2.61411000 -3.59701900
C -8.76672200 3.36668700 -2.88491400
H -10.37064100 3.09546300 -4.27754600
H -8.73794300 4.44820400 -2.99660500
C -6.87774900 -0.77496400 -0.75979600
C -7.81532900 -1.46652600 0.07855300
C -5.87568200 -1.49596000 -1.39274500
C -7.68439500 -2.88329300 0.25053100
C -5.72012000 -2.90363500 -1.20647800
C -6.62040000 -3.56246500 -0.39784600
H -6.52120000 -4.63535000 -0.24639500
C -4.57934000 -3.64975300 -1.87507100
H -4.75422600 -4.72361000 -1.73444500
H -4.59964400 -3.47591500 -2.95681500
C -8.87558900 -0.80128700 0.75719700
C -9.75909600 -1.49921800 1.55254700
H -8.98441500 0.27201500 0.64012800
H -10.56208400 -0.97043700 2.05928300
C -8.61200400 -3.57256600 1.07777500
C -9.62974300 -2.89924000 1.71548800
H -8.49919800 -4.64731500 1.20077800
H -10.33187400 -3.43787300 2.34614000
O -4.95499100 -0.84855300 -2.19099700
O -5.12703200 0.94923900 0.63012700
C -5.32903100 -0.71280700 -3.56377100
H -5.49238000 -1.68864900 -4.04106800
H -6.23682600 -0.10958700 -3.67660200
H -4.49727700 -0.20649900 -4.06074400
C -5.56327800 0.71415200 1.97159900
H -5.92040700 1.63591600 2.45046900
H -6.35893100 -0.03760100 2.00987000
H -4.69033900 0.34389700 2.51460100

[6]FP-2-EDA
ub3lyp/def2tzvp,
el. energy = -5584.991732 a.u.

N -3.34313000 2.28615500 1.22993300
Fe -4.29761200 0.42949000 0.92062800
C -2.27679200 -2.64434300 -3.37590800
C -4.72394600 3.67483400 -0.29499700
C -6.01294200 -0.77714600 -1.88977300
C -5.90636700 0.61977100 -1.73923500
C -6.65102100 1.58214500 -2.51733200
C -6.30465900 2.81865200 -2.06440500
C -5.33712900 2.62848900 -1.01017200
N -5.11727200 1.28075400 -0.82487500
H -7.35751100 1.34321300 -3.29857300
H -6.67530000 3.77305000 -2.40878600
C -3.06827000 4.56856100 1.38620300
C -2.38608800 2.56688600 2.17870900
C -2.21619400 3.99766700 2.28394400
H -3.19935600 5.62118700 1.18176100
H -1.53315400 4.49891500 2.95514700
C -5.42561000 -3.15275700 -1.26114300
C -4.11961600 -2.63968300 0.50754300
C -4.67637200 -3.71876000 -0.27523100
H -5.96610500 -3.65994400 -2.04681900
H -4.49123700 -4.76995900 -0.10918200
C -1.66389900 1.62089700 2.93317900
C -3.24595000 -2.81998700 1.59826300
C -1.58011200 -1.97101600 3.29307700
C -1.83268700 0.22766200 2.83619200
C -1.11054700 -0.73965400 3.63104200

H -1.25740200 -2.92404000 3.68658500
H -0.34450700 -0.50567800 4.35575200
C -2.56873000 -1.77821200 2.25705500
C -3.77520600 3.49480900 0.72777000
C -5.35120800 -1.72011200 -1.08278600
N -4.53360100 -1.43609200 -0.01186200
N -2.71081800 -0.42942000 1.99973700
C -1.45389500 -2.46868700 -2.18790500
O -1.25788300 -3.34718000 -1.35562500
O -0.95024000 -1.22612900 -2.16056200
C 0.01526100 -0.88130600 -1.12647100
H -0.36301800 0.03999100 -0.67623400
O -5.67774300 0.48152800 2.10610100
C -5.81541300 0.80179300 3.46003300
H -5.39474800 1.79360600 3.68804600
H -6.88165300 0.81576800 3.73157000
H -5.31341600 0.06058700 4.10184700
H -2.44957900 -1.88596300 -4.12643100
C -0.65992200 2.12890400 3.93105200
C -0.96914900 2.07519400 5.29643300
C 0.60488100 2.63768000 3.53785800
C -0.06587500 2.50286400 6.26866700
H -1.94027200 1.68652500 5.59049400
C 1.51670400 3.06205400 4.51958400
C 1.17753800 2.99209300 5.86935100
H -0.33095500 2.45065700 7.32074500
H 2.48385100 3.43123700 4.21046100
H 1.89845200 3.32627800 6.61089800
C -5.09001600 5.08216500 -0.65972500
C -4.71138900 5.62996100 -1.89629800
C -5.81646900 5.88429500 0.23555400
C -5.04921900 6.94333100 -2.22778000
H -4.14342900 5.02411000 -2.59711200
C -6.15624600 7.19682400 -0.09738900
H -6.12116900 5.47114700 1.19332400
C -5.77296600 7.73068600 -1.32962800
H -4.74237100 7.35139800 -3.18736800
H -6.72310300 7.80055200 0.60650400
H -6.03629100 8.75283000 -1.58830200
C -6.89353600 -1.29258600 -2.98727000
C -8.07325600 -1.99656600 -2.69479700
C -6.55604100 -1.07940900 -4.33415400
C -8.89244300 -2.47159600 -3.72048200
H -8.35146600 -2.16078600 -1.65753700
C -7.37435000 -1.55618600 -5.35952200
H -5.64525800 -0.53749800 -4.57426500
C -8.54530700 -2.25410200 -5.05567400
H -9.80447500 -3.00928100 -3.47483200
H -7.09475700 -1.38432500 -6.39577100
H -9.18341700 -2.62452300 -5.85355500
C -3.09714500 -4.21559200 2.13178500
C -1.91083000 -4.97499800 2.05459200
C -4.21432700 -4.78644700 2.77003500
C -1.86465200 -6.25067900 2.63949200
C -4.16210400 -6.05221200 3.34632800
H -5.13046400 -4.20541600 2.82635700
C -2.97407200 -6.78397600 3.28576000
H -0.94514800 -6.82069500 2.57443500
H -5.03847000 -6.45998300 3.84236200
H -2.91315200 -7.77370900 3.73011500
H 0.02479600 -1.66735100 -0.37186000
N -0.76223000 -4.49769500 1.36920500
N 0.88577900 2.72690700 2.15929700
C 0.50248200 -4.54753000 1.91644500
O 0.70176500 -4.81010600 3.10201100
C 2.05634600 3.09390800 1.53193800
O 3.11623300 3.28988300 2.12577400
C 1.96091100 3.24361400 0.03809000
C 3.15660700 3.14522400 -0.69028400
C 0.76477800 3.52779600 -0.63465400
C 3.17504400 3.29006500 -2.07786600
H 4.07200600 2.94966900 -0.14430500
C 0.77306100 3.68235900 -2.02238700
H -0.16449300 3.67531900 -0.09226000
C 1.96330800 3.55642100 -2.73608000
H -0.15222900 3.91047100 -2.54463300
H 1.95725400 3.67585000 -3.81767400
C 1.64623100 -4.28286500 0.97982400
C 2.83532000 -3.78551100 1.52818500
C 1.59615500 -4.59878500 -0.38585000
C 3.97451300 -3.58115200 0.74282700
H 2.85962100 -3.56921200 2.59245900
C 2.72969300 -4.40933100 -1.17533300
H 0.69136300 -5.00444100 -0.82477600
C 3.90629200 -3.90193700 -0.61937600
H 2.70072200 -4.66682200 -2.23109700
H 4.77812000 -3.75882100 -1.25022500
H 0.12483700 2.45068200 1.55322000
H -0.89506200 -4.03995100 0.46854600
C 1.38059700 -0.68041800 -1.75701300
H 1.34911400 0.10100500 -2.52298100
H 2.10564700 -0.37990800 -0.99354400
H 1.73871400 -1.60968500 -2.21198300
C 5.25855600 -3.09332000 1.41308900
H 5.72441800 -3.95137500 1.91688000
H 4.98282400 -2.38881500 2.20320700
C 6.28775200 -2.47153500 0.49301000
C 6.21449800 -1.08715800 0.14647300
C 7.29798000 -3.23501800 -0.05171300
C 7.11375900 -0.50238500 -0.73840200
C 8.24469100 -2.69337900 -0.95816100
H 7.37388700 -4.28833000 0.21097200
C 8.14656700 -1.31074100 -1.32416500
C 9.08293900 -0.80028100 -2.26847800
C 10.06627200 -1.60483800 -2.80282600
H 9.01725100 0.24035600 -2.56705400
H 10.76983500 -1.19115700 -3.52059900
C 10.16964300 -2.96515000 -2.42500100
C 9.27417200 -3.49452100 -1.52344700
H 10.95197800 -3.58760000 -2.85090600
H 9.33704100 -4.54032000 -1.23122900
C 6.97804000 0.94965700 -1.08088900

C 7.92163300 1.91848300 -0.59398000
C 5.90325400 1.38203700 -1.84650400
C 7.74104100 3.30096100 -0.92885600
C 5.69315600 2.76169800 -2.14863900
C 6.61165300 3.68335400 -1.69679800
H 6.46738500 4.73862700 -1.91973500
C 4.45787900 3.20065400 -2.90297500
H 4.65306100 4.18846100 -3.34098500
H 4.27174600 2.52713700 -3.74726400
C 9.03284600 1.56858000 0.22519100
C 9.92063300 2.52541800 0.66799100
H 9.17759800 0.53056800 0.50369900
H 10.76063400 2.23241700 1.29231300
C 8.67765700 4.26191800 -0.46009700
C 9.74844700 3.88616000 0.31889100
H 8.52620000 5.30587300 -0.72479400
H 10.45667700 4.63015300 0.67337400
O 4.95769300 0.48725000 -2.30145000
O 5.18772900 -0.34864900 0.68896400
C 5.29772200 -0.19045800 -3.51229500
H 5.45002300 0.51491000 -4.34143800
H 6.20259600 -0.79747100 -3.39516100
H 4.45321800 -0.84324000 -3.74708100
C 5.52602800 0.41288100 1.85438600
H 5.81806000 -0.23992800 2.68868600
H 6.34174400 1.11515100 1.65126000
H 4.63133200 0.97523700 2.13016900
N -2.86820600 -3.79750300 -3.53832300
N -3.37266200 -4.80720800 -3.66840100

^{2}TS2-2
ub3lyp/def2tzvp,
el. energy = -5584.944754 a.u.
im. frequency -309.24

N -3.44476900 2.14686500 0.73354500
Fe -3.96867000 0.21576100 0.37835400
C -2.32032200 0.21285800 -0.71552600
C -4.61964900 3.22214000 -1.17096700
C -6.03832400 -1.39822600 -1.87873400
C -5.88226000 -0.00928200 -2.00056200
C -6.59792200 0.80522600 -2.95497500
C -6.17073100 2.08366900 -2.78275300
C -5.20736200 2.06365600 -1.70513000
N -5.03944000 0.77733300 -1.25314100
H -7.33651800 0.44178400 -3.65417300
H -6.49755800 2.96826600 -3.30942000
C -3.28159200 4.44238800 0.57128800
C -2.70159400 2.63321500 1.78531900
C -2.61446500 4.07179500 1.69776500
H -3.41758300 5.44149400 0.18414300
H -2.10686400 4.71080300 2.40606700
C -5.41244200 -3.61590100 -0.87675100
C -4.00275300 -2.80578700 0.68323300
C -4.59024100 -4.00699100 0.13043400
H -6.01974400 -4.23785700 -1.51790700
H -4.39983600 -5.01098400 0.48079000
C -2.09190200 1.86713400 2.79222600
C -3.15034200 -2.80164600 1.79863300
C -1.79407700 -1.63919700 3.55921100
C -2.16167800 0.46676200 2.84051000
C -1.50292200 -0.34195100 3.84095200
H -1.48048800 -2.52215100 4.09731600
H -0.89976400 0.03999600 4.65153800
C -2.62975400 -1.63927100 2.38140900
C -3.81889200 3.23875700 -0.01976500
C -5.32868900 -2.17385900 -0.95195200
N -4.44221300 -1.70782800 -0.01088600
N -2.83687500 -0.34636000 1.95570300
C -1.05166300 -0.50160200 -0.33347000
O -0.85699600 -1.69332700 -0.48443400
O -0.20174200 0.36718500 0.21726300
C 1.07096500 -0.16097000 0.72450800
H 1.33027000 0.52244900 1.53430600
O -5.49729300 0.32933700 1.36291500
C -5.62614400 0.95402300 2.60275400
H -5.41104300 2.03448300 2.56307800
H -6.66580900 0.83695600 2.94892500
H -4.97128900 0.51087100 3.37136700
H -2.13759500 1.11623000 -1.29982200
C -1.37369900 2.57482000 3.90749200
C -1.97074700 2.59936800 5.17592500
C -0.11259100 3.20419800 3.73995500
C -1.35890400 3.21866300 6.26455900
H -2.93703600 2.11864900 5.29877100
C 0.50537100 3.82367200 4.84020900
C -0.11773900 3.82829600 6.08636600
H -1.84681700 3.22285800 7.23505200
H 1.47113800 4.28752500 4.70326300
H 0.37944800 4.31444400 6.92167400
C -4.90105000 4.52622200 -1.85735600
C -4.33375900 4.80713000 -3.11071800
C -5.74299300 5.48585700 -1.27234800
C -4.59431300 6.01602200 -3.75859200
H -3.68221300 4.07329800 -3.57778900
C -6.00538600 6.69422900 -1.92088800
H -6.19796300 5.27629500 -0.30815200
C -5.43087700 6.96364600 -3.16511400
H -4.14143700 6.21705500 -4.72607600
H -6.66327200 7.42292900 -1.45461200
H -5.63498700 7.90427800 -3.66971600
C -7.00769600 -2.09120800 -2.78724700
C -8.19645100 -2.63621800 -2.27518300
C -6.75075900 -2.21304700 -4.16255800
C -9.10341100 -3.28377300 -3.11594600
H -8.40975700 -2.54289100 -1.21390700
C -7.65727100 -2.86218800 -5.00285000
H -5.83099700 -1.80347900 -4.57175200
C -8.83659500 -3.39913100 -4.48202300
H -10.02047400 -3.69518700 -2.70228100
H -7.43869800 -2.95138100 -6.06390300
H -9.54258300 -3.90403200 -5.13610700
C -2.90920600 -4.11106600 2.49696300

C -1.72259000 -4.86725800 2.35747400
C -3.92881700 -4.60101400 3.32919200
C -1.60107700 -6.08707800 3.04934900
C -3.79934900 -5.80301700 4.01958300
H -4.83560400 -4.01132400 3.43197200
C -2.62637800 -6.54407700 3.87107400
H -0.69403700 -6.66463700 2.94555100
H -4.60160800 -6.15323700 4.66289400
H -2.50312300 -7.48891300 4.39394900
H 0.89133000 -1.15452200 1.13677100
N -0.69578600 -4.42450000 1.48921000
N 0.47359500 3.19785600 2.45543300
C 0.64092600 -4.76459800 1.59490700
O 1.10240800 -5.36659600 2.56219700
C 1.67774800 3.73700100 2.04961300
O 2.51093100 4.21026800 2.81915100
C 1.92550600 3.70449100 0.56603300
C 3.26089800 3.70241800 0.13788500
C 0.89447800 3.73622700 -0.38481700
C 3.58627700 3.70255900 -1.22151200
H 4.04241600 3.70604400 0.89105400
C 1.20898500 3.74020900 -1.74317200
H -0.14583200 3.80193100 -0.07990100
C 2.54089400 3.71257600 -2.15605000
H 0.41316200 3.77599400 -2.48256500
H 2.77476700 3.71540000 -3.21817900
C 1.52875900 -4.39323900 0.44104900
C 2.90342000 -4.31205900 0.70635900
C 1.07482000 -4.23088800 -0.87474200
C 3.83417100 -4.07032700 -0.30596200
H 3.23605900 -4.46578200 1.72845500
C 1.99637200 -3.98837000 -1.89484000
H 0.01985400 -4.31709300 -1.11271400
C 3.36191600 -3.90653600 -1.61591000
H 1.64797300 -3.87336000 -2.91796000
H 4.06580600 -3.71955700 -2.42251400
H -0.07496000 2.73484200 1.74155300
H -0.94217100 -3.70537400 0.81571900
C 2.11335100 -0.17237600 -0.37467200
H 2.23294200 0.82146400 -0.81437700
H 3.08015200 -0.48003900 0.03605800
H 1.84161800 -0.88288700 -1.16113800
C 5.32201700 -4.08739800 0.02769200
H 5.69945900 -5.10320900 -0.15142000
H 5.43047700 -3.91509100 1.10364300
C 6.21007000 -3.12813200 -0.74023800
C 6.21759800 -1.73104700 -0.43272300
C 7.04489000 -3.58719600 -1.73550900
C 7.03540100 -0.83345400 -1.10445200
C 7.91106700 -2.72010800 -2.45001000
H 7.05662800 -4.64791600 -1.97802000
C 7.91555200 -1.32321200 -2.13074500
C 8.79908000 -0.47354200 -2.85547500
C 9.62618600 -0.97653200 -3.83688000
H 8.81712400 0.58661100 -2.62693200
H 10.29357500 -0.30753000 -4.37380200
C 9.61583100 -2.35650000 -4.15056100
C 8.77409300 -3.20663800 -3.46921100
H 10.27248400 -2.74046200 -4.92653100
H 8.75753600 -4.26931100 -3.70036800
C 7.01961100 0.62876300 -0.76518600
C 8.02134400 1.17961100 0.10580200
C 6.06054700 1.47176600 -1.31015300
C 8.00273300 2.58208800 0.39735200
C 6.04430700 2.87611400 -1.03735500
C 7.00199400 3.39522500 -0.19387600
H 7.00765800 4.46231100 0.01913400
C 5.02897900 3.78664600 -1.70291200
H 5.37439900 4.81936700 -1.56222000
H 5.03470000 3.61486400 -2.78492300
C 9.04263400 0.38499300 0.69989900
C 9.98723500 0.94588400 1.53259300
H 9.07154100 -0.67904500 0.49063800
H 10.75740700 0.31861400 1.97367800
C 8.98999500 3.12931600 1.26097100
C 9.96378800 2.33169100 1.81853300
H 8.96018600 4.19525100 1.47427900
H 10.71337600 2.76117100 2.47760000
O 5.05052700 0.97432600 -2.10736300
O 5.33424700 -1.29646600 0.53348600
C 5.35255100 0.83052100 -3.49731900
H 5.74808000 1.76035700 -3.92729800
H 6.07271900 0.02519900 -3.67507900
H 4.40891400 0.58146300 -3.99006200
C 5.85970000 -1.16435600 1.85867800
H 6.36256100 -2.08359200 2.18622700
H 6.56215500 -0.32811700 1.93201400
H 5.00270600 -0.97294200 2.50910500
N -2.62522700 -0.81076500 -2.36607800
N -3.02675500 -1.47356100 -3.15325200

Reaction coordinates: MECP

MECP-53 (toluene)
ub3lyp/6-31g(d) & LanL2DZ,
C -1.80926200 0.95345500 2.18517000
N -1.06237000 1.31949400 1.09747800
H -3.68909300 1.75924900 3.11673400
C -1.67571800 2.42388000 0.56823500
C -2.85865400 2.75173100 1.32593500
H -3.52294300 3.58189900 1.11538300
C -2.94145100 1.83437300 2.33567500
C -1.20991300 3.14142700 -0.53403100
N 0.81383700 1.81988300 -1.00169200
C 1.72468100 1.83797600 -2.03499600

C 1.43785400 2.93127600 -2.94220300
H 2.01054100 3.15841900 -3.83396400
C 0.32739400 3.55405200 -2.46665300
H -0.20254000 4.40187300 -2.88524900
C -0.06809400 2.84483900 -1.26630600
C -1.50640300 -0.10937600 3.03759100
H -2.18602800 -0.29294700 3.86567100
H 1.37653700 -3.65896400 3.62962500
C 0.90464500 -2.75271400 3.26781400
C 1.34802300 -1.99429400 2.11451600
H -0.81043500 -2.39067400 4.60354900
N 0.53766600 -0.89860000 1.92074100
C -0.42406800 -0.96826300 2.90258500
C -0.19216800 -2.11676700 3.75645700
C 2.73766900 0.91059800 -2.23974100
H 3.38397700 1.06249100 -3.10020000
H 4.53310400 -2.99434000 -0.53160600
C 3.91670100 -2.11821100 -0.69611700
C 4.01534900 -1.18702600 -1.69161500
H 4.72856100 -1.14713200 -2.50663300
C 2.96986900 -0.22144100 -1.45745700
N 2.23852700 -0.57028900 -0.35183300
C 2.81416500 -1.71307100 0.14006300
C 2.40454600 -2.37522900 1.29818500
H 2.94866100 -3.27438600 1.57606700
C -1.12097900 -2.03752000 -1.36976800
C -2.46446900 -2.12590600 -1.92067600
O -2.80411400 -2.80980500 -2.87444600
O -3.30100300 -1.33042400 -1.21585500
C -4.67188500 -1.30271000 -1.66133100
H -5.08910700 -2.31439000 -1.60177400
H -4.69960200 -0.99290100 -2.71165900
N 0.62923100 -3.32658800 -2.48301500
N -0.17976800 -2.72189800 -1.96056000
H -1.80232800 3.99233700 -0.86116900
Fe 0.78310000 0.56628100 0.57125200
C -5.41943700 -0.33138700 -0.76856200
H -4.98326300 0.67086200 -0.82945500
H -6.46896100 -0.27529400 -1.08107500
H -5.38641500 -0.65291000 0.27780800
H -0.83216200 -1.42042200 -0.52758200
O 1.91475700 1.59109200 1.82998800
C 2.55021400 2.77521100 1.54492800
H 2.90296900 3.28901400 2.46956800
H 3.46321100 2.66056600 0.91301100
H 1.91609200 3.52399800 1.01887500

MECP-31 (toluene)
ub3lyp/6-31g(d) & LanL2DZ,
C -2.11872500 -1.14787300 -1.43718700
N -0.84014300 -1.30413200 -0.96235200
H -3.70516500 -2.59302600 -2.11337800
C -0.59968600 -2.65429200 -0.95071600
C -1.76376400 -3.37541400 -1.41641800
H -1.83061000 -4.45394800 -1.49591300
C -2.70418600 -2.43988900 -1.72678000
C 0.60416500 -3.24992100 -0.58790100
N 1.87382600 -1.20212600 -0.12318000
C 3.17335300 -0.95456400 0.23881800
C 3.89822800 -2.19763800 0.38064900
H 4.94045800 -2.27532500 0.66702100
C 3.01513800 -3.19980400 0.11305000
H 3.18425800 -4.27001600 0.12494700
C 1.75508500 -2.56765400 -0.20696400
C -2.77709100 0.06726200 -1.59812800
H -3.78865300 0.03474300 -1.99428200
H -2.35263300 4.61390400 -0.89168400
C -2.16481500 3.54809900 -0.94992500
C -0.92665300 2.90478500 -0.56786900
H -4.00555000 2.64957300 -1.77409600
N -1.01451300 1.55230400 -0.75845300
C -2.26327000 1.31934000 -1.26829800
C -2.99420100 2.56165900 -1.39422600
C 3.71719900 0.30410300 0.48633000
H 4.76553200 0.34378000 0.76999300
H 2.65863900 4.79416900 0.74375400
C 2.60968800 3.72029500 0.60323700
C 3.60247700 2.80015900 0.75282900
H 4.63369900 2.96099900 1.04439200
C 3.02296500 1.50946500 0.44288000
N 1.70210300 1.65102800 0.10878900
C 1.42747100 2.99182400 0.19241500
C 0.20127700 3.58032700 -0.10120100
H 0.12776100 4.65986700 0.00375500
C -0.22981300 0.12359300 1.83357200
C -1.43809400 -0.69086800 2.06028000
O -1.45991200 -1.86145600 2.40263400
O -2.56222600 0.05156900 1.87316600
C -3.80643400 -0.65667700 2.01850500
H -3.79763800 -1.20829600 2.96468600
H -3.89654800 -1.38777200 1.20727300
N 1.47375900 -1.25394400 2.89815700
N 0.85694400 -0.34441800 2.52575700
H 0.65424100 -4.33506700 -0.61751800
Fe 0.44980700 0.17133300 -0.49478800
C -4.92656200 0.36670800 1.98039900
H -4.92763900 0.91301000 1.03169500
H -5.89499500 -0.13577500 2.09285600
H -4.82184300 1.09357300 2.79405500
H -0.33730600 1.19947900 1.86244400
O 0.95784700 0.46172900 -2.28001100
C 1.39551800 -0.56178500 -3.10133000
H 1.58774000 -0.15502700 -4.11448200
H 2.34264000 -1.03374600 -2.77041800
H 0.66351700 -1.38292200 -3.23407500

MECP-62 (toluene)
ub3lyp/6-31g(d) & LanL2DZ,
C 0.52078600 3.10714600 -0.08220000
N 0.72825400 1.86926800 0.48316400
H 1.78197500 4.95351700 -0.25712800
C 2.00110400 1.89667800 1.00629500

C 2.60600700 3.18449700 0.77083700
H 3.60542000 3.46227500 1.08142400
C 1.68770900 3.93513000 0.09885100
C 2.61884800 0.83935200 1.66529200
N 0.78818000 -0.79003000 1.49574100
C 0.63176400 -2.09144500 1.91678700
C 1.82917300 -2.54277500 2.58254400
H 1.96595300 -3.53309900 2.99838600
C 2.71048100 -1.50352200 2.56155600
H 3.71638500 -1.46560900 2.96044400
C 2.05332500 -0.41221500 1.88559600
C -0.62735800 3.49938300 -0.76329800
H -0.64937300 4.51214300 -1.15419700
H -4.73218500 1.99159600 -2.24439900
C -3.75652000 2.05834000 -1.77922600
C -3.11681600 0.98774000 -1.05343500
H -3.03338700 4.10061600 -2.19049500
N -1.88256100 1.39300700 -0.60238800
C -1.73753200 2.69889500 -1.01009300
C -2.90207400 3.11932600 -1.75190800
C -0.49993500 -2.87491700 1.71894200
H -0.47598300 -3.88646200 2.11267300
H -4.65117700 -2.90468800 -0.30158400
C -3.67986300 -2.60557900 0.07185800
C -2.78750300 -3.33770300 0.79427900
H -2.87562900 -4.36155100 1.13524400
C -1.64390800 -2.48797800 1.02951800
N -1.84252100 -1.25672500 0.45334700
C -3.08375400 -1.30656800 -0.13410100
C -3.68045000 -0.26521800 -0.83568100
H -4.66852900 -0.44467300 -1.24843500
C 0.56745000 -1.01720000 -2.50141200
C 1.88753400 -1.57635900 -2.22863000
O 2.13536500 -2.76190100 -2.08864000
O 2.80353400 -0.58566400 -2.16798200
C 4.16650600 -1.00249000 -1.91999400
H 4.43137900 -1.79072900 -2.63135800
H 4.22722400 -1.42540200 -0.91174700
N -1.27159400 -2.60785700 -2.73268700
N -0.42520000 -1.85821900 -2.62342600
H 3.62811100 1.00153900 2.03186500
Fe -0.65960000 0.39419000 0.70531000
C 5.05114900 0.21909700 -2.07413200
H 4.76176300 1.00593100 -1.36962600
H 6.09409400 -0.05417500 -1.87718500
H 4.98861000 0.62427000 -3.08990200
H 0.34277700 0.03538000 -2.60515700
O -1.47129700 0.96219300 2.21280200
C -0.79110800 1.56950800 3.27900800
H -1.46084100 1.57486200 4.15284200
H 0.12470500 1.03108400 3.56483300
H -0.52449400 2.61436300 3.05622000

Reaction coordinates: Redox potential investigation

^{6}FP-OMe (gas phase)
ub3lyp/cc-pVTZ & LanL2DZ,
el. energy = -1227.384531 a.u.

N -1.39194300 1.44271800 -0.29418000
Fe 0.03943300 0.00001600 0.25774000
C -3.37857600 0.00150400 -0.42391300
C 0.05521900 -3.42924500 -0.30149600
C -1.18860800 -2.79988400 -0.33673000
C -2.45733700 -3.47964900 -0.45712000
C -3.42244300 -2.51666600 -0.49322900
C -2.74901400 -1.24267000 -0.39418000
N -1.39321000 -1.44144700 -0.29420000
H -2.58090600 -4.55309600 -0.51838700
H -4.49269600 -2.64546100 -0.58969000
C -3.42022300 2.51970600 -0.49332400
C -1.18615200 2.80097700 -0.33668300
C -2.45427900 3.48184600 -0.45719400
H -4.49035800 2.64942800 -0.58984900
H -2.57691700 4.55539900 -0.51849000
C 2.57366100 -3.48254000 -0.28607700
C 2.85823100 -1.24524300 -0.21307400
C 3.53833800 -2.51959200 -0.25869100
H 2.70075300 -4.55632300 -0.33165900
H 4.61281000 -2.64774500 -0.27688500
C 0.05822100 3.42924300 -0.30135200
C 3.48882700 -0.00150400 -0.19981900
C 3.54054500 2.51655200 -0.25847100
C 1.30210600 2.79981400 -0.25725400
C 2.57670300 3.48033700 -0.28588800
H 4.61512600 2.64379300 -0.27662900
H 2.70471700 4.55401100 -0.33146000
C 2.85933400 1.24279400 -0.21294900
C -2.74791400 1.24512300 -0.39424000
C 1.29965500 -2.80090600 -0.25743000
N 1.50032200 -1.44409100 -0.20968900
N 1.50159600 1.44282000 -0.20955500
O -0.02416500 -0.00019000 2.06908900
C -1.01459700 0.00009700 3.05570200
H -1.65804300 -0.88933200 2.97878200
H -0.54790200 -0.00213000 4.05069700
H -1.65491300 0.89200100 2.98131800
H -4.46103400 0.00198600 -0.50800300
H 0.05570800 -4.51421700 -0.34255700
H 4.57452000 -0.00198800 -0.20489500
H 0.05967200 4.51421400 -0.34240400

^{6}FP-OMe (toluene)
ub3lyp/cc-pVTZ & LanL2DZ,
el. energy = -1227.410308 a.u.

N -1.16306400 1.65362300 -0.27950400

Fe 0.03999600 0.00477400 0.23562900
C -3.34373700 0.52831200 -0.41245200
C -0.46714200 -3.38761500 -0.31957500
C -1.60189300 -2.57613900 -0.34721600
C -2.95940700 -3.05317300 -0.47003300
C -3.76728900 -1.95391400 -0.49880100
C -2.90907100 -0.79732500 -0.39280900
N -1.59859600 -1.20186200 -0.29360300
H -3.24458500 -4.09515700 -0.53852600
H -4.84482000 -1.91783200 -0.59514300
C -3.00482100 3.02675900 -0.45815900
C -0.75297500 2.96503300 -0.30667800
C -1.90418100 3.83141200 -0.41411500
H -4.04350400 3.31767400 -0.54893800
H -1.86278600 4.91197200 -0.46219000
C 2.01603200 -3.82191800 -0.30795500
C 2.63676900 -1.65285700 -0.23196400
C 3.11556800 -3.01575600 -0.27948500
H 1.97909500 -4.90274200 -0.35371300
H 4.15854400 -3.30482500 -0.29712900
C 0.57319200 3.39632400 -0.26791200
C 3.44807600 -0.51786700 -0.21131900
C 3.87893200 1.96562000 -0.23786800
C 1.70840300 2.58514100 -0.23425000
C 3.07118700 3.06464000 -0.25174200
H 4.96066300 1.92949700 -0.25188600
H 3.35997200 4.10744700 -0.27996800
C 3.01419300 0.80830800 -0.21155600
C -2.53327400 1.66351700 -0.37569400
C 0.85909300 -2.95593000 -0.27800600
N 1.26400800 -1.64514400 -0.22933300
N 1.70185800 1.21236400 -0.20705200
O 0.00298700 0.00161300 2.05418200
C -0.98021900 -0.09672700 3.04330800
H -1.63705700 -0.96490400 2.88258300
H -0.50793300 -0.21040800 4.03034100
H -1.61052900 0.80561200 3.07663000
H -4.41388500 0.69194700 -0.49462200
H -0.63187100 -4.45979100 -0.36523600
H 4.52120400 -0.68234200 -0.21565500
H 0.73962400 4.46888200 -0.29424800

^{5}FP-OMe^{-} (gas phase)
ub3lyp/cc-pVTZ & LanL2DZ,
el. energy = -1227.457250 a.u.

N -1.21261000 1.63316400 -0.30772500
Fe 0.03500700 0.00069900 0.41868600
C -3.34511800 0.42694600 -0.46903500
C -0.36584200 -3.40481200 -0.36305300
C -1.53454400 -2.63106500 -0.39076200
C -2.88057900 -3.15461300 -0.55098300
C -3.71829900 -2.07733200 -0.58071600
C -2.88322400 -0.89657300 -0.43862400
N -1.57606400 -1.26913100 -0.31499200
H -3.13838500 -4.20351600 -0.64150100
H -4.79560000 -2.07247700 -0.70001300
C -3.09006300 2.94706900 -0.55675600
C -0.83723400 2.94350700 -0.36681900
C -2.01300300 3.78446700 -0.51735300
H -4.13552800 3.20882600 -0.67227300
H -2.00470300 4.86559200 -0.59439600
C 2.13948600 -3.78325800 -0.36535200
C 2.68943800 -1.59400900 -0.24367200
C 3.21646000 -2.94621500 -0.32724900
H 2.13627200 -4.86467200 -0.43845900
H 4.26763700 -3.20805700 -0.36327100
C 0.48583400 3.40531500 -0.33071800
C 3.46444300 -0.42611000 -0.22697200
C 3.84477700 2.07838300 -0.30162900
C 1.65261700 2.63019000 -0.27636300
C 3.00705200 3.15518400 -0.33087000
H 4.92807000 2.07378900 -0.33687800
H 3.27016400 4.20470400 -0.39483200
C 3.00110300 0.89693800 -0.22944000
C -2.57115400 1.59536500 -0.43013000
C 0.95587800 -2.94133300 -0.30466400
N 1.32614700 -1.63105800 -0.22263900
N 1.68895100 1.26836700 -0.20549400
O 0.00458100 0.00137300 2.30795800
C -1.06991100 -0.00901300 3.17361300
H -1.83087700 -0.77993400 2.92921000
H -0.75130000 -0.21629300 4.21687400
H -1.61627200 0.95796900 3.21090900
H -4.41952400 0.56179100 -0.57359100
H -0.49763700 -4.48245000 -0.43235400
H 4.54367400 -0.56088900 -0.24923500
H 0.62353900 4.48288500 -0.38846200

^{5}FP-OMe^{-} (toluene)
ub3lyp/cc-pVTZ & LanL2DZ,
el. energy = -1227.515493 a.u.

N 1.29273300 -1.56925600 -0.30790300
Fe -0.03642500 -0.00113300 0.39373000
C 3.36755400 -0.26389300 -0.46542100
C 0.20889700 3.42632400 -0.33980200
C 1.41317600 2.70789200 -0.37083300
C 2.73437000 3.29361800 -0.52003200
C 3.62114900 2.25615900 -0.55955300
C 2.84262700 1.03637000 -0.43313100
N 1.51759700 1.34708200 -0.31007500
H 2.94451500 4.35454800 -0.59725200
H 4.69837000 2.30287700 -0.67415100
C 3.23014100 -2.79468100 -0.55066200
C 0.97867300 -2.89741300 -0.36381800
C 2.19286100 -3.68149200 -0.50913300
H 4.28716900 -3.00857300 -0.66307300
H 2.23538300 -4.76250300 -0.58193600
C -2.31246100 3.68513200 -0.34283900
C -2.76075400 1.47067600 -0.24829100
C -3.34938100 2.79782600 -0.31461400
H -2.36067300 4.76674000 -0.40163700
H -4.41195700 3.01137400 -0.34634200

C -0.32143500 -3.42238900 -0.32801600
C -3.48044700 0.26678400 -0.23743300
C -3.74120600 -2.25457900 -0.30010200
C -1.52492100 -2.70362300 -0.28012800
C -2.85341600 -3.29131500 -0.32357200
H -4.82401500 -2.30213000 -0.32947500
H -3.06786200 -4.35289700 -0.37582300
C -2.95545600 -1.03374000 -0.24203200
C 2.64968100 -1.46822800 -0.42924100
C -1.09040000 2.90047100 -0.29358300
N -1.39903000 1.57188100 -0.22855200
N -1.62585900 -1.34292400 -0.22260800
O -0.03723300 -0.01900500 2.29335300
C 1.04341700 -0.00798800 3.14931300
H 1.71260500 0.86827300 3.01090800
H 0.72007200 0.02404900 4.21211200
H 1.69062400 -0.90715600 3.05921900
H 4.44757100 -0.34706000 -0.56657000
H 0.29042600 4.50979500 -0.39494200
H -4.56493300 0.35102500 -0.25541900
H -0.40649900 -4.50582100 -0.37791300

^{2}EDA$^+$ (gas phase)
ub3lyp/cc-pVTZ,
el. energy = -415.769919 a.u.
C -1.31552000 -0.75995700 -0.34433600
C -0.18194800 0.20046000 -0.15801200
O -0.45611800 1.38875000 -0.15973300
O 0.96377500 -0.40769700 -0.09052900
C 2.19455300 0.44264000 0.00465900
H 2.02046000 1.15664000 0.81298100
H 2.26492600 0.98113100 -0.94309200
N -3.52833500 -0.01450900 0.43976800
N -2.52489800 -0.35484900 0.06482000
C 3.35693900 -0.48430700 0.25690900
H 3.48014200 -1.20130200 -0.55821700
H 4.26818000 0.11774900 0.32077300
H 3.23978300 -1.02503600 1.19884400
H -1.28625600 -1.68511600 -0.91663600

^{2}EDA$^+$ (toulene)
ub3lyp/cc-pVTZ,
el. energy = -415.826516 a.u.
C -1.28207900 -0.83613500 -0.09620600
C -0.19088800 0.20140000 -0.05379300
O -0.46159200 1.38182800 -0.01856400
O 0.97000400 -0.40888200 -0.07721300
C 2.17979500 0.45059700 -0.06129900
H 2.05020200 1.17908200 0.74278700
H 2.20035400 0.97878100 -1.01859000
N -3.56148800 0.05817000 0.13603200
N -2.53130600 -0.37374800 0.02645000
C 3.36999700 -0.45282200 0.14146700
H 3.45236100 -1.19199200 -0.65980800
H 4.27573000 0.16115700 0.13387200
H 3.31705900 -0.97117500 1.10250100
H -1.17438500 -1.90861700 -0.25292100

^{1}EDA (gas phase)
ub3lyp/cc-pVTZ,
el. energy = -416.102649 a.u.
C -1.29512900 -0.79393100 -0.00002600
C -0.22107700 0.19529400 0.00000500
O -0.36869400 1.40273600 -0.00008000
O 0.97687200 -0.43686800 0.00014600
C 2.13414600 0.43054900 0.00008100
H 2.09254800 1.07661600 0.88252700
H 2.09231900 1.07676800 -0.88223200
N -3.59283900 0.03746400 0.00001800
N -2.52714600 -0.35868500 -0.00001300
C 3.36458600 -0.45556400 -0.00010300
H 3.38641800 -1.09512900 -0.88700600
H 4.26668000 0.16390700 -0.00016100
H 3.38658000 -1.09517300 0.88676700
H -1.14523300 -1.86346300 -0.00019800

^{1}EDA (toluene)
ub3lyp/cc-pVTZ,
el. energy = -416.106687 a.u.
C -1.29499000 -0.80005400 -0.00022400
C -0.22281300 0.19021000 -0.00014200
O -0.37838000 1.39886700 -0.00007800
O 0.97482100 -0.43417400 -0.00024300
C 2.13637800 0.43238100 -0.00006200
H 2.09753400 1.07640700 0.88395000
H 2.09793200 1.07637100 -0.88408900
N -3.58658100 0.04326900 0.00035400
N -2.52331200 -0.35887500 0.00003600
C 3.36531400 -0.45238400 0.00031000
H 3.39216100 -1.09203000 -0.88709000
H 4.26506100 0.17148100 -0.00071500
H 3.39299800 -1.09030600 0.88892400
H -1.15130000 -1.87113900 -0.00043600